FUNDAMENTALS OF MACHINING AND MACHINE TOOLS

SECOND EDITION

GEOFFREY BOOTHROYD
WINSTON A. KNIGHT

Fundamentals of Machining and Machine Tools

Second Edition

Geoffrey Boothroyd
Winston A. Knight

University of Rhode Island
Kingston, Rhode Island

Preface

This book is intended primarily for those studying and teaching the principles of machine tools and metal machining in universities and colleges. It should also prove useful to those concerned with manufacturing in industry.

The mathematical content of the book is deliberately limited. Those who have taken basic courses in statics and dynamics and who have had an introduction to calculus should have no difficulty in comprehending the material.

Many of the present texts dealing with the same material are purely descriptive. In this book, the approach is to illustrate, through fundamentals and analysis, the causes of various phenomena and their effects in practice. Emphasis is given to the economics of machining operations and the design of components for economic machining.

A significant portion of the book is based on a previous text written by one of the authors (Geoffrey Boothroyd) and published by McGraw-Hill. While much of this material has been retained, recent developments have been included where appropriate. Several new chapters have been introduced and others largely rewritten. The section on tool materials has been expanded to include the modern materials that are contributing significantly to increases in productivity in industry. A new chapter on

machine tool vibrations has been included, which covers the fundamental aspects of machine tool chatter, the dynamic testing of machine tools, and the practical means of improving machine tool stability. The chapter on grinding has been expanded to include thermal aspects of the process and a description of new grinding processes, including creep feed grinding.

New emphasis in the book has been placed on the utilization of machine tools through the inclusion of chapters on manufacturing systems and automation and on computer-aided manufacturing, together with an expanded chapter on design for machining, which serves as an introduction to an area of growing importance, that of design for manufacturability. Various types of automation in machine tools are outlined and an introduction to cellular plant layouts and flexible manufacturing systems is included. Aspects of the programming of numerical control machine tools are discussed in some detail. Finally, because of their growing importance, the main nonconventional machining processes are described and examples of their application given.

We are indebted to those with whom we have been associated in recent years and who have assisted both directly and indirectly in the preparation of this book, including colleagues and graduate students whose work has been helpful in the preparation of this book. Finally, we would like to thank Ms. Kathleen Yorkery for typing the manuscript.

GEOFFREY BOOTHROYD
WINSTON A. KNIGHT

Contents

f

Conventions Used in This Book

STANDARDIZATION

Every attempt is made in this book to follow the latest International Organization for Standardization (ISO) recommendations for units and definitions. The most important of these is, of course, the International System (SI) of basic and derived units. The basic system is described in ISO Standard 1000, and recommendations for its application are specified in ISO Recommendation R31. The latter document includes suggested symbols for the various derived units.

In addition, numerous standards are becoming available covering various aspects of machining and are followed as closely as possible. Unfortunately, some of these new standards include symbols and definitions that are at variance with the SI; this variance leads to a certain amount of duplication. For example, the recommended symbol for the feed applied in a machining operation is f, which is also the recommended symbol for frequency of vibration. Confusion among measurements and symbols is avoided, however, by the use of appropriate suffixes and subscripts, respectively.

This book is written entirely in SI units because the U.S. manufacturing industry is already in the process of conversion to the SI system.

Table S1.1   Units Derived from the Basic SI Units

Unit being measured	Symbol	Name of unit	Symbol for unit
Angle, plane	α, β, γ, etc.	Radian	rad
Angular velocity	ω	–	rad/s
Angular acceleration	α	–	rad/s^2
Frequency	f	Hertz	Hz
Rotational frequency	n	Reciprocal second	s^{-1}
Area	A	–	m^2
Volume	V	–	m^3
Velocity	v	–	m/s
Acceleration	a	–	m/s^2
Density	ρ	–	kg/m^3
Force	F	Newton	kg$\cdot$m/s^2, or N
Energy, work, heat	W	Joule	N$\cdot$m, or J
Pressure, stress	p	Pascal	N/m^2, or Pa
Power	P	Watt	J/s, or W
Temperature difference	θ	Degree Celsius	K $-$ 273.15, or °C

Where SI units are specified in the text, the approximate English (U.S. Customary System [USCS]) equivalents are given in parentheses. Graphs and results from previously published work are reproduced with the original scales in English (USCS) units, and the corresponding SI scales are added at the right and along the top where appropriate. Graphs produced specifically for this book are given in SI units with the equivalent English units added at the right and along the top.

Table S1.2   Prefixes Used with SI Units

Multiple and submultiple[a]	Prefix	Symbol
10^9, or E + 09	giga	G
10^6, or E + 06	mega	M
10^3, or E + 03	kilo	k
10^{-3}, or E − 03	milli	m
10^{-6}, or E − 06	micro	μ
10^{-9}, or E − 09	nano	n
10^{-12}, or E − 12	pico	p

[a]$E \pm ab = 10^{\pm ab}$

Table SI.3 USCS-SI Conversion Table

Quantity	To convert from	To	Multiply by[a]	
Length	inch (in.)	meter (m)	2.54*	$E-02$
	foot (ft)	meter (m)	3.048*	$E-01$
Mass	pound (lb)	kilogram (kg)	4.535 924	$E-01$
Time	minute (min)	second (s)	6.0*	$E+01$
	hour (hr)	second (s)	3.6*	$E+03$
Force	pound force (lbf)	newton (N)	4.448 222	$E+00$
Speed	foot per minute (ft/min)	meter per second (m/s)	5.08*	$E-03$
	inch per second (in./sec)	meter per second (m/s)	2.54*	$E-02$
	inch per minute (in./min)	meter per second (m/s)	4.233*	$E-04$
	revolution per minute (rpm)	radian per second (rad/s)	1.047 192	$E-01$
Acceleration	foot per second per second (ft/sec^2)	meter per second per second (m/s^2)	3.048*	$E-01$
	inch per second per second (in./sec^2)	meter per second per second (m/s^2)	2.54*	$E-02$
Area	square inch (in.^{2})	square meter (m^2)	6.451 6*	$E-04$
Volume	cubic inch (in.^{3})	cubic meter (m^3)	1.638 706	$E-05$
Volume flow rate	cubic inch per minute (in.^{3}/min)	cubic meter per second (m^3/s)	2.731 177	$E-07$
Density	pound per cubic inch (lb/in.^{3})	kilogram per cubic meter (kg/m^3)	2.767 991	$E+04$
Pressure, stress	pound force per square inch (lbf/in.^{2})	newton per square meter (N/m^2)	6.894 757	$E+03$
Energy, work heat	British thermal unit (Btu)	newton-meter (N-m), or joule (J)	1.055 06	$E+03$
Power	horsepower (hp)	joule per second (J/s), or watt (W)	7.457	$E+02$
	foot-pound force per minute (ft-lbf/min)	joule per second (J/s), or watt (W)	2.259 697	$E-02$
Thermal conductivity	Btu in./hr ft^2°F	joule per second meter kelvin (J/smK), or watt per meter kelvin (W/mK)	1.442 279	$E-01$
Specific heat capability	Btu/lb°F	joule per kilogram kelvin (J/kgK)	4.184	$E+03$

[a]Values followed by an asterisk are exact conversions.

INTRODUCTION TO THE INTERNATIONAL (SI) SYSTEM OF UNITS

In 1960 the General Conference of Weights and Measures on the International System of Units formally approved the system of units known as the International (SI) System of Units. This system is now being adopted throughout the world and is currently being adopted by the United States. In practice the system is convenient because it obviates the need for the insertion of conversion factors into equations and eliminates many of the ambiguities present in other systems. The basic SI units encountered in engineering are defined as follows:

1. The unit of length l is the meter, m, which is the length equal to 1, 650, 763.73 wavelengths in vacuo of the radiation corresponding to the transition between the levels $2p_{10}$ and $5d_5$ of the krypton-86 atom.
2. The unit of mass m is the kilogram, kg, which is equal to the mass of the international prototype of the kilogram.
3. The unit of time t is the second, s, which is the duration of 9, 192, 631, 770 periods of the radiation corresponding to the transition between the two hyperfine levels of the ground state of the cesium-133 atom.
4. The unit of temperature T is the kelvin, K, which is 1/273.16 of the thermodynamic temperature of the triple point of water.
5. The unit of electric current l is the ampere, A, which is that constant current which, if maintained in two straight parallel conductors of infinite length, of negligible, circular cross section and placed 1 meter apart in a vacuum, would produce between these conductors a force equal to 2×10^{-7} newton per meter of length.

To encourage the student or reader to become familiar with SI units, most of the problems presented at the end of each chapter are given in SI units without the English equivalents. It is hoped that the student or reader will thereby discover that the new system is considerably easier to work with than the U.S. Customary System (pounds, feet, etc.).

For those not sufficiently familiar with the SI system the tables introduce the basic and derived units and their definitions and recommended symbols. Useful conversions are also given.

Table SI.1 presents a selection of derived units.

The most common prefixes for SI units are listed in Table SI.2. It should be noted that

1. The prefix refers to the whole unit; for example, the m (milli) in m · N/ m² means m(N/m²), not mN/m². The dot is used to indicate multiplication when confusion could arise.
2. Prefixes in denominators are avoided, except for k in kg (kilogram).

Useful conversion factors are given in Table SI.3.

1
Machine Tools and
Machining Operations

1.1 INTRODUCTION

The history of metal cutting dates from the latter part of the eighteenth century. Before that time machine tools did not exist, and the following extract from the diary of an English engineer, Richard Reynolds, dated October 1760, gives some idea of the manufacturing problems that had to be faced. Richard Reynolds was attempting to produce a cylinder for a fire engine for drawing water from a coal pit. The cylinder, of cast brass, had a length of 9 ft and a bore 28 in. in diameter. He wrote:

> Having hewed two balks of deal to a suitable shape for the cylinder to lie therein solidly on the earth in the yard, a plumber was procured to cast a lump of lead of about three hundred weight, which being cast in the cylinder, with a dike of plank and putty either side, did make it of a curve to suit the circumference, by which the scouring was much expedited. I then fashioned two iron bars to go around the lead, whereby ropes might be tied, by which the lead might be pulled to and fro by six sturdy and nimble men harnessed to each rope, and by smearing the cylinder with emery and train oil through which the lead was pulled, the circumference of the cylinder on which the lead lay was presently made of a superior smoothness; after which the cylinder

being turned a little, and that part made smooth, and so on, until with exquisite pains and much labour the whole circumference was scoured to such a degree of roundness as to make the longest way across less than the thickness of my little finger greater than the shortest way; which was a matter of much pleasure to me, as being the best that we so far had any knowledge of.

In 1776 James Watt built the first successful steam engine, and one of his greatest difficulties in developing this machine was the boring of the cylinder casting. His first cylinder was manufactured from sheet metal, but it could not be made steamtight. Even attempts to fill the gap between the piston and the cylinder with cloth, leather, or tallow were of no avail. The problem was eventually solved by John Wilkinson when he invented the horizontal-boring machine. This machine consisted of a cutting tool mounted on a boring bar that was supported on bearings outside the cylinder. The boring bar could be rotated and fed through the cylinder, thus generating, with the tool points, a cylindrical surface independent of the irregularities of the rough casting (Fig. 1.1). This boring machine was the first effective machine tool, and it enabled James Watt to produce a successful steam engine.

Metal cutting as we know it now started with the introduction of this first machine tool. Today, machine tools form the basis of our industry and are used either directly or indirectly in the manufacture of all the products of modern civilization.

1.2 GENERATING MOTIONS OF MACHINE TOOLS

The principle used in all machine tools is one of generating the surface required by providing suitable relative motions between the cutting tool and the workpiece. The cutting edge or edges on the cutting tool remove a layer of work material; the removed material is called a shaving or a chip. The simplest surfaces to generate are flat surfaces and internal or external cylindrical surfaces. For example, if a tool is reciprocated backward and forward in a straight line and a workpiece is incrementally fed beneath the tool in a direction at right angles to the motion of the tool, a flat surface will be generated on the workpeice. Similarly, a cylindrical surface can be generated by rotating the workpiece and feeding the tool parallel to the axis of workpiece rotation. Thus, in general, two kinds of relative motion must be provided by a metal-cutting machine tool. These motions are called primary motion and feed motion and are defined as follows:

The primary motion is the main motion provided by a machine tool or manually to cause relative motion between the tool and workpiece so
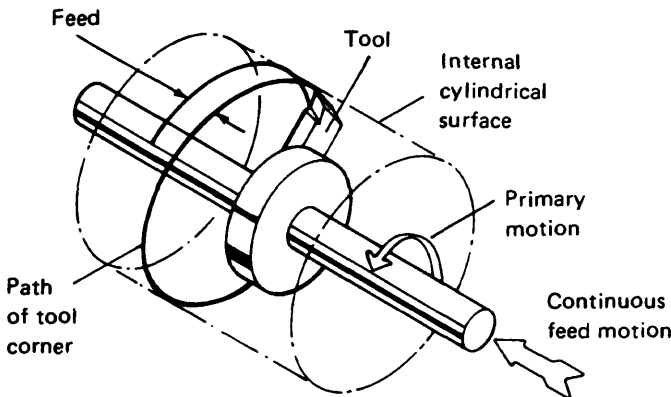
Figure 1.1   Generation of a cylindrical surface in horizontal boring.

that the face of the tool approaches the workpiece material. Usually, the primary motion absorbs most of the total power required to perform a machining operation.

The feed motion is a motion that may be provided to the tool or workpiece by a machine tool which, when added to the primary motion, leads to a repeated or continuous chip removal and the creation of a machined surface with the desired geometric characteristics. This motion may proceed by steps or continuously; in either case it usually absorbs a small proportion of the total power required to perform a machining operation.

To facilitate the descriptions of machine tool motions it is useful to employ a system of machine tool axes recommended by the International Organization for Standards [1]. Although this system was established for the purposes of programming numerically controlled machine tools, it is likely to be adopted as a general system for all machine tools. The system is based on the right-hand coordinate system shown in Fig. 1.2a and refers to the possible motions of a tool in a machine tool. The three coordinate axes X, Y, and Z refer to possible linear motions of the tool, and the motions A, B, and C refer to possible rotary motions of the tool about these axes, respectively. To understand the right-hand screw sign convention used in this system it is helpful to imagine a right-hand screw thread aligned with each axis. If a screwed nut mounted on any axis is rotated such that it moves along the axis in a positive direction away from the origin, that rotary motion is positive.

A particular machine tool can move the tool in only a few of the possible directions shown in Fig. 1.2a. However, before the actual directions of
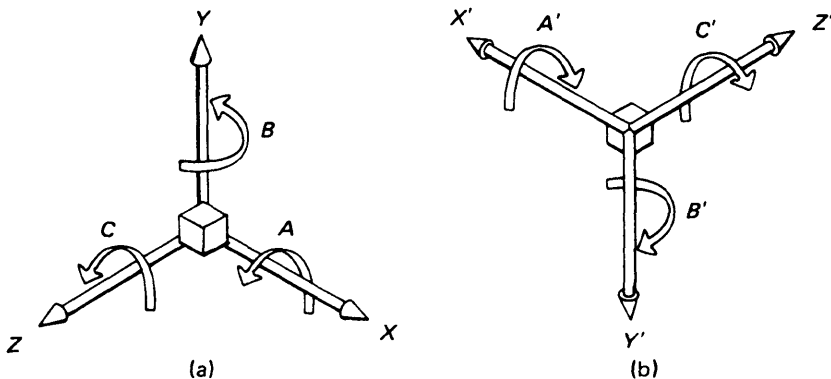
Figure 1.2 Coordinate system for specification of machine tool motions. (a) Motions of tool; (b) motions of workpiece.

motion in a particular machine tool can be labeled, it is necessary to orient the coordinate system relative to that machine tool. The coordinate system is oriented as follows:

The Z axis of motion is arranged parallel to the axis of the machine spindle, which provides primary motion. If the machine has no spindle, the Z axis is arranged perpendicular to the work-holding surface. Positive Z motion increases the distance between the workpiece and toolholder.

Where possible, the X axis is horizontal and parallel to the work-holding surface. On machines with no main spindle the X axis is parallel to and positive in the principal direction of cutting (primary motion). On machines with rotating workpieces, the X motion is radial and parallel to the cross slide. (Positive X motion is defined as the motion of a tool when it recedes from the axis of rotation of the workpiece.) On machines with rotating tools:

1. If the Z axis is horizontal, positive X motion is to the right when viewed from the main spindle toward the workpiece.
2. If the Z axis is vertical, positive X motion is to the right when viewed from the main spindle toward the machine column.

Positive Y motion is selected to complete the coordinate system shown in Fig. 1.2a.

For motion of the workpiece in a machine tool a similar set of axes and motions is employed (Fig. 1.2b), but the appropriate letter is primed, and the sign convention is reversed. The reason for the prime and reversed sign is that if, for example, a tool can be made to approach a workpiece by

motion in the positive X direction, the same effect can be obtained by moving the workpiece in the positive X' direction.

In the following sections some common low-production machine tools will be described and their generating motions illustrated. These machine tools can be divided into three groups:

1. Those using single-point tools
2. Those using multipoint tools
3. Those using abrasive wheels

Machines using single-point tools will be described first, starting with the most common, the engine lathe. The description of the engine lathe and some of the operations that can be performed on it will be used to introduce numerous terms and definitions that are applicable to all types of machining operations. This description is therefore necessarily quite lengthy, but it is important even for those familiar with machining operations because of the new international terminology used.

For the present purposes the term *machining* will be taken to mean any process in which material is removed gradually from a workpiece, including metal cutting with single-point and multipoint tools and grinding with abrasive wheels.
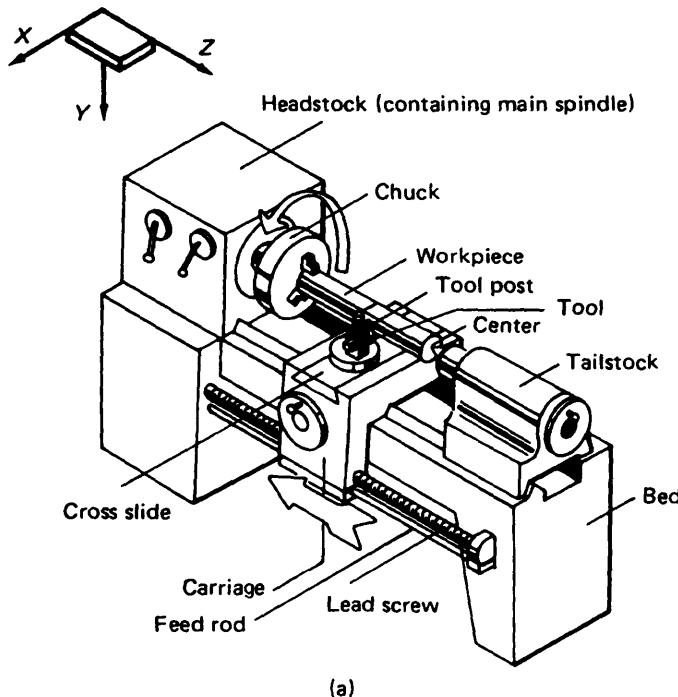
For each machining operation, equations are developed to estimate the time taken to perform the operation and the power required. At the end of the chapter a summary of these equations is presented, together with typical characteristics of the machines described (including speed range, feed range, power, efficiency, size, and accuracy) and characteristics of various work materials.

1.3   MACHINES USING SINGLE-POINT TOOLS
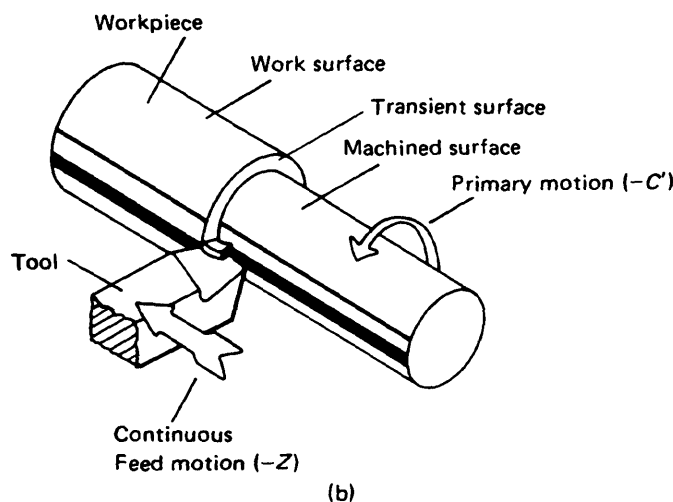
1.3.1   Engine Lathe (Center Lathe)

An engine lathe is shown diagrammatically in Fig. 1.3a; it consists of a horizontal bed supporting the headstock, the tailstock, and the carriage. All machine tools must have a means of supporting or holding the workpiece. In Fig. 1.3 the workpiece is gripped at one end by a chuck mounted on the end of the main spindle of the machine and is supported at the other end by a center mounted in the tailstock. The tailstock can be clamped at various positions along the bed to accommodate workpieces of various lengths. Short workpieces need only be gripped by the chuck.

Primary motion, the rotation of the workpiece (motion C'), is provided by the movement of a series of gears driving the main spindle, the gears being driven by an electric motor mounted at the rear of the machine. The

(a)

(b)

Figure 1.3   (a) An engine lathe; (b) cylindrical turning on an engine lathe.

main spindle and the gears are all mounted in the headstock. Levers on the front of the headstock allow various rotational speeds to be selected.

The single-point cutting tool is held in a toolholder or tool post, which is mounted on a cross slide, which in turn is mounted on the carriage. The carriage is driven along the bed (motion Z) by a lead screw (for screw cutting) or a rack, pinion gear, and feed rod (for turning); both the lead screw and the feed rod are connected to the main spindle through a train of gears. Alternatively the carriage can remain stationary on the bed, and the gear train can be used to drive the toolholder across the carriage (motion X) using a lead screw in the cross slide.

Figure 1.3b shows a cylindrical surface being generated on a workpiece by the rotation of the workpiece ($-C'$ motion) and the movement of the carriage along the lathe bed ($-Z$ motion); this operation is known as cylindrical turning.

The feed motion setting on the lathe is the distance moved by the tool during each revolution of the workpiece. Once chosen, the feed setting remains constant regardless of the spindle speed because of the geared drive between the main spindle and the feed rod. The feed f for all machine tools is defined as the displacement of the tool relative to the workpiece, in the direction of feed motion, per stroke or per revolution of the workpiece or tool. Thus, to turn a cylindrical surface of length l_w, the number of revolutions of the workpiece is l_w/f, and the machining time t_m is given by

$$t_m = \frac{l_w}{fn_w} \qquad (1.1)$$

where n_w is the rotational frequency of the workpiece.

It should be emphasized at this point that n_w is the time for one pass of the tool (one cut) along the workpiece. This single pass does not necessarily mean, however, that the machining operation is completed. If the first cut is designed to remove a large amount of material at high feed (roughing cut), the forces generated during the operation will probably have caused significant deflections in the machine structure. The resulting loss of accuracy will necessitate a further machining operation at low feed (finish cut) to bring the workpiece diameter within the limits specified and provide a smooth machined surface. For these reasons, it is usual to machine the workpiece oversize deliberately during the roughing cut, leaving a small amount of material that will subsequently be removed during the finishing cut.

Before discussing the operation of the lathe further, it will be helpful to describe some of the features of the single-point tool used in the lathe and in several other types of machine tools.

1.3.2   Single-Point Tools

Single-point tools are cutting tools having one cutting part (or chip-producing element) and one shank. They are commonly used in lathes, turret lathes, planers, shapers, boring mills, and similar machine tools. A typical single-point tool is illustrated in Fig. 1.4. The most important features are the cutting edges and adjacent surfaces. These are shown in the figure and defined as follows:

1.   The face is the surface or surfaces over which the chip flows.
2.   The flank is the tool surface or surfaces over which the surface produced on the workpiece passes.
3.   The cutting edge is that edge of the face which is intended to perform cutting. The tool major cutting edge is that entire part of the cutting edge which is intended to be responsible for the transient surface on the workpiece. The tool minor cutting edge is the remainder of the cutting edge.
4.   The corner is the relatively small portion of the cutting edge at the junction of the major and minor cutting edges; it may be curved or straight, or it may be the actual intersection of these cutting edges.

   In general, when a tool is applied to a workpiece, its motion relative to the workpiece has two components:

1.   The motion resulting from the primary motion of the machine tool, which can be called the primary motion of the tool
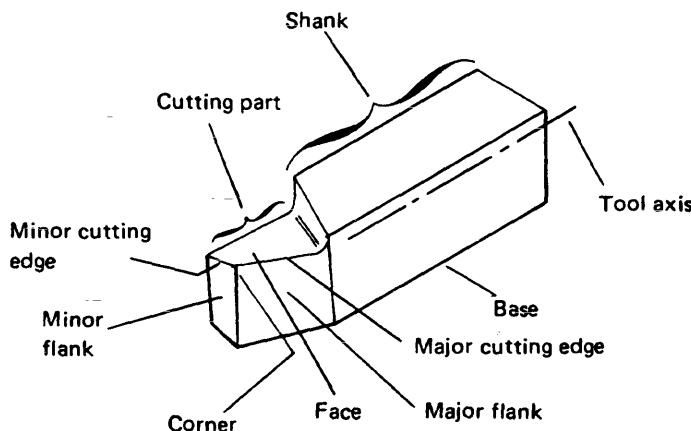
Figure 1.4   Typical single-point tool.

2. The motion resulting from the feed motion of the machine (Fig. 1.5)

The resultant of these two tool motions is called the resultant cutting motion and is defined as the motion resulting from simultaneous primary and feed motions.

It should be noted that in machine tools where the feed is applied while the tool is not engaged with the workpiece (as in shaping or planing, for example), the resultant cutting motion is identical to the primary motion. Where the feed motion is applied continuously, the angle between the direction of primary motion and the resultant cutting direction is called the resultant cutting-speed angle η. This angle is usually extremely small and for most practical purposes can be assumed to be zero. Further, the cutting speed v, the instantaneous velocity of the primary motion of the selected point on the cutting edge relative to the workpiece, can vary along the major cutting edge. The feed speed v_f, the instantaneous velocity

Tool-primary-motion vector

Resultant cutting-speed angle

Resultant cutting-motion vector

Tool feed motion vector

Selected point on the cutting edge
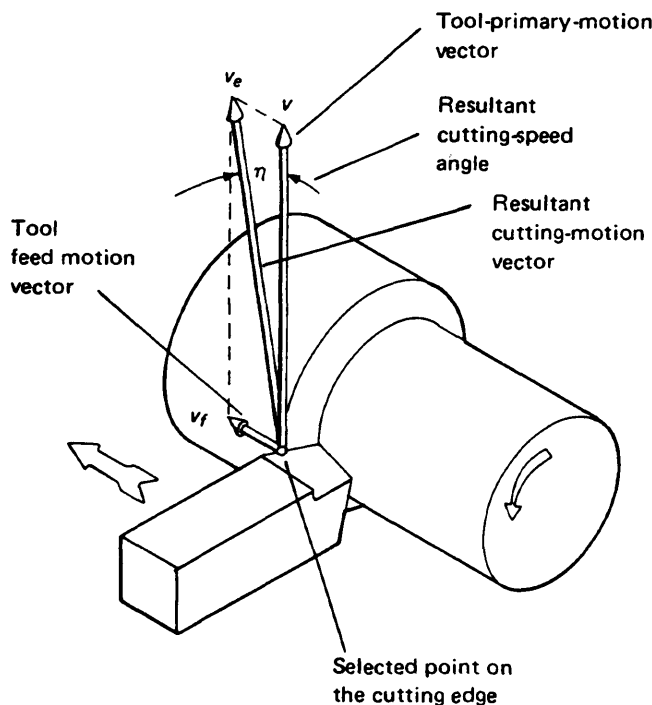
Figure 1.5   Resultant cutting motion in cylindrical turning.

of the feed motion of the selected point on the cutting edge relative to the workpiece, is constant.

Finally, the resultant cutting speed v_e, the instantaneous velocity of the resultant cutting motion of the selected point on the cutting edge relative to the workpiece, is given by

$$v_e = \frac{v}{\cos \eta} \tag{1.2}$$

but since for most practical operations η is very small, it can generally be assumed that

$$v_e = v \tag{1.3}$$

One of the important tool angles when considering the geometry of a particular machining operation is the angle in Fig. 1.6 called the major cutting-edge angle κ_r. The thickness of the layer of material being removed at the selected point on the cutting edge, known as the undeformed chip thickness a_c, significantly affects the power required to perform the operation. Strictly, this dimension should be measured both normal to the cutting edge and normal to the resultant cutting direction. However, for all practical purposes, since η is small, as described above, a_c can be measured normal to the direction of primary motion; thus in Fig. 1.6 and all subsequent figures, a_c will be measured this way. From Fig. 1.6, therefore, a_c is given by $a_f \sin \kappa_r$, where a_f is the feed engagement, the instantaneous engagement of the tool cutting edge with the workpiece measured in the direction of feed motion. For single-point cutting operations a_f is equal to the feed f, and therefore

$$a_c = f \sin \kappa_r \tag{1.4}$$

The cross-sectional area A_c of the layer of material being removed (cross-sectional area of the uncut chip) is approximately given by

$$A_c = f a_p \tag{1.5}$$

where a_p is the back engagement, previously known as depth of cut. The back engagement is the instantaneous engagement of the tool with the workpiece, measured perpendicular to the plane containing the directions of primary and feed motion (Fig. 1.5). In general the back engagement determines the depth of material removed from the workpiece in a single-point cutting operation.
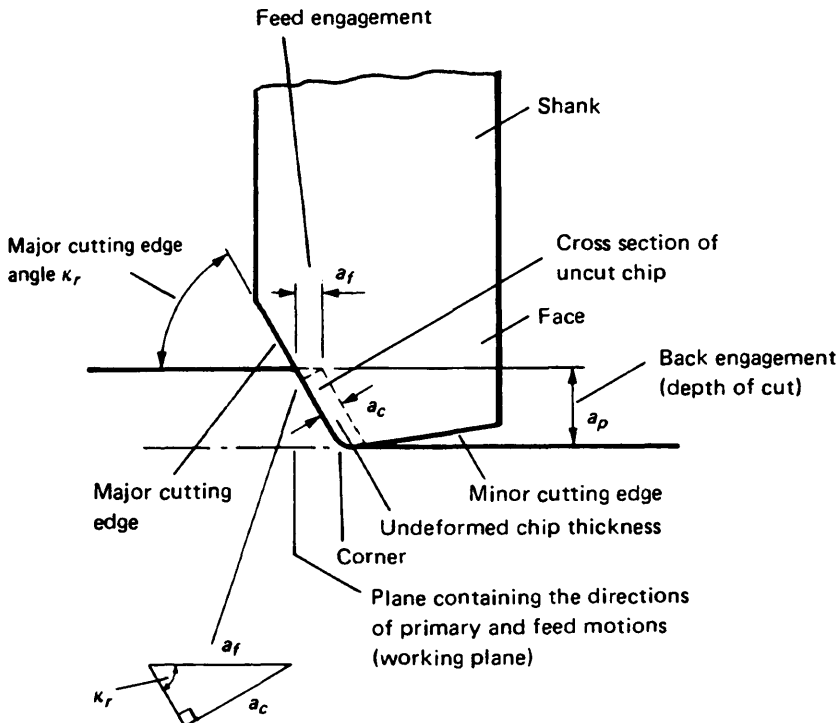
Figure 1.6 Single-point tool operation, where $a_c = a_f \sin \kappa_r$.

1.3.3 Typical Lathe Operations

Figure 1.7 illustrates five typical lathe operations: cylindrical turning, facing, boring, external threading, and cutoff. In each case the primary motion and the feed motion, together with certain other terms and dimensions, are indicated. In any machining operation the workpiece has three important surfaces:

1. The work surface, the surface on the workpiece to be removed by machining
2. The machined surface, the desired surface produced by the action of the cutting tool
3. The transient surface, the part of the surface formed on the workpiece by the cutting edge and removed during the following cutting stroke, during the following revolution of the tool or workpiece, or, in other cases (as, for example, in a thread-turning operation) (Fig. 1.7d) during the following pass of the tool

In Fig. 1.7a, which shows the geometry of a cylindrical-turning operation, the cutting speed at the tool corner is given by $\pi d_m n_w$, where n_w is the rotational frequency of the workpiece, and d_m is the diameter of the machined surface. The maximum value of the cutting speed is given by $\pi d_w n_w$, where d_w is the diameter of the work surface. Thus the average, or mean, cutting speed v_{av} is given by

$$v_{av} = \frac{\pi n_w (d_w + d_m)}{2} \qquad (1.6)$$

The metal removal rate Z_w is the product of the mean cutting speed and the cross-sectional area of the uncut chip A_c. Thus

$$Z_w = A_c v_{av}$$

$$= \frac{\pi a_f a_p n_w (d_w + d_m)}{2}$$

$$= \pi f a_p n_w (d_m + a_p) \qquad (1.7)$$

This same result could have been obtained by dividing the total volume of metal removed by the machining time t_m.
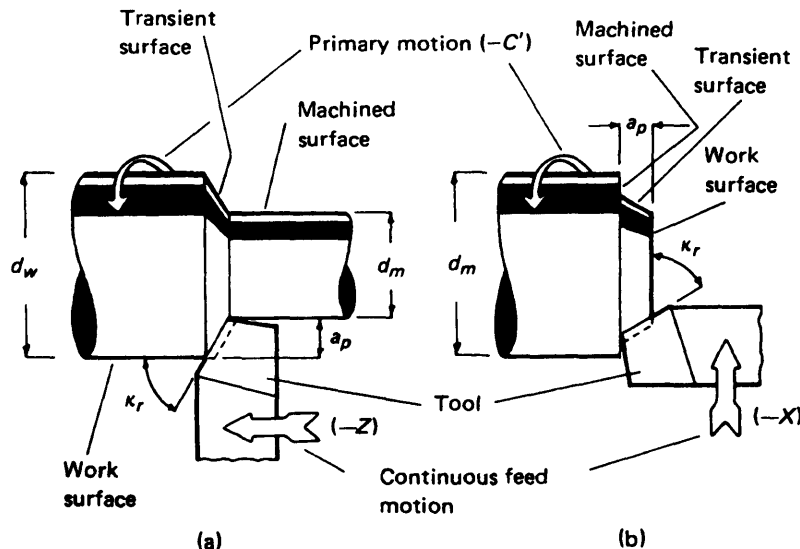
Figure 1.7 Lathe operations: (a) Cylindrical turning; (b) facing.
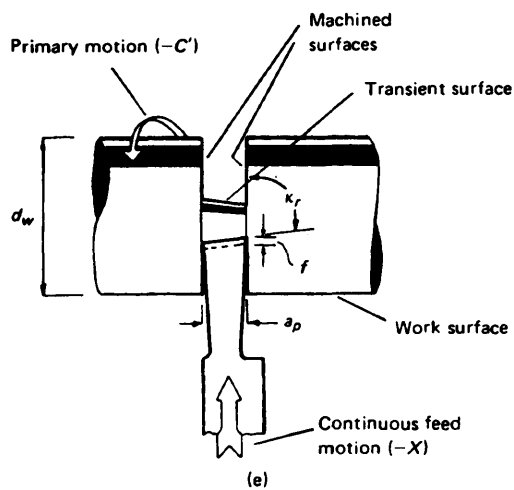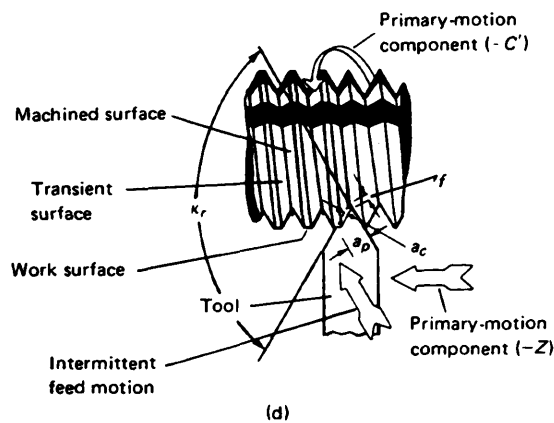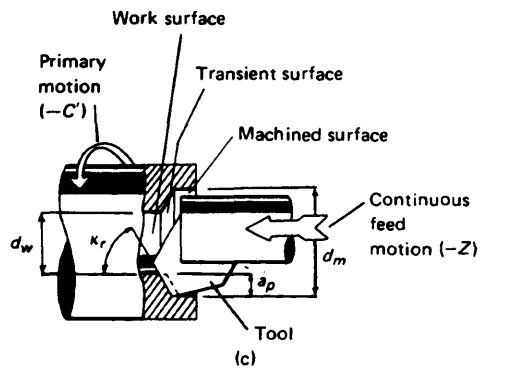
Figure 1.7 (continued) Lathe operations: (c) boring; (d) external threading; (e) parting or cutoff.

For operations where the back engagement a_p is small compared to the diameter of the machined surface d_m, the metal removal rate is approximately given by

$$Z_w \cong \pi f a_p n_w d_m \qquad (1.8)$$

For a given work material machined under given conditions, the energy required to remove a unit volume of material, p_s, can be measured. This factor is mainly dependent on the work material, and if its value is known, the power P_m required to perform any machining operation can be obtained from

$$P_m = p_s Z_w \qquad (1.9)$$

Finally, if the overall efficiency of the machine tool motor and drive systems is denoted by η_m, the electrical power P_e consumed by the machine tool is given by

$$P_e = \frac{P_m}{\eta_m} \qquad (1.10)$$

Approximate values of p_s for various work materials and various values of the underformed chip thickness are presented at the end of this chapter.

An operation in which a flat surface is generated by an engine lathe is shown in Fig. 1.7b and can be performed by feeding a tool in a direction at right angles ($-X$ motion) to the axis of workpiece rotation. In this operation, known as facing, the cutting speed at the tool corner varies from a maximum at the beginning of the cut to zero when the tool reaches the center of the workpiece. Clearly this operation can only be performed when the workpiece does not require support by the tailstock center.

The undeformed chip thickness a_c and the cross-sectional area of the uncut chip A_c are given, as in cylindrical turning, by Eqs. (1.4) and (1.5), respectively.

The machining time t_m is given by

$$t_m = \frac{d_m}{2 f n_w} \qquad (1.11)$$

The maximum cutting speed $v_{\max}$ and the maximum metal removal rate $Z_{w_{\max}}$ are given by

$$v_{max} = \pi n_w d_m \tag{1.12}$$

$$Z_{w_{max}} = \pi f a_p n_w d_m \tag{1.13}$$

Figure 1.7c shows an internal cylindrical surface being generated on a lathe. This operation is termed *boring* and can only be used to enlarge an existing hole in the workpiece. If the diameter of the work surface is d_w and the diameter of the machined surface is d_m, the mean cutting speed is given by Eq. (1.6) and the metal-removal rate by

$$Z_w = \pi f a_p n_w (d_m - a_p) \tag{1.14}$$

Finally the machining time t_m is given by Eq. (1.1) if l_w is taken as the length of the hole to be bored.

The lathe operation illustrated in Fig. 1.7d is known as external threading, or screw cutting. In this operation the primary motion of the tool is considered to be a combination of the motions $-C'$ and $-Z$. This motion generates a helix on the workpiece and is obtained by setting the gears that drive the lead screw to give the required pitch of the machined threads. The machining of a thread necessitates several passes of the tool along the workpiece, each pass removing a thin layer of metal from one side of the thread. The feed is applied in increments, after each pass of the tool, in a direction parallel to the machined surface. In calculating the production time, allowance must be included for the time taken to return the tool to the beginning of the cut, to increment the feed, and to engage the lathe carriage with the lead screw.

The last lathe operation to be illustrated (Fig. 1.7e) is used when the finished workpiece is to be separated from the bar of material gripped in the chuck. It is known as a parting, or cutoff, operation and produces two machined surfaces simultaneously. As with a facing operation, the cutting speed and hence the metal removal rate varies from a maximum at the beginning of the cut to zero at the center of the workpiece. The machining time is given by Eq. (1.11) and the maximum metal removal rate by Eq. (1.13).

1.3.4   Work and Tool Holding in an Engine Lathe

In the most common method of work holding the chuck has either three or four jaws (Fig. 1.8) and is mounted on the end of the main spindle. A three-jaw chuck is used for gripping cylindrical workpieces when the operations to be performed are such that the machined surface is concentric with the work surfaces. The jaws have a series of teeth that mesh with spiral grooves on a circular plate within the chuck. This plate can be
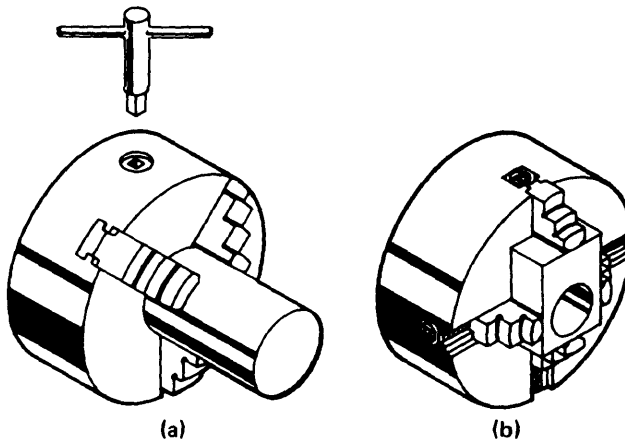
Figure 1.8   Lathe work holding using chucks. (a) Three-jaw chuck; (b) independent four-jaw chuck.

rotated by the key inserted in the square socket, resulting in simultaneous radial motion of the jaws. Since the jaws maintain an equal distance from the chuck axis, cylindrical workpieces are automatically centered when gripped.

With the four-jaw chuck, each jaw can be adjusted independently by rotation of the radially mounted threaded screws. Although accurate mounting of a workpiece can be quite time-consuming, a four-jaw chuck is often necessary for noncylindrical workpieces.

For very complicated shapes a circular faceplate can be used. The faceplate has radial slots that provide a means of bolting the workpiece to the faceplate.

For small lathes employed extensively for work on material provided in bar form, collets are often used. These collets are effectively split sleeves that fit snugly over the workpiece and have a taper on their outer surface. Drawing the collet into a matching tapered hole in the end of the spindle has the effect of squeezing the collet and gripping the workpiece.

For accurate turning operations or in cases where the work surface is not truly cylindrical, the workpiece can be turned between centers. This form of work holding is illustrated in Fig. 1.9. Initially the workpiece has a conical center hole drilled at each end to provide location for the lathe centers. Before supporting the workpiece between the centers (one in the headstock and one in the tailstock), a dog (a clamping device) is secured at the headstock end. The dog is arranged so that the tip is inserted in a slot

Headstock
Drive plate
Tailstock
Center
Dog
Center
Cavity for
Workpiece   clearance
60°
Taper hole to
accept center
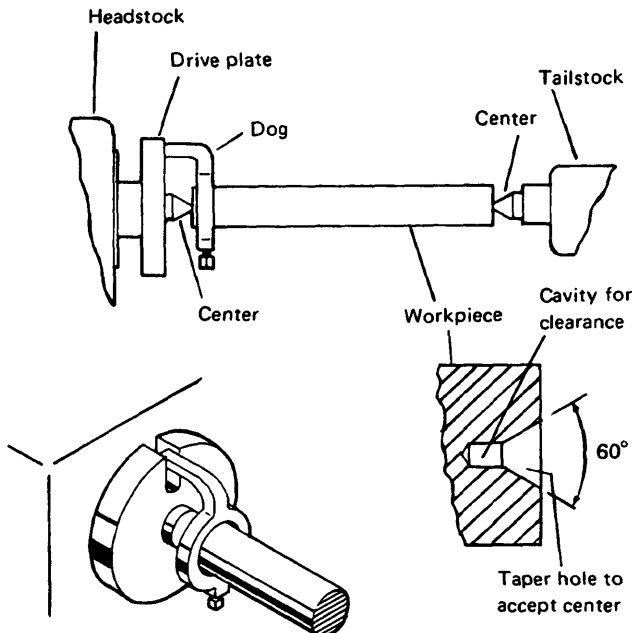
Figure 1.9   Work holding when turning between centers.

in the drive plate mounted on the main spindle, ensuring that the workpiece will rotate with the spindle.

The simplest form of tool holder is illustrated in Fig. 1.10 and is suitable for holding one single-point tool. Immediately below the tool is a curved block resting on a concave spherical surface; this method of support provides an easy way of inclining the tool so that its corner is at the correct height for the machining operation. In the figure the tool post is shown mounted on a compound rest. The rest is a small slideway that can be clamped in any angular position in the horizontal plane and is mounted on the cross slide of the lathe. The compound rest allows the tool to be hand-fed at an oblique angle to the lathe bed and is required, for example, in screw-threading operations and the machining of short tapers or chamfers.

Another common form of tool post is shown in Fig. 1.11; it also would be mounted on the compound rest. This four-way tool post can, as its name suggests, accommodate as many as four cutting tools. Any cutting tool can be quickly brought into position by unlocking the tool post with the lever provided, rotating the tool post, and, finally, reclamping with the lever.
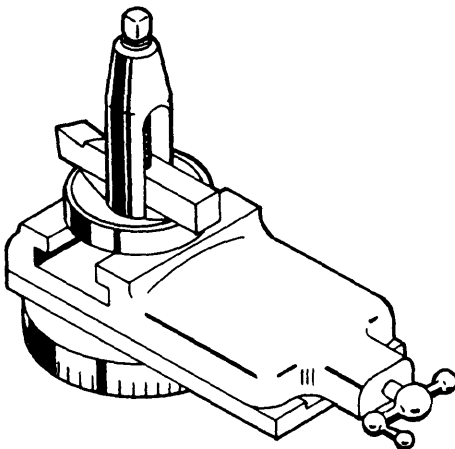
Figure 1.10   Typical lathe tool post and compound rest.

1.3.5   Other Types of Lathes

The engine lathe is the most common machine tool used in low-produc-
tion work. Several other kinds of lathes are available: for medium-
production work, turret lathes are widely employed. In a turret lathe the
tailstock is replaced with a rotary-indexing, hexagonal turret which can be
driven along the bed by the lead screw. A variety of tools can be mounted
on the faces of the turret (in some turret lathes two or more tools can be
mounted on the one face) and are brought into operation by manually in-
dexing the turret and engaging the feed drive.

Single-spindle and multispindle automatic lathes are suitable for
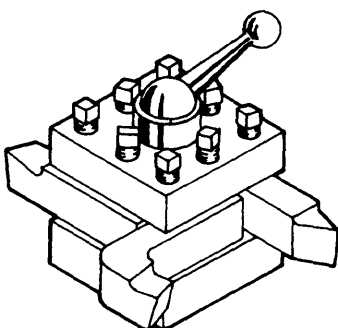
Figure 1.11   Four-way tool post.

high-volume or mass production of small components machined from work material in bar form. The various motions of these lathes are controlled by specially machined cams, and the operations are completely automatic, including the gradual feeding of the workpiece through the hollow spindle to the collet. The machine needs attention only when a new bar of material is required. Items such as small screws needed in large quantities are manufactured on this type of lathe.

1.3.6   Vertical-Boring Machine (Vertical Borer)

A horizontal-spindle lathe is not suitable for turning heavy, large-diameter workpieces. The axis of the machine spindle would have to be so elevated that a machinist could not easily reach the tool- and work-holding devices. In addition, it would be difficult to mount the workpiece on a vertical faceplate or support it between centers; for this reason a machine that operates on the same principle as a lathe but has a vertical axis is used and is known as a vertical-boring machine (Fig. 1.12). Like the lathe, this machine rotates the workpiece (motion C') and applies continuous, linear feed motion to the tool. This motion can be either at right angles to the axis of workpiece rotation (motion X) or parallel to it (motion Z).

Single-point tools are employed and mounted in a toolholder similar to the four-way tool post shown in Fig. 1.11 but without the rapid-indexing feature. The operations carried out are generally limited to turning ($-Z$ motion), facing ($-X$ motion), and boring ($-Z$ motion). These operations were illustrated in Fig. 1.7a to c; the geometry described and equations developed still apply.

The horizontal work-holding surface, which facilitates the positioning of large workpieces, consists of a rotary table having radial T slots for clamping purposes. Two typical work-holding methods are illustrated in Fig. 1.13.

1.3.7   Horizontal-Boring Machine (Horizontal Borer)

The last type of machine described here that uses single-point tools and has a rotary primary motion is a horizontal-boring machine (Fig. 1.14). This machine is needed mostly for heavy noncylindrical workpieces in which an internal cylindrical surface is to be machined. In general, the words *horizontal* or *vertical* used when describing a machine tool refer to the orientation of the machine spindle that provides primary motion (main spindle). Thus, in the horizontal borer the main spindle is horizontal.

The principal feature of the machine is that the workpiece remains
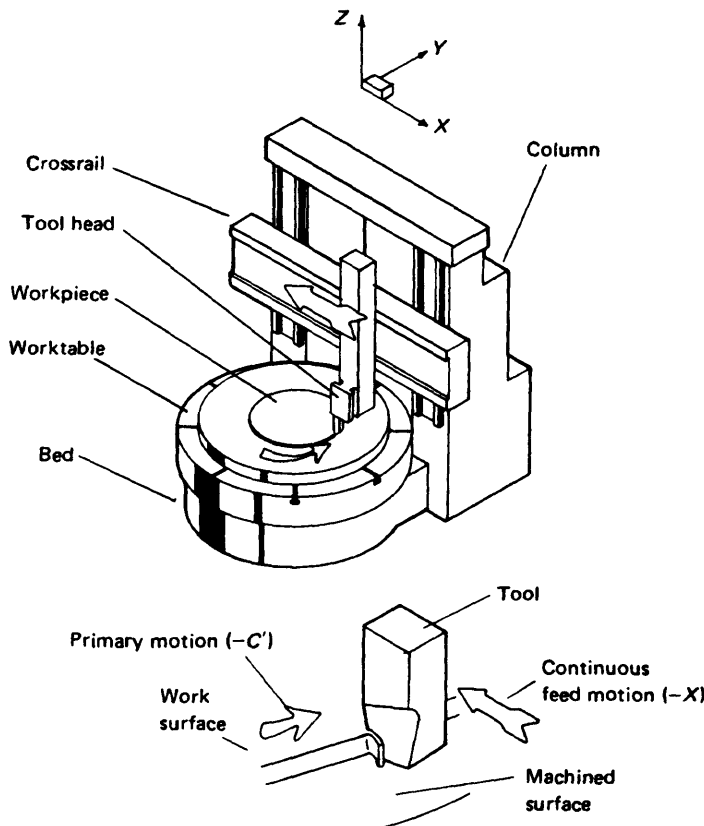
Figure 1.12   Facing on a vertical-boring machine.

stationary during machining, and all the generating motions are applied to the tool. The most common machining process is boring and is shown in the figure; boring is achieved by rotating the tool, which is mounted on a boring bar connected to the spindle (motion C), and feeding the spindle, boring bar, and tool along the axis of rotation (motion Z). The machine tool motions which can be used to move the workpiece are for positioning of the workpiece and are not generally employed while machining is taking place. A facing operation can be carried out by using a special toolholder (Fig. 1.15) that feeds the tool radially as it rotates.

The worktable has T slots to facilitate clamping of the workpiece. Several common methods of using these T slots are shown in Fig. 1.16.

Again, the equations developed earlier for the undeformed chip thick-
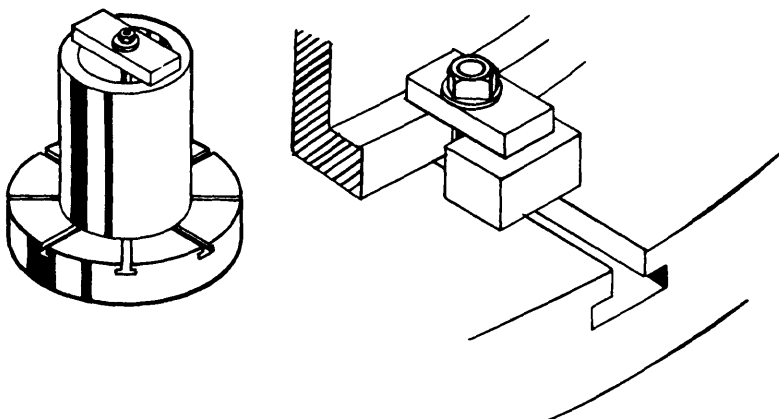
Figure 1.13 Workholding in vertical-boring machines.

ness, the machining time, and the metal removal rate in boring and facing apply.

1.3.8 Shaping Machine (Shaper)

The shaper is a small machine on which the primary motion is linear (Fig. 1.17). The single-point tool is gripped in a toolhead mounted on the end of a ram. The ram is made to move backward and forward (X motion) either by a mechanical drive system or a hydraulic piston and cylinder. The cutting stroke is the forward stroke, and with either mechanical or hydraulic shapers the forward ram speed is slower than the speed on the return stroke, causing the production time to be reduced as much as possible. A quick-return mechanism often used in mechanical shapers is shown in Fig. 1.18. In all shapers the length of the stroke can be adjusted to suit the particular workpiece being machined. The feed is applied to the workpiece in increments at the end of the return stroke of the ram by a rachet-and-pawl mechanism driving the lead screw in the crossrail.

Shapers are most commonly used to machine flat surfaces on small components and are only suitable for low-batch quantities. For the machining of a horizontal surface (Fig. 1.17), the workpiece is fed horizontally (Y' motion); for vertical surfaces, the workpiece is fed vertically (Z' motion).

Typical tool- and work-holding methods are illustrated in Fig. 1.19, where it can be seen that the toolhead is similar to the tool post and compound rest used on a lathe. The toolhead can be rotated and clamped in various positions in the vertical plane to allow inclined surfaces to be
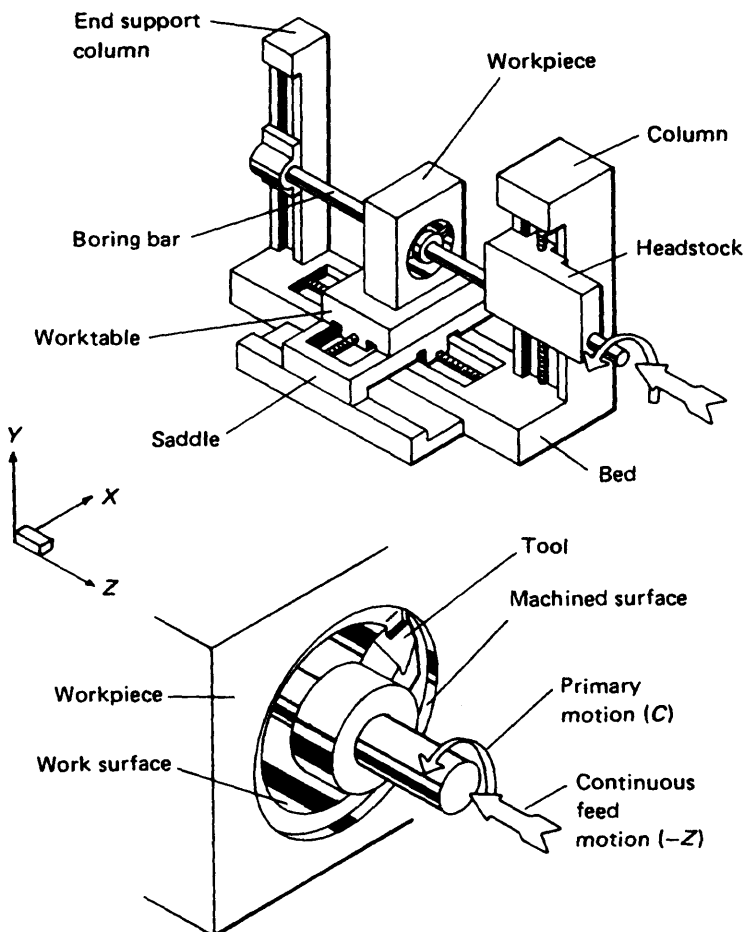
Figure 1.14   Boring on a horizontal-boring machine.

generated by hand feeding of the tool. An essential feature of the shaper toolhead is the clapper box. Effectively the tool post is pivoted on a horizontal pin and the tool is free to rotate forward, thereby lifting the tool corner during the return stroke of the ram. This action is brought about simply by the force exerted by the workpiece on the tool as the tool is dragged backward across the work surface. The workpiece is generally conveniently held in a vise bolted to the surface of a table provided with T slots for this purpose.

   The geometries when shaping horizontal, vertical, and inclined flat
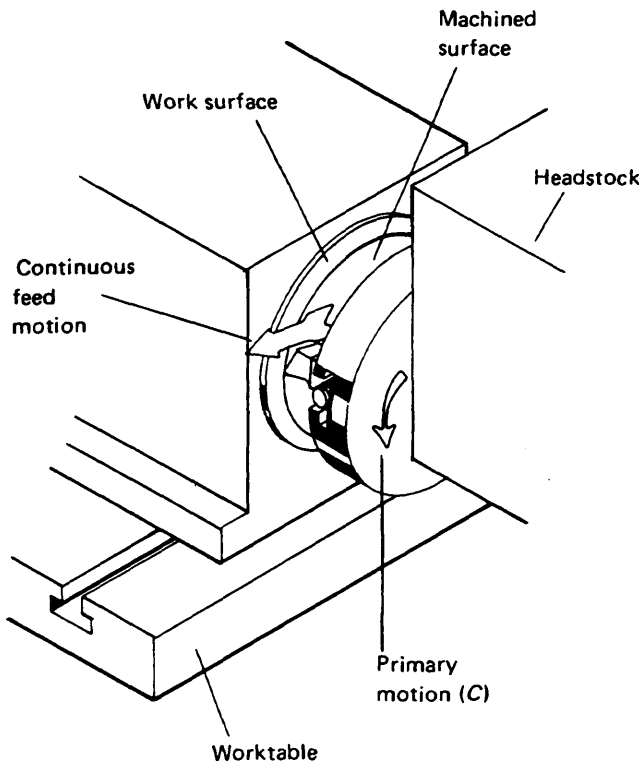
Figure 1.15   Facing on a horizontal-boring machine.

surfaces are shown in Fig. 1.20. For a surface of width b_w the machining time t_m is given by

$$t_m = \frac{b_w}{fn_r} \tag{1.15}$$

where n_r is the frequency of reciprocation or cutting strokes and f is the feed.

The metal removal rate Z_w during cutting will be given by

$$Z_w = A_c v = f a_p v \tag{1.16}$$

where v is the cutting speed and a_p is the back engagement. The undeformed chip thickness a_c will be given by

Step block
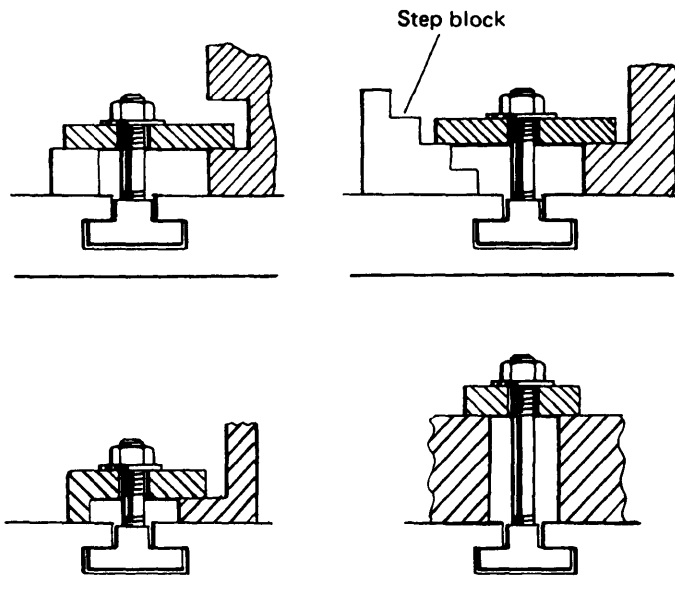
Figure 1.16 Work-holding methods for machine tables having T slots.

$$a_c = f \sin \kappa_r \qquad\qquad\qquad (1.17)$$

1.3.9   Planing Machine (Planer)

The shaper is unsuitable for generating flat surfaces on very large parts because of limitations on the stroke and overhang of the ram. This problem is solved in the planer (Fig. 1.21) by applying the linear primary motion to the workpiece (motion X') and feeding the tool at right angles to this motion (motion Y or Z). The primary motion is normally accomplished by a rack-and-pinion drive using a variable-speed motor. As with the shaper, the tool posts are mounted on clapper boxes to prevent interference between the tools and workpiece on the return stroke, and the feed motion is intermittent. The work is held on the machine table using the T slots provided. The machining time, metal removal rate, and undeformed chip thickness can be estimated using the equations developed for the shaper.

The planer is the last of the machine tools employing single-point cutting tools to be described here. The next section describes machines designed to apply multipoint cutting tools to the workpiece.
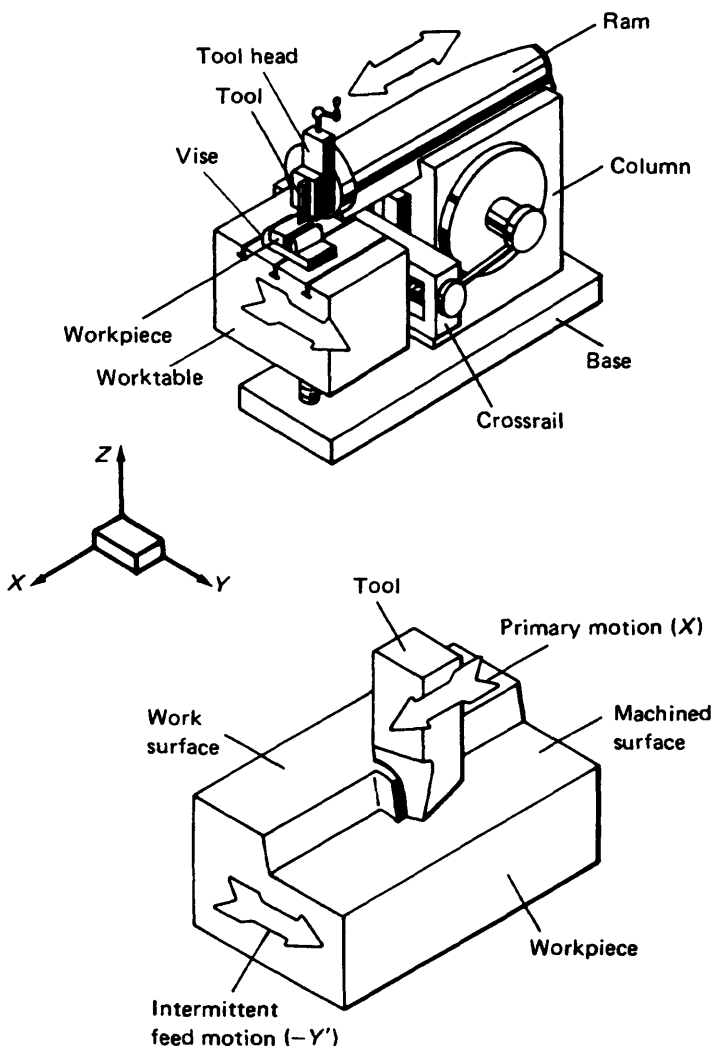
Figure 1.17 Production of a flat surface on a shaper.
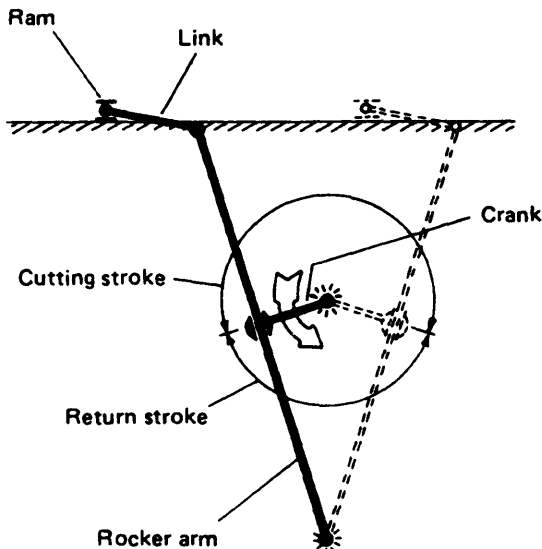
Figure 1.18   Quick-return mechanism for a mechanical shaper.

1.4   MACHINES USING MULTIPOINT TOOLS

1.4.1   Multipoint Tools

A multipoint tool can be regarded as a series of two or more cutting parts (chip-producing elements) secured to a common body. The majority of multipoint tools (milling cutters, drills, etc.) are intended to be rotated and have either a taper (conical) or parallel (cylindrical) shank for holding purposes or a bore through which a spindle or arbor can be inserted. The terms such as face, flank, and cutting edges, defined earlier for single-point tools, are still applicable, and the cutting action at a selected point on one of the cutting edges is the same.

The common multipoint tools—drills, reamers, milling cutters, and broaches—will be introduced along with descriptions of the machine tools on which they are most often used.

1.4.2   Drilling Machine (Drill Press)

A drill press (Fig. 1.22) can perform only those operations where the tool is rotated (motion C) and fed along its axis of rotation (motion Z). The workpiece always remains stationary during the machining process. On many drill presses the tool is fed by the manual operation of a lever to the
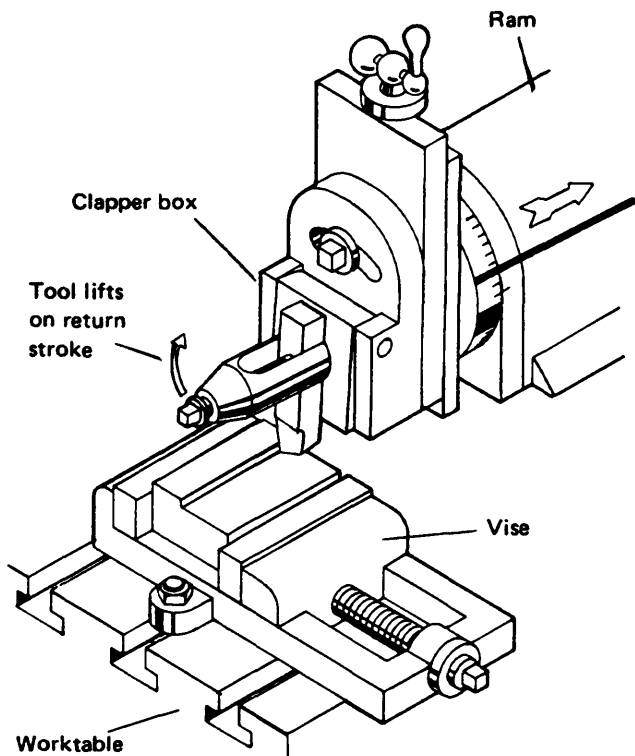
Figure 1.19 Tool and work holding in a shaper.

right of the head. Both the worktable and the head can be raised and lowered to accommodate workpieces of different heights.

The most common operation performed on this machine is drilling with a twist drill to generate an internal cylindrical surface. A twist drill with a taper shank, together with the geometry of the drilling operation, is shown in Fig. 1.23. This tool has two cutting edges, each of which is expected to remove its share of the work material. Thus the feed per tooth (the depth of material removed by each tooth and measured parallel to the direction of feed motion) is the feed engagement a_f and is equal to one-half of the feed f. By geometry therefore

$$a_c = \frac{f}{2} \sin \kappa_r \tag{1.18}$$

where κ_r is the major cutting-edge angle.
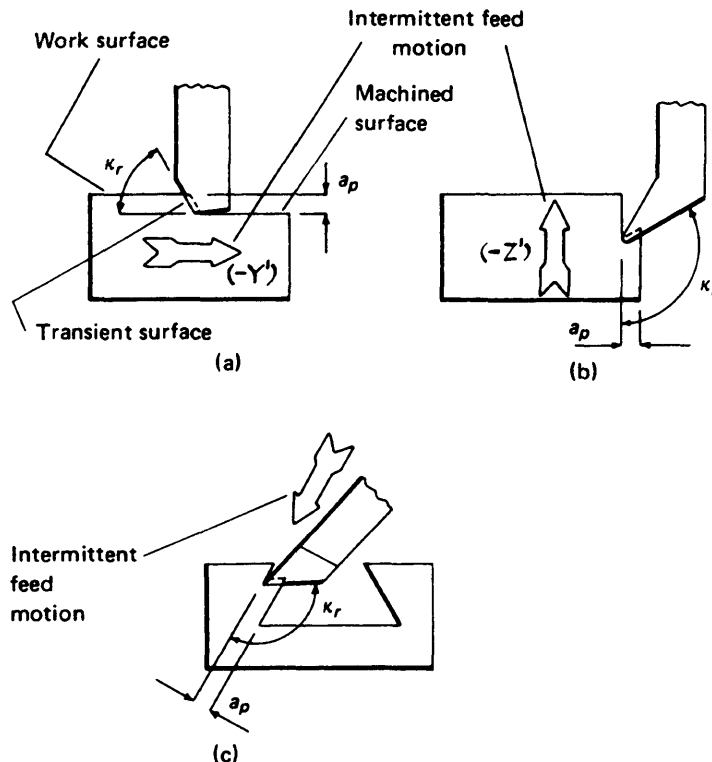
Figure 1.20 Shaping operations. (a) Horizontal surface; (b) vertical surface; (c) inclined surface.

The machining time t_m is given by

$$t_m = \frac{l_w}{fn_t} \tag{1.19}$$

where l_w is the length of the hole produced and n_t is the rotational frequency of the tool.

The metal removal rate Z_w may be obtained by multiplying the feed speed v_f by the cross-sectional area of the hole produced. Thus

$$Z_w = \frac{\pi}{4}d_m^2 v_f = \frac{\pi f d_m^2 n_t}{4} \tag{1.20}$$

where d_m is the diameter of the machined surface. If an existing hole of diameter d_w is being enlarged,

Column

Cross-rail

Tool heads

Workpiece

Worktable

Base

Z

X Y

Tool

Work
surface

Intermittent
feed motion $(-Y)$

Machined
surface

Primary
motion (X')

Workpiece
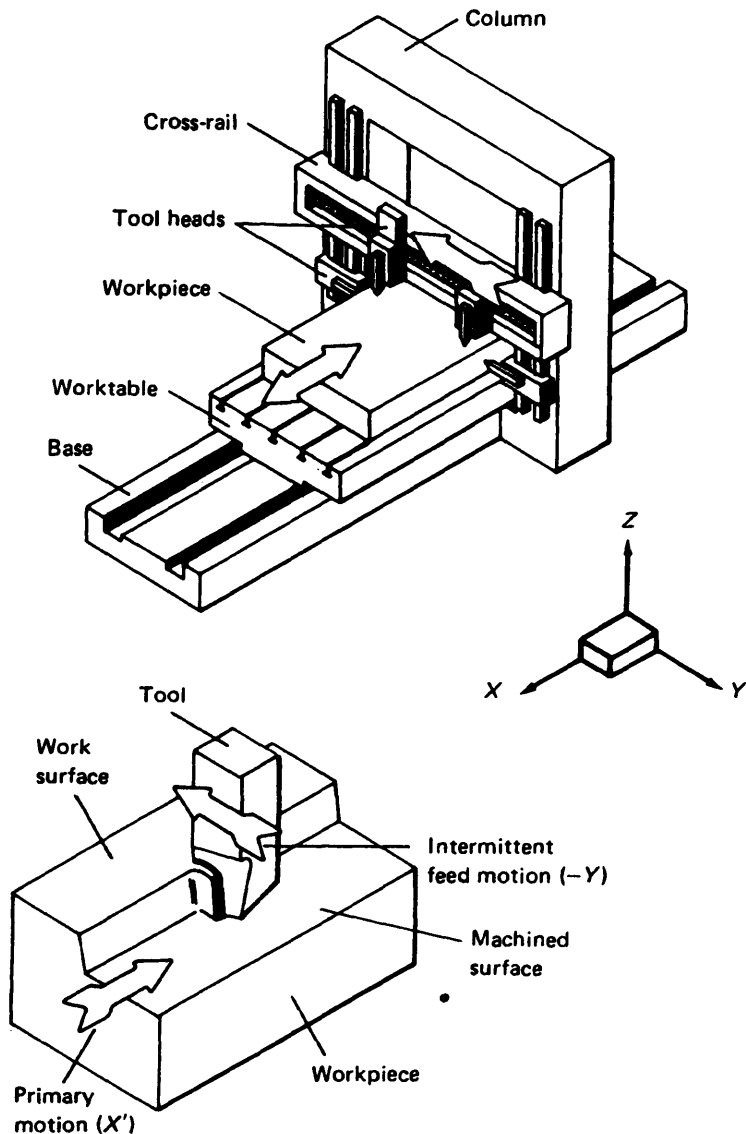
Figure 1.21   Production of a flat surface on a planer.
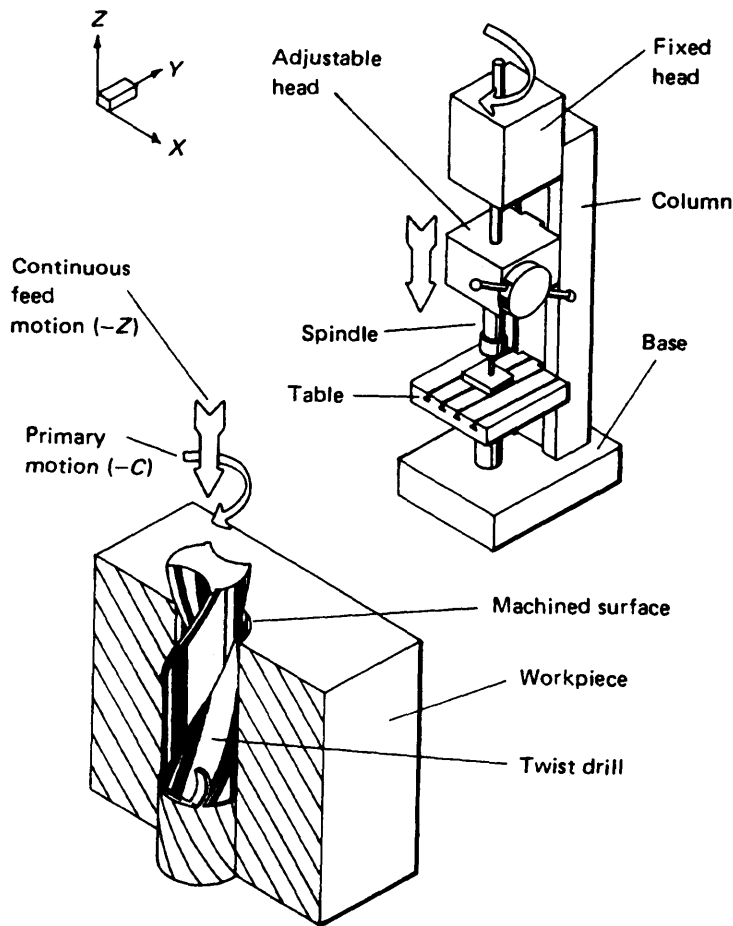
Figure 1.22   Drilling on a drill press.

$$Z_w = \frac{\pi f (d_m^2 - d_w^2) n_t}{4} \tag{1.21}$$

Clearly the cutting speed will be a maximum at either corner (the outer radius of the major cutting edges) and will be zero at the tip of the drill, which is in the form of a short chisel edge. In drilling a new hole, this chisel edge must force its way through the work material, effectively pushing the material outward to be removed by the cutting edges. The poor cutting conditions in this region have little effect on the quality of the hole

Tongue

Body

Major
flank

Shank

Tool axis

Flute

Face

Minor cutting
edge

Major
cutting
edge

Corner

a_p

$a_f = \dfrac{f}{2}$

a_c

κ_r
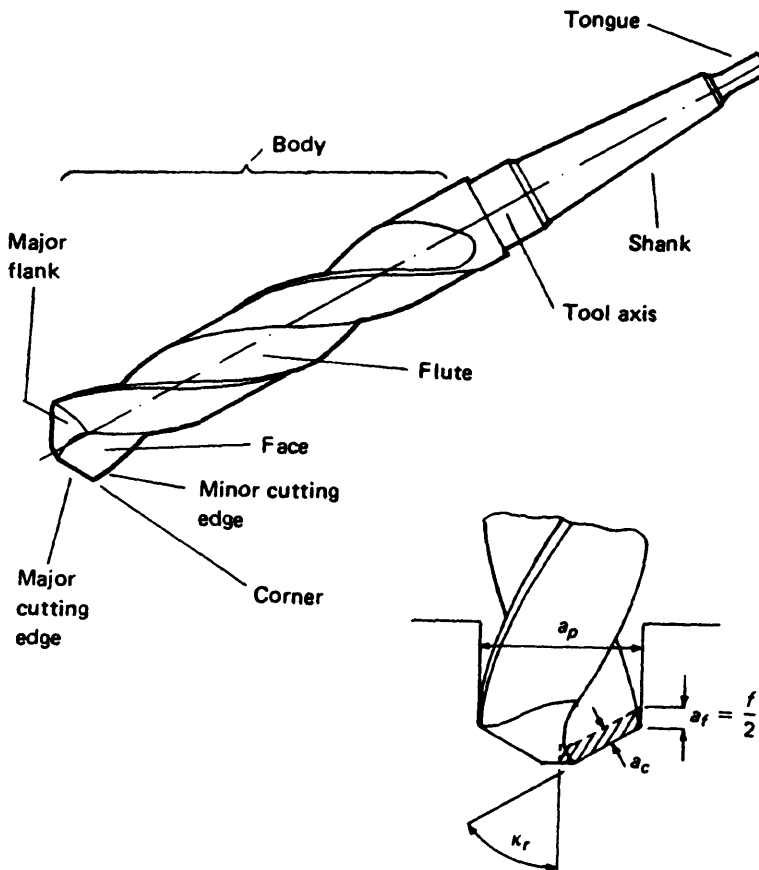
Figure 1.23   Twist drill, where $a_c = a_f \sin \kappa_r$.

produced, which is mainly determined by the conditions at the minor cutting edges. The chips removed by the cutting edges take a helical form and travel up the drill flutes.

Twist drills are usually considered suitable for machining holes having a length less than five times their diameter. Special drills requiring special drilling machines are available for drilling deeper holes and are not described here.

The workpiece is often held in a vise bolted to the machine worktable. The drilling of a concentric hole in a cylindrical workpiece, however, is often carried out on an engine lathe with the drill held either in the

tailstock (for hand feeding) or in a special drill holder mounted on the carriage.

Large twist drills are usually provided with a taper shank, as shown in Fig. 1.23. This shank is designed to be inserted in a corresponding taper hole in the end of the machine spindle. The tongue on the end of the shank is inserted in a slot at the bottom of the hole in the spindle and prevents rotation of the drill relative to the spindle during machining. The drill is removed by tapping a wedge (drift) into the slot in the machine spindle, as illustrated in Fig. 1.24.

Small twist drills have a parallel shank and are held in a three-jaw chuck of the familiar type used in hand drills. These chucks are provided with a taper shank for location in the drill-press spindle or in the tailstock of a lathe.

Several other machining operations can be performed on a drill press, and some of the more common ones are illustrated in Fig. 1.25. The center-drilling operation produces a shallow, conical hole with clearance at the bottom. This center hole can provide a location for a lathe center when the workpiece is subsequently to be supported between centers (Fig. 1.9) or can provide a guide for a subsequent drilling operation to prevent the drill point from "wandering" as the hole is started. The reaming operation is intended for finishing a previously drilled hole. The reamer is similar to a drill but has several cutting edges and straight flutes. It is intended to remove a small amount of work material only, but it considerably improves the accuracy and surface finish of a hole. The spot-
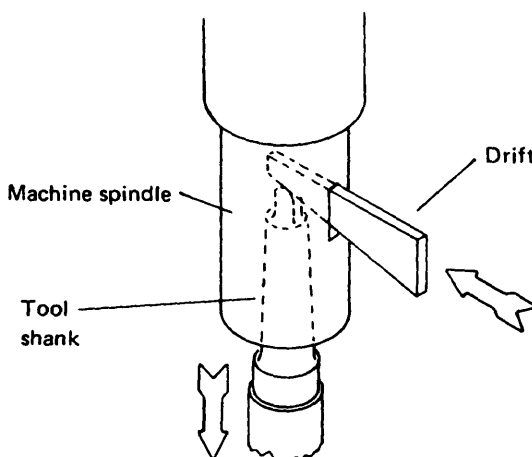
Figure 1.24 Releasing a taper-shank tool.
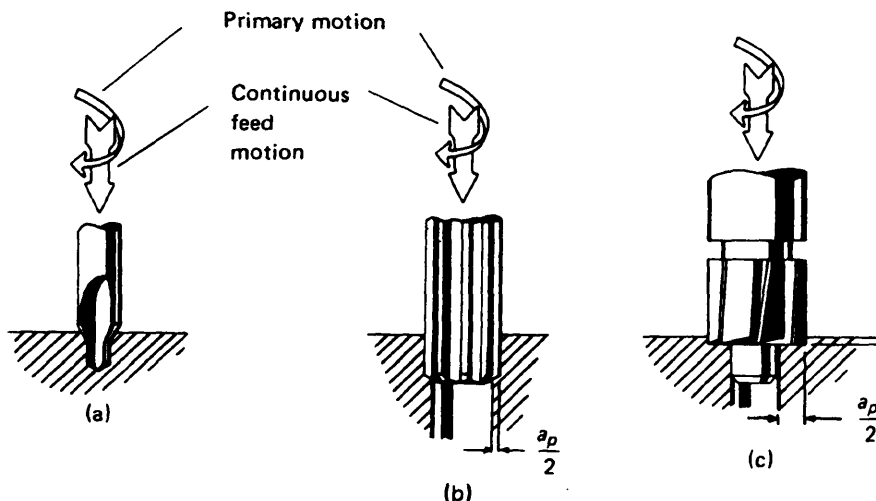
Figure 1.25 Some drill-press operations. (a) Center drilling; (b) reaming; (c) spot-facing.

facing operation is designed to provide a flat surface around the end of a hole and perpendicular to its axis; this flat surface provides a suitable seating for a washer and nut.

For large workpieces a radial-arm drilling machine is used (Fig. 1.26). In this machine the drilling head and motor can be positioned along an arm that is free to swing in a horizontal plane about the column, allowing large areas to be covered. The radial-arm drilling machine is particularly suitable for drilling large numbers of holes in heavy workpieces.

1.4.3 Horizontal-Milling Machine (Horizontal Miller)

There are two main types of milling machines: horizontal and vertical. These words again refer to the orientation of the main spindle. In the horizontal-milling machine shown in Fig. 1.27 the milling cutter is mounted on a horizontal arbor driven by the main spindle. The tools are therefore rotated (motion C) and the work fed continuously (motions X' or Y').

The simplest operation, slab milling, is used to generate a horizontal surface on the workpiece, as shown in Fig. 1.27. The figure shows the conventional slab-milling operation; if the workpiece had been fed in the opposite direction, it would tend to climb onto the work surface, and this type of slab milling is called "climb" milling. Some evidence suggests that
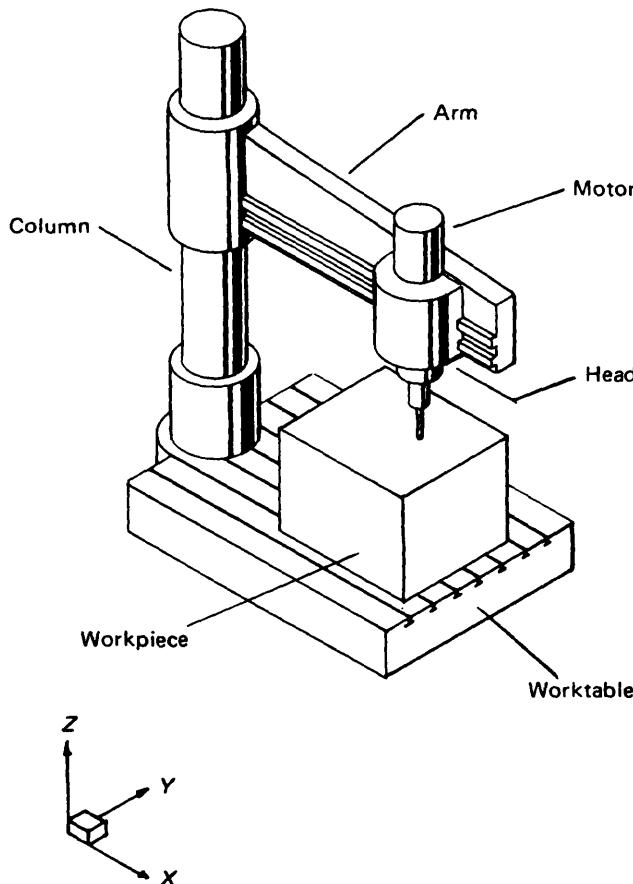
Figure 1.26 Radial-arm drill.

the forces and power consumption are less in climb milling than in conventional milling. However, high rigidity of the machine tool and work- and tool-holding devices is required for this oepration.

The geometry in conventional slab milling is shown in Fig. 1.28. The feed f, which is equal to the distance moved by the workpiece during one revolution of the tool, is given by

$$f = \frac{v_f}{n_t} \tag{1.22}$$

where v_f is the feed speed of the workpiece and n_t is the rotational fre-
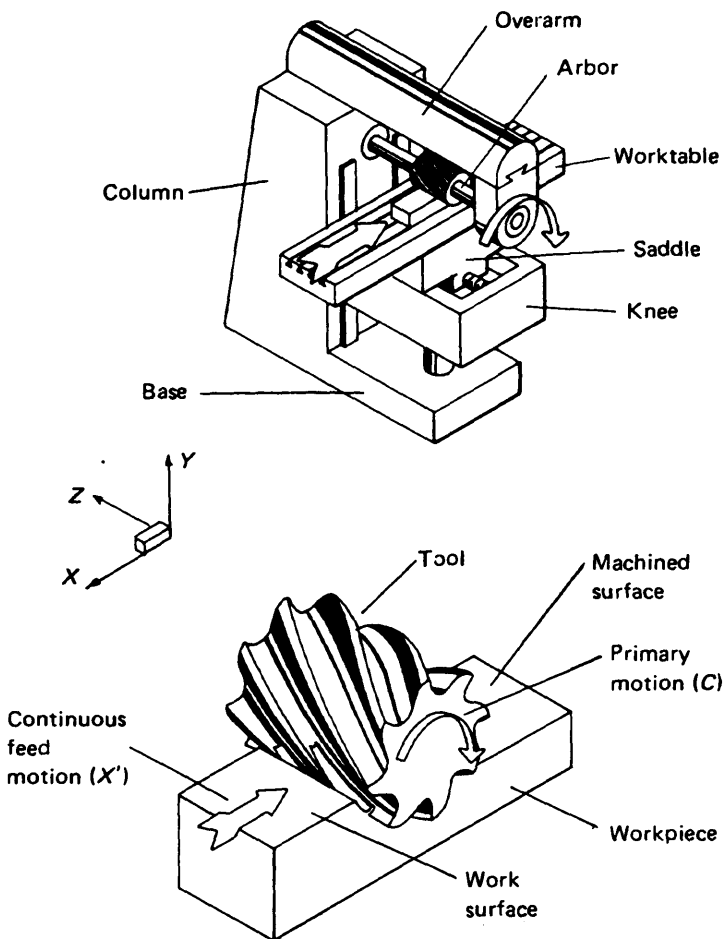
Figure 1.27 Slab milling on a knee-type horizontal-milling machine.

quency of the cutter. The feed engagement a_f, which is equal to the thickness of a chip removed by one tooth and measured parallel to the feed direction (feed per tooth), is given by f/N, where N is the number of teeth on the cutter. The maximum undeformed chip thickness $a_{c_{max}}$ (measured normal to the direction of primary motion) is therefore given by

$$a_{c_{max}} = \frac{v_f \sin \theta}{N n_t} \tag{1.23}$$

where θ is given by (Fig. 1.28)
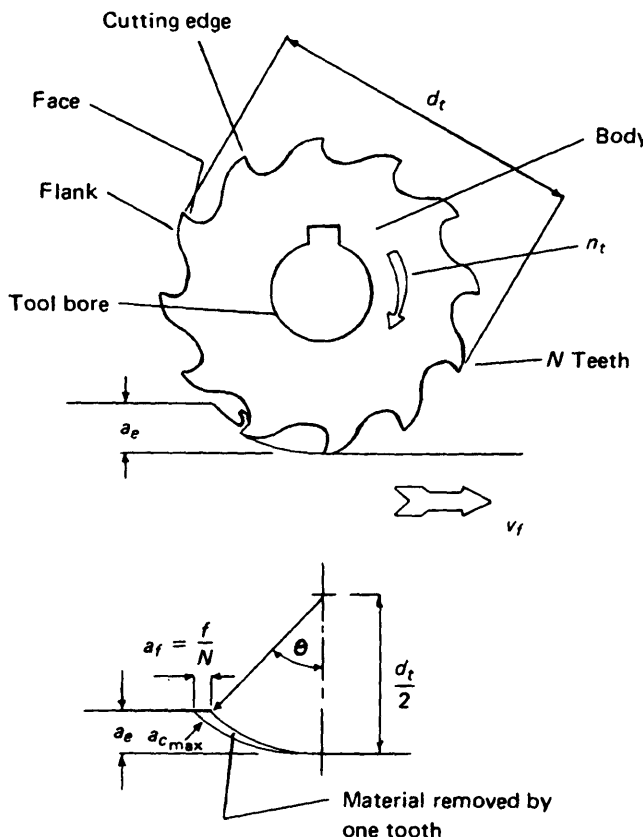
Figure 1.28 Geometry of a slab-milling operation, where $a_{c_{max}}$ = $(2v_f/Nn_t)\sqrt{a_c/d_t}$.

$$\cos\theta = 1 - \frac{2a_e}{d_t} \tag{1.24}$$

where d_t is the diameter of the cutter and a_e is the working engagement (the instantaneous engagement of the tool with the workpiece), measured in the plane containing the directions of primary and feed motion and perpendicular to the direction of feed motion. In slab milling the working engagement was known as depth of cut.

Now

$$\sin\theta = \sqrt{1 - \cos^2\theta}$$

$$= 2 \sqrt{\frac{a_e}{d_t} - \left(\frac{a_e}{d_t}\right)^2} \qquad (1.25)$$

and substitution of (1.25) in (1.23) gives

$$a_{c_{\max}} = \frac{2v_f}{Nn_t} \sqrt{\frac{a_e}{d_t}\left(1 - \frac{a_e}{d_t}\right)} \qquad (1.26)$$

Finally, if a_e/d_t is small,

$$a_{c_{\max}} = \frac{2v_f}{Nn_t} \sqrt{\frac{a_e}{d_t}} \qquad (1.27)$$

When estimating the machining time t_m in a milling operation, it should be remembered that the distance traveled by the cutter will be larger than the length of the workpiece. This extended distance is illustrated in Fig. 1.29 in which it can be seen that the cutter travel distance is given by $l_w + \sqrt{a_e(d_t - a_e)}$ where l_w is the length of the workpiece. Thus the machining time is given by

$$t_m = \frac{l_w + \sqrt{a_e(d_t - a_e)}}{v_f} \qquad (1.28)$$

The metal removal rate Z_w will be equal to the product of the feed speed and the cross-sectional area of the metal removed, measured in the direction of feed motion. Thus, since the back engagement a_p is equal to the workpiece width,
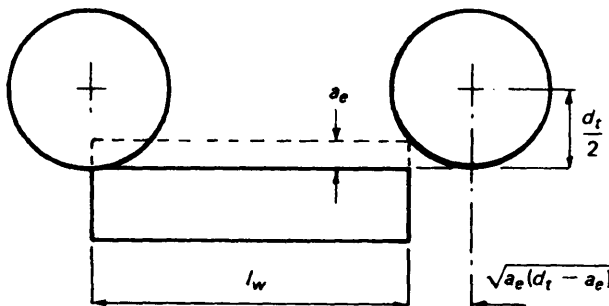
Figure 1.29 Relative motion between a slab-milling cutter and the workpiece during machining time.

$$Z_w = a_e a_p v_f \tag{1.29}$$

Figure 1.30 shows some further horizontal-milling operations. In form cutting, the special cutter has cutting edges shaped to form the cross section required on the workpiece. Because these cutters are generally expensive to manufacture, form milling is used only when the quantity of production is sufficiently large. In slotting, a standard cutter with minor cutting edges at each end of the major cutting edges is used to produce a
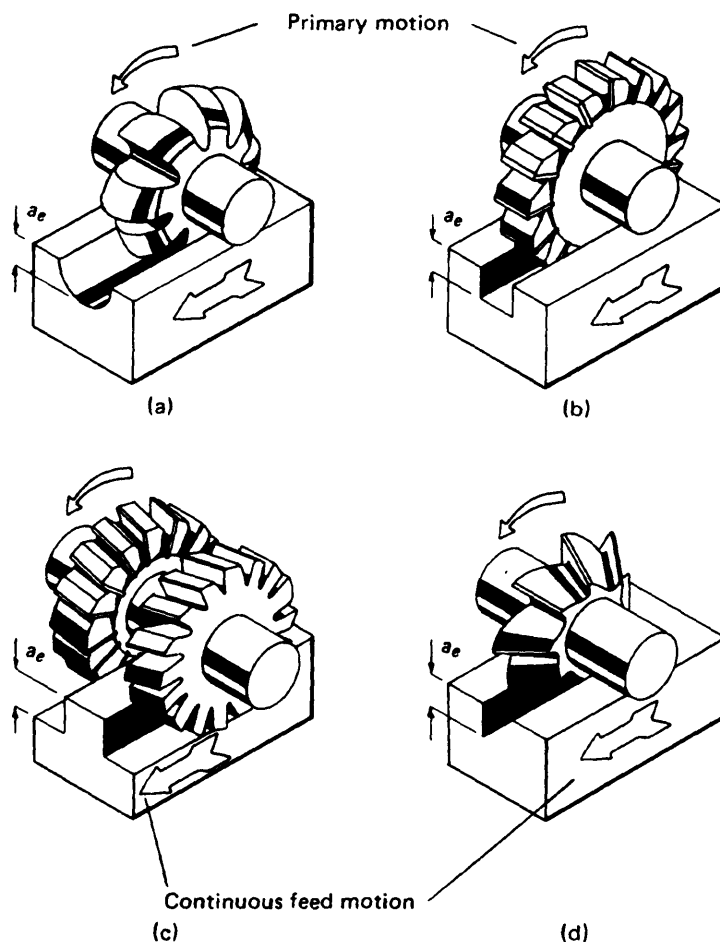
Figure 1.30 Some horizontal milling operations. (a) Form cutting; (b) slotting; (c) straddle milling; (d) angular milling.

rectangular slot in a workpiece. Similarly, in angular milling a standard cutter machines a triangular slot. The straddle-milling operation shown in the figure is only one of an infinite variety of operations that can be carried out by mounting more than one cutter on the machine arbor. In this way combinations of cutters can machine a wide variety of cross-sectional shapes. When cutters are used in combination, the operation is often called gang milling.

In horizontal milling the tools are mounted on a spindle or arbor (Fig. 1.31) and constrained by a key. The arbor has a tapered section at one end that is designed to fit into a corresponding tapered bore or socket in the end of the main spindle. A drawbar passed through the hollow main spin-
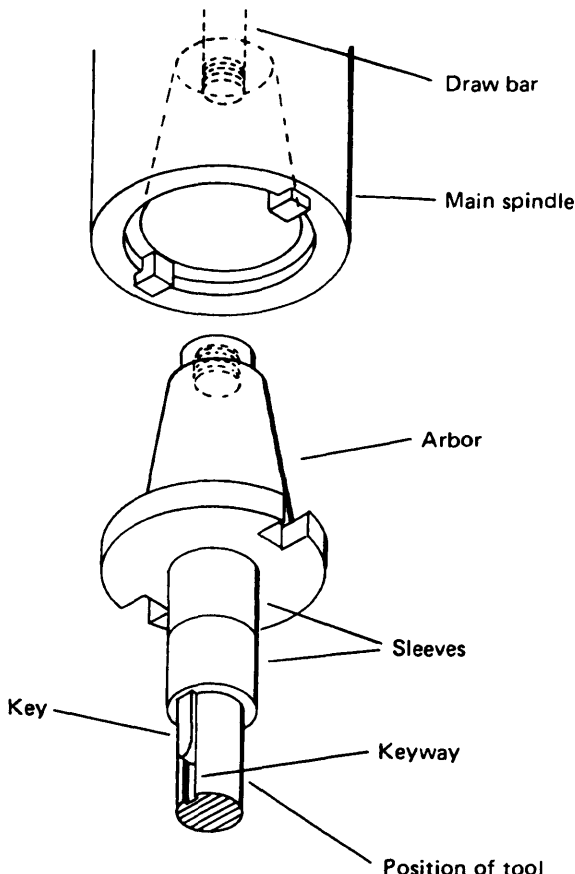
Figure 1.31 Tool holding in horizontal milling.

dle from the rear of the machine is screwed into the end of the arbor, which results in the arbor being drawn tightly into the spindle socket. Sleeves are used as spacers to locate the tool in its required axial position on the arbor. The free end of the arbor is supported in a bearing mounted at the end of the overarm, as illustrated in Fig. 1.27.

Work holding is accomplished by either using a machine vise bolted to the worktable or by bolting the workpiece directly onto the worktable using the T slots provided.

1.4.4   Vertical-Milling Machine (Vertical Miller)

A wide variety of operations involving the machining of horizontal, vertical, and inclined surfaces can be performed on a vertical-milling machine. As the name of the machine implies, the spindle is vertical. In the knee-type machine illustrated in Fig. 1.32 the workpiece can be fed either

1.   Along the vertical axis (Z' motion) by raising or lowering the knee
2.   Along a horizontal axis (Y' motion) by moving the saddle along the knee
3.   Along a horizontal axis (X' motion) by moving the table across the saddle

In larger vertical-milling machines the saddle is mounted directly on the bed, and relative motion between the tool and workpiece along the vertical axis is achieved by motion of the head up or down the column (Z motion); these machines are called bed-type, vertical-milling machines.

A typical face-milling operation, where a horizontal flat surface is being machined, is shown in Fig. 1.32. The cutter employed, known as a face-milling cutter, is shown in Fig. 1.33, which also illustrates the geometry of the operation.

The feed f is the distance the cutter advances across the workpiece during one revolution. Thus

$$f = \frac{v_f}{n_t} \tag{1.30}$$

where v_f is the feed speed and n_t is the rotational speed of the cutter.

If the tool axis passes over the workpiece, the undeformed chip thickness increases to a maximum value and then decreases during the time each tooth is engaged with the workpiece; its maximum value, $a_{c_{max}}$, is equal to the feed engagement, which is equal to f/N, where N is the number of teeth on the cutter. Thus
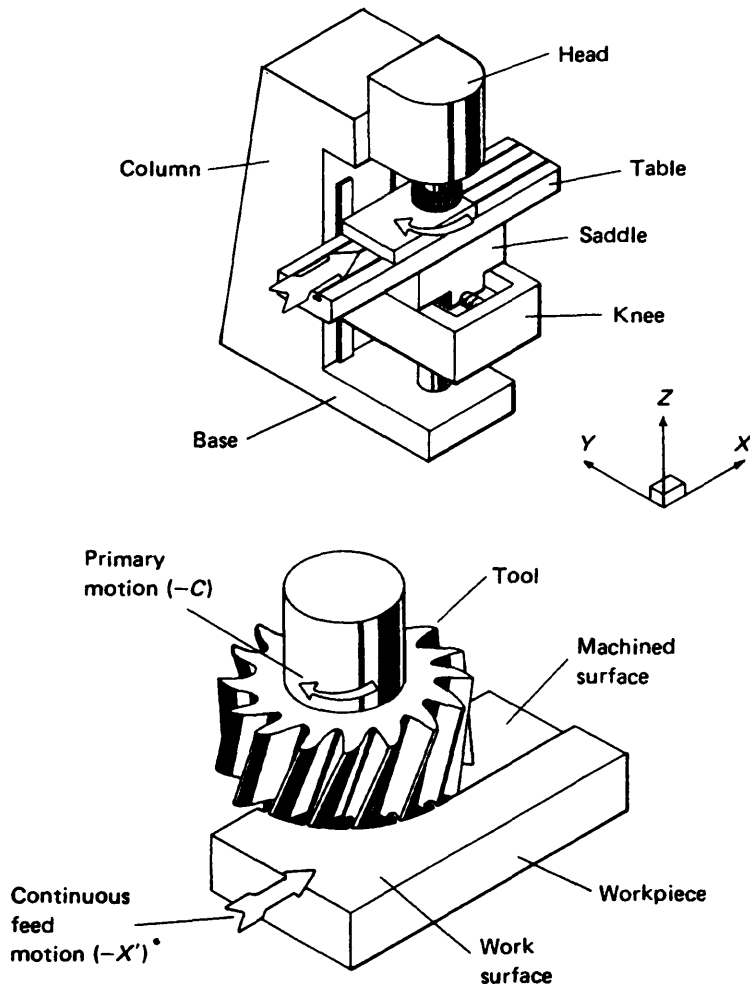
Figure 1.32 Face milling on a knee-type milling machine.

$$a_{c_{max}} = \frac{v_f}{N n_t} \tag{1.31}$$

In estimating the machining time t_m allowance should again be made for the additional relative motion between the cutting tool and workpiece. As can be seen in Fig. 1.34, the total motion when the path of the tool axis passes over the workpiece is given by $(l_w + d_t)$ and therefore the machining time is given by
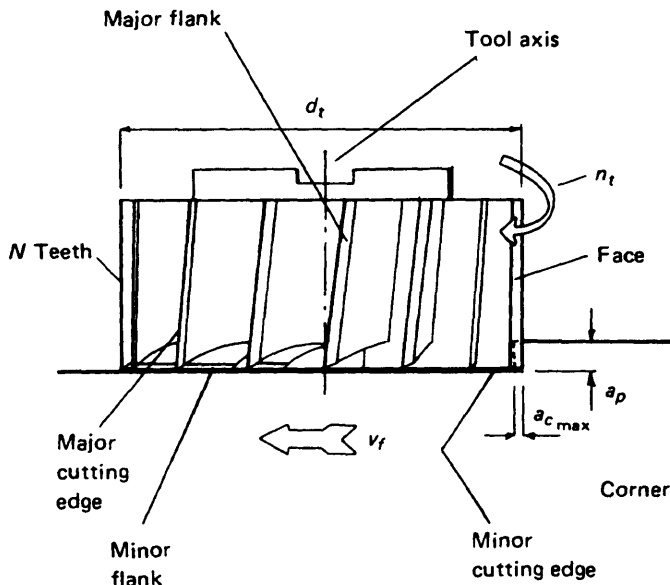
Figure 1.33 Geometry of face milling, where $a_{c_{max}} = v_f/Nn_t$.

$$t_m = \frac{(l_w + d_t)}{v_f} \tag{1.32}$$

where l_w is the length of the workpiece and d_t is the diameter of the cutter.

When the path of the tool axis does not pass over the workpiece,

$$t_m = \frac{l_w + 2\sqrt{a_e(d_t - a_e)}}{v_f} \tag{1.33}$$

where a_e is the working engagement. In this case the operation is similar to slab milling with a large working engagement, and the maximum value of the undeformed chip thickness is given by Eq. (1.26).

The metal removal rate Z_w in both cases is given by Eq. (1.29).

A variety of vertical-milling machine operations is illustrated in Fig. 1.35. It can be seen that in one pass of the tool, several combinations of machined surfaces can be produced.

Milling cutters for vertical-milling machines generally have either a bore or a straight shank. Those having a bore are called shell end mills and are secured to an arbor (Fig. 1.36) held in a socket in the machine
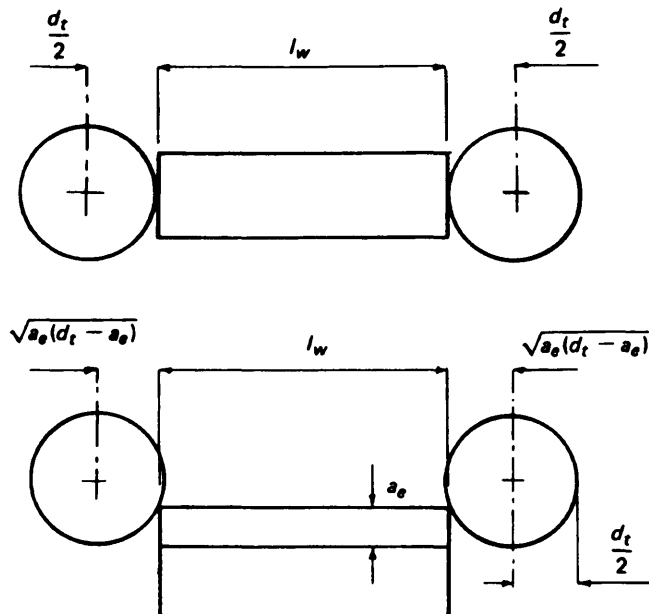
Figure 1.34 Relative motion between the face-milling cutter and the workpiece during machining time.

spindle with a drawbar. Those having a straight shank are either gripped in a chuck or held in the spindle by a screw bearing on a flat surface, machined into the shank.

Work holding is again accomplished by a machine vise or by using the T slots in the machine table.

1.4.5   Broaching Machine (Broacher)

The last machine using multipoint tools to be described here is the broaching machine. A vertical-broaching machine suitable for machining shaped slots in the workpiece is shown in Fig. 1.37. In broaching, the machine provides the primary motion (usually hydraulically powered) between the tool and workpiece (motion X), and the feed is provided by the staggering of the teeth on the broach, each tooth removing a thin layer of material. Since the machined surface is usually produced during one pass of the tool, the machining time t_m is given by

$$t_m = \frac{l_t}{v} \tag{1.34}$$
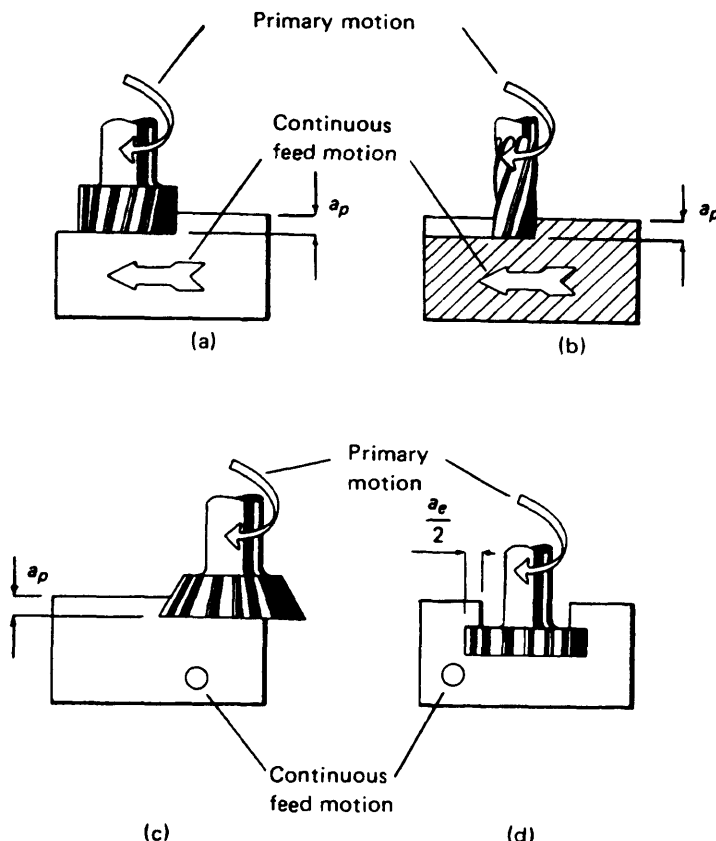
Figure 1.35 Some vertical-milling-machine operations. (a) Horizontal surface; (b) slot; (c) dovetail; (d) T slot.

where l_t is the length of the broach and v is the cutting speed. The feed f in broaching is defined as the motion an imaginary single cutting edge would have to be given by the machine tool to produce the same result as the array of cutting edges with which the tool or machine is actually provided. The undeformed chip thickness a_c at a selected point on the cutting edge is therefore equal to the feed or the feed engagement; thus

$$a_c = a_f = f \qquad (1.35)$$

The average metal removal rate Z_w can be estimated by dividing the total volume of metal removed by the machining time.
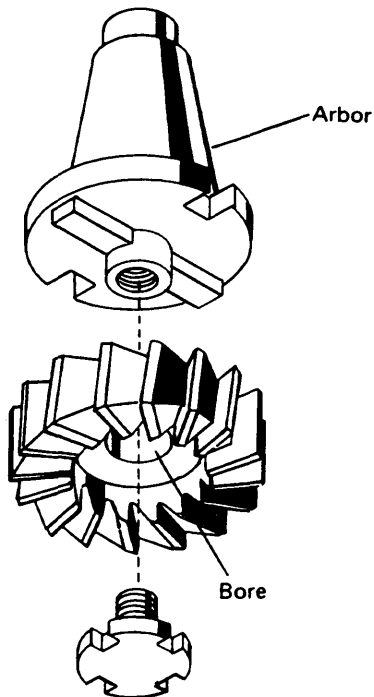
Figure 1.36   Tool holding for a shell end mill.

Broaching is widely used to produce noncircular holes. In these cases the broach can be either pulled or pushed through a circular hole to enlarge the hole to the shape required or to machine a keyway, for example (Fig. 1.38). Broaches must be designed individually for the particular job and are expensive to manufacture. It follows that broaching can be justified only when a very large batch of components (100,000 to 200,000) are to be machined.

1.4.6   Taps and Dies

The production of internal and external screw threads can be accomplished by the use of taps and dies. These multipoint tools can be thought of as helical broaches, and because the amount of material removed is quite small, they can often be operated by hand.

In Fig. 1.39 a tap is fed into a prepared hole and rotated at low speed. The relative motion between a selected point on a cutting edge and the workpiece is therefore helical; this motion is the primary motion. All the
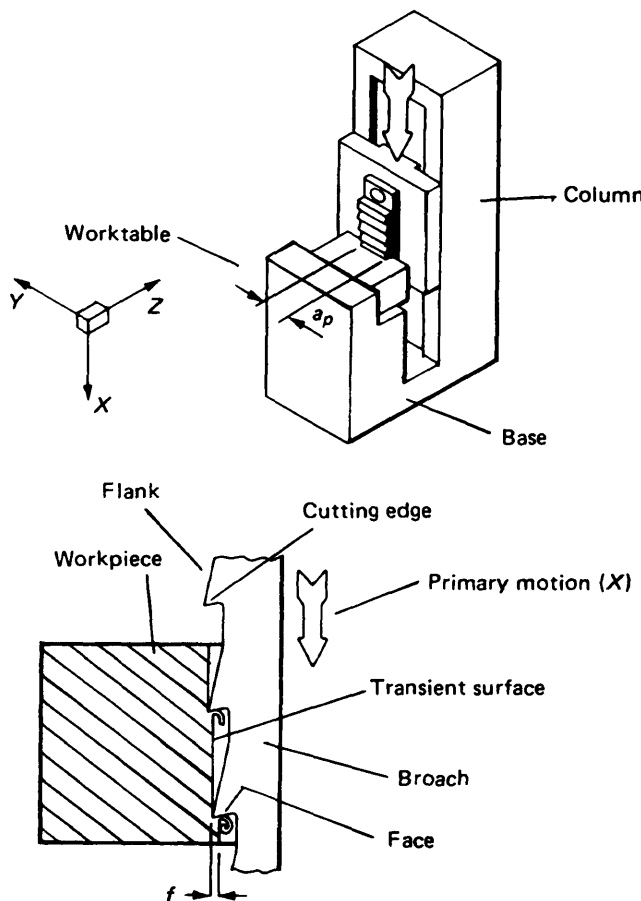
Figure 1.37   Broaching on a vertical-broaching machine, where $a_c = f$.

machining is done by the lower end of the tap, where each cutting edge removes a small layer of metal (Fig. 1.39, inset) to form the thread shape; the fully shaped thread on the tap serves to clear away fragments of chips which may collect. A die has the same cutting action as a tap but is designed to produce an external thread.

Internal threading using taps can be carried out on turret lathes and drill presses. External threading using dies can be carried out on turret lathes and special screw-cutting machines.
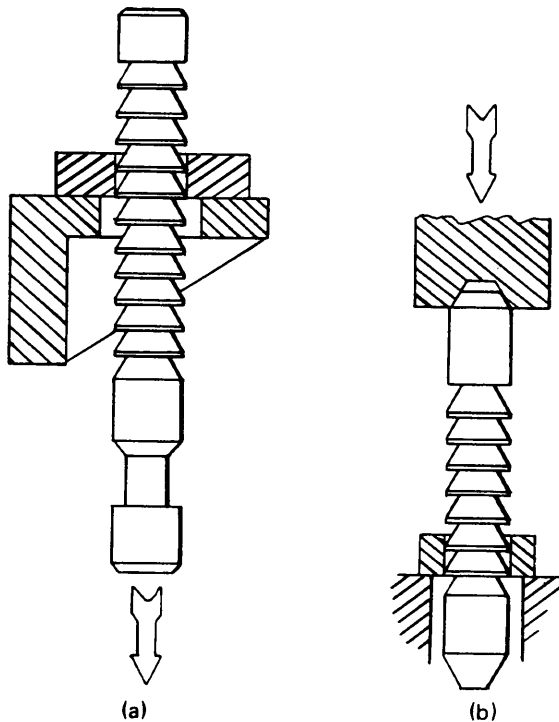
Figure 1.38   Methods of broaching a hole. (a) Pull broach; (b) push broach.

1.5   MACHINES USING ABRASIVE WHEELS

1.5.1   Abrasive Wheels

Abrasive wheels (or grinding wheels) are generally cylindrical, disc-shaped, or cup-shaped (Fig. 1.40). The machines on which they are used are called grinding machines, or grinders; they all have a spindle which can be rotated at high speed and on which the grinding wheel is mounted. The spindle is supported by bearings and mounted in a housing; this assembly is called the wheel head. A belt drive from an electric motor provides power for the spindle. The abrasive wheel consists of individual grains of very hard material (usually silicon carbide or aluminum oxide) bonded in the form required.

Abrasive wheels are sometimes used in rough grinding where material removal is the important factor; more commonly, abrasive wheels are

Primary motion

Major flank

Face

Material removed by one tooth

a_c

Minor cutting edge

Material removed during one revolution

Minor flank

Major cutting edge

Work surface

A

View of tap in direction of arrow A
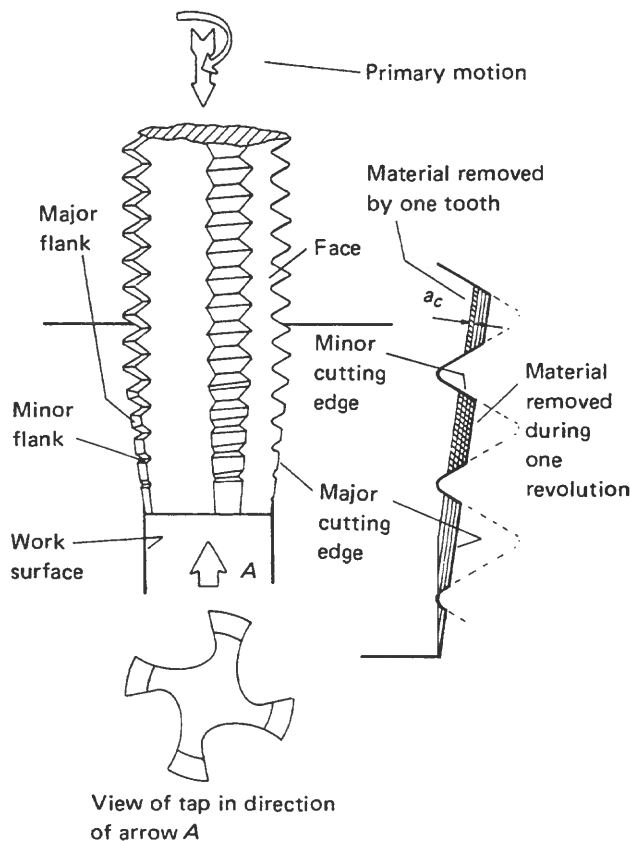
Figure 1.39 Tapping.
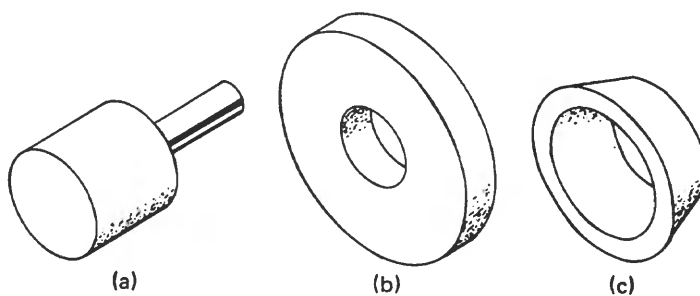
Figure 1.40 Common shapes of abrasive wheels. (a) Cylindrical; (b) disc; (c) cup.

(a)   (b)   (c)

used in finishing operations where the resulting surface finish is the criterion.

In the metal-cutting machine tools described earlier, generation of a surface is usually obtained by applying a primary motion to either the tool or workpiece and a feed motion to either the tool or the workpiece. In grinding machines, however, the primary motion is always the rotation of the abrasive wheels, but often two or more generating (feed) motions are applied to the workpiece to produce the desired surface shape.

It is difficult to estimate the undeformed chip thickness in grinding because the individual grains in the wheel are so irregular. As a rough guide, values of 0.00025 to 0.025 mm (0.00001 to 0.001 in.) can be assumed if it is remembered that a closely packed grain structure, small grains, a high cutting speed, a low feed or feed rate, and a small depth of cut will all tend to result in a low value of the undeformed chip thickness. Further, because of the relatively inefficient cutting conditions in grinding, the specific cutting energy p_s tends to be considerably higher in grinding than in metal-cutting processes.

1.5.2   Horizontal-Spindle Surface-Grinding Machine (Horizontal-Spindle Surface Grinder)

The horizontal-spindle surface grinder (Fig. 1.41) has a horizontal spindle that provides primary motion to the wheel (motion C). The principal feed motion is the reciprocation of the worktable on which the work is mounted (motion X'); this motion is known as the traverse and is hydraulically operated. Further feed motions may be applied either to the wheel head, by moving it down the column (motion $-Y$) (known as infeed), or to the table, by moving it parallel to the machine spindle (motion Z') (known as cross-feed). In Fig. 1.41 a horizontal surface is being generated on a workpiece by a cross-feed motion (motion $-Z'$). This feed motion, which is intermittent, is usually hydraulically operated and applied after each stroke or pass of the table. The amount of cross-feed f may therefore be defined as the distance the tool advances across the workpiece between each cutting stroke. The operation is known as traverse grinding.

Figure 1.42 shows the geometries of both traverse grinding and plunge grinding on a horizontal-surface grinder. From Fig. 1.42a, the metal removal rate in traverse grinding is given by

$$Z_w = f a_p v_{trav} \tag{1.36}$$

where

f = cross-feed per cutting stroke
a_p = back engagement
v_{trav} = traverse speed

The machining time t_m is given by

$$t_m = \frac{b_w}{2fn_r} \tag{1.37}$$

where n_r is the frequency of reciprocation and b_w is the width of the
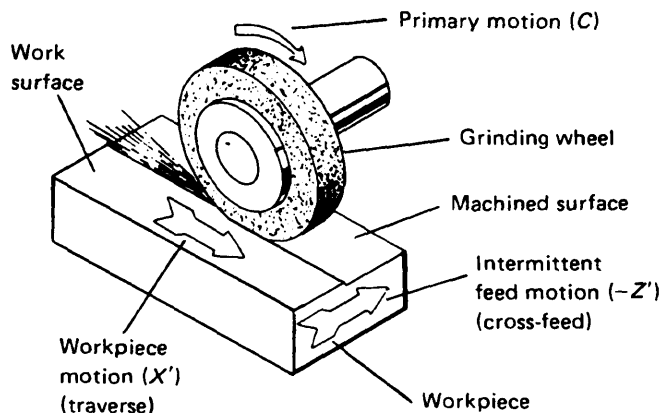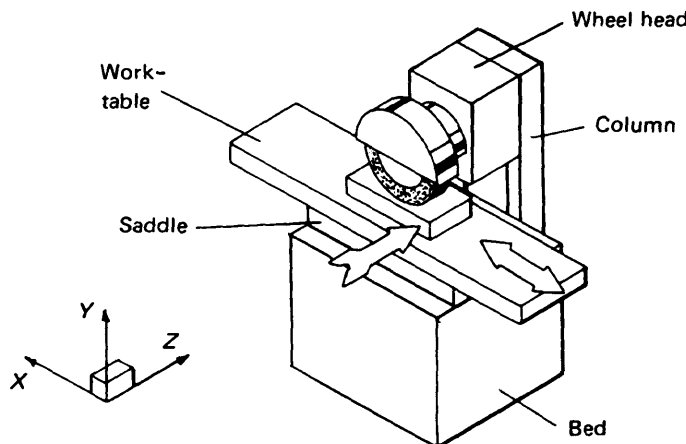
Figure 1.41 Surface grinding on a horizontal-spindle surface grinder.
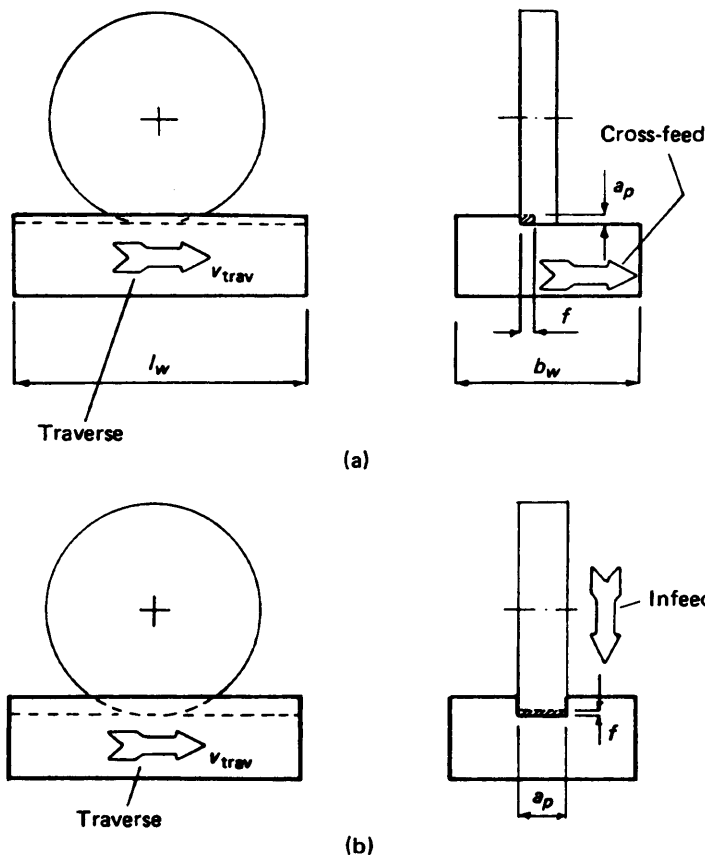
Figure 1.42 Horizontal-spindle surface-grinding operations. (a) Traverse grinding; (b) plunge grinding.

workpiece. The frequency of reciprocation depends on the traverse speed setting and on the stroke setting. Typical relationships between these parameters will be presented later. In a similar way, for the plunge-grinding operation (Fig. 1.42b), the metal removal rate is given by Eq. (1.36).

Before estimating the machining time in the plunge-grinding operation, it is necessary to describe a phenomenon known as "sparking-out." In any grinding operation where the wheel is fed in a direction normal to the work surface (infeed), the feed f, which is the depth of the layer of material removed during one cutting stroke, will initially be less than the nominal feed setting on the machine. This feed differential results from the deflection of the machine tool elements and workpiece under the forces generated during the operation. Thus, on completion of the theoretical number of cutting strokes required, some work material will still have to be removed. The operation of removing this material, called sparking-out, is achieved by continuing the original grinding operation with no further application of feed until metal removal becomes insignificant (no further sparks appear). If the time for sparking-out is denoted by t_s, the machining time in plunge grinding is given by

$$t_m = \frac{a_t}{2fn_r} + t_s \qquad (1.38)$$

where a_t is the total depth of work material to be removed.

Typical tool and work holding in a surface-grinding machine are illustrated in Fig. 1.43. Tool holding is generally accomplished by mounting the wheel on the end of the machine spindle between two flanges. Work holding is often achieved by use of a magnetic vise controlled by a lever that can be placed in the "on" or "off" position. When "off," the magnetic field is short-circuited. Motion of the lever to the "on" position slides the magnet into a position where the magnetic field passes through the workpiece. Clearly, this type of vise is suitable only for workpieces of ferromagnetic material and for finishing operations where the forces generated during grinding are small. In other situations a mechanical vise or other direct clamping means would be employed.

1.5.3   Vertical-Spindle Surface-Grinding Machine (Vertical-Spindle Surface Grinder)

The vertical-spindle surface grinder (Fig. 1.44) employs a cup-shaped abrasive wheel and performs an operation similar to face milling. The worktable is reciprocated (X' motion) and the tool fed intermittently downward

(a)

(b)
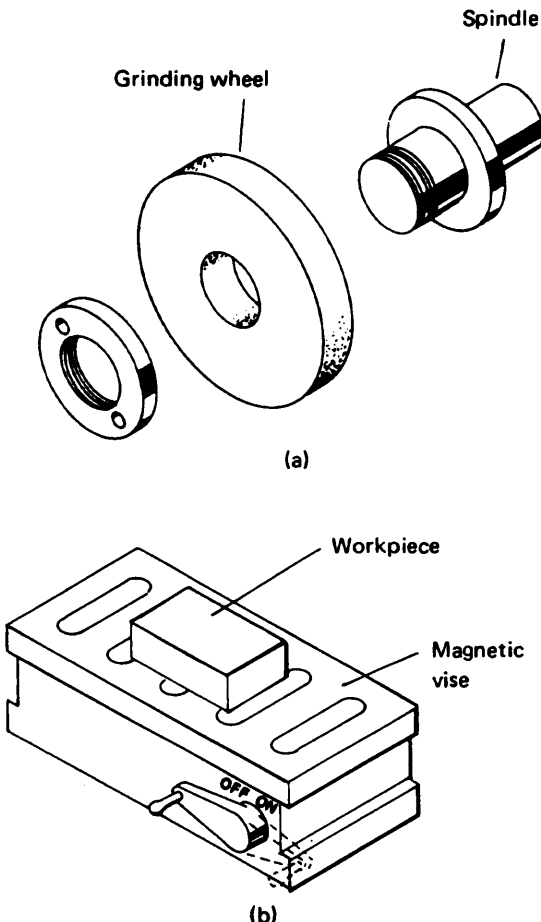
Figure 1.43   Tool and work holding in surface grinding. (a) Tool holding; (b) work holding.

($-Z$ motion); these motions are known as traverse and infeed, respectively. A horizontal surface is generated on the workpiece, and because of the deflection of the machine structure, the feed f will initially be less than the feed setting on the machine tool. This means that sparking-out is necessary, as in plunge grinding on a horizontal-spindle machine.

The metal removal rate is given by

$$Z_w = f a_p v_{trav} \tag{1.39}$$
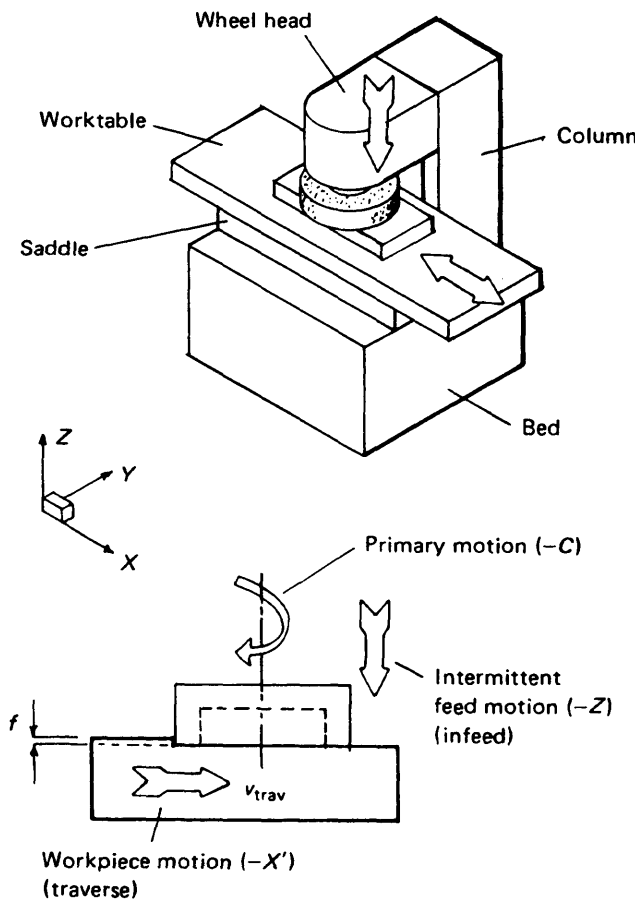
Figure 1.44 Surface grinding on a vertical-spindle surface grinder.

where a_p, the back engagement, is equal to the width of the workpiece, and v_{trav} is the traverse speed.

The machining time is given, as in plunge grinding on a horizontal-spindle machine, by Eq. (1.38).

For vertical-spindle surface grinders with a horizontal, rotary worktable on which several workpieces can be mounted the machining time is given by

$$t_m = \frac{a_t}{fn_w} + t_s \tag{1.40}$$

where n_w is the rotational frequency of the worktable.

1.5.5 Cylindrical-Grinding Machine (Cylindrical Grinder)

In the cylindrical-grinding machine (Fig. 1.45) the workpiece is supported and rotated between centers. The headstock provides the low-speed rotational drive (C' motion) to the workpiece and is mounted, together with the tailstock, on a worktable that is reciprocated horizontally (Z' motion) using a hydraulic drive. The grinding-wheel spindle is horizontal and parallel to the axis of workpiece rotation, and horizontal, hydraulic
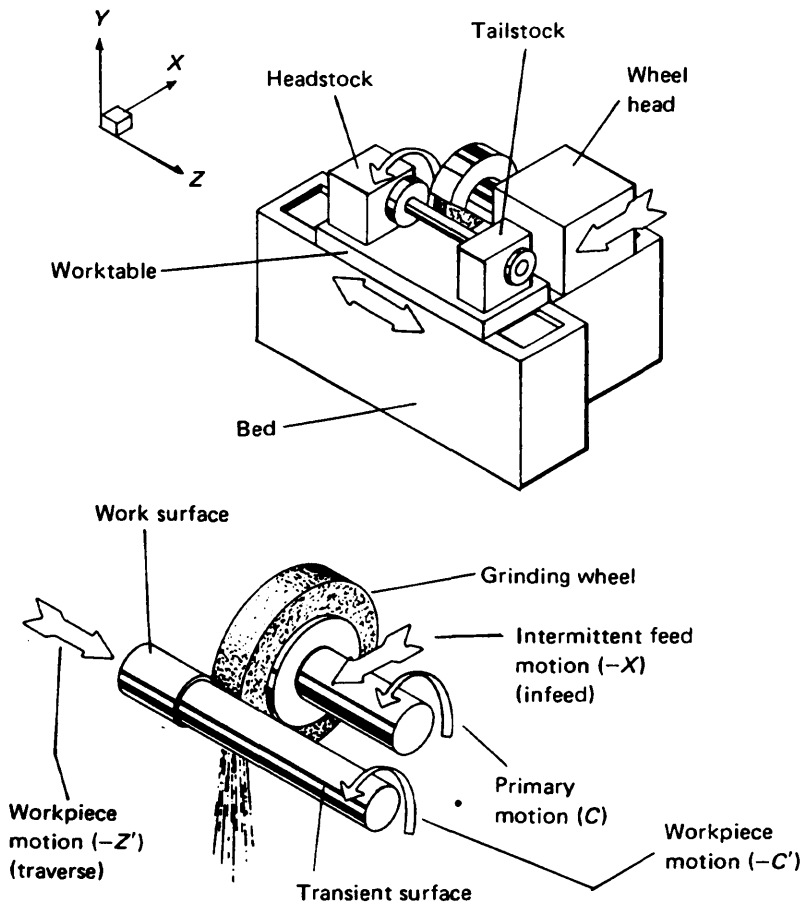
Figure 1.45 Cylindrical grinding.

feed can be applied to the wheel head in a direction normal to the axis of workpiece rotation ($-X$ motion); this motion is known as infeed.

Figure 1.45 shows a cylindrical surface being generated using the traverse motion; an operation which can be likened to cylindrical turning, where the single-point cutting tool is replaced by a grinding wheel. In fact, grinding attachments are available that allow this operation to be performed on an engine lathe.

The geometries of traverse and plunge grinding on a cylindrical grinder are shown in Fig. 1.46. In traverse grinding, the maximum metal removal rate is closely given by

$$Z_{w_{max}} = \pi f d_w v_{trav} \qquad (1.41)$$

where

d_w = diameter of the work surface
v_{trav} = traverse speed
f = feed per stroke of the machine table (usually extremely small compared to d_w)

The machining time will be given by Eq. (1.38).

In the plunge-grinding operation shown in Fig. 1.46b, the wheel is fed into the workpiece, without traverse motion applied, to form a groove. If v_f is the feed speed of the grinding wheel, d_w the diameter of the work surface,
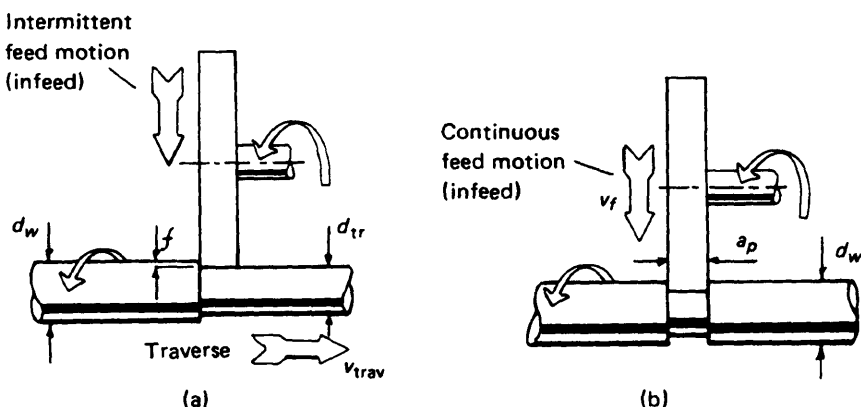
Figure 1.46 Cylindrical-grinding operations. (a) Traverse grinding; (b) plunge grinding.

and a_p the back engagement (the width of the grinding wheel), the maximum metal removal rate is given by

$$Z_{w_{max}} \cong \pi a_p d_w v_f \qquad (1.42)$$

and the machining time will be

$$t_m = \frac{a_t}{v_f} + t_s \qquad (1.43)$$

where a_t is the total depth of material to be removed and t_s is the sparking-out time.

1.5.6 Internal-Grinding Machine (Internal Grinder)

The last machine to be described here is the internal grinder (Fig. 1.47), which is designed to produce an internal cylindrical surface. The wheel head supports a horizontal spindle and can be reciprocated (traversed) in a direction parallel to the spindle axis (Z motion). A small cylindrical grinding wheel is used and is rotated at very high speed. The workpiece is mounted in a chuck or on a magnetic faceplate and rotated (motion C'). Horizontal feed is applied to the wheel head in a direction normal to the wheel spindle (motion X); this motion is known as infeed. Again, traverse and plunge grinding can be performed, the geometries of which are shown in Fig. 1.48.

Traverse grinding is shown in Fig. 1.48a, and the maximum removal rate, which occurs at the end of the operation, is given by

$$Z_{w_{max}} = \pi f d_m v_{trav} \qquad (1.44)$$

where

   f = feed
v_{trav} = traverse speed
  d_m = diameter of the machined surface

The machining time is again given by Eq. (1.38).
Finally, in plunge grinding (Fig. 1.48b) the maximum removal rate is given by

$$Z_{w_{max}} = \pi a_p d_m v_f \qquad (1.45)$$

and the machining time by Eq. (1.43).

Headstock   Chuck

Wheel
head

Bed

Workpiece

Workpiece
motion (−C')

Grinding wheel

Intermittent feed
motion (X)
(infeed)

Primary motion (−C)

Work
surface

Spindle
motion (−Z)
(traverse)

Transient
surface
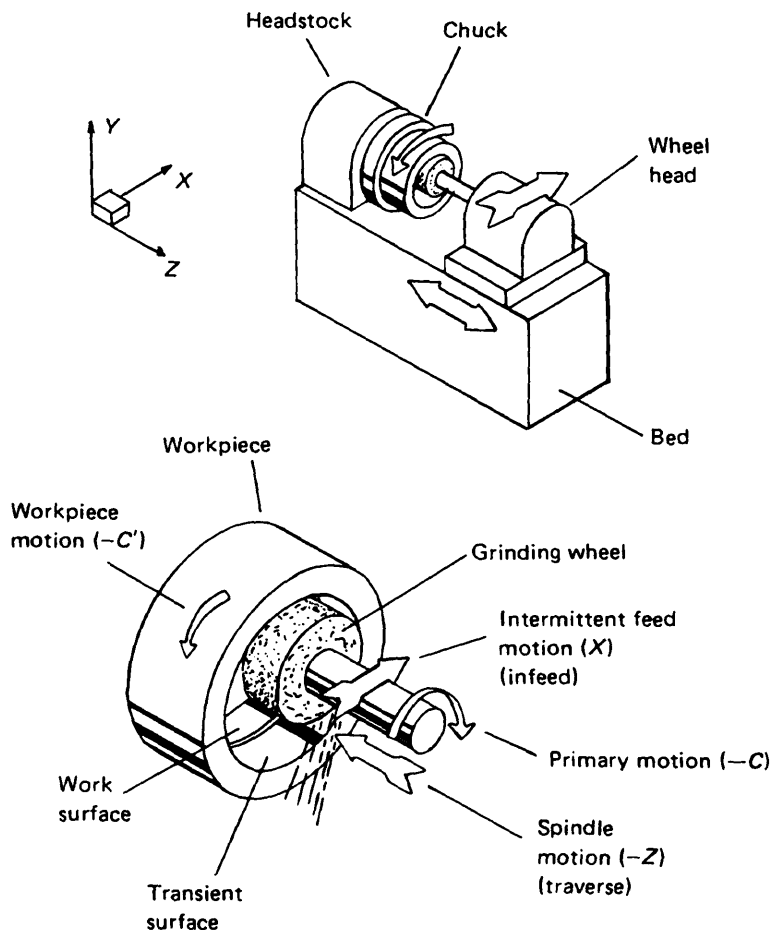
Figure 1.47   Internal grinding.

1.6   SUMMARY OF MACHINE TOOL CHARACTERISTICS AND MACHINING EQUATIONS

In this section a summary of the equations derived for each machining operation is presented with empirical information that allow rough estimates to be made of machining times and power consumption.

First, however, Tables 1.1 to 1.3 present characteristics and capabilities of typical machine tools. Table 1.1 lists the common machines that employ single-point tools and shows the nature of the primary motion
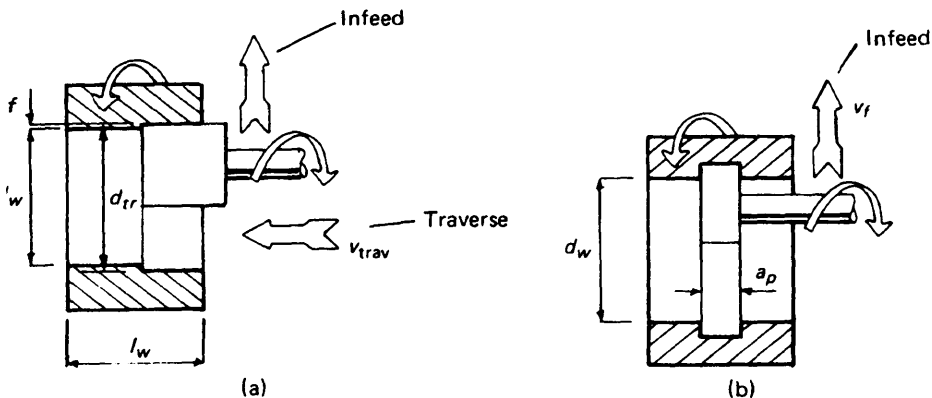
Figure 1.48 Internal-grinding operations. (a) Traverse grinding; (b) plunge grinding.

and its typical speed range; the nature of the feed motion and the range of feed f; the power available P_e; the overall efficiency η_m of the machine drive system; the capacity of the machine in terms of the maximum workpiece dimensions that can be accommodated; and, finally, an estimate of the machining accuracy that can be achieved without special techniques.

Tables 1.2 and 1.3 present similar information for machines employing multipoint tools and grinding machines, respectively. It should be noted that for each type of machine a wide range of sizes is generally available; the tables give details of only one typical machine within the range.

Table 1.4 summarizes the equations developed earlier for the machining time t_m, the metal removal rate Z_w, and the mean undeformed chip thickness $a_{c_{av}}$ for metal-cutting operations. Table 1.5 summarizes the equations for the machining time and the metal removal rate for grinding operations.

The machining time is an important factor when considering the economics and production rate of an operation, but it should be remembered that the time spent by the operator on loading and unloading workpieces, changing tools, and positioning the workpiece or tool before engaging the feed is not included. To estimate the machining time for those machines having a reciprocating motion, it is necessary to know the relationships between the frequency of reciprocation n_r, the cutting speed v (or traverse speed v_{trav} in grinding machines), and the length of the workpiece l_w. Typical relationships presented in Fig. 1.49 allow a rough es-

Table 1.1 Typical Characteristics of Machines Using Single-Point Tools

Machine	Primary motion				Feed motion			Power P_e	Overall efficiency η_m	Maximum size of workpiece	Machining accuracy
	Type	Axis	Applied to	Range of speed	Type	Applied to	Range of feed f				
Engine lathe	Rotary	Horizontal	Workpiece	0.3–27 s^{-1} (20–1 600 rpm)	Continuous	Tool	0.05–2.5 mm (0.002–0.1 in.)	4 kW (5 hp)	70	$l_w < 760$ mm (30 in.) $d_w < 360$ mm (14 in.)	0.013 mm (0.000 5 in.)
Vertical borer	Rotary	Vertical	Workpiece	0.07–3.3 s^{-1} (4–200 rpm)	Continuous	Tool	0.05–2.5 mm (0.002–0.1 in.)	15 kW (20 hp)	70	$d_w < 1.2$ m (48 in.)	0.025 mm (0.001 in.)
Horizontal borer	Rotary	Horizontal	Tool	0.3–27 s^{-1} (20–1 600 rpm)	Continuous	Tool	0.05–0.75 mm (0.002–0.03 in.)	7.5 kW (10 hp)	70	$l_w < 1.2$ m (48 in.)	0.025 mm (0.001 in.)
Shaper	Linear	Horizontal	Tool	To 0.75 m/s (150 ft/min)	Intermittent	Workpiece	0.05–0.75 mm (0.002–0.03 in.)	4 kW (5 hp)	70	$l_w < 410$ mm (16 in.) $b_w < 410$ mm (16 in.)	0.075 mm (0.003 in.)
Planer	Linear	Horizontal	Workpiece	To 1.5 m/s (300 ft/min)	Intermittent	Tool	0.05–2.5 mm (0.002–0.1 in.)	30 kW (40 hp)	80	$l_w < 7.6$ m (25 ft) $b_w < 1.2$ m (48 in.)	0.064 mm (0.002 5 in.)

Key: b_w = width of workpiece; d_w = diameter of workpiece; l_w = length of workpiece.

Table 1.2 Typical Characteristics of Machines Using Multipoint Tools

Machine	Primary motion				Feed motion			Power P_e	Overall efficiency η_m	Maximum size of workpiece	Maximum size of tool	Machining accuracy
	Type	Axis	Applied to	Speed range	Type	Applied to	Range of feed v_f or f					
Upright drill press	Rotary	Vertical	Tool	1–10 s^{-1} (60–600 rpm)	Continuous	Tool	0.15–0.64 mm (0.006–0.025 in.)	3.7 kW (5 hp)	70	600 × 600 mm (24 × 24 in.)	25-mm-dia. (1-in.) drill	0.013 mm (0.005 in.)
Radial-arm drill	Rotary	Vertical	Tool	1–10 s^{-1} (60–600 rpm)	Continuous	Tool	0.15–0.64 mm (0.006–0.025 in.)	3.7 kW (5 hp)	70	1.2 × 1.2 m (48 × 48 in.)	25-mm-dia. (1-in.) drill	0.013 mm (0.005 in.)
Bench drill press	Rotary	Vertical	Tool	12–83 s^{-1} (700–5 000 rpm)	Hand-operated	Tool	. . .	250 W (0.33 hp)	85	250 × 250 mm (10 × 10 in.)	8-mm-dia. ($\frac{5}{16}$-in.) drill	0.05 mm (0.002 in.)
Horizontal miller	Rotary	Horizontal	Tool	0.3–8.3 s^{-1} (20–500 rpm)	Continuous	Workpiece	0.2–8.5 mm/s (0.5–20 in./min)	3.7 kW (5 hp)	50	$l_w < 915$ mm (36 in.) $b_w < 250$ mm (10 in.)	200 mm dia. (8 in.)	0.076 mm (0.003 in.)
Vertical knee-type miller	Rotary	Vertical	Tool	0.3–8.3 s^{-1} (20–500 rpm)	Continuous	Workpiece	0.2–8.5 mm/s (0.5–20 in./min)	3.7 kW (5 hp)	50	$l_w < 915$ mm (36 in.) $b_w < 250$ mm (10 in.)	15 mm dia. (6 in.)	0.076 mm (0.003 in.)
Vertical bed-type miller	Rotary	Vertical	Tool	0.3–8.3 s^{-1} (20–500 rpm)	Continuous	Workpiece	0.2–8.5 mm/s (0.5–20 in./min)	15 kW (20 hp)	50	760 × 760 mm (30 × 30 in.)	250 mm dia. (10 in.)	0.076 mm (0.003 in.)
Broacher	Linear	Vertical or horizontal	Tool	To 0.5 m/s (100 ft/min)	Provided by cutting edges	Tool	0.013–0.13 mm (0.000 5–0.005 in.)	19 kW (25 hp)	80	$l_w < 460$ mm (18 in.)	915 mm long (36 in.)	0.013 mm (0.000 5 in.)

Key: b_w = width of workpiece; l_w = length of workpiece.

Table 1.3 Typical Characteristics of Machines Using Abrasive Wheels

Machine	Rotary primary motion applied to wheel		Traverse			Rotary motion of workpiece		Intermittent feed		Power P_s	Overall efficiency η_m	Maximum size of workpiece	Machining accuracy
	Axis	Speed	Axis	Applied to	Maximum feed	Axis	Speed	Applied to	Maximum feed f				
Horizontal-spindle surface grinder	Horizontal	33 s^{-1} (2 000 rpm)	Horizontal	Workpiece	0.75 m/s (150 ft/min)	. . .	. . .	Workpiece	6.4 mm (0.25 in.)	1 kW (1.5 hp)	85	l_w < 600 mm (24 in.) b_w < 200 mm (8 in.)	0.002 5 (0.000 1 in.)
Vertical-spindle surface grinder	Vertical	33 s^{-1} (2 000 rpm)	Horizontal	Workpiece	0.75 m/s (150 ft/min)	. . .	. . .	Wheel	1.5 mm (0.06 in.)	3.7 kW (5 hp)	85	l_w < 760 mm (30 in.) b_w < 250 mm (10 in.)	0.025 mm (0.001 in.)
Vertical-spindle surface grinder with rotary table	Vertical	33 s^{-1} (2 000 rpm)	. . .	. . .	. . .	Vertical	1.7 s^{-1} (100 rpm)	Wheel	0.25 mm (0.01 in.)	1 kW (1.5 hp)	85	400-mm-dia. (16 in.) table	0.002 5 mm (0.000 1 in.)
Cylindrical grinder	Horizontal	33 s^{-1} (2 000 rpm)	Horizontal	Workpiece	0.5 m/s (100 ft/min)	Horizontal	1.7 s^{-3} (100 rpm)	Wheel	0.4 mm (0.015 in.)	1 kW (1.5 hp)	85	l_w < 600 mm (24 in.) d_w < 250 mm (10 in.)	0.002 5 mm (0.000 1 in.)
Internal grinder	Horizontal	1700 s^{-1} (100 000 rpm)	Horizontal	Wheel	0.75 m/s (150 ft/min)	Horizontal	3.3 s^{-1} (200 rpm)	Wheel	0.025 mm (0.001 in.)	1 kW (1.5 hp)	85	l_w < 200 mm (8 in.) d_w < 150 mm (6 in.)	0.000 25 mm (0.000 01 in.)

Key: b_w = width of workpiece; d_w = diameter of workpiece; l_w = length of workpiece.

Table 1.4 Summary of Equations for Cutting Operations

Operation	Figure	Machining time t_m	Metal removal rate Z_w or $Z_{w_{max}}$	Mean undeformed chip thickness, $a_{c_{av}}$
Turning	1.7(a)	$\dfrac{l_w}{fn_w}$	$\pi f a_p n_w (d_m + a_p)$	
Boring	1.7(c)		$\pi f a_p n_w (d_m - a_p)$	
Facing	1.7(b)	$\dfrac{d_m}{2fn_w}$	$\pi f a_p n_w d_m$	$f \sin \kappa_r$
Parting	1.7(e)			
Shaping and planing	1.20	$\dfrac{b_w}{fn_r}$	$f a_p v$	
Drilling	1.23	$\dfrac{l_w}{fn_t}$	$\dfrac{\pi f d_m^2 n_t}{4}$	$\dfrac{f}{2} \sin \kappa_r$
Slab milling	1.28 1.29	$\dfrac{l_w + \sqrt{a_e(d_t - a_e)}}{v_f}$		$\dfrac{v_f}{Nn_t} \sqrt{\dfrac{a_e}{d_t}}$
Face milling	1.33 1.34	$\dfrac{l_w + d_t}{v_f}$	$a_e a_p v_f$	$\dfrac{v_f}{Nn_t}$
Side and face milling	1.33 1.34	$\dfrac{l_w + 2\sqrt{a_e(d_t - a_e)}}{v_f}$		$\dfrac{v_f}{Nn_t} \sqrt{\dfrac{a_e}{d_t}\left(1 - \dfrac{a_e}{d_t}\right)}$
Broaching	1.37	$\dfrac{l_t}{v}$	$f a_p v$ per engaged cutting edge	f

Key: a_e = working engagement; a_p = back engagement; b_w = width of surface to be machined; d_m = diameter of machined surface; d_t = diameter of tool; f = feed; l_t = length of tool; l_w = length of surface or hole to be machined; n_r = frequency of reciprocation; n_t = rotational frequency of tool; n_w = rotational frequency of workpiece; N = number of teeth on cutter; v = cutting speed; v_f = feed speed; κ_r = major cutting edge angle.

timate to be made of the rate of reciprocation n_r for use in the equations in Tables 1.4 and 1.5.

Although the cost of the power consumed in a machining operation is not usually an important economic factor, it is necessary to be able to estimate the quantity of power required because of the limitations which may be imposed by the power available to operate a particular machine tool. The ability to estimate power requirements is important because, for rough-machining operations, it is usually desirable to remove metal at the highest rate possible. It was shown earlier [Eq. (1.9)] that the power required for machining P_m can be found from

$$P_m = p_s Z_w$$

Table 1.5 Summary of Equations for Grinding Operations

Machine		Operation	Figure	Machining time t_m	Metal removal rate Z_w or $Z_{w_{max}}$
Horizontal-spindle surface grinder		Traverse	1.42(a)	$\dfrac{b_w}{2fn_r}$	$f a_p v_{trav}$
		Plunge	1.42(b)	$\dfrac{a_t}{2fn_r} + t_s$	
Vertical-spindle surface grinder	Reciprocating worktable	Traverse	1.44	$\dfrac{a_t}{2fn_r} + t_s$	
	Rotary worktable	Traverse		$\dfrac{a_t}{fn_w} + t_s$	
Cylindrical grinder		Traverse	1.46(a)	$\dfrac{a_t}{2fn_r} + t_s$	$\pi f d_w v_{trav}$
		Plunge	1.46(b)	$\dfrac{a_t}{v_f} + t_s$	$\pi a_p d_w v_f$
Internal grinder		Traverse	1.48(a)	$\dfrac{a_t}{2fn_r} + t_s$	$\pi f d_m v_{trav}$
		Plunge	1.48(b)	$\dfrac{a_t}{v_f} + t_s$	$\pi a_p d_m v_f$

Key: a_p = back engagement; a_t = total depth of material to be removed; b_w = width of workpiece to be machined; d_m = diameter of machined surface; d_w = diameter of work surface; f = feed; n_r = frequency of reciprocation; n_w = rotational frequency of workpiece; t_s = spark-out time; v_f = feed speed; v_{trav} = traverse speed.

In practice the specific cutting energy p_s depends mainly on the hardness of the work material and the mean value of the undeformed chip thickness $a_{c_{av}}$. A guide to the relationships between p_s and $a_{c_{av}}$ for various work materials is presented in Fig. 1.50 and can be used with the equations in Tables 1.4 and 1.5 to estimate P_m. It should be noted that for slab milling and face milling the mean value of a_c has been approximated roughly by $a_{c_{max}}/2$ ($a_{c_{max}}$ is the maximum value of a_c), except in face milling, where the workpiece width is smaller than the tool diameter. In face milling the mean value of a_c is approximately equal to $a_{c_{max}}$. For all other cases $a_{c_{av}}$ is equal to a_c.

For a particular machine, the power available for machining can be estimated from

$$P_m = P_e \eta_m \tag{1.46}$$

v or v_f, ft/min
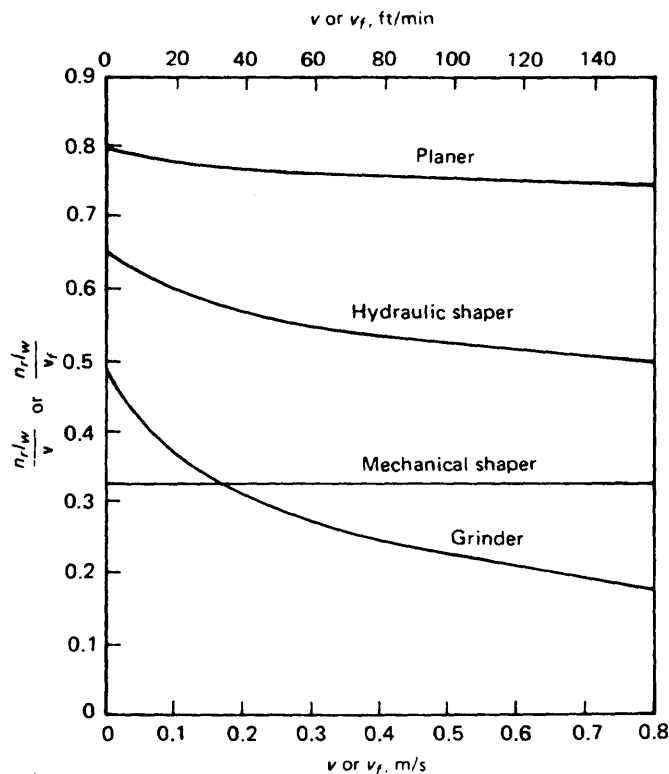
Figure 1.49   Typical characteristics of machine tools having a reciprocating motion, where n_r = frequency of reciprocation, l_w = length of workpiece, v = cutting speed, and v_{trav} = traverse speed (for grinders).
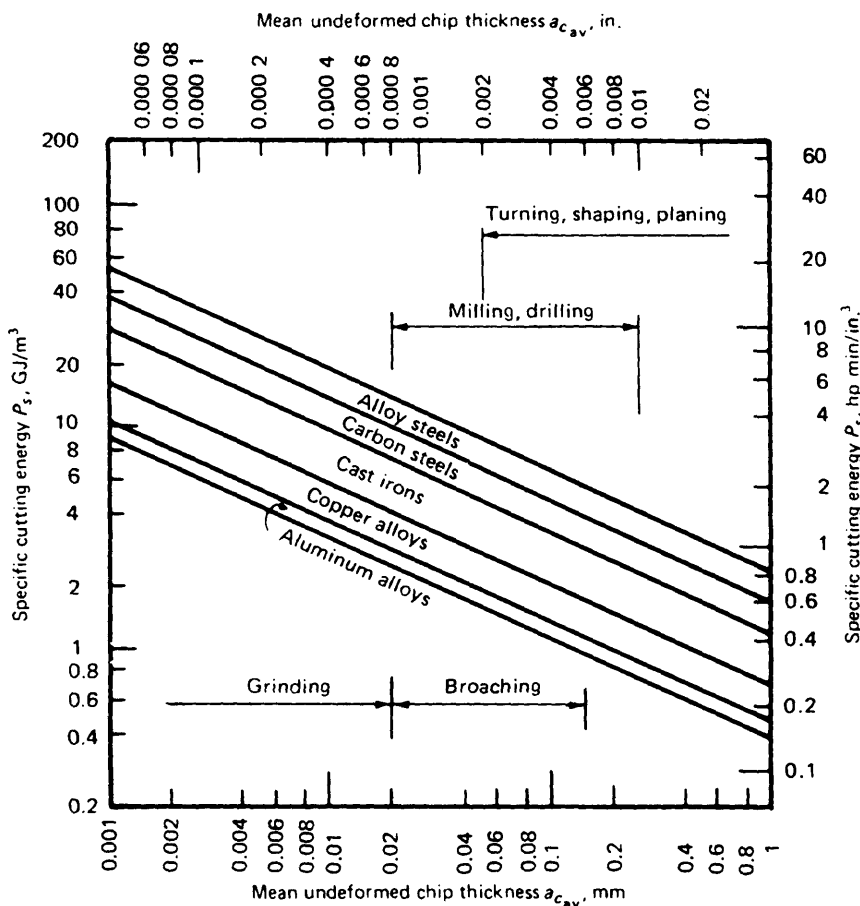
Figure 1.50 Approximate values of the specific cutting energy p_s for various materials and operations.

where P_e is the electrical power available and η_m is the overall efficiency of the drive system.

PROBLEMS

1. Two thousand bars 80 mm in diameter and 300 mm long must be turned down to 65 mm diameter for 150 mm of their length. The surface-finish and accuracy requirements are such that a heavy roughing cut (removing most of the material) followed by a light

finishing cut are needed. The roughing cut is to be taken at maximum power. The light finishing cut is to be taken at a feed of 0.13 mm, a cutting speed of 1.5 m/s, and at maximum power.

    If the lathe has a 2-kW motor and an efficiency of 50 percent, calculate the total production time in kiloseconds (ks) for the batch of work. Assume that the specific cutting energy for the work material is 2.73 GJ/m^3, the time taken to return the tool to the beginning of the cut is 15 s, and the time taken to load and unload a workpiece is 120 s.

2.   A workpiece in the form of a bar 100 mm in diameter is to be turned down to 70 mm diameter for 50 mm of its length. A roughing cut using maximum power and a depth of cut of 12 mm is to be followed by a finishing cut using a feed of 0.1 mm and a cutting speed of 1.5 m/s.

    It takes 20 s to load and unload the workpiece and 30 s to set the cutting conditions, set the tool at the beginning of the cut, and engage the feed.

    The specific cutting energy for the material is 2.3 GJ/m^3 and the lathe has a 3-kW motor and a 70 percent efficiency. Estimate:

a.   The machining time for the rough cut
b.   The machining time for the finish cut
c.   The total production time for each workpiece

3.   A 50-mm-diameter bar is to be screw-threaded, for 250 mm of its length, on a lathe. The included angle of the thread is 60 deg, the pitch is 2.5 mm, and the outside diameter of the threaded portion is to be 50 mm.

a.   If the undeformed chip thickness is limited to 0.13 mm, how many passes of the tool will be required to complete the operation?
b.   If the rotational frequency of the workpiece is 0.8 s^{-1} and it takes 20 s to return the tool and engage the carriage with the lead screw after each pass, what will be the total production time?

4.   A 1.5-m-diameter disc with a 600-mm-diameter hole in the center is to be faced, starting at the outside, on a vertical-boring machine. The rotational frequency of the table is 0.5 s^{-1}, the feed is 0.25 mm, and the back engagement (depth of cut) is 6 mm. The specific cutting energy for the work material and the particular cutting conditions is 3.5 GJ/m^3. Calculate

a.   The machining time, in kiloseconds
b.   The power consumption (in kW) at the beginning of the operation
c.   The power consumption just before the end of the operation

5. In a pipe flange facing operation carried out on a lathe, the depth of cut is 12 mm, and the inside and outside diameters of the flange are 250 mm and 500 mm, respectively. The specific cutting energy of the work material is 2.6 GJ/m³, the maximum rotational frequency of the lathe spindle is 6 s⁻¹, and the maximum feed that can be applied is 0.25 mm. The major cutting-edge angle of the tool is 60 deg. Find:
    a. The maximum power required for machining when the machine is operating at maximum capacity
    b. The cutting force
    c. The machining time

6. Fifty 1-m-diameter discs having an 80-mm-diameter hole in the center are to be faced on a vertical-boring machine with a feed of 0.25 mm and a back engagement (depth of cut) of 5 mm. The machine has an automatic control device by which the cutting speed is continuously adjusted to allow maximum power utilization at the cutting tool of 3 kW. However, the maximum rotational frequency of the spindle is limited to 0.7 s⁻¹.

    If the specific cutting energy for the work material is 2.27 GJ/m³ and it takes 600 s to unload a machined disc, load an unmachined disc, and return the tool to the beginning of the cut, calculate the total production time for the batch, in kiloseconds (ks).

7. In a facing operation carried out on a lathe the end of a carbon steel cylindrical workpiece 300 mm diameter is to be faced with a high-speed steel tool having a major cutting-edge angle of 60 deg. The depth of cut (back engagement) is 10 mm and the feed 0.1 mm.
    a. What is the maximum rotational frequency for the lathe if the power available for machining is 4 kW? (Find the specific cutting energy for the work material from Fig. 1.50.)
    b. What is the machining time?

8. In a particular mechanical shaper mechanism, the length of the rocker arm is 1.4 m, the rocker-arm pivot is 1.4 m below the connection between the link and the ram, the radius of the crank is 150 mm, and the crank pivot is 700 mm above the rocker-arm pivot. If the crank is rotated at 0.3 s⁻¹, calculate
    a. The time for a forward stroke of the ram
    b. The time for a return stroke of the ram
    c. The maximum cutting speed, in meters per second (m/s), during the forward stroke

9. The cross-feed on a shaper consists of a lead screw having 0.2 threads per millimeter. A ratchet and pawl on the end of the lead screw is driven from the shaper crank such that the pawl indexes the ratchet by one tooth during each return stroke of the ram. If the shaper is

operating at one stroke per second and the ratchet on the cross-feed lead screw has 20 teeth, calculate

 a. The feed, in millimeters (mm)

 b. The shortest time to machine the surface of a rectangular workpiece 130 mm long by 100 mm wide

10. A shaper is operated at two cutting strokes per second and is used to machine a workpiece 150 mm in length at a cutting speed of 0.5 m/s using a feed of 0.4 mm and a back engagement (depth of cut) of 6 mm. Calculate

 a. The total machining time to produce 800 components each 100 mm in width

 b. The percentage of this time during which the tool is not contacting the workpiece

 c. The metal removal rate during actual machining.

11. A shaper is operated at a frequency of reciprocation of 1.5 s^{-1} and is used to machine a 4-mm layer of material from the top of a rectangular low-carbon steel workpiece. The width of the workpiece is 150 mm and its length is 200 mm. The tool has a major cutting-edge angle of 30 deg and is contacting the workpiece for 72 percent of the time. The feed is 0.25 mm. Find:

 a. The undeformed chip thickness

 b. The total time to complete the operation neglecting setup, loading, and unloading

 c. The metal removal rate during machining

 d. The power required during machining (use Fig. 1.50 to obtain the specific cutting energy)

12. In a drilling operation using a twist drill, the rotational frequency of a drill is 5 s^{-1}, the feed 0.25 mm, the major cutting-edge angle 60 deg, and the drill diameter 12 mm. Assuming that the specific cutting energy for the work material is 2 GJ/m^3, calculate

 a. The maximum metal removal rate

 b. The undeformed chip thickness

 c. The drill torque, in Newton-meters (N-m)

13. In a slab-milling operation, the width of the medium carbon steel workpiece is 75 mm, its length is 200 mm, and a 5-mm layer is to be removed in one pass.

 a. What feed speed (mm/s) could be used if the power available for cutting is 3 kW and the specific cutting energy for the work material is 3.6 GJ/m^3?

 b. If the cutter diameter is 100 mm and the ideal surface roughness is 1.5 micrometers (μm), what should be the rotational frequency of the cutter?

    c.   What is the cutting speed?

    d.   What is the machining time?

14.   In a slab-milling operation, the cutter has 20 teeth and is 100 mm in diameter. The rotational frequency of the cutter is 5 s^{-1}, the workpiece feed speed is 1.3 mm/s, the working engagement (depth of cut) is 6 mm, and the back engagement (width of the workpiece) is 50 mm. The relationship between the maximum undeformed chip thickness $a_{c_{max}}$ and the specific cutting energy p_s, in gigajoules per cubic meter (GJ/m^3), for the work material is

$$p_s = 1.4[1 + (25 \times 10^{-6})/a_{c_{max}}]$$

Estimate

    a.   The maximum metal removal rate

    b.   The maximum power, in kilowatts (kW), required at the cutter

15.   In a slab-milling operation, the length of the workpiece is 150 mm, its width is 50 mm, and a layer 10 mm in thickness is to be removed from its upper surface. The diameter of the cutter is 40 mm and it has 10 teeth. The workpiece is of medium carbon steel, the feed speed selected is 2 mm/s, and the cutter speed is 2.5 rev/s. Estimate:

    a.   The power required (in kW)

    b.   The machining time for the operation

Note: Use Fig. 1.50 to obtain the specific cutting energy.

16.   In a face-milling operation the back engagement (depth of cut) is 5 mm, the work feed speed is 0.65 mm/s, and the working engagement (width of the workpiece) is 50 mm. The cutter has a diameter of 100 mm and has 20 teeth. If the cutting speed is to be 1 m/s, calculate

    a.   The rotational frequency of the cutter

    b.   The maximum metal removal rate

    c.   The time taken to machine 1000 workpieces of length 150 mm if it takes 180 s to load and unload a workpiece and return the cutter to the beginning of the cut

17.   In a finish-surface-grinding operation on a horizontal-spindle surface grinder, the length of the workpiece is 100 mm and its width 50 mm. The cross-feed is applied every stroke of the worktable and is set at 0.25 mm, the back engagement (depth of cut) is 0.1 mm, and the maximum traverse speed is 250 mm/s. The frequency of worktable reciprocation is 1 s^{-1}. Calculate

    a.   The machining time

    b.   The maximum metal removal rate

    c.   The maximum power consumption in watts (W) if the specific cutting energy for the conditions employed is 25 GJ/m^3

    d. The maximum tangential force on the grinding wheel if its diameter is 150 mm and has a rotational frequency of 60 s^{-1}.

REFERENCE

1. Axis and Motion Nomenclature for Numerically Controlled Machine Tools: ISO Recommendation R841, 1st ed., October 1968.

2
Mechanics of Metal Cutting

2.1 INTRODUCTION

Research in metal cutting did not start until approximately 70 years after the introduction of the first machine tool. It is not proposed to give here a complete history of research in metal cutting but to indicate some of the more important steps that have been made.

According to Finnie, who published a historical review of work in metal cutting [1], early research in metal cutting started with Cocquilhat in 1851 [2] and was mainly directed toward measuring the work required to remove a given volume of material in drilling. In 1873 tabulations of the work required in cutting metal were presented by Hartig [3] in a book that seems to have been the authoritative work on the subject for several years.

The shavings, or swarf, removed during the cutting of metal are called chips, and the first attempts to explain how chips are formed were made by Time [4] in 1870 and the famous French scientist Tresca [5] in 1873. Some years later, in 1881, Mallock [6] suggested correctly that the cutting process was basically one of shearing the work material to form the chip and emphasized the importance of the effect of friction occurring on the cutting-tool face as the chip was removed (Fig. 2.1a). He produced
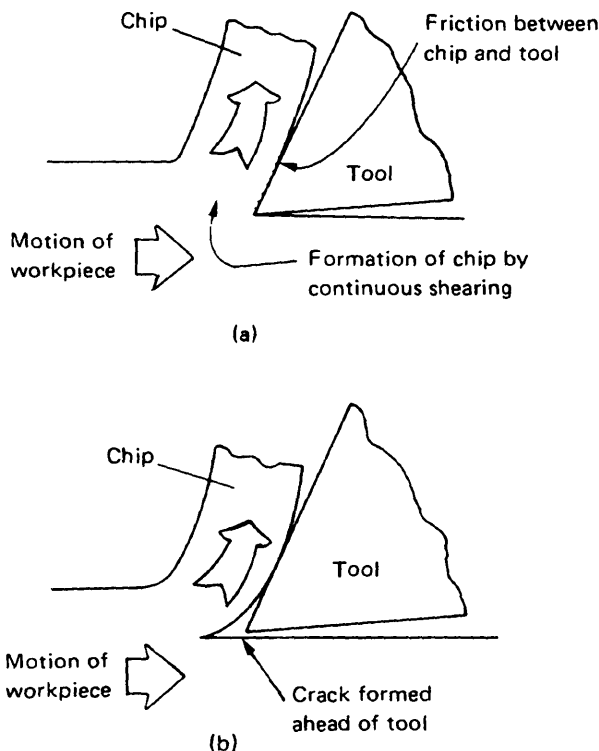
Figure 2.1 Models of the cutting process. (a) Present-day model; (b) earlier misconception.

drawings of chip formation from polished and etched specimens of partly formed chips; in addition, he observed the effect of cutting lubricants, the effect of the tool sharpness on the cutting process, and the reasons for instability in the cutting process that leads to undesirable vibrations, or "chatter." Many of these observations are surprisingly close to the accepted modern theories and are still being repeated more than 100 years later.

Finnie [1] reports that a step backward in the understanding of the metal-cutting process was taken in 1900 when Reuleaux [7] suggested that a crack occurred ahead of the tool and that the process could be likened to the splitting of wood. This theory suggests a model of cutting similar to that shown in Fig. 2.1b and is a misconception that found popular support for many years.

About this time the now-famous paper by Taylor [8] was published, which reported the results of 26 years of research investigations and exper-

ience. Taylor was interested in the application of piecework systems in machine shops, where a time allowance was set for a particular job and a bonus was given to the workman performing his task in the allocated time. To assist in the application of such a system Taylor investigated the effect of tool material and cutting conditions on tool life during roughing operations. The principal object was to determine the empirical laws that allow optimum cutting conditions to be established. In a biographical note at the beginning of the paper it was reported that with a combination of the development of a heat-treatment process to produce high-speed, steel-cutting tools (known as the Taylor–White process of heat treatment) and the results of empirical research to improve shop methods, Taylor was able to increase the production of the Bethlehem Steel Company's machine shop by 500 percent. It is of interest to note that the empirical law governing the relationship between cutting speed and tool life suggested by Taylor is still used today and employed as the basis for many recent studies of machining economics. One fundamental discovery made by Taylor was that the temperature existing at the tool cutting edge controlled the tool wear rate.

Since 1906 when Taylor's paper was published, empirical and fundamental work on metal cutting has gradually increased in volume. Most of the fundamental work has been carried out since the publication of the well-known paper by Ernst and Merchant [9] in 1941, dealing with the mechanics of the process. The main results of this more recent work are discussed in Chaps. 2 through 6 of this book.

2.2 TERMS AND DEFINITIONS

All metal-cutting operations can be likened to the process shown in Fig. 2.2, where the tool is wedge-shaped, has a straight cutting edge, and is constrained to move relative to the workpiece in such a way that a layer of metal is removed in the form of a chip. Figure 2.2b depicts the general case of cutting known as oblique cutting. A special case of cutting, where the cutting edge of the tool is arranged to be perpendicular to the direction of relative work-tool motion (Fig. 2.2a), is known as orthogonal cutting. Since orthogonal cutting represents a two-dimensional rather than a three-dimensional problem, it lends itself to research investigations where it is desirable to eliminate as many of the independent variables as possible. The relatively simple arrangement of orthogonal cutting is therefore widely used in theoretical and experimental work.

The wedge-shaped cutting tool basically consists of two surfaces intersecting to form the cutting edge (Fig. 2.3). The surface along which the chip flows is known as the rake face, or more simply as the face, and that
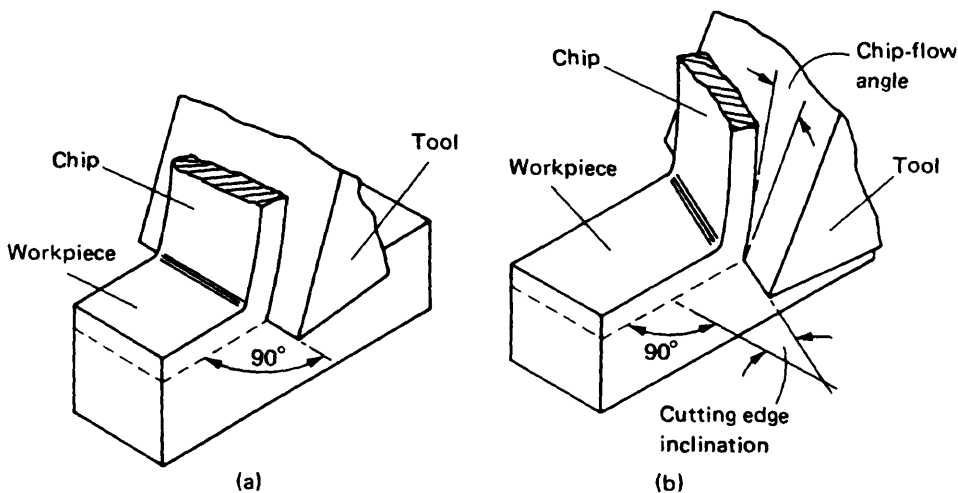
Figure 2.2 Orthogonal and oblique cutting. (a) Orthogonal cutting; (b) oblique cutting.

surface ground back to clear the new or machined workpiece surface is known as the flank. Thus, during cutting a wedge-shaped "clearance crevice" exists between the tool flank and the new workpiece surface.

The depth of the individual layer of material removed by the action of the tool is known as the undeformed chip thickness (Fig. 2.3), and although in practical cutting operations this dimension often varies as cutting proceeds, for simplicity in research work it is usually arranged to be constant.

One of the most important variables in metal cutting is the slope of the tool face, and this slope, or angle, is specified in orthogonal cutting by the angle between the tool face and a line perpendicular to the new work surface (Fig. 2.3). This angle is known as the rake angle or, in accordance with ISO terminology, the working normal rake, and Fig. 2.3 illustrates how the sign of the angle is defined.

The tool flank plays no part in the process of chip removal; however, the angle between the flank and the new workpiece surface can significantly affect the rate at which the cutting tool wears and is defined as the clearance angle or, more precisely, the working normal clearance.

Thus from Fig. 2.3 the sum of the rake, clearance, and wedge angles is equal to 90 deg, where the wedge angle is the included angle between the face and the flank.

Undeformed
chip thickness

Tool face

Chip

Tool

Clearance
crevice

New
workpiece
surface

Cutting
edge

Tool flank

Working normal
rake γ_{n_e}

Wedge
angle

$-\gamma_{n_e}$

α_{n_e}

Working normal
clearance

(a) (b)
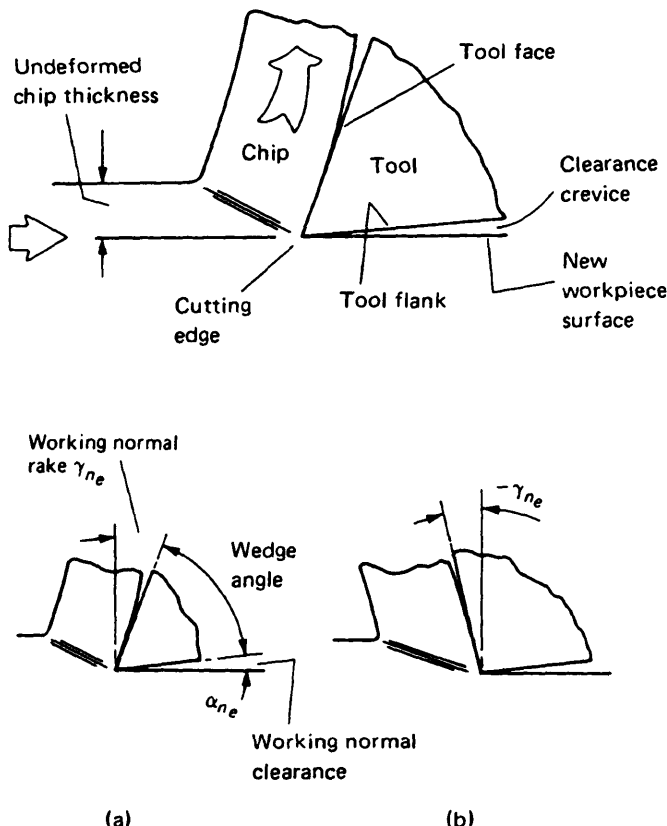
Figure 2.3 Terms used in metal cutting. (a) Positive rake; (b) negative rake.

2.3 CHIP FORMATION

The type of chip produced during metal cutting depends on the material being machined and the cutting conditions used. One of the most useful techniques for a study of chip formation is the quick-stopping device. With this device it is possible to "freeze" or suddenly stop the cutting action and allow subsequent microscopic examination of the chip removal process. A typical quick-stopping device, designed for use in a shaping machine, is depicted in Fig. 2.4. Here the workpiece is gripped in a vise that is free to slide in the guide block. During cutting the vise is constrained by the holding ring, which is held in position by shear pins passing through both the guide block and the holding ring. The shear pins are designed to carry the force required to remove the chip. When the cut is
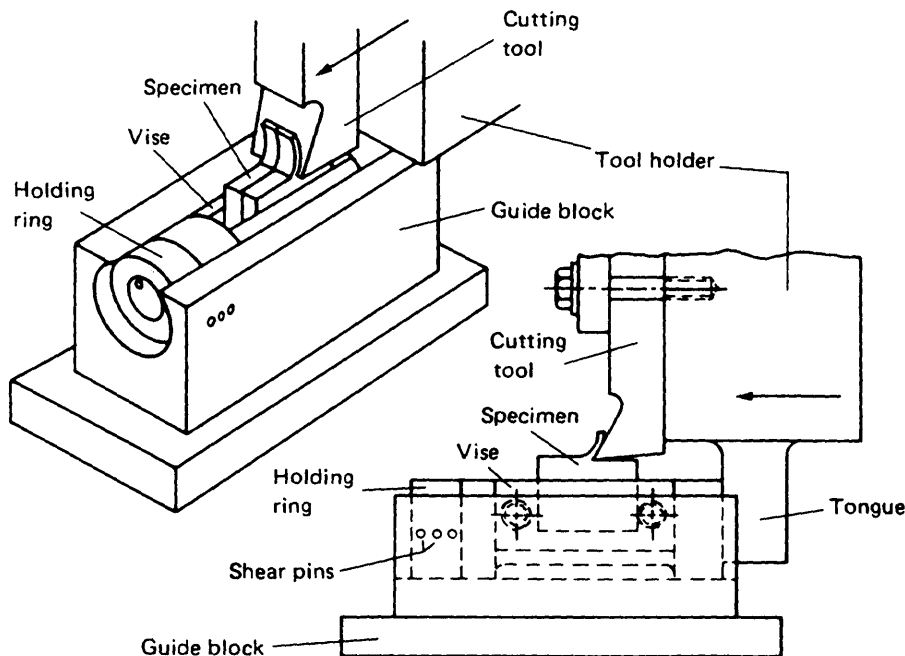
Figure 2.4 Quick-stopping device.

partly completed, a tongue on the toolholder contacts the vise, shears the pins, and pushes the vise and holding ring forward. This action of the tongue stops the cutting action by accelerating the speed of the workpiece rapidly to the speed of the cutting tool. With carefully designed devices the effective stopping time is extremely small. For example, in the device described above, the stopping time was estimated [10] to be 0.00017 s when the cutting speed is 0.8 m/s. Several other quick-stop mechanisms have been devised, including the use of explosive action, such as in humane killer guns, to propel a lathe tool away from the cutting position at very high speeds [11, 12].

After the use of a quick-stop device, a segment of the workpiece, with the chip attached, can be cut out and examined in detail at any required magnification. The specimens may be mounted, polished, and etched to reveal the internal action of cutting. In some cases the photographic deposition of a fine grid on the outside surface can aid the determination of the extent of the deformation zone and the material strain during cutting [12]. Since each quick-stop specimen illustrates the cutting action at only one instant in time, several specimens must be prepared to cover a range of cutting conditions.

Examples of specimens obtained with the quick-stopping device shown in Fig. 2.4 are depicted in Figs. 2.5 to 2.7. The specimens shown in Figs. 2.5 to 2.7 were chosen because they depict the three basic types of chip formation occurring in practice: the continuous chip, the continuous chip with built-up edge, and the discontinuous chip. In each case the cutting speed is 0.8 m/s, which means that during the retardation of the cutting action the tool travels a distance of only 0.07 mm relative to the specimen, which, in Fig. 2.5, is equal to about one-tenth of the undeformed chip thickness. These calculations support the assumption that the specimens obtained with this technique are representative of chip formation during cutting.

2.3.1 Continuous Chip

Figure 2.5 shows the formation of a continuous chip. This type of chip is common when most ductile materials, such as wrought iron, mild steel, copper, and aluminum, are machined. It can be seen that cutting under these conditions is a steady-state process. For this reason most of the research conducted into metal cutting has dealt with continuous-chip production. Basically this operation is one of shearing the work material to form the chip and sliding of the chip along the face of the cutting tool. The formation of the chip takes place in the zone extending from the tool cutting edge to the junction between the surfaces of the chip and workpiece; this zone is known as the primary deformation zone (Fig. 2.5). To deform the material in this manner the forces that must be transmitted to the chip across the interface between the chip and the tool are sufficient to deform
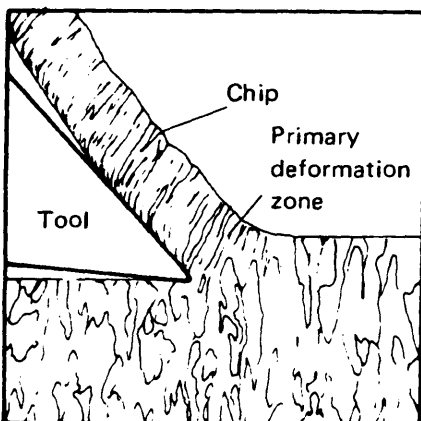
Figure 2.5   Continuous chip.

the lower layers of the chip as it slides along the tool face (secondary deformation zone).

2.3.2   Continuous Chip with Built-up Edge

Under some conditions, usually at relatively low cutting speeds, the friction between the chip and the tool is so great that the chip material welds itself to the tool face. The presence of this welded material further increases the friction, and this friction leads to the building up of layer upon layer of chip material. The resulting pile of material is referred to as a built-up edge (Fig. 2.6).

Often the built-up edge continues to grow and then breaks down when it becomes unstable, the broken pieces being carried away by the underside of the chip and the new workpiece surface. Figure 2.6 shows the rough workpiece surface obtained under these conditions. A study of built-up-edge formation in metal cutting is most important as it is one of the principal factors affecting surface finish and can have a considerable influence on cutting-tool wear. These effects will be discussed later.

2.3.3   Discontinuous Chip

During the formation of a chip the material undergoes severe strain, and, if the work material is brittle, fracture will occur in the primary deformation zone when the chip is only partly formed. Under these conditions the chip is segmented (Fig. 2.7), and the condition is referred to as discontinuous-chip formation. Discontinuous chips are always produced when
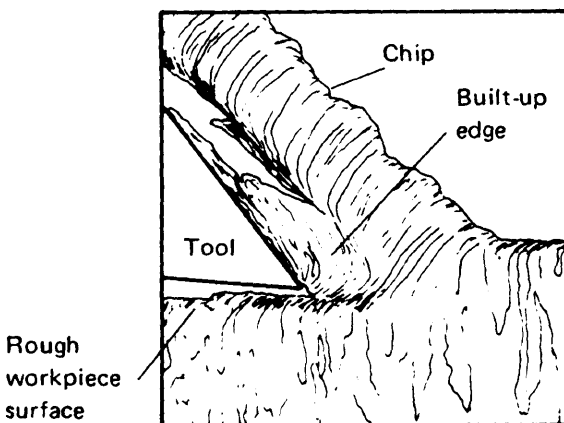
Figure 2.6   Continuous chip with built-up edge.
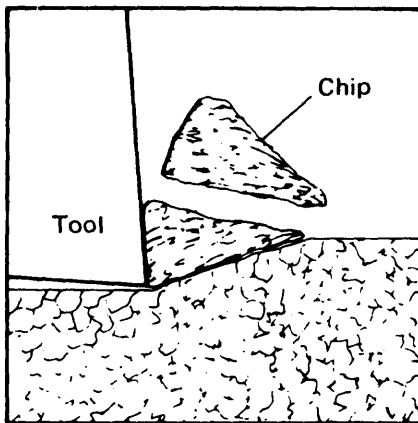
Figure 2.7   Discontinuous chip.

machining such materials as cast iron or cast brass but may also be produced when machining ductile materials at very low speeds and high feeds.

2.4   THE FORCES ACTING ON THE CUTTING TOOL AND THEIR MEASUREMENT

In orthogonal cutting the resultant force F, applied to the chip by the tool lies in a plane normal to the tool cutting edge (Fig. 2.8). This force is usually determined, in experimental work, from the measurement of two orthogonal components: one in the direction of cutting (known as the cutting force F_c), the other normal to the direction of cutting (known as the thrust force F_t). The accurate measurement of these two components of the resultant tool force has been the subject of considerable effort in the past, and several types of cutting-force dynamometers have been developed.

In most metal-cutting-force dynamometers the tool force is determined by measuring the deflections or strains in the elements supporting the cutting tool. It is essential that the instrument should have high rigidity and high natural frequencies so that the dimensional accuracy of the cutting operation is maintained and the tendency for chatter, or vibrations, to occur during cutting is minimized. The dynamometer must, however, give strains or displacements large enough to be measured accurately. The design of the dynamometer depends, to a large extent, on the strain- or deflection-measuring device and instrumentation employed. Figure 2.9 shows a simple type of two-component, cutting-force dynamometer,
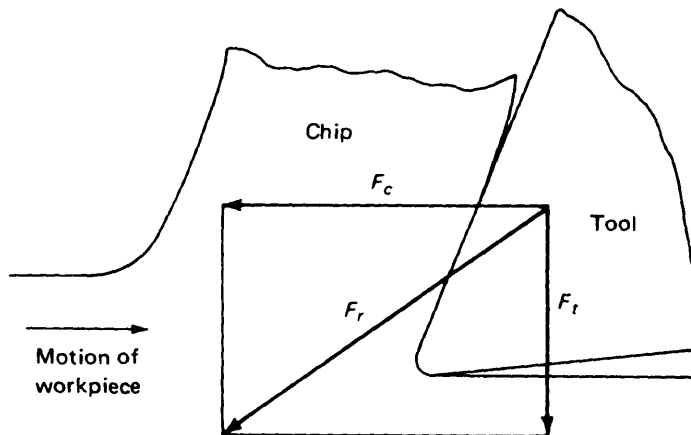
Figure 2.8 Cutting (F_c) and thrust (F_t) components of resultant tool force (F_r).

where the cutting tool is supported at the end of a cantilever. The vertical and horizontal components of the deflection of the cantilever under the action of the resultant tool force are taken as a measure of the two force components. Many effective dynamometer designs have been developed using a range of deflection-measuring methods, including strain gauges and piezoelectric load cells, for increased resolution and stiffness.

The two components F_c and F_t of the resultant tool force F_r measured with a dynamometer may be used to calculate many important variables in the process of continuous-chip formation.

2.5 SPECIFIC CUTTING ENERGY

The rate of energy consumption during machining P_m is the product of the cutting speed v and the cutting force F_c. Thus,

$$P_m = F_c v \qquad (2.1)$$

Both the rate of energy consumption and the metal removal rate are proportional to the cutting speed. A parameter giving an indication of the efficiency of the process, independent of the cutting speed, is therefore the energy consumed per unit volume of metal removed, referred to as the specific cutting energy p_s. This parameter is given by

$$p_s = \frac{P_m}{Z_w} = \frac{F_c}{A_c} \qquad (2.2)$$

Cutting tool
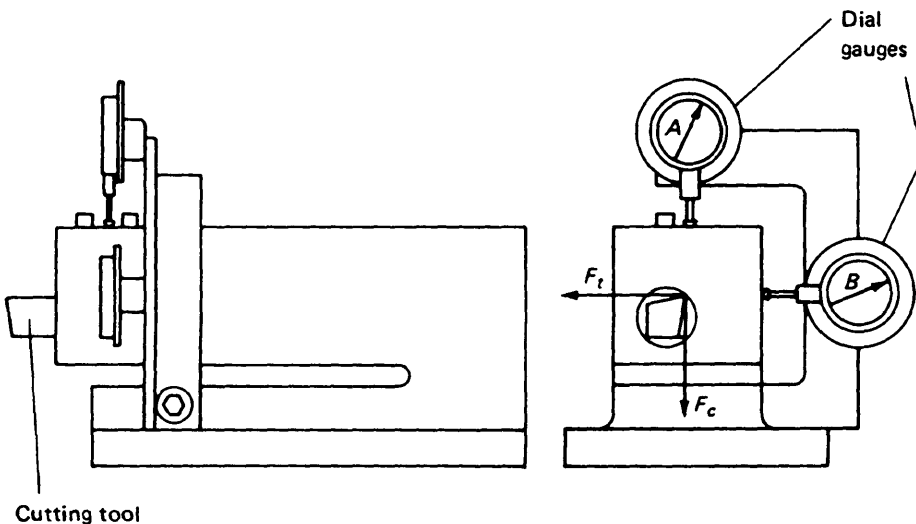
Figure 2.9 Simple two-component cutting-force dynamometer for use on a lathe, where dial gauge A gives a measure of F_c and dial gauge B gives a measure of F_t.

where Z_w is the metal removal rate and A_c is the cross-sectional area of the uncut chip.

The specific cutting energy can vary considerably for a given material and is affected by changes in cutting speed, feed, tool rake, and so on. However, for a given tool rake at high cutting speeds and large feeds the specific cutting energy tends to become constant, as can be seen in Fig. 2.10. This constant value can be a useful guide, in practice, to the forces required to cut a given material at large speeds and feeds, and for the results presented in Fig. 2.10 for a low-carbon steel, p_s approaches 1 GN/m².

2.6 PLOWING FORCE AND THE "SIZE EFFECT"

The resultant tool force in metal cutting is distributed over the areas of the tool that contact the chip and workpiece. No cutting tool is perfectly sharp, and in the idealized picture shown in Fig. 2.11 the cutting edge is represented by a cylindrical surface joining the tool flank and the tool face. Observations in the past [13] have shown that the radius of this edge varies from 0.005 to 0.03 mm for a freshly ground high-speed steel tool. As the tool edge "plows" its way through the work material, the force that acts on the tool cutting edge forms only a small proportion of the cutting force at large

Cutting speed v, ft/min
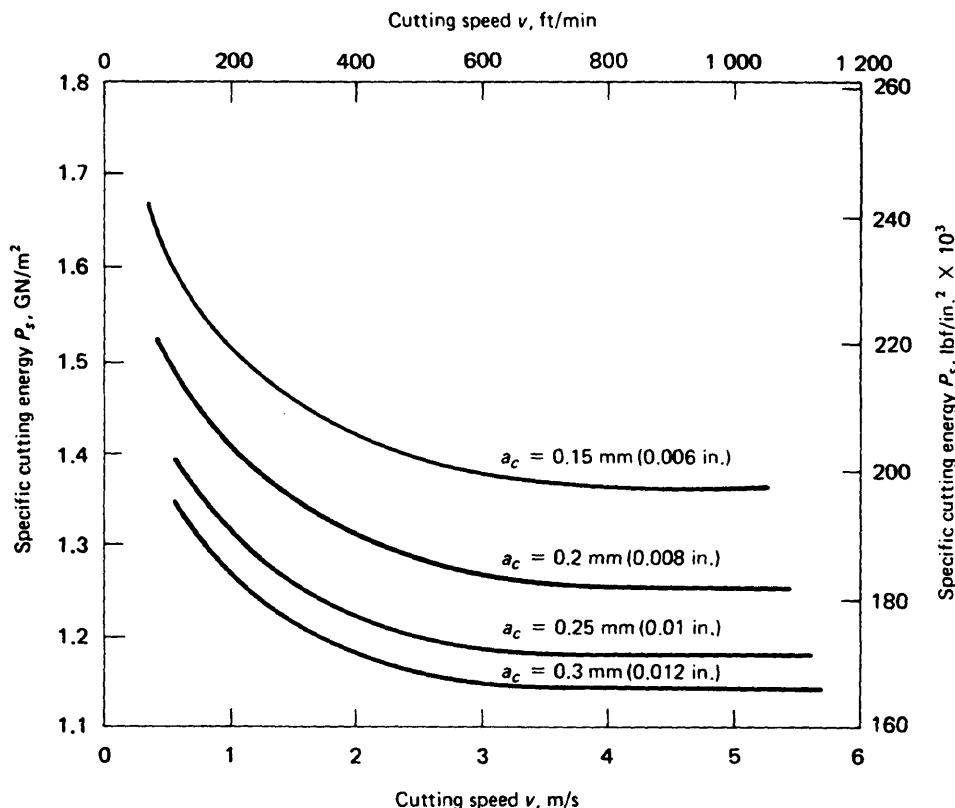
Figure 2.10 Effect of cutting speed and undeformed chip thickness on specific cutting energy, where p_s = specific cutting energy, v = cutting speed, and a_c = undeformed chip thickness and the material is mild steel, the normal rake is 10 deg, and the width of the chip is 1.25 mm.

values of the undeformed chip thickness a_c. At small values of a_c, however, the force that acts on the tool edge is proportionately large and cannot be neglected.

Because of the high stresses acting near the tool cutting edge, deformation of the tool material may occur in this region. This deformation would cause contact between the tool and the new workpiece surface over a small area of the tool flank. Thus when sharp cutting tools are used, a frictional force may act in the tool-flank region, this force again forming a small proportion of the cutting force at high feeds.

Neither the force acting on the tool edge nor the force that may act on
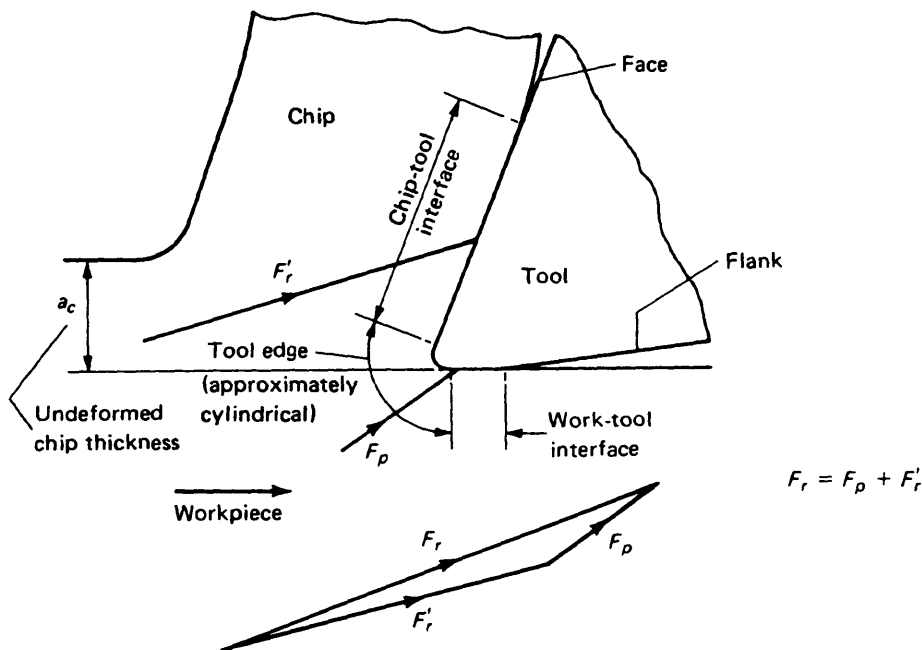
Figure 2.11 Contact regions on a cutting tool, where F_r = resultant tool force, F_r' = force required to remove the chip, and F_p = plowing force (acting on the tool edge and work–tool interface region).

the tool flank contributes to removal of the chip, and these forces will be referred to collectively as the plowing force F_p.

The existence of the plowing force results in certain important effects and can explain the so-called size effect. This term refers to the increase in specific cutting energy (the energy required to remove a unit volume of metal) at low values of undeformed chip thickness. For example, in Fig. 2.12 the mean specific cutting energy is plotted against undeformed chip thickness for a slab-milling operation. At the relatively small values of chip thickness occurring in this process, the specific cutting energy p_s increases rapidly with decreasing chip thickness. It is thought that the plowing force F_p is constant and therefore becomes a greater proportion of the total cutting force as the chip thickness decreases. When the total cutting force is divided by the undeformed-chip cross-sectional area to give p_s, the portion of p_s contributing to chip removal will remain constant, and the portion resulting from the plowing force F_p will increase as the chip thickness decreases. The increase in specific cutting energy, p_s, as the chip

Maximum undeformed chip thickness $a_{c_{max}}$, in. $\times 10^{-3}$

Maximum undeformed chip thickness $a_{c_{max}}$, mm
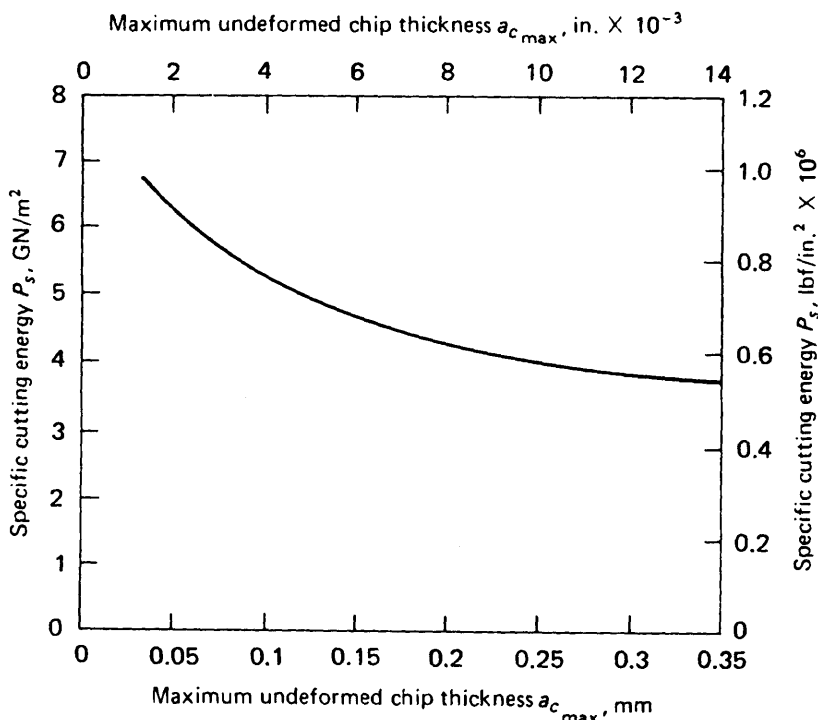
Figure 2.12 Effect of maximum undeformed chip thickness $a_{c_{max}}$ on specific cutting energy p_s during slab milling, where the material is steel, 57 ton/in², UTS.

thickness decreases explains why (as shown in Fig. 1.50) those processes, such as grinding, that produce very thin chips require greater power to remove a given volume of metal.

2.7 THE APPARENT MEAN SHEAR STRENGTH OF THE WORK MATERIAL

Many analyses of the metal-cutting processes have been developed, but with only limited success. In general, assumptions have to be made which are often valid only for a restricted range of conditions. A particular difficulty in formulating an analysis of the metal-cutting process is the lack of constraint in the process, which reduces the range of boundary conditions that can be applied. It has been suggested [14] that a unique solution does not exist for a particular set of cutting conditions and further

that parameters such as the cutting forces, cutting ratio, and so on, that occur in a particular case depend on the conditions that exist when the tool first contacts the workpiece. However, the analyses of metal cutting developed do predict many of the general trends observed in the process. Figure 2.13 shows the idealized model of continuous-chip formation employed in much of the previous work on the mechanics of the cutting process. Two of the earliest workers to employ this model were Ernst and Merchant [9], who suggested that the shear zone, or primary deformation zone, could be reasonably represented by a plane, called the shear plane. The angle of inclination of the shear plane to the direction of cutting, called the shear angle φ, could be determined as shown in Eqs. 2.3 to 2.5.

From Fig. 2.13, the length of the shear plane is given by

$$l_s = \frac{a_c}{\sin \phi} = \frac{a_0}{\cos (\phi - \gamma_{n_e})} \tag{2.3}$$

Thus,
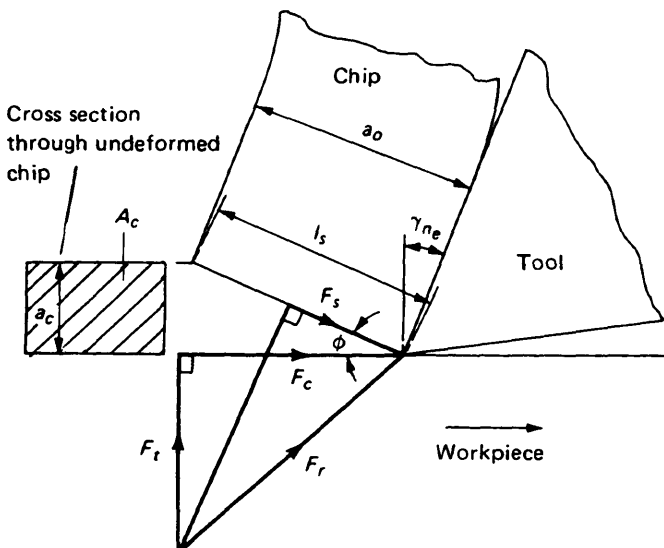
Figure 2.13 Shear-plane model of continuous chip formation, where F_r = resultant tool force, F_c = cutting force, F_t = thrust force, F_s = shear force on shear plane, ϕ = shear angle, γ_{n_e} = working normal rake, a_c = undeformed chip thickness, a_0 = chip thickness, A_c = cross-sectional area of uncut chip, and l_s = length of shear plane.

$$\frac{a_c}{a_0} \cos{(\phi - \gamma_{n_e})} = \sin{\phi}$$

and after rearrangement,

$$\tan{\phi} = \frac{(a_c/a_0) \cos{\gamma_{n_e}}}{1 - (a_c/a_0) \sin{\gamma_{n_e}}} \tag{2.4}$$

The ratio a_c/a_0 is known as the cutting ratio and is denoted by r_c. Thus,

$$\tan{\phi} = \frac{r_c \cos{\gamma_{n_e}}}{1 - r_c \sin{\gamma_{n_e}}} \tag{2.5}$$

where

ϕ = shear angle
r_c = cutting ratio (given by a_c/a_0)
a_c = undeformed chip thickness
a_0 = chip thickness
γ_{n_e} = working normal rake

In experimental work the working normal rake and the undeformed chip thickness are known, and the chip thickness can either be measured either directly with a ball-ended micrometer or obtained from the weight of a known length of chip as follows:

$$a_0 = \frac{m_c}{l_c a_w \rho} \tag{2.6}$$

where

m_c = mass of the chip specimen
l_c = length of the chip specimen
a_w = width of the chip
ρ = density of the workpiece material

If the resultant tool force is resolved in a direction parallel to the shear plane, the force F_s required to shear the work material and form the chip is obtained. As shown in Fig. 2.13, this force may be expressed in terms of the cutting (F_c) and thrust (F_t) components of the resultant tool force:

$$F_s = (F_c \cos \phi) - (F_t \sin \phi) \tag{2.7}$$

The area of shear A_s is given by

$$A_s = \frac{A_c}{\sin \phi} \tag{2.8}$$

and thus the apparent shear strength of the material τ_s on the shear plane may be obtained:

$$\tau_s = \frac{F_s}{A_s} = \frac{[(F_c \cos \phi) - (F_t \sin \phi)] \sin \phi}{A_c} \tag{2.9}$$

Experimental work [10] has shown that τ_s, calculated in this way, remains constant for a given work material over a wide variety of cutting conditions. It has been observed, however, that at small feeds τ_s increases with a decrease in feed (or undeformed chip thickness). This exception to the constancy of τ_s can be explained by the existence of a constant plowing force F_p. If F_p is subtracted from the resultant cutting force F_r, then F'_r, the force required to remove the chip and acting on the tool face, is obtained (see Fig. 2.11):

$$F'_r = F_r - F_p \tag{2.10}$$

It has been shown [15] that if the components of F'_r are used to calculate the apparent shear strength of the work material, this apparent shear strength remains constant with respect to changes in feed. Thus,

$$\tau'_s = [(F'_c \cos \phi) - (F'_t \sin \phi)] \frac{\sin \phi}{A_c} \tag{2.11}$$

where

F'_c = cutting component of F'_r
F'_t = thrust component of F'_r
τ'_s = constant property of the work material

Studies of the deformation of metals at high strain rates have shown that a material deforms at a constant stress when the strain rate is sufficiently large. In metal cutting, the strain rates are thought to be on the order of 10^3 to 10^5 s^{-1}, and under these conditions the shear strength of the metal would be expected to be constant and independent of strain rate,

strain, and temperature. These shear-strength characteristics, it is suggested, explain why in metal cutting the value of τ_s', the mean shear strength of the work material, is constant and independent of the cutting speed and rake angle under the range of these conditions normally encountered in metal cutting.

2.8   CHIP THICKNESS

The chip thickness a_0 in metal cutting is not only governed by the geometry of the cutting tool and the undeformed-chip thickness a_c, but, as will be seen, it can also be affected by the frictional conditions existing at the chip–tool interface. Because the cutting process is affected by these factors, it differs fundamentally from other metal deformation processes, where the final shape of the deformed material is determined by the shape or setting of the tool used. In metal cutting, before predictions of cutting forces can be made, the chip thickness a_0 must be determined in order that the geometry of the process will be known.

It has been shown [Eq. (2.5)] that knowledge of the shear angle ϕ allows a_0 to be estimated for a given set of cutting conditions. Experimentally, ϕ, and hence the cutting ratio r_c, depends on the work and tool materials and the cutting conditions. A number of attempts have been made, in the past, to establish a theoretical law that predicts the shear angle ϕ, and two of these attempts are considered below.

2.8.1   Theory of Ernst and Merchant

Although Piispanen attempted to solve this problem in 1937, the first complete analysis resulting in a so-called shear-angle solution was presented by Ernst and Merchant [9]. In their analysis the chip is assumed to behave as a rigid body held in equilibrium by the action of the forces transmitted across the chip–tool interface and across the shear plane.

For convenience, in Fig. 2.14 the resultant tool force F_r is shown acting at the tool cutting edge and is resolved into components F_n and F_f in directions normal to and along the tool face, respectively, and into components F_{ns} and F_s normal to and along the shear plane, respectively. The cutting (F_c) and thrust (F_t) components of the resultant tool force are also shown.

It is assumed that the whole of the resultant tool force is transmitted across the chip–tool interface and that no force acts on the tool edge or flank (i.e., the plowing force is zero).

The basis of Ernst and Merchants' theory was the suggestion that the shear angle ϕ would take up such a value as to reduce the work done in
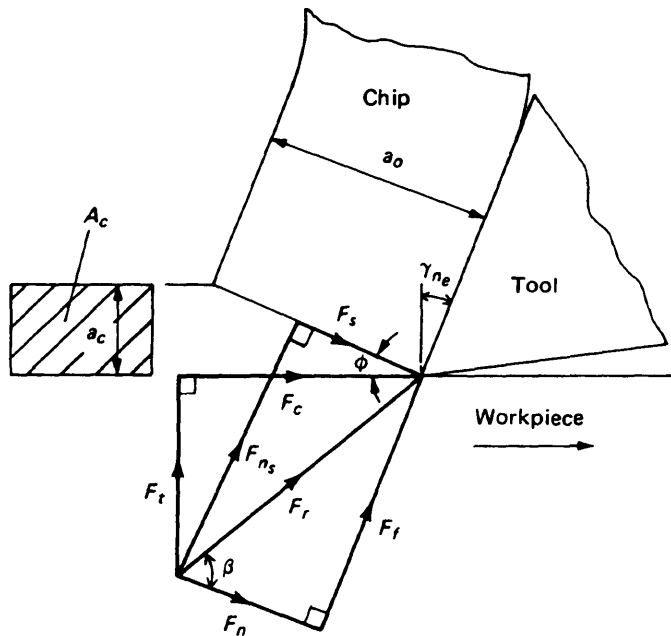
Figure 2.14 Force diagram for orthogonal cutting, where F_r = resultant tool force, F_c = cutting force, F_t = thrust force, F_s = shear force on shear plane, F_{n_s} = normal force on shear plane, F_f = frictional force on tool face, F_n = normal force on tool face, ϕ = shear angle, γ_{n_e} = working normal rake, β = mean friction angle on tool face, A_c = cross-sectional area of uncut chip, a_c = undeformed chip thickness, and a_0 = chip thickness.

cutting to a minimum. Since, for given cutting conditions, the work done in cutting was proportional to F_c, it was necessary to develop an expression for F_c in terms of ϕ and then to obtain the value of ϕ for which F_c is a minimum.

From Fig. 2.14

$$F_s = F_r \cos (\phi + \beta - \gamma_{n_e}) \tag{2.12}$$

and

$$F_s = \tau_s A_s = \frac{\tau_s A_c}{\sin \phi} \tag{2.13}$$

where

τ_s = shear strength of the work material on the shear plane
A_s = area of the shear plane
A_c = cross-sectional area of the uncut chip
β = mean angle of friction between chip and tool (given by arctan F_f/F_n)
γ_{n_e} = working normal rake

From Eqs. (2.12) and (2.13)

$$F_r = \frac{\tau_s A_c}{\sin \phi} \frac{1}{\cos (\phi + \beta - \gamma_{n_e})} \tag{2.14}$$

Now by geometry

$$F_c = F_r \cos (\beta - \gamma_{n_e}) \tag{2.15}$$

Hence from Eqs. (2.14) and (2.15)

$$F_c = \frac{\tau_s A_c}{\sin \phi} \frac{\cos (\beta - \gamma_{n_e})}{\cos (\phi + \beta - \gamma_{n_e})} \tag{2.16}$$

Equation (2.16) may now be differentiated with respect to ϕ and equated to zero to find the value of ϕ for which F_c is a minimum. The required value is given by

$$2\phi + \beta - \gamma_{n_e} = \frac{\pi}{2} \tag{2.17}$$

Merchant [16] found that this theory agreed well with experimental results obtained when cutting synthetic plastics but agreed poorly with experimental results obtained for steel machined with a sintered carbide tool.

It should be noted that in differentiating Eq. (2.16) with respect to ϕ, it was assumed that A_c, γ_{n_e}, and τ_s would be independent of ϕ. On reconsidering these assumptions, Merchant decided to include in a new theory the relationship

$$\tau_s = \tau_{s_0} + k\sigma_s \tag{2.18}$$

which indicates that the shear strength of the material τ_s increases linearly with increase in normal stress, σ_s, on the shear plane (Fig. 2.15); at zero
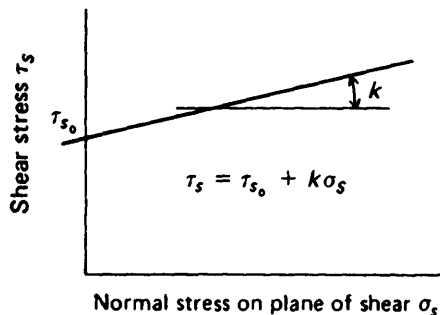
Figure 2.15 Dependence of τ_s on σ_s assumed in Merchant's second theory.

normal stress τ_s is equal to τ_{s_0}. This assumption agreed with the work of Bridgman [17], where, in experiments on polycrystalline metals, the shear strength was shown to be dependent on the normal stress on the plane of shear.

Now from Fig. 2.14

$$F_{n_s} = F_r \sin (\phi + \beta - \gamma_{n_e}) \qquad (2.19)$$

and

$$F_{n_s} = \sigma_s A_s = \frac{\sigma_s A_c}{\sin \phi} \qquad (2.20)$$

From Eqs. (2.19) and (2.20)

$$\sigma_s = \frac{\sin \phi}{A_c} F_r \sin (\phi + \beta - \gamma_{n_e}) \qquad (2.21)$$

Combining Eqs. (2.14) and (2.21),

$$\tau_s = \sigma_s \cot (\phi + \beta - \gamma_{n_e}) \qquad (2.22)$$

and from Eqs. (2.18) and (2.22)

$$\tau_s = \frac{\tau_{s_0}}{1 - k \tan(\phi + \beta - \gamma_{n_e})} \qquad (2.23)$$

This equation shows how the value of τ_s may be affected by changes in

ϕ and is now inserted in Eq. (2.16) to give a new equation for F_c in terms of ϕ:

$$F_c = \frac{\tau_{s_0} A_c \cos(\beta - \gamma_{n_e})}{\sin \phi \cos(\phi + \beta - \gamma_{n_e})[1 - k \tan(\phi + \beta - \gamma_{n_e})]} \qquad (2.24)$$

It is now assumed that k and τ_{s_0} are constants for the particular work material and that A_c and γ_{n_e} are constants for the cutting operation. Thus Eq. (2.24) may be differentiated to give the new value of ϕ. The resulting expression is

$$2\phi + \beta - \gamma_{n_e} = C \qquad (2.25)$$

where C is given by arccot k and is a constant for the work material. (As mentioned earlier, however, more recent experimental work indicates that τ_s remains constant for a given material over a wide range of cutting conditions, and therefore k would be expected to be zero.)

2.8.2 Theory of Lee and Shaffer

The theory of Lee and Shaffer [18] was the result of an attempt to apply the plasticity theory to the problem of orthogonal metal cutting. In dealing with problems using the plasticity theory, it is necessary to make certain assumptions regarding the behavior of the work material under stress as follows:

1. The material is rigid plastic, which means that the elastic strain is negligible during deformation and that once the yield point is exceeded, deformation takes place at constant stress. The stress–strain curve for a rigid-plastic material is shown in Fig. 2.16, where it is seen that the material does not work-harden.
2. The behavior of the material is independent of the rate of deformation.
3. The effects of temperature increases during deformation are neglected.
4. The inertia effects resulting from acceleration of the material during deformation are neglected.

These assumptions have led to useful solutions of many problems in plasticity. They should closely approximate the actual behavior of the work material during metal cutting because of the very high strains and strain rates that occur in the cutting process. It is known that the rate of work hardening of most metals decreases rapidly with increasing strain
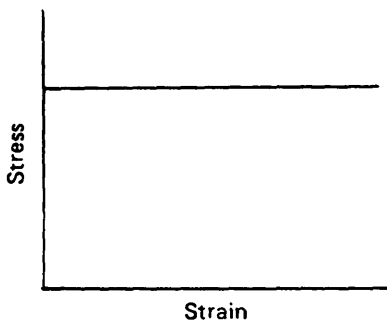
Stress

Strain

Figure 2.16 Stress–strain curve for a rigid-plastic material.

and that the effect of a high strain rate is to raise the yield strength of the metal with respect to its ultimate stress. Also, with the high strains encountered, the elastic strain would form a negligible proportion of the total strain. Thus, the stress-strain curve for the work material would correspond approximately to the ideal case, as shown in Fig. 2.16.

In the solution of a problem in plasticity, the construction of a slip-line field is necessary; this field consists of two orthogonal families of lines (called slip lines), indicating, at each point in the plastic zone, the two orthogonal directions of maximum shear stress.

The slip-line field proposed by Lee and Shaffer for the orthogonal cutting of a continuous chip is shown in Fig. 2.17. It can be seen that Lee and Shaffer have employed the idealized shear-plane model of cutting, where all the deformation takes place in a plane extending from the tool cutting edge to the point of intersection of the free surfaces of the work and chip. Consideration is given, however, to the manner in which the cutting forces applied by the tool are transmitted through the chip to the shear plane. This transmission of forces results in the triangular plastic zone *ABC*, where no deformation occurs but the material is stressed to its yield point. Thus, the maximum shear stress throughout this zone is τ_s, the shear stress on the shear plane, and the two directions of this maximum shear stress are indicated by the two orthogonal sets of straight lines (slip lines).

If the boundaries of this triangular zone are considered, it is clear that the shear plane *AB* must give the direction of one set of slip lines since the maximum shear stress must occur along the shear plane. Also, since no forces act on the chip after it has passed through the boundary *AC*, no stresses can be transmitted across this boundary. Thus, *AC* can be regarded as a free surface, and since the directions of maximum shear stress always meet a free surface at $\pi/4$, the angle *CAB* is equal to $\pi/4$. Finally,
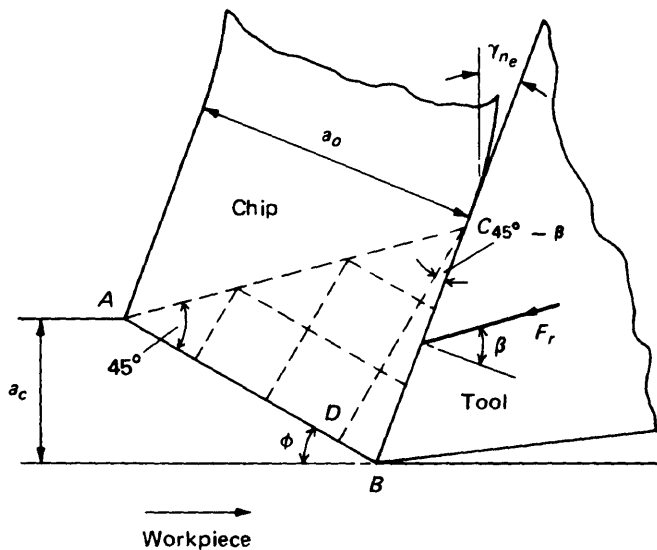
Figure 2.17 Lee and Shaffer's slip-line field for orthogonal cutting, where F_r = resultant tool force, ϕ = shear angle, γ_{n_e} = working normal rake, β = mean friction angle on tool face, a_c = undeformed chip thickness, and a_0 = chip thickness.

assuming that the stresses acting at the chip–tool interface are uniform (an unreasonable assumption, as shown later), the principal stresses at the boundary BC will meet this boundary at angles β and $[\beta + \pi/2]$ (where β is given by $\arctan F_f/F_n$ and is the mean chip–tool friction angle). Directions of maximum shear stress lie at $\pi/4$ to the directions of principal stress, and thus the angle BCD is given by $[\pi/4] - \beta$.

It now follows from Fig. 2.17 that

$$\phi + \frac{\pi}{4} + \beta - \gamma_{n_e} = \frac{\pi}{2}$$

Thus,

$$\phi + \beta - \gamma_{n_e} = \frac{\pi}{4} \tag{2.26}$$

which is the required shear-angle solution.

Lee and Shaffer realized that Eq. (2.26) could not apply where β is

equal to $\pi/4$ and γ_{n_e} is zero since with these values, ϕ would be zero. They considered, however, that such conditions of high friction and low rake angle were just those conditions that lead to the formation of a built-up edge in practice. To support this point, a second solution was presented for the new geometry where a built-up edge is present on the tool face [18].

2.8.3 Experimental Evidence

The theories outlined above were compared with the results of independently conducted experiments [19]. Figure 2.18 shows the most convenient way of making such comparisons; that is, the shear angle ϕ is plotted against $\beta - \gamma_{n_e}$. On such a graph, the relationships obtained by the Ernst and Merchant and the Lee and Shaffer theories both form straight lines. It can be seen that neither of these theories approach quantitative agreement with any of the experimental relationships for the various materials tested. However, if these theories are compared qualitatively with the experimental results, both the theories and the experimental results show that a linear relationship exists between ϕ and $\beta - \gamma_{n_e}$ and that a decrease
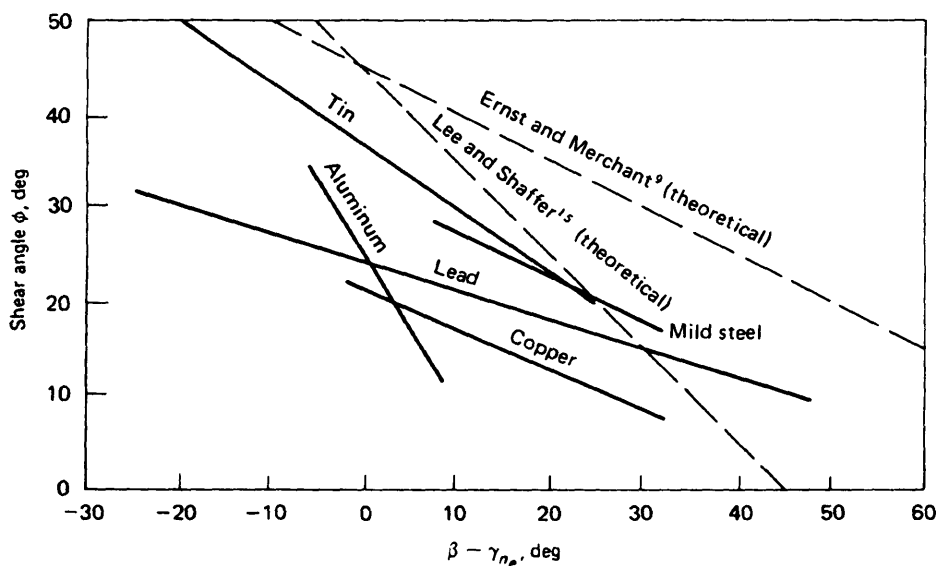
**Figure 2.18** Comparison of theoretical and experimental shear-angle relationships for orthogonal metal cutting, where ϕ = shear angle, β = mean friction angle on tool face, and γ_{n_e} = working normal rake. [After Pugh [19].)

in $\beta - \gamma_{n_e}$ always results in an increase in ϕ. Thus, for a given rake angle γ_{n_e}, a decrease in β, the mean friction angle on the tool face, results in an increase in ϕ, the shear angle, with a corresponding decrease in the area of shear. Since the mean shear strength of the work material in the shear zone remains constant, the force required to form the chip will be reduced. An increase in rake γ_{n_e} always results in an increase in the shear angle ϕ and hence a reduction in the cutting forces. This increase in shear angle, however, is usually accompanied by a relatively small increase in the friction angle β, an effect that will be discussed later.

The comparison in Fig. 2.18 shows that no unique relationship of the kind predicted by the Ernst and Merchant and the Lee and Shaffer theories could possibly agree with all the experimental results. Even the modified Merchant theory in which the shear stress on the shear plane is assumed to be linearly dependent on the normal stress could not agree with all the results. The modified Merchant theory yielded the relationship

$$2\phi + \beta - \gamma_{n_e} = C \qquad (2.27)$$

where C is a constant depending on the work material. Substituting various values of C in Eq. (2.27) could only give a series of parallel lines on the graph in Fig. 2.18. Clearly, the experimental lines are not parallel and could not be represented by Eq. (2.27).

It is not difficult to produce reasons why the theories of Ernst and Merchant and of Lee and Shaffer do not find agreement with experimental results. The assumption that the cutting tool is perfectly sharp (i.e., the plowing force F_p is negligible) could be a very rough approximation to actual conditions, particularly at small values of undeformed chip thickness. Further, it has been shown that the primary deformation zone cannot be regarded as a shear plane under a wide variety of cutting conditions. For example, Palmer and Oxley [20], using cinephotography to observe the flow of grains in a steel workpiece during slow-speed cutting, found that the primary deformation zone had the form shown in Fig. 2.19. Nakayama [21] showed that this wide deformation zone had constant proportions for cutting speeds as high as 2.5 m/s. In Nakayama's experiments the side of the specimen workpiece was coated with lampblack, and a series of lines was inscribed on the prepared surface parallel to the cutting direction. During cutting, these lines formed stationary material flow lines and could be photographed. It was therefore possible to plot the boundaries of the primary deformation zone. Similar observations have been made using a variety of techniques, including quick-stop tests using photodeposited grids on the work surface to determine the extent of the deformation zone [12].
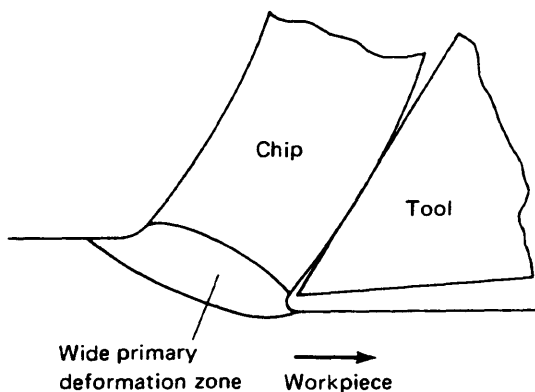
Figure 2.19   Model of an orthogonal cutting process. (After Palmer and Oxley [20].)

A number of analyses of the metal-cutting process using a thick shear-zone model have been attempted. Many of these models are complex and apply only to a limited range of conditions. The shear plane in the model developed by Ernst and Merchant is a velocity discontinuity and consequently the effects of strain hardening and strain rate, which is very high in actual cutting, cannot be taken into account. Oxley and his co-workers [12,22] have, based on experimental observations, utilized a parallel-sided, thick, shear zone model as shown in Fig. 2.20. This model, retains many of the features of the single shear-plane model, but allows the effects of strain hardening, strain rate, and temperature to be included in the analysis.

The shear-angle theories of Ernst and Merchant and of Lee and Shaffer and experimental results such as those in Fig. 2.18 indicate that the friction on the tool face is a most important factor in metal cutting. In many of the metal-cutting theories produced, the simplifying assumption has been made that chip–tool frictional behavior can be represented by a single value of the mean coefficient of friction on the tool face. It is therefore important to consider in detail the nature of the frictional conditions between the chip and the tool in metal cutting.

2.9   FRICTION IN METAL CUTTING

It is clear from the preceding discussion that, by some mechanism not completely understood, the frictional behavior on the tool face affects the geometry of the cutting process. Before the frictional conditions in metal
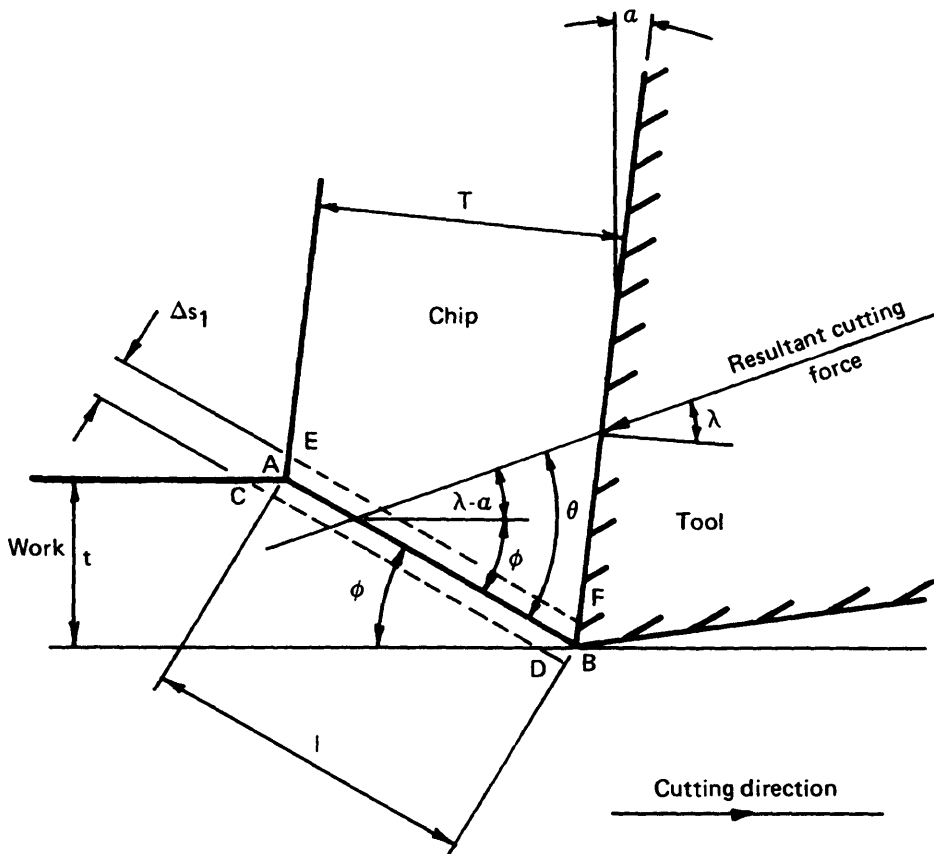
Figure 2.20 Parallel-sided, thick, shear zone model of orthogonal cutting. (After Fenton and Oxley [22].)

cutting are considered, it is necessary to discuss the nature of friction between dry sliding surfaces.

Amontons' laws of friction, formulated in 1699 [23], state that friction is independent of the apparent area of contact and proportional to the normal load between the two surfaces. In 1785, Coulomb [24] verified these laws and made a further observation: that the coefficient of friction is substantially independent of the speed of sliding. The work of Bowden and Tabor [25] has contributed much to the explanation of these empirical laws.

Microscopic examination shows that even the most carefully prepared "flat" metallic surfaces consist of numerous hills and valleys. When

two surfaces are placed together, contact is established at the summits of only a few irregularities in each surface (Fig. 2.21a). If a normal load is applied, yielding occurs at the tips of the contacting asperities, and the real area of contact A_r increases until it is capable of supporting the applied load. For the vast majority of engineering applications this real area of contact A_r is only a small fraction of the apparent contact area A_a and is given by

$$A_r = \frac{F_n}{\sigma_y} \qquad (2.28)$$

where F_n is the normal force and σ_y is the yield pressure of the softer metal.

The adhesion resulting from the intimate metallic contact of these asperities has been termed *welding*, and when sliding takes place, a force is required for continual shearing of the welded junctions at the tips of these asperities. The total frictional force F_f is therefore given by

$$F_f = \tau_f A_r \qquad (2.29)$$

where τ_f is the shear strength of the softer metal.

Thus, from Eqs. (2.28) and (2.29) the coefficient of friction is given by
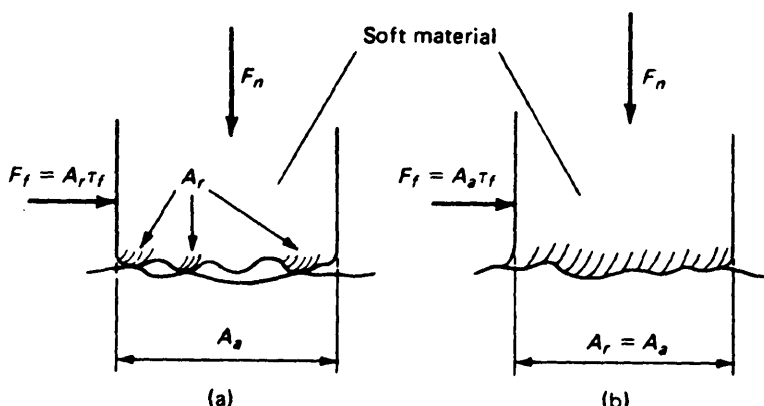

Figure 2.21 Suggested frictional behavior for a "soft" slider, where F_f = frictional force, F_n = normal force, A_r = real area of contact, A_a = apparent area of contact, and τ_f = shear strength of softer metal. (a) Sliding friction; (b) sticking friction.

$$\mu = \frac{F_f}{F_n} = \frac{\tau_f}{\sigma_y} \tag{2.30}$$

Equation (2.30) shows that the coefficient of friction is independent of the apparent contact area, and since the ratio τ_f/σ_y would be expected to be constant for a given metal, the frictional force is proportional to the normal load (i.e., μ is constant). These results are consistent with the laws of dry sliding friction.

During metal cutting, it has generally been observed that the mean coefficient of friction between the chip and the tool can vary considerably and is affected by changes in cutting speed, rake angle, and so on. This variance of the mean coefficient of friction results from the very high normal pressures that exist at the chip–tool interface. For example, when steel is machined, these normal pressures can be as high as 3.5 GN/m^2 and can cause the real area of contact to approach, or become equal to, the apparent contact area over a portion of the chip–tool interface (i.e., A_r/A_a equals unity). Thus, under these circumstances A_r has reached its maximum value and is constant. The frictional force F_f is still given by Eq. (2.29) but is now independent of the normal force F_n, and the ordinary laws of friction no longer apply. Under these conditions the shearing action is no longer confined to surface asperities but takes place within the body of the softer metal (Fig. 2.21b).

Consideration of frictional behavior in metal cutting has led [26] to the model of orthogonal cutting with a continuous chip and no built-up edge shown in Fig. 2.22. Here the normal stresses between the chip and the tool are sufficiently high to cause A_r/A_a to approach unity over the region of length l_{st}, adjacent to the tool cutting edge, termed the *sticking region*. In the length $l_f - l_{st}$, extending from the end of the sticking region to the point where the chip loses contact with the tool, the ratio A_r/A_a is less than unity, and therefore the coefficient of friction is constant; this region has been termed the *sliding region*.

In previous work [15], evidence of the sticking mode of frictional contact was produced by examination of the undersurface of the chip on specimens where the cutting action had suddenly been stopped. It was observed that in a region adjacent to the tool cutting edge, the grinding marks on the tool face were imprinted on the undersurface of the chip, indicating that no relative motion between the chip and the tool had occurred and that the real and apparent areas of contact are equal in this region. These observations have been confirmed optically using transparent sapphire tools and high-speed photography [25,28].

Under conditions of sticking friction, the mean angle of friction β on the tool face will depend on the form of the normal stress distribution, the
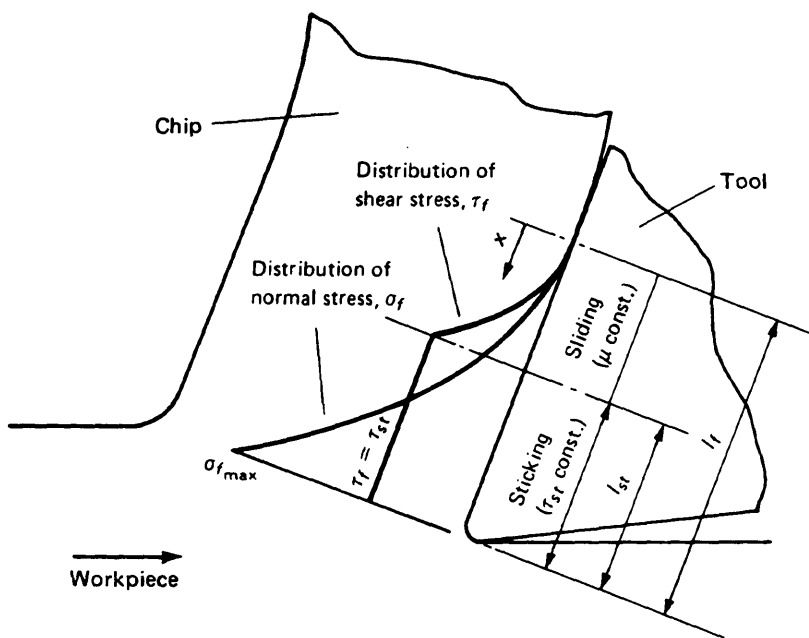
Figure 2.22 Model of chip–tool friction in orthogonal cutting, where $\sigma_{f_{max}}$ = maximum normal stress, σ_f = normal stress, τ_f = shear stress, τ_{st} = shear strength of chip material in the sticking region, l_f = chip–tool contact length, and l_{st} = length of sticking contact region. (After Zorev [26].)

chip–tool contact length l_f, the mean shear strength of the chip material in the sticking region, and the coefficient of friction in the sliding region. Clearly, a single value of the mean angle of friction is insufficient to describe completely the frictional conditions on the tool face.

An analysis of the stress distribution on the tool face shown in Fig. 2.22 has been presented by Zorev [26]. It was shown that the mean angle of friction is mainly dependent on the mean normal stress on the tool face, and this result may be used to explain the effect of changes in working normal rake γ_{n_e} on the mean friction angle β. As γ_{n_e} increases, the component of the resultant tool force normal to the tool face will decrease, and therefore the mean normal stress will decrease. However, the mean shear stress remains roughly constant and therefore an increase in γ_{n_e} would be expected to increase the mean angle of friction β. This result is in accordance with the findings of experimental work [18], where an increase in γ_{n_e} has been shown to result in an increase in β for a wide variety of work

materials. The general form of the rake face stress distributions shown in Fig. 2.22 have been observed experimentally from photoelastic measurements and using split-tool dynamometers [30]. These methods do not allow the stresses to be determined very close to cutting edge, but there is some evidence to indicate that the normal stress may be constant in the sticking region close to the cutting edge [30].

PROBLEMS

1. In an orthogonal cutting test on mild steel the following results were obtained:

    a_c = 0.25 mm $\qquad$ F_c = 900 N
    a_0 = 0.75 mm $\qquad$ F_t = 450 N
    a_w = 2.5 mm $\qquad$ γ_{n_e} = 0
    l_f = 0.5 mm

    Calculate
    a. The mean angle of friction on the tool face β
    b. The mean shear strength of the work material τ_s
    c. The mean frictional stress on the tool face τ_f

2. In an orthogonal cutting test the following conditions were noted:

    Width of chip (width of cut) = 2.5 mm
    Undeformed chip thickness = 0.25 mm
    Chip thickness = 1.0 mm
    Working normal rake = −5 deg
    Cutting force = 900 N
    Thrust force = 900 N

    Calculate
    a. The shear angle
    b. The mean shear strength of the work material

3. In an experimental turning operation where low-carbon steel was being machined using a carbide tool the following data were taken:

    Cutting force F_c = 1 kN
    Thrust force F_t = 0.5 kN
    Working normal rake γ_{n_e} = 20 deg
    Feed f = 0.141 mm
    Working major cutting-edge angle κ_r = 45 deg
    Depth of cut (back engagement) a_p = 5 mm
    Cutting speed v = 2 m/s
    Cutting ratio r_c = 0.2

Workpiece diameter d_w = 100 mm
Workpiece machined length l_w = 300 mm

Estimate from the data given:
a. The specific cutting energy of the work material p_s
b. The power required for machining P_m
c. The undeformed chip thickness a_c
d. The width of cut a_w
e. The shear angle ϕ
f. The mean angle of friction on the tool face β
g. The time taken to complete the machining operation

4. Show that in metal cutting when the working normal rake is zero, the ratio of the shear strength of the work material τ_s to the specific cutting energy p_s is given by

$$\frac{\tau_s}{p_s} = \frac{(1 - \mu r_c)r_c}{1 + r_c^2}.$$

where μ is the coefficient of chip–tool friction and r_c is the cutting ratio.

5. In an orthogonal machining operation with a rake angle of 5 deg and an undeformed chip thickness of 1 mm, the chip thickness is found to be 3 mm. What will the chip thickness be if the rake angle is increased to 15 deg assuming Ernst and Merchant's first theory holds, that is,

$$2\phi + \beta - \gamma_{n_e} = \pi/2$$

Assume the friction coefficient is not influenced by changes in rake angle.

6. Derive an expression for the specific cutting energy p_s in terms of the shear angle ϕ and the mean shear strength of the work material τ_s in orthogonal cutting. Assume that the shear-angle relationship of Ernst and Merchant applies, that is,

$$2\phi + \beta - \gamma_{n_e} = \pi/2$$

7. Assuming that the shear angle theory of Lee and Shaffer applies, namely,

$$\phi + \beta - \gamma_{n_e} = \pi/4$$

Show that the specific cutting energy p_s will be given by

$$p_s = \tau_s(1 + \cot \phi)$$

where τ_s is the mean shear strength of the work mateiral.

8. For the orthogonal cutting of a particular work material, it is found that the length of chip-tool contact is always equal to the chip thickness a_0 and that the mean shear stress at the chip-tool interface is equal to the mean shear stress on the shear plane. Show that, under these circumstances, the mean coefficient of friction on the tool face μ must be equal to or less than 4/3 and that when it is equal to unity, the shear angle ϕ is equal to the working normal rake γ_{n_e}.

9. In cutting experiments using a sharp tool with zero rake, it was found that the chip-tool contact length was equal to the chip thickness a_0. It was also found that the shear stress along the tool face was constant and was a constant proportion R of the shear strength of the work material on the shear plane.

   a. Derive an expression for the cutting force F_c in terms of a_c, a_w, τ_s, R, and ϕ.

   b. Differentiate the expression to obtain the value of ϕ to give minimum F_c.

10. Assume that in an orthogonal cutting operation, the frictional force F_f on the tool face is given by $K\tau_s A_0$ where K is a constant, τ_s is the apparent shear strength of the work material, and A_0 is the cross-sectional area of the chip. Show that the following relationship exists between the mean coefficient of friction μ on the tool face, the shear angle ϕ, and the working normal rake γ_{n_e}

$$\mu = \frac{K \cos^2(\phi - \gamma_{n_e})}{K \sin(\phi - \gamma_{n_e}) \cos(\phi - \gamma_{n_e}) + 1}$$

11. For the machining of a particular work material it is found that the shear angle ϕ is always equal to the working normal rake γ_{n_e}. Assuming that the shear strength of the work material in the sticking-friction region on the tool face is the same as the shear strength τ_s of the material on the shear plane and that the length of the sticking region is equal to the chip thickness a_0, derive expressions for the cutting force F_c and the thrust force F_t in terms of τ_s, γ_{n_e}, and the cross-sectional area of the uncut chip A_c. Also, calculate the value of γ_{n_e} for which F_t would be zero. Neglect the forces in the sliding-friction region on the tool face.

12. In machining tests it was found that for a particular material, the following relation applied

$$2\phi + \beta - \gamma_{n_e} = \pi/2$$

Also, when the rake angle γ_{n_e} was 20 deg, the coefficient of friction was 1.2.

a. What would the chip thickness be if in a turning operation, the feed was 0.15 mm and the major cutting-edge angle was 60 deg?

b. If the cutting force is limited to 3 kN and the specific cutting energy of the work material is 2 GJ/m^3, what maximum depth of cut can be taken?

13. Assuming that in orthogonal machining the distribution of normal stress along the tool rake face is linear, becoming maximum at the cutting edge and reducing to zero at the end of the chip–tool contact length, derive an expression for the mean coefficient of friction μ between the chip and tool in terms of: the maximum normal stress σ_m, the normal stress σ_0 at which real and apparent areas of contact become equal, and the coefficient of friction in sliding region μ_s.

REFERENCES

1. Finnie, I.: Review of the metal cutting analyses of the past hundred years, *Mech. Eng.,* vol. 78, no. 8, p. 715, 1956.
2. Cocquilhat, M.: Experiences sur la resistance utile produite dans le forage, *Ann. Trav. Publ. en Belgique,* vol. 10, p. 199, 1851.
3. Hartig, E.: Versuche uber Leistung und Arbeitsverbrauch der Werkzeng-maschine, 1873.
4. Time, I.: Soprotivlenie Metallov i Dereva Rezaniju, St. Petersburg, 1870.
5. Tresca, H.: Memoire sur le rabotage des metaux, *Bull. Soc. d'Encouragement pour l'Industrie Nationale,* pp. 585, 685, 1873.
6. Mallock, A.: The action of cutting tools, *Proc. Roy. Soc. Lond.,* vol. 33, p. 127, 1881–1882.
7. Reuleaux, F.: Uber den Taylor Whiteschen Werkzengstahl, in Verein zur Beforderung des Gewerbefleisses in Preussen, *Sitzungsberichte,* vol. 79, p. 179, 1900.
8. Taylor, F. W.: On the art of cutting metals, *Trans. ASME,* vol. 28, p. 31, 1906.
9. Ernst, H., and M. E. Merchant: Chip formation, friction and high quality machined surfaces, in *Surface Treatment of Metals,* Vol. 29. American Society of Metals, New York, 1941, p. 299.
10. Wallace, P. W.: An Investigation on the Friction Between Chip and Tool in Metal Cutting, fellowship thesis, Department of Mechanical Engineering, University of Salford, England, 1962.
11. Trent, E. M.: *Metal Cutting,* 2nd ed., Butterworths, London 1984.

12. Stevenson, M. G., and P. L. B. Oxley: An experimental investigation of the influence of speed and scale on the strain-rate in a zone of intense plastic deformation, *Proc. Inst. Mech. Eng.*, vol. 184, p. 561, 1970.

13. Toups, R. M.: An Analysis of the Natural Sharpness Radius of Cutting Tools, Master's thesis, Department of Mechanical Engineering, Georgia Institute of Technology, Atlanta, September, 1961.

14. Dewhurst, P.: On the non-uniqueness of the machining process, *Proc. Roy. Soc. Lond.*, vol. A360, p. 587, 1978.

15. Wallace, P. W., and G. Boothroyd: Tool forces and tool-chip friction in orthogonal machining, *J. Mech. Eng. Sci.*, vol. 6, no. 1, p. 74, 1964.

16. Merchant, M. E.: Mechanics of the metal cutting process, *J. Appl. Phys.*, vol. 16, no. 5, p. 267, and no. 6, p. 318, 1945.

17. Bridgman, P. W.: *Phys. Rev.*, vol. 48, p. 825, 1935; *Proc. Amer. Acad. Arts Sci.*, vol. 71, p. 386, 1937; *J. Appl. Phys.*, vol. 8, no. 5, p. 328, 1937; *J. Appl. Phys.*, vol. 14, no. 6, p. 273, 1943; *The Physics of High Pressure*, G. Bell & Sons, Ltd., London, 1949.

18. Lee, E. H., and B. W. Shaffer: The theory of plasticity applied to a problem of machining, *J. Appl. Mech.*, vol. 18, no. 4, p. 405, 1951.

19. Pugh, H. D.: Mechanics of the cutting process, *Proc. IME Conf. Tech. Eng. Manufacture*, London, 1958, p. 237.

20. Palmer, W. B., and P. L. B. Oxley: Mechanics of orthogonal machining, *Proc. IME*, vol. 173, p. 623, 1959.

21. Nakayama, K.: Studies on the Mechanism of Metal Cutting, *Bull. Fac. Eng. Yokohama Nat. Univ. (Japan)* vol. 7, p. 1, 1958.

22. Fenton, R. G., and Oxley, P. L. B.: Mechanics of orthogonal machining: Predicting chip geometry and cutting forces from work-material properties and cutting conditions, *Proc. Inst. Mech. Eng.*, vol. 184, p. 927, 1970.

23. Amontons: Histoire de l'Academie Royale des Sciences avec les Memoires de Mathematique et de Physique, 1969.

24. Coulomb, C. A.: Memoires de Mathematique et de Physique de l'Academie Royale des Sciences, Paris, 1785.

25. Bowden, F. P., and D. Tabor: *Friction and Lubrication of Solids*, Oxford University Press, London, 1954.

26. Zorev, N. N.: Interrelation between Shear Processes Occurring Along Tool Face and on Shear Plane in Metal Cutting, International Research in Product Engineering, 1963, p. 42 (presented at the International Product Engineering Research Conference, Pittsburgh, Pa., 1963).

27. Doyle, E. D., et al: Frictional interaction in continuous chip formation, *Proc. Roy. Soc. Lond.*, vol. A366, p. 173, 1979.

28. Wright, P. K.: Frictional interactions in machining: Comparison between transparent sapphire and steel cutting, *J. Metals Technol.*, vol. 8, p. 150, 1981.

29. Amini, E.: Photo elastic analysis of stresses and forces in steady cutting, *J. Strain Analysis*, vol. 3, p. 206, 1968.

30. Barrow, G., et al: Determination of rake face stress distribution in orthogonal machining, *Int. J. Mach. Tool Dev. Res.*, vol. 22, p. 25, 1982.

3
Temperatures in Metal Cutting

During the cutting of metal, high temperatures are generated in the region of the tool cutting edge, and these temperatures have a controlling influence on the rate of wear of the cutting tool and on the friction between the chip and tool. Because of the effect on tool wear, considerable attention has been paid in the past to the determination of the temperatures in the tool, chip, and workpiece in metal cutting.

3.1   HEAT GENERATION IN METAL CUTTING

It has been stated earlier that the rate of energy consumption during machining P_m is given by

$$P_m = F_c v \tag{3.1}$$

where F_c is the cutting component of the resultant tool force and v is the cutting speed.

When a material is deformed elastically, the energy required for the operation is stored in the material as strain energy, and no heat is generated. However, when a material is deformed plastically, most of the energy used is converted into heat. In metal cutting the material is subjec-

109

ted to extremely high strains, and the elastic deformation forms a very small proportion of the total deformation; therefore it may be assumed that all the energy is converted into heat.

Conversion of energy into heat occurs in the two principal regions of plastic deformation (Fig. 3.1): the shear zone, or primary deformation zone, AB and the secondary deformation zone BC. If, as in most practical circumstances, the cutting tool is not perfectly sharp, a third heat source BD would be present owing to friction between the tool and the new workpiece surface. However, unless the tool is severely worn, this heat source would be small and is neglected in the present analysis. Thus,

$$P_m = P_s + P_f \tag{3.2}$$

where P_s is the rate of heat generation in the primary deformation zone (shear-zone heat rate) and P_f is the rate of heat generation in the secondary deformation zone (frictional heat rate).

P_f is given by $F_f v_0$ where F_f is the frictional force on the tool face and v_0 is the velocity of chip flow, which is given by $v r_c$. Thus, if P_f and P_m are known, P_s may be obtained from Eq. (3.2).

To understand how heat is removed from these zones by the workpiece, chip, and tool materials it is first necessary to consider the transfer of heat in a material moving relative to a heat source.

3.2   HEAT TRANSFER IN A MOVING MATERIAL

Consider the element $ABCD$ (Fig. 3.2), which has unit thickness and through which the material flows in the x direction. The point A has coor-
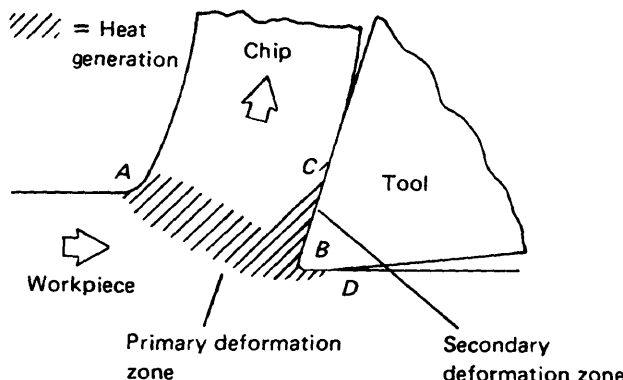

**Figure 3.1**   Generation of heat in orthogonal cutting.

$B(x, y + \delta y)$ $C(x + \delta x, y + \delta y)$

$\left[\theta + \dfrac{\partial\theta}{\partial y}\, \delta y\right]$ $\left[\theta + \dfrac{\partial\theta}{\partial y}\, \delta y + \dfrac{\partial\theta}{\partial x}\, \delta x\right]$

δy

Velocity of material v

δx $D(x + \delta x, y)$

$A(x, y)$
$[\theta]$

$\left[\theta + \dfrac{\partial\theta}{\partial x}\, \delta x\right]$
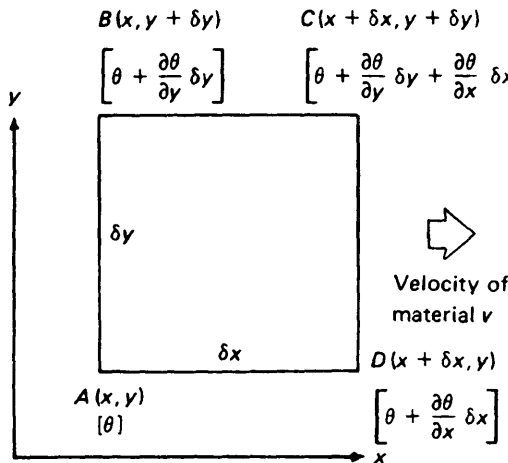
Figure 3.2   Element through which heated material flows.

dinates x, y, and the material at this point is assumed to have an instantaneous temperature θ. Coordinates and temperatures at points B, C, and D are shown in Fig. 3.2.

Heat is transferred across the boundaries AB and CD by conduction because of the temperature gradients in the x direction and by transportation because of the flow of heated material across these boundaries. Across BC and AD, heat can only be transferred by conduction because there is no flow of material across these boundaries. It can be shown that if the net heat flow into the element is zero (no heating within the element), then

$$\frac{\partial^2\theta}{\partial y^2} + \frac{\partial^2\theta}{\partial x^2} - \frac{R}{a}\frac{\partial\theta}{\partial x} = 0 \tag{3.3}$$

where R is given by $\rho c v a/k$ and is known as the thermal number and where

k = thermal conductivity
c = specific heat capacity
ρ = density
v = velocity of the material relative to the heat source

In metal cutting the thermal number is taken to be $\rho c v a_c/k$, where v is the cutting speed and a_c is the undeformed chip thickness.

The solution of Eq. (3.3) is possible for only the simplest boundary conditions. It is useful to consider the solution of this equation for a one-dimensional case, and this one-dimensional case is depicted in Fig. 3.3 for a metal moving at high speed. Here it is seen that a point in the material approaching the heat source is heated very rapidly, reaches its maximum temperature at the heat source, and then remains at constant temperature. With this result in mind temperature distribution in metal cutting will now be considered.

3.3   TEMPERATURE DISTRIBUTION IN METAL CUTTING

Figure 3.4 shows the experimentally determined temperature distribution in the workpiece and the chip during orthogonal metal cutting [1]. As a point X in the material, which is moving toward the cutting tool, approaches and passes through the primary deformation zone, it is heated until it leaves the zone and is carried away within the chip. Point Y, however, passes through both deformation zones, and it is heated until it has left the region of secondary deformation. It is then cooled as the heat is conducted into the body of the chip, and eventually the chip achieves a uniform temperature throughout. Thus the maximum temperature occurs along the tool face some distance from the cutting edge. Point Z, which remains in the workpiece, is heated by the conduction of heat from the primary deformation zone. Some heat is conducted from the secondary deformation zone into the body of the tool. Thus,
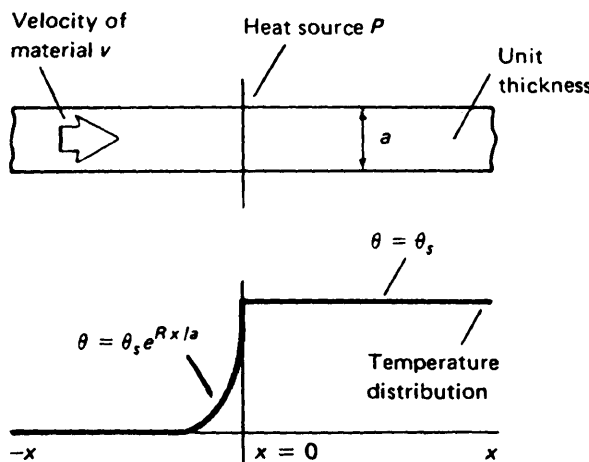

Figure 3.3   Temperature distribution in a fast-moving material for a one-dimensional case, where $\theta_s = P/\rho c v a$.
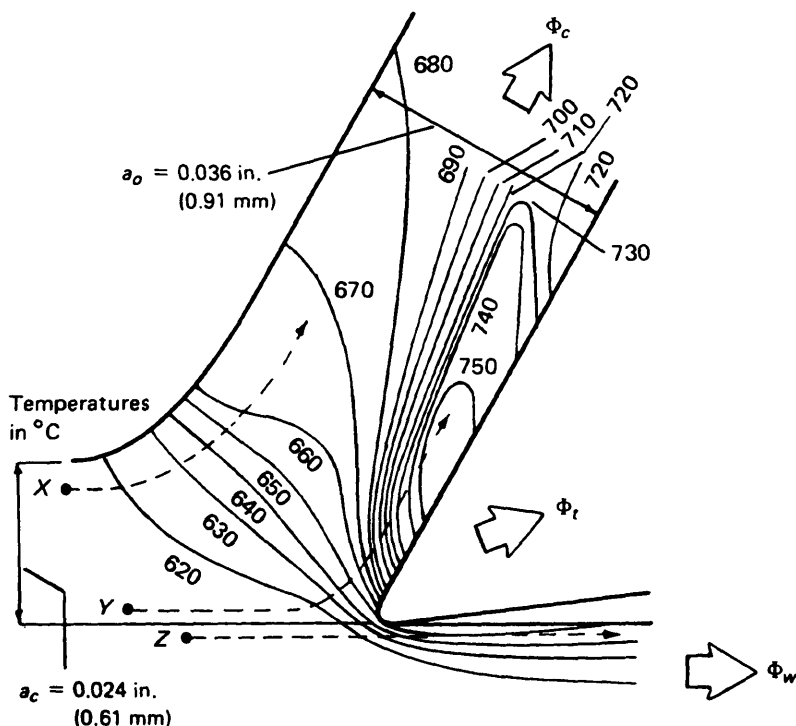
Figure 3.4 Temperature distribution in workpiece and chip during orthogonal cutting (obtained from an infrared photograph) for free-cutting mild steel where the cutting speed is 75 ft/min (0.38 m/s), the width of cut is 0.25 in. (6.35 mm), the working normal rake is 30 deg, and the workpiece temperature is 611°C. (After Boothroyd [1].)

$$P_m = \Phi_c + \Phi_w + \Phi_t \qquad\qquad (3.4)$$

where

P_m = total rate of heat generation

Φ_c = rate of heat transportation by the chip

Φ_w = rate of heat conduction into the workpiece

Φ_t = rate of heat conduction into the tool

Because the chip material near the tool face is flowing rapidly, it has a much greater capacity for the removal of heat than the tool. For this reason Φ_t usually forms a very small proportion of P_m and may be neglected except at very low cutting speeds.

3.3.1 Temperatures in the Primary Deformation Zone

The rate of heat generation in the primary deformation zone is P_s, and a fraction of this heat, Γ, is conducted into the workpiece; the remainder, $[1 - \Gamma]P_s$, is transported with the chip. Thus, the average temperature rise θ_s of the material passing through the primary deformation zone is given by

$$\theta_s = \frac{(1 - \Gamma)P_s}{\rho c v a_c a_w} \tag{3.5}$$

where a_w is the width of the chip.

Equation (3.5) shows that if Γ is known for a given set of cutting conditions, θ_s may be determined.

Several theoretical analyses of the temperatures in the workpiece and shear zone have been carried out, two of the more successful being those of Weiner [2] and Rapier [3]. Figure 3.5 shows the idealized model of the cutting process employed; it was assumed that the primary deformation zone could be regarded as a plane heat source of uniform strength, that no heat was lost from the free surfaces of the workpiece and chip, and that the thermal properties of the work material were constant and independent of temperature. The problem was to solve Eq. (3.3), the basic heat transfer
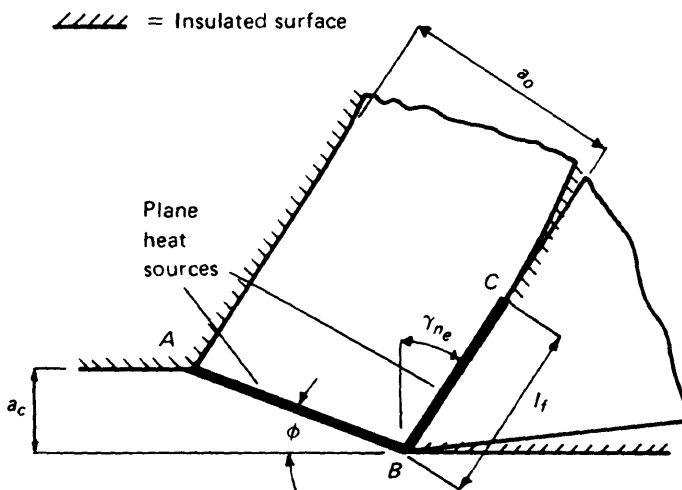

Figure 3.5 Idealized model of cutting process employed in theoretical work on cutting temperatures.

equation, within the boundaries of the workpiece. An exact solution to this problem was not found possible and further assumptions were necessary. The most useful suggestion was made by Weiner [2], who assumed that no heat was conducted in the material in the direction of its motion. This assumption was shown to be justified in metal cutting because at high speeds the transfer of heat in the direction of motion is mainly by transportation, and the conduction term can be neglected. This means that Eq. (3.3) can be rewritten as

$$\frac{\partial^2 \theta}{\partial y^2} - \frac{R}{a} \frac{\partial \theta}{\partial x} = 0 \qquad (3.6)$$

Weiner was able to solve Eq. (3.6) within the stipulated boundary conditions for the workpiece, and he produced an equation expressing Γ (the proportion of P_s conducted into the workpiece) as a unique function of R tan ϕ (where ϕ is the shear angle). This theoretical relationship between Γ and R tan ϕ is compared with experimental data in Fig. 3.6, where it is seen that the theory has slightly underestimated results at high values of R tan ϕ (i.e., at high speeds and feeds). In the theory where a plane heat source was assumed, heat can only flow into the workpiece by conduction, whereas in
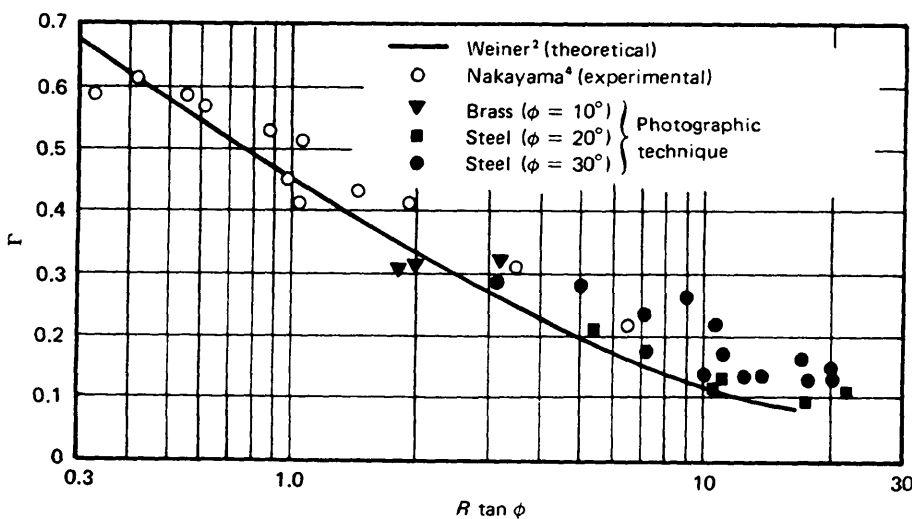

Figure 3.6 Effect of R tan ϕ on division of shear-zone heat between chip and workpiece, where Γ = the proportion of shear zone heat conducted into the workpiece, R = thermal number, and ϕ = shear angle. (After Boothroyd [1].)

reality heat is generated over a wide zone, part of which extends into the workpiece. The effect of this wide heat generation zone becomes increasingly important at high speeds and feeds and explains the slight disagreement between theory and experiment at high values of $R \tan \phi$.

3.3.2   Temperatures in the Secondary Deformation Zone

The maximum temperature in the chip occurs where the material leaves the secondary deformation zone (point C, Fig. 3.1) and is given by

$$\theta_{max} = \theta_m + \theta_s + \theta_0 \tag{3.7}$$

where

> θ_m = temperature rise of the material passing through the secondary deformation zone
> θ_s = temperature rise of the material passing through the primary deformation zone [given by Eq. (3.5)]
> θ_0 = initial workpiece temperature

In an analysis of the chip temperatures Rapier [3] assumed that the heat source resulting from friction between the chip and tool was a plane heat source of uniform strength (Fig. 3.5) and was able to solve Eq. (3.6) within the boundary conditions shown. The following expression was obtained:

$$\frac{\theta_m}{\theta_f} = 1.13 \sqrt{\frac{R}{l_0}} \tag{3.8}$$

where

> θ_m = maximum temperature rise in the chip owing to the frictional heat source in the secondary deformation zone
> l_0 = length of the heat source divided by the chip thickness (l_f/a_0)
> R = thermal number

The average temperature rise of the chip resulting from the secondary deformation θ_f (frictional heat source) is given by

$$\theta_f = \frac{P_f}{\rho c v a_c a_w} \tag{3.9}$$

A later comparison of Eq. (3.8) with experimental results [1] showed that Rapier's theory considerably overestimated θ_m, and it was suggested that this overestimation occurred because during cutting, the friction between the chip and tool causes severe deformation of the chip material and the resulting heat source extends some distance into the chip. The boundary conditions shown in Fig. 3.7 are thought to approximate more closely the real conditions, and an analysis based on this revised model [1] yielded results which agreed with experimental data. These results, shown in Fig. 3.8, indicate the effect of variations in the width of the uniformly distributed heat source. When these curves are used, l_0 can be estimated from the wear on the tool face, and the width of the heat source can be estimated from a photomicrograph of the chip cross section. A typical chip cross section is shown in Fig. 3.9; where the lines of maximum grain elongation are curved, it may be assumed that the material has passed through the secondary deformation zone.

3.3.3 Example

To illustrate the application of the theories and equations derived in this chapter a worked example is now presented. In this example the max-
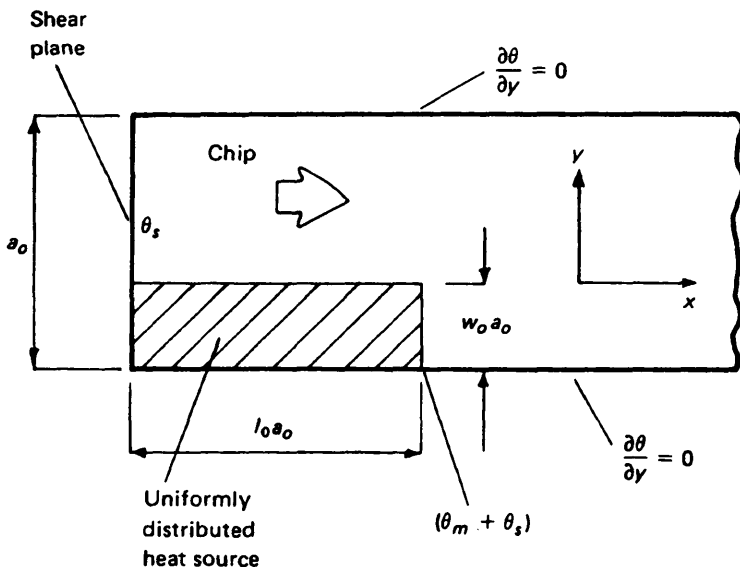

**Figure 3.7**   Revised boundary conditions for chip.
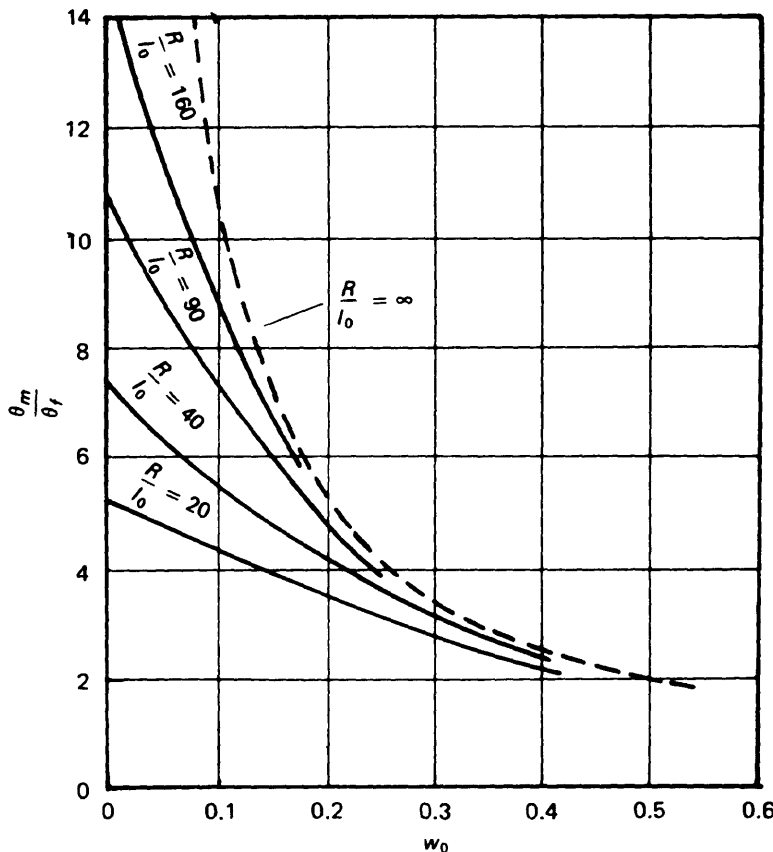
Figure 3.8 Effect of width of secondary deformation zone on chip temperatures, where R = thermal number, $l_0 a_0$ = chip-tool contact length, $w_0 a_0$ = width of secondary deformation zone, θ_m = maximum temperature rise in chip, and θ_f = mean temperature rise in chip. (After Boothroyd [1].)

imum temperature along the tool face is estimated for the following conditions during the orthogonal cutting of mild steel:

Working normal rake γ_{n_e} = 0
Cutting force F_c = 890 N (200 lbf)
Thrust force F_t = 667 N (150 lbf)
Cutting speed v = 2 m/s (394 ft/min)
Undeformed chip thickness a_c = 0.25 mm (0.009 8 in.)
With of cut a_w = 2.5 mm (0.098 in.)
Cutting ratio r_c = 0.3
Length of contact between chip and tool l_f = 0.75 mm (0.03 in.)
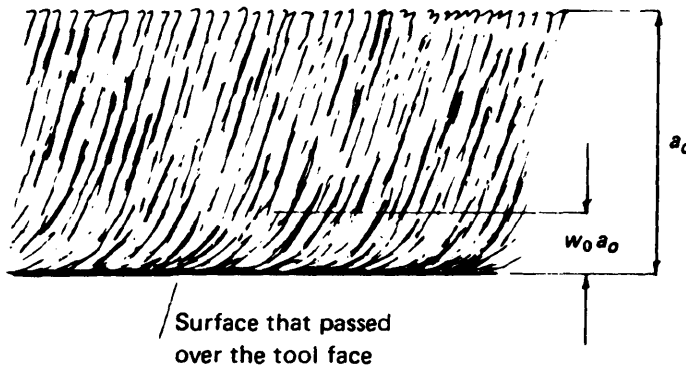
Figure 3.9   Grain deformation in chip cross section.

The total heat generation rate is given by Eq. (3.1). Thus,

$$P_m = F_c v = 890(2)$$

$$= 1780 \text{ J/s} \ (100 \text{ Btu/min})$$

The rate of heat generated by friction between the chip and tool is given by

$$P_f = F_f v_0 = F_f v r_c$$

In the present example γ_{ne} equals 0, and therefore F_f equals F_t. Thus,

$$P_f = F_t v r_c$$

$$= 667(2)(0.3)$$

$$= 400 \text{ J/s} \quad (22.7 \text{ Btu/min})$$

The rate of heat generation from shearing is given by Eq. (3.2). Thus,

$$P_s = P_m - P_f = 1380 \text{ J/s} \quad (77.3 \text{ Btu/min})$$

To estimate the temperature rise θ_s using Eq. (3.5) it is first necessary to obtain Γ from Fig. 3.6; to obtain Γ the value of $R \tan \phi$ is required.

The thermal number R is given by $\rho c v a_c / k$ and assuming that for mild steel ρ is 7200 kg/m³ (0.26 lb/in.³), k is 43.6 J/smK [302.6 Btu (in.)/ (h)(ft²)(°F)], and c is 502 J/kgK [0.12 Btu/(lb)(°F)]:

$$R = \frac{7200(502)(2)(0.00025)}{43.6} = 41.5$$

When the rake angle γ_{n_e} equals 0, tan ϕ equals r_c. Thus,

$R \tan \phi = 41.5(0.3) = 12.45$

The proportion of the shearing heat conducted into the workpiece is now obtained from Fig. 3.6. Thus,

$\Gamma = 0.1$

If the appropriate values are substituted into Eq. (3.5),

$$\theta_s = \frac{(1 - \Gamma)P_s}{\rho c v a_c a_w}$$

$$= (1 - 0.1)(1380)/(7200)(502)(2)(0.00025)(0.0025)$$

$$= 275°C (495°F)$$

This value (275°C, or 495°F) is the mean temperature rise in the primary deformation zone, and since it is a temperature difference, it can be expressed in either degrees Centigrade (°C) or kelvin (K).

The mean temperature rise of the chip from the secondary deformation zone (frictional heat source) is given by Eq. (3.9).

Thus, neglecting the heat conducted into the cutting tool,

$$\theta_f = \frac{400}{4.518} = 88.5°C (159.3°F)$$

To obtain the ratio θ_m/θ_f and hence θ_m from Fig. 3.8, it is necessary to estimate the values of w_0 and R/l_0.

The width of the secondary deformation zone divided by the chip thickness w_0 is assumed to be 0.2 for mild steel under unlubricated cutting conditions. Also,

$$l_0 = \frac{l_f r_c}{a_c} = \frac{0.75(0.3)}{0.25} = 0.9$$

Therefore,

$$R/l_0 = \frac{41.5}{0.9} = 46.1$$

The ratio θ_m/θ_f may now be obtained from Fig. 3.8; thus,

$$\theta_m = 4.2(88.5) = 372°C \ (670°F)$$

If it is assumed the workpiece is at a room temperature θ_0 of 22°C (72°F), the maximum temperature along the tool rake face is given by Eq. (3.7). Thus,

$$\theta_{max} = \theta_m + \theta_s + \theta_0$$
$$= 372 + 275 + 22$$
$$= 669°C \quad (1234°F)$$

It should be noted that in these calculations the thermal properties of the material are assumed to be constant and independent of temperature. With many engineering materials, however, the specific heat capacity and thermal conductivity vary considerably with changes in temperature. If more accurate predictions of tool temperatures are required, the relationships between the thermal properties of the material and temperature must be known and care taken to use the appropriate values in the calculations.

3.3.4   Effect of Cutting Speed on Temperatures

If the tool forces and the cutting ratio do not vary with changes in cutting speed, for the conditions used in the preceding example the relationships between temperature and cutting speed shown in Fig. 3.10 are obtained. Here it is seen that the mean shear-zone temperature θ_s increases slightly with increasing cutting speed and then tends to become constant, whereas the maximum tool face temperature ($\theta_m + \theta_s$) increases rapidly with increasing cutting speed.

3.4   THE MEASUREMENT OF CUTTING TEMPERATURES

A number of methods have been developed for the measurements of temperatures in metal cutting. Some of these methods only make it possible for the average cutting temperatures to be determined, but effective methods are available for determining temperature distributions in the workpiece, chip, and tool near the cutting edge.

3.4.1   Work-Tool Thermocouple

The technique most widely used to study cutting temperatures is the work-tool thermocouple technique. In this technique the emf generated at
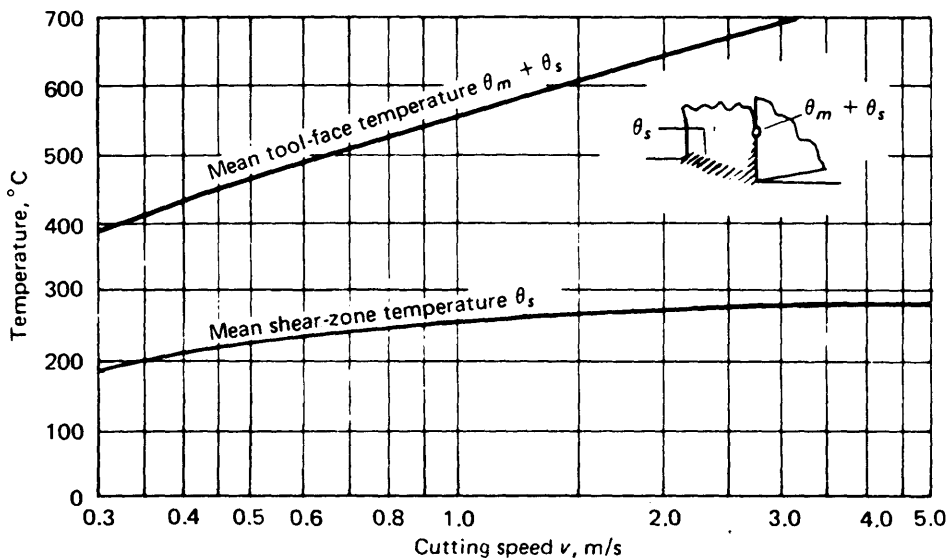
Figure 3.10 Effect of cutting speed on cutting temperatures (theoretical).

the junction between the workpiece and tool is taken as a measure of the temperatures in this region. A typical work–tool thermocouple arrangement on a lathe is shown in Fig. 3.11. It is important when using this technique to insulate the thermocouple circuit from the machine and to use the same circuit when calibrating the thermocouple. It may be assumed that the reading given by this method is an indication of the mean temperature along the chip–tool interface. This technique has been used extensively in the past to investigate the effects of changes in cutting conditions on cutting temperatures and to obtain empirical relationships between temperature and cutting-tool wear rate. However, the work–tool thermocouple method is limited because it gives no indication of the distribution of temperature along the tool rake face.

There are a number of sources of error in using the work–tool thermocouple. In particular, the tool and work materials are not ideal elements for a thermocouple. Consequently, the emf tends to be low and the emf/temperature calibration nonlinear. The work–tool thermocouple must be calibrated against a standard thermocouple. Each tool and workpiece material combination must be calibrated separately. In addition, it is unlikely that the emf determined with a stationary tool, used for
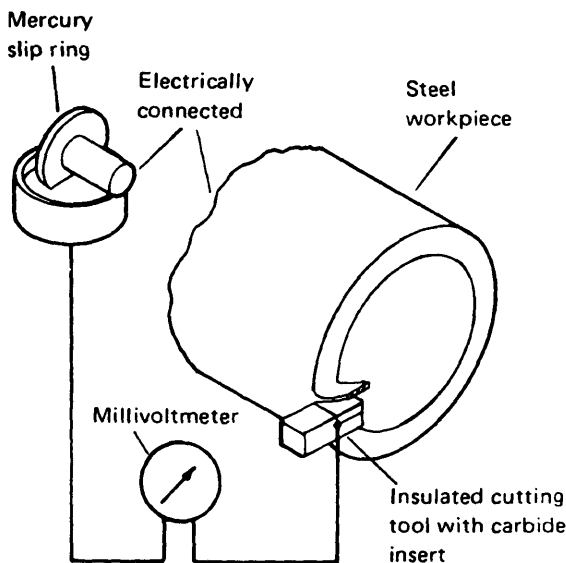
Figure 3.11   Work-tool thermocouple circuit.

calibration, is the same as that obtained for an equivalent temperature during cutting when the work material is being severely strained.

3.4.2   Direct Thermocouple Measurements

Direct thermocouple measurements can be made during cutting. The results shown in Fig. 3.6 were obtained [4] using the thermocouple technique illustrated in Fig. 3.12. In these experiments the rig was first run without cutting, and the reading on the millivoltmeter resulting from the rubbing action of the constantan wire on the workpiece was noted.

This reading was subsequently subtracted from the readings taken while cutting was in progress. With this method, the temperatures at selected points around the end face of the tubular workpiece were measured and then used to calculate the proportion of the shear-zone heat conducted into the workpiece.

Direct measurement can be made by making a hole in the tool close to the cutting edge and inserting a thermocouple to measure the temperature at a particular position. This can then be repeated with holes in various positions to give an estimate of the temperature distributions. Significant errors may occur where the temperature gradients are steep, as the holes for the thermocouples may cover a considerable range of temperature.
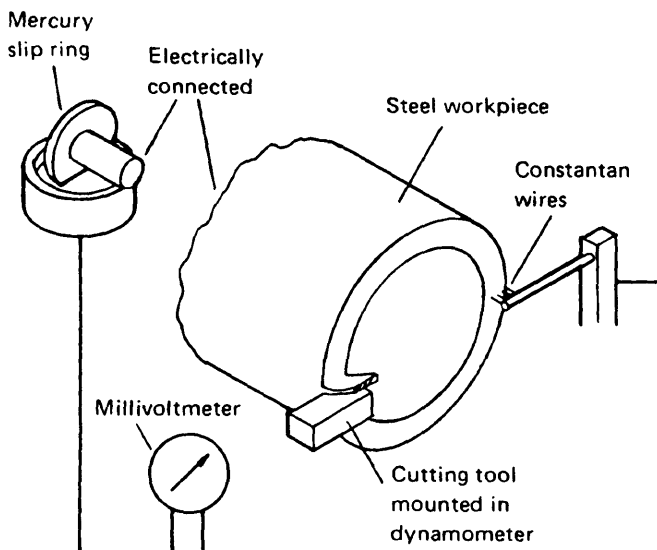
Figure 3.12 Arrangement for measurement of workpiece temperatures using the thermocouple technique. (After Nakayama [4].)

3.4.3 Radiation Methods

When the tool–workpiece area can be observed directly, cameras and film sensitive to infrared radiation can be used to determine temperature distributions. The result shown in Fig. 3.4 was obtained from an infrared photograph of the cutting operation [1]. In the technique used to produce this result a furnace of known temperature distribution was photographed simultaneously with the cutting operation using an infrared-sensitive plate, enabling the optical density of the plate to be calibrated against temperature. Some of the experimental results are shown in Fig. 3.6 and experimental confirmation of the curves in Fig. 3.8 were obtained by this method.

For the result shown in Fig. 3.4 the workpiece was preheated because of the relatively low sensitivity of the infrared photographic plates available at that time. Improvements in infrared-sensitive films and development of thermal imaging video cameras now make it possible to determine temperature distributions for workpieces at room temperature.

3.4.4 Hardness and Microstructure Changes in Steel Tools

The room-temperature hardness of hardened steel decreases after reheating and the loss in hardness is related to the temperature and time of heat-

ing. The hardness decrease is the result of changes in the microstructure of the steel. These structural changes can be observed using optical and electron microscopes. These changes provide an effective means of determining temperature distributions in the tool during cutting. Microhardness measurements on tools after cutting can be used to determine constant-temperature contours in the tool [5], but the technique is time-consuming and requires very accurate hardness measurements.

The structural changes in the material take place gradually, but it has been observed that for some high-speed steels distinct modifications occur at approximately 50°C intervals between 600 and 900°C [6]. This permits temperature measurements with an accuracy of +/−25°C within the heat-affected region. Metallographic examination of the tool after cutting makes it possible for temperature distributions in the tool to be determined, but requires experienced interpretation of the observed structural changes. This method has been used to study temperature distributions in high-speed steel lathe tools and drills [6–8]. The main limitations of this method of temperature estimation is that it can be used only within the range of cutting conditions suitable for high-speed steel and when relatively high temperatures are generated.

PROBLEMS

1. If, when machining at high cutting speeds, the heat conducted into the cutting tool becomes negligible and the heat conducted into the workpiece is 4 percent of the total heat generated, derive an expression for the final chip temperature θ in terms of the
   a. Specific cutting energy p_s
   b. Specific heat capacity of the work material c
   c. Density of the work material ρ
2. a. Show that when cutting metal orthogonally with a tool of zero rake angle, the rate of heat generation P_s in the shear zone is given by

   $$P_s = F_c v(1 - \mu r_c)$$

   where

   F_c = cutting force
   v = cutting speed
   μ = mean coefficient of friction on the tool face
   r_c = cutting ratio

   b. For the same conditions, calculate the mean shear-zone tempera-

ture rise θ, when the metal has a specific cutting energy of 2.8 GN/m^2, $\mu = 1.0$, $r_c = 0.2$, and 10 percent of the shear-zone heat is conducted into the workpiece. Assume for the work material that $\rho = 7200$ kg/m^3 and $c = 500$ J/kgK.

  c. What would be the value of θ, if the cutting speed were doubled and the proportion of shear-zone heat conducted into the workpiece remained the same?

3. During some machining experiments, it was found that for the range of conditions studied, the following assumptions could be made:

  a. The heat conducted into the cutting tool was negligible.

  b. The proportion of the heat generated in the shear zone conducted into the workpiece was 0.2.

  c. The maximum temperature rise in the chip due to the frictional heat source θ_m followed the relation

$$\theta_m = \theta_f \sqrt{R}$$

  where θ_f is the mean temperature rise of the chip due to the frictional heat source and R is the thermal number.

  d. The heat generated due to friction was equal to 20 percent of the heat generated in the shear zone.

  Derive an expression for the maximum temperature in the chip above the initial workpiece temperature in terms of the specific cutting energy of the workpiece p_s, the specific heat c, and density ρ of the workpiece and the thermal number R.

4. It was found from experiments where the chips produced during shaping were caught in a calorimeter that the mean chip-temperature rise was 500°C. The cutting conditions were as follows:

Cutting speed = 1 m/s
Undeformed chip thickness = 0.5 mm
Width of chip = 5 mm
Working normal rake = 45 deg
Cutting force = 6000 N
Thrust force = 0
Chip thickness = 1.2 mm
Length of workpiece = 300 mm

After 100 strokes of the shaper, the insulated workpiece was immersed in a calorimeter and its additional heat content found to be 30 kJ. Neglecting the heat conducted into the cutting tool, calculate the proportion of the shear-zone heat conducted into the workpiece.

REFERENCES

1. Boothroyd, G.: Temperatures in orthogonal metal cutting, *Proc. IME,* vol. 177, p. 789, 1963.
2. Weiner, J. H.: Shear plane temperature distribution in orthogonal cutting, *Trans. ASME,* vol. 77, no. 8, p. 1331, 1955.
3. Rapier, A. C.: A theoretical investigation of the temperature distribution in the metal cutting process, *Br. J. Appl. Phys.,* vol. 5, no. 11, p. 400, 1954.
4. Nakayama, K.: Temperature rise of workpiece during metal cutting, *Bull. Fac. Eng. Yokohama Nat. Univ. (Japan),* vol. 5, no. 1, 1956.
5. Trent, E. M.: *Metal Cutting,* 2nd ed., Butterworth, London, 1986.
6. Wright, P. K., and E. M. Trent: Metallographic methods of determining temperature gradients in cutting tools, JISI, vol. 211, p. 364, 1973.
7. Mills, B., D. W. Wakeman, and A. Aboukhushaba: A new technique for determining the temperature distribution in high-speed steel cutting tools using scanning electron microscopy, *Ann. CIRP,* vol. 29, p. 73, 1980.
8. Mills, B., and T. D. Mattishaw: The application of scanning electron microscopy to the study of temperatures and temperature distributions in M2 high-speed-steel twist drills, *Ann. CIRP,* vol. 30, p. 15, 1981.

4
Tool Life and Tool Wear

4.1   INTRODUCTION

Cutting-tool life is one of the most important economic considerations in metal cutting. In roughing operations the various tool angles, cutting speeds, and feed rates are usually chosen to give an economical tool life. Conditions giving a very short tool life are uneconomical because tool-grinding and tool replacement costs are high. On the other hand, the use of very low speeds and feeds to give long tool life is uneconomical because of the low production rate. Clearly, any tool or work material improvements that increase tool life will be beneficial. To form a basis for such improvements much effort has been made to understand the nature of tool wear and other forms of tool failure.

The life of a cutting tool can be brought to an end in various ways, but these ways may be separated into two main groups:

1.   The gradual or progressive wearing away of certain regions of the face and flank of the cutting tool
2.   Failures bringing the life of the tool to a premature end

4.2 PROGRESSIVE TOOL WEAR

The fundamental nature of the mechanism of wear can be very different under different conditions. In metal cutting, three main forms of wear are known to occur: adhesion, abrasion, and diffusion wear.

In adhesion wear [1], the wear is caused by the fracture of welded asperity junctions between the two metals. In metal cutting, junctions between the chip and tool materials are formed as part of the friction mechanism; when these junctions are fractured, small fragments of tool material can be torn out and carried away on the underside of the chip or on the new workpiece surface. The conditions that exist in metal cutting are well suited to adhesive wear as new material surfaces uncontaminated with oxide films are continually produced, and this facilitates the formation of welded asperity junctions.

The form of wear known as abrasion wear occurs when hard particles on the underside of the chip pass over the tool face and remove tool material by mechanical action. These hard particles may be highly strain-hardened fragments of an unstable built-up edge, fragments of the hard tool material removed by adhesion wear, or hard constituents in the word material.

Solid-state diffusion occurs when atoms in a metallic crystal lattice move from a region of high atomic concentration to one of low concentration. This process is dependent on the existing temperature, and the rate of diffusion increases exponentially with increases in temperature. In metal cutting, where intimate contact between the work and tool materials occurs and high temperatures exist, diffusion can occur where atoms move from the tool material to the work material. This process, which takes place within a very narrow reaction zone at the interface between the two materials and causes a weakening of the surface structure of the tool, is known as diffusion wear.

4.3 FORMS OF WEAR IN METAL CUTTING

The progressive wear of a tool takes place in two distinct ways (Fig. 4.1):

1. Wear on the tool face characterized by the formation of a crater and resulting from the action of the chip flowing along the face
2. Wear on the flank where a wear land is formed from the rubbing action of the newly generated workpiece surface

4.3.1 Crater Wear

The crater formed on the tool face conforms to the shape of the chip underside and is restricted to the chip–tool contact area (Fig. 4.1). In addi-
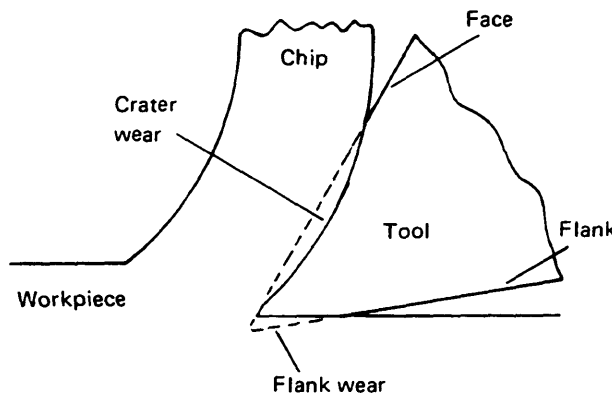
Figure 4.1 Regions of tool wear in metal cutting.

tion, the region adjacent to the cutting edge where sticking friction or a built-up edge occurs is subjected to relatively slight wear.

It was seen in Chap. 3 that in metal cutting, the highest temperatures occur some distance along the tool face; at high cutting speeds these temperatures can easily reach the order of 1000°C. Under these high-temperature conditions high-speed steel tools wear very rapidly because of thermal softening of the tool material. Although carbide-tool materials retain their hardness at these high temperatures, solid-state diffusion can cause rapid wear.

In experimental work the maximum depth of the crater is usually a measure of the amount of crater wear and can be determined by a surface-measuring instrument.

Under very-high-speed cutting conditions, crater wear is often the factor that determines the life of the cutting tool: the cratering becomes so severe that the tool edge is weakened and eventually fractures. However, when tools are used under economical conditions, the wear of the tool on its flank, known as flank wear, is usually the controlling factor.

4.3.2   Flank Wear

Wear on the flank of a cutting tool is caused by friction between the newly machined workpiece surface and the contact area on the tool flank. Because of the rigidity of the workpiece, the worn area, referred to as the flank wear land, must be parallel to the resultant cutting direction. The width of the wear land is usually taken as a measure of the amount of wear and can be readily determined by means of a toolmaker's microscope.

Figure 4.2 shows a typical graph of the progress of flank wear land
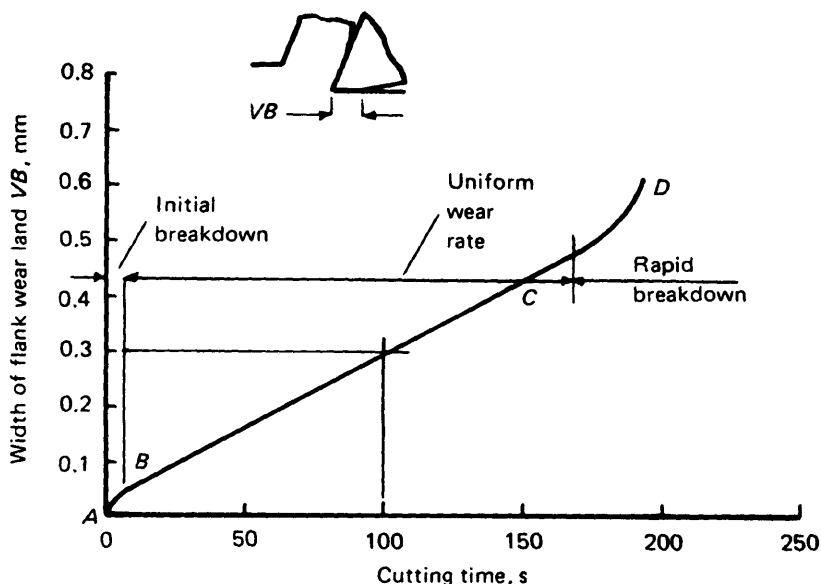
Figure 4.2 Development of flank wear with time for a carbide tool at a cutting speed of 1 m/s.

width *VB* with time or distance cut. The curve can be divided into three regions:

1. The region *AB* where the sharp cutting edge is quickly broken down and a finite wear land is established
2. The region *BC* where wear progresses at a uniform rate
3. The region *CD* where wear occurs at a gradually increasing rate

Region *CD* is thought to indicate the region where the wear of the cutting tool has become sensitive to the increased tool temperatures caused by the presence of a wear land of such large proportions. Clearly, in practice, it would be advisable to regrind the tool before the flank wear enters the last region (region *CD* in Fig. 4.2) where rapid breakdown occurs.

4.3.3 Tool-Life Criteria

A tool-life criterion is defined as a predetermined threshold value of a tool-wear measure or the occurrence of a phenomenon. In practical machining operations the wear of the face and flank of the cutting tool is not uniform along the active cutting edge; therefore it is necessary to specify the locations and degree of the wear when deciding on the amount

of wear allowable before regrinding the tool. Figure 4.3 shows a typical worn single-point tool. As shown in the figure, the amount of cratering varies along the active cutting edge, and the crater depth KT is measured at the deepest point of the crater (section A-A). It can be seen that flank wear is usually greatest at the extremities of the active cutting edge. Conditions at the tool corner tend to be more severe than those in the central part of the active cutting edge because of the complicated flow of chip material in that region. The width of the flank wear land at the tool corner (zone C) is designated VC. At the opposite end of the active cutting edge (zone N) a groove or wear notch often forms, because in this region the work material tends to be work-hardened from the previous processing operation. The width of the wear land at the wear notch is designated VN.

In the central portion of the active cutting edge (zone B), the wear land is usually fairly uniform. However, to allow for variations that may occur,
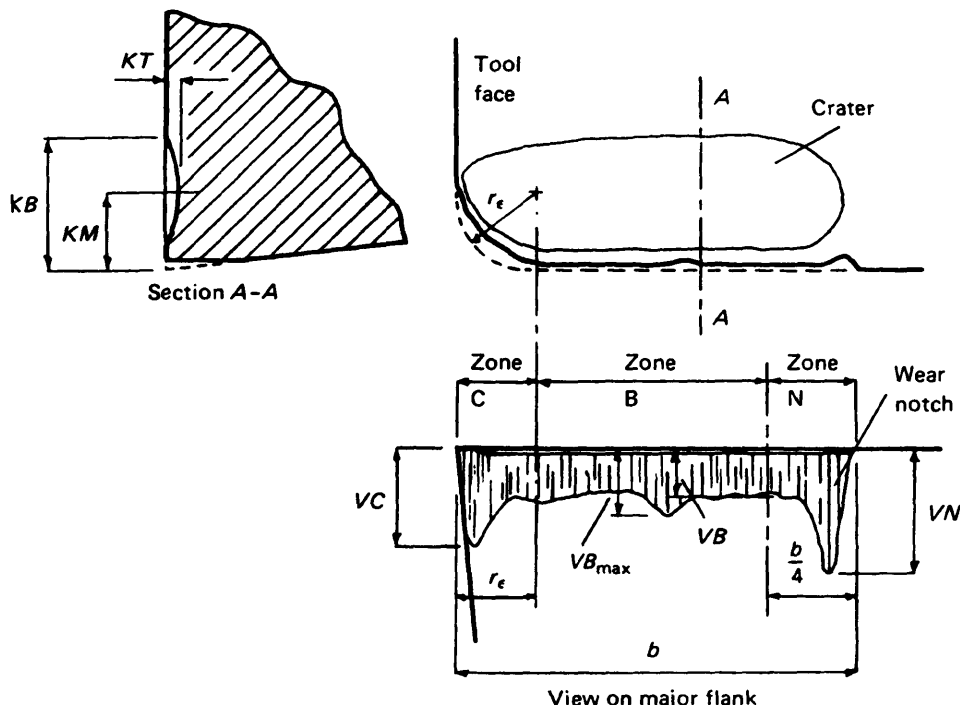

Figure 4.3   Some features of single-point-tool wear in turning operations. (After ISO 5th Draft Proposal [2].)

the average wear-land width in this region is designated VB, and the maximum wear-land width is designated VB_{max}.

The criteria recommended in the new ISO standard dealing with tool-life testing [2] follow.

4.3.4   Common Criteria for High-Speed Steel or Ceramic Tools

The criteria recommended by the ISO to define the effective tool life for high-speed steel tools or ceramic tools are

1. Catastrophic failure, or
2. $VB = 0.3$ mm if the flank is regularly worn in zone B, or
3. $VB_{max} = 0.6$ mm if the flank is irregularly worn, scratched, chipped, or badly grooved in zone B

4.3.5   Common Criteria for Sintered-Carbide Tools

For sintered-carbide tools, one of the following criteria is recommended:

1. $VB = 0.3$ mm, or
2. $VB_{max} = 0.6$ mm if the flank is irregularly worn, or
3. $KT = 0.06 + 0.3f$, where f is the feed

4.3.6   Tool Life

Tool life is defined as the cutting time required to reach a tool-life criterion. The most significant factor affecting tool life when the work material, tool material, and tool shape are chosen for a particular machining operation is the cutting speed.

In studying the optimization of machining processes it is necessary therefore to know the relationship between tool life and cutting speed for the conditions under examination. Early work on this subject was carried out by Taylor [3], who produced an empirical equation that can be written as follows:

$$\frac{v}{v_r} = \left(\frac{t_r}{t}\right)^n \qquad\qquad (4.1)$$

where

n = constant
v = cutting speed
t = tool life
v_r = reference cutting speed giving a known tool life of t_r

Referring again to Fig. 4.2, which shows the results of a tool-wear test, it can be seen that the tool life for a criterion of VB equal to 0.3 mm is 100 s. If this test were repeated for various cutting speeds, each test would give a different value of tool life for a mean wear-land width of 0.3 mm. If all the results were then plotted on logarithmic scales, a graph similar to that shown in Fig. 4.4 would result. It can be seen that the points fall on a straight line and therefore can be represented by Eq. (4.1), where $-(1/n)$ is the slope of the line and (v_r, t_r) is one point on the line.

Thus from the graph n is 0.25 and if the reference speed v_r is chosen arbitrarily as 1 m/s, t_r is 100 s. Equation (4.1) now becomes

$$vt^{0.25} = 100^{0.25} = 3.16$$

It will be shown later, in Chap. 6, how such information can be used in the optimization of machining processes.

4.3.7 Premature Tool Failure

Many cutting tools, particularly single-point cutting tools, are provided with carbide inserts, either brazed to the shank or attached mechanically (in the latter case they are known as "throwaway" inserts). These carbide
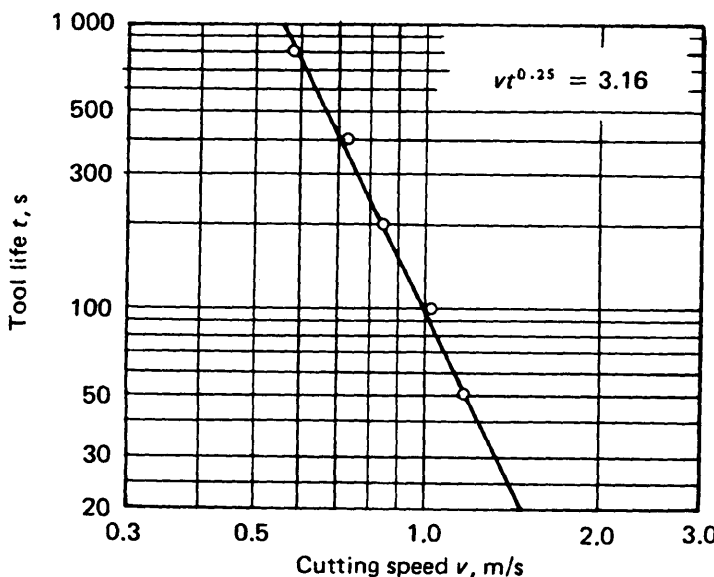

Figure 4.4 Typical relationship between tool life and cutting speed.

inserts are extremely brittle, and the tools should be handled carefully since sudden loads caused by dropping the tool or engaging a large cut suddenly may fracture the insert. These tools are also susceptible to fracture from transient thermal stresses, such as those occurring during intermittent cutting (as in the milling operation) or from localized cooling when coolant is inadequately applied during cutting. Damage may also be caused by careless grinding or incorrect brazing techniques, where cracks may be formed by thermal stresses, thus weakening the cutting edge.

Although most research work on tool wear has dealt, in the past, with the progressive flank and crater wear of cutting tools, the ways in which the life of a tool may be prematurely brought to an end can be extremely important in practice.

4.3.8   The Effect of a Built-up Edge

The presence of a built-up edge on the tool face during cutting can affect the tool-wear rate in various ways, sometimes decreasing the life of a cutting tool and sometimes increasing it. With an unstable built-up edge the highly strain-hardened fragments, which adhere to the chip undersurface and the new workpiece surface, can increase the tool-wear rate by abrading the tool faces. However, when very hard materials (such as cast iron) are cut, the presence of a stable built-up edge can be beneficial [4]. A stable built-up edge protects the tool surface from wear and performs the cutting action itself (Fig. 4.5).

A built-up edge can also contribute to sudden tool failures when tools with carbide inserts are used. For example, when a tool is suddenly disengaged, a portion of built-up edge (welded during cutting to the tool face)
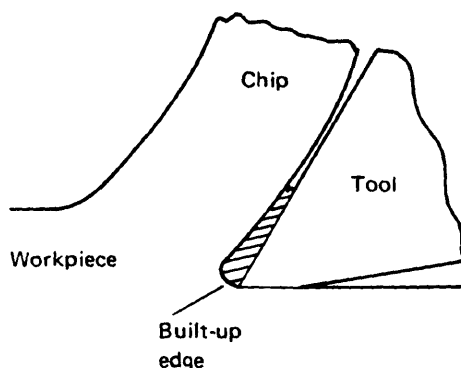

Figure 4.5   Built-up edge protecting tool face. (After Trent [4].)

may be torn off, taking with it a fragment of tool material. A built-up edge can also be detrimental to tool life during the cooling of the tool at the end of a cut. Because the coefficient of linear expansion of steel is approximately twice that of a carbide tool material, cracks may be introduced in the insert where the attached portion of built-up edge has contracted, during cooling, by an amount greater than the contraction of the carbide [4] (Fig. 4.6).

4.3.9 The Effect of Tool Angles

In general, it can be said that poor cutting conditions giving increased specific cutting energies and increased tool temperatures result in higher tool-wear rates. Because an increase in rake usually leads to an improvement in cutting conditions, a longer tool life would be expected. However, when the tool rake is large, the cutting edge is mechanically weak, resulting in higher wear rates and shorter tool life. Therefore, for an otherwise constant set of cutting conditions, an optimum rake exists giving a maximum tool life.

A typical relationship between rake angle and tool life is shown in Fig. 4.7, where the optimum rake is approximately 14 deg when cutting high-strength steel with a high-speed steel tool [5]. Experience has shown that the optimum rake is roughly constant for given work and tool materials, and in practice the values given in Table 4.1 are used.

In certain circumstances, for example, when milling with carbide cutters, where the impact loading at each revolution of the cutter might tend to fracture the insert, a negative rake is used to achieve greater strength.

Experience has shown that the width of the flank wear land is usually the limiting factor determining the life of the cutting tool. However, it has been shown [6] that the physical conditions of stress, temperature, and speed that determine the wear rate on the tool flank are constant along the
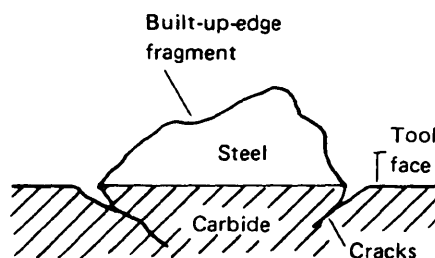

**Figure 4.6** Cracks forms in carbide insert during cooling. (After Trent [4].)
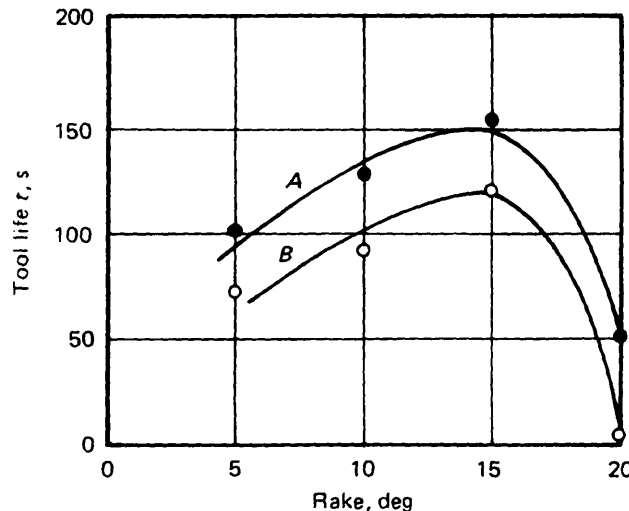
Figure 4.7 Effect of tool rake on tool life, where the work material is high-strength steel and the tool material is high-speed steel. In curve *A* the feed is 0.127 mm (0.005 in.) and the cutting speed is 0.66 m/s (130 ft/min); in curve *B* the feed is 0.508 mm (0.02 in.) and the cutting speed is 0.41 m/s (80 ft/min). (After Cherry [5].)

wear land, and for reasonably small wear lands these physical conditions are not greatly affected by changes in the wear-land width. For these two reasons it would be expected that the wear rate of the tool material normal to the resultant cutting direction would be constant and independent of the normal clearance. Figure 4.8 shows that the rate of increase of flank wear-land width, on the other hand, is dependent on the flank clearance.

From the figure, with zero tool rake,

$$(VB) = (NB) \cot \alpha_{n_e}$$

$$\frac{VB}{NB} = \frac{\dot{VB}}{\dot{NB}} = \cot \alpha_{n_e} \tag{4.2}$$

where

 $\dot{VB}$ = rate of increase of flank wear-land length
    $\dot{NB}$ = rate of removal of tool material normal to the cutting direction
    γ_{n_e} = working normal clearance

Table 4.1 Recommended Normal Rake for Roughing
Operations

Work material	High-speed steel, deg	Carbide, deg
Cast iron, cast brass	0	0.0
Brass and bronze	8	3.5
Soft brass and high-tensile steel	14	3.5
Mild steel	27	3.5
Light alloys	40	13.0

Hence, for an assumed constant wear rate normal to the cutting direction, the flank wear rate $\dot{VB}$, which determines the tool life, is proportional to clearance cot γ_{n_e}. The relationship is illustrated in Fig. 4.8, where it is seen that for small values of clearance an increase in clearance will give a significantly reduced wear rate. It is clear, however, that in practice the normal clearance cannot be made too large without running the risk of weakening the tool edge. Experience has shown that with most work
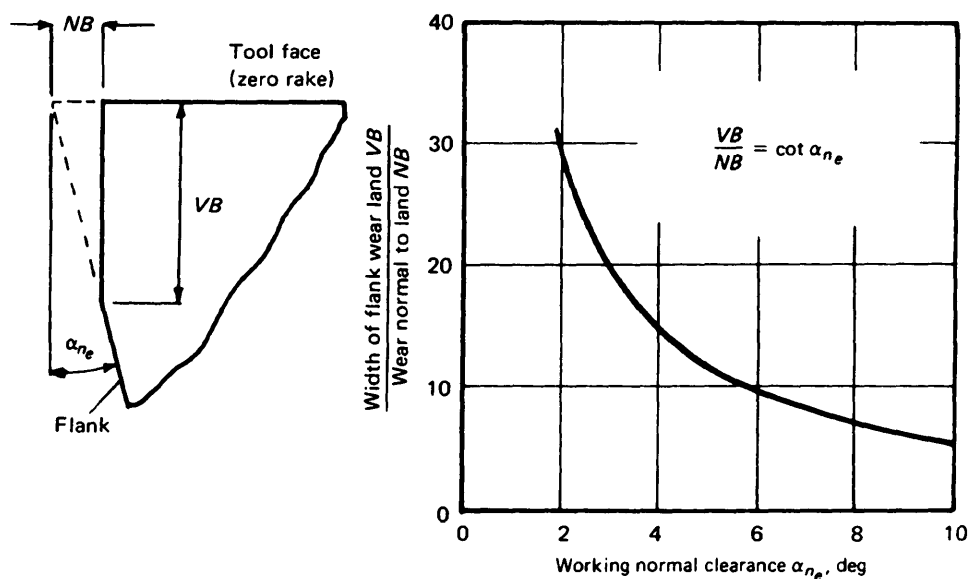
Figure 4.8 Effect of normal clearance on flank wear.

materials, clearance angles of 8 deg with high-speed steel tools and 5 deg with carbides give the best compromise between these conflicting requirements.

4.3.10 The Effect of Speed and Feed on Cratering and Built-up-Edge Formation

In metal cutting, increases of speed or feed result in an increase in the temperature on the tool face. At low speeds increases in tool-face temperatures tend to reduce friction at the chip–tool interface and hence tend to prevent the formation of a built-up edge; at high speeds increases in tool-face temperatures tend to increase the rate of crater wear. The relative effects of changes in speed and feed are shown clearly by graphs prepared by Trent [4]; two examples of the effects of changes in feed and speed are presented in Fig. 4.9. These graphs show, for a given work and tool material combination, the ranges of speed and feed where a built-up edge occurs, where rapid cratering occurs, and where, under very severe conditions, extremely rapid breakdown of the tool occurs because of deformation of the tool at the cutting edge (a result of high temperatures and stresses). Such graphs are extremely useful when comparing the performance of various tool materials. The results in Fig. 4.9 show, for example, that when titanium is added to a tungsten–carbide tool material, crater wear occurs at a significantly higher range of speeds and feeds when carbon steel is machined. Thus the useful range of speeds and feeds is increased by the use of tungsten–titanium–carbide tool materials for machining carbon steels.

4.4 THE TOOL MATERIAL

4.4.1 Basic Requirements of Tool Materials

Cutting tools are required to operate under high loads at elevated temperatures, often well in excess of 1000°C. In addition, severe frictional conditions occur between the tool and chip and between the tool and the newly machined workpiece surface. The main requirements for cutting tool materials are:

1. High-temperature physical and chemical stability; high-hot hardness is of particular importance
2. High wear resistance
3. High resistance to brittle fracture

   High performance in all of these three attributes is generally not pos-
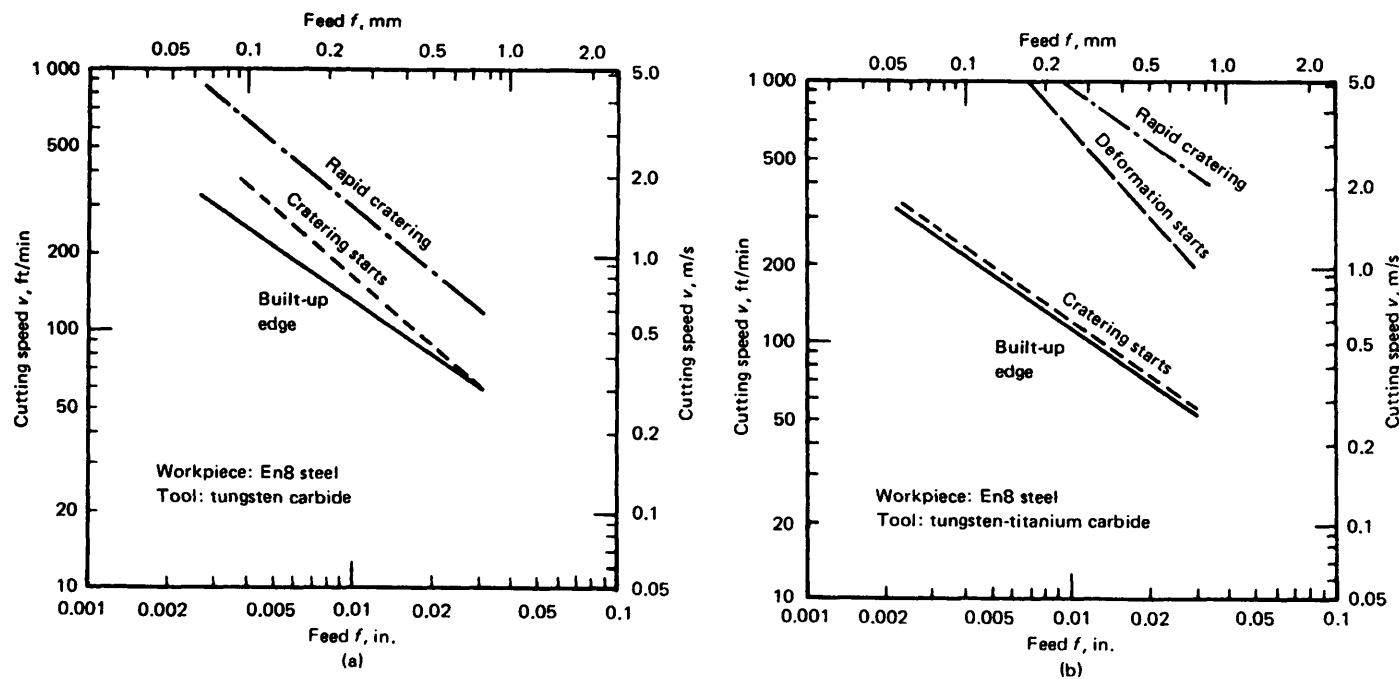
Figure 4.9 (a) Tool-wear chart for a tungsten–carbide tool. (b) Tool-wear chart for a tungsten–titanium–carbide tool. (After Trent [4].)

sible. For example, materials with increased high-temperature resistance and high wear resistance will also have reduced resistance to brittle fracture.

Other factors which influence the performance of cutting tools are:

1. Relative hardness of the tool and work material
2. Abrasive particles, such as scale, on the surface of the workpiece
3. Chemical compatibility of the tool and work material
4. Cutting temperatures
5. Condition of the machine tool, rigidity, for example;
6. Type of machining operation, in particular whether continuous or interrupted cuts occur, which is important for materials with a low resistance to brittle fracture.

4.4.2 Major Classes of Tool Materials

The major types of cutting-tool materials are shown in Table 4.2. The earliest materials used were hardened carbon steels, but these are restricted to low cutting speeds and temperatures, as the martensite present, which gives the material its hardness, softens at 250°C and above. Consequently, carbon steel tools are now only used for machining soft materials, as in woodworking.

One of the greatest steps forward in the machining of metals was made when Taylor [3] discovered the heat-treatment process used in producing high-speed steel-cutting tools. Use of these cutting tools made higher metal removal rates possible owing to the improved tool-wear behavior. Since Taylor's heat-treatment discovery, developments in metallurgical science and technology have led to other new tool materials, such as cast alloys, cemented carbides, and, more recently, sintered oxides or ceramics.

Practical experience has shown which tool materials are most suited to particular operations. With single-point tools, where tool manufacturing problems are not serious, the desirable property is a high hardness value that is maintained at high temperatures. Unfortunately an increase in hardness is usually accompanied by a decrease in the impact strength of the material; an increase in hardness also increases tool manufacturing problems. Consequently, the materials found most suitable for continuous cutting with single-point cutting tools often cannot be used for multipoint cutting tools. Since single-point cutting tools form only a small proportion of the total number of cutting tools used in practice, most metal cutting is still performed with tools manufactured from high-speed steel.

The materials shown in Table 4.2 are arranged in order of increased

Table 4.2   Major Classes of Tool Material

Hot hardness	Wear resistance		Toughness
↓	↓	1. Carbon steels 2. High-speed steels 3. Cast alloys 4. Tungsten carbides 5. Cermets 6. Titanium carbides 7. Ceramics 8. Polycrystalline diamond and cubic boron nitride 9. Single-crystal diamond	↑

temperature resistance and hot hardness. Figure 4.10 shows the effect of temperature on the hardness of some of these materials [7]. All of these materials, with the exception of single-crystal diamond, consist of a softer phase separating very hard particles. Increasing the proportion of the harder-phase material increases the hardness but reduces the toughness of the material. Recent developments in tool materials have included the coating of these basic materials with thin, high-wear-resistant layers to improve performance, particularly for high-speed steel and tungsten carbide tools. The main classes of tool materials will now be discussed in greater detail.

4.4.3   High-Speed Steel

High-speed steels (HSS) are alloy steels with alloying elements consisting mainly of tungsten (about 18 percent) and chromium (about 4 percent); they may also contain cobalt, vanadium, or molybdenum. During the heat-treatment process carbides of the alloying elements are formed and dispersed throughout the material as very hard particles. Over 20 grades of HSS tool materials are in common use, each with its own advantages and limitations [8]. High-speed steel-cutting tools are relatively inexpensive and tough, but have limited hot hardness and can only be used for cutting temperatures up to 550°C. High-speed steel can be hot-rolled and forged to rough shapes, then machined, prior to heat treatment and finish grinding. It is still the most common tool material, particularly for monolithic tools such as drills, milling cutters, and so on.

In recent years high-speed steel cutting tools have been available with a thin (1 to 2 μm) coating of titanium nitride (TiN), which has an equivalent hardness of Rockwell C 80–85. The high-speed steel provides a relatively ductile, shock-resistant core to the tool, while the coating has ex-
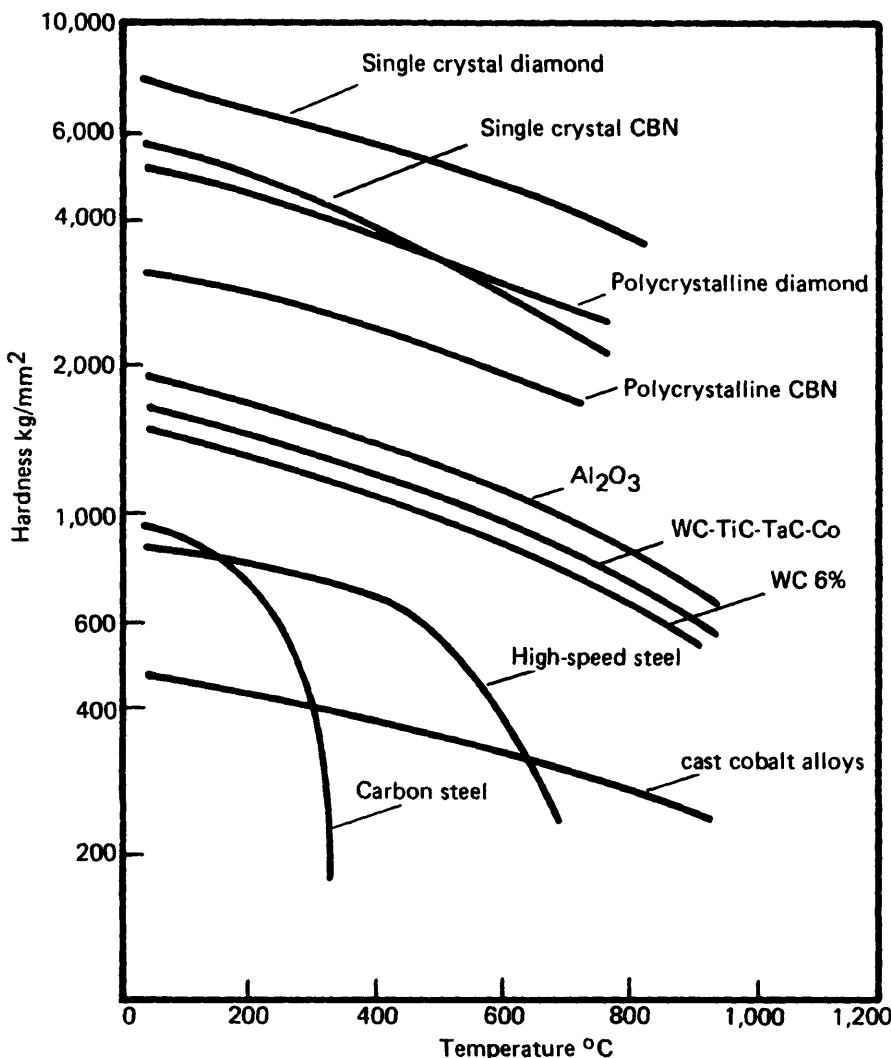
Figure 4.10 Variation of hardness with temperature for some tool materials. (Adapted from Almond [7].)

ceptional wear resistance and lower friction than the uncoated high-speed steel.

4.4.4 Cast Alloy Tools

Cast-alloy tools contain no iron and are cast into their final shape. They consist of cobalt, chromium, tungsten, and carbon, the carbide phase being about 25 to 30 percent, by volume, of the matrix. These tools can usually be used at slightly higher speeds than high-speed steels and have less tendency to form a built-up edge during machining. They find the widest applications in the machining of cast iron, malleable iron, and the hard bronzes.

4.4.5 Cemented Carbide Tools

Cemented carbides are usually made by mixing tungsten powder and carbon at high temperatures in the ratio of 94 and 6 percent respectively, by weight. This compound is then combined with cobalt, and the resulting mixture is compacted and sintered in a furnace at about 1400°C. This tungsten–carbide–cobalt material can maintain high hardness values at temperatures as high as 1200°C and can therefore be used at much higher cutting speeds than high-speed steel or cast-alloy tool materials. However, as mentioned earlier, cemented carbides are not as tough and cannot be shaped after sintering. For this reason they usually take the form of inserts, either brazed on or clamped on (Fig. 4.11). The clamped-on inserts are thrown away after all the cutting edges have been worn. Straight tungsten carbides are the strongest and most wear resistant but are subject to rapid cratering when machining steels. To improve resistance to cratering, tantalum carbide and titanium carbide are added to the basic composition, resulting in tungsten–tantalum carbide or tungsten–titanium carbide.

   More recently, cemented titanium carbide has been available in the form of disposable inserts. This material is more wear resistant than straight tungsten carbide but has the disadvantage of lower strength. However, developments in the manufacture of this material have led to the production of superior grades that allow cutting speeds approaching those of ceramics; these superior grades can be used in the semirough cutting of steels and certain cast irons. Some believe that by the end of this decade at least one-half of all steel machining will be carried out using cemented titanium carbide [9].

   Cemented carbides are available in many different grades [8], which differ in hardness and wear resistance. In general, increasing the cobalt content of the material increases the toughness but reduces the hardness.
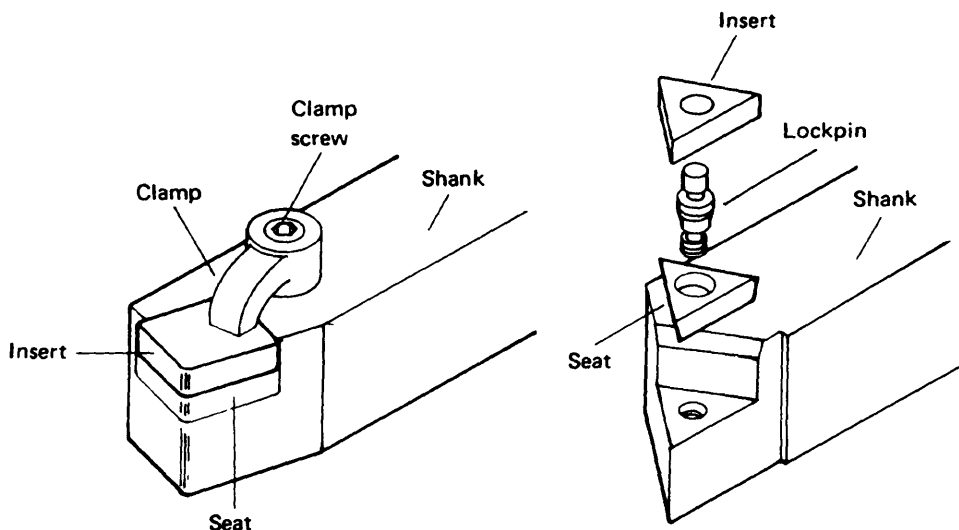
Figure 4.11 Typical styles of clamped-on (throwaway) insert tools.

All cemented carbides can be used at elevated temperatures compared to high-speed steel, but these materials are relatively brittle and can fracture easily when interrupted cuts are used.

4.4.6 Coated Carbides

The basic requirement for the efficient rough machining of steel is a tool material that exhibits the toughness of the tungsten carbide while giving the superior wear resistance of titanium carbide. For this reason much interest is being shown in the coating of cemented tungsten carbides with a thin layer of harder material. These coatings are between 5 and 8 μm thick and are found to practically eliminate interdiffusion between the chip and the tool. The coatings are usually applied by chemical vapor deposition. Eventually when the coating has been worn away by abrasion, the wear rate becomes the same as that for the uncoated tool.

Successes have been reported with coatings of titanium carbide [10], titanium dioxide [11], and titanium nitride [12]. More recently, new coatings with improved properties have been introduced, including aluminum oxide (Al_2O_3) hafnium nitride (HfN), and zirconium nitride (ZrN) [13]. The newest coatings consist of multiple layers of different materials. For example, layers of Al_2O_3 and TiN can be combined. The outer layers of TiN provide a low friction and chemically inert surface for a new tool. As the TiN wears through, the additional wear-resistant layer of Al_2O_3 is exposed.

4.4.7 Ceramic and Cermet Tools

Ceramic tool materials are made from sintered aluminum oxide (Al_2O_3) and various other boron and silicon nitride powders; these powders are mixed together and sintered at about 1700°C. Sintered oxides can be used at cutting speeds two to three times those employed with tungsten carbides, are very hard, and have a high compressive strength and low thermal conductivity. They are, however, extremely brittle and can only be used where shock and vibrations do not occur. They are only available in the form of throwaway inserts, and their widest applications are in high-speed finish turning.

Three types of ceramic cutting tools are mainly used; aluminum oxide (Al_2O_3), Sialon (a combination of silica, aluminum, oxygen, and nitrogen), and silicon nitride (Si_3N_4). Aluminum oxide is the most common and performs best for finishing and semifinishing, with noninterrupted cuts. Sialon offers greater resistance to mechanical shock and possesses the ability to withstand the higher thermal shocks that arise from the use of coolants. Sialon cannot be used with carbon steels because of chemical incompatibility [14]. Silicon nitride tools have attributes similar to Sialon, but with improved toughness and the ability to withstand high temperatures and loads.

Cermet tools are made from 70 percent Al_2O_3 and 30 percent titanium carbide. These materials are tougher and more fracture resistant than ceramics, but somewhat softer. The high toughness and hardness of cermets allow them to be used at speeds several times higher than those for carbides, and they also have the ability to perform interrupted cuts.

The most recent developments involving ceramic tools are ceramic-ceramic composites, which consist of an Al_2O_3 matrix reinforced by tiny silicon carbide wiskers. These wiskers distribute the cutting forces more evenly, which results in a considerable increase in fracture toughness compared to cermets. These composite materials are suitable for roughing and finishing cuts and appear particularly useful for machining nickel-based alloys, cast iron, and steels.

4.4.8 Polycrystalline Tools

Polycrystalline cutting tools are fabricated by compacting small particles of diamond (synthetic and natural) or cubic boron nitride (CBN) under high pressure and temperature conditions. Single-crystal diamonds are used for fine-finishing operations. Although natural diamonds are the hardest materials known, their crystalline structure results in nonuniform strength. Polycrystalline tool materials are more homogeneous, with improved strength and durability, but with slightly reduced hardness com-

pared to natural diamond. Cubic boron nitride is less expensive than diamond, but over 20 times more costly than carbide. The high cost is counterbalanced by a considerably increased tool life (up to 50 times longer than carbide). Polycrystalline CBN tools are becoming commonly applied in grinding operations such as machining hardened steel parts, machine beds, and steel mill rolls [13].

4.5 THE WORK MATERIAL

The term *machinability* is often applied to work materials to describe their machining properties; it can have several meanings depending on the cutting process under consideration. When it is stated that material A is more machinable than material B, this can mean that a lower tool-wear rate is obtained with material A, or a better surface finish can be achieved with material A, or that less power is required to machine material A. Clearly, with finishing processes, tool wear and surface finish are the most important considerations; with roughing operations, tool wear and power consumption are important.

It should be noted that any statement regarding machinability may only apply under the particular set of circumstances existing when the observation was made. For example, under a given set of condtiions a better surface finish may be obtained with material A than material B; however, under another set of conditions, say with a different tool material, the situation may be reversed. Similar behavior can occur with the other criteria of machinability, tool-wear rate, and power consumption. To complicate the situation further, a certain group of materials may be placed in one order of machinability on a tool-wear basis, but in a different order if surface-finish or power-consumption criteria are applied. Clearly, the term machinability can have little meaning except in a loose qualitative sense.

Even though the term is meaningful only in a loose qualitative sense, many attempts have been made to obtain a quantitative measure of machinability—a machinability index or number. A method for producing such an index, if the results were meaningful, would be most helpful, particularly to steel manufacturers who must check the machining properties of their work materials and therefore would welcome a quick and reliable checking method. Many ingenious methods for producing machinability data have been proposed, and some are still used today. Although these methods are of doubtful meaning, they can be used to measure the variation in some machining property of materials having the same specification. It would be most difficult to prove that the results of these tests yield quantitative information on machining properties of

practical interest, although experience has shown that these results do give some guide.

4.5.1   Tool Wear and Machinability Testing

The production of such tool-wear data as those shown in Figs. 4.2, 4.4, and 4.9 is extremely tedious and involves a series of carefully taken measurements over long periods of time. These tests, of necessity, consume a considerable amount of work material and often several experimental tools. The additives and inclusions in commercial work materials can vary due to segregation in such a manner that considerable variations in tool-wear rate occur from the inside of the specimen to the outside; variations can also occur along the length of a specimen. Considerable variations between tool materials of nominally the same specification can also occur. With carbide tools, specimen inserts placed together in the furnace during the sintering process are known to exhibit different wear performances. With high-speed steel tools, the problem is even greater: the tempering temperatures are so critical that the slightest variation in heat-treatment conditions results in large variations in performance.

For the reasons given above, the results of extended tool-wear tests can often be misleading because of the danger that the properties of both the workpiece and specimen tools may vary during a series of tests. The ISO-recommended tool-life test for turning [2] attempts to minimize these problems by specifying the tool and work materials and the test conditions very closely. However, some method of rapid wear testing, consuming a small quantity of work material and requriing only one specimen tool, is clearly desirable and several testing methods have been proposed.

One method of rapid testing is known as the accelerated wear test, and one example of this type of test involves a facing operation in a lathe. In this test the workpiece is rotated at high speed, and the tool is traversed from the workpiece center line radially outward. Conditions are chosen such that complete failure of the tool occurs before the tool reaches the outside diameter of the workpiece. The radial distance machined is taken as a measure of the machining characteristics of the particular tool-workpiece combination. Although this method is useful as a comparative test for various work or tool materials, the results yield little information regarding the fundamental nature of wear in machining and do not give an absolute measure of the performance of the tool, a measure which could be related to its behavior in practical circumstances.

Another type of rapid wear test involves a special technique for measuring extremely small amounts of wear. In this method the working

surfaces of the cutting tool are carefully prepared and polished, the tool is then used to cut the test workpiece for a short time, and the small amount of wear occurring on the tool flank is measured. The disadvantage of this method is that the wear characteristics measured are those occurring in the initial tool breakdown period and may not always be representative of the behavior of a tool in the later stages of wear. A further technique for measuring small amounts of tool wear is the radioactive-tracer technique. In this method the test cutting tool is irradiated by a radioactive source before the cutting test. The chips produced during the test are collected and their activity measured with a radioactivity counter; the reading is taken as a measure of the wear rate of the cutting tool. This method is also suitable only as a comparative test.

In a more recent proposal for rapid wear testing, the tool is initially prepared by grinding an artificial wear land on its flank. Increases in the magnitude of this wear land from a small amount of machining are measured, and thus the wear rate of the tool in the central linear portion of the wear curve (Fig. 4.2) is obtained. In this test, care must be taken to grind the initial wear land with a slightly negative "clearance" to establish the required frictional contact between the tool and workpiece at the beginning of the test.

In all the theories of progressive tool wear, the rate of wear would be expected to increase both with increased metallic contact at the interface and with increased temperature; thus it might be expected that some relationship exists between tool wear and chip–tool friction and between tool wear and temperature. That a relationship of this type does exist was found true in the past and explains why, under many conditions, measurements of chip–tool friction or cutting temperatures can give a useful guide to the wear behavior of a given work–tool combination. Such measurements are used as machinability tests and have the great advantage that they require very little work material.

4.5.2   Factors Affecting the Machinability of Metals

In general it can be said that high hardness will give poor machinability because power consumption and temperatures and hence tool-wear rates will be high. However, many other factors affect machinability, and it can also be said in general that pure metals tend to adhere to the working surfaces of the cutting tool and give high friction and high tool-wear rates. For example, when pure iron is machined, cutting forces and tool-wear rates are extremely high, almost as high as those obtained when some of the very tough alloy steels are machined.

The deliberate addition of sulfur, lead, and tellurium to nonferrous

metals as well as steels makes possible increased production rates and improved surface finish, but how these additives function is not completely understood. It appears certain that these additives reduce the metallic contact between the tool and work material; hence they reduce friction adn tool-wear rates. These constituents do not greatly affect the room-temperature mechanical properties of the parent metal, but the high-temperature properties can be seriously affected. The effect of sulfur, lead, or tellurium on the high-temperature properties of metals of course limits the use of these so-called free-machining metals, but nevertheless they find wide application and demand for them is high. The lack of theory on the effects of the workpiece material on tool wear creates difficulties for engineers and metallurgists involved in production. For example, with increasing automation in machining processes it becomes more important to maintain consistent tool-wear characteristics, but it is well known that very large differences in tool wear occur when cutting metals of nominally the same specification. These differences are usually not related to the material properties normally measured.

Particular difficulties are encountered with metals developed for high-temperature applications, such as those metals used in turbines. Addition of free-machining elements is not usually possible with these metals, and therefore it is left to the tool engineer and production engineer to solve the machining problems. Some of these problems are becoming so difficult that other machining techniques, such as electrochemical machining have become more economical to use; these techniques are discussed in Chap. 14.

PROBLEMS

1. A single-point cutting tool has a zero rake angle and a clearance angle of 2 deg. By what percentage would the life of the tool between regrinds be increased if a clearance angle of 8 deg were provided? (Asume the tool is reground after a specified amount of flank wear has taken place and that the rate of wear of the tool normal to the wear land is constant.)

2. From the results of tests for a tool clearance of 8 deg, it was found that the tool life was 240 s for a cutting speed of 1 m/s, and 12 s for a cutting speed of 5 m/s. Assuming that Taylor's tool-life relationship holds, that is,

$$vt^n = v_r t_r^n$$

Estimate:

a. The constant n
b. The percentage change in tool life if the tool clearance angle is decreased from 8 to 3 deg.
c. The new value of v_r when $t_r = 1$ (after the change in clearance angle)

3. In a multipass rough-turning operation the tool life is observed to obey an equation

$$t = v^{-3} f^{-0.8} a_p^{-0.1}$$

where v, f, and a_p are the cutting speed, feed, and depth of cut, respectively, in SI units. The system normally operates with $v = 1$ m/s, $f = 0.5$ mm, and $a_p = 10$ mm. Estimate the effect (percent increase or decrease) on tool life, cutting force, and power of doubling the metal removal rate by increasing (a) the speed, (b) the feed, (c) the depth of cut.

REFERENCES

1. Bowden, F. P., and D. Tabor: *Friction and Lubrication of Solids*, Oxford University Press, London, 1954.
2. Tool Life Testing with Single-Point Turning Tools, ISO 5th Draft Proposal, ISO/TC 29/WG22 (Secretariat 37), vol. 91, March 1972.
3. Taylor, F. W.: On the art of cutting metals, *Trans. ASME,* vol. 28, p. 31, 1906.
4. Trent, E. M.: Tool wear and machinability, *Prod. Eng. (Lond.)*, vol. 38, no. 3, p. 105, 1959.
5. Cherry, J.: Practical investigation in metal cutting, *Prod. Eng. (Lond.)*, vol. 41, no. 2, p. 90, 1962.
6. Boothroyd, G., J. M. Eagle, and A. W. J. Chisholm: Effect of tool flank wear on the temperatures generated during metal cutting, *Adv. Mach. Tool Des. Res.,* Vol. 7., p. 667, 1967.
7. Almond, E. A.: Towards improved tests based on fundamental properties, in *Towards Improved Tool Performance,* National Physical Laboratory Conference, Metals Society, London, 1982.
8. Drozda, T. J., and C. Wick, eds.: *Tool and Manufacturing Engineers Handbook,* Vol. 1: *Machining,* 4th ed. Society of Manufacturing Engineers, 1983.
9. Kalish, H. S.: The potential of titanium carbide for machining steel, *Cutting Tool Eng.,* vol. 24, no. 9–10, pp. 6–9, 1972.
10. Horlin, N. A.: TiC coated cemented carbides—their introduction and impact on metal cutting, *Prod. Eng. (Lond.)*, vol. 50, no. 4–5, pp. 153–159, 1971.
11. Suh, N. P., and B. J. Sanghvi: Frictional characteristics of oxide-treated and untreated tungsten carbide tools, J. Eng. Ind., series B, vol. 93, no. 2, pp. 455–460, 1971.

12. Feinberg, B.: Longer life from TiN tools, *Mfg. Eng. Manag.,* vol. 67, no. 1, pp. 16–18, 1971.
13. Kalish, H. S.: Status report: cutting tool materials, *Carbide Tool J.,* p. 3, May/June 1984.
14. Drozda, T. J.: Ceramic tools find new applications, *Manuf. Eng.,* p. 34, May, 1985.

5
Cutting Fluids and
Surface Roughness

5.1 CUTTING FLUIDS

Cutting fluids, usually in the form of a liquid, are applied to the chip formation zone to improve the cutting conditions (compared to dry cutting conditions). These improvements can take several forms, depending on the tool and work materials, the cutting fluid, and to a large extent the cutting conditions. The two most important ways in which a cutting fluid can act are as a coolant and as a lubricant. Most practical cutting fluids have a mineral- or vegetable-oil base, mineral oil being the more widely used. Some of these oils are made to be applied as an emulsion with water (water-miscible cutting fluids); the remainder are used neat (undiluted with water), either plain or having various additives. In general, oil-and-water emulsions are used when cooling action is the most important requirement because these emulsions have a much larger heat-conducting capacity than neat oils. With almost 90 percent of machine tools an oil-and-water emulsion is used. Neat oils are used when lubricating action is the most important consideration; their use is usually confined to slow-speed cutting operations such as screw cutting, broaching, and gear cutting.

5.2   THE ACTION OF COOLANTS

Several advantages are to be gained by applying a coolant to the cutting process:

1.   An increase in tool life through temperature reduction in the region of the tool cutting edge
2.   Easier handling of the finished workpiece
3.   A reduction in the thermal distortion caused by temperature gradients generated wtihin the workpiece during machining

The last two factors are most important in the grinding process. A secondary and sometimes overlooked advantage of cutting-fluid application is the flushing action, which assists the removal of chips from the cutting area. Properly placed fluid nozzles can help prevent the packing of chips in flutes of drills or milling cutters.

Quantitative information on the effect of a coolant on cutting-tool life has been obtained mainly from drill life tests; these tests clearly demonstrated improvements in drill life owing to the application of a coolant. It seems most likely that these improvements are caused by some reduction in temperature in the region of the drill point, but work on cutting temperatures described in Chap. 3 suggests that the heat losses from the exposed surface of the tool and workpiece have quite a small effect on the temperatures in the region of the tool cutting edge. It can only be assumed, therefore, that the tool-wear rate is extremely sensitive to the small changes in temperature in the region of the wearing surfaces that result from the application of a coolant.

Holmes [1] has described the various general characteristics of water-miscible cutting fluids (Table 5.1) and has developed the guide to their selection presented in Table 5.2.

5.3   THE ACTION OF LUBRICANTS

5.3.1   Boundary Lubrication

Bowden and Tablor [2] have shown that under conditions of high temperature and pressure and low sliding velocity a hydrodynamic film cannot be maintained, and thus direct contact occurs. Frictional resistance to motion under these conditions arises from a combination of asperity shearing and viscous shearing of the fluid; this is known as boundary lubrication and is greatly affected by the nature of the adsorbed fluid layer (boundary layer), a few molecules thick, on the surfaces of the sliding metals. A lubricant boundary layer functions by reducing the area of in-

Table 5.1 General Characteristics of Water-Miscible Cutting Fluids[a]

Type of lubricant	Characteristics
Emulsifiable, soluble oils	
General-purpose	Used at dilutions between 1:10 and 1:40 and give a milky emulsion. Used for general-purpose machining.
Clear-type	Used at dilutions between 1:20 and 1:60. Their high emulsifier content results in emulsions that vary from translucent to clear. Used for grinding or general-purpose machining.
Fatty	Used at concentrations similar to those for general-purpose soluble oils and give a similar (milky-emulsion) appearance. Their fat content makes them particularly effective for general machining operations on nonferrous metals.
Extreme-pressure	Generally contain sulfurized or chlorinated extreme-pressure additives. Used at dilutions between 1:10 and 1:20 where a higher performance than that given by general-purpose, clear-type, or fatty soluble oil is required.
Chemical solutions	
Grinding fluids	Essentially solutions of chemical rust inhibitors in water. Used at dilutions between 1:50 and 1:100 for grinding operations on iron and steel.
General-purpose, synthetic cutting fluids	Contain mainly water-soluble rust inhibitors and surface-active load-carrying additives. Used at dilutions between 1:10 and 1:40 for cutting and higher dilutions for grinding. Most are suitable for both ferrous and nonferrous metals.
Extreme-pressure, synthetic cutting fluids	Similar in characteristics to general-purpose, synthetic cutting fluids but containing extreme-pressure additives to give higher machining performance when used with ferrous metals.

[a]After Holmes [1].

timate metallic contact between the two surfaces. Some lubricants having "reactive ingredients" (extreme-pressure additives of sulfur, phosphorus, or chlorine) can offer considerably greater surface protection during sliding by the formation of a solid-lubricant layer. This layer of solid lubricant, often the product of a chemical reaction between the lubricant and the metal surface, remains effective at temperatures to its melting point.

When two metallic surfaces, each having an adsorbed solid-lubricant

Table 5.2 Guide to the Selection of Water-Miscible Cutting Fluids[a]

Machining operation	Free-machining nonferrous alloys	Tough nonferrous alloys	Free-machining and low-carbon steels	Medium-carbon steels	High-carbon and alloy steels	Stainless and heat-resistant alloys
Grinding	General-purpose or clear-type, soluble oils		Clear-type, soluble oil or chemical grinding fluid			
Turning	General-purpose, soluble oil	General-purpose or fatty, soluble oils	General-purpose, soluble oil or synthetic fluid		Extreme pressure, soluble oil or synthetic fluid	
Milling		General-purpose or fatty, soluble oils		Extreme-pressure, soluble oil or synthetic fluid	Extreme-pressure, soluble oil or synthetic fluid (neat cutting oils may be necessary)	
Drilling	General-purpose or fatty, soluble oils		Fatty or extreme-pressure, soluble oils; synthetic fluids			
Gear shaping			Extreme-pressure, soluble oil or synthetic fluid		Neat cutting oils preferable	
Hobbing			Extreme-pressure, soluble oil or synthetic fluid			Neat cutting oils preferable
Broaching			. Extreme-pressure soluble oil or synthetic fluid		Neat cutting oils preferable	
Tapping	General-purpose or fatty, soluble oils (neat cutting oils may be preferable)		Extreme-pressure, soluble oil or synthetic fluid (neat cutting oils may be preferable)			

[a]After Holmes [1].

layer, are placed together and a normal load applied, the resulting deformation of the surface asperities causes some penetration of the lubricant layer, and metallic contact is established (Fig. 5.1).

If the real area of contact A_r is thought of as the area supporting the load and γ_m is the proportion of this area in which metallic contact occurs, the frictional force F_f required to continually shear the junctions between surface asperities can be written as

$$F_f = A_r[\gamma_m \tau_1 + (1 - \gamma_m)\tau_2] \tag{5.1}$$

where τ_1 and τ_2 are the shear strengths of the softer metal and the softer lubricant layer, respectively. Thus, if γ_m remains essentially constant for given values of τ_1 and τ_2, the frictional force will be proportional to A_r, so that Amontons' law will hold as for unlubricated sliding surfaces. If the temperature at the interface rises until the lubricant layer melts, the layer loses its rigidity, and a large increase in metallic contact occurs; if τ_1 is greater than τ_2, F_f increases. As the interface temperature increases further, the frictional force and surface damage become characteristic of unlubricated sliding contact, although the lubricant is visibly present on the surface. The lubricant layer is now said to be desorbed or completely mobile. Thus in Eq. (5.1), as the melting point of the lubricant boundary layer is exceeded, γ_m tends to unity and F_f tends to $A_r \tau_1$, thus approaching dry, sliding-friction conditions.

5.3.2 Lubrication in Metal Cutting

Under certain conditions the application of a lubricant to the cutting process can result in a reduction in friction on the tool face; this friction
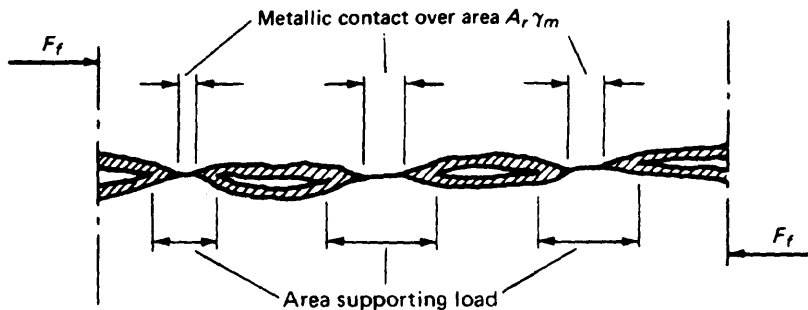
Figure 5.1 Sliding between surfaces with solid lubricant layer, where F_f = friction force, τ_1 = shear strength of softer metal, and τ_2 = shear strength of lubricant layer.

reduction on the tool face can cause a reduction in power consumption, an increase in tool life, and, most important, an improvement in the surface finish of the machined component by reducing the occurrence of a built-up edge. The action of cutting lubricants has in the past provided a fascinating topic for fundamental research. It has been known for some time that a considerable reduction in the mean coefficient of friction on the tool face can be achieved, under certain conditions, by application of the correct lubricant. However, many accepted engineering lubricants can have little or no effect on the cutting operation. It has also been shown that other fluids and chemicals (e.g., carbon tetrachloride), never used as lubricants in normal engineering applications, can have startling effects on the cutting process, reducing power consumption by as much as 60 percent in certain cases.

The extremely high pressures existing in the region of the chip–tool interface during machining do not allow complete hydrodynamic lubrication, where the chip and tool would be separated by a thin film of fluid. Indeed, it has been known for some time that the lubricating action of cutting fluids is mainly of a chemical nature. For example, note the lubricating effect of carbon tetrachloride (CCl_4) when copper is machined; it can be seen from Fig. 5.2 that at low cutting speeds friction at the chip–tool
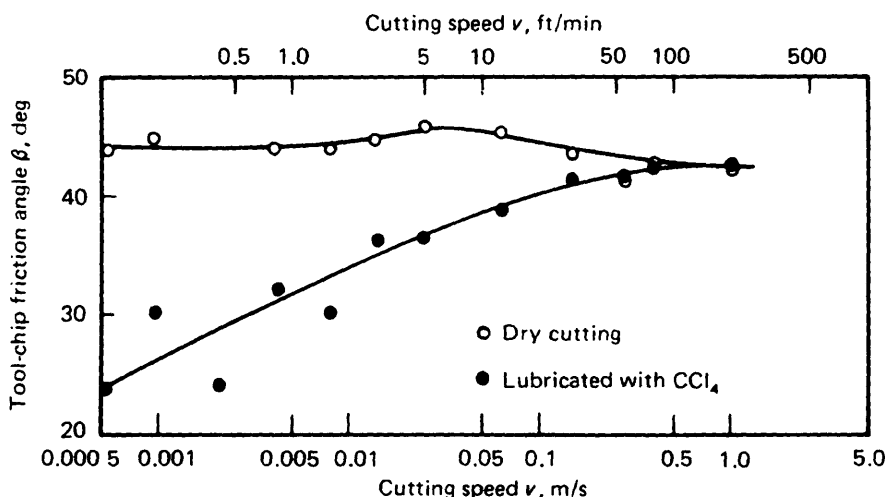
Figure 5.2 The effect of cutting speed on the lubricating action of carbon tetrachloride, where the work material is copper, the undeformed chip thickness is 0.25 mm (0.01 in.), the chip–tool contact length is 0.3 mm (0.012 in.), and the tool rake is 45 deg. (After Cassin and Boothroyd [3].)

interface is reduced considerably by the application of the fluid. It has been shown that this effect results from formation of a low-shear-strength film of copper chloride at the chip–tool interface, which acts as a boundary lubricant, preventing, to a large extent, intimate metallic contact between the chip and tool. Under dry cutting conditions the intimate contact between chip and tool results in an extensive secondary deformation zone that has the appearance of a stable built-up edge. The effect of the lubricant is to reduce the intimacy of chip–tool, contact, thereby eliminating the built-up edge and secondary deformation. This elimination of the built-up edge and secondary deformation causes a reduction in friction at the chip–tool interface, reducing the forces required to form the chip.

Characteristics of an Efficient Lubricant in Metal Cutting

The work of Cassin and Boothroyd [3] has led to the suggestion that for a pure chemical compound to act as an efficient lubricant in metal cutting it should

1. Have a small molecular size to allow rapid diffusion and penetration to the chip–tool interface
2. Contain a suitable reactive ingredient that, on reaction with the work material, forms a compound of lower shear strength that acts as a boundary lubricant
3. Be sufficiently unstable to be broken down under the temperatures and pressures existing at the chip–tool interface

Carbon tetrachloride (CCl_4), chloroform ($CHCl_3$), trichloroethane (CH_3CCl_3), and certain other chlorinated hydrocarbons have been found to be efficient lubricants when cutting many metals at low speeds. One important exception to this, however, is the machining of lead. The compound formed when machining lead in the presence of a chlorinated fluid is lead chloride, and this compound has a higher shear strength than lead itself. Thus under these circumstances an increase in the tool–chip friction occurs following application of the fluid.

The main disadvantage in using pure compounds such as those mentioned above is their toxicity. The use of carbon tetrachloride in any process involving high temperatures is out of the question since when heated, carbon tetrachloride gives off a very poisonous gas (phosgene). However, one form of methyl chloroform (inhibited trichloroethane), an extremely efficient lubricant under low-speed conditions, has been found to have relatively low toxicity, and successes with its use in practice have been reported in broaching and tapping.

Figure 5.3 indicates the magnitude of the lubricating effect when copper is machined with a variety of compounds and two commercial fluids
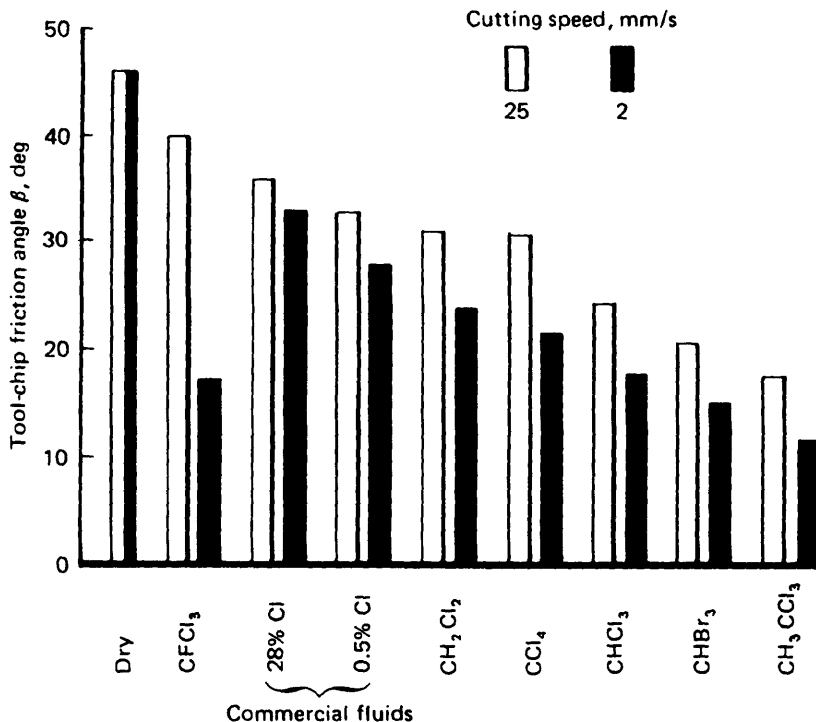
Figure 5.3 The lubricating action of various fluids, where the work material is copper, the undeformed chip thickness is 0.25 mm (0.01 in.), and the tool rake is 45 deg. (All fluids are applied liberally.) (After Cassin and Boothroyd [3].)

containing chlorinated additives. It can be seen that the lubricating effect of the commercial fluids is relatively small, and this small effect probably results from insufficient penetration of these fluids to the chip–tool interface during machining. Clearly, greater benefits could be obtained if a neat compound could be found that is safe to use under a range of practical cutting conditions.

The effectiveness of all cutting lubricants diminishes as the cutting speed is increased. An example of this is illustrated in Fig. 5.2 where the application of CCl_4 during the machining of copper had no effect on the chip–tool friction angle at cutting speeds greater than 0.5 m/s (100 ft/min). This diminished effect may be explained partly by a loss of penetration of the fluid to the chip–tool interface at these higher speeds and partly by the increased temperatures, which, according to the discussion in Sec. 5.3.1,

would be expected to reduce the effectiveness of the solid boundary lubricant formed.

The preceding discussion has been concerned with the effect of a lubricant on tool–chip friction during machining, which in itself is of little interest to the practical machinist. The machinist is more interested in the resulting surface finish, particularly at low cutting speeds where the effect of a built-up edge would be most pronounced. Clearly, a reduction in chip–tool friction would imply a reduction in the size of a built-up edge or its complete elimination, and this would give an improved surface finish. It may be accepted, therefore, that measurements of the effects of lubricants on tool–chip friction give an adequate guide to their performance in practice.

Tables 5.3 and 5.4 present the characteristics of neat cutting oils and a guide to their selection.

5.4 APPLICATION OF CUTTING FLUIDS

The cutting fluid cannot perform its function unless it is effectively delivered to the cutting zone. Fluids selected for lubricating properties

Table 5.3 Characteristics of Neat Cutting Oils[a]

Oil no.	Description	Viscosity (μm^2/s at 38°C)
1	Very-low-viscosity, inactive oil containing fatty and chlorinated additives	5.5
2	Inactive oil containing sulfurized fatty extreme-pressure additive	22.5
3	Inactive oil similar to No. 2 but with higher additive content	19.7
4	Multipurpose, chlorinated extreme-pressure oil with anti-stick-slip additives	37.8
5	Active oil containing free sulfur and sulfurized fat	25.0
6	Similar to No. 5 but with higher additive content	19.7
7	Inactive, extreme-pressure oil containing chlorinated and fatty additives; light in color	40.2
8	Low-viscosity, active oil containing free sulfur and sulfurized fatty additives	12.5
9	Special-purpose, highly chlorinated, active extreme-pressure oil	12.5

[a]After Holmes [1].

Table 5.4 Guide to the Selection of Neat Cutting Oils[a,b]

Machining operation	Workpiece material					
	Free-machining, nonferrous alloys	Tough, nonferrous alloys	Free machining and low-carbon steels	Medium-carbon steels	High-carbon and alloy steels	Stainless and heat-resistant alloys
Thread or form grinding	2	3	5	6 or 7		7
Turning	2 or 4	3 or 4		3, 4, or 5	6 or 4	6 or 7
Milling				4 or 5	6 or 7	
Drilling				5 or 6	6 or 8	8 or 9
Gear shaping				5 or 6		7 or 8
Hobbing	3		3 or 5	6 or 8		7 or 9
Broaching	3 or 4		6		8 or 9	9
Tapping	2	2 or 3			6 or 8	8 or 9

[a]The numbers refer to the oils listed in Table 5.3.
[b]After Holmes [1].

must be applied in such a way that a film can form on the sliding surfaces. Fluids chosen for cooling must gain access to the region of the tool cutting edge. This is usually achieved by flooding the cutting area with fluid, which effectively removes the heat generated by deformation of the work material. Additional problems occur in the application of cutting fluids in the grinding process owing to the high wheel speeds, and these are discussed in Chap. 9.

Continuous application of cutting fluids is generally preferred to intermittent applications, which cause temperature fluctuations. These temperature variations can lead to the formation of microcracks in hard and brittle tool materials, which may ultimately reduce the life of the cutting tools. Three main fluid application methods are used in practice for general cutting operations: manual, flood, and mist application.

5.4.1 Manual Application

Cutting fluids and lubricants are often applied manually, particularly for small-batch and jobbing shop production. Manual application with a brush by the operator is the easiest and least expensive method of fluid delivery. The main disadvantages of manual application are: (1) intermittent fluid application, (2) poor chip removal, and (3) limited access of the fluid to the cutting zone.

5.4.2 Flood Application

The most common method of fluid application is to flood the tool, workpiece, and cutting zone with fluid delivered from a low-pressure nozzle directed appropriately. Flood application allows a continuous flow of fluid to the cutting zone and helps to remove chips from the cutting zone. The cutting fluid drains into a sump in the base of the machine, where it is filtered before being pumped back to the delivery nozzle.

The effectiveness of flood application of cutting fluids depends on the geometry of the cutting process being used. Careful orientation of the delivery nozzles is necessary to ensure that the cutting fluid is not deflected away from the cutting zone by the rotating workpiece or tool.

5.4.3 Mist Application

Cutting fluids can be applied as an air-carried mist. Mist application is usually applicable to processes for which cutting speeds are high and the uncut chip thicknesses are relatively small, such as end-milling operations. This form of application can be used effectively when flooding is impractical, and it sometimes provides a means of applying cutting fluids

to otherwise inaccessible areas. The main disadvantage of mist application is the health risk due to inhalation of fluid droplets by the operator; consequently good ventilation is required.

5.5 SURFACE ROUGHNESS

The final surface roughness obtained during a practical machining operation may be considered as the sum of two independent effects:

1. The "ideal" surface roughness, which is a result of the geometry of the tool and the feed or feed speed
2. The "natural" surface roughness, which is a result of the irregularities in the cutting operation

5.5.1 Ideal Surface Roughness

The ideal surface roughness represents the best possible finish that may be obtained for a given tool shape and feed and can be approached only if built-up edge, chatter, inaccuracies in machine-tool movement, and so on, are eliminated. The ideal surface finish (which would be obtained under these ideal conditions) for the turning operation where a sharp-cornered tool is used is illustrated in Fig. 5.4a.

For the purposes of quantitative comparisons and analysis it is useful to be able to express the roughness of machined surfaces in terms of a single factor or index. The index most commonly used is known as the arithmetical mean value R_a and may be found as follows.

In the curve in Fig. 5.4b, which shows a cross section through the surface under consideration, a mean line is first found that is parallel to the general surface direction and divides the surface in such a way that the sum of the areas formed above the line is equal to the sum of the areas formed below the line. The surface roughness R_a is now given by the sum of the absolute values of all the areas above and below the mean line divided by the sampling length.

Thus, for the example in Fig. 5.4, the surface roughness value is given by

$$R_a = \frac{|\text{area } abc| + |\text{area } cde|}{f} \tag{5.2}$$

where f is the feed.

Since the areas abc and cde are equal,

$$R_a = \frac{2}{f}(\text{area } abc) = \frac{R_{\max}}{4} \tag{5.3}$$
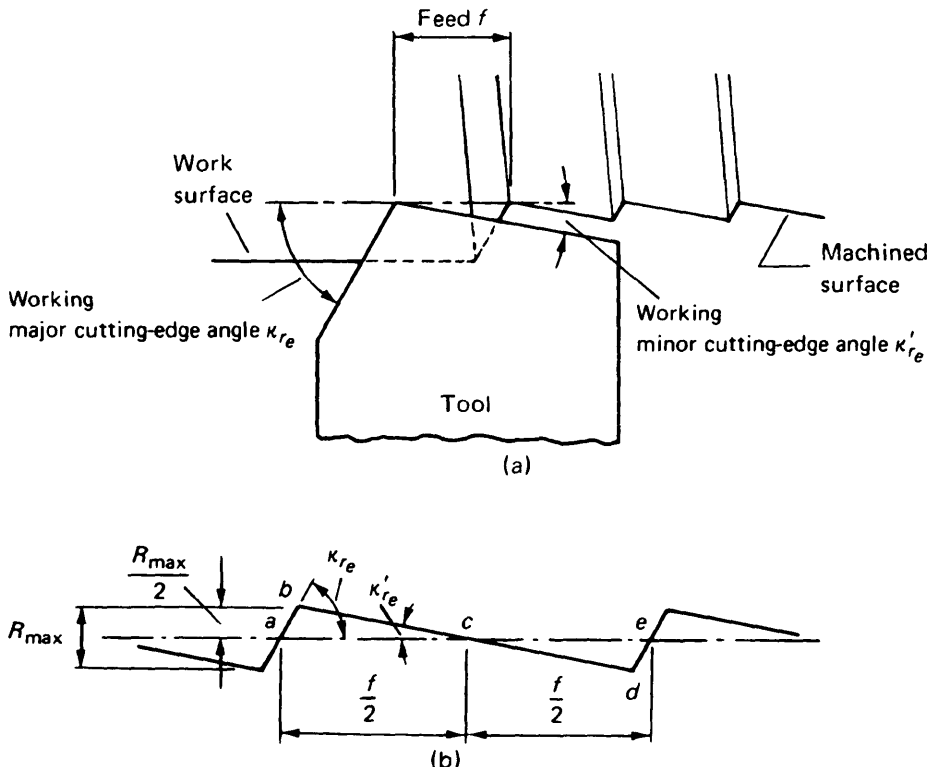
Figure 5.4 Idealized model of surface roughness for a cutting tool with a sharp corner, where κ_{r_e} = working major-cutting-edge angle, κ'_{r_e} = working minor cutting edge angle, and f = feed. (a) Surface produced; (b) cross section through surface irregularities.

where $R_{max}/2$ is the height of triangle *abc*.

It is interesting to note at this stage that the arithmetical mean value of surface roughness for a surface having uniform triangular irregularities is equal to one-quarter the maximum height of the irregularities.

Now by geometry

$$R_{max} = \frac{f}{\cot \kappa_{r_e} + \cot \kappa'_{r_e}} \tag{5.4}$$

where κ_{r_e} and κ'_{r_e} are the working major and minor cutting-edge angles, respectively.

Substitution of Eq. (5.4) in Eq. (5.3) gives

$$R_a = \frac{f}{4(\cot \kappa_{r_e} + \cot \kappa'_{r_e})} \tag{5.5}$$

Equation (5.5) shows that the arithmetical mean value for such a surface is directly proportional to the feed, and the curve in Fig. 5.5 [where Eq. (5.5) is plotted for a given feed and working major-cutting-edge angle] shows how the arithmetical mean value is affected by the working minor-cutting-edge angle.

Practical cutting tools are usually provided with a rounded corner, and Fig. 5.6 shows the surface produced by such a tool under ideal conditions. Deriving a theoretical equation giving the arithmetical mean value for such a surface is rather more difficult than in the preceding example, but it can be shown that this roughness value is closely related to the feed and corner radius by the following expression:

$$R_a = \frac{0.0321 f^2}{r_\varepsilon} \tag{5.6}$$

where r_ε is the corner radius.

In Fig. 5.7 the theoretical relationship between the surface-roughness value and the feed given by Eq. (5.5) is compared with experimental results. In these experiments, work material (copper) and cutting conditions were carefully chosen such that the natural surface roughness was extremely low, and no imperfections from the cutting action (chatter, built-up edge, etc.) were visible on the specimens. The operation was one of turning, and before each test the tools were carefully ground with the correct corner radius. Figure 5.7 shows that in these experimental results the actual roughness of the specimens was close to the "ideal" for each feed used.

5.5.2 Natural Surface Roughness

In practice, it is not usually possible to achieve conditions such as those described above, and normally the natural surface roughness forms a large proportion of the actual roughness. One of the main factors contributing to natural surface roughness is the occurrence of a built-up edge. The built-up edge may be continually building up and breaking down, the fractured particles being carried away on the undersurface of the chip and on the new workpiece surface. Thus, it would be expected that the larger the built-up edge, the rougher would be the surface produced, and factors tending to reduce chip–tool friction and to eliminate or reduce the built-up edge would give improved surface finish. Such factors would therefore
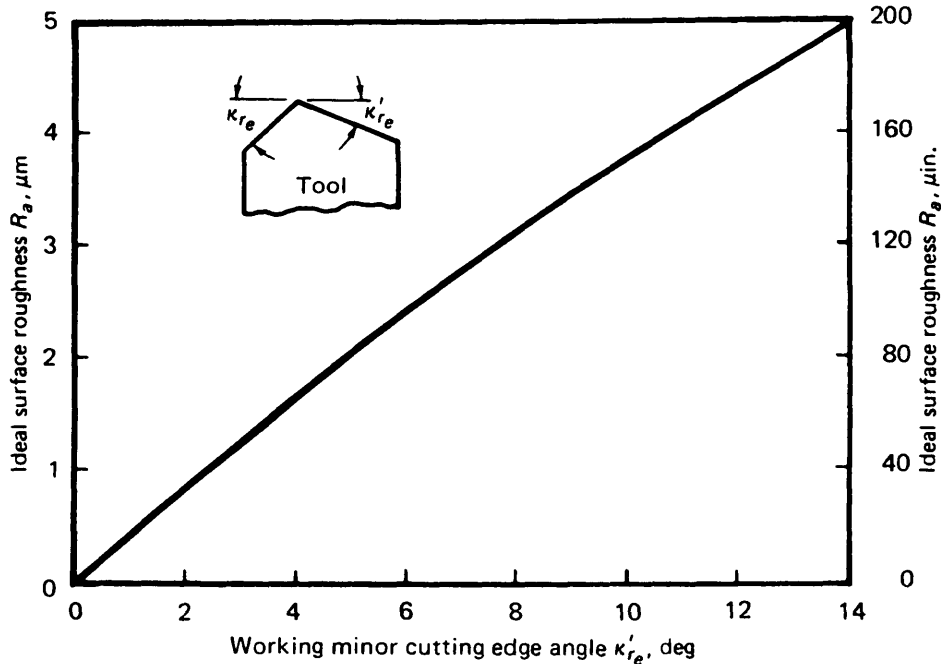
Figure 5.5 Effect of the minor-cutting-edge angle on an idealized model of surface roughness, where $\kappa_{r_e} = 45$ deg and $f = 0.1$ mm (0.004 in.).
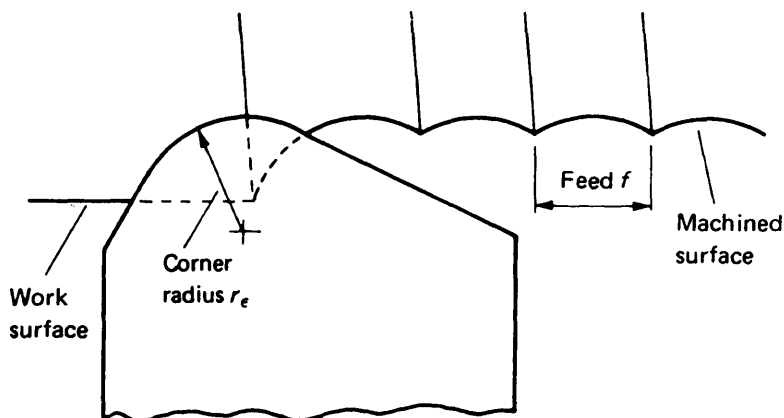
Figure 5.6 Idealized model of surface roughness for a tool with a rounded corner, where r_ε is the corner radius.
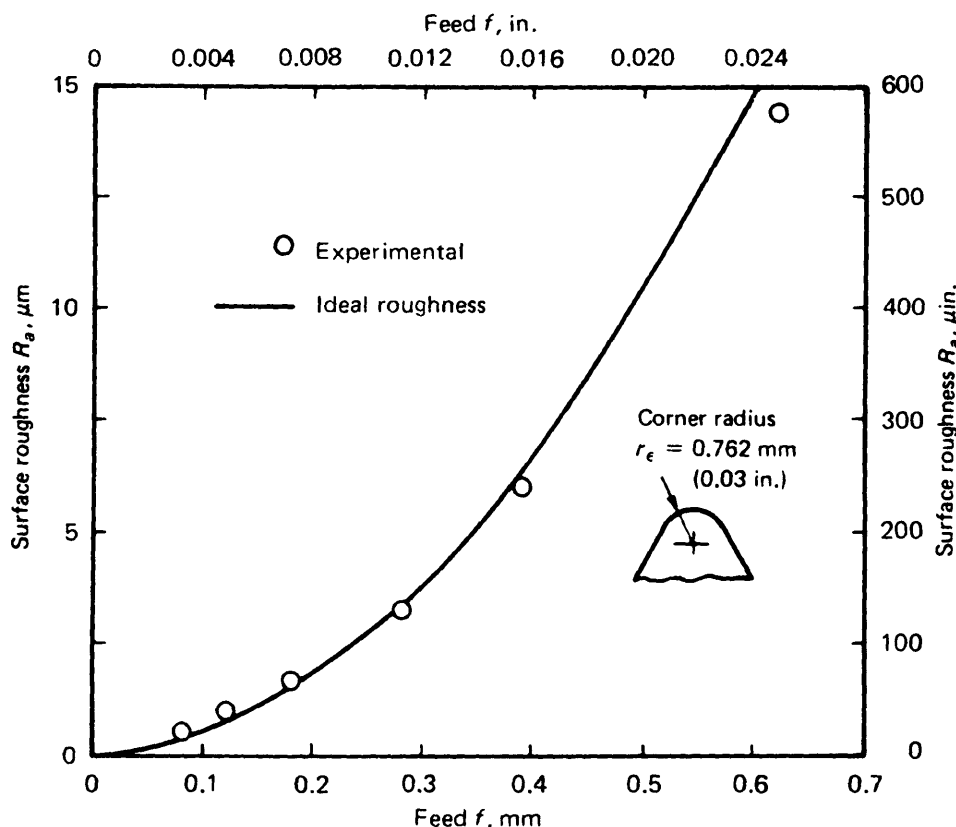
Figure 5.7 Comparison of experimental results with an idealized model of surface roughness.

be an increase in cutting speed, a change from, say, high-speed steel tool material to cemented carbide, the introduction of free machining materials such as leaded or resulfurized steels, the application of the correct cutting lubricant at low cutting speeds, and so on. An example of the effect of cutting speed is shown in Fig. 5.8, where the actual surface roughness for a turned component is large at low cutting speeds and becomes reduced as the cutting speed is increased, until it approaches the ideal surface roughness at high cutting speeds.

Other factors that commonly contribute to natural surface roughness in practice are

1. The occurrence of chatter or vibrations of the machine tool

Cutting speed v, ft/min
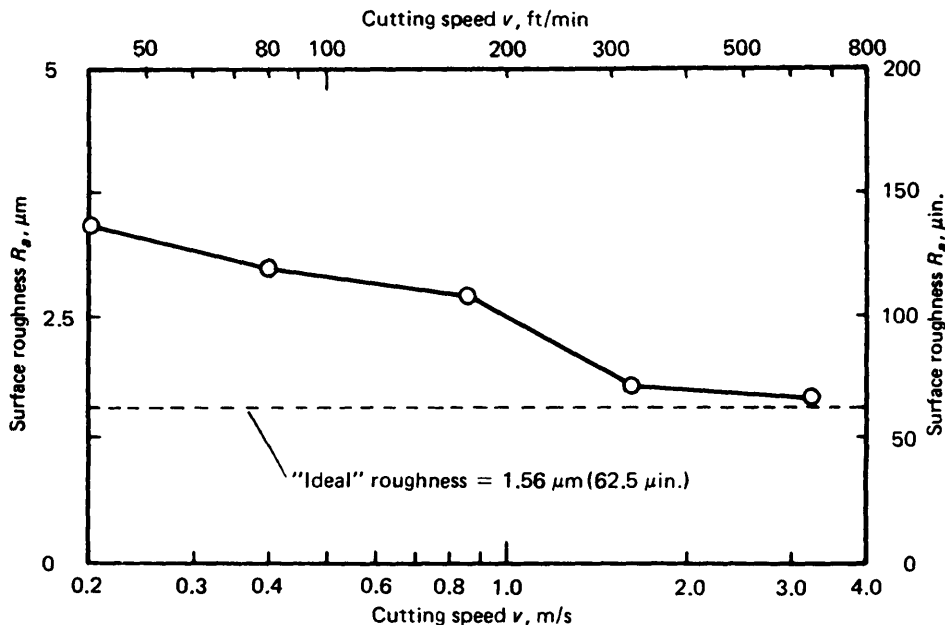
Figure 5.8 Effect of cutting speed on the surface roughness of turned specimens of mild steel.

2. Inaccuracies in machine tool movements such as the movement of the saddle on a lathe
3. Irregularities in the feed mechanism
4. Defects in the structure of the work material
5. Discontinuous chip formation when machining brittle materials
6. Tearing of the work material when ductile metals are cut at low cutting speeds
7. Surface damage caused by such factors as chip flow

The preceding discussion has been confined to the surface roughness produced by single-point tool operations. When consideration is given to the surface produced by multipoint cutting tools, it must be realized that because of the slight inaccuracies in the manufacture of the cutting tools or because of the inaccuracies of the primary motion of the machine tool, one tooth on the cutter plays a dominant role in generating the machined surface. Thus, in a slab-milling operation, for example, the surface roughness obtained under ideal conditions can be obtained by assuming that the cutting tool has only one tooth. Making the appropriate substitutions in Eq. (5.6) leads to the expression

$$R_a = \frac{0.0642}{d_t} \left(\frac{v_f}{n_t}\right)^2 \tag{5.7}$$

where

v_f = feed speed
d_t = diameter of the cutter
n_t = rotational frequency of the cutter

As a rough guide it can be stated that, in general, grinding processes will give surface roughnesses from 0.05 to 2.5 μm (2 to 100 μin.), diamond turning will give surface roughnesses from 0.1 to 1.0 μm (4 to 40 μin.), and milling and turning operations will give surface roughnesses greater than 1 μm (40 μin.).

5.5.3 Measurement of Surface Roughness

Before discussing the measurement of surface roughness, it is important to realize that other kinds of deviation from a perfectly smooth surface can occur. These deviations are called surface flaws and waviness. *Surface flaws* are widely separated irregularities that occur at random over the surface. They may be scratches, cracks, or similar flaws. *Waviness* is a form of regular deviation where the wavelength is greater than a specified magnitude (usually about 1 mm). Roughness is a finer irregularity than waviness and is superimposed upon waviness. A further term used in surface measurement is the lay. The *lay* of a surface is the direction of the predominant surface pattern and is usually determined by the machining method used to produce the surface. Measurements of a surface are made at right angles to the lay.

Instruments can be used to obtain an enlarged tracing of the surface irregularities; this tracing is known as the *surface profile*. These instruments operate by amplifying the vertical motion of a stylus as it is drawn across the surface; they can produce, in addition to a continuous recording of the profile on a strip of paper, a direct reading of the arithmetical-mean surface-roughness value. The arithmetical-mean surface-roughness value is obtained by a full-wave-rectifying and smoothing circuit connected to a galvanometer, and waviness is automatically eliminated by a frequency-cutoff device.

The ISO has recommended [4] a series of preferred roughness values and corresponding roughness grade numbers to be used when specifying surface roughness on drawings. The relationship between these numbers and the roughness values is shown in Table 5.5.

Table 5.5 ISO-recommended Roughness Values and Grade Numbers for the Specification of Surface Roughness

Roughness values R_a		Roughness grade numbers
µm	µin.	
50	2000	N12
25	1000	N11
12.5	500	N10
6.3	250	N9
3.2	125	N8
1.6	63	N7
0.8	32	N6
0.4	16	N5
0.2	8	N4
0.1	4	N3
0.05	2	N2
0.025	1	N1

PROBLEMS

1. A turning tool with a sharp corner and a major-cutting-edge angle of 60 deg is to be used at a feed of 0.05 mm. What minor cutting edge should be provided to obtain an arithmetical mean surface roughness under ideal conditions of 3 µm?

2. What corner radius should be ground on a tool with a rounded corner to give an arithmetical mean surface roughness of 10 µm when turning under ideal conditions with a feed of 0.25 mm?

3. A 150-mm-diameter slab-milling cutter has 10 teeth and is used at a feed speed of 1.5 mm/s. Estimate the "ideal" arithmetical mean surface roughness when the rotational frequency of the cutter is $3s^{-1}$.

REFERENCES

1. Holmes, P. M.: Factors affecting the selection of cutting fluids, *Ind. Lubr. Tribol.*, vol. 23, no. 2, pp. 47–55, 1971.

2. Bowden, F. P., and D. Tabor: *Friction and Lubrication of Solids*, Oxford University Press, London, 1954.

3. Cassin, C., and G. Boothroyd: The lubricating action of cutting fluids, *J. Mech. Eng. Sci. (GB)*, vol. 7, no. 1, pp. 67–81, 1965.

4. Technical Drawings—Methods of Indicating Surface Texture on Drawings, ISO Recommendation R1302, 1st ed., January 1971.

6
Economics of
Metal-Cutting Operations

6.1 INTRODUCTION

Of vital interest to the manufacturing engineer are production costs and
production rates. Although in practice a high production rate would prob-
ably mean low production costs, it should be pointed out that these two
factors must be considered separately and that the manufacturing con-
ditions giving maximum production rate will not be identical to those
conditions giving minimum cost of production.

Analysis of production costs and production rates can be a com-
plicated subject, and in many cases the analysis will apply only to the par-
ticular operation in question. However, experience gained over the years
has led to certain empirical rules or guiding principles for choosing the
optimum cutting conditions for a given machining operation, and it is the
object of this chapter to illustrate how these principles can be used.

In the following discussion the production time is defined as the aver-
age time taken to produce one component, and the production cost is
defined as the total average cost of performing the machining operation
on a component using one machine tool.

In general, the production of a component will involve several
machining operations using a variety of machine tools. Hence, the total

175

manufacturing costs, apart from the cost of the material, involve many items. For example, the raw material must be brought to the first machine and placed in the machine, and then when the first machining process is completed, the component must be removed, stacked, or stored temporarily, transported eventually to the second machine tool, and so on. It is found in practice that the cost of handling components between machines can represent a substantial proportion of total manufacturing costs. However, it is not proposed here to discuss the problem of materials handling but to analyze those factors involved in a particular machining operation. It will be assumed that the components are stacked next to the machine tool ready to be grasped by the operator and that the operator will stack the machined components conveniently near to the machine tool.

Assuming the appropriate tool and cutting fluid were chosen for the machining of a batch of components, the only cutting conditions to be determined are the cutting speed and feed.

For the purposes of this discussion it is necessary to explain that feed is the distance moved by the tool relative to the workpiece in the feed direction for each revolution of the tool or workpiece or each stroke of the tool or workpiece. Confusion may arise in certain multipoint tool operations, such as milling, where the feed settings on the machine refer to the relative speed between the tool axis and the workpiece in the feed direction (the feed speed).

Thus, if the feed speed in a milling operation is v_f and the rotational frequency of the tool is n_t, the workpiece feed during each revolution of the cutter is given by v_f/n_t and the maximum cutting speed v in a milling operation is given by $\pi d_t n_t$, where d_t is the tool diameter. It now follows that if it is required to double the cutting speed in a milling operation while keeping the feed constant, it will be necessary to double both the rotational frequency of the cutter n_t and the feed speed v_f.

With these considerations in mind it may be stated that in any operation, when either the cutting speed or feed are increased while the other condition is held constant, the actual machining time will be reduced, and the tool-wear rate will increase. Thus, very low speeds and feeds will result in a high production time because of the long machining time. Alternatively, very high speeds and feeds will result in a high production time because of the frequent need to change cutting tools. Clearly, an optimum condition will exist giving minimum production time. Similarly, an optimum condition will arise for minimum production cost. At low speeds and feeds costs will be high because of the cost of using the machine and operator for the long machining times. At high speeds and feeds costs will be high because of the cost of frequent tool replacement. The manufactur-

ing engineer's problem is how to minimize both the production time and the production cost. Since, in general, these objectives cannot be reached simultaneously, a compromise must be sought.

In this chapter the appropriate choice of feed will be discussed first. It will be shown that the correct feed to use in roughing operations is the highest the machine tool can withstand in terms of tool forces and power consumption. Next, optimum cutting-speed conditions will be analyzed for those operations involving constant cutting speeds (cylindrical turning, for example), and the optimum spindle-speed conditions will be analyzed for those operations involving variable cutting speeds (facing, for example). Finally, the analyses will be applied to practical machining operations and the advantages of modern tool materials and tool design will be illustrated.

6.2 CHOICE OF FEED

When a finishing cut is to be taken, the appropriate feed will be that which gives an acceptable surface finish. In this case the choice of feed is in the hands of the designer, who will have specified the surface finish requirements.

To explain how the appropriate feed is chosen in a roughing operation, it is first necessary to consider the relative effects of cutting speed and feed on tool life.

It can be concluded from the work in Chap. 3 that if changes in cutting speed affect neither the geometry of the cutting operation nor the specific energy consumption, the tool temperatures are a function of the thermal number, $\rho c v a_c / k$. Thus, equal changes in speed or feed should affect tool temperatures by the same amount. However, an increase in feed will not affect the relative speed of sliding at the wearing surface of the tool, whereas the speed of sliding will change in proportion to the cutting speed. Since tool wear is a function of both temperature and relative speed of sliding, it can be appreciated that increases in cutting speed will result in a greater reduction in tool life than similar increases in feed.

This conclusion agrees with practical experience and means that if an increased production rate is required in rough machining, it will always be preferable to increase the feed rather than increase the speed. Of course, this procedure will not always be practical since, in general, an increase in feed will increase the tool forces, whereas an increase in cutting speed will not. A limit on feed increase will therefore exist and will depend on the maximum tool force the machine tool is able to withstand. The guiding principle in choosing optimum cutting conditions in a roughing operation is that the feed should always be set at the maximum possible.

6.3 CHOICE OF CUTTING SPEED

Two distinct criteria can be used in choosing the cutting speed for a machining operation: minimum production cost and minimum production time. The optimum cutting speed giving minimum production cost in a constant-cutting-speed operation such as cylindrical turning will first be considered. In this case the time spent by the operator and his machine in producing a batch of components N_b can be separated into three items:

1. The nonproductive time, given by $N_b t_l$, where t_l is the time taken to load and unload each component and to return the tool to the beginning of the cut
2. The total machining time, given by $N_b t_m$, where t_m is the machining time for the component
3. The total time involved in changing worn tools, given by $N_t t_{c_t}$, where t_{c_t} is the tool changing time and N_t is the number of tools used

Thus, if M is the total machine and operator rate (including overheads), the total machine and operator costs will be

$$M(N_b t_l + N_b t_m + N_t t_{c_t}) \tag{6.1}$$

To this cost must be added the cost of the tools used, given by $N_t C_t$, where C_t is the cost of each tool. The average production cost C_{pr} for each component can now be written

$$C_{pr} = Mt_l + Mt_m + M\frac{N_t}{N_b}t_{c_t} + \frac{N_t}{N_b}C_t \tag{6.2}$$

The first item in this expression is the nonproductive cost, which is constant for the particular operation. The second item is the machining cost, which is reduced as the cutting speed is increased at constant feed. The final items are the tool costs, which increase as the cutting speed increases.

To calculate the number of tools used in producing the batch of components it is necessary to know the relationship between cutting speed and tool life. The work of Taylor [1] showed that an empirical relationship exists between these variables (Fig. 6.1), namely,

$$\frac{v}{v_r} = \left(\frac{t_r}{t}\right)^n \tag{6.3}$$

where
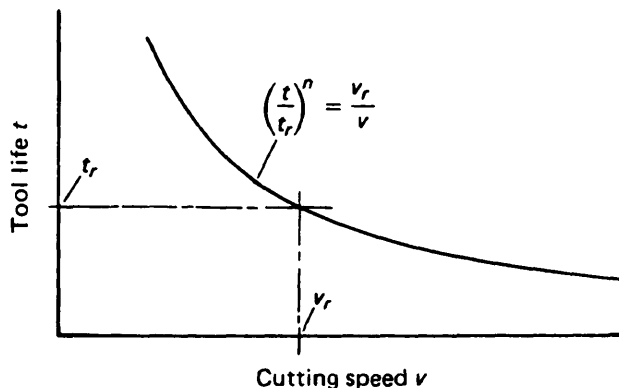
Figure 6.1 Taylor's tool-life relation, where n is a constant.

v = cutting speed
t = tool life
n = constant
t_r = measured tool life for a given cutting speed v_r

The value of t_r may be found for a particular workpiece and tool material and a particular feed either by experiment or from published empirical data. The index n depends mainly on the tool material; for high-speed steel $n \sim 0.125$, for carbide $0.25 < n < 0.3$, and for ceramics $0.5 < n < 0.7$. Figure 6.2 gives approximate ranges for the values of v_r for various tool and work materials when the tool life is 60 s.

The tool life t for a particular situation is therefore given by

$$t = t_r \left(\frac{v_r}{v} \right)^{1/n} \tag{6.4}$$

Traditionally, the Taylor tool-life equation has been applied in English units in the form

$$vt^n = C \tag{6.5}$$

where v is measured in feet per minute, t in minutes, and C, the cutting speed for 1 min of tool life, in feet per minute.

From Eq. (6.3), therefore,

$$\frac{v_r}{C} = \left(\frac{1 \text{ min}}{t_r} \right)^n \tag{6.6}$$

Brinnel hardness number
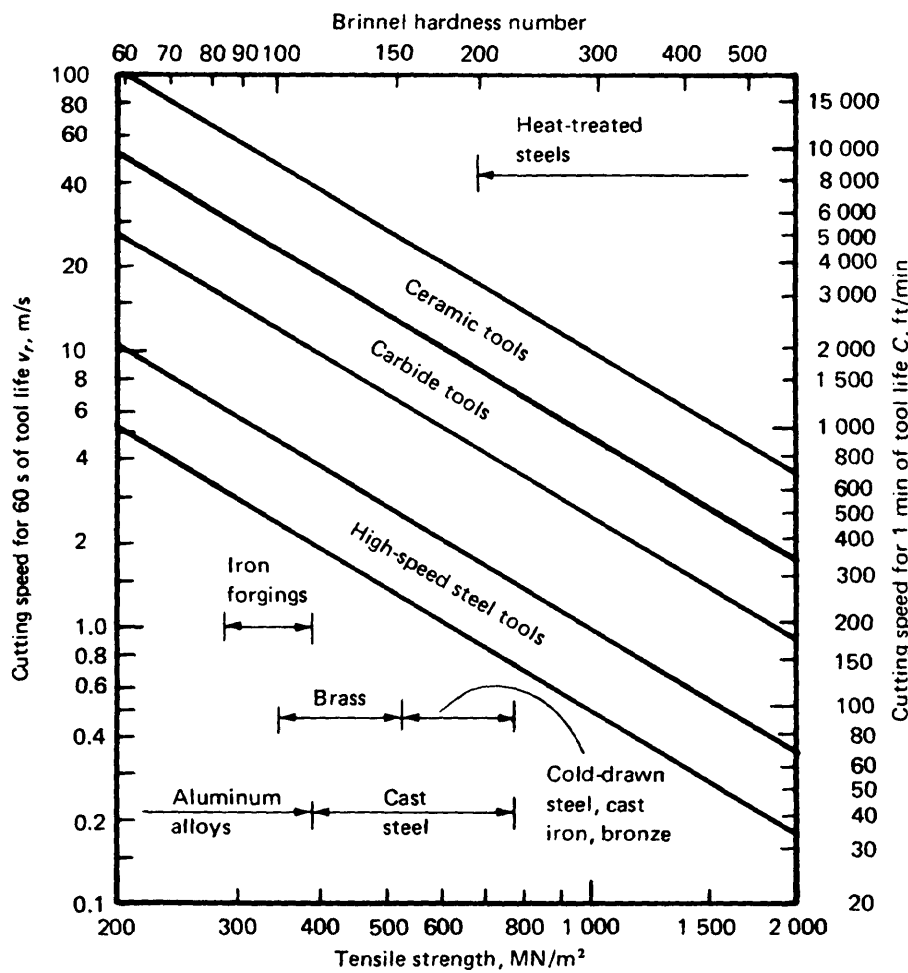
Figure 6.2 Approximate values of the cutting speed v_r when tool life $t_r = 60$ s.

Thus, the equation

$$\frac{197v_r}{C} = \left(\frac{60}{t_r}\right)^n \tag{6.7}$$

can be employed to convert previously published data to SI units.

The number of tools N_r used in machining the batch of components is given by $N_b t_m/t$, asuming that the tool is engaged with the workpiece during the entire machining time. Thus,

$$\frac{N_t}{N_b} = \frac{t_m}{t} = \frac{t_m}{\bar{t_r}} \left(\frac{v}{v_r}\right)^{1/n} \tag{6.8}$$

Finally, the machining time for one component is given by

$$t_m = \frac{K}{v} \tag{6.9}$$

where v is the cutting speed and K is a constant for the particular operation. In cylindrical turning, for example, the value of K will be given by $\pi d_w l_w / f$, where l_w is the length to be turned, d_w is the diameter of the workpiece, and f is the feed. In general, K can be regarded as the distance moved by the tool corner relative to the workpiece during the machining operation.

The relationship between the production cost and the cutting speed can now be obtained by substitution of Eqs. (6.8) and (6.9) in Eq. (6.2):

$$C_{pr} = Mt_l + MKv^{-1} + \frac{K}{v_r^{1/n}t_r} (Mt_{c_t} + C_t)v^{(1-n)/n} \tag{6.10}$$

To find the cutting speed v_c for minimum cost, Eq. (6.10) must now be differentiated with respect to v and equated to zero. Thus,

$$v_c = v_r \left(\frac{n}{1-n} \frac{Mt_r}{Mt_{c_t} + C_t}\right)^n \tag{6.11}$$

The effect of cutting speed on the cost of production can more clearly be shown in the form of a graph such as that in Fig. 6.3. In the figure the three individual cost items represented by the terms in Eq. (6.10), the nonproductive cost, the machining cost, and the tool costs, are plotted separately and show how an optimum cutting speed arises for a given set of conditions. It will be noted, from Eq. (6.11), that the optimum cutting speed is independent of the batch size and the nonproductive times involved.

To find the cutting speed giving maximum production rate (or minimum production time) it is necessary to follow a similar procedure to that described above. In this case inspection of Eq. (6.2) shows that the average production time for one component is given by

$$t_{pr} = t_l + t_m + \frac{N_t}{N_b} t_{c_t} \tag{6.12}$$
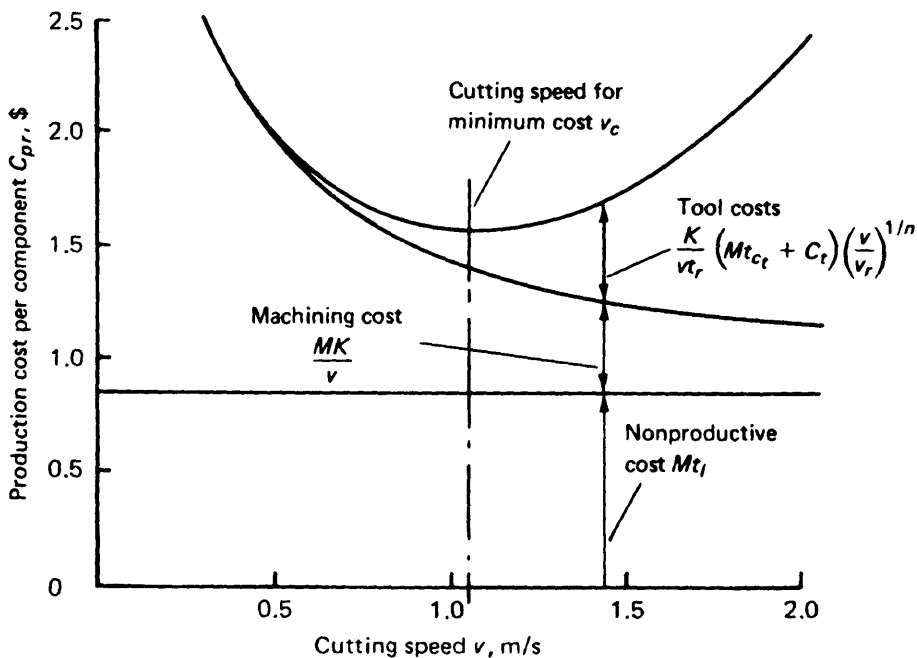
Figure 6.3 Variation in production cost per component C_{pr} with cutting speed v for a typical turning operation, where M = \$0.0028/s, C_t = \$2.1, t_{ct} = 240 s, n = 0.25, t_l = 300 s, K = 192 m, t_r = 60 s, and v_r = 2.75 m/s.

Substitution of Eqs. (6.8) and (6.9) in (6.12) and differentiation gives the cutting speed v_p for minimum production time. Thus

$$v_p = v_r \left(\frac{n}{1-n} \frac{t_r}{t_{c_t}} \right)^n \tag{6.13}$$

Comparison of Eqs. (6.11) and (6.13) shows that application of the criteria for minimum cost and minimum production time yield different conditions, and therefore the final choice of cutting speed requires a compromise. This compromise will be considered later.

6.4 TOOL LIFE FOR MINIMUM COST AND MINIMUM PRODUCTION TIME

In analyzing practical machining operations it is convenient to employ expressions for the optimum tool life for minimum cost t_c and the op-

timum tool life for minimum production time t_p. These expressions can be obtained by substitution of Eqs. (6.11) and (6.13), respectively, in Taylor's tool-life equation, Eq. (6.4). Thus,

$$t_c = \frac{1-n}{n}\left(t_{c_t} + \frac{C_t}{M}\right) \tag{6.14}$$

and

$$t_p = \left(\frac{1-n}{n}\right)t_{c_t} \tag{6.15}$$

For practical use the factor $(1-n)/n$ in Eqs. (6.14) and (6.15) is given the value 7 for high-speed steel, 3 for carbide, and 1 for oxide or ceramic. With these values the approximate expressions for the optimum tool life for various tool materials becomes for

High-speed steel:

$$t_c = 7\left(t_{c_t} + \frac{C_t}{M}\right) \tag{6.16}$$

$$t_p = 7t_{c_t} \tag{6.17}$$

Carbide:

$$t_c = 3\left(t_{c_t} + \frac{C_t}{M}\right) \tag{6.18}$$

$$t_p = 3t_{c_t} \tag{6.19}$$

Oxide or ceramic:

$$t_c = t_{c_t} + \frac{C_t}{M} \tag{6.20}$$

$$t_p = t_{c_t} \tag{6.21}$$

Finally, the corresponding optimum cutting speeds can be found from

$$v_c = v_r\left(\frac{t_r}{t_c}\right)^n \tag{6.22}$$

and

$$v_p = v_r \left(\frac{t_r}{t_p}\right)^n \tag{6.23}$$

From these equations it can be seen that before optimum conditions can be chosen, it is necessary to know the tool changing time t_{c_i}, the cost of providing a sharp tool C_t, the machine and operator costs M, and the cutting speed v_r for a particular tool life t_r. The following discussion indicates how some of these factors can be estimated.

6.5   ESTIMATION OF FACTORS NEEDED TO DETERMINE OPTIMUM CONDITIONS

The machine and operator costs include the operator's rate of pay plus the overhead associated with his or her employment and the depreciation rate of the machine tool plus the overhead associated with its use. The method of calculating these costs varies from factory to factory, but the following expression would be applicable in most cases:

$$M = W_o + \left(\frac{\text{percent operator overhead}}{100}\right) W_o$$
$$+ M_t + \left(\frac{\text{percent machine overhead}}{100}\right) M_t \tag{6.24}$$

where W_o is the operator's wage rate and M_t is the depreciation rate of the machine tool. Operator overhead can vary from 100 to 300 percent and includes the worker's benefits provided by the company, the cost of providing the working facilities, and the cost of the administrators necessary to employ the worker. Machine overhead includes the cost of the power consumed by the machine, the cost of servicing the machine, and possibly the cost of providing the location for the machine.

It is usual when calculating the machine depreciation rate to assume that its initial value can be written off, or amortized, after a certain number of years (amortization period). This period can vary from 2 to 10 years, depending on the type of machine and the tax depreciation rates determined by the Internal Revenue Service. The following expression would generally be used to estimate the machine depreciation rate:

$$M_t = \frac{\text{initial cost of machine}}{\text{number of working hours per year} \times \text{amortization period}} \tag{6.25}$$

The method used to estimate tool costs depends on the type of tool used. For regrindable tools the following expression can be used to estimate the cost of providing a sharp tool:

$$C_t = \text{cost of grinding} + \frac{\text{cost of tool}}{\text{average number of regrinds possible}} \qquad (6.26)$$

It should be realized that although a particular tool might theoretically be reground 20 times, the actual number of regrinds will generally be less because the tool becomes damaged or chipped through factors other than gradual wear during machining. In practice the actual number of regrinds might be less than one-half the theoretical number.

For disposable-insert tools, the cost of providing a sharp tool can be estimated from the following equation:

$$C_t = \frac{\text{cost of insert}}{\text{average number of cutting edges used per insert}}$$

$$+ \frac{\text{cost of holder}}{\text{number of cutting edges used during life of holder}} \qquad (6.27)$$

Again, it should be realized that the average number of cutting edges used per insert will generally be fewer than the number available, and an effort should be made to estimate the true figure.

The tool-changing time is the time required to remove the tool from the machine, place a new tool in the machine, set the new tool in its correct position, and restart the machining process. If a disposable-insert tool is used, the following expression applies:

$$t_{c_t} = \frac{\begin{array}{c}\text{time to index insert} \times \text{(average number of cutting}\\ \text{edges used per insert} - 1) + \text{time to replace insert}\end{array}}{\text{average number of cutting edges used per insert}} \qquad (6.28)$$

The cutting speed v, for a particular tool life t, depends on the tool material, tool shape, work material, and cutting conditions used. Values of v, can be obtained from values of C (the cutting speed for 1 min of tool life) for various materials and conditions tabulated in machining handbooks. A rough guide to the values is presented in Fig. 6.2.

6.6   EXAMPLE OF A CONSTANT-CUTTING-SPEED OPERATION

To illustrate the application of the expressions developed thus far it will be assumed that a large batch of steel shafts are to be rough-turned to a 76-

mm diameter for 300 mm of their length at a feed of 0.25 mm. A brazed-type carbide tool is to be used, and the appropriate constants in Taylor's tool-life equation for the conditions employed are as follows: $n = 0.25$, and $v_r = 4.064$ m/s when $t_r = 60$ s ($C = 800$ ft/min). The initial cost of the machine was \$10,800 and is to be amortized over 5 years. The operator's wage will be assumed to be \$0.0015/s (\$5.40/hr), and the operator and machine overheads are 100 percent. Tool-changing and resetting time on the machine is 300 s and the cost of regrinding the tool is \$2.00. The initial cost of a tool is \$6.00, and, on the average, it can be reground 10 times. Finally, the nonproductive time for each component is 120 s.

The first step in these calculations is to estimate the magnitudes of the relevant factors:

1. *The machine and operator rate M:* If the machine is to be used on an 8-hr shift per day, 5 days per week, and 50 weeks per year, each year will contain 7.2 Ms (7 $\times$ 10^6 s) of working time. The machine depreciation rate [Eq. (6.25)] is therefore

$$M_t = \frac{10,800}{7.2 \times 10^6 \times 5} = \$0.0003/s$$

and thus the machine and operator rate [Eq. (6.24)] is

$$M = 0.0003 + 0.0003 + 0.0015 + 0.0015 = \$0.0036/s$$

2. *The cost of providing a sharp tool C_t:* This cost can be found from Eq. (6.26) thus:

$$C_t = \$2.60$$

3. *The tool-changing time t_{c_t}:* This value is given as

$$t_{c_t} = 300 \text{ s}$$

It is now possible to estimate the tool life t_c and cutting speed v_c for minimum cost and the tool life t_p and cutting speed v_p for minimum production time. Thus from Eq. (6.18) for minimum cost

$$t_c = 3\left(t_{c_t} + \frac{C_t}{M}\right) = 3\left(300 + \frac{2.6 \times 10^3}{3.6}\right)$$

$$= 3.07 \text{ ks (51.2 min)}$$

and the corresponding cutting speed is given by Eq. (6.22):

$$v_c = v_r\left(\frac{t_r}{t_c}\right)^n = 4.064\left(\frac{60}{3070}\right)^{0.25}$$

$$= 1.52 \text{ m/s (299 ft/min)}$$

From Eq. (6.19), for minimum production time,

$$t_p = 3t_{c_t} = 900 \text{ s}$$

and the corresponding cutting speed [Eq. (6.23)] is

$$v_p = v_r\left(\frac{t_r}{t_p}\right)^n = 4.064\left(\frac{60}{900}\right)^{0.25}$$

$$= 2.065 \text{ m/s (407 ft/min)}$$

Unless conditions dictate that either the economics of the operation or production time is to be given priority, it is generally considered that any cutting speed between v_c and v_p will result in efficient machining. Since the majority of machine tools are provided with a limited selection of spindle speeds, a spindle speed giving a cutting speed within this range will be chosen; most probably the spindle speed selected would be the one giving a cutting speed closest to the cutting speed for minimum cost. In pursuing the present example it will be assumed that cutting speeds equal to both v_c and v_p can be obtained.

It is of interest to calculate the cost per component and the production time corresponding to the two criteria of minimum cost and minimum production time.

For minimum cost the time taken to machine one component t_m is given by Eq. (6.9), which for turning becomes

$$t_m = \frac{\pi d_w l_w}{vf} = \frac{\pi \times 76 \times 10^{-3} \times 300 \times 10^{-3}}{1.52 \times 0.25 \times 10^{-3}}$$

$$= 189 \text{ s (3.15 min)}$$

Since the tool life is 3070 s, each tool will produce 16 components, and the ratio N_t/N_b in the cost equation [Eq. (6.2)] will be equal to 0.0625. Thus, for each component

Nonproductive cost $= Mt_l = 3.6 \times 10^{-3} \times 120 = \$0.432$

$$\text{Machining cost} = Mt_m = 3.6 \times 10^{-3} \times 189 = \$0.68$$

$$\text{Tool cost} = \left(\frac{N_t}{N_b}\right)(Mt_{c_t} + C_t) = 0.0625[(3.6 \times 10^{-3} \times 300)$$

$$+ 2.6] = \$0.23$$

Finally the total cost C_{pr} is $1.34.

The production time can be found from Eq. (6.12). Thus, for each component

$$\text{Nonproductive time} = t_l = 120 \text{ s}$$

$$\text{Machining time} = t_m = 189 \text{ s}$$

$$\text{Tool changing time} = \left(\frac{N_t}{N_b}\right)t_{c_t} = 0.0625 \times 300$$

$$= 18.75 \text{ s}$$

Finally, the total production time t_{pr} is 328 s (5.5 min).

The conditions for minimum production time can be obtained in a similar way. In this case the machining time t_m is found to be 139.1 (2.32 min), the corresponding production cost C_{pr} is $1.55, and the production time 309 s (5.15 min). In this example it can be seen that use of the cutting speed giving minimum production time rather than minimum cost results in a reduction of the production time of 5.8 percent and an increase in the production cost of 15.7 percent. Whether this reduction in production time is worthwhile depends on the way the operation is financed. For example, if it is assumed that the factory is going to receive a fixed price for machining each component and that there is a high demand for the components, it is possible to calculate the profit involved in the operation of the particular machine over a given time period. Suppose the company is to receive $1.75 for each component; at minimum cost conditions over 1 year $(7.2 \times 10^6 \text{ s})$ the profit would theoretically be $9000. For minimum production time the figure would be $4660. Clearly, the minimum cost conditions would be preferable, and although the comparison will depend on many factors other than those considered above, this example illustrates a possible basis for establishing the compromise between minimum cost and minimum production time. The idea of machining at maximum efficiency is pursued in the next section.

6.7 MACHINING AT MAXIMUM EFFICIENCY

It has already been shown that if in a machining operation the minimum cost condition is chosen, production time will be greater than the mini-

mum. Also, if the condition for minimum production time is chosen, the cost of production will be higher than the minimum. To compromise between these two conditions the maximum rate of profit may be considered.

If S denotes the amount of money the machine shop receives for each component machined, the profit per component is given by $S - C_{pr}$, and the rate of profit P_r is given by

$$P_r = \frac{S - C_{pr}}{t_{pr}} \tag{6.29}$$

Substituting for C_{pr} and t_{pr} from Eqs. (6.10) and (6.12),

$$P_r = \frac{S - Mt_l - MKv^{-1} - Kv_r^{-1/n}t_r^{-1}(Mt_{c_t} + C_t)v^{(1-n)/n}}{t_l + Kv^{-1} + Kv_r^{-1/n}t_r^{-1}t_{c_t}v^{(1-n)/n}} \tag{6.30}$$

If Eq. (6.30) is now differentiated with respect to v, equated to zero, and combined with Eq. (6.3), the tool life t_{ef} for maximum efficiency (maximum rate of profit) is obtained. Thus,

$$t_{ef} = \frac{1 - n}{n}\left(t_{c_t} + \frac{t_l C_t}{S}\right) + \frac{C_t K}{nSv_r}\left(\frac{t_{ef}}{t_r}\right)^n \tag{6.31}$$

Unfortunately this equation can only be solved by numerical methods. However, a simple method would be to assume a value of t_{ef}^n equal to 6.5 s^n for carbide tools or 2.5 s^n for high-speed steel tools and substitute this value in the right side of Eq. (6.31) to obtain a new value of t_{ef}. This iteration procedure can be continued and will rapidly converge to a sufficiently close approximation.

One most interesting feature of Eq. (6.31) is that the condition for maximum efficiency is independent of the machine rate M. The ability to determine optimum machining conditions without a knowledge of M would be most helpful in practice because it is the uncertainty of overheads and amortization periods that makes M a difficult constant to estimate.

Figure 6.4 shows for a particular case how the rate of profit P_r varies with cutting speed (or tool life) for various values of the amount S charged for machining each component. Also shown on the graph are the conditions for minimum cost [Eq. (6.14)], minimum production time [Eq. (6.15)], and maximum efficiency [Eq. (6.31)].

It can be seen that if a profit is made, the condition for maximum efficiency always lies between the conditions for minimum cost and max-
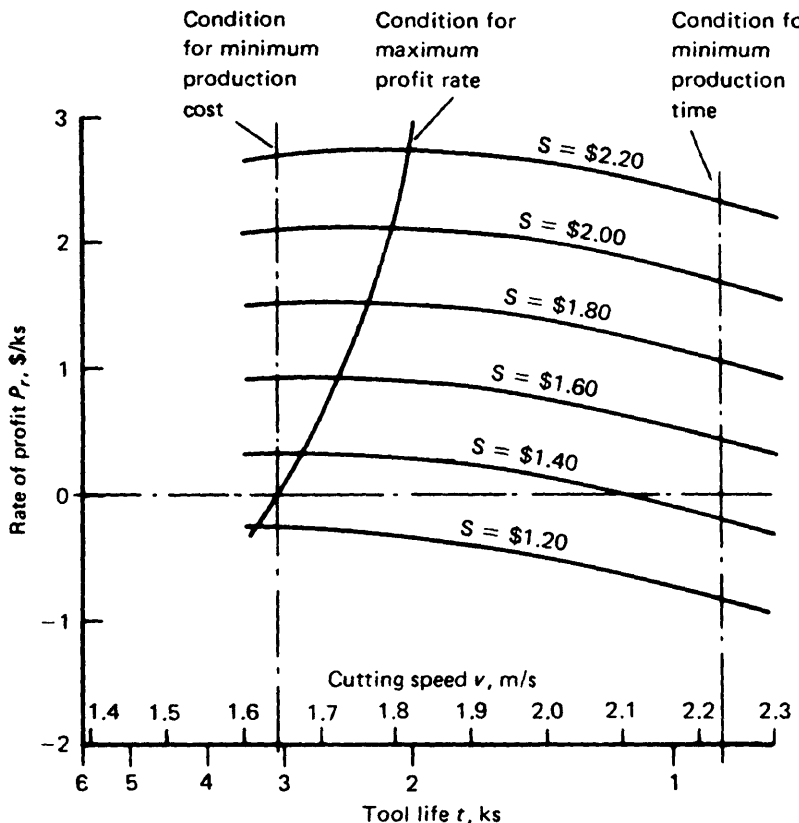
Figure 6.4 Effect of cutting speed v and tool life t on rate of profit P_r for a typical turning operation, where $M = \$0.00334/s$, $C_t = \$2.60$, $t_{c_t} = 300$ s, $n = 0.25$, $t_l = 60$ s, $K = 328$ m, $t_r = 1$ s, and $v_r = 12.2$ m/s.

imum production rate and that when the profit is zero, the condition for maximum efficiency becomes equal to the condition for minimum cost. It can also be seen that unless the profit is very high, the optimum condition for maximum profit lies close to the minimum-cost condition.

Before the equations already developed are used to compare the economics of different tool materials and tool designs, the optimum conditions for facing operations and operations involving interrupted cuts will be analyzed.

6.8 FACING OPERATIONS

Most machine tools are designed to operate at constant spindle speed. In a cylindrical-turning operation constant spindle speed gives a constant cutting speed, and the cutting speeds for minimum cost, minimum production time, and maximum efficiency can be calculated using the equations previously developed. In a facing operation, however, a constant spindle speed results in a variable cutting speed.

A facing operation is shown in Fig. 6.5. In this operation the cutting speed varies linearly with the radius of the cut r; the cutting speed is maximum at the periphery of the workpiece and minimum at the end of the operation. The tool-wear rate (the rate of increase of the flank wear-land width) will thus be maximum at the beginning of the cut and decrease as cutting proceeds. Figure 6.6 shows the flank wear-land width plotted against time as a tool is used to face several workpieces. In this graph the increase in tool flank wear-land width (VB) during the machining of each component is $(VB)_0$. Thus,

$$\frac{(VB)_0}{(VB)_m} = \frac{t_m}{t} \tag{6.32}$$

where $(VB)_m$ is the width of the wear land when the tool must be reground. Assuming the tool wears at a uniform rate at a given cutting speed, Taylor's tool-life equation (6.4) can be written

Feed f

Rotational frequency n_s
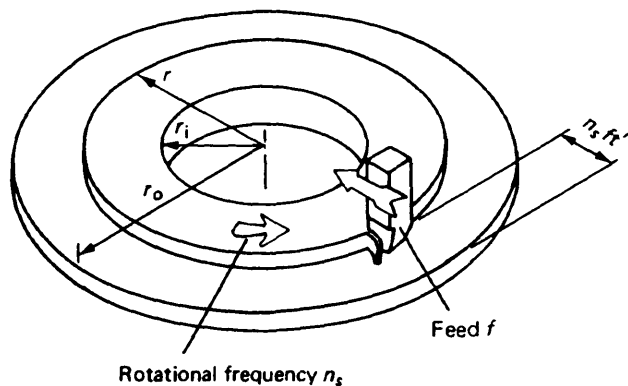
Figure 6.5 Facing operation.
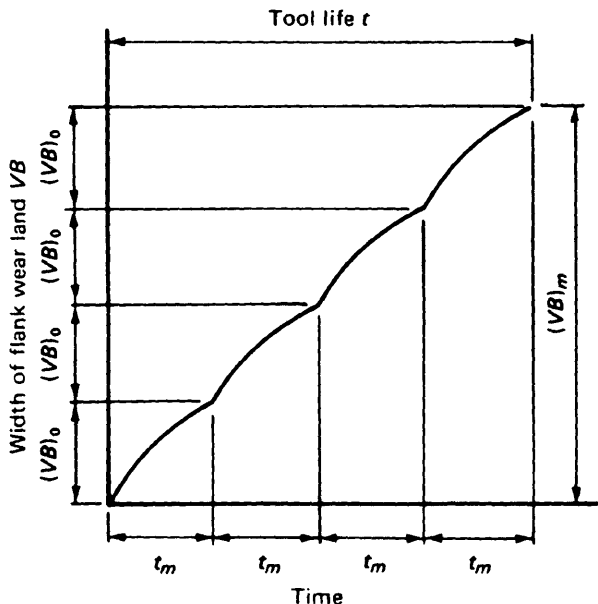
Figure 6.6 Tool wear during the facing of several components, where $(VB)_0$ = increase in wear-land width per component, $(VB)_m$ = maximum wear-land width, t = tool life, and t_m = machining time per component.

$$\frac{(VB)_m}{d(VB)/dt'} = t_r \left(\frac{v_r}{v}\right)^{1/n} \tag{6.33}$$

where $d(VB)dt'$ is the rate of increase of wear-land width.

The instantaneous cutting speed v is given by

$$v = 2\pi n_s r \tag{6.34}$$

where n_s is the rotational frequency of the machine spindle and the instantaneous radius at which cutting is taking place, r, is given by

$$r = r_o - n_s f t' \tag{6.35}$$

where

f = feed
r_o = outside radius of the workpiece
t' = time

Combination of Eqs. (6.33) and (6.34) and integration gives

$$\int_0^{(VB)_0} d(VB) = \int_0^{t_m} \frac{(VB)_m}{t_r} \left(\frac{2\pi n_s r}{v_r} \right)^{1/n} dt'$$

(6.36)

Substitution of

$$dr = -n_s f \, dt'$$

(6.37)

from Eq. (6.35), integration, and rearrangement yields

$$\frac{(VB)_0}{(VB)_m} = \frac{t_m}{t} = \frac{N_t}{N_b} = \left(\frac{2\pi n_s}{v_r} \right)^{1/n} \frac{n}{f n_s t_r (n + 1)} (r_o^{(n+1)/n} - r_i^{(n+1)/n})$$

(6.38)

Finally, the machining time t_m is given by

$$t_m = \frac{r_o - r_i}{n_s f}$$

(6.39)

To find the optimum spindle speed n_{s_c} giving minimum cost of production, Eqs. (6.38) and (6.39) can be substituted in Eq. (6.2), which is then differentiated with respect to n_s and equated to zero. Thus,

$$n_{s_c} = \frac{v_r}{2\pi r_o} \left(\frac{1 + n}{1 - n} \frac{M t_r}{M t_{c_t} + C_t} \frac{1 - a_r}{1 - a_r^{(n+1)/n}} \right)^n$$

(6.40)

where a_r is equal to r_i/r_o. The tool life t_c for minimum cost is given by combining Eqs. (6.38) through (6.40). Thus,

$$t_c = \frac{1 - n}{n} \left(t_{c_t} + \frac{C_t}{M} \right)$$

(6.41)

Similarly, the tool life t_p for minimum production time and t_{ef} for maximum efficiency are found to be identical to those for constant-cutting-speed operations.

The corresponding spindle speed must, however, be obtained from

$$n_{s;c,p,ef} = \frac{v_{c,p,ef}}{2\pi r_o} \left[\left(1 + \frac{1}{n} \right) \left(\frac{1 - a_r}{1 - a_r^{(n+1)/n}} \right) \right]^n$$

(6.42)

where $v_{c,p,ef}$ is the cutting speed for a constant-cutting-speed operation cor-

responding to a tool life of t_c, t_p, or t_{ef}. In Fig. 6.7, Eq. (6.42) is plotted for values of n of 0.125, 0.25, and 0.5. It can be seen that when a_r approaches unity, $n_{s;c,p,ef}$ approaches $v_{c,p,ef}/2\pi r_o$.

6.9 OPERATIONS WITH INTERRUPTED CUTS

In all milling, shaping, and planing operations the cutter tooth is in contact with the workpiece for only a proportion of the machining time. If the tool life t_c for minimum cost, the tool life t_p for minimum production time, and the tool life t_{ef} for maximum efficiency are thought of as the life of the tool while the machine tool is operating, the expressions for these quantities derived earlier will still hold. However, when the cutting speeds that result in these values of tool life are calculated, it is necessary to correct for the proportion Q of the machining time t_m during which the cutting edge is engaged with the workpiece. Thus the tool life t_c, t_p, or t_{ef} should be multiplied by Q as shown in Eq. (6.43) before the cutting speed is calculated:
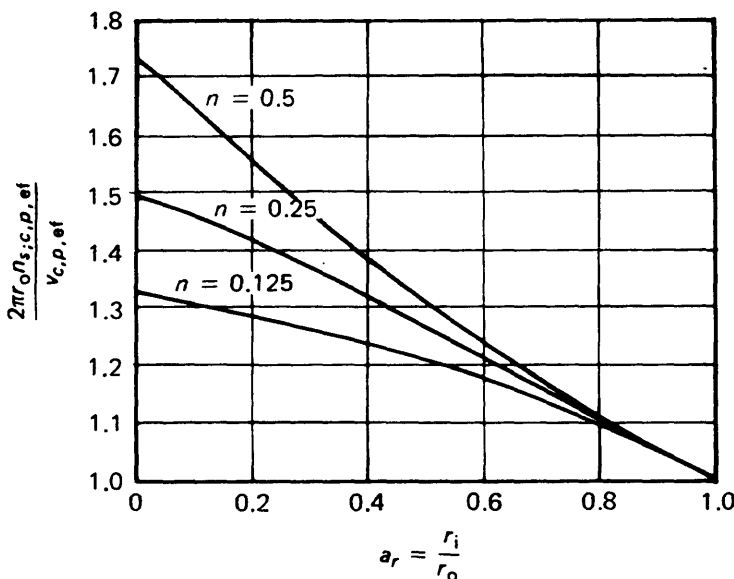
Figure 6.7 Effect of radius ratio a_r on the relation between optimum rotational frequency $n_{s;c,p,ef}$ for a constant spindle-speed operation and the cutting speed $v_{c,p,ef}$ for a constant-cutting-speed operation, where r_i = inside radius of surface to be faced and r_o = outside radius of surface to be faced.

$$v_{c,p,ef} = v_r \left(\frac{t_r}{Q t_{c,p,ef}} \right)^n \tag{6.43}$$

The values of q for slab milling, face milling, and side milling can be obtained from the geometries shown in Fig. 6.8.

Thus, for slab milling (Fig. 6.8a)

$$Q = \frac{\theta}{2\pi} = \frac{1}{4} + \frac{1}{2\pi} \arcsin\left(\frac{2a_e}{d_t} - 1 \right) \tag{6.44}$$

where a_e is the working engagement and d_t is the tool diameter. For side milling (Fig. 6.8b)

$$Q = \frac{\theta}{2\pi} = \frac{1}{4} + \frac{1}{2\pi} \arcsin\left(\frac{2a_e}{d_t} - 1 \right) \tag{6.45}$$

and for face milling (Fig. 6.8c)

$$Q = \frac{\theta}{\pi} = \frac{1}{\pi} \arcsin \frac{a_e}{d_t} \tag{6.46}$$

unless a_e is greater than or equal to d_t when Q is 0.5.

6.10 ECONOMICS OF VARIOUS TOOL MATERIALS AND TOOL DESIGNS

The principal tool materials of interest are high-speed steel, cemented carbide, and ceramics in increasing order of hardness and reducing order of toughness. The material most commonly used in practice is high-speed steel because it can be used in the manufacture of cutting tools of complicated shapes (for example, reamers, drills, taps, dies, and various milling cutters). Owing to the need to form it in its final shape and its high cost, cemented carbide is limited to applications where the individual inserts can be either brazed or clamped onto a steel body or toolholder. Thus, cemented carbide is generally limited to rough- or finish-turning and face-milling operations. Ceramic tool material (aluminum oxide) must also be manufactured in insert form and is used in disposable-insert single-point tools. Also, because it is brittle it cannot withstand the high forces involved in roughing operations and is generally used only in finish-turning operations.
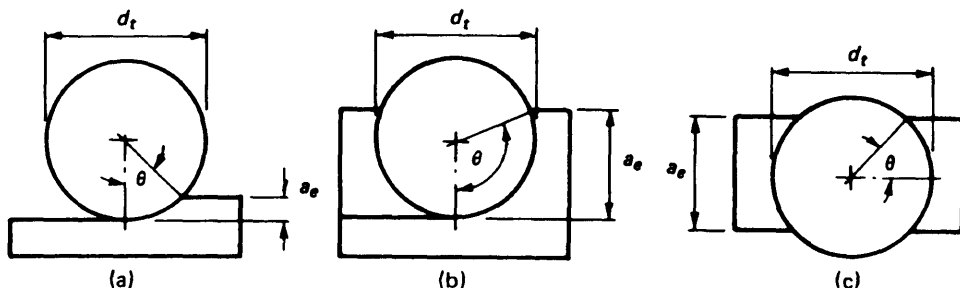
Figure 6.8 Determination of proportion Q of machining time when the cutting edge is engaged with the workpiece during milling, where a_e = working engagement and d_t = diameter of tool. (a) Slab milling; (b) side milling; (c) face milling.

For economic comparison, only those conditions giving minimum cost will be employed. Three comparisons are made in this section:

1. A rough-turning operation using both a high-speed steel tool and a brazed-carbide tool
2. A finish-turning operation using both a brazed- and a disposable-insert carbide tool and an aluminum oxide disposable-insert tool
3. A milling operation and a shaping operation

The first comparison, presented in Table 6.1, shows that although the optimum tool life for minimum cost was similar for both a high-speed-steel tool and a brazed-carbide tool, the production time using the high-speed-steel tool material was roughly twice that obtained with carbide. It can also be seen that although the cost of providing a sharp carbide tool was seven times the cost of providing a sharp high-speed-steel tool, the lower production time reduced the total production costs by 44 percent.

Table 6.2 shows an economic comparison between three different tools used in a finish-turning operation. The first tool is a brazed-carbide tool, the second is a disposable-insert carbide tool, and the third is a disposable-insert ceramic tool. The advantages of the disposable-insert tools are immediately evident: lower tool costs and shorter tool-changing time. Comparison of the first two columns, where the same tool material (carbide) is used, shows that disposable-insert tools hold considerable economic advantages: production time is decreased by 19 percent and production cost by 20 percent. This reduction of time and cost illustrates why the introduction of disposable-insert-type tools is one of the most important developments in the machining process.

Table 6.1 Minimum Production Costs and Corresponding Production Times for a Rough-Turning Operation Using High-Speed Steel and Brazed-Carbide Tools

Production costs and times	Type of tool	
	High-speed steel	Brazed carbide
Proportion of machining time when cutting edge is engaged Q	1.0	1.0
Machine and operator rate M, \$/s	0.0028	0.0028
Cost of sharp tool C_t, \$	0.30	2.10
Tool-changing time t_{c_t}, s	240	240
Tool-life index n	0.125	0.25
Tool life for minimum cost, $t_c = [(1/n) - 1]$ $[t_{c_t} + (C_t/M)]$, ks	2.43	2.97
Cutting speed for 1 min of tool life v_r, m/s	0.508	2.73
Cutting speed for minimum cost $v_c = v_r(60/Qt_c)^n$, m/s	0.32	1.03
Distance moved by cutting edge relative to workpiece K, m	200	200
Machining time $t_m = K/v_c$, s	625	194
Number of components produced per tool $= t_c/t_m$	4	15
Nonproductive time per component t_l, s	300	300
Tool-changing time per component $= (t_m/t_c)t_{c_t}$, s	60	16
Nonproductive cost per component, Mt_l, \$	0.84	0.84
Tool cost per component $= (t_m/t_c)(C_t + Mt_{c_t})$, \$	0.243	0.185
Machining cost per component Mt_m, \$	1.75	0.543
Total production time t_{pr}, s	985	510
Total cost per component C_{pr}, \$	2.83	1.57

The last column, disposable-ceramic tools, illustrates the advantages of ceramic tools for finishing operations. The much-higher cutting speeds possible with this material considerably reduce machining time and the costs. However, the extremely high cutting speeds required present a difficulty because most machine tools are not designed to operate under these conditions.

Table 6.3 compares a slab-milling operation and a shaping operation. Both of these operations involve interrupted cutting, and the tool life required correction before the cutting speed was calculated. This comparison is for the removal of an 18-mm- (0.71 in.) deep layer from the surface of a rectangular block 80 mm (3.15 in.) wide and 150 mm (5.9 in.) long. The feed in the shaping operation was limited to 0.13 mm (0.005 in.)

Table 6.2   Minimum Production Costs and Corresponding Production Times for a Finish-Turning Operation Using Brazed-Carbide, Disposable-Carbide, and Disposable-Ceramic Tools

	Type of tool		
Production costs and times	Brazed carbide	Disposable carbide	Disposable ceramic
Proportion of machining time when cutting edge is engaged Q	1.0	1.0	1.0
Machine and operator rate M, \$/s	0.003	0.003	0.003
Cost of sharp tool C_t, \$	2.00	0.25	0.40
Tool-changing time t_{c_t}, s	240	60	60
Tool-life index n	0.25	0.25	0.50
Tool life for minimum cost, $t_c = [(1/n) - 1][t_{c_t} + (C_t/M)]$, ks	2.72	0.43	0.193
Cutting speed for 1 min of tool life v_r, m/s	6	6	50
Cutting speed for minimum cost $v_c = v_r(60/Qt_c)^n$, m/s	2.35	3.73	28.3
Distance moved by cutting edge relative to workpiece K, m	1000	1000	1000
Machining time $t_m = K/v_c$, s	432	273	35.9
Number of components produced per tool $= t_c/t_m$	6	1	5
Nonproductive time per component t_l, s	240	240	240
Tool-changing time per component $= (t_m/t_c)t_{c_t}$, s	40	60	12
Nonproductive cost per component, Mt_l, \$	0.72	0.72	0.72
Tool cost per component $= (t_m/t_c)(C_t + Mt_{c_t})$, \$	0.453	0.43	0.116
Machining cost per component Mt_m, \$	1.296	0.819	0.108
Total production time t_{pr}, s	712	573	288
Total cost per component C_{pr}, \$	2.47	1.97	0.94

Table 6.3 Minimum Production Costs and Corresponding Production Times for the Machining of a Flat Surface 150 mm long and 80 mm wide Using a Horizontal Milling Machine and a Shaper

Production costs and times	Machining operation	
	Milling	Shaping
Proportion of machining time when cutting edge is engaged Q	0.14	0.75
Machine and operator rate M, \$/s	0.004	0.0025
Cost of sharp tool C_t, \$	20.00	0.50
Tool-changing time t_{c_t}, s	600	120
Tool-life index n	0.125	0.125
Tool life for minimum cost, $t_c = [(1/n) - 1]$ $[t_{c_t} + (C_t/M)]$, ks	39.2	2.24
Cutting speed for 1 min of tool life v_r, m/s	1.0	1.0
Cutting speed for minimum cost $v_c = v_r(60/Qt_c)^n$, m/s	0.57	0.66
Machining time $t_m = K/v_c$, s	140.4	186.4
Number of components produced per tool $= t_c/t_m$	279	12
Nonproductive time per component t_l, s	120	120
Tool-changing time per component $= (t_m/t_c)t_{c_t}$, s	2	10
Nonproductive cost per component, Mt_l, \$	0.48	0.300
Tool cost per component $= (t_m/t_c)(C_t + Mt_{c_t})$, \$	0.08	0.067
Machining cost per component Mt_m, \$	0.562	0.466
Total production time t_{pr}, s	262.4	316.4
Total cost per component C_{pr}, \$	2.12	0.833

because of the maximum cutting force the machine could provide. The feed speed in the milling operation was limited to 1.3 mm/s (3.07 in./min) because of the power available. In the milling operation a 100-mm- (3.94 in.) diameter cutter was employed. The calculation shows that the much-higher tool costs in milling result in a long economic tool life, but that since each cutter produces a large number of components, the tool costs per component are reasonably low. In this comparison the costs of the shaping operation are less than those for milling. This result is probably reasonable for such simple operations as the one used in the example. However, this operation should not be taken as typical: quite complicated shapes can be milled in one pass using "ganged" milling cutters or form milling cutters. Using a shaper in these situations would not be economic, prticularly if the batch size were large. In fact, a shaper is not considered to be a production machine tool and is generally only used when very small batches are to be machined because of the relatively low set-up time.

6.11   MACHINABILITY DATA SYSTEMS

The methods for determining the optimum feeds and speeds described in this chapter are based on the Taylor tool-life relationship [Eq. (6.5)]. In applying this equation a different value of the constants C and n exist for each tool–workpiece material combination utilized and for different cutting fluids used. Establishing the tool-life equation for a particular set of conditions requires lengthy cutting tests and wear measurements, which must be done for the whole range of tool and work materials under consideration. The extent of this task can be reduced by utilizing data found in handbooks [e.g., 2] or more recently in computer-based machinability data systems [3,4].

Two different types of machinability data systems can be identified: (1) data base systems and (2) mathematical model systems.

6.11.1   Data Base Systems

Data base systems incorporate a data base of large quantities of information from laboratory experiments and workshop experience. The data base can be accessed to determine the required items for the particular tool–work combination under consideration. Generally these systems include cost information as well as cutting parameter values.

6.11.2   Mathematical Model Systems

Mathematical model systems go a stage further than data base systems and incorporate the types of analysis methods described in this chapter for determining optimum feeds, speeds, and so on. Based on stored machinability data, the constants for the appropriate tool-life equations are determined and the optimum feeds and speeds are then determined using appropriate economic or production rate equations for the particular operation being considered.

PROBLEMS

1.   For single-shift working in a particular turning operation, the cost of the labor and machine time in resetting a cutting edge is $0.20, the cost of each throwaway insert having four cutting edges is $0.80, and the depreciation of the insert holder per insert is $0.08. The initial cost of the lathe was $20,000, which is amortized for 5 years. Machine running costs including labor and overhead but neglecting depreciation are estimated at $6.00/hr.

     If the Taylor tool-life index for the carbide inserts is 0.25, calcu-

late, for minimum-cost conditions, the tool life, in seconds (s), and cutting speed, in meters per second (m/s), if the machine is to be used on a

a. Single-shift, 40 hr/wk basis
b. Double-shift, 80 hr/wk basis

Assuming 50 working weeks per year, a cutting speed of 7.6 m/s, for 60 s tool life and a nonproductive time for loading and unloading a component of 3 min.

2. A batch of 1000 components is to be rough-turned to an 80-mm diameter for 300 mm of their length using a feed of 0.25 mm per revolution. The Taylor tool-life equation for the particular carbide tool–workpiece combination was found by experiment to be

$$vt^{0.25} = 28$$

where v is the cutting speed (in m/s) and t is the tool life (in s). If the cost per cutting edge for the particular throwaway-type insert tool is \$0.50 (including the tool depreciation and cost of resetting the cutting edge) and the total machine rate, including operator costs, is \$8.00/hr, calculate

a. The tool life (in s) to give minimum production costs
b. The cutting speed (in m/s) that will result in this optimum tool life
c. The total production time (in ks, assuming that the time taken to load and unload a component is 1 min, that the time taken to reset a cutting edge is 30 s, and that the initial setup time for the batch is 1 hr)
d. The total production cost, in dollars

3. A tool used in a turning operation is of the brazed-carbide-tip type. Its cost is \$10.00, and on the average it can be reground 10 times. The cost of regrinding is \$1.00. The lathe cost \$20,000 and is used for 8 hr per day, 5 days per week, 50 weeks per year. Its cost is to be amortized over 10 years, and the machine overheads are 100 percent. The operator's wage is \$5.00/hr, and operator overheads are 100 percent. The relation between cutting speed and tool life for the conditions employed is

$$vt^{0.25} = 7$$

where v is the cutting speed (in m/s) and t is the tool life (in s). The tool-changing time is 4 min, and the handling time per component is 5 min. The cutting distance per component is 200 m. Calculate the

a. Minimum production cost, in dollars
b. Minimum production time, in seconds

4. For the conditions of Prob. 3 calculate the tool life, in s, and cutting speed (in m/s), for maximum rate of profit and the corresponding production cost and production time. (Assume that the machine shop receives $4.00 for each component.)

5. From tool-life tests with a particular disposable-insert carbide tool and carbon steel workpiece the tool life was found to be 11.6 ks for a cutting speed of 1 m/s and 363 s for a speed of 2 m/s.

    The cost of the insert is $8 and it has four cutting edges. Indexing time is 10 s and insert replacement time is 30 s.

    a. For a machine and labor rate of $30/hr, what is the tool life for minimum cost (ks)? (*Note:* Neglect tool holder depreciation.)
    b. What cutting speed will give this tool life?

6. a. In a certain operation the high-speed-steel drills used cost $1.00 and under the conditions presently used have a life of 1500 s. The time to replace a worn drill is 30 s. If the machine plus operator and overheads cost $10/hr, by what percentage should the spindle speed be increased or decreased to maximize production rate.

    b. A turning operation is run under conditions of minimum cost with carbide tools. The tool-changing time is 100 s and the cost of a new tool edge is $0.50. If, as a result of a wage increase, the machine rate including operator and overheads rises from $12/hr to $16/hr, by what percentage should the cutting speed be increased or decreased.

7. The machining time in a particular turning operation is 200 s and the tool requires changing every five components. The nonproductive time (loading and unloading) is 300 s per component and the tool changing time is 150 s. The cutting speed is 2.5 m/s and the tool is a brazed-type carbide ($n = 0.25$) that requires an expenditure of $2.50 for regrinding (including depreciation).

    a. What should the cutting speed be changed to in order to operate at minimum cost? (Assume a machine depreciation rate of $5 per hour, operator wages of $6 per hour, and 100 percent overheads on operator and equipment.)
    b. How much would be saved per component by operating at minimum cost?

8. At present it takes 30 s to turn a workpiece and the tool must be reground after 80 workpieces. The Taylor tool-life relation for the tool–workpiece combination is:

$$vt^{0.25} = 7$$

where v is the cutting speed (in m/s) and t is the tool life (in seconds).

a. If the loading and unloading of a workpiece takes 20 s (including the time to return the tool to the beginning of the cut and if it takes 200 s to change a worn tool, what is the present average production time per component?

b. If the cutting speed is tripled, what will the new production time be?

c. If the cutting speed for maximum production rate were used, what would the tool life be (in seconds)?

9. In a slab-milling operation, four milling cutters are "ganged" to produce a shaped surface on a steel workpiece 200 mm in length. The largest cutter has a diameter of 150 mm, and all cutters are of high-speed steel. It takes 5 min to change the cutters, and the tool-life–cutting relationship is

$$vt^{0.125} = 2.65$$

where v is the cutting speed (in m/s) and t is the tool life (in s). The working engagement (depth of cut) for the largest cutter is 14 mm, and the machine and operator rate is $24.00/hr. Two of the milling cutters cost $80.00 each and cost $10.00 each to regrind; the remaining two cutters cost $100.00 each and cost $12.00 each to regrind. All cutters can be reground 20 times on the average. The time to remove and replace a component and return the cutters to the start of the cut is 3 min. Estimate the minimum production cost (in $) and the corresponding production time (in s), when the feed speed is 2 mm/s. Also, estimate the minimum production cost and corresponding production time if the machine is fitted with a special swivel vise that allows a new component to be positioned in the machine while the previous component is being machined. (Assume that this allows the nonproductive time per component to be reduced to 30 s.)

10. At present, on a single-spindle, deep-hole drilling machine one drill can drill six holes in a boiler end plate between regrinds. The drill speed is 25 s^{-1} and the drill has a carbide tip for which n in Taylor's tool-life relation is 0.25. The machining time per hole is 6 min. The machine cost $100,000 dollars and is to be amortized over 50,000 hours. The machine overheads are 70 percent, the operator's wage is $4.00/hr, and the operator overheads are $10.00/hr. The initial cost of

one drill is $50.00; it can be reground 10 times on the average at a cost of $2.00 per regrind. Drill-changing time is 6 min. Neglecting the drill-repositioning time, calculate the

    a. Cost per hole under present conditions, in dollars

    b. Drill speed to give minimum cost per hole, in reciprocal seconds (s^{-1})

    c. Cost per hole under minimum cost conditions, in dollars

11. A company is to purchase a new three-spindle deep-hole drilling machine at a cost of $250,000. The efficiency with which the three spindles can be employed is 90 percent because it will not always be possible to drill three holes simultaneously. Tool-changing time per drill will be 2 min, and the remaining costs will be the same as for the old machine described in Prob. 10. Calculate, for the new machine,

    a. The total cost per hole, in dollars, if the machine is operated at the present drill speed of 25 s^{-1}.

    b. The drill speed, in reciprocal seconds (s^{-1}), to give minimum cost per hole

    c. The total cost, in dollars, per hole under optimum conditions

REFERENCES

1. Taylor, F. W.: On the art of cutting metals, *Trans. ASME,* vol. 28, p. 31, 1906.

2. Partons, N. R., ed.: *N.C. Machinability Data Systems,* SME, Dearborn, MI, 1971.

3. Pressman, R. S., and J. E. Williams: *Numerical Control and Computer Aided Manufacturing,* Wiley, New York, 1977.

4. Groover, M. P., and E. W. Zimmers: *CAD/CAM,* Prentice-Hall, Englewood Cliffs, NJ, 1984.

7

Nomenclature of Cutting Tools

7.1 INTRODUCTION

The most important features of a cutting tool are the two cutting edges:

1. The major cutting edge, which usually removes the bulk of metal
2. The minor cutting edge, which mainly controls the final surface finish of the workpiece

and the faces and flanks that intersect to form the cutting edges. Figure 7.1 specifies the important features of a single-point cutting tool and the nomenclature describing these features. The figure also shows the application of a single-point cutting tool in a turning operation.

The geometry and nomenclature of cutting tools, even single-point cutting tools, are surprisingly complicated subjects. It is difficult, for example, to determine the appropriate planes in which the various angles of a single-point cutting tool should be measured; it is especially difficult to determine the slope of the tool face. A number of systems of geometric arrangements and nomenclature exists. To appreciate the advantages and disadvantages of different systems of cutting-tool nomenclature (e.g., the ISO-recommended system, the British maximum rake systems, or the
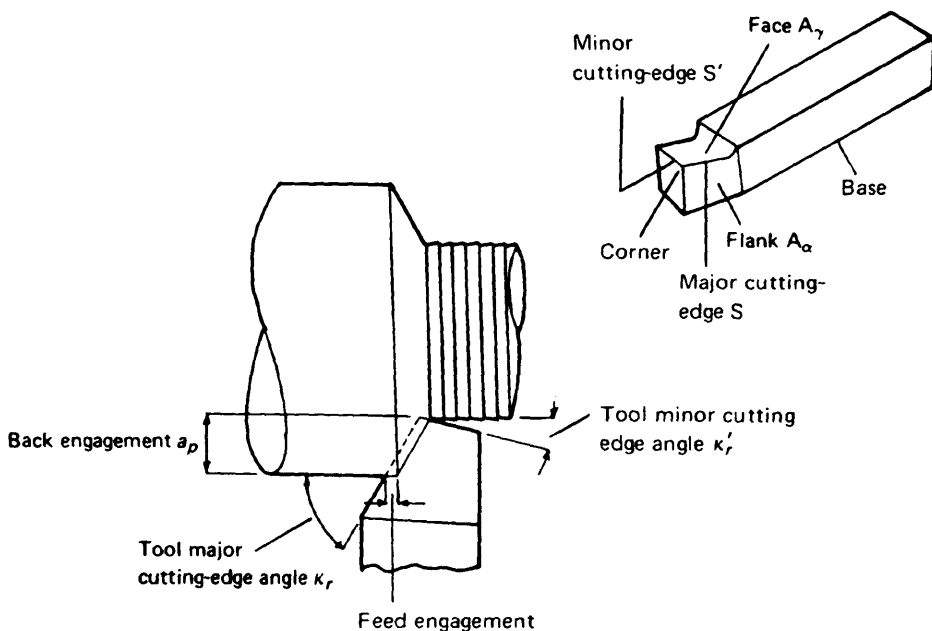
Figure 7.1 Terms applied to single-point tools and the single-point cutting operation.

American Standards Association system) it is necessary first to understand how the tool shape affects the direction in which the chip flows.

In much research work consideration is given only to the somewhat-artificial geometric arrangement known as orthogonal cutting. In the orthogonal arrangement shown in Fig. 7.2a the straight cutting edge of the wedge-shaped cutting tool is at right angles to the direction of cutting. Rarely in practice, however, is the cutting edge at right angles to the direction of cutting; most cutting operations involve oblique cutting, where the cutting edge is inclined. In the oblique arrangement shown in Fig. 7.2b the cutting edge is inclined at an angle λ_s (known as the cutting-edge inclination) to a line drawn at right angles to the direction of cutting. The cutting-edge inclination is measured in the plane of the new workpiece surface and in orthogonal cutting, $\lambda_s = 0$. With oblique cutting the chip flows up the tool face in a direction forming an angle λ_γ (chip-flow angle) with a line drawn on the face at right angles to the cutting edge. Figure 7.3 shows a development of the chip produced during oblique cutting: the part of the diagram below the line denoting the cutting edge is a view normal to the new workpiece surface, and that part above the cutting edge is a view nor-
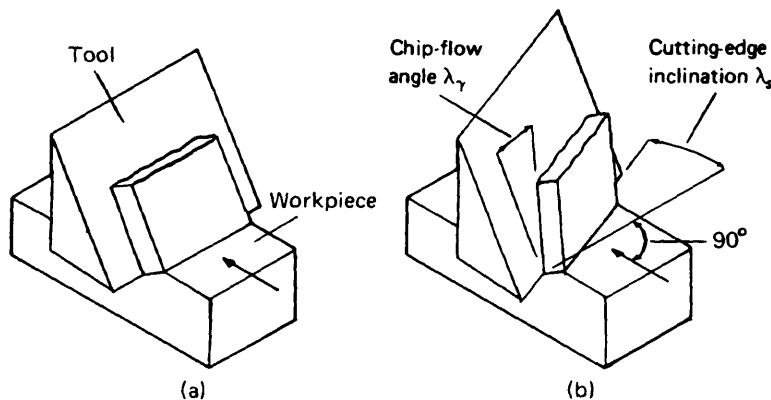
Figure 7.2 Basic cutting operations. (a) Orthogonal cutting; (b) oblique cutting.

mal to the tool face. The diagram shows that if the chip does not change in width during its formation,

$$\lambda_s = \lambda_\gamma \tag{7.1}$$

Experiments have shown that variations from this equality of inclination and chip-flow angles may occur in practice, but for most circumstances Eq. (7.1) gives an adequate approximation. It is of interest to note that Eq. (7.1) was proposed by Stabler [1] and is commonly known as Stabler's chip-flow law. The important result of Stabler's law is that the inclination of the cutting edge λ_s is a major parameter determining the direction of chip flow away from the cutting region and is, therefore, one important consideration in the design of practical cutting tools. Thus, any acceptable system of tool nomenclature should include a definition of cutting-edge inclination to give the system physical meaning in relation to the cutting process. A second important consideration in choosing a system of nomenclature related to the grinding of cutting tools is that it should be possible to set the specified tool angles directly onto the grinding vise or jig. With these two important points in mind, the various systems of cutting-tool nomenclature used in the past are now considered.

7.2   SYSTEMS OF CUTTING-TOOL NOMENCLATURE

7.2.1   British Maximum-Rake System

Figure 7.4 illustrates the old British system (1886), where the slope of the tool face was measured in a plane normal to the tool base and to the tool
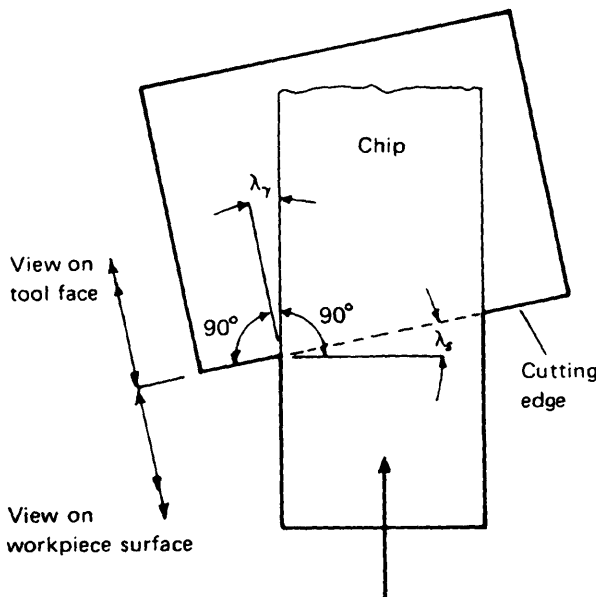
Figure 7.3   Demonstration of Stabler's chip-flow law ($\lambda_s = \lambda_\gamma$).

face, that is, in the direction of maximum slope. This method had the advantage that the specified angles could be set on a grinding vise and the face ground to the specified angle. The difficulty with this system was that the angles specified were quite independent of the position of the cutting edge, and, therefore, complicated expressions or a set of curves had to be used to estimate the direction of chip flow. It has been suggested that the system developed from the idea that the chip flows in the direction of maximum slope of the tool face. Since this idea is not even approximately true, the system had no physical significance in relation to the cutting process.

7.2.2   American Standards Association System

The American Standards Association (ASA) system (Fig. 7.5a) specified the tool face by defining its slope in two orthogonal planes: one parallel to and the other perpendicular to the axis of the cutting tool, both planes being perpendicular to the base of the tool. The two angles thus specified are known as the tool back rake and tool side rake (Fig. 7.5a).

In this system, as in the British maximum-rake system, the angles were specified independently of the position of the cutting edge and,

Tool-face orthogonal
plane P$_g$ (perpendicular
to tool base and tool face)

Tool geometric rake γ_g
(previously maximum rake)

Section on P$_g$

View normal to
tool base
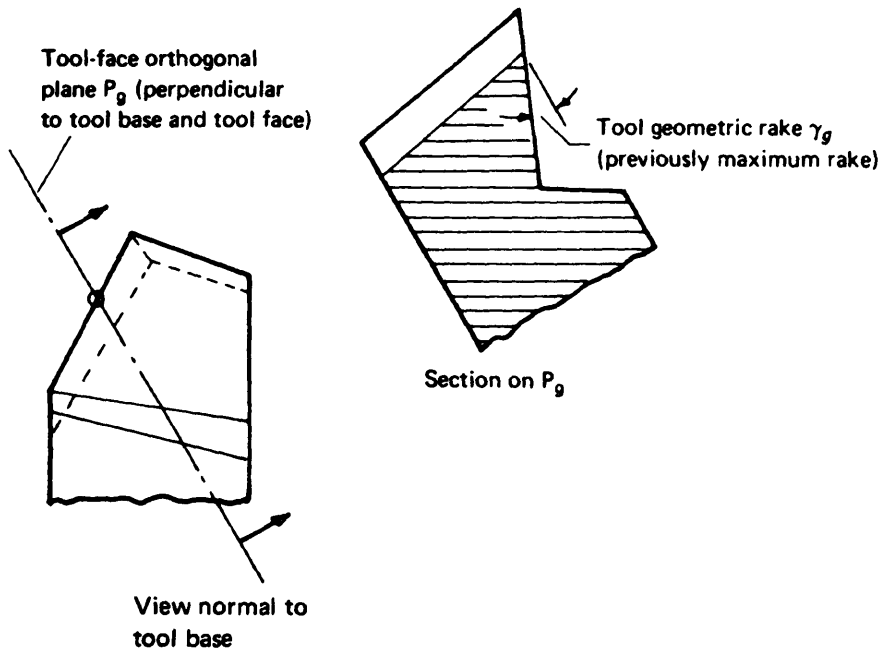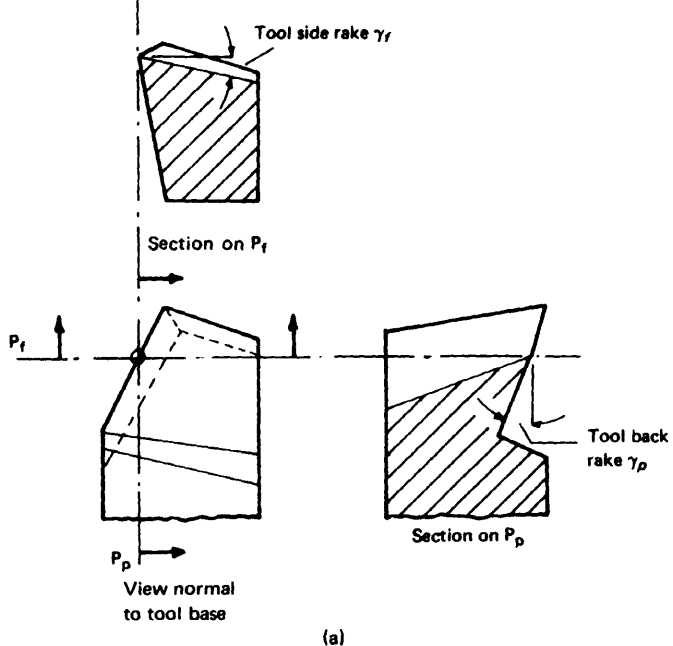
Figure 7.4 Early British maximum-rake system.

therefore, gave no indication of the behavior of the tool in practice. The advantage of the system was always considered to be the simplicity of its use in the grinding of single-point cutting tools; yet a tool cannot be ground accurately to the back rake and side rake without using equations or curves.

For example, suppose a two-axis vise is used when the tool is being ground. The vise has protractor axes A and B perpendicular to each other, and both lie in horizontal planes when set at zero. The tool is mounted in the vise in such a way that the upper of the two axes, A, is parallel to the tool axis. If the tool face is to be surface-ground, the vise must be used to arrange the future tool face in a horizontal plane. If axis B is used first to tilt the tool forward through an angle γ_p to set the tool back rake (Fig. 7.5b), the axis A may be used to rotate the tool about its own axis through an angle γ_f equal to the tool side rake. Unfortunately this last operation will also have rotated the plane in which the back rake should be measured; therefore, the back rake setting should be adjusted accordingly. Consideration of Fig. 7.5b shows that if the required tool back rake is γ_p, axis B
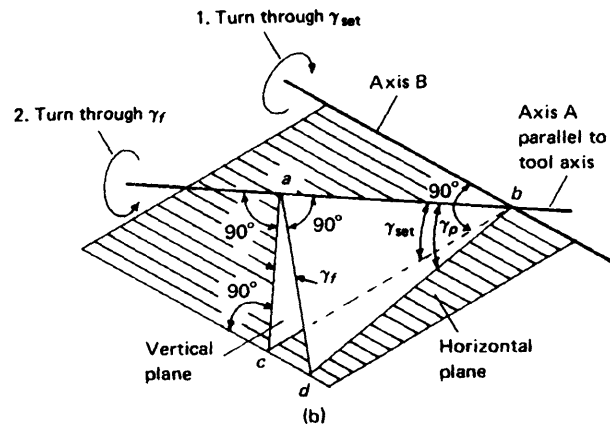
Figure 7.5 (a) Early American Standards Association (ASA) system; (b) construction to determine tool back-rake compensation owing to the tool side-rake setting, where $ab = ac \cot \gamma_{set}$, $ab = ad \cot \gamma_p$, and $ac/ad = \cos \gamma_f = \tan \gamma_{set} \tan \gamma_p$. (Axis A is the upper axis on the vise.)

should have been set at γ_{set}, which may be obtained from the following expression:

$$\tan \gamma_{set} = \cos \gamma_f \tan \gamma_p \tag{7.2}$$

where γ_f is the tool side rake.

In practice, this compensation was nearly always ignored, and when the two angles were small, the resulting error was negligible. Nevertheless the system still had the main disadvantage that the angles were independent of the cutting edge.

7.2.3 German System

The German (DIN) system also specified two rake angles, called back rake and side rake (Fig. 7.6), but in the German system the angles were related to the position of the cutting edge. The German back rake was the slope of the cutting edge measured in a plane containing this edge and perpendicular to the tool base; the German side rake was the slope of the tool face measured in a plane that was both perpendicular to the plane in which back rake was measured and perpendicular to the tool base. This system had some physical meaning in relation to the cutting process because both angles were specified in relation to the edge of the tool that performs the cutting operation.

A difficulty arose, however, when the system was used for grinding a cutting tool. The problem is similar to that occurring in the American system. The procedure for grinding a tool to the German system was as follows:

1. The tool was clamped in a universal vise with three orthogonal protractor axes A, B, and C set at zero.
2. The desired major cutting-edge angle was set on the top vertical axis A such that the future cutting edge lay parallel to the third bottom axis C.
3. The desired German back rake was set on the second, horizontal axis B in order to bring the future cutting edge in a horizontal plane.
4. The next step was to set the German side rake on the bottom axis C, but it will be seen that rotation of this axis rotated the tool about the future cutting edge. Thus, the side rake was being measured in a plane normal to the cutting edge and not perpendicular to the tool base. For accurate grinding, the setting on axis C should have been adjusted (depending on the setting of axis B) using equations or curves in a manner similar to that of the American system.

Clearly, these difficulties can be avoided if the side rake is measured

Tool orthogonal rake γ_o
(previously German side rake)

Section on P_o

View normal
to tool base

Tool cutting-edge
inclination, λ_s (previously
German back rake)

View in P_s
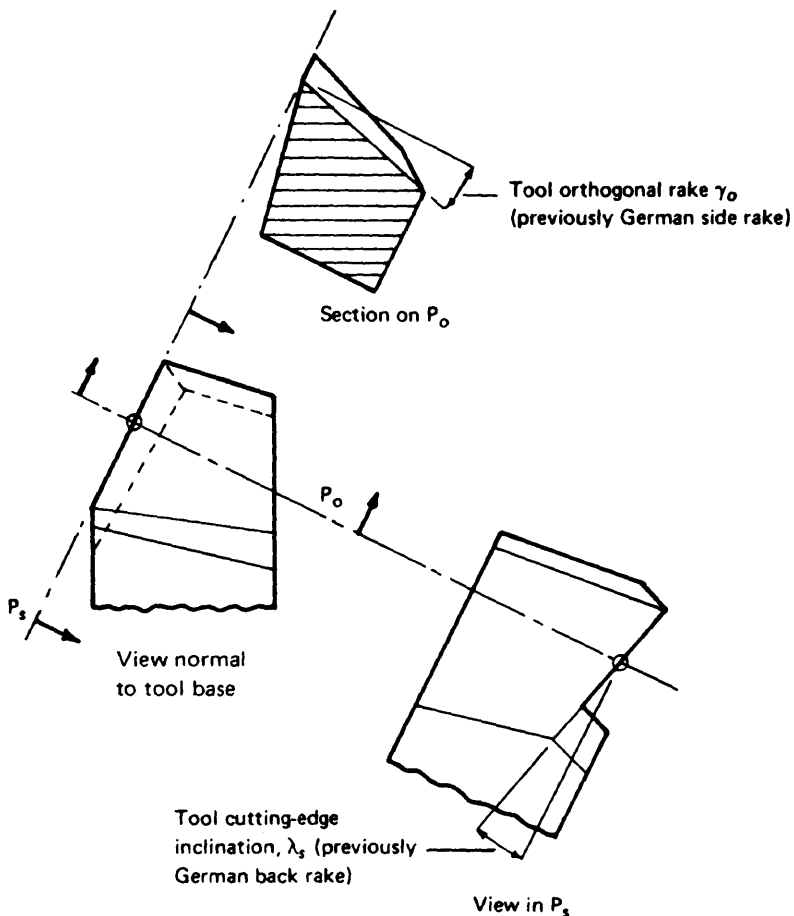
Figure 7.6   Early German (DIN) system.

in a plane normal to the tool cutting edge. The side-rake angle could then be set on the third axis C without the need for compensations. This idea forms the basis for a system of cutting-tool nomenclature called the normal-rake system, which has now been adopted as the new ISO standard and the standard in America, Great Britain, and Germany. It is of interest to note that the normal-rake system of cutting-tool nomenclature was first proposed by Stabler in 1955 [2].

7.3 INTERNATIONAL STANDARD

7.3.1 Tool-in-Hand and Tool-in-Use Systems

The ISO recommendation for the nomenclature of cutting tools [3] first establishes systems of planes that can be used to define the various angles of the faces and flanks of the tool. It should be understood that two systems of angles and planes are required. The first system is the tool-in-hand system of planes and angles and refers to a cutting tool that is held in the hand and is used for the purposes of grinding and sharpening the tool. The second system is the tool-in-use system of planes and angles and refers to the cutting tool being used in a machining operation.

The reason two systems are required is twofold: First, in a simple turning operation as the feed is increased, the effective rake angles increases, and the effective clearance decreases (Fig. 7.7); second, it is possible that a cutting tool (particularly a single-point cutting tool) can be held in a machine tool in various orientations, thereby altering the effective angles of the tool. Thus, the tool-in-hand system is defined in relation to the tool base (or, for rotating tools, to the tool axis). The tool-in-use system, on the other hand, is defined in relation to the resultant cutting direction and the direction of feed motion.

Figures 7.8 through 7.11 shows the two systems of planes necessary for defining the tool shape with respect to a selected point on the major cut-
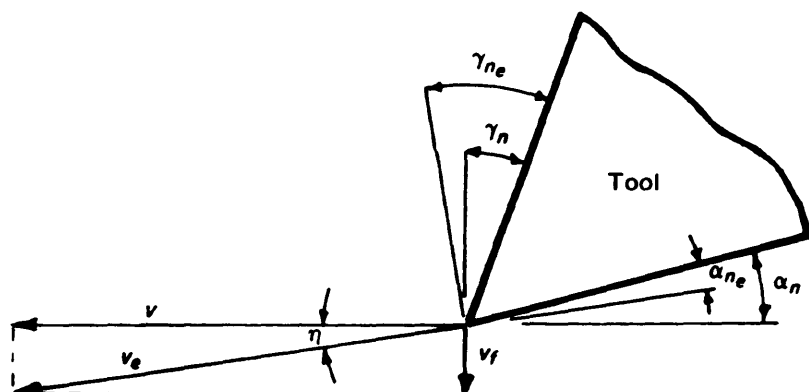
Figure 7.7 Effect of resultant cutting-speed angle η on normal rake and normal clearance in orthogonal cutting, where v = cutting speed, v_f = feed speed, v_e = resultant cutting speed, γ_n = tool normal rake, γ_{ne} = working (effective) normal rake, γ_n = tool normal clearance, and γ_{n_e} = working (effective) normal clearance.
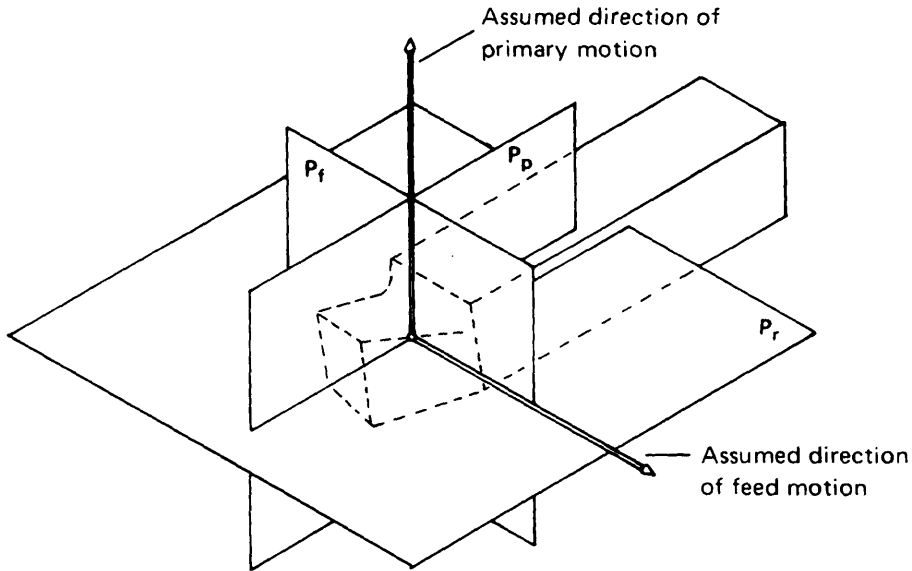
Figure 7.8   Tool-in-hand planes P_r, P_f, and P_p for the major cutting edge of a single-point tool, where P_r, the tool reference plane, is parallel to the tool base; P_f, the assumed working plane, is perpendicular to the tool reference plane P_r, perpendicular to the tool axis, and parallel to the assumed direction of feed motion, and P_p, the tool back plane, is perpendicular to the tool reference plane P_r and perpendicular to the assumed working plane P_f.

ting edge of a single-point tool. Table 7.1 shows how, using these systems of planes, the various angles are defined; it should be noted that the planes and angles in the tool-in-hand system are prefixed by the work *tool* and those in the tool-in-use system are prefixed by the word *working*, except for those planes or angles that are the same in either system. For example, it can be seen from the table that the tool normal rake γ_n is the angle between the tool face A_γ and the tool reference plane P_r, measured in the cutting-edge normal plane P_n.

Each plane is provided with a symbol consisting of the letter P with a subscript to denote the plane's identity. In all the planes and angles defined here it is assumed that the selected point of reference lies on the major cutting edge (S). If, however, the selected point were on the minor cutting edge, the name of the plane or angle would include the words *minor cutting edge* and the symbol would bear a prime. For example P'_s would be the total minor cutting-edge plane, and γ'_n would be the tool minor cutting-edge normal rake.
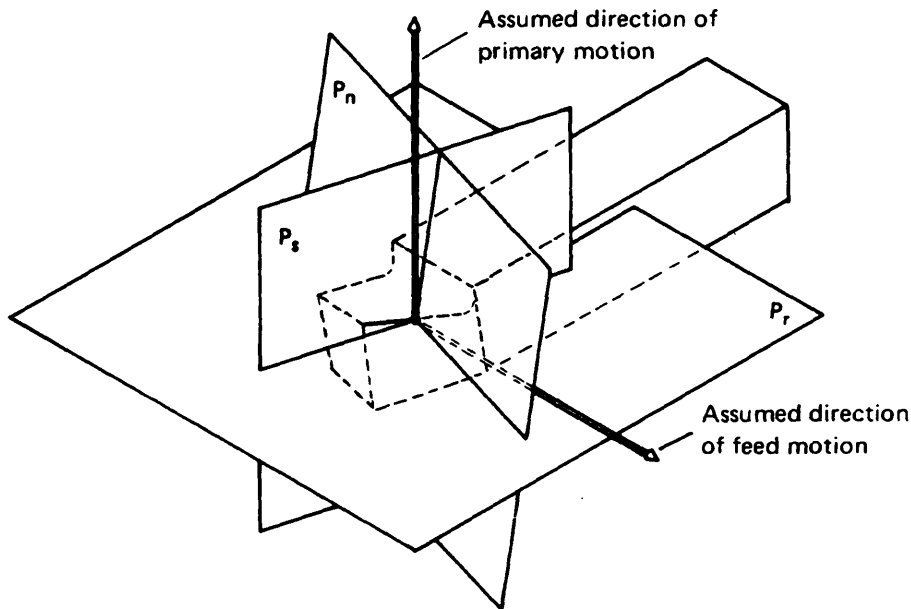
Figure 7.9 Tool-in-hand planes P_r, P_s, and P_n for the major cutting edge of a single-point tool, where P_r, the tool reference plane, is parallel to the tool base; P_s, the tool cutting-edge plane, is tangential to the cutting edge and perpendicular to the tool reference plane P_r; and P_n, the cutting-edge normal plane, is perpendicular to the cutting edge.

The symbol for a plane or angle in the tool-in-use system bears an additional subscript, e, for *effective*. For example, P_{s_e} would be the working cutting-edge plane and γ_{n_e} would be the working normal rake.

Figures 7.12 and 7.13 show the various tool and working angles for a single-point cutting tool. The signs of the various angles are all positive in these figures.

As explained in Chap. 1, in practice the angle between the resultant cutting direction and the direction of primary motion, the resultant cutting speed angle η, is usually very small; therefore if the tool is clamped in the machine in its most natural position (e.g., as in Fig. 7.1 for cylindrical turning), the tool-in-use system and tool-in-hand system almost coincide and corresponding angles are almost identical. However, if the tool is oriented differently from its most natural position, the working angles will be different from the tool angles. To relate one system to another it is necessary to define the orientation of the tool in the machine tool, and for

Direction of
primary motion

Resultant cutting
direction

P_{fe}

P_{pe}

P_{re}

Direction of feed motion
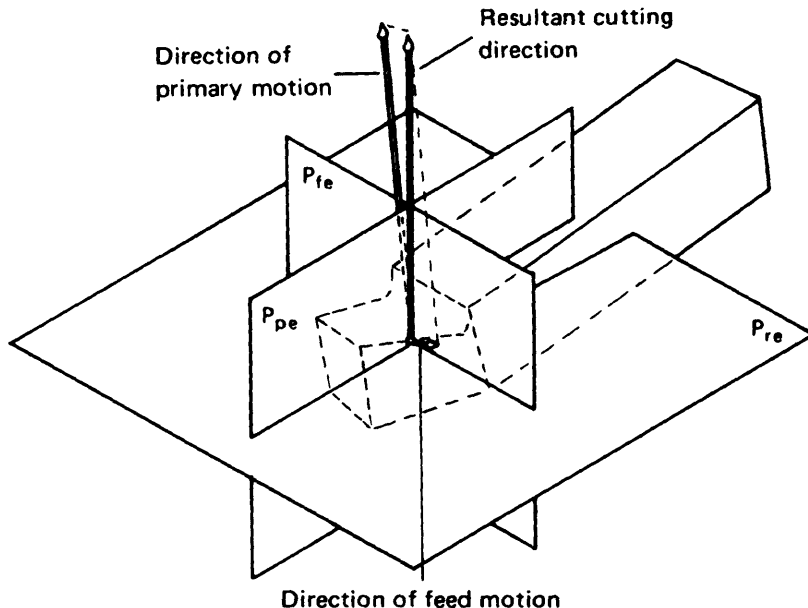
Figure 7.10 Tool-in-use planes P_{re}, P_{fe}, and P_{pe} for the major cutting edge of a single-point tool, where P_{re}, the working reference plane, is perpendicular to the resultant cutting direction; P_{fe}, the working plane, is perpendicular to the working reference plane P_{re} and contains the directions of the primary and feed motions; and P_{pe}, the working back plane, is perpendicular to the working reference plane P_{re} and perpendicular to the working plane P_{fe}.

this purpose another system of planes and angles, called the setting system of planes and angles, is required.

7.3.2 Setting System

To complete the relationship between the tool and working system it is necessary to define two sets of angles:

1. Those angles defining the position of the tool in the machine tool (called setting angles)
2. Those angles defining the orientation of the resultant cutting direction and direction of feed motion relative to the machine tool

In the present discussion only the first set of angles will be defined; the definitions will provide sufficient information to obtain the working angles from the tool angles when the resultant cutting speed angle η is
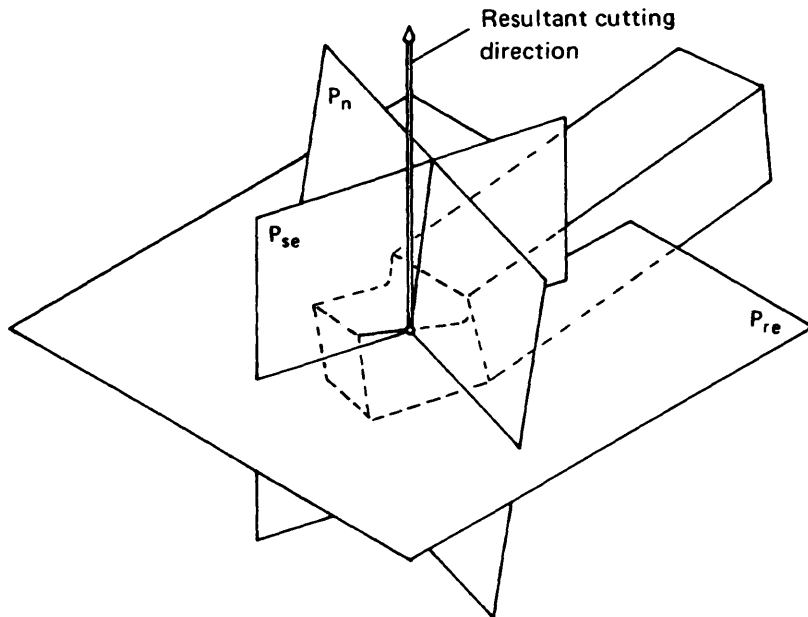
Figure 7.11 Tool-in-use planes P_{re}, P_{se}, and P_n for the major cutting edge of a single-point tool, where P_{re}, the working reference plane, is perpendicular to the resultant cutting direction; P_{se}, the working cutting edge plane, is tangential to the cutting edge and perpendicular to the working reference plane P_{re}; and P_n, the cutting-edge normal plane, is perpendicular to the cutting edge.

Table 7.1 Tool and Working Angles, Definitions

Angle	Is the angle between	And	Measured in plane
Tool normal rake γ_n	A_γ	P_r	P_n
Working normal rake γ_{n_e}	A_γ	P_{r_e}	$P_{n_e}(\equiv P_n)$
Tool normal clearance α_n	A_α	P_s	P_n
Working normal clearance α_{n_e}	A_α	P_{s_e}	$P_{n_e}(\equiv P_n)$
Tool cutting-edge angle κ_r	P_s	P_f	P_r
Working cutting-edge angle κ_{r_e}	P_{s_e}	P_{f_e}	P_{r_e}
Tool cutting-edge inclination λ_s	S	P_r	P_s
Working cutting-edge inclination λ_{s_e}	S	P_{r_e}	P_{s_e}
Tool-included angle ε_r	P_s	P_s'	P_r
Normal wedge angle $\beta_n(\equiv\beta_{n_e})$	A_γ	A_α	$P_n(\equiv P_{n_e})$

Key: A_γ = tool face; A_α = tool flank; S = major cutting edge.

217
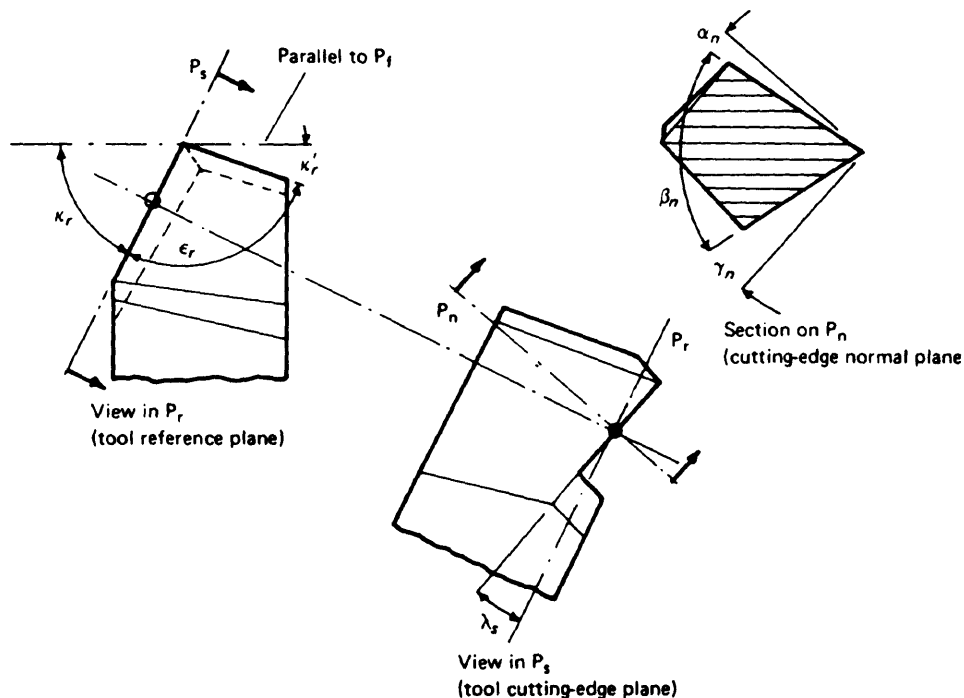
Figure 7.12 Tool angles for a single-point tool, where κ_r = tool cutting-edge angle, κ_r' = tool minor cutting-edge angle, λ_s = tool cutting-edge inclination, γ_n = tool normal rake, α_n = tool normal clearance, β_n = normal wedge angle, and ε_r = tool-included angle.

assumed to be zero. Neglecting the effect of the resultant cutting speed angle η simplifies the mathematical analysis, but it should be remembered that for situations where the angle η is significant (say, greater than 1 deg), more complicated equations must be employed.

The setting angles are defined in Fig. 7.14 for a single-point tool. The figure also indicates the signs of the angles determined from the right-hand-screw rule. The axes X, Y, and Z correspond to the machine-tool axes defined and illustrated for various machine tools in Chap. 1.

7.3.3   Mathematical Relationships Between Tool and Working Systems

Equations (7.3) through (7.11) allow the working angles to be calculated when a single-point tool is held in a machine tool in any orientation and
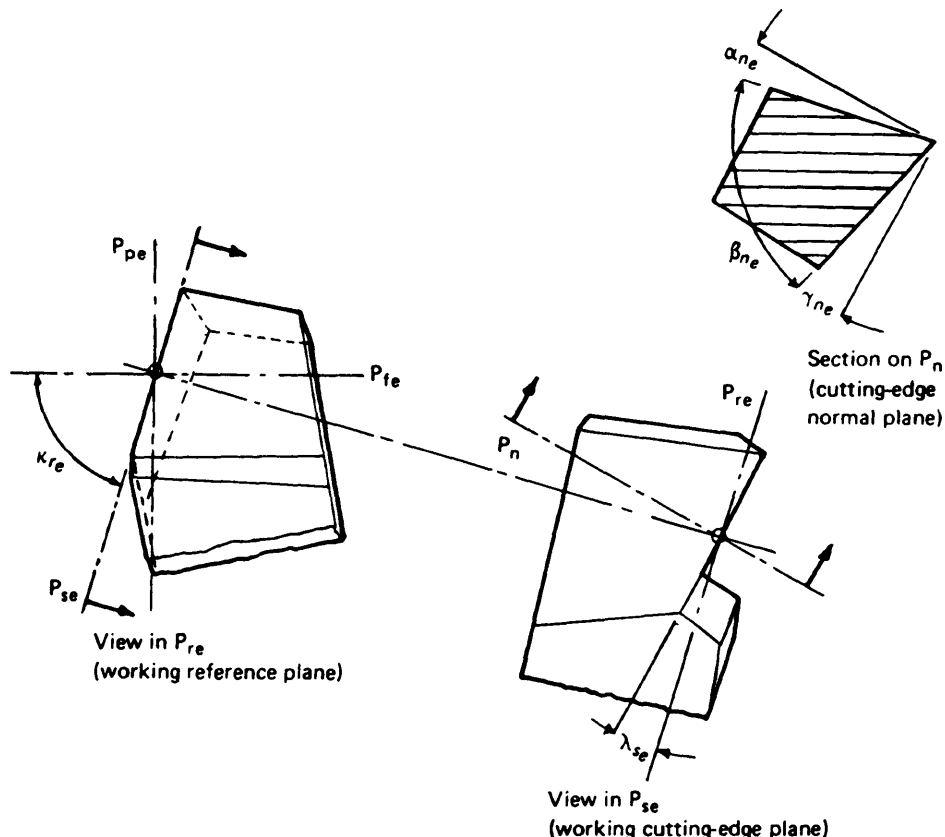
Figure 7.13 Working angles for a single-point tool, where κ_{r_e} = working cutting-edge angle, λ_{s_e} = working cutting edge inclination, γ_{n_e} = working normal rake, α_{n_e} = working normal clearance, β_{n_e} = normal wedge angle (= β_n), and ε_{r_e} = working included angle.

when it can be assumed that the resultant cutting-speed angle η is zero (Fig. 7.7). Each working angle is calculated in three steps, each step corresponding to moving the tool from its most natural position through each of the three setting angles in turn. Thus, in each group of equations the suffix G, H, or L refers to the effect of the appropriate setting angle. It should be noted that the resulting angles are the true working angles only when the working plane P_{f_e} coincides with the machine plane P_{yz} and when the effect of feed is negligibly small, that is, $\eta = 0$. Also, under certain conditions (e.g., when drilling or turning with a high feed), the effect of the resultant cutting speed angle η must be taken into account.
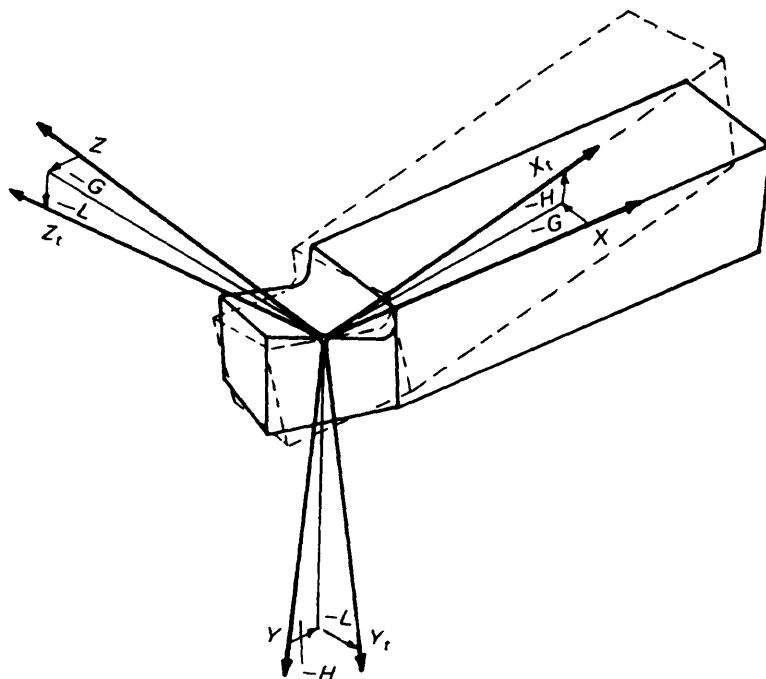
Figure 7.14 Setting planes and angles, where X, Y, and Z are the machine axes as defined in Chap. 1; X_t, Y_t, and Z_t are the tool-in-hand axes and correspond to the intersections of the tool-in-hand planes as follows, $X_t(P_r P_p)$, $Y_t(P_p P_f)$, $Z_t(P_f P_r)$, as well as to the machine axes when the tool is in its most "natural" position on the machine tool; G is the plane-setting angle and is positive if it has the effect of decreasing κ; H is the elevation-setting angle and is positive if it has the effect of increasing the angle λ; L is the roll-setting angle and is positive if it has the effect of decreasing the angle γ. (*Note:* For the right-hand tool shown, the signs of the setting angles obey the right-hand-screw rule.)

The equations for calculating the cutting-edge angle are

$$\kappa_{r_L} = \arctan \frac{\sin \kappa_r}{(\cos \kappa_r \cos L) - (\tan \lambda_s \sin L)} \qquad (7.3)$$

$$\kappa_{r_H} = \arctan \frac{(\sin \kappa_{r_L} \cos H) - (\tan \lambda_{s_L} \sin H)}{\cos \kappa_{r_L}} \qquad (7.4)$$

$$\kappa_{r_G} = \kappa_{r_H} - G = \kappa_{r_e} \qquad (7.5)$$

for the cutting-edge inclination

$$\lambda_{s_L} = \arcsin[(\sin \lambda_s \cos L) + (\cos \kappa_r \cos \lambda_s \sin L)] \qquad (7.6)$$

$$\lambda_{s_H} = \arcsin[(\sin \lambda_{s_L} \cos H) + (\sin \kappa_{r_L} \cos \lambda_{s_L} \sin H)] \qquad (7.7)$$

$$\lambda_{s_G} = \lambda_{s_H} = \lambda_{s_e} \qquad (7.8)$$

and for the normal rake

$$\gamma_{n_L} = \gamma_n - \arctan \frac{\sin \kappa_r \sin L}{(\cos \lambda_s \cos L) - (\cos \kappa_r \sin \lambda_s \sin L)} \qquad (7.9)$$

$$\gamma_{n_H} = \gamma_{n_L} + \arctan \frac{\cos \kappa_{r_L} \sin H}{(\cos \lambda_{s_L} \cos H) - (\sin \kappa_{r_L} \sin \lambda_{s_L} \sin H)} \qquad (7.10)$$

$$\gamma_{n_G} = \gamma_{n_H} = \gamma_{n_e} \qquad (7.11)$$

The effect of setting angles on normal clearance is numerically the same as for normal rake except the change is in the opposite sense.

7.3.4 Example

A lathe tool is to be placed in a machine such that the plane setting angle G is -20 deg, the elevation setting angle H is -10 deg, and the roll setting angle L is zero. Also, the tool-in-hand angles (Fig. 7.12) are as follows:

1. The tool major-cutting-edge angle κ_r is 30 deg.
2. The tool major-cutting-edge inclination λ_s is 5 deg.
3. The tool major-cutting-edge normal rake γ_n is 10 deg.
4. The tool major-cutting-edge normal clearance α_n is 5 deg.

From Eqs. (7.3), (7.6), and (7.9) when $L = 0$,

$$\kappa_{r_L} = \kappa_r = 30°$$

$$\lambda_{s_L} = \lambda_s = 5°$$

$$\gamma_{n_L} = \gamma_n = 10°$$

$$\alpha_{n_L} = \alpha_n = 5°$$

From Eqs. (7.4) and (7.5)

$$\kappa_{r_e} = \kappa_{r_H} - G$$

$$= \arctan \left[\frac{(\sin 30° \cos 10°) + (\tan 5° \sin 10°)}{\cos 30°} \right] + 20°$$

$$= 30.3° + 20° = 50.3°$$

From Eqs. (7.7) and (7.8)

$$\lambda_{s_e} = \lambda_{s_H}$$

$$= \arcsin [(\sin 5° \cos 10°) - (\sin 30° \cos 5° \sin 10°)]$$

$$= 0$$

From Eqs. (7.10) and (7.11)

$$\gamma_{n_e} = \gamma_{n_H}$$

$$= 10° + \arctan \left[\frac{-\cos 30° \sin 10°}{(\cos 5° \cos 10°) + (\sin 30° \sin 5° \sin 10°)} \right)$$

$$= 10° - 8.9° = 1.1°$$

and finally since the normal rake has been reduced by the setting angles, the normal clearance would be increased by the same amount. Thus,

$$\alpha_{n_e} = \alpha_n + 8.9 \text{ deg} = 5 \text{ deg} + 8.9 \text{ deg} \approx 13.9 \text{ deg}$$

7.3.5 Calculation of Tool Angles from Working Angles

It is often desired to calculate the tool angles when the required working angles and the setting angles are specified. To calculate the tool angles (when the effect of feed is neglected and when the working plane P_{fe} coincides with the machine plane P_{yz}) the appropriate equations are as follows:

For the cutting-edge angle

$$\kappa_{r_G} = \kappa_{r_e} - G \tag{7.12}$$

$$\kappa_{r_H} = \arctan \frac{(\sin \kappa_{r_G} \cos H) - (\tan \lambda_{s_G} \sin H)}{\cos \kappa_{r_G}} \tag{7.13}$$

$$\kappa_{r_L} = \arctan \frac{\sin \kappa_{r_H}}{(\cos \kappa_{r_H} \cos L) - (\tan \lambda_{s_H} \sin L)} = \kappa_r \tag{7.14}$$

for the cutting-edge inclination

$$\lambda_{s_G} = \lambda_{s_e} \tag{7.15}$$

$$\lambda_{s_H} = \arcsin \left[(\sin \lambda_{s_G} \cos H) + (\sin \kappa_{r_G} \cos \lambda_{s_G} \sin H) \right] \tag{7.16}$$

$$\lambda_{s_L} = \arcsin \left[(\sin \lambda_{s_H} \cos L) + (\cos \kappa_{r_H} \cos \lambda_{s_H} \sin L) \right] = \lambda_s \tag{7.17}$$

and for the normal rake

$$\gamma_{n_G} = \gamma_{n_e} \tag{7.18}$$

$$\gamma_{n_H} = \gamma_{n_G} + \arctan \frac{\cos \kappa_{r_G} \sin H}{(\cos \lambda_{s_G} \cos H) - (\sin \kappa_{r_G} \sin \lambda_{s_G} \sin H)} \tag{7.19}$$

$$\gamma_{n_L} = \gamma_{n_H} - \arctan \frac{\sin \kappa_{r_H} \sin L}{(\cos \lambda_{s_H} \cos L) - (\cos \kappa_{r_H} \sin \lambda_{s_H} \sin L)} = \gamma_n \tag{7.20}$$

The effect of setting angles on normal clearance is numerically the same as for normal rake except the change is in the opposite sense.

All of the equations relating the tool and working systems were derived by Verma [4].

PROBLEMS

1. A tool bit is to be mounted in the standard straight tool holder shown in Fig. 7.15. The shank of the tool holder is to be mounted horizontally and perpendicular to the spindle axis of a lathe with the tool corner at the same level as the spindle axis. Calculate the tool angles for the bit to give the following working angles:
   a. A working major cutting-edge angle κ_{r_e} of 45 deg
   b. A working major cutting-edge inclination λ_{s_e} of 0
   c. A working major cutting-edge normal rake γ_{n_e} of 5 deg
   d. A working major cutting-edge normal clearance α_{n_e} of 3 deg
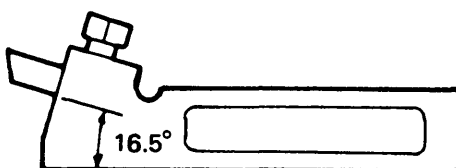
Figure 7.15 Standard straight tool holder.

2. If the tool holder of Prob. 1 had been a right-hand tool holder with the front part bent to the left through an angle of 10 deg in the plan view, what tool angles for the bit would be required?

REFERENCES

1. G. V. Stabler, The fundamental geometry of cutting tools, *Proc. IME,* vol. 165, p. 14, 1951.
2. G. V. Stabler, The basic nomenclature of cutting tools, *J. Inst. Prod. Eng.,* vol. 34, p. 264, 1955.
3. Geometry of the Active Parts of Cutting Tools—General Terms, Reference Systems, Tool and Working Angles, Draft International Standard ISO/DIS 3002, 1973.
4. D. K. Verma, Nomenclature of Cutting Tools, M.S. Thesis, Department of Mechanical Engineering University of Massachusetts, Amherst, 1969.

8
Chip Control

8.1 INTRODUCTION

Before the advent of carbide tools and the use of high cutting speeds, continuous chips produced in metal cutting did not present a serious problem. At low cutting speeds, these chips usually have a natural curl and tend to be brittle. However, cutting speeds have now increased to such an extent that chip control has become necessary. In turning operations, where the tool is continuously removing metal for a long period, a continuous chip can become entangled with the tool, the workpiece, or the machine-tool elements. This type of chip can be hazardous to the operator and, unless controlled properly, can result in mechanical chipping of the cutting edge. If coolant is being applied, the chip may interfere with the flow of coolant, causing alternate heating and cooling of the cutting edge. The resulting thermal stresses can reduce the life of cemented-carbide tools.

The handling of continuous chips in bulk can present a major economic problem. A handling characteristic of chips can be expressed by the bulk ratio, the total volume occupied by the chips divided by the volume of solid chip material. Unbroken, continuous chips have a bulk ratio of approximately 50, tightly wound chips a bulk ratio of approx-

imately 15, and well-broken chips a bulk ratio of approximately 3. The volume occupied by well-broken chips is therefore about one-seventeenth the volume of unbroken chips, a considerable advantage when it comes to handling and disposal.

Figure 8.1 shows the various forms of chips that may be produced in a cutting operation together with the first two digits of a proposed international standard-coding system [1]. The dangers and difficulties that result from the formation of long chips has necessitated the study and development of various means to control chips and break them into small coils or fragments as they are produced.

8.2   CHIP BREAKERS

The controlling and breaking of chips is accomplished by a chip breaker, which is defined as a modification of the face to control or break the chip, consisting of either an integral groove or an integral or attached obstruction.

There are basically two kinds of chip breaker: the groove type and the obstruction type. These chip breakers together with the important dimensions are illustrated in Figs. 8.2 and 8.3.

A chip breaker acts by controlling the radius of the chip and directing the chip in such a way that it breaks into short lengths. In addition to an appropriate chip-breaker design it is necessary to have the correct tool geometry so that the chip will follow the proper path across the tool face. It was seen in Chap. 7 that the direction of chip flow is controlled mainly by the working major cutting-edge inclination. When this angle is zero, the condition is known as orthogonal cutting, and the chip will usually form a spiral, as shown in Fig. 8.4a. Under orthogonal conditions and with the chip initially tightly curled, the radius of chip curvature will be forced to increase gradually as cutting proceeds. This gradual increase in chip-curvature radius will impose gradually increasing stresses in the chip, eventually causing breakage and resulting in spiral chips. If the chip does not have a natural curl (the case at high cutting speeds) and no chip breaker is present, straight or ribbon chips are produced that can become snarled if the cutting process is continuous. With a chip breaker present, the chip will be curled, but because of the restrictions imposed on its path, it will strike the transient surface of the workpiece and continuously break into small fragments (Fig. 8.4b). These fragments, which take the form of loose arc chips, often fly violently from the cutting region and present a hazard to the machine operator.

In the more common situation of oblique cutting (when the working major cutting-edge inclination is not zero) long chips are usually tubular,
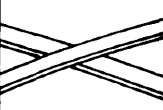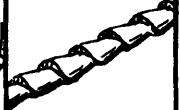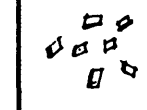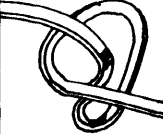
1. Ribbon chips	2. Tubular chips	3. Spiral chips	4. Washer-type helical chips	5. Conical helical chips	6. Arc chips	7. Elemental chips	8. Needle chips
1.1 Long	2.1 Long	3.1 Flat	4.1 Long	5.1 Long	6.1 Connected		
1.2 Short	2.2 Short	3.2 Conical	4.2 Short	5.2 Short	6.2 Loose		
1.3 Snarled	2.3 Snarled		4.3 Snarled	5.3 Snarled			

Figure 8.1 Chip forms produced in machining operations.
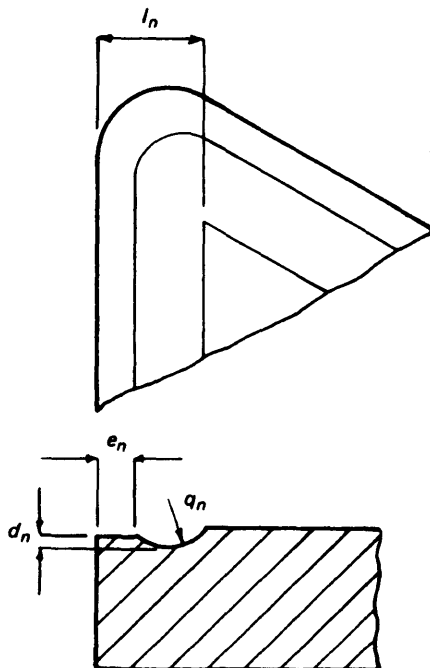
Figure 8.2   Groove-type chip breaker, where d_n = chip-breaker-groove depth, e_n = chip-breaker land width, l_n = chip-breaker distance, and q_n = chip-breaker-groove radius.

washer-type helical, or conical helical (Fig. 8.1) and can become snarled. In the production of tubular chips (Fig. 8.4c) the helix angle of the chip will be equal to the chip-flow angle and therefore approximately equal to the working major cutting-edge inclination. However, in many situations the cutting speed can vary considerably along the major cutting edge of the tool (in drilling, for example), and washer-type or conical-helical-type chips are produced. To provide chip breaking under any of these conditions the radius of the chip must be controlled by a chip breaker; in addition, the working major cutting-edge angle and the working major cutting-edge inclination must be such that the free end of the chip strikes one of the surfaces on the workpiece or the tool flank. The most common situation is shown in Fig. 8.4d, where the free end of the chip clears the transient surface and strikes the work surface at some point A. The free end of the chip is then carried down by the rotation of the workpiece and eventually strikes the tool flank at B. Further chip production, with the free end effectively fixed at B, results in an increasing radius of chip curva-
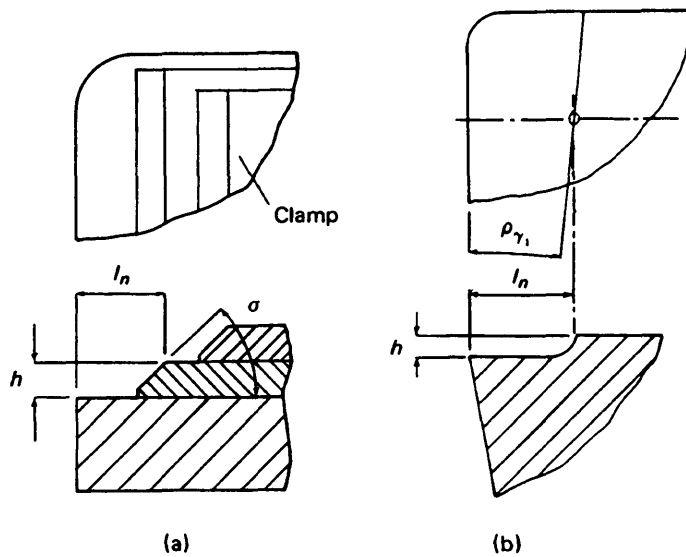
Figure 8.3 Obstruction-type chip breakers, where h = chip-breaker height, l_n = chip-breaker distance, σ = chip-breaker wedge angle, and $\rho_{\gamma 1}$ = chip-breaker angle. (a) Attached; (b) integral.
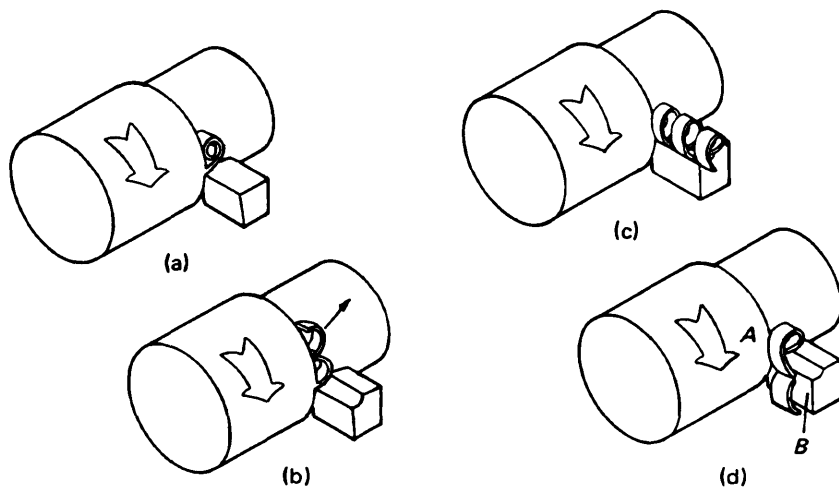
Figure 8.4 Production of various chip forms in turning. (a) Orthogonal cutting, flat spiral chips; (b) orthogonal cutting, loose-arc chips; (c) oblique cutting, long tubular chips; (d) oblique cutting, connected-arc chips.

ture, increasing stresses, and, eventually, fracture of the chip. This process results in the production of arc-type chips (Fig. 8.1). Under these circumstances the radius of chip curvature is critical. If this radius is too large, the free end of the chip may not strike the tool flank but rather coil around the tool. If this radius is too small, the chip may clear the tool face and form a tubular or helical chip. In the latter case the chip may eventually break because of its weight and motion.

Hendriksen [2] classified chips into three categories: overbroken, efficiently broken, and underbroken. Generally, connected arc chips are considered to be efficiently broken. In turning operations with a proper chip-former geometry and tool shape, the type of broken chip produced can usually be controlled by the feed. A change in feed affects both the chip thickness and radius of chip curvature, the rule being that to change from an underbroken to an efficiently broken chip, the feed should be increased. Several analyses [3,4,5] were made to determine the conditions under which various types of chip breaking will occur. The principal parameters were found to be the radius of chip curvature, the thickness of the chip, and the properties of the workpiece material. However, limited success has been achieved in correlating these analyses with experimental data such as that obtained by Nakayama [4] (shown in Fig. 8.5). This figure illustrates how the feed and radius of chip curvature affect the efficiency of the chip-breaking operation.

8.3 PREDICTION OF RADIUS OF CHIP CURVATURE

Although no method has yet been found possible to predict the actual chip-breaking performance of various tool designs, some success has been experienced [6] in predicting the radius of chip curvature when a chip breaker is employed.

For any of the obstruction-type chip breakers it is only necessary to realize that the chip starts to curl away from the tool face at the end of the chip-tool contact region and that the chip then maintains a constant radius of curvature until it clears the chip breaker. From the geometry of Fig. 8.6 it can be deduced that for an integral obstruction-type chip breaker, the radius of chip curvature, r_{chip}, at the defined point is given by

$$r_{chip} = \frac{(l_n - l_f)^2}{2h} + \frac{h}{2} \tag{8.1}$$

where

l_n = chip-breaker distance
l_f = length of chip–tool contact
h = chip-breaker height

Creveling, Jorden, and Thomsen [7] investigated the length of chip-tool contact and concluded that

$$\frac{l_f}{a_0} = K \tag{8.2}$$

where K is a constant for a given material and a_0 is the chip thickness.
Hence, Eq. (8.1) becomes

$$r_{\text{chip}} = \frac{(l_n - Ka_0)^2}{2h} + \frac{h}{2} \tag{8.3}$$

These authors found that for steel K equals unity, and although K is prob-
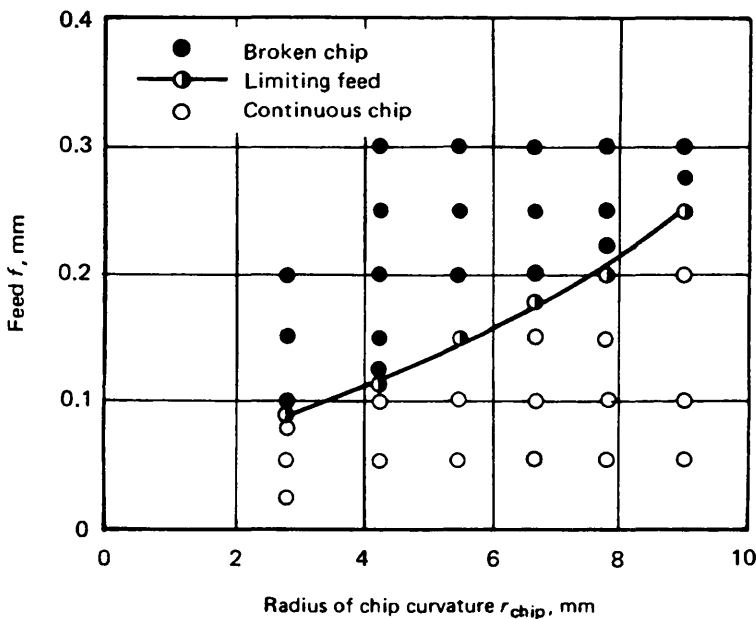
Figure 8.5 Effects of radius of chip curvature and feed on chip breaking for S45C at a cutting speed of 1.83 m/s. (After Nakayama [4].)
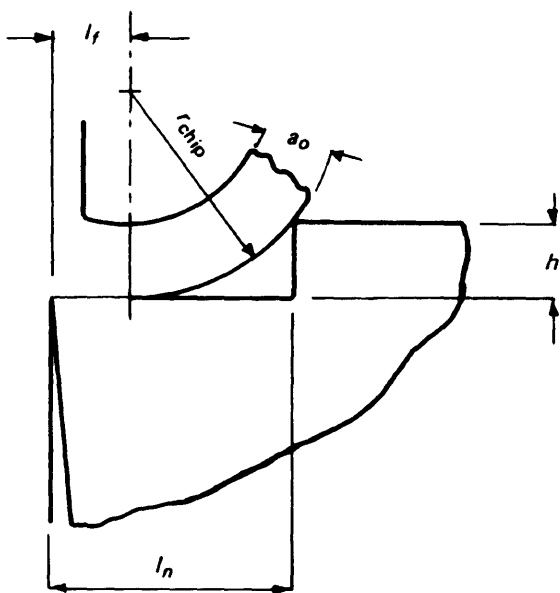
Figure 8.6 Construction to determine radius of chip curvature for an integral obstruction-type chip breaker, where l_f = contact length between the chip and tool, l_n = chip-breaker distance, h = chip-breaker height, a_0 = chip thickness, and r_{chip} = chip-curvature radius.

ably not equal to unity for all conditions and materials, it seems unlikely that the value of K will vary considerably. For practical purposes, therefore, it is reasonable to assume that l_f/a_0 equals unity and Eq. (8.3) becomes

$$r_{chip} = \frac{(l_n - a_0)^2}{2h} + \frac{h}{2} \tag{8.4}$$

Figure 8.7 shows that Eq. (8.4) agrees closely with experimental results.

For an attached obstruction-type chip breaker (Fig. 8.8), the equation for the radius of chip curvature can be developed in a similar way:

$$r_{chip} = [(l_n - l_f) - (h \cot \sigma)] \cot \frac{\sigma}{2} \tag{8.5}$$

where σ is the chip-breaker wedge angle, and when l_f equals a_0 this equation becomes

Chip thickness a_o, mm
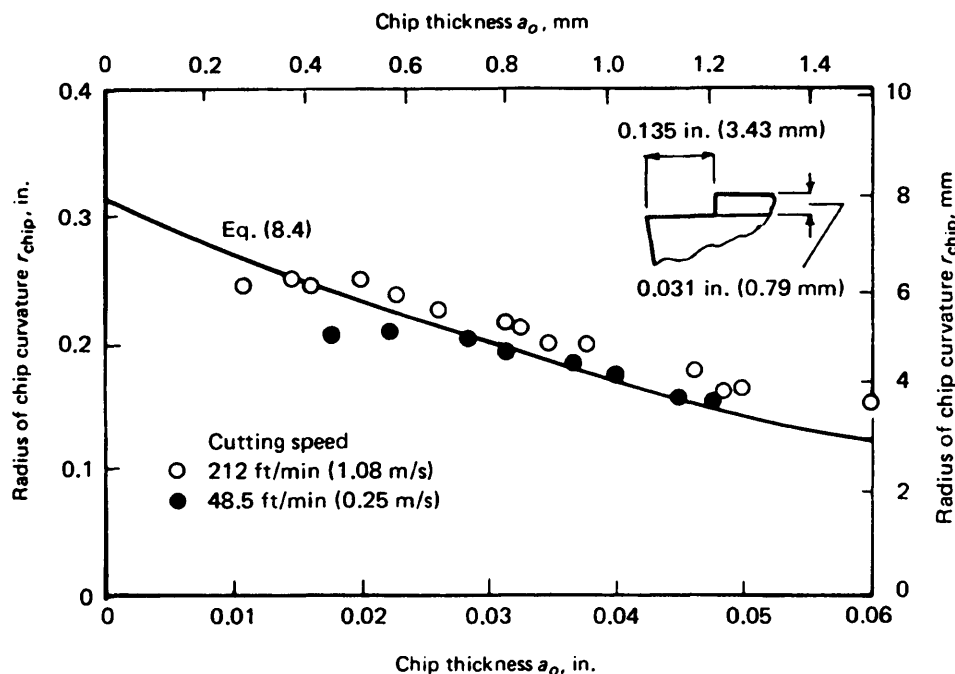
Figure 8.7 Effect of chip thickness on radius of chip curvature when 85/15 brass is cut. (After Trim and Boothroyd [6].)

$$r_{chip} = [(l_n - a_0) - (h \cot \sigma)] \cot \frac{\sigma}{2} \qquad (8.6)$$

For a groove-type chip breaker no chip control is obtained unless the chip-breaker land width e_n is less than the length of chip–tool contact l_f. When e_n is less than l_f, the chip will try to flow down into the groove and conform to the chip-breaker groove radius q_n (Fig. 8.9). If, however, q_n is too small, the chip will not follow the groove contour until tool wear is significant. Thus, if l_f is assumed equal to a_0 and the choice of chip-breaker groove radius q_n is appropriate,

$$r_{chip} = q_n \qquad (8.7)$$

when e_n is less than a_0.

Equations (8.4), (8.6), and (8.7) allow the radius of chip curvature to be estimated for a chip breaker of given dimensions, and the chip thickness a_0 always appears as a significant parameter. It can therefore be ap-
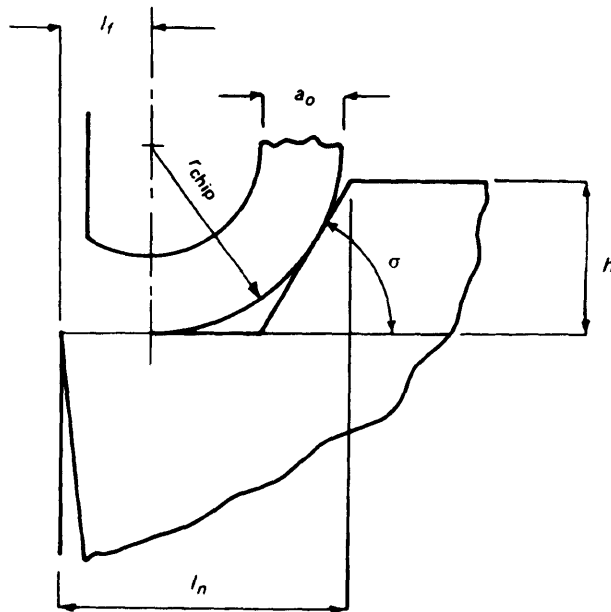
Figure 8.8 Construction to determine radius of chip curvature for an attached obstruction-type chip breaker, where l_f = contact length between the chip and tool, l_n = chip-breaker distance, h = chip-breaker height, a_0 = chip thickness, r_{chip} = chip-curvature radius, and σ = chip-breaker wedge angle.

preciated why both r_{chip} and a_0 have a controlling influence on the efficiency of chip breaking.

8.4 TOOL WEAR DURING CHIP BREAKING

As a tool wears, a crater forms on its face. The shape of this crater conforms to the shape of the curled chip, and thus the presence of a chip breaker will affect the wear process. Conversely, as a crater forms on a plain tool, the crater can eventually act as a chip breaker. Figure 8.10 shows the results of some experiments [8] where the progress of tool wear was studied for three tools under identical cutting conditions. In each test the shape of the worn face of the tool was observed at intervals of 4 min (240 s).

In the first test (Fig. 8.10a) a plain tool was used. Initially the chip was a long ribbon chip that became snarled. Gradually a crater formed that caused the chip to curl, and after only 8 min (480 s) this crater started to act as a chip breaker.
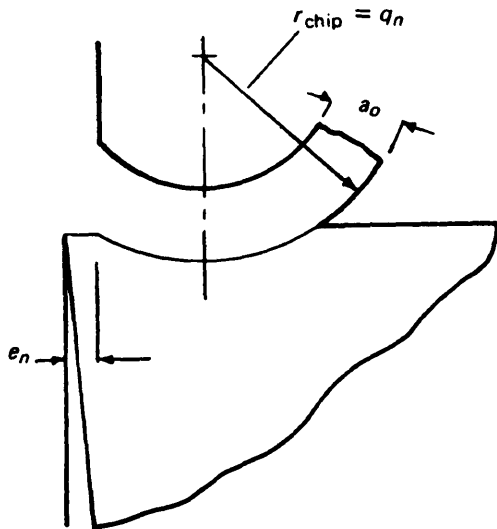
Figure 8.9 Chip radius of curvature when $e_n < a_0$ for a groove-type chip breaker, where e_n = chip-breaker land width, a_0 = chip thickness, and r_{chip} = chip-curvature radius.

In the second test (Fig. 8.10b) an attached obstruction-type chip breaker was employed. It can be seen that in addition to controlling the radius of chip curvature and the breaking of the chips, this obstruction-type chip breaker caused the rate of wear on the tool face to decrease substantially. However, as wear progressed, the radius of chip curvature decreased, until after 11 min (660 s) the chips became overbroken.

Finally, in the third test (Fig. 8.10c) a groove-type chip breaker was employed. Again after about 11 min (660 s) chip breaking became unsatisfactory, and the chips were overbroken because of the reduced radius of chip curvature. In this test the rate of wear was comparable to that of the plain tool but the effect of the groove-type chip breaker was to eliminate the initial period where no chip breaking occurred.

It appears from these tests that the obstruction-type chip breaker causes a reduced rate of wear on the tool face. However, since satisfactory chip breaking occurred for the first 11 min (660 s) only, this amount of time became the effective tool life, even though a wear land of only 0.01 in. (0.25 mm) in width had developed on the tool flank.

It can be concluded that the effective life of a cutting tool can be shortened considerably using a chip breaker, simply because the chip-breaking action may become ineffective before the tool itself is significantly worn.

Scale: 0.1 mm

0.1 mm

Time t', s

240 480 720 960 1 200

(a)

Time t', s

Chip breaker

240 480 720 960 1 200

(b)

Time t', s

Groove

240 480 720 960 1 200

(c)
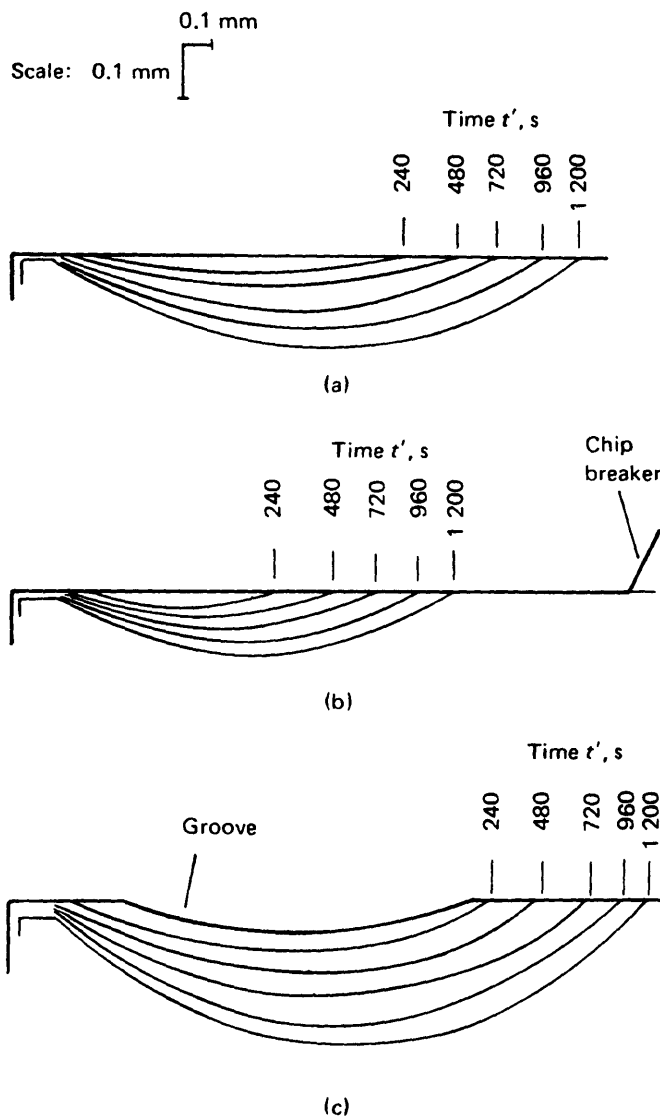
Figure 8.10 History of crater wear during turning for a work material of AISI 1045 hot-rolled steel and a tool material of carbide (Kennametal-K4H), where the cutting speed is 550 ft/min (2.8 m/s), the feed is 0.014 in. (0.356 mm), and the major-cutting-edge angle is 75 deg. (a) Plain tool; (b) attached obstruction-type chip breaker; (c) groove-type chip breaker. (After Reinhart and Boothroyd [8].)

PROBLEMS

1. A single-point cutting tool is fitted with an integral obstruction-type chip breaker and is provided with positive, working major cutting-edge inclination so that a chip of helical form is produced. The chip-breaker height is 0.5 mm and the chip-breaker distance is 1.5 mm. The undeformed chip thickness is 0.05 mm and the cutting ratio is 0.2. If the chip width is 2 mm, estimate the minimum working major cutting-edge inclination that will ensure that the successive chip coils will not overlap. (Assume that the chip–tool contact length is equal to the chip thickness.)

2. An integral obstruction-type chip breaker has a chip-breaker height of 1 mm and a chip-breaker distance of 4 mm. It is found that the chip is broken satisfactorily when the chip thickness is 0.8 mm. What chip-breaker distance should be provided for an attached obstruction-type chip breaker to give the same performance as the integral obstruction-type chip breaker if the chip breaker height is 2 mm and the chip-breaker wedge angle is 45 deg? (Assume that the chip–tool contact length is equal to the chip thickness.)

REFERENCES

1. Tool Life Testing with Single-Point Turning Tools, 5th Draft Proposal, ISO/ TC 29/WG 22 (Secretariat 37) 91, March 1972.
2. Hendriksen, E. K.: Chip breaking—A study of three dimensional chip flow, *ASME Paper* 53-S-9.
3. Okushima, K., T. Hoshi, and T. Fujinawa: On the behavior of chip in steel cutting, Part 2, In the case of the parallel type chip breaker, *Bull. J. Soc. Mech. Eng.,* vol. 3, no. 10, p. 199, 1960.
4. Nakayama, K.: A study of chip breaker, *Bull. J. Soc. Mech. Eng.,* vol. 5, no. 17, p. 142, 1962.
5. Subramanian, T. L., and A. Bhattacharyya: Mechanics of chip breakers, *Int. J. Prod. Res.,* vol. 4, no. 1, 1965.
6. Trim, A. R., and G. Boothroyd: Action of obstruction type chip former, *Int. J. Prod. Res.,* vol. 6, no. 3, p. 227, 1968.
7. Creveling, J. M., T. F. Jorden, and E. G. Thomsen: Some studies of angle relationships in metal cutting, *Trans. ASME,* vol. 79, no. 1, pp. 127–137, January 1957.
8. Reinhart, L. E., and G. Boothroyd: Effect of Chip Forming Devices on Tool Wear in Metal Cutting, *Proc. 1st No. Amer. Metalworking Res. Conf.,* Hamilton, Ontario, vol. 2, p. 13, May 1973.

9
Machine Tool Vibrations

9.1 INTRODUCTION

The machine, cutting tool, and workpiece form a structural system having complicated dynamic characteristics. Under certain conditions vibrations of the structural system may occur, and as with all types of machinery, these vibrations may be divided into three basic types:

1. *Free or transient vibrations:* resulting from impulses transferred to the structure through its foundation, from rapid reversals of reciprocating masses, such as machine tables, or from the initial engagement of cutting tools. The structure is deflected and oscillates in its natural modes of vibration until the damping present in the structure causes the motion to die away.
2. *Forced vibrations:* resulting from periodic forces within the system, such as unbalanced rotating masses or the intermittent engagement of multitooth cutters (milling), or transmitted through the foundations from nearby machinery. The machine tool will oscillate at the forcing frequency, and if this frequency corresponds to one of the natural frequencies of the structure, the machine will resonate in the corresponding natural mode of vibration.

239

3. *Self-excited vibrations:* usually resulting from a dynamic instability of the cutting process. This phenomenon is commonly referred to as machine tool chatter and, typically, if large tool–work engagements are attempted, oscillations suddenly buildup in the structure, effectively limiting metal removal rates. The structure again oscillates in one of its natural modes of vibration.

It is important to limit vibrations of the machine tool structure as their presence results in poor surface finish, cutting-edge damage, and irritating noise. The causes and control of free and forced vibrations are generally well understood and the sources of vibration can be removed or avoided during operation of the machine. Chatter vibrations are less easily controlled and metal removal rates are frequently limited because the operator must stop the machine to change the cutting conditions, which often means reducing the depth of cut or feed rate. The causes of machine tool chatter are generally well understood and the vibrations occur because of the basic interaction between the cutting process and the machine tool structure [1,2,3]

9.2   FORCED VIBRATIONS

A machine structure that is subjected to a periodic force will vibrate at the forcing frequency. Several basic results can be illustrated, first by considering a single-degree-of-freedom system.

9.2.1   Single-Degree-of-Freedom System

For the one-degree-of-freedom system shown in Fig. 9.1 the equation of motion is

$$m_e \frac{d^2x}{dt'^2} + c_d \frac{dx}{dt'} + S_e x = F_{max} \cos \omega_f t' \tag{9.1}$$

where

x = displacement
t' = time
m_e = equivalent mass
c_d = damping force per unit velocity (viscous damping constant)
S_e = restoring force per unit displacement (spring stiffness)
F_{max} = peak value of the external harmonic force
ω_f = angular frequency of the external harmonic force
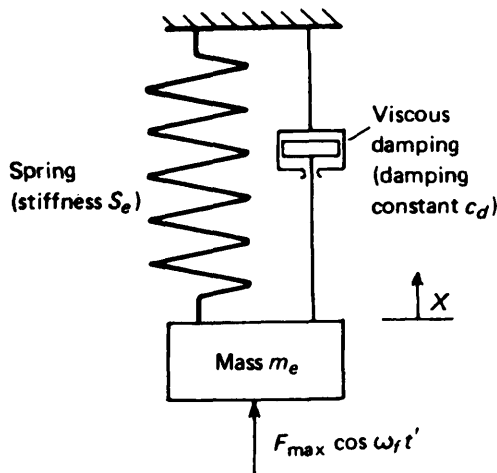
Figure 9.1 Model of one-degree-of-freedom mass–spring system with viscous damping.

The steady-state vibration of this system is given by

$$x = \frac{F_0 \cos (\omega_f t' - \phi_f)}{\sqrt{4\zeta^2\omega_f^2 - (\omega_n^2 - \omega_f^2)}} \qquad (9.2)$$

where

$F_0 = F_{max}/m_e$
ω_n = the natural angular frequency
ζ = the damping ratio

Equation (9.2) represents a motion of angular frequency ω_f at an amplitude given by:

$$a_v = \frac{F_0}{\sqrt{4\zeta^2\omega_f^2 + (\omega_n^2 - \omega_f^2)^2}} \qquad (9.3)$$

and lagging the disturbing force by a phase angle ϕ_f where

$$\phi_f = \tan^{-1} \frac{2\zeta\omega_n}{(\omega_n^2 - \omega_f^2)} \qquad (9.4)$$

Resonance occurs when ω_f equals ω_n and the amplitude at resonance

is $F_0/2\zeta\omega_n$. These results are shown in Fig. 9.2, where Eqs. (9.3) and (9.4) are plotted for various values of the damping ratio ζ.

It can be seen from these results that to minimize the amplitude of vibration of a damped mass–spring system, the damping should be as large as possible and the natural frequency of the system should be significantly less than the frequency of the disturbing force.

Forced vibration in machine tools are most often caused by cyclic variations in the cutting forces. Such variations will occur in side or face milling, for example, where the frequency of the forced vibration equals the product of the tool rotational frequency and the number of teeth on the tool.

Figure 9.3 shows the variation in spindle torque during a slab-milling operation for cutters having various numbers of teeth. It can be seen that as the number of teeth increases, the frequency of the torque variations increases and the peak torque decreases.

The machine tool designer will be able to estimate from data such as that presented in Fig. 9.3 the magnitudes and frequencies of the disturbing forces likely to occur during the operation of the machine tool. With this information the designer will be better able to design the machine so that the natural frequencies of the various parts of the structure do not approach the forcing frequencies.

The response curves for the single-degree-of-freedom system shown in Fig. 9.2 can be plotted in polar form on a single diagram (Fig. 9.4). As can be seen, the resulting curve is approximately circular, with the resonant frequency occurring when the phase lag of the displacement is around 90 deg. Such a frequency response diagram is referred to as the harmonic response locus or harmonic receptance of the system. This representation of the frequency response is useful when considering complex structures with many degrees of freedom and in particular for the analysis of machine tool chatter [1,2,3].

9.2.2 Complex Structures

It is possible to simulate the behavior of complex structures by considering numerous masses, springs, and damping elements connected together, although in practice choosing the appropriate values for each element is difficult. However, if the structure is excited with a periodic force, it will behave in a similar manner to the single-degree-of-freedom system considered in Sec. 9.2.1. As the frequency of the exciting force is varied, the structure will resonate with large-amplitude vibrations as before, but with a number of important differences:

1.   A complex structure will exhibit several resonances or natural fre-
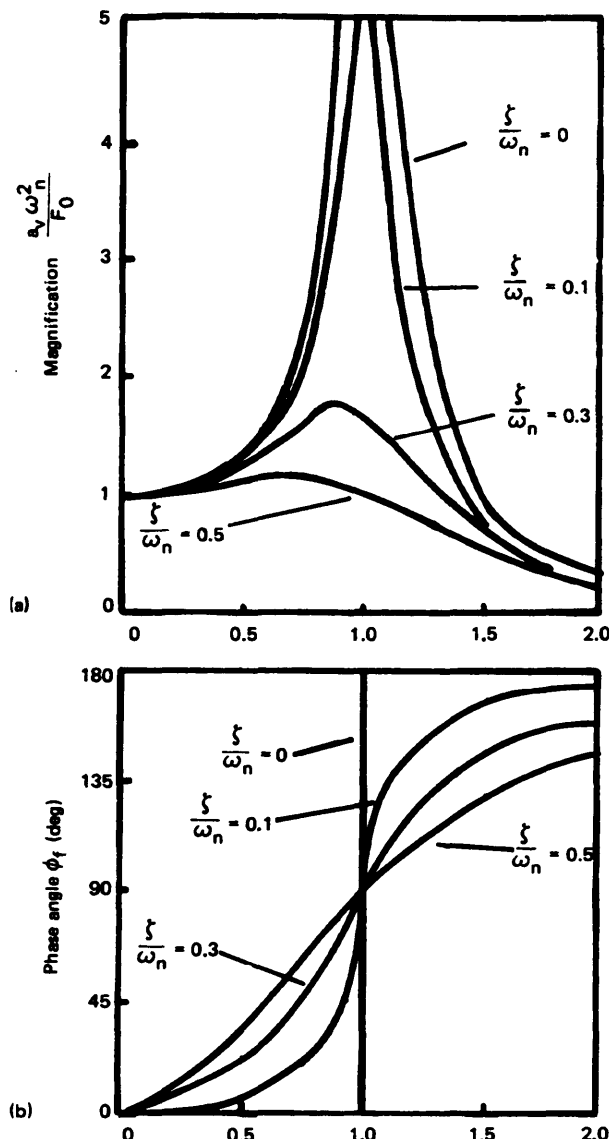
Figure 9.2 Response curves for the system in Fig. 9.1, where a_v = amplitude of the vibration, F_0 = peak value of disturbing force divided by the mass, ω_f = angular forcing frequency, ω_n = angular natural frequency of the system, ζ = damping ratio, and ϕ_f is the phase angle between the displacement and the disturbing force.
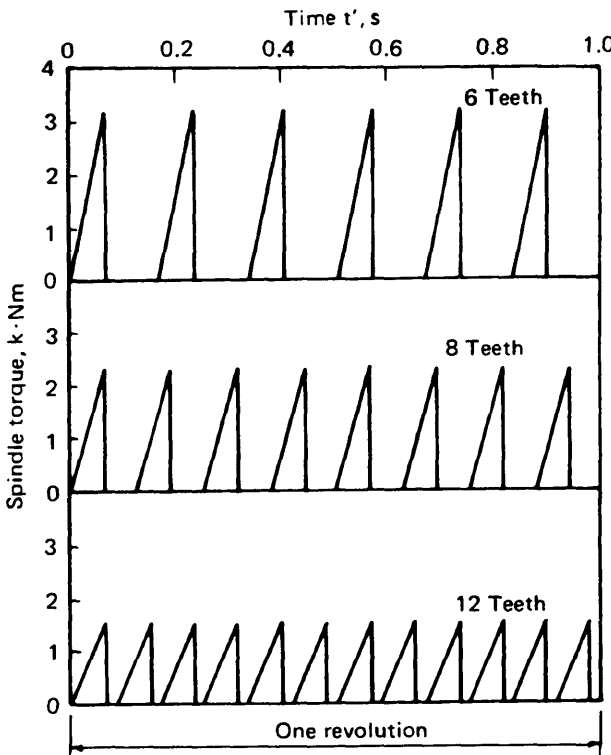
Figure 9.3 Variations in spindle torque during slab milling with a straight-tooth cutter, where the cutter diameter d_t = 100 mm, the work engagement (depth of cut) a_e = 5 mm, the back engagement (width of cut) a_p = 200 mm, the rotational frequency of the cutter n_t = 1 s^{-1} and the feed speed v_f = 17 mm/s.

quencies and the frequency response curve will have several peaks corresponding to each resonance. For example, Fig. 9.5 shows the resonance curves for a machine tool structure and Fig. 9.6 shows the corresponding harmonic response locus. Each resonance produces a loop of approximately circular form in the curve.

2. At each resonance the contribution of the various elements of the structure to the overall response will vary. Some parts will be moving with large amplitudes at some frequencies, but hardly moving at all for others. Each resonance will have a corresponding mode of vibration or mode shape that the structure adopts. The modes of vibration can be represented graphically by considering the motion of various points on the structure and indicating the amplitude and relative phase of the motion of

these points on a picture of the structure. Figure 9.7 shows some of the mode shapes for a horizontal-milling machine structure [4]. The important modes of vibration are those that result in relative displacements of the tool and workpiece, as these will have a detrimental effect on the surface finish of the workpiece. If two modes of vibration occur at frequencies close to each other, these are closely coupled modes of vibration.
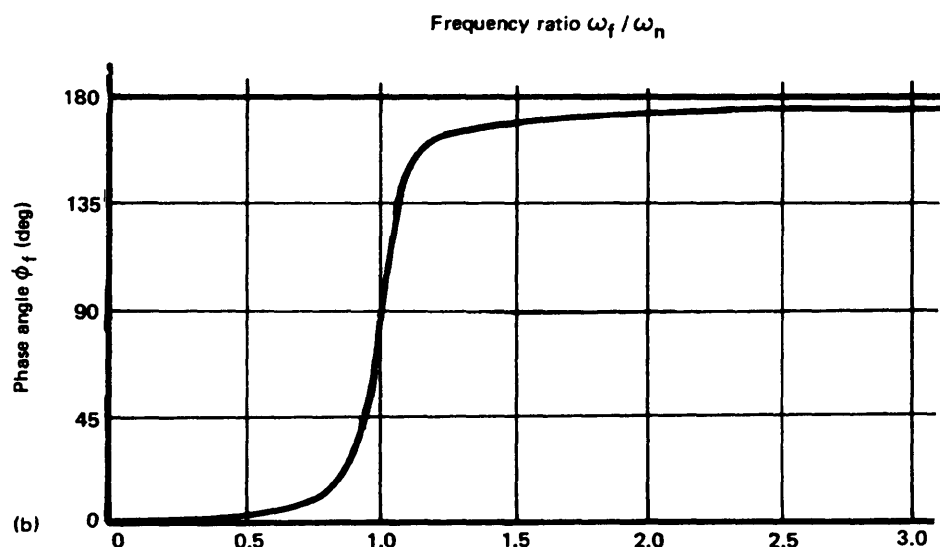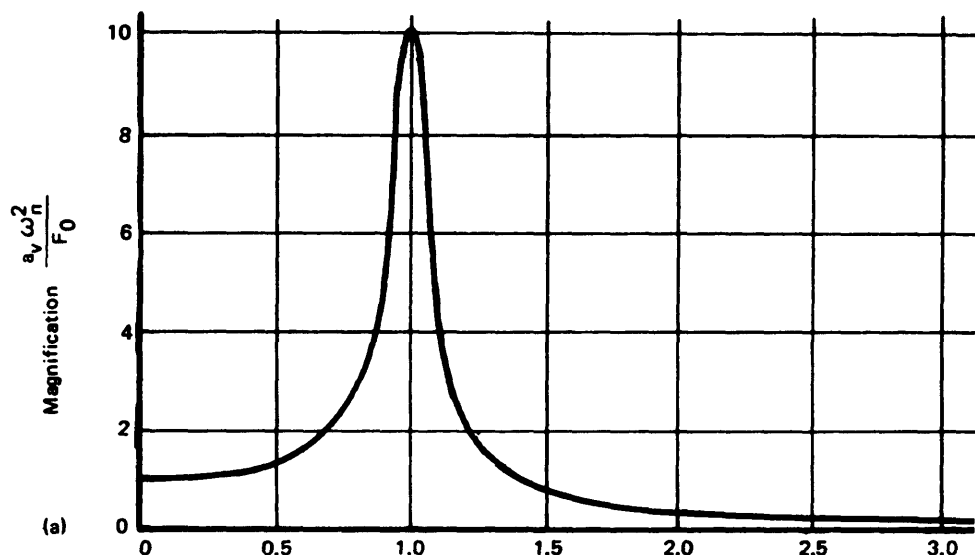
3. A machine tool is a three-dimensional structure and consequently the points of application and the direction of the exciting force and the measured vibration are important. For the single-degree-of-freedom system discussed in Sec. 9.2.1, the direction and point of application of the exciting force F_{max} corresponded to the measured vibration x. The resulting frequency response is referred to as a direct response, since these two directions correspond. However, in a complex three-dimensional structure it is obviously possible to apply the exciting force at a particular point in one direction and then to measure the displacement at another point in a different direction. The resulting frequency response curve will again exhibit resonances as before and is referred to as a cross-frequency response. This is important because forces applied at certain points and directions may result in only some of the modes of vibrations being excited.

9.3   SELF-EXCITED VIBRATIONS (CHATTER)

9.3.1   Interaction of the Cutting Process and Machine Structure

The basic cause of chatter is the dynamic interaction of the cutting process and the machine tool structure. A schematic representation of an orthogonal machining operation is presented in Fig. 9.8, which depicts a cutting tool and workpiece connected by an elastic structure. During cutting, a force F_r is generated between the tool and workpiece, which acts at an angle to the cut surface. The magnitude of this cutting force depends largely on the tool–work engagement and depth of cut. The cutting force strains the structure elastically and can cause a relative displacement of the tool and workpiece, which alters the tool–work engagement (undeformed chip thickness). Thus, during cutting the machine tool behaves as a closed-loop feedback system, as shown in Fig. 9.9. A disturbance in the cutting process (e.g., because of a hard spot in the work material) will cause a deflection of the structure, which may alter the undeformed chip thickness, in turn altering the cutting force. There is a possibility for the initial vibration to be self-sustaining (unstable) and build up, with the machine oscillating in one of its natural modes of vibration.

The closed-loop cutting-process structural system will become un-

(a)

Frequency ratio ω_f / ω_n

(b)
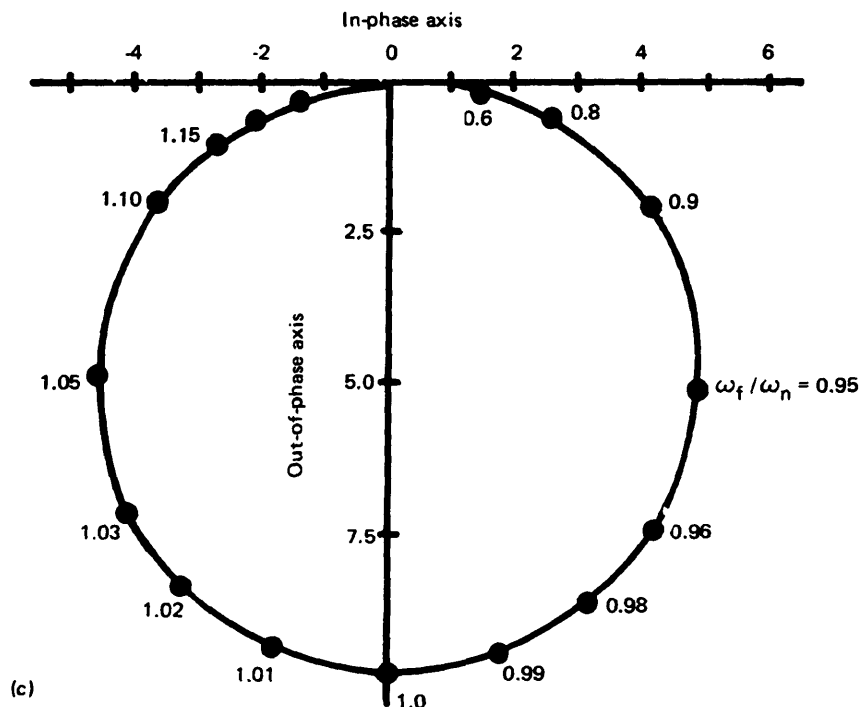
Figure 9.4 Relation between resonance and phase curves and harmonic re-
sponse locus: (a) resonance curve; (b) phase curve; (c) harmonic response locus of
a system with one degree of freedom with viscous damping corresponding to
$\zeta = 0.05$.
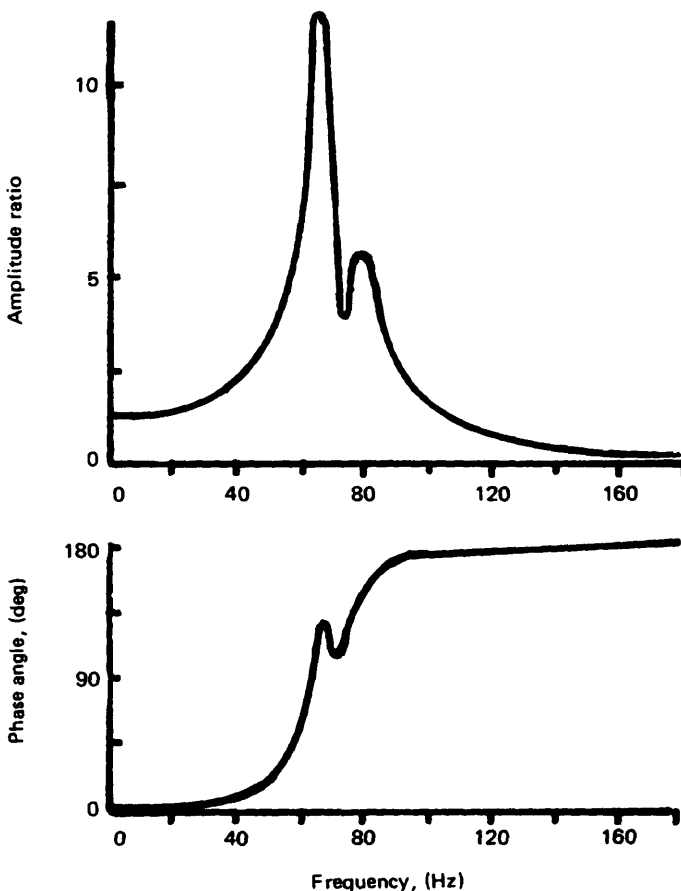
Figure 9.5 Frequency response of a machine tool structure.

stable if a mechanism exists for transferring energy into the structure to sustain the vibration. Two major effects can cause instability: the regenerative effect, which is the dominant cause, and the mode-coupling effect.

Regenerative Instability

Regenerative instability can occur when successive passes of the cutting tool overlap, that is, when the tool at any instant is removing a surface that was cut on the previous pass of the tool or revolution of the workpiece (Fig. 9.10). A disturbance in the cutting process will cause a wavy surface to be generated on the workpiece. During the next pass of the tool the un-
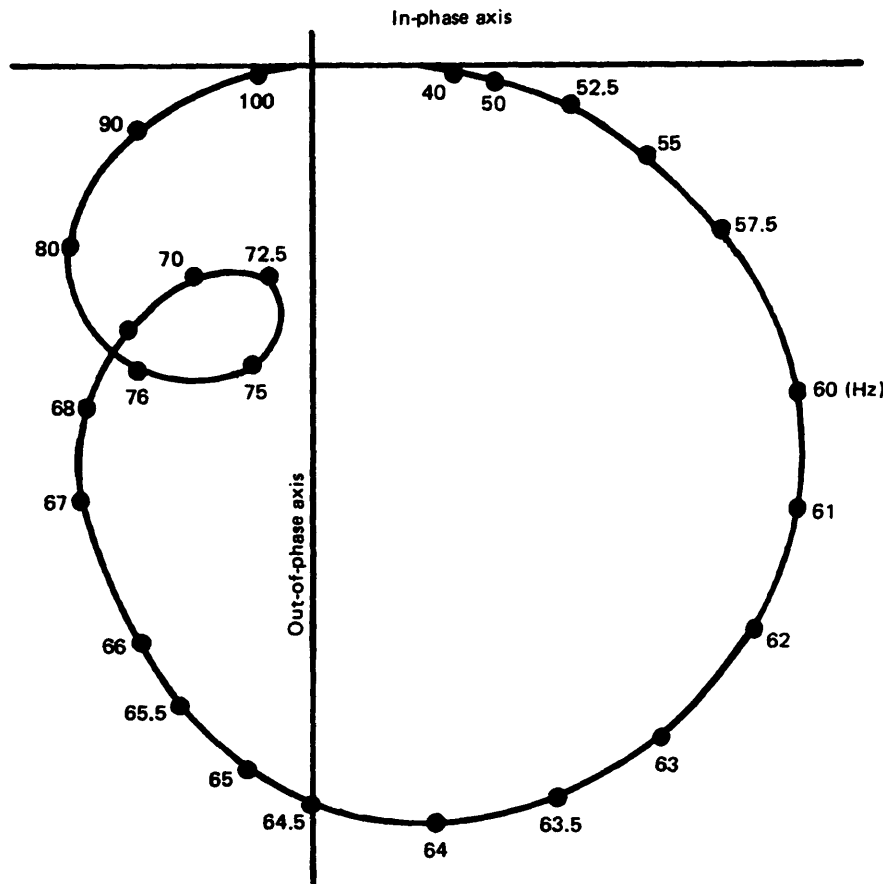
Figure 9.6   Polar frequency response locus corresponding to Fig. 9.5.

deformed chip thickness will depend on the current motion of the tool and the wave cut on the surface during the previous pass. Depending on the phase between these waves, the force variation may increase after successive passes of the tool and the vibration will build up, until limited by some nonlinearity such as the tool leaving the workpiece during part of the vibration cycle.

Mode-Coupling Instability

Mode-coupling instability can occur when successive passes of the tool do not overlap, such as in screw cutting, and results from a particular motion of the tool relative to the workpiece in the presence of closely coupled

(a)

(b)

(c)

(d)
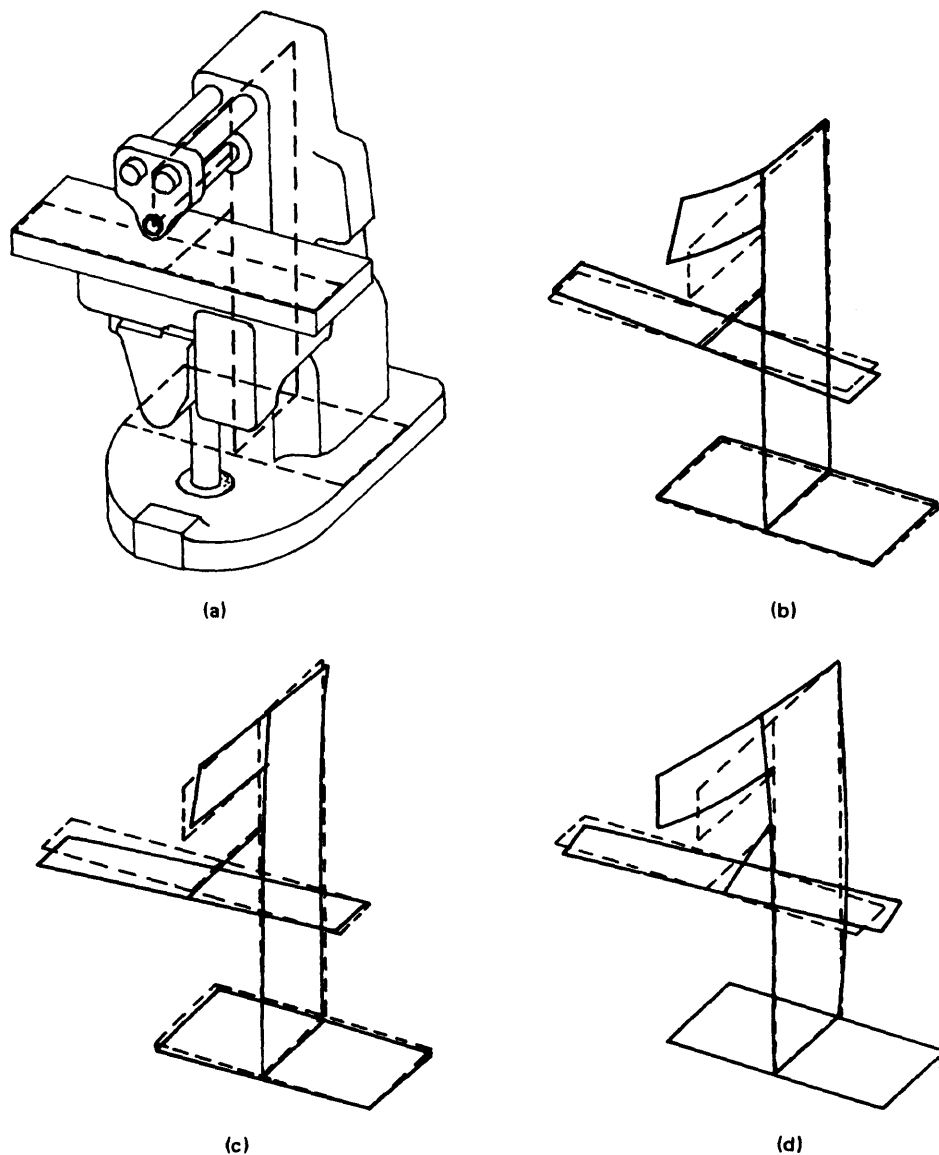
Figure 9.7   Modal shapes of a horizontal-milling machine structure. (a) Grid for describing modal shapes; (b) distortion for 97-Hz mode; (c) distortion for 107-Hz mode; (d) distortion for 112-Hz mode.
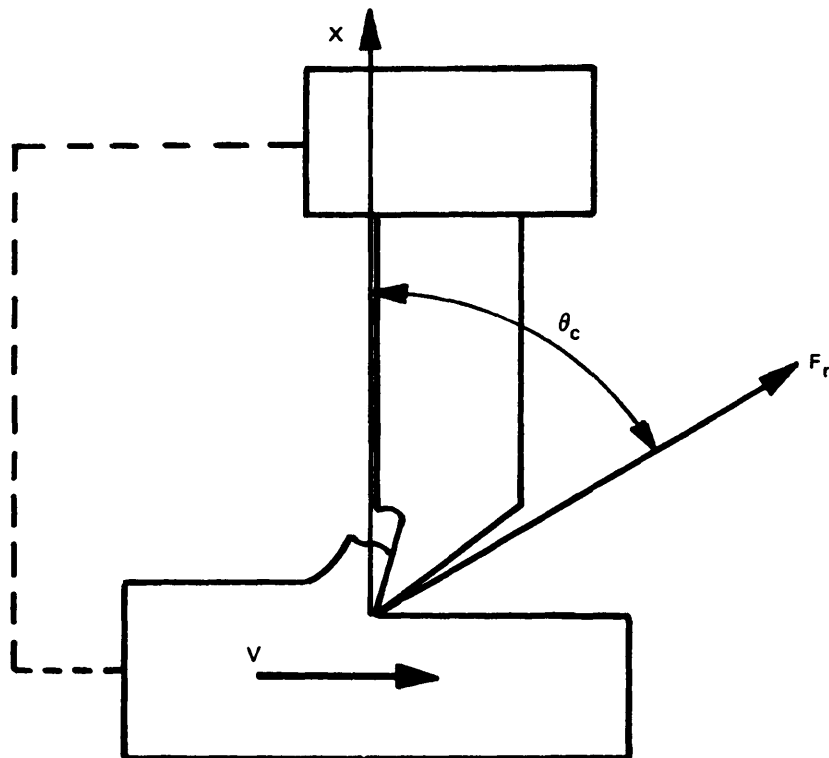
Figure 9.8 Idealized orthogonal cutting system.

modes of vibration of the structure. The characteristics of the structure can be such that a free vibration of the structure causes the tool to follow an elliptical path relative to the workpiece when disturbed, as illustrated in Fig. 9.11. The cutting force F_r, does work during this periodic motion when F_r opposes the motion. It will put work into the system during half of the cycle and take work out during the other half. Over the lower part of the elliptical path, the undeformed chip thickness is greater and consequently the value of F_r is higher. Thus, more work may be put into the system over the lower part of the cycle elliptical path than is taken out in the upper part, resulting in a net input of energy and causing the amplitude of vibration to increase.

9.3.2 Stability Charts

The stability of a machine tool can be represented graphically in the form of a chart, which depicts the effect on stability of the width of cut, drill
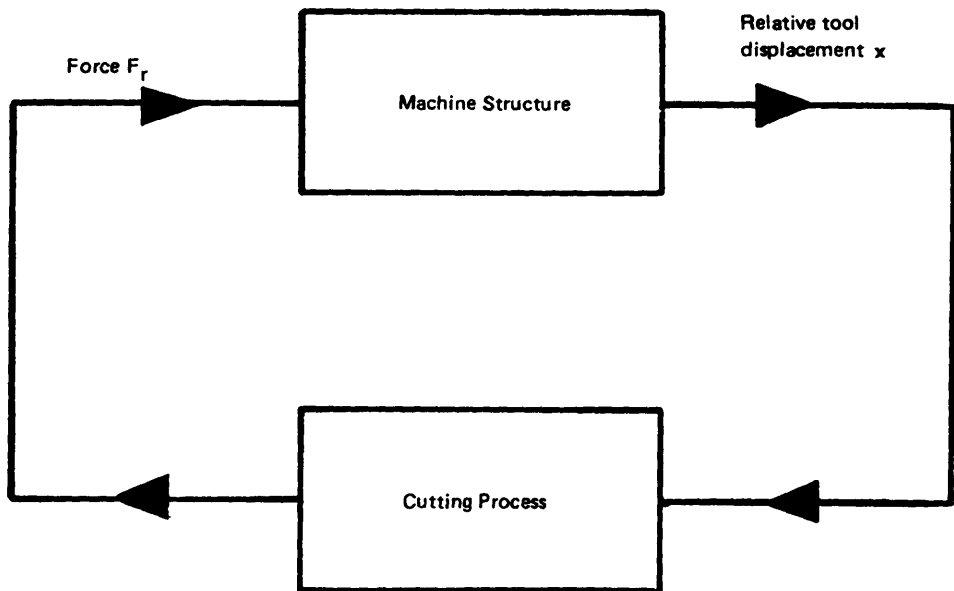
Figure 9.9 Closed-loop representation of the machine tool structure and cutting-process system.

diameter, and so on, and the rotational speed of the tool or workpiece. A typical experimental stability chart for a horizontal-milling machine is shown in Fig. 9.12, with the unstable ranges shown as lobed areas. This chart was obtained by cutting at different widths of cut and rotational speeds of the cutter and noting the conditions at which instability occurs and vibrations build up. This type of stability chart, with the unstable regions forming lobes, is typical of that obtained when chatter is caused by the regenerative effect. A number of important features should be noted:

1. The lobes lie on an envelope forming a boundary below which the machine is stable for all rotational speeds.
2. The stability of the machine increases at low speeds.
3. The envelope b_w of the unstable regions has a horizontal asymptote, b_{w0}, which represents a width of cut below which the machine is always stable.
4. A judicious selection of cutting speed can increase the chatter-free width of cut, that is, points lying between the lobes of the stability chart.

First pass   Second pass   Third pass

Fourth pass

Wave cut on previous tool pass

Current tool oscillation
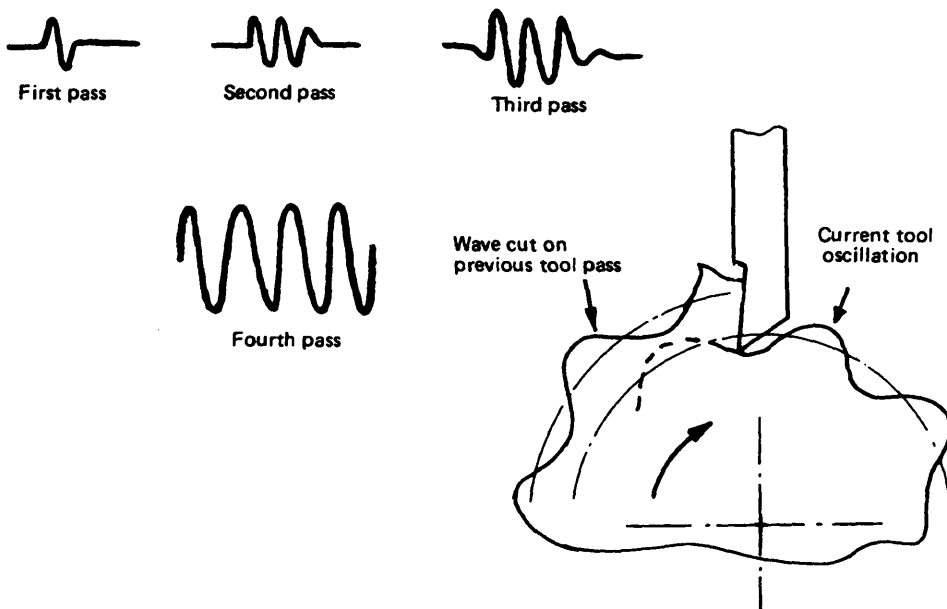
Figure 9.10   Regenerative instability.

9.3.3   Analysis of Machine Tool Chatter

An analysis of machine tool instability is based on the condition at the threshold of stability, assumed to be the point at which a disturbance in the cutting process neither grows nor decays in magnitude, that is, a small amplitude harmonic vibration persists. Considering the closed-loop system of Fig. 9.9, this requires a representation of the response of the machine structure and the response of the cutting process itself to such vibrations, in other words:

1. A transfer function between a harmonic force input and a relative displacement output of the structure
2. A transfer function for the cutting process between a vibrational displacement input and a force output

For simplicity, the analysis will consider initially an orthogonal-turning operation, as indicated in Fig. 9.13.

Cutting Process

Under steady-state conditions the cutting force F, remains reasonably constant and acts at an angle θ_c to the normal to the cut surface (Fig. 9.8).
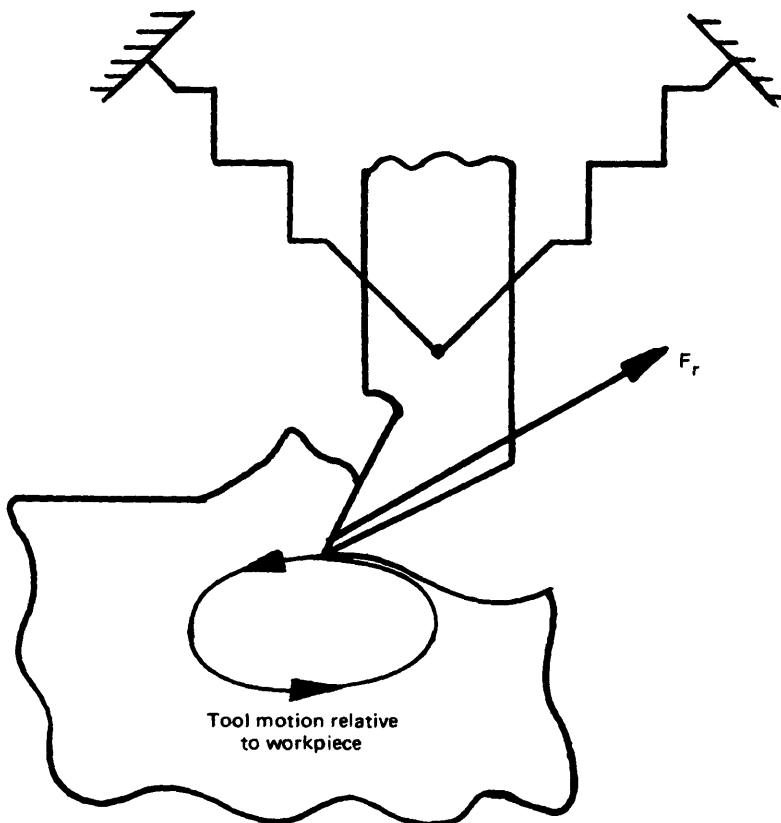
Figure 9.11 Mode coupling suitability.

When the tool oscillates relative to the workpiece, some of the cutting-process parameters (undeformed chip thickness, relative tool geometry, etc.) undergo cyclic variations and a cyclic force variation dF_r is superimposed on the mean force F_r. The magnitude of dF_r is dependent on the nature of the tool motion and the way it affects the parameters governing the cutting force. The cutting-force variation is determined mainly by relative oscillations normal to the cut surface, and this case is illustrated in Fig. 9.13. Oscillations parallel to the cut surface and torsional oscillations of the drive system cause changes in the cutting speed, and these have been shown to have little effect on the onset of instability [5]. If the situation shown in Fig. 9.13 is considered, it can be seen that the depth of cut is dependent on both the current motion of the tool x_t and the wave left on the surface during the previous tool pass $x_{(t'-T)}$. Note that x is the displacement
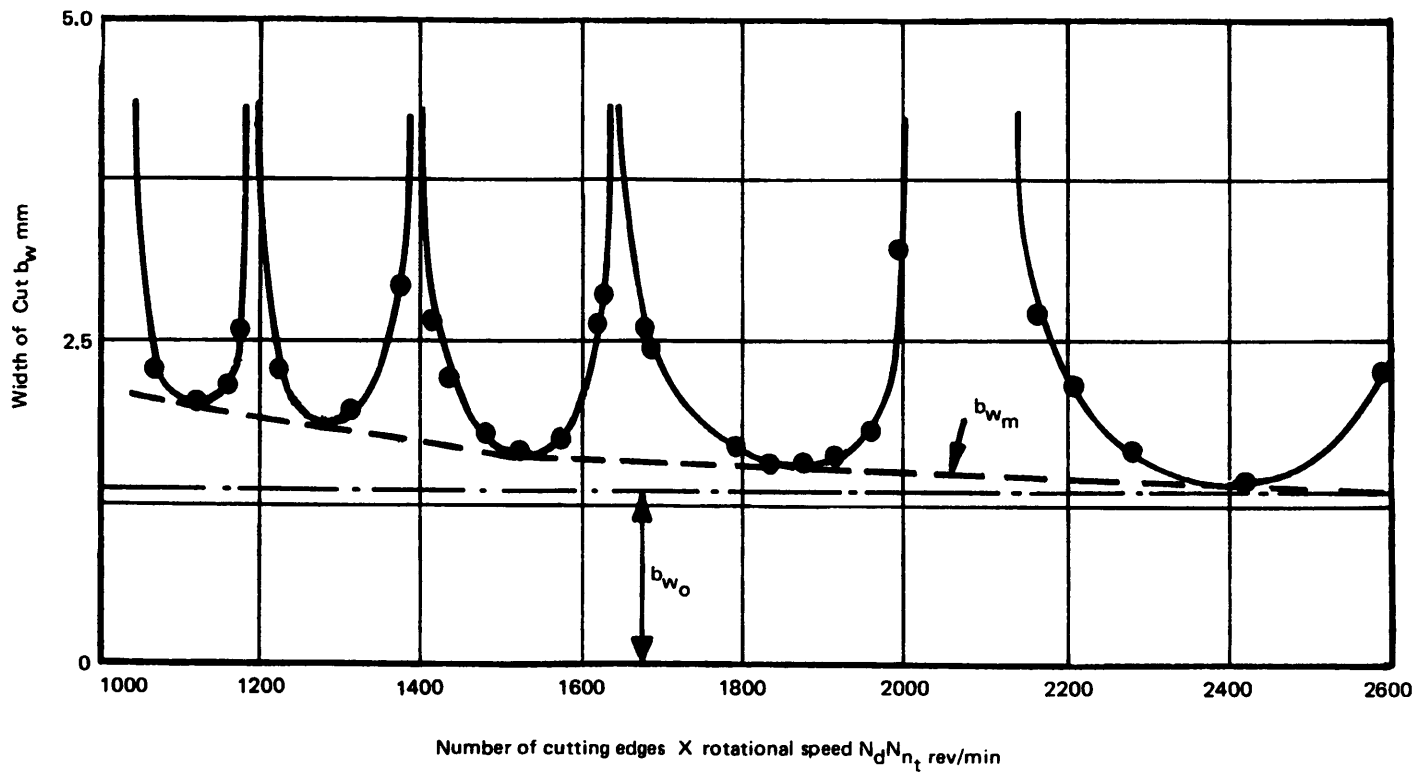
Figure 9.12 Experimental stability chart of a horizontal milling machine, feed speed = 0.79 mm/rev and depth of cut = 5.24 mm. (Adapted from Sadek and Tobias [10].)
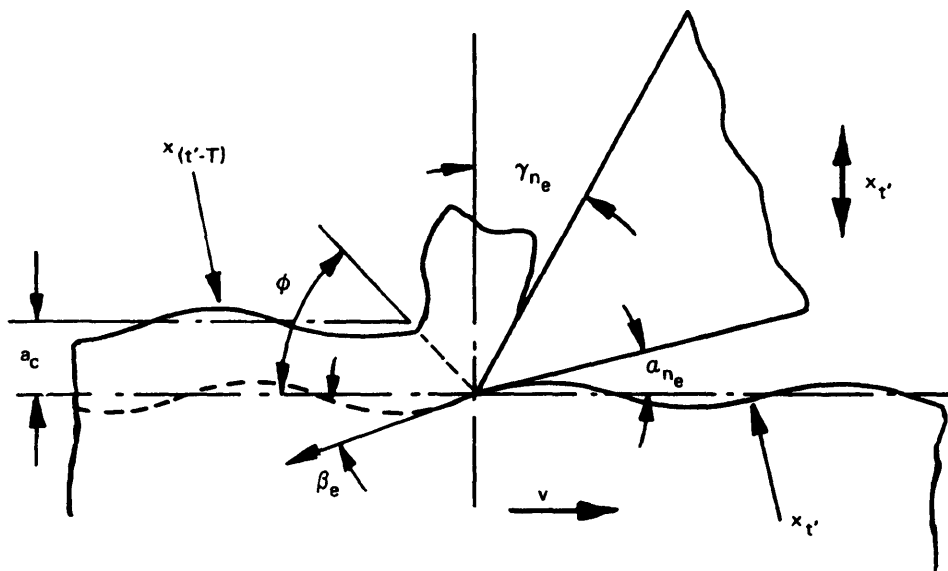
Figure 9.13 Effect of oscillations of the tool in the normal direction during orthogonal cutting.

of the tool perpendicular to the mean cutting direction, t' is time, and T is the time for one pass of the tool or revolution of the workpiece. The presence of a vibration normal to the mean cutting direction causes variations in a number of the parameters known to influence the cutting force, as indicated in Table 9.1 [6]. The actual influence of each of these parameter variations on the cutting force is difficult to determine. Several analyses of the dynamic cutting process have been attempted [7–9] and these are mostly modifications of the basic shear-plane model discussed in Chap. 2. However, examination of the entries in Table 9.1 indicates that the cutting-force variation should be divided into a portion that is in phase with the displacement $x_{t'}$ and another portion that is out of phase with $x_{t'}$, dependent on the derivative of $x_{t'}$.

The in-phase force variation can be expressed as

$$dF_1 = k_1(x_{t'} - x_{(t'-T)}) \tag{9.5}$$

where k_1 is the chip-thickness coefficient or cutting stiffness, which is proportional to the width of cut, drill diameter, and so on. This expression applies when successive passes of the cutting tool completely overlap. For

Table 9.1   Dynamic Variation of Cutting Parameters Resulting from the Normal Tool Motion $x_{t'}$.[a]

Parameter	Dynamic value
In-phase element:	
Uncut chip thickness a_c	$da_c = x_{t'} - x_{(t'-T)}$
Out-of-phase elements:	
Cutting speed v	Negligible change due to $x_{t'}$ in the normal direction
Tool rake angle γ_{n_e}	$d\gamma_{n_e} = -x_{t'}/v$
Tool clearance angle α_{n_e}	$d\alpha_{n_e} = x_{t'}/v$
Instantaneous cutting direction β_e	$d\beta_e = x_{t'}/v$
Free surface slope δ_c	$d\delta_e = x_{t'}/v - x_{(t'-T)}/v$
Shear angle ϕ	$d\phi = f(x_{t'})/v$

[a]Adapted from Das et al. [6].

cases when successive passes do not overlap completely, an overlap factor μ_c can be introduced, which can have a value of from zero to one, and Eq. (9.5) becomes

$$dF_1 = k_1(x_{t'} - \mu_c x_{(t'-T)}) \tag{9.6}$$

Several of the parameters in Table 9.1 depend on the derivative of the tool motion and the cutting speed, but the individual contribution of each parameter is difficult to determine. However the effect of all these parameter variations can be combined into one out-of-phase force variation of the following form:

$$dF_2 = k_2 \frac{2\pi}{\Omega} \dot{x}_{t'} \tag{9.7}$$

where k_2 is a constant and Ω is the rotational speed of the workpiece (rad/s).

The total force variation due to the tool oscillation relative to the workpiece is

$$dF_r = dF_1 + dF_2 = k_1(x_t' - \mu_c x_{(t'-T)}) + k_2 \frac{2\pi}{\Omega} \dot{x}_{t'} \tag{9.8}$$

which can be used to analyze the conditions at the limit of stability.

Machine Structure

At the threshold of stability the transfer function for the structure is its frequency response. Since for most cutting operations, the cutting force acts in a direction different from the normal to the cut surface, the relevant frequency response is the cross response between these two directions. This may be represented as a polar diagram (Fig. 9.14) and is called the operative receptance. This polar diagram represents the in-phase and out-of-phase components of the response at each frequency and can be expressed as a complex number. Thus, at each frequency
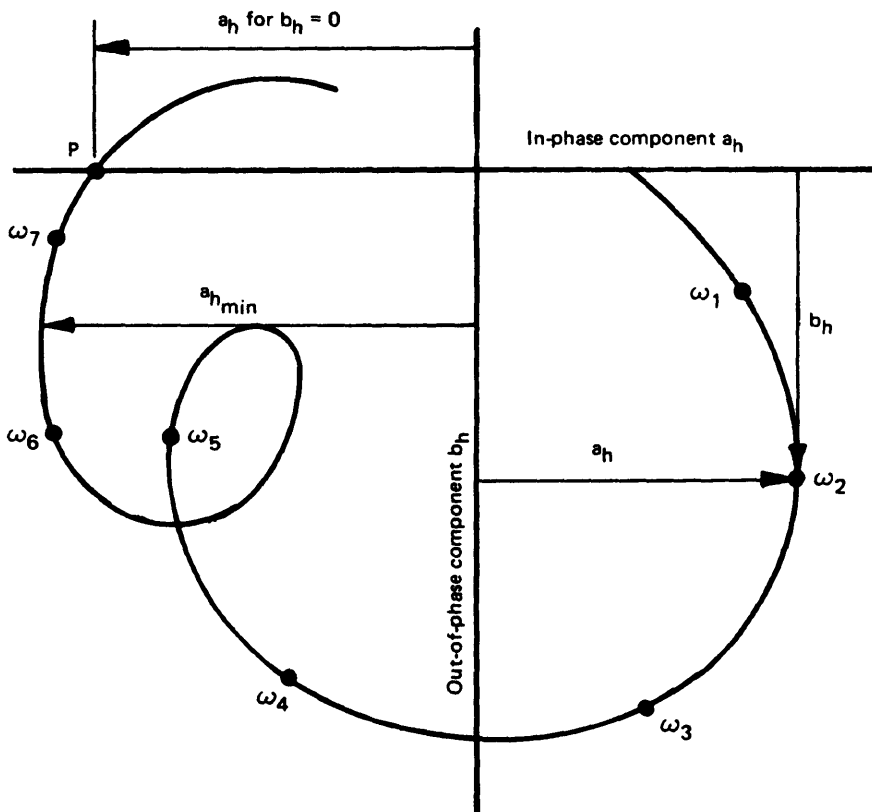
Figure 9.14 Cross-frequency response locus between cutting force direction and the normal to the cut surface (operative receptance locus).

$$x = (a_h + ib_h)F \qquad\qquad\qquad (9.9)$$

where $i = \sqrt{-1}, x$ and F are varying harmonically, and a_h and b_h depend on the magnitude of the vibrational frequency ω_f.

The required operative receptance depends on the cutting process and the particular cutting conditions (depth of cut, tool rake angle, etc.). Figure 9.15 shows the cutting force directions and normal to the cut surface for several machining processes. For multipoint operations such as milling, a mean direction for the force F_r must be used, because the number of teeth engaged with the workpiece varies as the tool rotates. Also, the effective normal direction to the cut surface must be known and is assumed to pass through the center of the arc joining the points of contact between the tool and workpiece [10]. As a result the direction of the normal to the cut surface is different for different values of the depth of cut in slab milling.

For the analysis of machine tool instability, the cross receptance between the applicable cutting force direction and the normal to the cut surface must be known, for conditions similar to those existing at the threshold of stability. Determination of this frequency response will be discussed later.

Stability Analysis

At the threshold of stability $x = dF_r(a_h + ib_h)$ or

$$x = -\left[k_1(x_{t'} - \mu_c x_{(t'-T)}) + k_2 \frac{2\pi}{\Omega}\right](a_h + ib_h) \qquad\qquad (9.10)$$

(a)   (b)   (c)
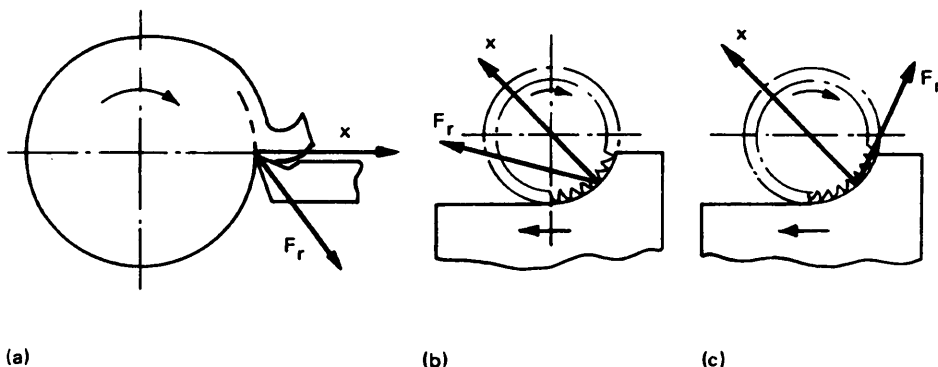
Figure 9.15   Forcing and response directions in some machining processes.

with the negative sign introduced because an increase in the displacement x causes a decrease in the cutting force F_r.

At the limit of stability x is harmonic, that is, $x = Xe^{i\omega t'}$, and therefore in Eq. (9.10)

$$Xe^{i\omega t'} = -\left[k_1(Xe^{i\omega t'} - \mu_c Xe^{i\omega(t'-T)}) + k_2 \frac{2\pi}{\Omega} i\omega Xe^{i\omega t'} \right](a_h + ib_h)$$

or

$$1 = -(a_h + ib_h)\left[k_1(1 - \mu_c e^{-i\omega T}) + k_2 \frac{2\pi}{\Omega} i\omega \right] \qquad (9.11)$$

However, $e^{-i\omega T} = \cos(\omega T) - i\sin(\omega T)$ and, therefore, expanding and equating real and imaginary parts

$$1 = b_h\left(k_1\mu_c \sin \omega T + k_2 \frac{2\pi}{\Omega} \right) - a_h k_1(1 - \mu_c \cos \omega T)$$

and

$$0 = a_h\left(k_1\mu_c \sin \omega T + k_2 \frac{2\pi}{\Omega} \right) + b_h k_1(1 - \mu_c \cos \omega T)$$

which, after replacing ωT by β_c and k_2/k_1 by C_c, assumed a constant, become

$$k_1 = \frac{1}{b_h \mu_c \sin \beta_c + \beta_c C_c b_h - a_h(1 - \mu_c \cos \beta_c)} \qquad (9.12)$$

and

$$0 = a_h(\mu_c \sin \beta_c + C_c \beta_c) + b_h(1 - \mu_c \cos \beta_c) \qquad (9.13)$$

These two equations define the limit of stability for a given frequency in terms of critical values of the cutting stiffness k_1 to which the width of cut is directly proportional.

Equations (9.12) and (9.13) must be solved numerically to give a stability chart. The procedure for this is as follows:

1. For a particular frequency, obtain the values of a_h and b_h from the frequency response locus (Fig. 9.14).

2. From Eq. (9.13), obtain the solutions for the phase angle β_c. There are a large number of these solutions and for each one $\beta_c = \omega T = 60\omega/n_w$, where n_w is the rotational frequency of the workpiece.
3. Substituting each solution for β_c into Eq. (9.12) gives a corresponding critical value of k_1.
4. Repeat these calculations for other values of the frequency ω.

The stability chart (k_1 versus n_w) may then be plotted and will be of the form shown in Fig. 9.16.

Modification for Multiedge Cutting Operations

The preceding equations were derived for a single-point turning operation, but can be readily modified for multipoint cutting tools by replacing k_1 by $N_d k_1$ and setting $\beta_c = \omega T/N$, where N is the number of cutting edges and N_d is the average number contacting the workplace at any time. Thus, for a drilling operation, $N = N_d = 2$. For a slab-milling operation the value of N_d depends on the tool radius and the depth of cut a_e (Fig. 9.17):

$$N_d = \frac{N}{2\pi} \cos^{-1} \frac{(d_t/2 - a_e)}{d_t/2} \qquad (9.14)$$

Special Cases

Two special cases of this analysis exist, from which some general conclusions can be drawn. First, a simplification can be made by assuming $C_c = 0$, $\mu_c = 1$, which means that the increased damping from the cutting
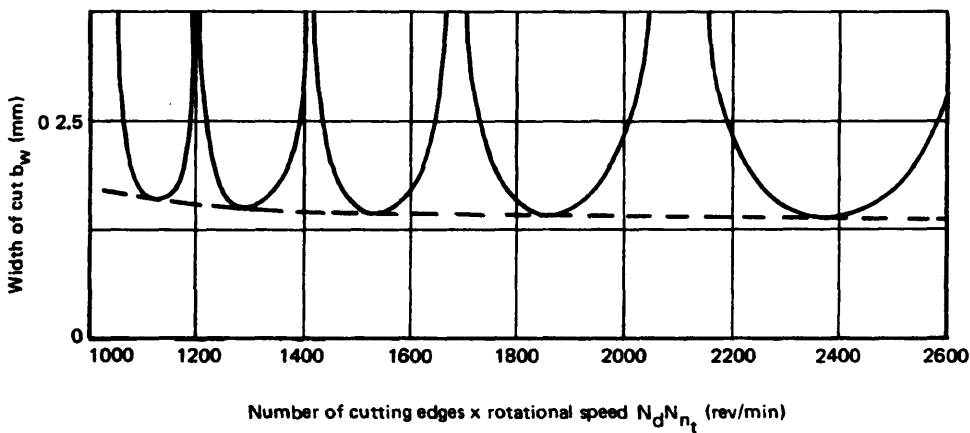
Figure 9.16 Predicted stability chart corresponding to Fig. 9.12, $C_c = 0.001$. (From Sadek and Tobias [10.)
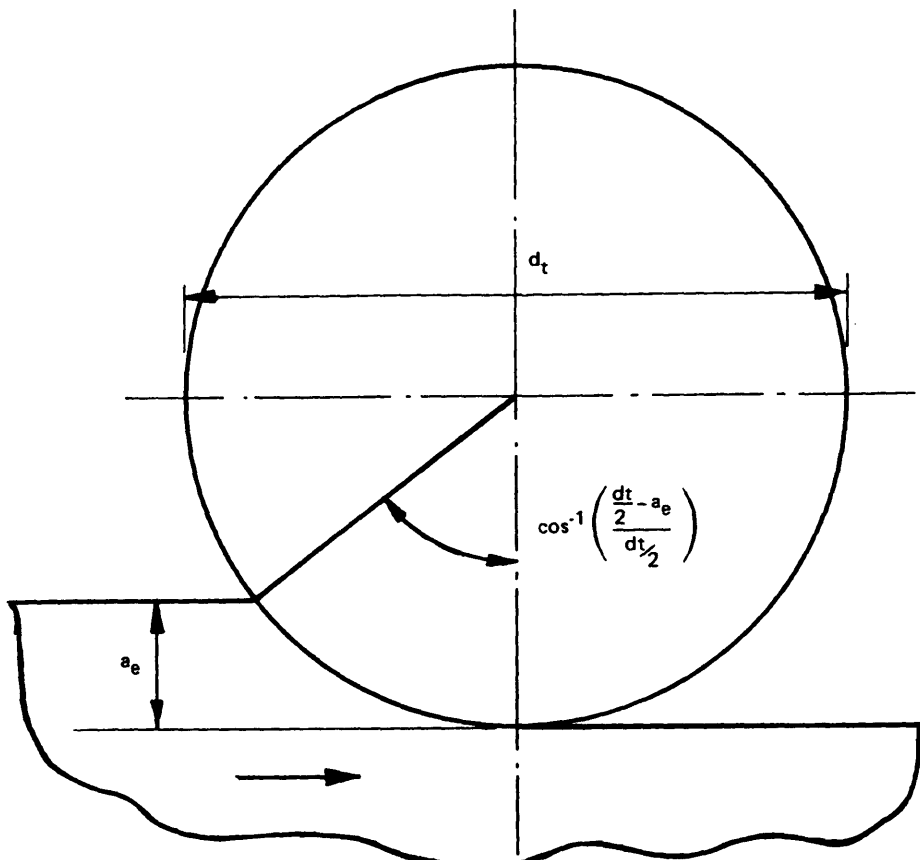
Figure 9.17 Arc of contact during slab milling, N_d = the average number of teeth in contact, N = number of teeth on the cutter, d_t = tool diameter, and a_e = the work engagement (depth of cut).

process is ignored at low speeds and successive cuts by the tool completely overlap. In this case Eq. (9.10) becomes

$$x_{t'} = -[k_1(x_{t'} - x_{(t'-T)})](a_h + ib_h) \tag{9.15}$$

or

$$\frac{x_{t'}}{x_{(t'-T)}} = \frac{k_1(a_h + ib_h)}{1 + k_1(a_h + ib_h)}$$

which has a magnitude of 1 at the threshold of stability and gives:

$$k_1 = -\frac{1}{2a_h} \quad \text{or} \quad \infty \tag{9.16}$$

Equation (9.13) becomes

$$a_h \sin \beta_c + b_h(1 - \mu_c \cos \beta_c) = 0 \tag{9.17}$$

This result allows some important conclusions to be drawn, which can be shown to apply also to the more general case when k_2 and therefore C_c has a finite value.

1.   Since the chip-thickness coefficient must be positive, instability can occur only for frequencies for which a_h is negative, that is, frequencies corresponding to the left-hand portion of the polar frequency response diagram (Fig. 9.14).

2.   The stability chart for this case is similar to Fig. 9.16, except the increase in stability at low speeds is not present (Fig. 9.18). The horizontal asymptote in both stability charts is the same.

3.   The lowest value of k_1 corresponds to the negative value of a_h of greatest magnitude. This gives the lowest point on each lobe of the stability chart and defines the horizontal asymptote in the stability charts. This is important because if cutting conditions are chosen such that k_1 is below this asymptote, the machine will be stable for all cutting speeds.
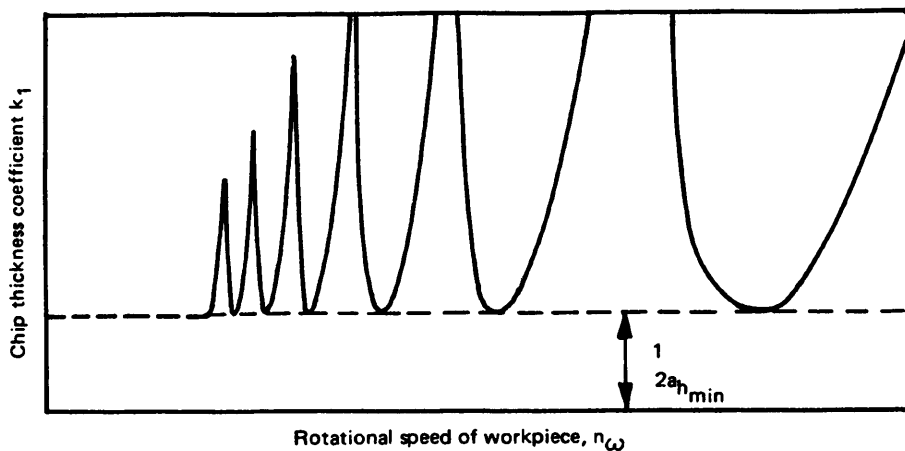
Figure 9.18   Form of the stability chart when $C_c = 0$ and $\mu_c = 1$.

This result can form the basis for a comparative dynamic acceptance test for machine tools.

The second special case is where $C_c = 0$ and $\mu_c = 0$. For this condition Eqs. (9.12) and (9.13) give $k_1 = -1/a_h$ and $b_h = 0$, which means that instability can occur only when a_h is negative and b_h is zero. This instability occurs at the frequency at which the locus crosses the negative in-phase axis (point P, Fig. 9.14). This stability condition is independent of cutting speed; thus, the stability chart is a horizontal line at $k_1 = -1/a_h$.

In general, for mode-coupling instability the operative response locus must cross the negative in-phase axis and this can occur only with a cross-frequency response locus for a structure with closely coupled modes of vibration. Also, mode-coupling instability cannot occur for cutting processes for which the cutting force direction corresponds to the normal to the cut surface, since the operative response locus is then a direct-frequency response, which will not cross the negative in-phase axis. This means, for example, that this type of instability is not possible for a drilling operation.

The value of k_1 and therefore the corresponding width of cut for mode-coupling instability is much greater than for regenerative instability. Thus, this type of instability will not be significant for conditions where successive passes of the cutting tool overlap each other.

9.4   DETERMINATION OF FREQUENCY RESPONSE LOCI

The analysis of machine tool stability requires knowledge of the cross-frequency response between the cutting-force direction and the normal to the cut surface. This response should be experimentally determined for the conditions prevailing at the threshold of stability, that is, when a small amplitude harmonic force exists between the tool and workpiece and a large mean cutting force is applied. In addition, the spindle of the machine should be rotating.

To determine the required cross-frequency response directly involves applying a harmonic force in the direction of the cutting force and measuring the response in the direction of the normal to the cut surface. A different setup would therefore be required for each possible direction of the cut force and direction of the normal to the cut surface. Fortunately, it is possible to deduce the cross response for any given direction of the applied force and direction of the measured response from experimentally measured responses in only a few directions. For example, we can consider the slab-milling process shown in Fig. 9.19 [11]. To determine the cross-frequency response between the direction of force F_r and the normal to the cut surface x, it is necessary to measure the direct-frequency re-

sponse in two directions (u and v), preferably orthogonal to each other, and the cross response between these two directions.

If R_{uu}, R_{vv}, R_{uv}, and R_{vu} are the direct- and cross-receptance loci for the u and v direction, respectively. By Maxwell's theorem of reciprocity, $R_{uv} = R_{vu}$. Figure 9.19c shows the force diagram in slab milling. The forces in the v and u directions are

$$F_v = \frac{F \sin (\alpha + \psi)}{\sin 2\alpha} \tag{9.18}$$

$$F_u = \frac{F \sin (\psi - \alpha)}{\sin 2\alpha} \tag{9.19}$$

The responses (deflections) in the v and u directions due to the force F become:

$$\delta_v = R_{uu}F_u + R_{vu}F_v \tag{9.20}$$

and

$$\delta_u = R_{vv}F_v + R_{uv}F_u \tag{9.21}$$

In the experimental set-up these deflections will be sensed by transducers mounted in the v and u directions and will arise because of a resultant displacement in the direction R (Fig. 9.19d)

$$\delta_R = \frac{\delta_v}{\cos (\alpha - \beta_R)} = \frac{\delta_\theta}{\cos (\alpha + \beta_R)} \tag{9.22}$$

The response sensed by a transducers in the direction x is given by

$$\delta_x = \delta_v \cos \alpha \cos \beta_R \tag{9.23}$$

From Eq. (9.22)

$$\frac{\delta_v}{\cos \alpha \cos \beta_R + \sin \alpha \sin \beta_R} = \frac{\delta_u}{\cos \alpha \cos \beta_R - \sin \alpha \sin \beta_R} \tag{9.24}$$

Substitution of Eqs. (9.18), (9.19), (9.20), (9.21) and (9.24) into Eqs. (9.23), we obtain

(a)

(b)
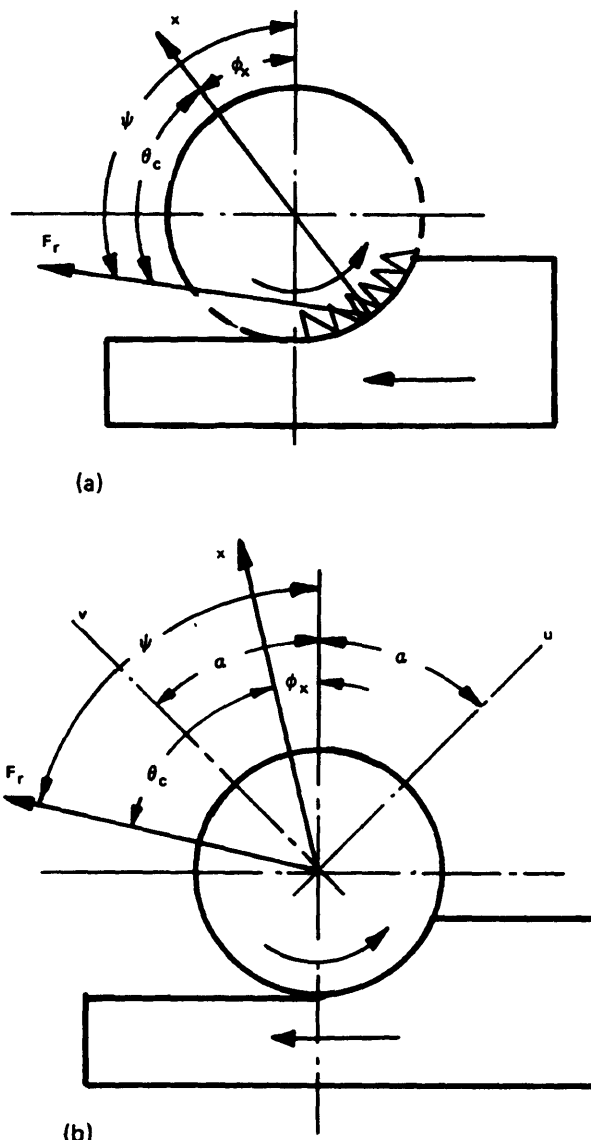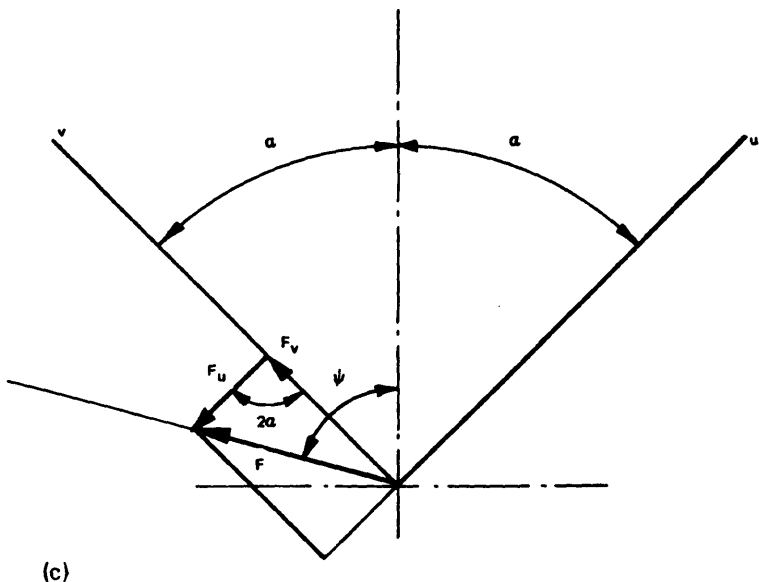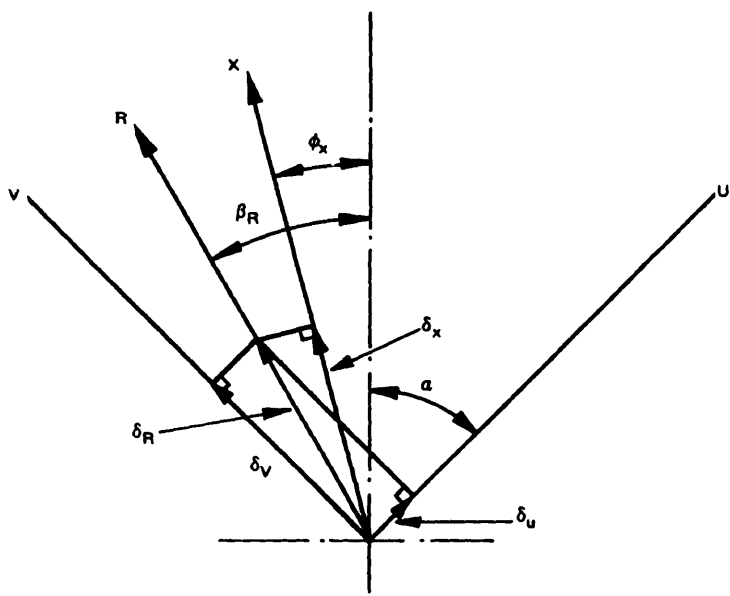
Figure 9.19 (a) Orientation of the cutting force F_r and the effective normal to the cut surface x in up-milling. (b) Orientation of two electromagnets u and v of the vibration exciter with the directions of F_r and x. (After Sadek and Tobias [10].) (c) Force components in the v and u directions. (d) Displacements in the u, v, R, and x directions.

(c)

(d)

$$\delta_x = \frac{F}{\sin^2 2\alpha} \left[R_{uu} \sin(\psi - \alpha) \sin(\alpha - \phi_x) \right.$$

$$+ R_{uv}\{\sin(\psi + \alpha) \sin(\alpha - \phi_x) + \sin(\psi - \alpha) \sin(\alpha - \phi_x)\}$$

$$+ R_{vv} \sin(\psi + \alpha) \sin(\alpha + \phi_x) \left. \right] \tag{9.25}$$

The cross receptance between the F and x directions is δ_x/F and it can be determined from Eq. (9.25).

In this way the operative receptance can be computed for any directions of F and x. For a three-dimensional cutting process, such as face milling, similar equations can be developed, but direct and cross receptances for three directions must then be measured.

Measurement of the required frequency responses under appropriate conditions can be readily carried out using electromagnetic vibrators of the type shown in Fig. 9.20. These exciters consist essentially of two U-shaped laminated electromagnets mounted on a base of nonmagnetic
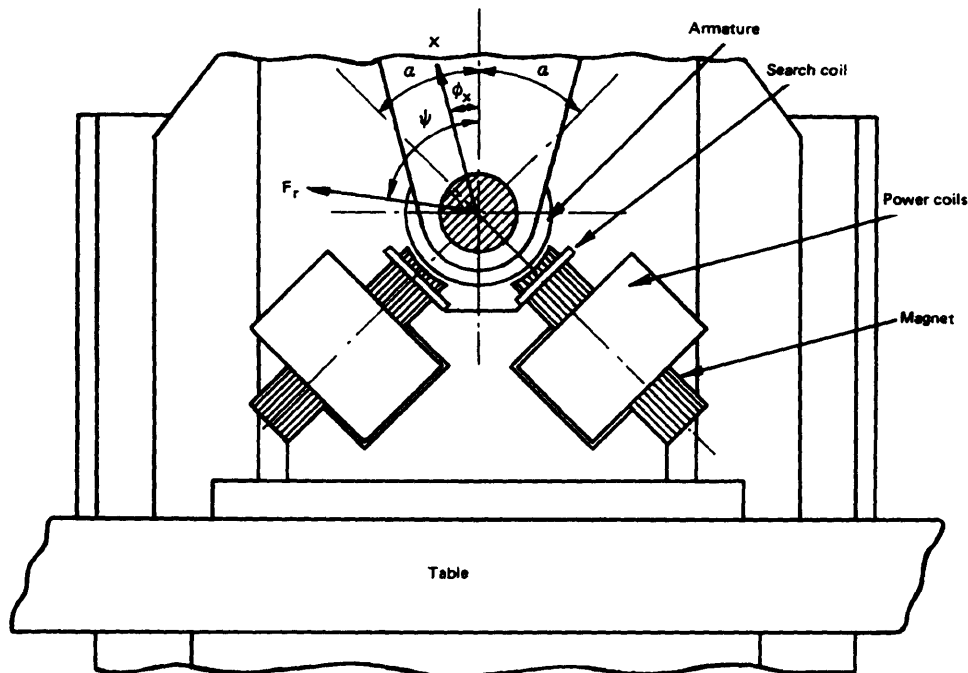
Figure 9.20 The electromagnetic exciter for milling machines. (From Sadek and Tobias [10].)

light alloy, which can be rigidly clamped either to the table of the milling machine or to the saddle of the lathe, with their forcing axes 30 or 45 deg to an axis of symmetry. The magnet acts on a rotor which replaces the workpiece on a lathe or the tool on a horizontal-milling machine.

The relative vibration induced by the magnetic force between the magnet poles and the rotor (armature) can be measured by a capacitance transducer rigidly mounted midway between the poles of each magnet, with its axis parallel to the forcing axis of the magnet. These transducers are also used for setting up the clearance between the poles and armature. Search coils placed around each arm of the U-shaped magnets, near their poles, are used for measuring the exciting-force component.

The main advantages of this form of vibration exciter are:

1. Low weight and high rigidity to minimize the effect of the mass and flexibility of the exciter on the response of the machine tool structure
2. Capacity for providing a harmonic exciting force superimposed on a constant load simulating the mean cutting thrust
3. Capacity for exciting the machine with the spindle rotating without physical contact between the vibrator and the rotating member.

The conditions existing at the threshold of stability are well simulated by these exciters. The necessary direct- and cross-frequency response data can be obtained directly in one setting by vibrating each set of magnets in turn.

9.5 DYNAMIC ACCEPTANCE TESTS FOR MACHINE TOOLS

The analysis of regenerative instability described earlier showed that the horizontal asymptote to the stability charts is given by Eq. (9.16) and depends only on the maximum negative in-phase magnitude of the operative receptance. This receptance can form the basis for a coefficient of merit for the dynamic assessment of machine tools, which is particularly useful for the comparison of the performance of similar machines [10]. Thus, from Fig. 9.14, the coefficient of merit can be defined as

$$COM = \tfrac{1}{2} a_{k_{min}} \qquad (9.26)$$

To compare the performance of alternative machines of a similar type it is necessary to determine the operative frequency response for each machine as described earlier and then to compute the coefficient of merit for each machine. An advantage of this approach is that machines can be compared for a wide range of cutting conditions from a single set of fre-

quency response loci. For example, in horizontal milling the relative stability can be determined for different depths of cut and directions of cutting. This is achieved by computing the operative receptances for the appropriate cutting force and normal to the cut surface directions and determining the coefficient of merit. Figure 9.21 shows values of the coefficient of merit determined for a typical horizontal-milling machine for different depths of cut and when the machine table is fed in opposite directions. This result shows that this particular machine is much more stable when the table is fed from left to right. In fact, the width of cut for unconditional stability is increased by more than a factor of 2.

9.6 IMPROVING MACHINE TOOL STABILITY

During the operation of a machine tool, particularly under numerical control, it is not always possible to avoid the conditions at which chatter vibrations may build up. A means of improving the stability of a machine may therefore be necessary, and several possibilities are available.

9.6.1 Structural Alterations

More damping and/or stiffness may be added to the structure to effectively reduce the magnitude of $a_{h_{min}}$ on the operative response locus (Fig. 9.14). Only those modes of vibration causing significant relative separation of the tool and workpiece need be considered. However, determination of where to apply additional damping most effectively may require careful analysis of the structure.

It may be possible, by redesign of portions of the structure, to alter the principal directions of the major modes of vibration so they do not coincide with the cutting force and/or the normal to the cut surface directions. In machines such as vertical-milling machines, the direction of the normal to the cut surface and cutting force changes continually during operation of the machine, so that this approach may not be effective. However in lathes, these directions remain relatively constant. Redesign of the tailstock of an engine lathe (Fig. 9.22) to alter the relationship between the principal directions of the modes of vibration and the normal to the cut surface has been found to result in improvements in stability [12].

9.6.2 Vibration Absorbers

A vibration absorber is a mass–spring system added to the structure and tuned so that its natural frequency coincides with that of the major vibration mode, thus reducing the effect of vibration in the major mode. Vibration absorbers can be considered for machine tools, but may be difficult to
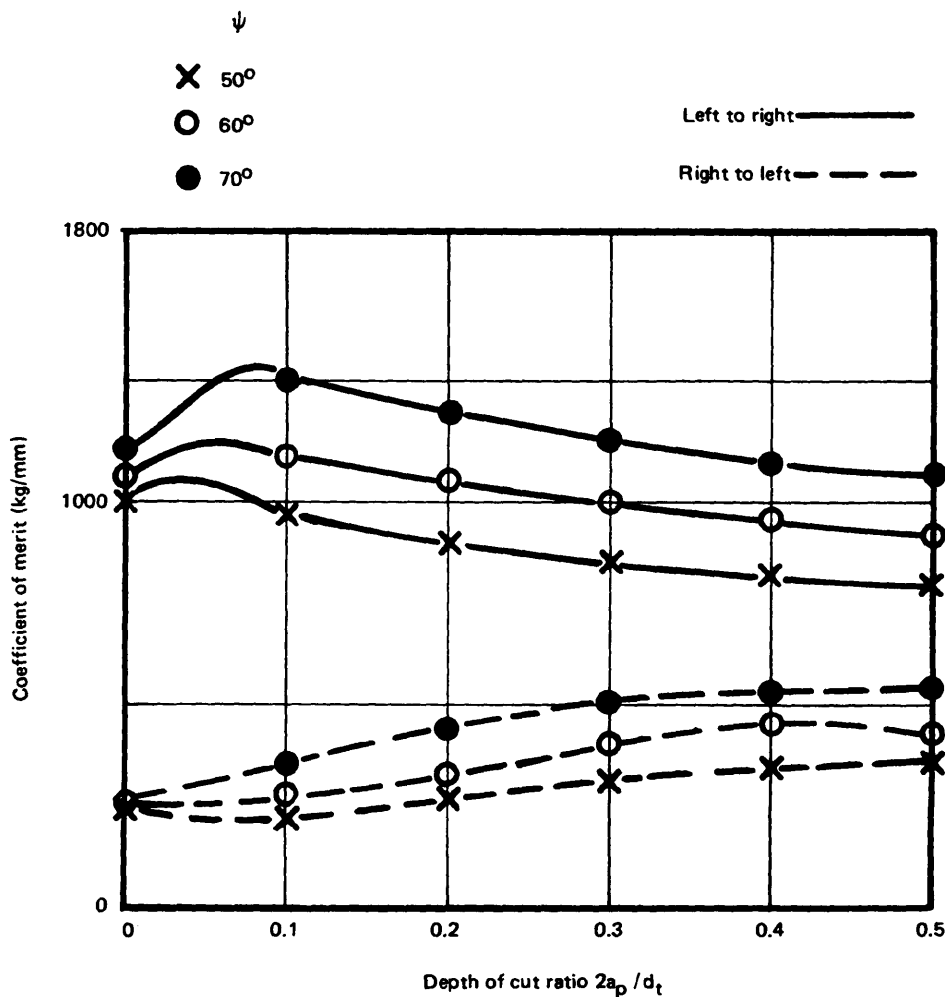
Figure 9.21   Variation of the coefficients of merit with different cutting conditions for horizontal milling. (From Sadek and Tobias [10].)
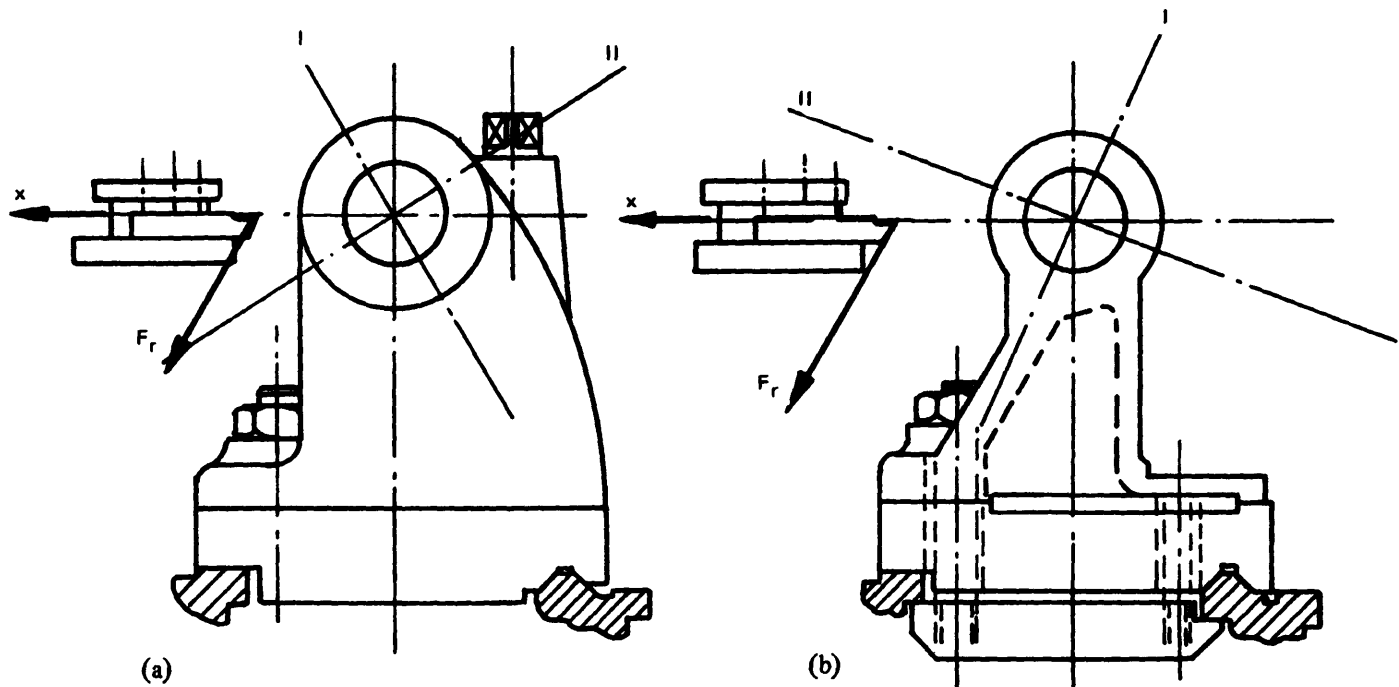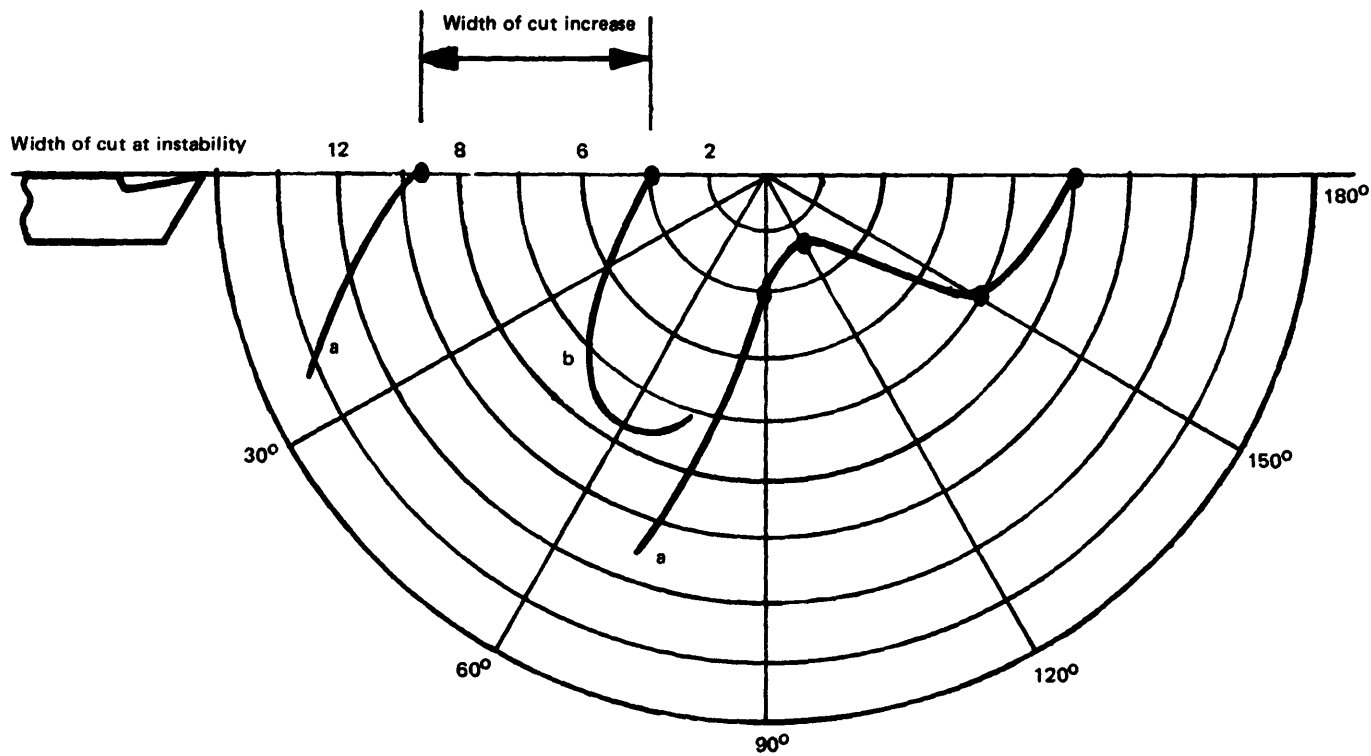
Figure 9.22 (a) Redesign of a lathe tailstock to reorient principal directions of vibration. (b) Improvements in the width of cut for instability. (Adapted from Tlusty [12].)

Width of cut increase

Width of cut at instability

12 8 6 2

180°

150°

120°

90°

60°

30°

a

b

a

use if several major modes of vibration exist. For machines with a single dominant mode of vibration these devices may be successful. Figure 9.23 shows the effect of adding an absorber to the overarm of a horizontal-milling machine. This resulted in considerable improvement in stability for the particular cutting conditions used.

9.6.3 Modification of the Regenerative Effect

Regenerative instability occurs when the phasing between successive waves cut on the surface of the workpiece by a vibrating tool reaches critical values. Consequently, a means of disturbing this phasing can improve stability. This can be done in several ways, as discussed in the following sections.

Variable-Pitch Milling Cutters

Several investigations of the use of milling cutters with variable pitch between successive teeth have been made [14–16], and this technique can lead to improvements in stability. Figure 9.24 shows the effect on stability charts of irregular tooth pitch for slab milling [14]. Such cutters result in different phasing between the waves cut by successive teeth on the cutter and can destroy the basic regenerative effect.

Another way to achieve irregular pitch for helical slab milling cutters is to use different helix angles on successive teeth. Figure 9.25 shows improvements in stability obtained using such cutters [16].

Superimposed Speed Variation

A second method to alter the phasing between successive waves cut on the work surface is to superimpose a variation in speed on the steady spindle rotation. Although difficult to achieve in practice, this approach can be effective for processes with a slow buildup of vibrations, such as some grinding operations.

9.6.4 Active Force Control

Several attempts have been made to control chatter vibrations by means of active feedback control, generally in connection with lathe turning. This is achieved by sensing vibrations of the tool or workpiece and then feeding this signal to a vibrator, usually electrohydraulic, connected to the tool post. The signal is modified so that the force applied opposes the motion of the tool and damps down any vibrations. This fairly complex instrumentation has been used effectively under laboratory conditions.
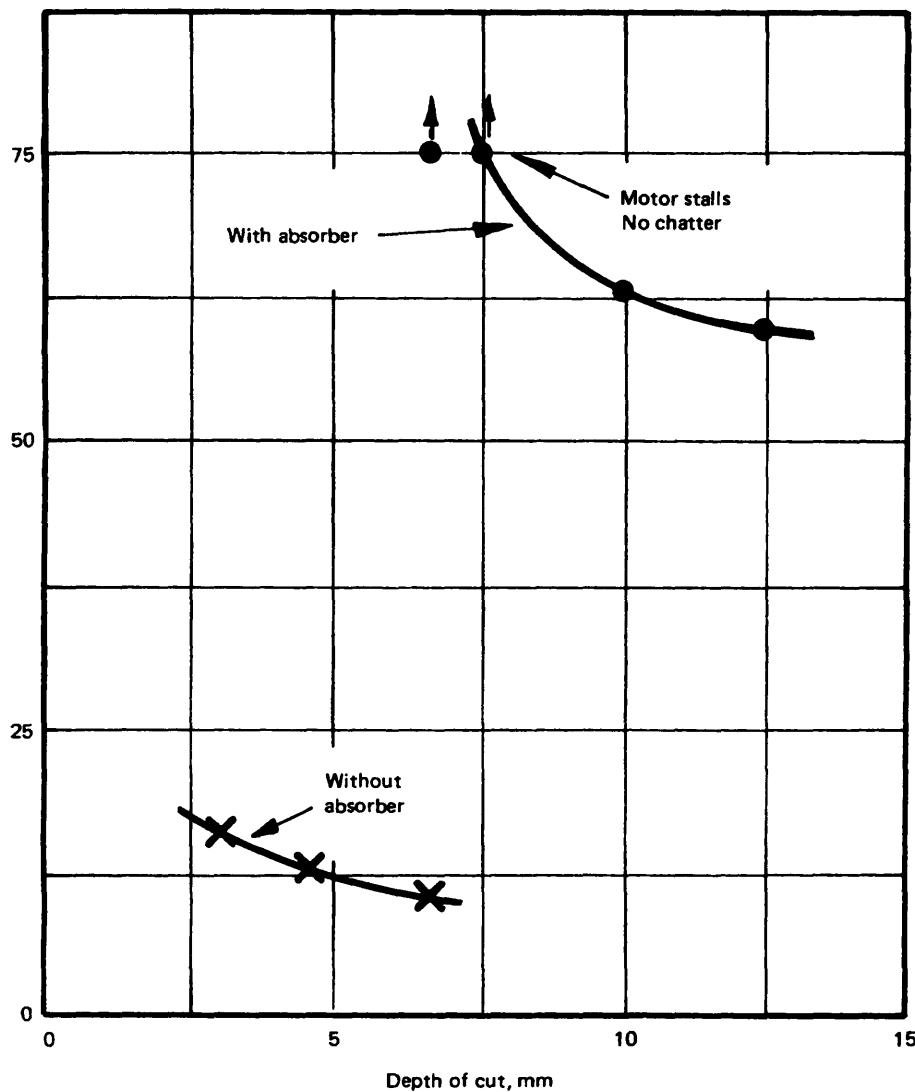
Figure 9.23   Improvement in the stability of a milling machine fitted with a vibration absorber. [From Stone and Andrew [13].)
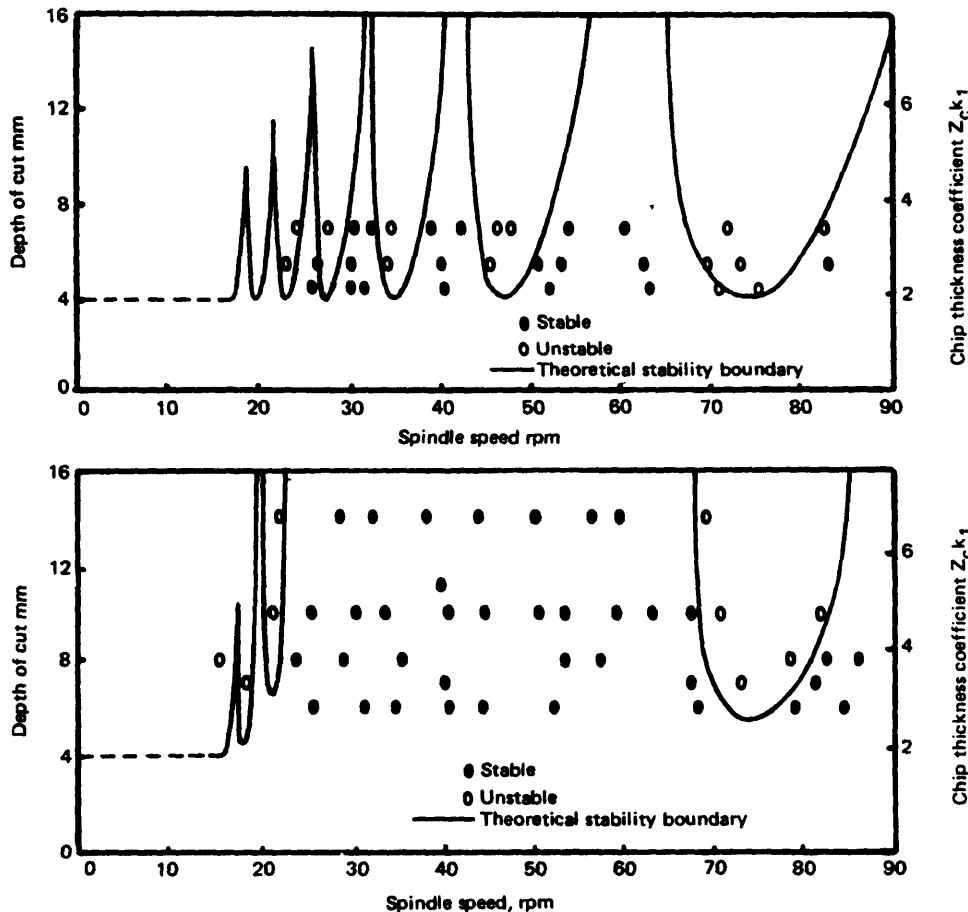
Figure 9.24 Stability charts for regular and irregular tooth pitch milling cutters. (From Opitz et al. [14].)
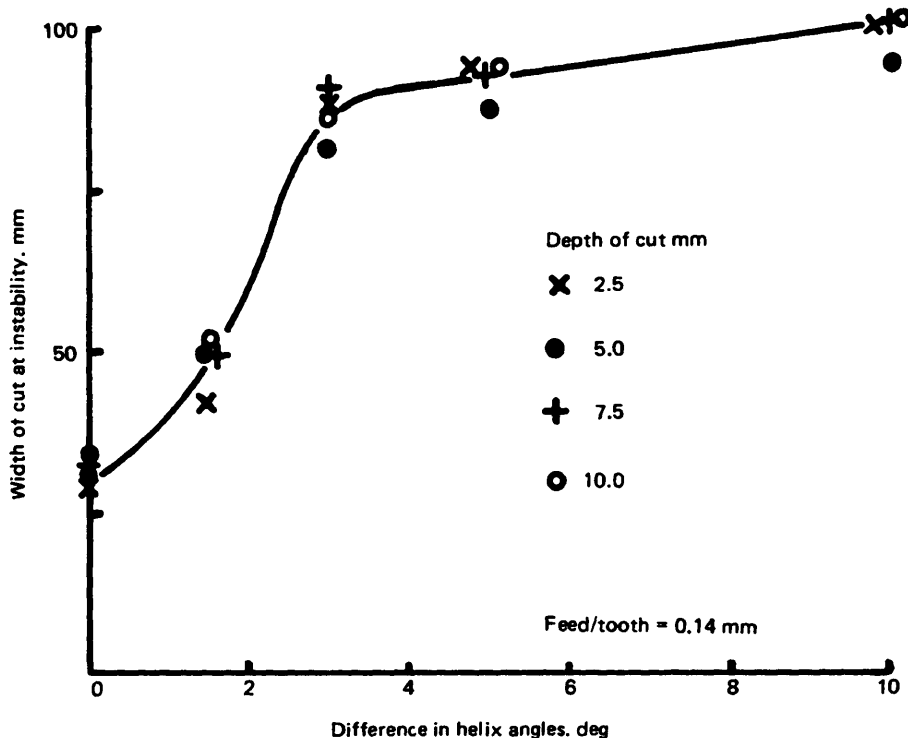
Figure 9.25 Width of cut at stability boundary for various differences in helix angles on helical milling cutters (rotational speed = 122 rpm). (From Stone [16].)

PROBLEMS

1. A simple lathe structure can be represented as a single degree of freedom system aligned along the direction of the normal to the cut surface, with an equivalent mass m_e, damping coefficient c_d, and stiffness S_e. If the direction of the cutting force is inclined at an angle θ_c to the normal to the cut surface, show that the limit of stability for fully regenerative chatter is defined by the following equations:

$$\frac{k_1}{S_e} = \frac{-(1 - (\omega/\omega_n)^2)}{(1 - \cos \beta_c) \cos \theta_c}$$

and
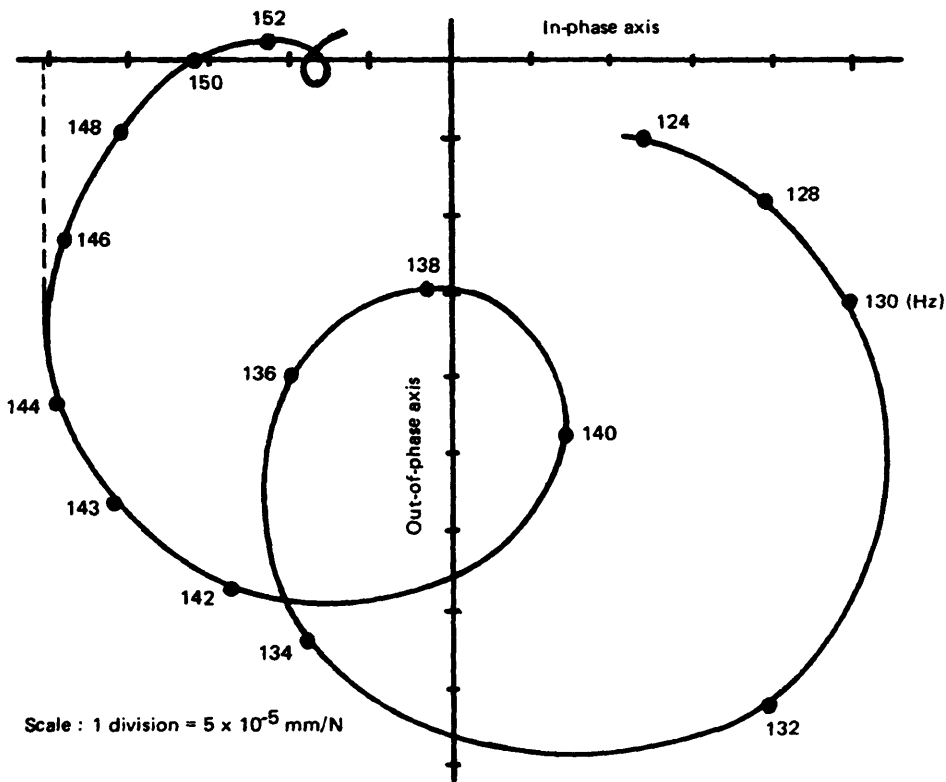
Figure 9.26 Operative frequency response locus for a machine tool structure.

$$\frac{k_1}{S_e} = \frac{-2\omega\zeta}{\omega_n \sin \beta_c \cos \theta_c}$$

where $\beta_c = \omega T$, T = the period between successive passes of the tool, ω_n is the natural frequency of the system and ζ is the damping ratio. It should be assumed that the cutting force varies only due to variations in the undeformed chip thickness and k_1 is the chip thickness coefficient (or cutting stiffness). If ω_n = 50 Hz, ζ = 0.5, and θ_c = 60 deg, plot the highest speed unstable region of the stability chart in terms of k_1/S_e and β_c.

2. Figure 9.26 shows the cross-frequency response (receptance) locus for a lathe between the cutting-force direction and the normal to the cut surface. It is assumed that variations in cutting force occur only because of variations in the undeformed chip thickness.

(a) Prepare a sketch of the stability chart for fully regenerative cutting conditions in terms of the critical values of the chip-thickness coefficient, indicating some of the cutting speeds for the minima on the chart and also the frequency range in which instability will occur.

(b) What will be the form of the stability chart for machining under conditions in which no overlapping of successive cuts occur?

(c) If, instead of a turning operation, the process were a slab-milling operation with a cutter having 20 teeth with an average of three engaged with the workpiece at any time, what difference would this make to the stability chart?

REFERENCES

1. Tobias, S. A.: *Machine-tool Vibrations*, Blackie and Son, London, 1965.

2. Tlusty, J., and K. M. Polacek: Experiences with analysing stability of machine-tool against chatter, *Proc. 9th International MTDR Conference*, Pergamon Press, New York, 1968.

3. Welbourne, D. B., and J. K. Smith: *Machine-tool Dynamics: An Introduction*, Cambridge University Press, New York, 1970.

4. Andrew, C.: Chatter in horizontal milling, *Proc. Inst. Mech. Eng. (London)*, vol. 179, p. 877, 1968.

5. Knight, W. A.: Torsional Vibrations and Machine-Tool Stability, Ph.D. thesis, University of Birmingham, Birmingham, England, 1967.

6. Das, M. K., W. A. Knight, and M. M. Sadek: A critical assessment of cutting force models in the analysis of machine-tool instability, *Proc. 11th International MTDR, Conference*, Pergamon Press, New York, 1970.

7. Das, M. K., The relationship between the static and dynamic cutting of metals, *Int. J. Mach. Tool Des. Res.*, vol. 7, 1965.

8. Nigm, M. M., M. M. Sadek, and S. A. Tobias: Prediction of dynamic cutting coefficients from steady state cutting data, *Ann. CIRP*, vol. 21, no. 1, p. 98, 1972.

9. Sarnicola, J. F., and G. Boothroyd: Machine-Tool Chatter: Factors Which Influence Cutting Forces During Wave Generating and Regenerative Chatter, *Proc. 2nd NAMR Conference*, Madison, Wisconsin, May 1974.

10. Sadek, M. M., and S. A. Tobias: Comparative dynamic acceptance tests for machine tools applied to horizontal milling machines, *Proc. Inst. Mech. Eng., (London)*, vol. 185, p. 319, 1971.

11. Choudhury, I., M. M. Sadek, and S. A. Tobias: Determination of the dynamic characteristics of machine tool structures, *Proc. Inst. Mech. Eng. (London)*, vol. 184, p. 943, 1970.

12. Tlusty, J.: New tailstock design improves stability of centre lathes, *Proc. 7th International MTDR Conference*, Pergamon Press, New York, 1966.

13. Stone, B. J., and C. Andrew: Vibration absorbers for machine-tools, *Proc. 9th International MTDR Conference,* Pergamon Press, New York, 1968.

14. Opitz, H., E. U. Dregger, and H. Roese: Improvement of the dynamic stability of the milling process by irregular tooth pitch, *Proc. 7th International MTDR Conference,* Pergamon Press, New York, 1966.

15. Slavicek, J.: The effect of irregular tooth pitch on stability of milling, *Proc. 6th International MTDR Conference,* Pergamon Press, New York, 1965.

16. Stone, B. J.: The Effect on Regenerative Chatter Behaviour of Machine Tools of Cutters with Different Approach Angles on Adjacent Teeth, MTIRA Report No. 34, MTIRA, England, July 1970.

10
Grinding

10.1 INTRODUCTION

Significant developments have recently been made in the grinding of
metals. Whereas a few years ago, grinding was considered a finishing
process, the development of new grinding wheels has led to such im-
provements in performance that in many cases grinding can now be eco-
nomically used for the bulk removal of metal. In addition, processes, such
as creep-feed grinding, have been developed for removing relatively large
amounts of stock material in a single pass. In the future an increasing pro-
portion of the total amount of metal removal will be accomplished by
grinding. It is believed, however, that grinding will never replace conven-
tional metal cutting as the principal method of machining components
[1].

10.2 THE GRINDING WHEEL

A grinding wheel essentially consists of a large number of abrasive par-
ticles, called grains, held together by a suitable agent called the bond (Fig.
10.1). It may be regarded as a multipoint cutting tool with a cutting action
similar to that of a milling cutter except that the cutting points are
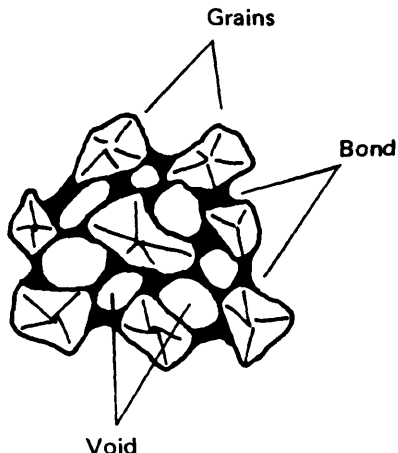
Figure 10.1   Grinding-wheel structure.

irregularly shaped and randomly distributed over the active face of the wheel. Cutting speeds in grinding are considerably higher than for other machining operations.

Those grains at the surface of the wheel that perform the cutting operation are called active grains. In peripheral grinding, each active grain removes a short chip of gradually increasing thickness in a way that is similar to the action of a tooth on a slab-milling cutter (Fig. 10.2). Because of the irregular shape of the grains, however, there is considerable interference, or plowing action, between each active grain and the new work surface. Each active grain is a small cutting tool with a large negative rake angle (−60 deg or larger) (Fig. 10.3), and this results in very low values for the shear angle during the removal of each chip. The plowing action results in progressive wear, causing the formation of worn areas on the active grains. As grinding proceeds, the number and size of these worn areas increase, thus increasing the interference or friction, resulting in an increase in the force acting on the grain. Eventually this force becomes large enough either to tear the worn grain from the bond of the wheel and thus expose a new unworn grain or to fracture the worn grain to produce new cutting edges. Thus, a grinding wheel has a self-sharpening characteristic, and the force a grain can withstand before being torn from the wheel or fractured is a most important factor when grinding-wheel performance is considered.

A wheel consisting of relatively tough grains strongly bonded together will only exhibit the self-sharpening characteristic to a small degree and
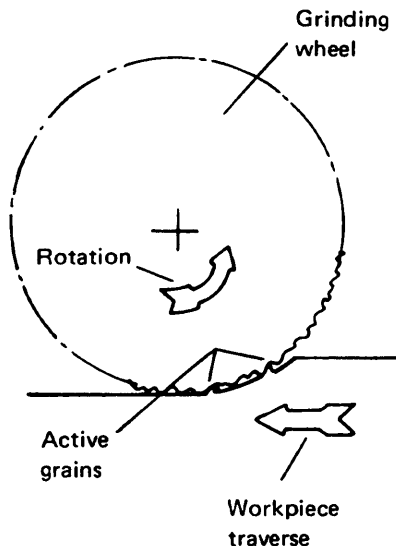
Figure 10.2   Action of a grinding wheel.

will quickly develop a glazed appearance during grinding. This glazed appearance is caused by the relatively large worn areas that develop on the active grains. These worn areas result in excessive friction and the consequent overheating of the workpiece. Grinding under these conditions is inefficient and necessitates "dressing" the wheel at frequent intervals to remove worn grains from the wheel surface. Dressing is usually carried out by passing a diamond-tipped dressing tool across the wheel surface while the wheel rotates. Dressing with a diamond-tipped tool removes or fractures the worn grains at the wheel periphery, thus generating a new and sharpened cutting surface. The need for frequent dressing to remove worn grains characterizes a hard wheel.

The opposite characteristic, where the grains in the wheel are torn out of the structure or fracture very rapidly during grinding, describes a soft wheel. Under the circumstances characterizing a soft wheel, the volume of wheel removed becomes significant compared to the volume of metal removed; the wheel will rapidly lose its shape and dressing will soon be necessary. Rapid fracturing represents inefficient grinding conditions, and thus the object in selecting a wheel for a particular operation is to achieve a compromise between the two extremes just described for hard and soft wheels.
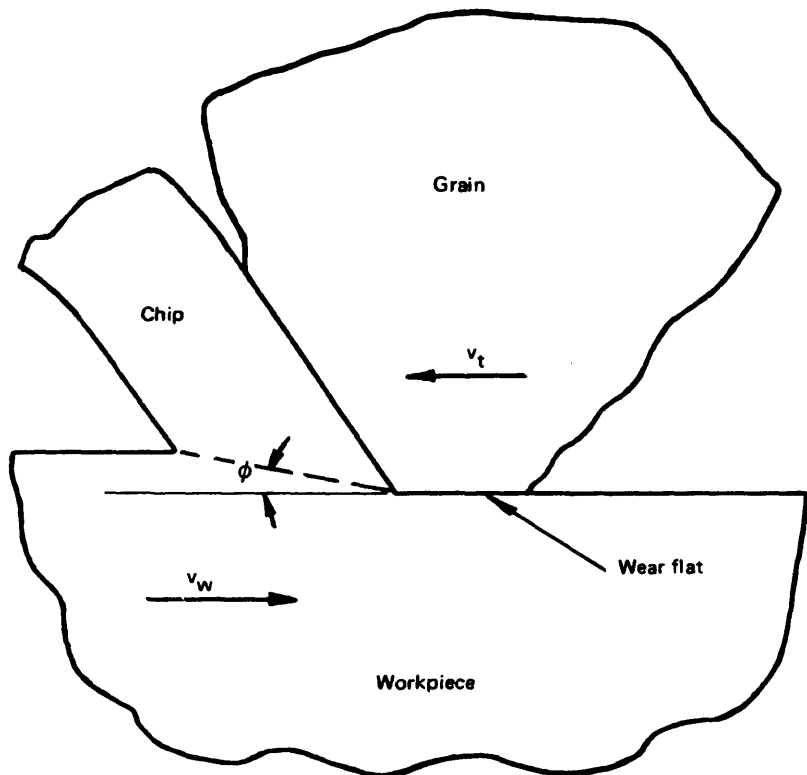
Figure 10.3   Chip formation by an abrasive grain, characterized by negative rake angle, small shear angle, and wear flat on the grain.

Several factors combine to determine whether a wheel behaves hard or soft, and some of these factors are discussed below.

10.2.1   Grain Type

Table 10.1 shows the hardness of various materials used for grains in grinding wheels, together with the hardness of some other materials for comparison. The hardest type of grain used in grinding wheels is diamond, and naturally this type of grain is used for grinding very hard materials, such as cemented carbides. This is followed by cubic boron nitride (CBN), which has now taken over some of the applications for which diamond was previously used. However, grains of aluminum oxide or silicon carbide are more commonly used in the manufacture of general-purpose grinding wheels. Silicon carbide grains are the tougher of the two

Table 10.1 Knoop Hardness for Various Materials and Abrasives

Common glass	300–500	Titanium carbide	1800–3200
Hardened steels	700–1300	Silicon carbide[a]	2100–3000
Tungsten carbide	1800–2400	Boron carbide	2800
Aluminum oxide[a]	2000–3000	Cubic boron nitride[a]	4000–5000
Titanium nitride	2000	Diamond[a]	7000–8000

[a]Used commonly as griding abrasives.

types, a property that makes them more efficient abrasives when used in such grinding materials as the hard cast irons. On the other hand, silicon carbide grains dull more rapidly than aluminum oxide grains when used in grinding steels. The general rule is to select aluminum oxide for surface grinding of steels of all kinds, including the hard stainless steels, annealed malleable iron, and tough bronzes and to select silicon carbide for surface grinding of gray iron, chilled iron, brass, soft bronze, aluminum, hard facing alloys, and the cemented carbides.

10.2.2 Grain Size

Grain size is determined mainly by the surface-finish requirement: the smaller the grain, the smoother the surface obtained. The grain size may also affect the relative hardness of the wheel. The size of grain is designated by the mesh of the screen through which it just passes. Thus, a grain of 20 grit passes through a mesh of 20 openings per inch. Grains are sorted into various sizes by a mechanical sifting machine.

10.2.3 Bond

Six principal types of bond are used for grinding wheels: vitrified, silicate, shellac, resinoid, rubber, and metallic.

A vitrified bond is a clay melted to a glasslike consistency. It is strong and rigid and is the most common type of bond used for grinding wheels. A silicate bond is essentially water glass, (sodium silicate) hardened by baking. It holds the grains more loosely than a vitrified bond, and therefore the wheel behaves softer. A resinoid bond is a thermosetting resin and a wide range of properties can be obtained by different mixes of the compound. It is strong but fairly flexible and is sometimes used for manufacturing large grinding wheels. A rubber bond consists of fairly hard vulcanized rubber; it can be used for the manufacture of thin, flexible wheels, used particularly for cutoff machines and similar applications. A shellac bond is used for grinding wheels employed in producing very smooth finishes on hard surfaces. A metallic bond is used for

grinding wheels with diamond or CBN grains and cannot be dressed in the usual way. Metallic-bonded wheels are produced by sintering compacted mixtures of the grains and metallic powders, usually of bronze.

10.2.4 Structure

The structure of a wheel is determined by the proportion and arrangement of the abrasive grains and bond. Some wheels have an open (porous) structure, while others have more tightly packed grains with the spaces between grains filled with the bonding material; this is known as a closed structure. A wheel with an open structure provides for easier swarf, or chip, removal but will tend to behave soft; on the other hand, a wheel with a closed structure will tend to clog with swarf and will behave hard.

10.2.5 Designation of Grinding Wheels

Table 10.2 shows the ISO standard marking system for grinding wheels. It can be seen that the grinding-wheel code consists of seven alphanumeric symbols referring to type of abrasive, nature of abrasive, grain size, wheel grade (relative hardness), structure, nature of bond, and finally a manufacturer's record. In general, the following guidelines can be used for the selection of a grinding wheel:

1. Choose aluminum oxide for steels and silicon carbide for carbides and nonferrous metals.
2. Choose a hard-grade wheel for soft materials and a soft-grade wheel for hard materials.
3. Choose a large grit for soft and ductile materials and a small grit for hard and brittle materials.
4. Choose a small grit for a good finish and a large grit for a maximum metal removal rate.
5. Choose a resinoid, rubber, or shellac bond for a good finish and a vitrified bond for a maximum metal removal rate.
6. For surface speeds greater than 32 m/s do not choose a vitrified bond.

10.3 EFFECT OF GRINDING CONDITIONS ON WHEEL BEHAVIOR

It has been seen that wheels of different types manufactured from different types of grain behave in different ways, and the choice of wheel type will depend on the material to be ground, the surface finish required, and the metal removal rate. However, grinding conditions also play an

Table 10.2   ISO Standard Marking System for Grinding Wheels[a]

Sequence	1	2	3	4	5	6
Type of abrasive	Nature of abrasive	Grain size	Grade	Structure	Nature of bond	Manufacturer's record
51	A	36	L	5	V	23
Manufacturer's symbol indicating exact type of abrasive						Manufacturers private marking to identify wheel

Aluminum oxide—A
Silicon carbide—C

Dense to open

Coarse	Medium	Fine	Very fine		
				0	8
				1	9
				2	10
10	30	70	220	3	11
12	36	80	240	4	12
14	46	90	280	5	13
16	54	100	320	6	14
20	60	120	400	7	etc.
24		150	500		
		180	600		

V — vitrified
S — silicate
R — rubber
RF — rubber with fabric reinforcement
B — resinoid (synthetic resins)
BF — resinoid (synthetic resins) reinforced
E — shellac
Mg — magnesia

Grade scale

Soft	Medium	Hard

A B C D E F G H I J K L M N O P Q R S T U V W X Y Z

[a]The sample grinding-wheel designation shown is 51A36L5V23.

important part in determining whether a wheel will behave hard or soft.

Figure 10.4 shows the approximate shape of the layer of material removed by a single grain during plunge grinding. The average length of a chip l_c during grinding is given approximately by

$$l_c = \frac{d_t}{2} \sin \theta \tag{10.1}$$

where d_t is the diameter of the wheel and

$$\cos \theta = \frac{(d_t/2) - f}{d_t/2} = 1 - \frac{2f}{d_t} \tag{10.2}$$

where f is the infeed. Now

$$\sin^2 \theta = 1 - \cos^2 \theta$$
$$= \frac{4f}{d_t} - \frac{4f^2}{d_t^2} \tag{10.3}$$

by substitution of Eq. (10.2). Substituting Eq. (10.3) in Eq. (10.1) and neglecting the second-order term,

$$l_c = (fd_t)^{0.5} \tag{10.4}$$

The metal removal rate Z_w during grinding is given by

$$Z_w = fa_p v_w \tag{10.5}$$

where a_p is the back engagement (width of the grinding path) and v_w is the surface speed of the workpiece.

If the chips have the triangular cross section shown in Fig. 10.4, the average volume V_0 of each chip is given by

$$V_0 = \tfrac{1}{6} a_{w_{max}} a_{c_{max}} l_c \tag{10.6}$$

where $a_{c_{max}}$ is the maximum undeformed chip thickness and $a_{w_{max}}$ is the maximum width of the chip and can be expressed by

$$a_{w_{max}} = r_g a_{c_{max}} \tag{10.7}$$

where r_g is the grain–aspect ratio.
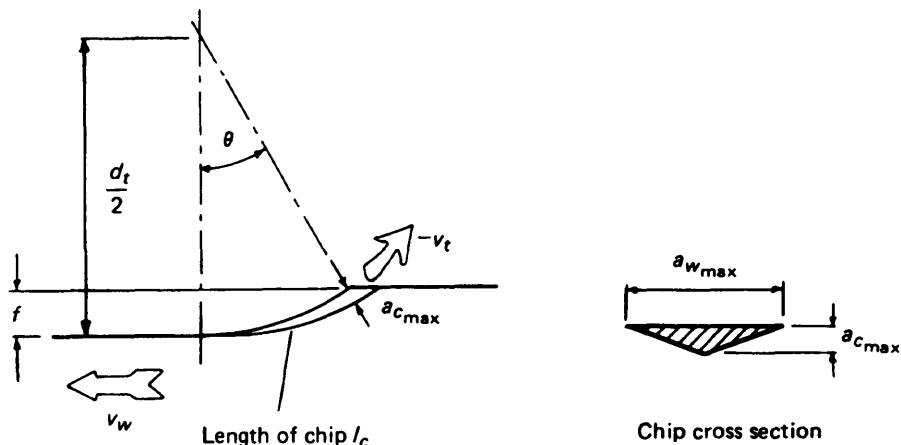
Figure 10.4 Geometry of chip removal in plunge grinding, where d_t = diameter of wheel, f = infeed, v_t = surface speed of wheel, v_w = surface speed of workpiece, $a_{c_{max}}$ = maximum undeformed chip thickness, and $a_{w_{max}}$ = maximum chip width.

The number of chips produced per unit time N_c is given by

$$N_c = v_t a_p C_g \tag{10.8}$$

where v_t is the surface speed of the wheel and C_g is the number of active grains per unit area on the wheel surface.

Finally, since $V_0 N_c$ is equal to Z_w, from Eqs. (10.4) to (10.7)

$$a_{c_{max}}^2 = \frac{K v_w}{v_t} f^{0.5} \tag{10.9}$$

where K is given by $6/(C_g r_g d_t^{0.5})$ and is a constant for the particular grinding wheel.

Since an increase in $a_{c_{max}}$ will result in an increase in the maximum force acting on each active grain during grinding, it follows that any change in grinding conditions tending to increase $a_{c_{max}}$ increases the self-sharpening process, and the grinding wheel tends to behave softer. Thus from Eq. (10.9) the following changes in grinding conditions would be expected to make a wheel behave soft [2]:

1. An increase in the work surface speed v_w
2. An increase in the infeed f
3. A decrease in the wheel surface speed v_t

10.4   DETERMINATION OF THE DENSITY OF ACTIVE GRAINS

If it is desired to evaluate the constant K in Eq. (10.9), it is necessary to measure the number of active grains per unit area of wheel surface C_g. In a method used by Backer, Marshall, and Shaw [3] the grinding wheel was rolled over a glass plate covered with a layer of carbon black. The resulting picture on the glass plate was enlarged photographically and C_g was determined by counting the number of marks per unit area.

A device [4] that may be used to measure the number of active grains passing one point on the workpiece surface during one revolution of the grinding wheel employs a thermocouple located at the surface of the workpiece. The thermocouple wire is insulated and passes through the workpiece. As each active grain passes, a thermocouple junction is formed between the wire and the workpiece, and a pulse is obtained from the high temperature developed. The pulses are displayed on an oscilloscope screen and counted.

A more direct method was employed by Grisbrook [5]. The surface of the grinding wheel was viewed on a projection microscope and the number of cutting points passing a line on the projection screen was counted as the wheel was rotated a given amount. The number of active grains determined in this manner was found to agree with the number of chips produced during one revolution of the wheel in grinding.

10.5   TESTING OF GRINDING WHEELS

An important factor in determining the characteristics of a grinding wheel is the force required to break the bond between grains. Much effort has been made to devise a method that will determine bond forces so that the operating performance of a grinding wheel may be predicted. A typical method [4] is to pass a sintered-metal carbide or diamond chisel over the wheel surface in such a way that it tears a layer of grains from the bond. The forces required to separate a layer of grains from the bond are taken as a measure of the strength of the bond, thus giving a guide to the behavior of the wheel in practice.

10.6   ANALYSIS OF THE GRINDING PROCESS

In the previous discussion it was shown that wheel wear is an essential phenomenon in grinding and provides the necessary self-sharpening characteristic. This variation in wheel surface means that wheel–workpiece engagements (width of grinding path and feed) will change as cutting proceeds. In addition, because the engagements are so small com-

pared to the grinding machine itself, structural deflections arising from the grinding forces can significantly affect the values of these engagements. In other words, machining conditions will be affected by the machining process, a phenomenon that cannot be neglected in the grinding process.

Figure 10.5 shows an idealized model of the cylindrical plunge-grinding process. The stiffness of the wheel-support system in the infeed direction is represented by a spring of stiffness S_t, the stiffness of the work-support system by a spring of stiffness S_w, and finally the stiffness of the wheel and work are designated by S_i. The wheel support is approaching the workpiece at the machine infeed rate of v_i, the radius of the wheel is being reduced at a rate $d_t/2$, and the radius of the workpiece is being reduced at a rate $d_w/2$ or v_f. Under steady-state conditions the force components generated at the wheel–workpiece contact zone are the cutting force F_c and the thrust force F_t.

It can be appreciated from the figure that at steady state, the feed speed v_f resulting from a given machine infeed rate v_i depends on the
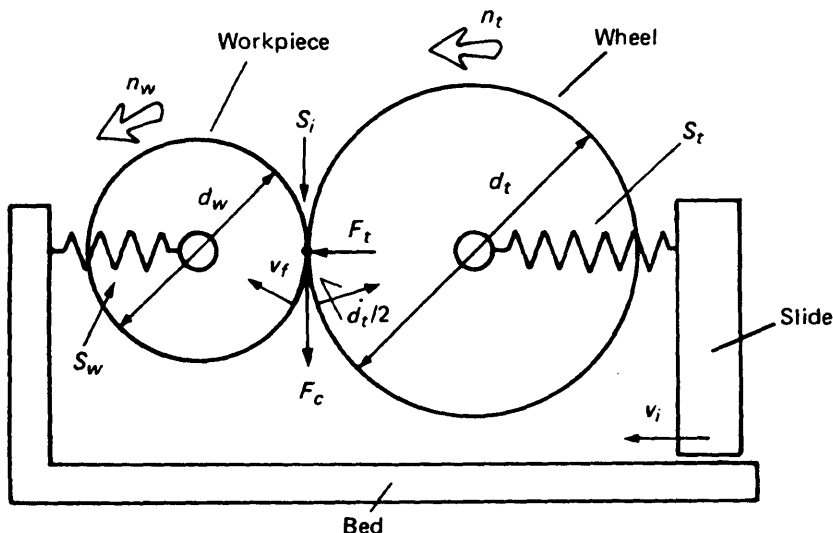
Figure 10.5   Idealized model of cylindrical plunge grinding, where S_w = stiffness of workpiece support, S_t = stiffness of wheel support, S_i = combined stiffness of workpiece and wheel, n_w = rotational frequency of workpiece, n_t = rotational frequency of wheel, d_w = diameter of workpiece, d_t = diameter of wheel, v_i = machine infeed speed, v_f = feed speed, F_c = cutting force, and F_t = thrust force.

stiffnesses of the machine tool, workpiece, and wheel and on the rate $d_t/2$ at which the wheel wears. Thus,

$$v_f = v_i - \frac{\dot{d}_t}{2} \tag{10.10}$$

To obtain quantitative relationships for the forces generated it is necessary to know the effect of the grinding conditions on the grinding forces. Figure 10.6 shows a relationship between the thrust force per unit width of cut and the feed. (It should be emphasized that the feed f is the advance of the wheel surface per revolution of the workpiece.) It can be seen that three distinct regions occur [6]:

1. When the thrust force per unit back engagement (width of cut) is very
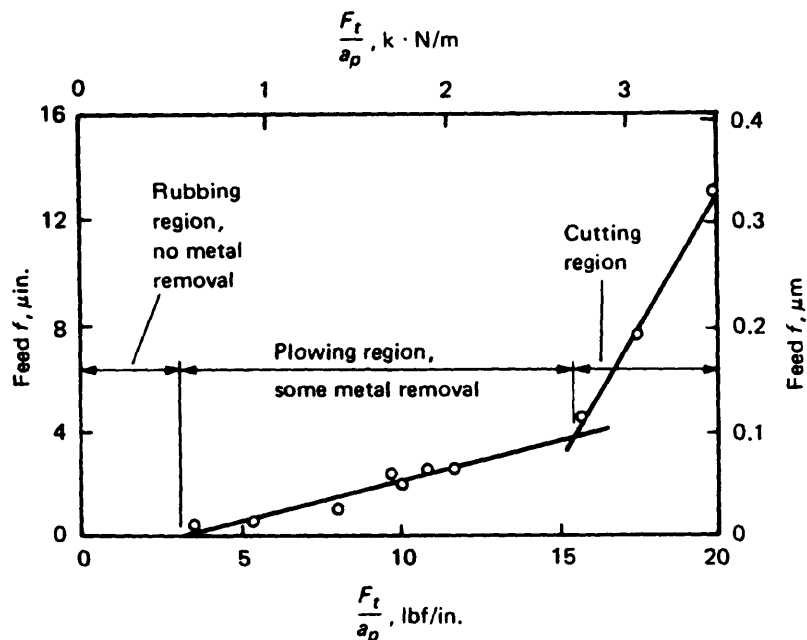
Figure 10.6 Effect of thrust force per unit width of cut on feed during internal, plunge, climb grinding of AISI 4150 at Rockwell C 53-55 using an A801L8V wheel with an equivalent wheel diameter of 2.09 in. (53 mm), where the wheel surface speed is 7700 ft/min (30 m/s), the workpiece surface speed is 540 ft/min (2.74 m/s), F_t = thrust force, a_p = back engagement (width of cut), and f = feed. (After Hahn and Lindsay [7].)

low, only rubbing occurs, where the grains rub on the work surface with essentially no material removal.

2. For low force values, plowing occurs, where the grains plow a furrow in the workpiece, with the extruded material broken off along the sides of the groove, giving a low metal removal rate.
3. For high force values, cutting occurs where the active grains produce chips (in the manner described in Sec. 10.3) giving high metal removal rates.

Clearly for rough grinding and for rapid stock removal it is desirable to operate under conditions where cutting occurs. The plowing region is important for obtaining a good surface finish during the final passes of the operation.

A more useful way of presenting the results of grinding experiments is shown in Fig. 10.7, where the metal removal rate Z_w and the wheel removal rate Z_t are plotted against the thrust force F_t. It can be seen that within the cutting region, the relationships for Z_w and Z_t are both linear. If the threshold thrust force at the beginning of the cutting region is designated F_{t_0} the following expressions can be written for Z_w and Z_t, respectively:

$$Z_w = \Lambda_w(F_t - F_{t_0}) \tag{10.11}$$

$$Z_t = \Lambda_t(F_t - F_{t_0}) \tag{10.12}$$

where Λ_w and Λ_t are the workpiece and wheel removal parameters [7], respectively, and can be regarded as the volume of workpiece or wheel removed per unit time per unit thrust force, respectively.

The metal removal rate Z_w can also be expressed by

$$Z_w = \pi d_w a_p v_f \tag{10.13}$$

where d_w is the diameter of the workpiece, a_p is the back engagement (width of cut), and v_f is the feed speed. Also, Z_t can be expressed by

$$Z_t = \frac{\pi d_t a_p \dot{d}_t}{2} \tag{10.14}$$

Thus, if Eqs. (10.11) to (10.14) are combined and substituted in Eq. (10.10),

$$v_f = \frac{v_i}{1 + (\Lambda_t d_w / \Lambda_w d_t)} \tag{10.15}$$
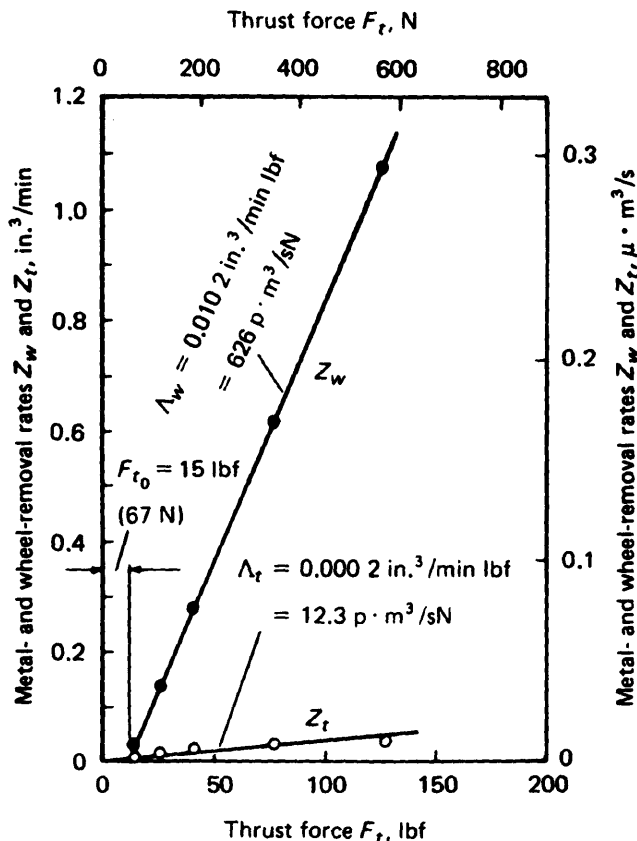
Figure 10.7 Effect of thrust force F_t on the metal and wheel removal rates Z_w and Z_t, respectively, during internal, plunge, climb grinding of an easy-to-grind material, AISI 52100 at Rockwell C 60-62, using an A70K8V wheel with an equivalent wheel diameter of 29 in. (737 mm), where the wheel surface speed is 12,000 ft/min (61 m/s) and the workpiece surface speed is 250 ft/min (1.27 m/s) and F_{t_0} = threshold force for grinding by "cutting," Λ_w = metal removal parameter, and Λ_t = wheel removal parameter. (After Hahn and Lindsay [1]).

For an easy-to-grind material the ratio Λ_w/Λ_t, referred to as the grinding ratio, would be on the order of 50; therefore, under steady-state conditions feed speed v_f approaches the machine infeed speed v_i quite closely. However, for a difficult-to-grind material the grinding ratio can be on the order of 3.0, and Eq. (10.15) must be used to estimate the actual feed speed.

10.6.1 Specific Cutting Energy for Grinding Processes

The specific cutting energy for grinding operations is considerably higher than for conventional cutting processes [8], as shown in Table 10.3. The total specific energy during cutting can be divided into three elements as follows:

1. Energy used in chip formation
2. Energy used in plastic deformation without cutting, that is, plowing
3. Energy expended in sliding friction, in particular on worn areas on
·   the active grains.

The specific cutting energy for grinding is higher than for single-point cutting for several reasons, including the following:

1. *The size effect:* the chips produced by the active cutting edges are very small, and it is well known that during deformation small pieces of material have proportionately greater strength than larger ones. Hence the specific cutting energy for chip formation will be larger.
2. *Effective cutting edge geometry:* the active grains have large negative rake angles and the chip formation involves large shear strains. The energy of plastic deformation is higher than for other cutting processes.
3. *Wear lands:* the size of the worn areas on the active grains is much larger proportionately than for single-point cutting. Consequently, the specific energy expended in sliding friction and plowing is greater.

Table 10.3   Specific Cutting Energy for Grinding and Conventional Cutting[a]

Material	Specific energy (W_s/mm^3)	
	Conventional cutting	Grinding
Aluminum alloys	0.44 − 1.09	6.8 − 27.3
Cast irons	1.64 − 5.46	11.29 − 60.0
Titanium alloys	3.0 − 5.0	16.4 − 54.6
Carbon steels	2.73 − 9.28	13.6 − 68.2

[a]Adapted from Kalpakjian [8].

10.6.2   Cylindrical Grinding Cycles

Cylindrical grinding processes are used to improve the tolerance, surface finish, and roundness of workpieces previously machined on lathes. In a typical cylindrical grinding cycle, the first contact with the workpiece is made at the high spots on the work. Consequently, during the first few revolutions or passes of the workpiece, wheel–work contact is intermittent. Each subsequent revolution or pass further improves the workpiece roundness geometry, but this can require several revolutions or passes and significant stock removal. This process is referred to as rounding up the workpiece. Computer-based analysis procedures, which take into account the dynamic behavior of the grinding machine, combined with grinding process equations, have been developed [8] that allow estimates to be made of the amount of stock removal and the time required to round up the workpiece to a required accuracy. The allowance left on workpieces prior to finish grinding must be large enough for the rounding-up process to be complete before the required finished size of the part is reached.

In a cylindrical plunge-grinding operation, the wheel is advanced to the position that, if wheel wear were negligible and the system rigid, would result in the removal of the desired stock from the workpiece. Thus, in the real situation the actual reduction in the workpiece radius when the infeed is stopped is less than that required because of the deflections of the structure and the wheel wear. Continuation of the grinding process without further application of feed results in the removal of the material left as a result of structural deflections; this procedure is known as spark-out. The results of an analysis of the sparking-out process [10] are presented in Fig. 10.8. This analysis applies to cylindrical grinding in which the contact force between the wheel and workpiece is gradually reduced as the elastic deflections of the machine and workpiece relax.

The solid line in Fig. 10.8 shows how grinding conditions affect the number of revolutions of the workpiece to remove 90 percent of the stock that remains after the machine infeed is disengaged. The linear portion of this relationship can be expressed by

$$m = \frac{2v_w a_p}{\Lambda_w S_e}$$

where v_w is the workpiece surface speed and S_e is the effective stiffness of the grinding-machine system given by $(S_w + S_i + S_t)$. The time taken for the spark-out operation t_s can therefore be obtained from

$$t_s = \frac{m}{n_w} \tag{10.16}$$

99.9% 99%

90%

100

ϵ

10

1

1 10 100

$$\frac{v_w a_p}{\Lambda_w S_e}$$
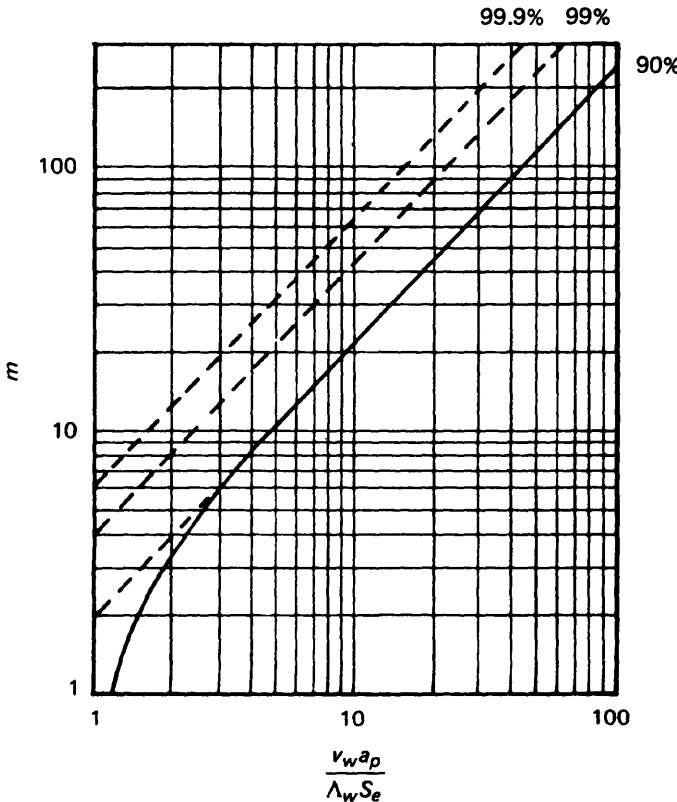
Figure 10.8 Effect of grinding conditions on the number of workpiece revolutions, or reciprocations, for spark-out and for various percentages of the material removed, where m = number of workpiece revolutions or reciprocations, v_w = workpiece surface speed, a_p = back engagement (width of cut), Λ_w = workpiece removal parameter, and S_e = system stiffness.

where n_w is the rotational frequency of the workpiece. The value of the constant in Eq. (10.16) depends on the percentage reduction in workpiece diameter; for the solid line in Fig. 10.7 this is 90 percent. The remaining lines shown dashed in the figure are for 99 and 99.9 percent removal of the metal remaining when the infeed is stopped.

It is interesting to note that the spark-out time given by Eq. (10.16) is independent of the magnitude of the infeed employed as well as the velocity of the workpiece. From this equation it is possible to reason that a decrease in back engagement (width of cut) a_p decreases the spark-out time and increases in the machine-workpiece-tool stiffness S_e or the

metal removal parameter Λ_w (easier-to-grind material) decrease the spark-out time.

It should be pointed out that wheel wear has not been taken into account in this analysis. For difficult-to-grind materials where wheel wear is significant compared to material removal, spark-out time is reduced and an oversize workpiece results.

In addition, toward the end of the spark-out process the thrust force F_t will fall to values below the plowing-cutting transition (Fig. 10.6). After this point the decay rate of the force becomes slower and the metal removal rate is reduced considerably. This final phase of spark-out produces the smooth surface finish required on the workpiece, but it is clearly necessary for the rounding up of the workpiece to be completed before the final phase of spark-out is reached. The spark-out process follows an exponential decay with different time constants corresponding to the cutting and plowing regions [9].

10.6.3 Surface Grinding Cycles

Similar effects occur during surface grinding, which is used to improve the flatness and surface finish of workpieces previously machined by milling or shaping machines. The finish allowance must again be sufficient for surface flatness to be improved before the required finish size is reached. During plunge grinding on a surface grinding machine a spark-out phase similar to that occurring in cylindrical grinding occurs. However, the analysis must be modified to account for the intermittent contact between the wheel and workpiece, which occurs at the end of each stroke of the machine.

10.6.4 Equivalent Diameters of Grinding Wheels

Before considering the material and wheel removal parameters further, it is necessary to explain the effect of conformity of the wheel and workpiece [11]. Figure 10.9 shows two situations: internal grinding and external cylindrical grinding. It can be seen that the contact area between the wheel and work is significantly greater during the internal-grinding operation. This amount of contact or conformity affects the grinding process and can be allowed for by estimating the equivalent diameter d_e of the grinding wheel [12].

The equivalent wheel diameter is the diameter of a grinding wheel used in plunge surface grinding that would give the same length of work–wheel contact for the same feed as that obtained in the grinding operation considered. It was shown earlier that the length of work–wheel contact in surface grinding would be given by $(fd_e)^{0.5}$. Figure 10.10 shows the
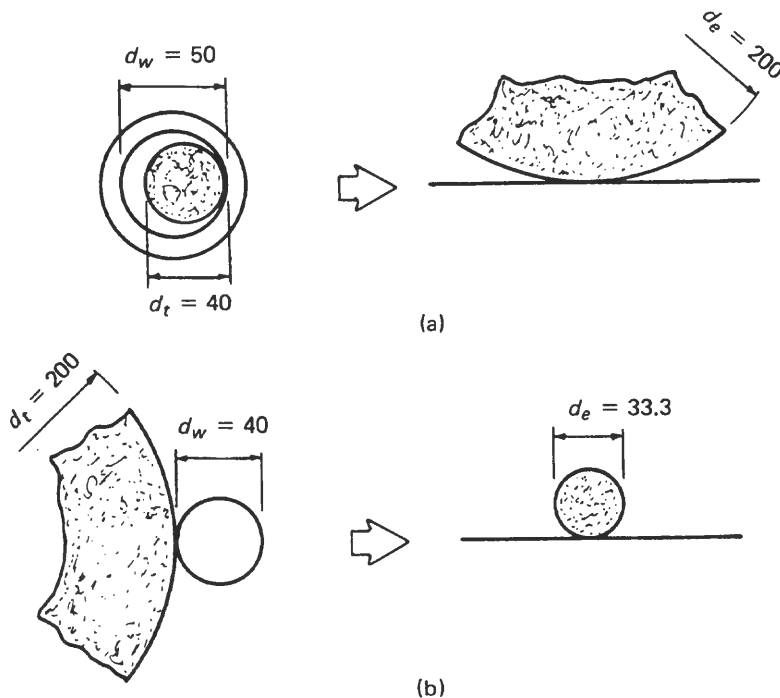
Figure 10.9 Equivalent diameter of wheel, where d_e = equivalent wheel diameter, d_t = wheel diameter, and d_w = workpiece diameter. (a) Internal grinding; (b) external cylindrical grinding.

geometry in external cylindrical grinding. It can be seen that the feed is given by

$$f = x_1 + x_2 \tag{10.17}$$

and the length of work–wheel contact a_b is approximately given by both $(x_1 d_w)^{0.5}$ and $(x_2 d_t)^{0.5}$ where d_w and d_t are the diameters of the workpiece and wheel, respectively. Therefore,

$$fd_e = (x_1 d_w)^{0.5} = (x_2 d_t)^{0.5} \tag{10.18}$$

Combining Eqs. (10.17) and (10.18) and rearranging gives

$$d_e = \frac{d_t}{1 + d_t/d_w} \tag{10.19}$$
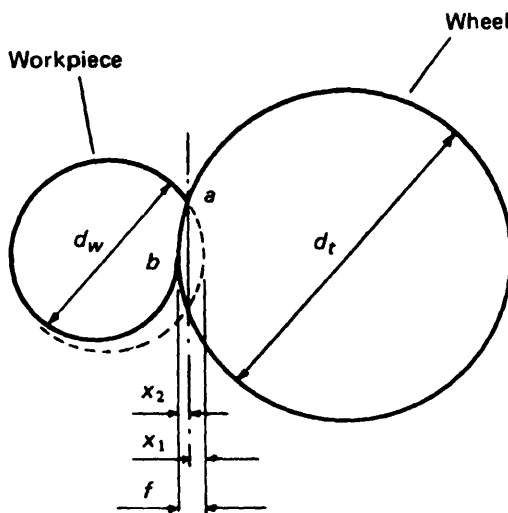
Figure 10.10 Geometry in external cylindrical grinding, where d_w = diameter of workpiece, d_t = diameter of wheel, and f = feed.

Similarly, it can be shown that for internal grinding the equivalent wheel diameter is

$$d_e = \frac{d_t}{1 - d_t/d_w} \tag{10.20}$$

Figure 10.9 gives the equivalent diameter calculated from Eqs. (10.19) and (10.20) for both external and internal cylindrical grinding. Use of the equivalent diameter of the wheel allows the conditions for a variety of grinding operations to be related and for measurements for one kind of operation to be employed in predicting the conditions for another.

10.6.5   Metal Removal Parameter for Easy-to-Grind Materials

It has been found from previous empirical work [7] that the metal removal parameter Λ_w for easy-to-grind materials is dependent on three main factors: wheel speed, workpiece hardness, and wheel-dressing conditions.

Previous studies [7] have shown that higher wheel speeds tend to increase the magnitude of the metal removal parameter and a higher workpiece hardness tends to decrease it. Also, it has been found [13] that wheel-dressing conditions can influence Λ_w. Figure 10.11 shows the
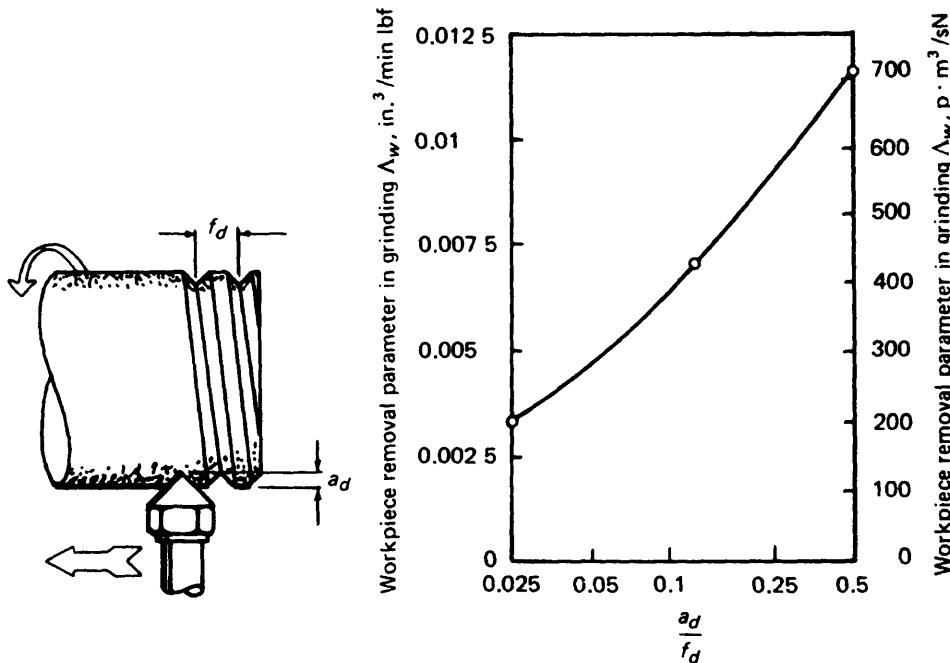
Figure 10.11 Geometry during wheel dressing and its effect on the metal removal parameter for AISI 4620 steel at Rockwell C 60-62, where the wheel surface speed is 12,000 ft/min (61 m/s), the workpiece surface speed is 800 ft/min (4.1 m/s), and the feed during dressing is 0.004 in. (0.1 mm) and a_d = depth of dress, f_d = feed during dressing, and Λ_w = metal removal parameter. (After Hahn and Lindsay [1].)

geometry during wheel dressing. The important parameter is found to be the ratio of the depth of the dress a_d and the feed f_d during dressing. It is found [7] that an increased value of a_d/f_d increases the magnitude of Λ_w as illustrated in Fig. 10.11.

Lindsay [14] has produced a semiempirical analysis resulting in the following expression for the metal removal parameter for easy-to-grind metals:

$$\Lambda_w = \frac{7.93 \times 10^5 \times (v_w/v_t)^{0.158}[1 + (4a_d/3f_d)]f_d^{0.58}v_t}{d_e^{0.14}V_b^{0.47}d_g^{0.13}R_{kc}^{1.42}} \text{ p} \cdot \text{m}^3/\text{sN}$$

$$(10.21)$$

where

v_w = workpiece surface speed, m/s

v_t = wheel surface speed, m/s

a_d = depth of dress, m

f_d = feed during dressing, m

d_e = equivalent wheel diameter, m

R_{kc} = Rockwell hardness number of the work material (C scale)

Also, d_g is the grain diameter given approximately by

$$d_g = \frac{0.0254}{\text{grain size}} \text{ m} \qquad (10.22)$$

and V_b is the percentage volume of bond material in the wheel given by

$$V_b = 1.33H_n + 2.2S_n - 8 \qquad (10.23)$$

where S_n is the wheel structure number and H_n, the wheel hardness number, is obtained from the following scale:

Wheel grade	H	I	J	K	L	M	$\cdots$
Wheel hardness number H_n	0	1	2	3	4	5	$\cdots$

Equation (10.21) has been found to give estimates of the metal removal parameter to within about ±20 percent [7].

10.6.6 Example

It is required to estimate the metal removal parameter Λ_w for the internal grinding of an R_{kc} 60, 52100 steel ring of internal diameter 95.25 mm with a grinding wheel 82.55 mm in diameter. The surface speeds of the wheel and workpiece are to be 63.5 m/s and 4 m/s, respectively. The wheel designation is A80M4V dressed with a feed of 0.1 mm at a depth of 0.0125 mm.

The wheel structure number S_n is 4, and the wheel hardness number H_n is 5. Therefore, from Eq. (10.23)

$$V_b = (1.33 \times 5) + (2.2 \times 4) - 8 = 7.45$$

The grain size is 80, and therefore from Eq. (10.22)

$$d_g = \frac{0.0254}{80} = 0.0003175$$

The equivalent wheel diameter for internal grinding is given by Eq. (10.20). Thus,

$$d_e = \frac{82.55}{1 - 82.55/95.25} = 619 \text{ mm}$$

Substitution of these, and the remaining figures, in Eq. (10.21) gives

$$\Lambda_w = \frac{7.93 \times 10^5 \times (4/63.5)^{0.158}}{0.619^{0.14} \times 7.45^{0.47}}$$

$$\times \frac{[1 + (4 \times 0.0125)/(3 \times 0.1)] \times 0.0001^{0.58} \times 63.5}{0.0003175^{0.13} \times 60^{1.42}}$$

$$= \frac{7.93 \times 10^5 \times 0.646 \times 1.167 \times 0.00479 \times 63.5}{0.935 \times 2.57 \times 0.35 \times 335}$$

$$= 645 \text{ p·m}^3/\text{sN} \ (0.0105 \text{ in}^3/\text{min lbf})$$

10.6.7 Metal Removal Parameter for Difficult-to-Grind Materials

Tool steels, high-strength alloys, carbides, and so on, are classed as difficult to grind. Figure 10.12 shows how the thrust force affects the metal and wheel removal rates for a difficult to grind material. Comparison of these data with those presented in Fig. 10.7 for an easy-to-grind material shows that for a difficult-to-grind material the threshold thrust force F_{t0} is higher (311 N compared with 67 N), the metal removal parameter Λ_w is lower (13.5 compared with 626 p · m^3/sN), and the grinding ratio, Λ_w/Λ_t, is lower (3.1 compared with 51). This means that higher forces and hence greater power are required and greater wheel wear occurs with the difficult-to-grind materials.

It has not yet been found possible to obtain an empirical equation for the metal removal parameter for difficult-to-grind materials, but as a guide Table 10.4 presents values of Λ_w for the rough grinding of some of these materials. The low figures are for low values of the thrust force per unit back engagement (width of cut) F_t/a_p, and the high figures are for high values of F_t/a_p

10.7 THERMAL EFFECTS IN GRINDING

The high cutting speeds in grinding result in temperatures at the grain tip that may be as high as 1700°C. As a result some of the chips may melt during formation. As mentioned already, the specific cutting energy for grinding is higher than for other cutting operations. A high proportion of this
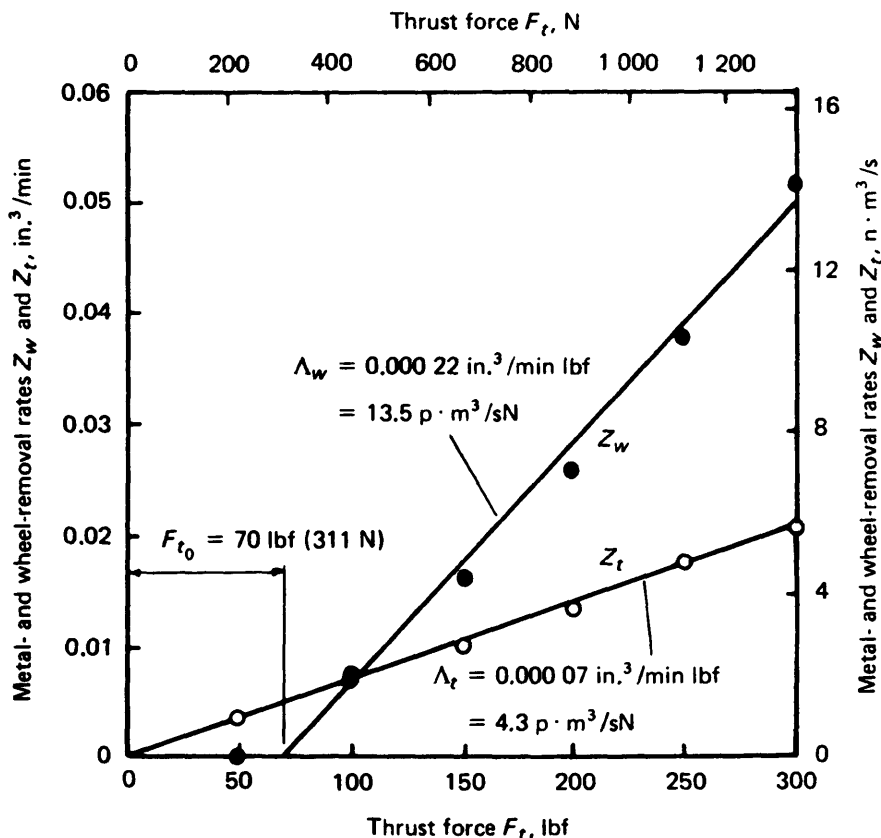
Figure 10.12   Effect of thrust force F_t on the metal and wheel removal rates Z_w and Z_t, respectively, during internal, plunge, climb grinding of a difficult-to-grind material, M-4 at Rockwell C 65, using an A80K4V wheel with an equivalent wheel diameter of 27.6 in. (701 mm), where the wheel surface speed is 12,000 ft/min (61 m/s), the workpiece surface speed is 250 ft/min (1.27 m/s), F_{t_0} = threshold force for grinding by cutting, Λ_w = metal removal parameter, and Λ_t = wheel removal parameter. (After Hahn and Lindsay [7].)

Table 10.4 Approximate Values of the Metal Removal Parameter Λ_w for Some Difficult-to-Grind Materials[a]

Material	Description	Metal removal parameter Λ_w	
		in.^{3}/min lbf	p · m^3/sN
T-15	High-speed steel, tungsten type	0.00015–0.0015	9–90
M-2	High-speed steel, molybdenum type	0.0004–0.0011	25–70
Inconel X	Nickel alloy	0.0006–0.0025	37–150
M-4	High-speed steel, molybdenum type	0.0002–0.002	12–120
M-50	High-speed steel, molybdenum type	0.0019–0.0045	120–280

[a]After Hahn and Lindsay [7].

energy appears as heat which flows into the work surface. It has been stated that 60 to 90 percent of the total energy consumed in grinding flows instantaneously into the workpiece, causing rapid local increases in temperature [15]. Increasing the specific metal removal rate reduces the proportion of total energy flowing into the workpiece, and dulling of the wheel increases this value. The proportion of the total energy flowing into the workpiece E has been expressed as [16]:

$$E = (0.6 + 0.05A_g)\ 100 \text{ percent} \tag{10.24}$$

where A_g is the relative contact area of the grains expressed as a percentage, ranging from 0 to 5 percent. The value of A_g increases as the wheel becomes less sharp.

Various forms of thermal damage may occur in grinding, as shown schematically in Fig. 10.13 [17], and the main effects are as follows:

1. *Dimensional errors:* The heat generated causes expansion of the workpiece, resulting in dimensional errors on cooling after the grinding process.

2. *Material structural changes:* Metallurgical changes may occur in the surface layers of the workpiece. Softening and tempering of the surface layers of hardened steel components may occur. Regions of untempered martensite may be formed because of rapid cooling after grinding in other steel components.

3. *Burning and surface cracking:* Excessive temperatures may cause surface oxidation and burning. Thermal cracking of the work surface may
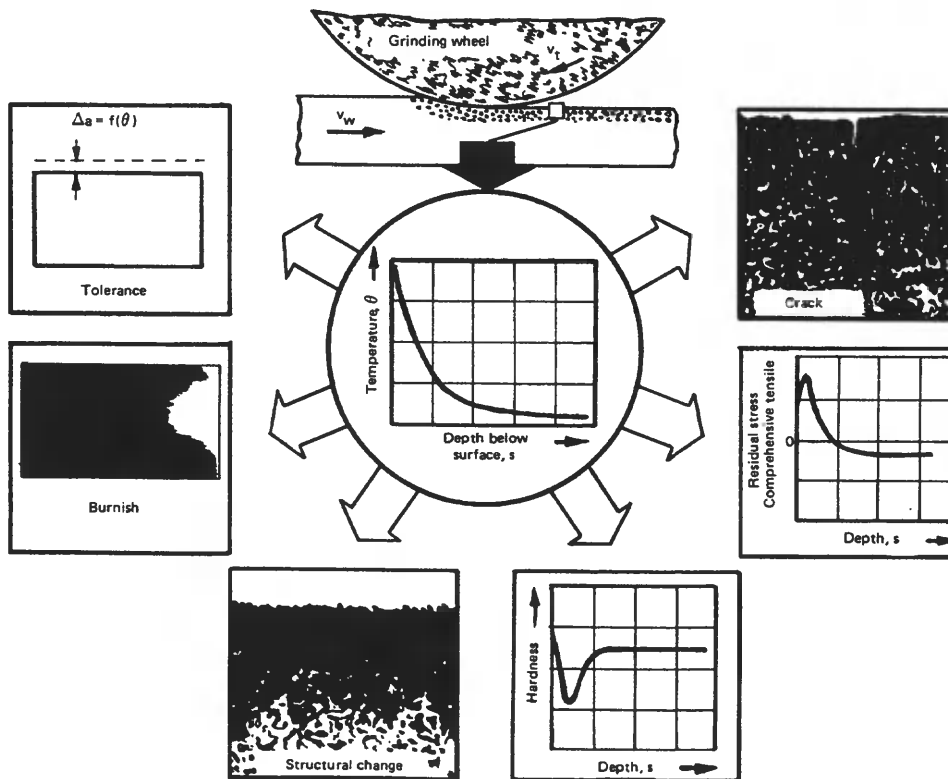
Figure 10.13   Thermal effects of grinding at the workpiece surface (Adapted from Konig et al. [17].)

result for some conditions. In severe cases such surface cracks may be readily visible, but for less critical conditions microscopic cracks may occur that reduce the fatigue and stress corrosion resistance of the workpiece.

4. *Residual stresses:*   The temperature changes and gradients in the work surface layers, together with the plastic deformation that takes place, results in residual stresses being set up in the workpiece. Such residual stresses, particularly if they are tensile at the surface, reduce the fatigue strength of the workpiece. These effects can be reduced by using softer grade wheels and lower wheel speeds.

Overall there is a threshold temperature above which significant thermal damage occurs. The principal factors that influence this temperature are wheel speed, work speed, force intensity, and wheel sharpness. In

general, higher work speeds and sharp wheels, allow higher force intensities and stock removal rates to be used without significant thermal damage occurring. Adaptive control methods for grinding have been developed in which the wheel sharpness and induced force intensity are monitored [9], with cutting conditions adjusted appropriately during the grinding cycle.

10.8 CUTTING FLUIDS IN GRINDING

10.8.1 General Discussion

Cutting fluids in grinding perform the same functions as in other cutting operations. These fluids lubricate the chip–grit and grit–workpiece interfaces, thereby reducing the power consumed and the heat generated. In addition, the workpiece is cooled, reducing the extent of the possible surface damage.

Neat oils provide the greatest lubrication, but only limited cooling. Consequently, neat oil use is restricted mainly to difficult-to-grind materials and to form grinding, partly because of higher costs, potential fire hazards, and operator health risks due to the release of toxic fumes. For general-purpose grinding, oil-and-water emulsions are used, with the lubricating properties regulated by adjusting the relative proportions of oil and water in the mixture.

10.8.2 Application of Grinding Fluids

For the grinding fluid to provide the necessary lubrication, it must penetrate into the contact zone between the wheel and workpiece. This is difficult because of the high wheel speeds used in grinding. It has been generally accepted that a thin air film barrier is formed around the rotating wheel that is difficult to penetrate and prevents the fluid from entering the grinding zone (e.g., [18]). However, some workers [19] have cast doubt on the validity of this air cushion effect and claim that if the stream of fluid has a velocity significantly different from the surface velocity of the wheel, the fluid forms turbulence and bounces off. If the velocities of the fluid and wheel are similar, then a laminar stream follows the contours of the wheel for some distance without forming turbulence, before finally leaving the wheel surface through centrifugal forces.

Several different methods for applying grinding fluids are used. Internal grinding is the most difficult type of grinding operation in which to obtain an adequate supply of fluid, mainly owing to the restricted access to the grinding zone and the greater work–wheel conformity.

1.   Flooding is the most common fluid application technique used. A large volume of fluid is applied at low pressure, and this generally gives acceptable results for conventional surface grinding.

2.   In jet application, high-pressure jets of fluid are applied through nozzles close to the wheel and workpiece in the direction of wheel rotation. It is generally assumed that the high-pressure jets are required to penetrate the air cushion on the wheel surface. However, the fluid velocity is also high and approaches the wheel speed, so that formation of a laminar stream on the wheel thus dragging fluid into the grinding zone is more likely to occur.

3.   Grinding wheels, particularly those with vitrified bonds, are porous and fluid can be applied through the wheel into the grinding zone. The fluid is normally applied through the spindle or by means of cupped flanges on the sides of the wheel. The method can be used in combination with flooding, with a neat oil applied through the wheel, to reduce friction in the grinding zone, and an oil–water emulsion applied externally, mainly to provide cooling.

4.   Chamber-type or air-deflector flood nozzles are being used increasingly for the low-pressure application of grinding fluids on surface grinding machines, high-speed grinding machines, and other types of cylindrical grinding machines. Figure 10.14 shows a typical configuration of this type of nozzle. Two alternative mechanisms for the effectiveness of chamber-type nozzles have been proposed. One explanation is that the air deflector removes the air cushion from the wheel and causes a low-pressure zone ahead of the grinding zone, pulling fluid from the nozzle into the wheel surface, which carries the fluid into the grinding zone. A second explanation [19] is that the fluid in the enlarged nozzle chamber is accelerated by the wheel itself, forming a laminar stream of coolant in contact with the wheel; this stream is carried into the grinding zone.

5.   Some benefits have been found from having radial or spiral grooves in the side faces of the grinding wheel, with the fluid applied to the side faces of the wheel [18]. The grinding fluid then flows radially along these grooves into the grinding zone.

10.9   GRINDING-WHEEL WEAR

The grinding ratio G_r is an important factor when the performance of grinding wheels is considered; it is given by

$$G_r = \frac{\Lambda_w}{\Lambda_t} \qquad\qquad (10.25)$$
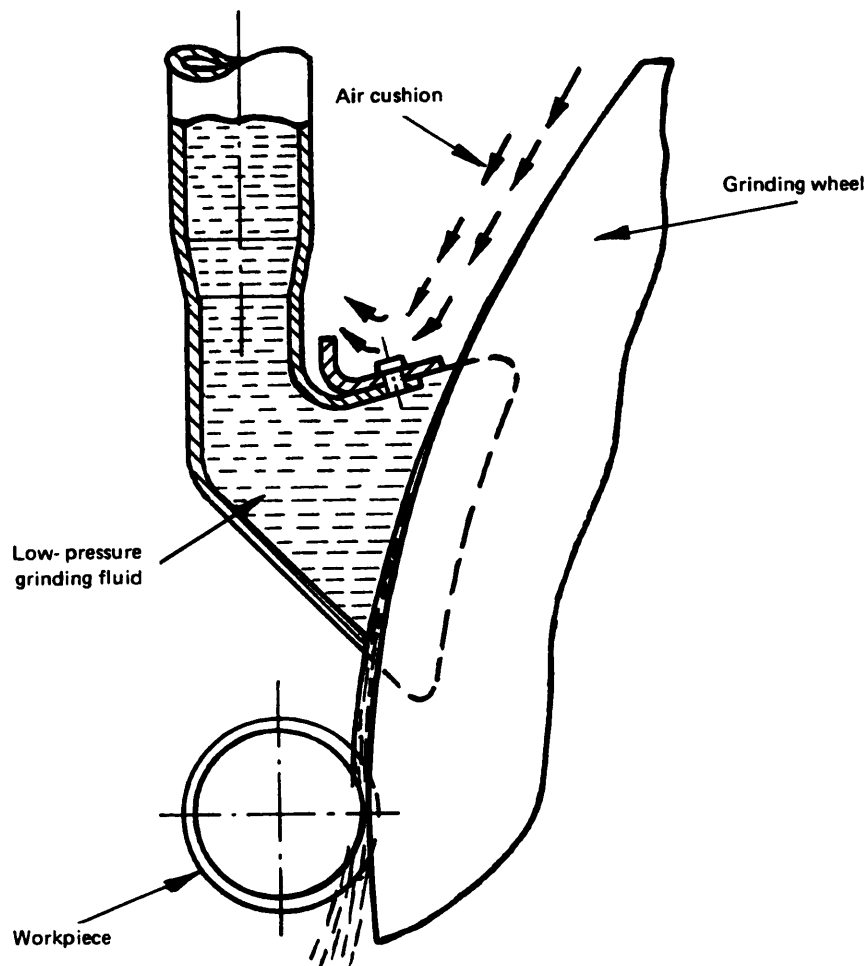
Figure 10.14 Air deflector nozzle or chamber-type nozzle used to increase grinding-fluid penetration into the grinding zone. (From Werner and Lauer-Schmaltz [19].)

or, in other words, it is the ratio of the volume of metal removed to the volume of wheel worn away. Curves relating the volume of wheel wear to the volume of metal removed (Fig. 10.15) are found to be similar to wear curves for a single-point cutting tool and exhibit an initial breakdown period followed by a region of uniform wear rate and finally a period of rapid breakdown. Ideally, the grinding wheel should be dressed at the end of the middle region of uniform wear.

As grinding proceeds and the active grains make repeated contact with the workpiece, the sharp edges are worn away, producing flat areas or wear scars on the grains; this type of wear is known as attritious wear. As this process continues, the forces on the active grains become sufficiently large either to fracture the grain or to tear it from the wheel bond; this type of wear is known as fracture wear. When a sufficiently large proportion of the active grains is fractured or torn from the wheel bond, the wear curve enters the final stage of rapid breakdown, and grinding becomes inefficient. A high grinding ratio is desirable, and Fig. 10.15 shows that an optimum grinding ratio will occur within the middle region of uniform wear rate, the grinding ratio being lower in the initial breakdown stage and in the final breakdown period.

The thrust force also affects the grinding ratio, as shown in Fig. 10.16. This result shows that the wheel removal rate becomes large, and hence the grinding ratio becomes small, when the thrust force is excessive. It is generally considered efficient to employ conditions where the wheel
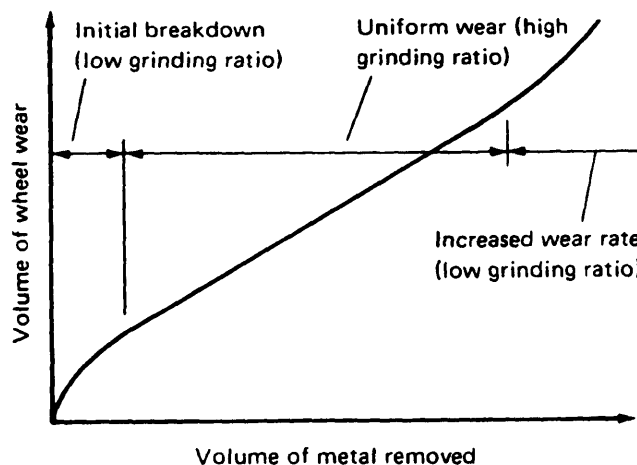
Figure 10.15   Wear of grinding wheels.
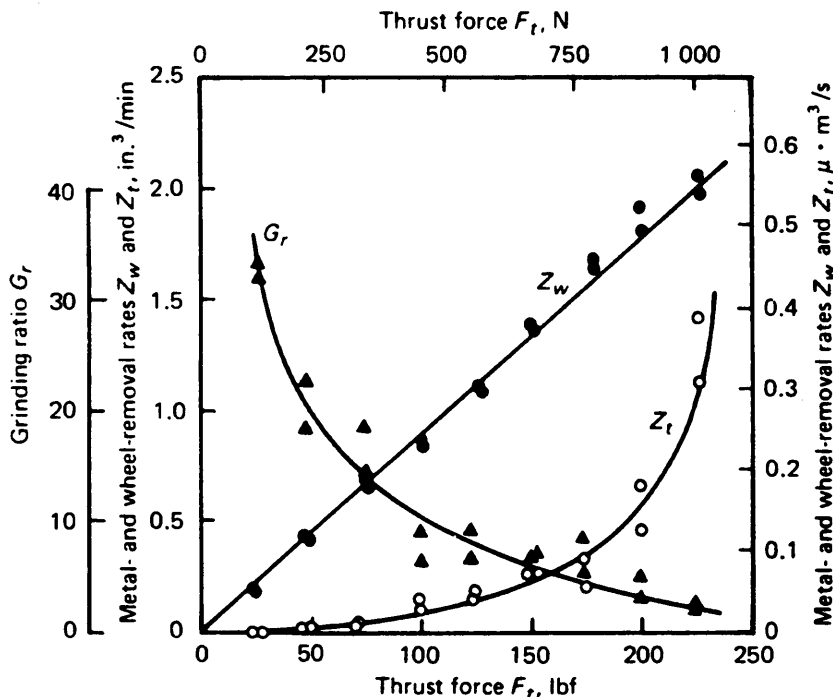
Figure 10.16 Effect of thrust force F_t on the metal and wheel removal rates Z_w and Z_t, respectively, and the grinding ratio G_r during surface grinding of an AISI 52100 steel ring at Rockwell C 60 with an equivalent wheel diameter of 3.25 in. (83 mm), where the wheel-surface speed is 12,000 ft/min (61 m/s) and the work-surface speed is 500 ft/min (2.54 m/s). (After Hahn and Lindsay [7].)

removal rate has just begun to rise steeply, that is, where F_t is between 150 and 200 lbf in Fig. 10.16.

10.10   NONCONVENTIONAL GRINDING OPERATIONS

10.10.1   High-Speed Grinding

It has been demonstrated that increasing grinding speeds well above those used conventionally, up to 180 m/s, can result in increased metal removal rates, without significant changes in grinding forces, specific cutting energies, and surface finish [20]. During early investigations of high-speed grinding, it was suggested that the process might be developed to compete with other machining operations for large stock removal applications.

However, production applications of high-speed grinding have not increased significantly and use of the process is largely restricted to groove grinding and the grinding of the more difficult-to-machine materials.

Considerable safety problems exist with high-speed grinding, because of the increased potential for bursting of the highly stressed wheels. Machines specifically designed to contain broken wheel fragments are required, together with special wheel designs, often of segmental construction.

10.10.2 Creep Feed Grinding

The production utilization of creep feed grinding has increased significantly, largely because of reduced machining times for large stock removal applications, which may be as low as fifty percent of the times for conventional grinding.

In creep feed grinding the operation is performed in a single pass with a large depth of cut (Fig. 10.17), but with low values of the infeed per revolution [21]. Compared to conventional grinding, creep feed grinding has the following characteristics.

1. Increased total grinding forces
2. Reduced average forces on the individual grains
3. Increased temperatures in the wheel–work contact zone
4. Reduced temperatures of the newly generated work surface

As a result, creep feed grinding machines must be more rigid than conventional grinding machines and high-efficiency grinding-fluid application systems are required. The wheel profile stability in creep feed grinding is good and typical applications are in grinding deep slots or the grinding of profiles, particularly those having high depth-to-width ratios or using difficult-to-grind materials. A typical application is the form grinding of turbine blade root profiles of high-temperature superalloys. Adaptation of the process to cylindrical grinding is known as deep grinding, and it involves initial plunge grinding into the stationary workpiece, before the workpiece is rotated slowly relative to the wheel. The complete stock removal is then completed in one revolution of the workpiece.

10.10.3 Low-Stress Grinding

By careful selection of grinding conditions the occurrence of tensile residual stresses near the surface of the workpiece can be largely eliminated [22]. Low-stress grinding is used on workpieces that will be subjected to high stress or stress corrosion environments.

For low-stress grinding soft and open wheels are used, at lower cutting
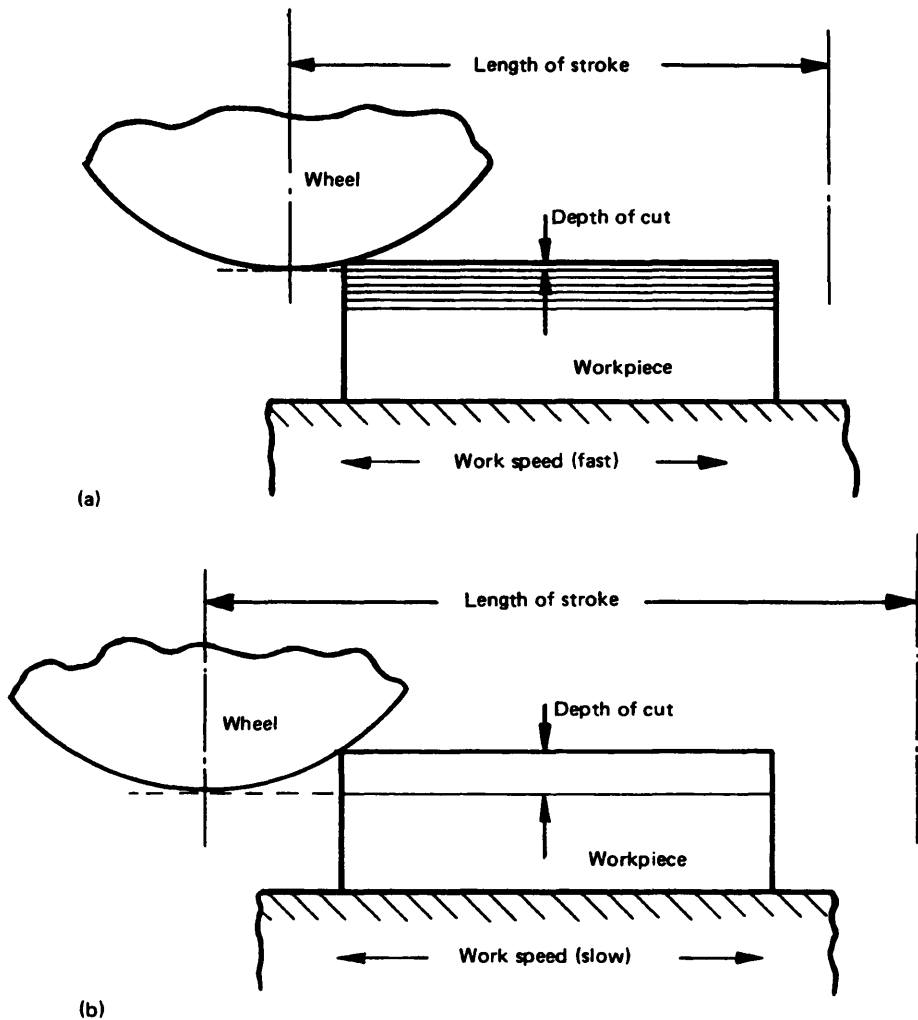
Figure 10.17 Feed, length of stroke, and depth of cut for (a) conventional surface grinding; (b) creep-feed grinding. (From Werner [21].)
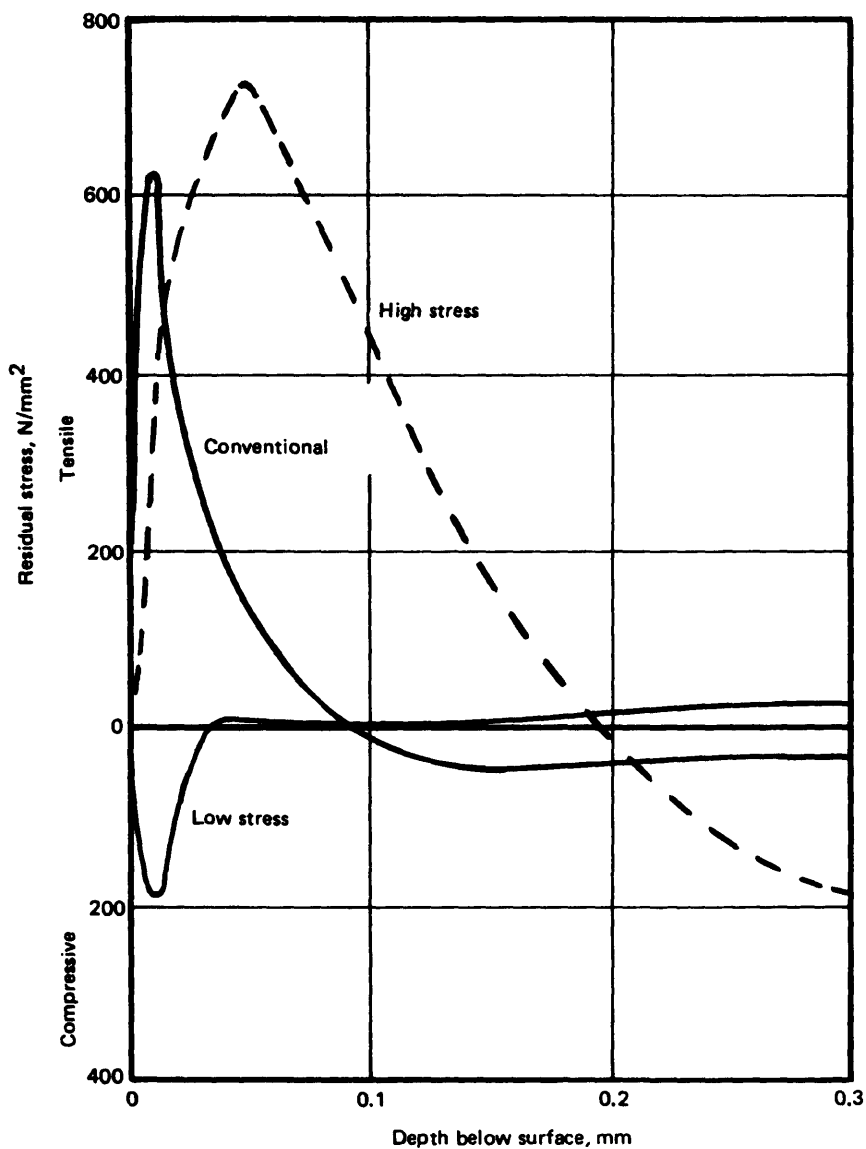
Figure 10.18 Residual stresses induced in the workpiece by various grinding conditions. (From

speeds than for conventional grinding, typically 18 m/s rather than 30 m/s. Oil-based grinding fluids are also used, with low infeed rates (0.005 mm per pass), to minimize frictional effects at the work surface. Figure 10.18 shows residual stresses for low-stress, conventional, and high-stress grinding conditions, the latter corresponding to dry grinding with a relatively hard wheel. For low-stress grinding conditions a small compressive residual stress is induced near the work surface, which can be beneficial to the fatigue resistance of the workpiece.

PROBLEMS

1. It is required to slit a 500-mm-square section block of tool steel on a large horizontal surface grinder using a grinding wheel 5 mm wide and 2 m in diameter. The workpiece removal parameter is 50 p · m^3/sN and the wheel removal parameter is 20 p · m^3/sN. Estimate the time taken to complete the operation if the downfeed is set at 2 mm per cutting stroke and the machine operates at 0.2 cutting stroke per second. Also, estimate the thrust force if the threshold thrust force is 900 N and if the workpiece traverse speed is 150 mm/s.

2. A 20-mm-wide groove in a 50-mm diameter steel shaft is to be plunge-ground on a cylindrical grinder. The depth of the groove is to be 10 mm and the material is easy to grind with a hardness of Rockwell C 60. The rotational frequencies of the workpiece and wheel are 10 and 200 s^{-1}, respectively. The wheel is designated A70D8V, has a diameter of 300 mm, and is dressed with a feed of 0.1 mm at a depth of 0.01 mm. If the machine infeed speed is set at 0.2 mm/s, estimate the total time for the operation, including spark-out, where 90 percent of the material remaining after the infeed is stopped is removed. Assume that the effective stiffness of the grinding system in the thrust force direction is 1.6 MN/m.

REFERENCES

1. Merchant, M. E.: Delphi-type forecast of the future of production engineering, *CIRP Ann.,* vol. 20/3, p. 213, 1971.
2. Shaw, M. C.: The Grinding of Metals, IME Proc. Conf. Tech. Engineering Manufacture, London, p. 433, 1958.
3. Backer, W. R., E. R. Marshall, and M. C. Shaw: The size effect in metal cutting, *Trans. ASME,* vol. 74, no. 1, p. 61, 1952.
4. Peklenik, J., and H. Opitz: Testing of grinding wheels, Adv. Machine Tool Des. Res., p. 163, 1962.
5. Grisbrook, H.: Cutting points on the surface of a grinding wheel and chips produced, Adv. Machine Tool Des. Res., p. 155, 1962.

6. Hahn, R. S.: On the nature of the grinding process, Adv. Machine Tool Des. Res., p. 129, 1962.

7. Hahn, R. S., and R. P. Lindsay: Principles of grinding, *Machinery*, July–November, 1971.

8. Kalpakjian, S. *Manufacturing Processes for Engineering Materials*, Addison-Wesley, Reading, Mass., 1984.

9. Hahn, R. S., A Survey on Precision Grinding for Improved Product Quality, Proc. 25th International MTDR Conference, Birmingham, p. 3, 1985.

10. Boothroyd, G.: *Fundamentals of Metal Machining and Machine Tools*, McGraw-Hill, New York, 1975.

11. Hahn, R. S.: The Effect of Wheel-Work Conformity in Precision Grinding, *ASME Paper* 54-A-178, 1954.

12. Lindsay, R. P.: The Effect of Conformity, Wheelspeed, Dressing and Wheel Composition on the Grinding Performance of Conventional and High Temperature Alloys, *SME Paper* MR70-803, 1970.

13. Lindsay, R. P.: Dressing and Its Effect on Grinding Performance, *SME Paper* MR69-568, 1969.

14. Lindsay, R. P.: On Metal Removal and Wheel Removal Parameters, Surface Finish, Geometry and Thermal Damage in Precision Grinding, Doctoral Dissertation, Department of Mechanical Engineering, Worcester Polytechnic Institute, Worcester, Mass., 1971.

15. Snoeys, R., M. Maris, and J. Peters: Thermally induced damage in grinding, *CIRP Ann.* vol. 27, no. 2, p. 571, 1978.

16. Malkin, S.: Thermal Aspects of Grinding, Part 1, Energy Partition, *Trans. ASME*, no. 73-WA/Prod., 1973.

17. Konig, W., W. Honscheid, and R. Lowin: Untersuchung der bein Schleifprozess entstehenden Temperaturen und ihre Auswirkungen auf das Arbeitsergebnis, *Forschungsb. Landes Nordrh. Nr.* 2648, Westdeutsches Verlag, 1977.

18. Radhakrishnan, V., and B. T. Achyutha: A method for reducing the corner wear in plunge grinding, *Proc. Inst. Mech. Eng.* vol. 200, no. B1, p. 19, 1986.

19. Werner, P. C., and H. Lauer-Schmaltz: Advanced Application of Coolant and Prevention of Wheel Loading in Grinding, Proc. International Symposium on Metal Working Lubrication, ASME, p. 228, 1980.

20. Brown, E. L., F. L. Schierloh, and A. R. McMillan: High Speed O.D. Plunge Grinding, *SME Technical Paper* MR 79-952, 1979.

21. Werner, P. C., Application and Technological Fundamentals of Deep and Creep Feed Grinding, *SME Technical Paper*, MR 79-319, 1979.

22. Kohls, J. B., and G. Bellows: Low stress grinding: Its parameters and potential, *Manuf. Eng.*, p. 38, October, 1976.

11
Manufacturing Systems and Automation

11.1 INTRODUCTION

The efficiency of a manufacturing facility can be measured in three basic ways: manufacturing cost, productivity, and profit.

Manufacturing cost involves not only the costs of machining, assembly, and so on, but also the costs of moving the component components from machine to machine and temporary storage. It can be affected by the efficiency of the various manufacturing processes used and the way these processes are integrated or arranged in the factory. It is also affected by labor costs and the quality of the product design.

Productivity, in contrast, refers only to the efficiency with which labor is utilized. It is generally taken to mean the average output per man-hour. Thus, if factory A produces 300 refrigerators per week and employs 300 workers and factory B can produce only 150 refrigerators per week with the same number of workers, the workers in factory A are twice as productive as those in factory B. This higher labor efficiency of factory A does not necessarily mean, however, that the refrigerators from factory A will be less expensive than those from factory B. Perhaps factory A is using much more expensive automated manufacturing equipment that offsets the savings in labor.

317

Finally, the profit made by the company will be affected by changes in manufacturing costs or productivity.

Manufacturing cost, productivity, and profit cannot be optimized simultaneously, as shown by the example in Chap. 6, where the conditions for minimum cost, minimum production time (maximum productivity), and maximum profit rate were all different.

The purpose of this chapter is to discuss the means of improving productivity in manufacturing by improved manufacturing systems and increased automation. Automation is defined here as any means of helping workers perform their tasks more efficiently.

Before discussing particulars, it is necessary to explain that the approach to automation depends heavily on the volume of production.

11.2 TYPES OF PRODUCTION

Usually, three categories are used in describing the volume of production: mass production, large-batch production, and small-batch production. It may be assumed that mass production involves a volume of more than 1 million components per year and small-batch production less than a few hundred in each production run. Estimates of the proportion of total production in the United States in the batch categories vary from 70 to 85 percent. Because of the large proportion of manufacturing in the batch categories, much attention is paid to automation in batch manufacturing.

The general characteristics of these types of production are as follows.

11.2.1 Mass or Continuous Production

Mass production is characterized by large numbers of components of the same configuration, for which the demand is relatively constant and predictable. The quantities required are sufficient to keep manufacturing equipment loaded continuously or for long periods of time. Consequently, special-purpose machines and tools are used, which closely match the features of the components to be produced. High levels of automation can be justified economically and high productivity can be achieved.

11.2.2 Large-Batch Production

In large-batch production large quantities of similar components are produced in batches. Some flexibility of operation of the machines is required, but many special-purpose machines and tooling, with associated long set-up times, can be justified.

11.2.3 Small-Batch Production

In small-batch production a wide variety of components for which the demand fluctuates must be produced in small batches. General-purpose machines, not specifically designed for particular components, must be used. These machines must be frequently reset for batches of different components, resulting in considerable loss of productive time. Automation for this section of industry must be flexible in operation and readily reprogrammed for a wide variety of components.

11.3 TYPES OF FACILITIES LAYOUT

Several different layouts of machine tools and equipment are used in manufacturing, and the appropriate type depends mainly on the quantities and type of product being processed.

11.3.1 Functional or Process Layout

The functional or process form of layout is used traditionally for batch manufacture. The plant is organized into sections with similar machines together, that is, a turning section, a milling section, and so on (Fig. 11.1). Since most components require a variety of operations, they must be transported frequently from one process-specialized section to another. This results in poor work flow and long and uncertain throughput times, giving rise to considerable problems with the scheduling and control of production. High levels of work in progress are also associated with this plant organization. Responsibility for manufacture is in the hands of several different supervisors.
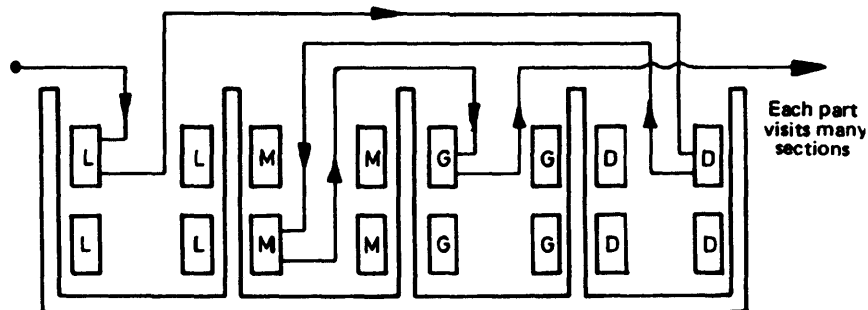
The functional or process layout is very flexible for situations of fluctuating demands, and some benefits are derived from grouping similar skills together in the individual sections.

11.3.2 Line Layout
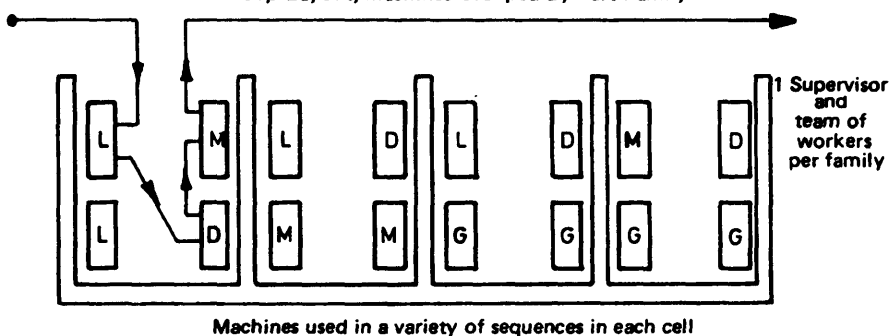
In the line layout, machines are arranged in the sequence of operations, so that parts flow from one machine to the next during processing. Large numbers of components with the same processing sequence are required, and consequently flow lines are usually restricted to mass and large-quantity production. Such flow lines are usually associated with high levels of dedicated automation.

Short, predictable throughput times are typical for line layouts, together with low levels of work in progress. As a result, production control is considerably simplified. Automatic flow lines require high capital
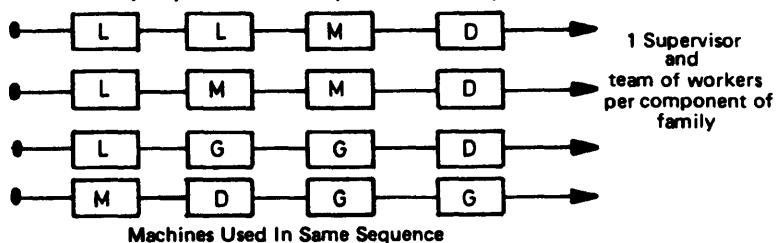
Functional Layout, Machines Grouped By Process

Each part
visits many
sections

Group Layout, Machines Grouped By Part Family

1 Supervisor
and
team of
workers
per family

Machines used in a variety of sequences in each cell

Line Layout, 1 Line Per Component of Family

1 Supervisor
and
team of workers
per component of
family

Machines Used In Same Sequence

KEY: L = lathe M = miller G = grinder D = drill

Figure 11.1   Types of machine tool layout.

expenditure and considerable design and development costs. They are relatively inflexible and generally unsuitable for situations with variable product demand or frequent product design changes.

11.3.3 Group or Cellular Layout

The group or cellular form of layout can be used for small-batch production when a relatively stable distribution of component types exists. This is usually the case for companies involved in the manufacture of a particular type of product such as machine tools, hydraulic pumps, and so on. Cells or groups of machines are formed to process families of related parts, requiring similar processes in a variety of sequences (Fig. 11.1). If possible, components should be completely processed in the particular cell. Compared with the functional layout, the cellular layout results in improved work flow and lower throughput times, together with improved labor and machine utilization. Production control is generally easier and levels of work in progress are reduced.

The successful operation of a cellular layout requires increased labor mobility and flexibility, as there are usually more machines than operators in each cell. The key machines are fully loaded and each requires an operator, but several secondary machines may be used by fewer operators, who move from machine to machine as required. A full description of the design and operation of cellular layouts is given by Gallagher and Knight [1]. As will be seen later, an extension of this basic approach leads to modern flexible manufacturing systems.

Multiproduct or group flow lines may be used for some families of components, where each member of the family has a similar sequence of operations so that unidirectional flow lines can be utilized. General-purpose machine tools are used; usually with work handling performed by mechanical conveyors. Some resetting of machines is required for a change of product but advantage can be taken of the similarities between components to keep this to a low level.

Table 11.1 summarizes the general characteristics of the various types of facilities layouts used.

11.4 TYPES OF AUTOMATION

Automation used in manufacturing can be divided into two basic types: fixed automation and programmable automation.

11.4.1 Fixed Automation

This type of automation is dedicated to a specific task or a limited range of tasks. Cams and other mechanisms are often used to control motions.

Table 11.1 General Characteristics of Different Plant Layout Types

	Type of Layout		
Characteristics	Functional	Group	Line
Specialization	By process	By component type	By component type
Material flow between m/cs	In batches	Nearly continuous	Continuous
Material throughput time	Long	Short	Shorter
Stocks of work in progress	High	Low	Lower
Responsibility for quality	Many foremen per part	One foreman per part	One foreman per part
Responsibility for delivery by due date	Many foremen per part	One foreman per part	One foreman per part
Investment in special tooling	High: one set per operation/part	Low: one set per tooling family	High: one set per line; one line/part
Investment in buildings	High	Lower	Lower
Control of material flow	Complex	Simple	Simpler

This form of automation requires high initial investment and long set-up times. It is usually restricted to large-volume production for which high productivity can be achieved. The equipment is relatively inflexible and cannot be readily adapted to new tasks or products. Transfer lines and automatic lathes are examples of fixed or dedicated automation.

11.4.2 Programmable Automation

This form of automation can be used for lower-volume production since the equipment can be readily reprogrammed for new tasks and products. Two basic forms of programmable automation exist: program sequence control and numerical control.

Program Sequence Control

A sequence of motions or operations is controlled by timers, relays, or programmable controllers. The actual motions are limited by preset mechanical stops and limit switches. Many capstan and turret lathes use sequence control, programmed by plugboards or microprocessor-based controllers.

Numerical Control

The most important form of programmable automation for manufacturing is numerical control (NC). The machine controller is fed with a program of instructions, usually on paper tape. The position, velocity, and acceleration of the machine motions can be controlled, together with auxiliary functions such as tool changing, turning the coolant supply on-off, and so on. As NC for machine tools was being developed, programs initially consisted of numerical data only, hence the term numerical control. However, in modern controllers a mixture of alphabetic codes and numerical information makes up the program. Some details on the programming of NC machine tools are given in Chap. 12.

Numerically controlled machine tools are very flexible in operation and are highly suited to small-batch manufacturing. When the job changes, a new program of instructions is prepared and the changeover to the new task can be achieved quickly. Fixturing requirements are usually simple, which also facilitates the changeover from one component to another. Programming is carried out away from the machine tool and does not significantly interfere with production time.

Numerical control has been applied to a wide range of manufacturing equipment, including metal-cutting machine tools, welding, sheet metal working, tube bending, flame cutting, and many others. This discussion is limited to metal-cutting machine tools, the most widespread application of NC. Currently, around 20 percent of modern machine tools utilize this form of control.

Some different forms of automation in machine tools will now be discussed.

11.5   TRANSFER MACHINES

Transfer machines are often the most suitable method for a continuous flow of identical or very similar components in the mass production of consumer goods. They are basically special-purpose systems in which the components are automatically transferred from one machining head to another, often called unit head machines. Each machining head carries out one operation until, when the component has negotiated the complete transfer system, all the necessary operations have been completed.

With transfer machines the component is automatically transferred from one machining operation to the next either by a circular indexing table (the rotary-transfer system shown in Fig. 11.2a) or along a conveyor (the in-line transfer system shown in Fig. 11.2b). In the in-line system the component is held on a special pallet or fixture, and arrangements have to be made to return empty pallets to the beginning of the line. Often a rapidly moving return conveyor parallel to the main transfer line is used to return the empty pallets.

Transfer machines are often constructed in modular fashion; the machining heads for drilling, boring, and so on, are standard items and are added to the system at the appropriate stations. Rotary-transfer machines can usually accommodate only six or fewer stations because of restrictions on space. The size of an in-line machine can be almost unlimited, and in-line machines have been employed, for example, to perform all the machining operations on an automobile engine cylinder block. In addition to the machining operations, these systems also incorporate stations for inspection and sometimes assembly operations.

11.5.1   Economics of Transfer Machines

When the optimum machining conditions for transfer machines operating on the indexing principle are considered, it is necessary to account for the condition that when one machining station is stopped in order to change tools, the whole indexing transfer machine must stop. It must also be remembered that no advantage exists in having the machining time vary from station to station. If one station has a short machining time, the cutting speed at that station can be reduced without affecting the cycle time for the machine with the advantage that tool costs will be reduced at the station and down time reduced for the whole transfer machine.

For analysis, assume that on a transfer machine having N_s stations the same cutting-tool material is used at each station.
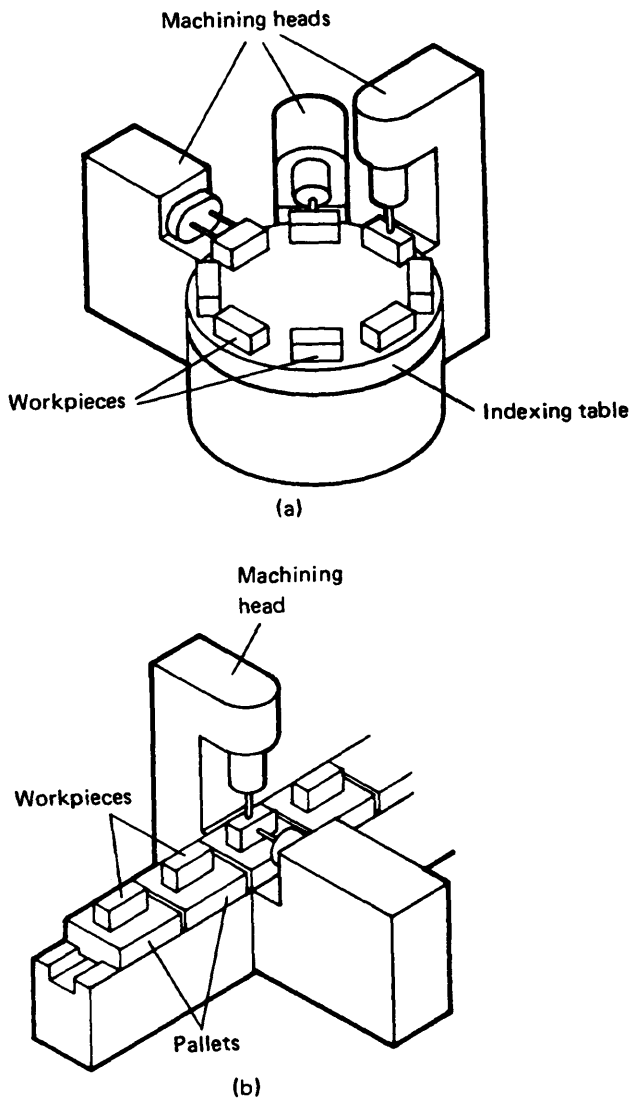
Figure 11.2   Transfer machines. (a) Rotary; (b) in-line.

For any station s, therefore, the tool-life relationship is

$$\frac{v_s}{v_{r_s}} = \left(\frac{t_{r_s}}{t_s}\right)^n \tag{11.1}$$

where

    v_s = cutting speed
    t_s = tool life
    v_{r_s} = cutting speed for a tool life of t_{r_s}

The machining time t_m for each operation is given by

$$t_m = \frac{K_s}{v_s} \tag{11.2}$$

where K_s is the distance moved by the tool corner relative to the workpiece during the machining time. If Eqs. (11.1) and (11.2) are combined,

$$t_s = t_{r_s}\left(\frac{v_{r_s} t_m}{K_s}\right)^{1/n} \tag{11.3}$$

The total time to produce N_b components is now given by

$$N_b(t_t + t_m) + N_b \sum (t_m t_{ct_s}/t_s) \tag{11.4}$$

where

    t_t = time taken to index the machine and advance and withdraw the tools
    t_{a_s} = tool changing time at any station s
    Σ = sum of the terms for all the stations on the machine

Thus, the average production time per component is

$$t_{pr} = t_t + t_m + \sum \frac{t_m t_{ct_s}}{t_s} \tag{11.5}$$

If the rate (cost per unit time) for each station (including the section of the transfer machine associated with that station) is M_s, the total rate for the transfer machine will be ΣM_s, and the production cost per component C_{pr} will be given by

$$C_{pr} = \sum (M_s t_{pr}) + \sum \frac{t_m C_{t_s}}{t_s} \tag{11.6}$$

where C_{t_s} is the cost of providing a new tool at station s.

Substitution of Eqs. (11.3) and (11.5) in Eq. (11.6) and rearrangement gives

$$C_{pr} = \sum M_s (t_t + t_m) + t_m^{1-(1/n)}$$

$$\times \left\{ \sum M_s \sum \left[\left(\frac{K_s}{v_{r_s}} \right)^{1/n} \frac{t_{ct_s}}{t_{r_s}} \right] + \sum \left[\left(\frac{K_s}{v_{r_s}} \right)^{1/n} \frac{C_{t_s}}{t_{r_s}} \right] \right\} \tag{11.7}$$

Equation (11.7) can now be differentiated with respect to t_m to find the machining time t_{m_c} giving minimum production costs. Thus,

$$t_{m_c} = \left(\left(\frac{1}{n} - 1 \right) \left\{ \sum \left[\left(\frac{K_s}{v_{r_s}} \right)^{1/n} \frac{t_{ct_s}}{t_{r_s}} \right] + \frac{\sum [(K_s/v_{r_s})^{1/n}(C_{t_s}/t_{r_s})]}{\sum M_s} \right\} \right)^n \tag{11.8}$$

The minimum production costs per component can now be found by substitution of t_{m_c} for t_m in Eq. (11.7), and the optimum tool life at each station can be obtained from Eq. (11.3).

To illustrate the effect of combining a series of machining processes on one indexing transfer machine it will now be assumed that a series of similar operations are to be performed at each station and that the parameters at each station are identical. In this case Eq. (11.8) becomes

$$t_{m_c} = \left\{ \left(\frac{1}{n} - 1 \right) \left[\left(N_s \frac{t_{ct}}{t_r} \right) + \frac{C_t}{M t_r} \right] \right\}^n \frac{K}{v_r} \tag{11.9}$$

Substitution of Eq. (11.9) in (11.3) now gives the optimum tool life at each station:

$$t_c = \left(\frac{1}{n} - 1 \right) \left(N_s t_{ct} + \frac{C_t}{M} \right) \tag{11.10}$$

Comparison of this result with the optimum tool life for a single operation (obtainable by writing $N_s = 1$ in Eq. [11.10]) indicates that as the number of stations on a transfer machine increases, so does the optimum tool life. Thus, the optimum cutting speeds would be lower on a transfer machine than those on a single machine tool.

11.5.2 Example

Assume that high-speed steel tools are used ($n = 0.125$) on a five-station indexing transfer machine, and that the values of $K_s, t_{a_s}, C_{t_s}, v_{r_s}$, and t_{r_s} for each station are as shown in Table 11.2. From these figures the following values are obtained:

$$\sum M_s = \$0.0155/s$$

$$\sum \left(\frac{K_s}{v_{r_s}}\right)^{1/n} \frac{t_{ct_s}}{t_{r_s}} = 1.49 \times 10^{19} \text{ s}^8$$

$$\sum \left(\frac{K_s}{v_{r_s}}\right)^{1/n} \frac{C_{t_s}}{t_{r_s}} = \$6.0 \times 10^{17} \text{ s}^7$$

From Eq. (11.8), the optimum machining time is

$$t_{m_c} = \left[7(1.49 \times 10^{19}) + \frac{6 \times 10^{17}}{0.0155} \right]^{0.125} = 373 \text{ s}$$

From Eq. (11.7) if the transfer time t_t is 12 s, the minimum production cost per component is

$$C_{min} = 0.0155(12 + 373) + \frac{(0.0155 \times 1.49 \times 10^{19}) + (6.0 \times 10^{17})}{10^{18}}$$

$$= 5.97 + 0.83 = \$6.80$$

where C_{min} is the minimum cost of production, that is, the minimum value of C_{pr}. Finally, the optimum cutting speed at each station can be obtained from Eq. (11.2); thus, for stations 1, 2, 3, 4, and 5 the cutting speeds are 0.49, 0.65, 0.16, 0.24, and 0.33 m/s, respectively.

11.6 AUTOMATIC MACHINES

Where transfer machines are used exclusively for mass production, the class of machine tool referred to as *automatic* is used in both mass and large-batch production. The most common of these machines is the automatic lathe, sometimes referred to simply as an "automatic."

Those single-spindle automatic lathes that are designed to produce components from bar stock will continually produce these components without needing attention, except for the replacement of the bar stock and the changing of worn tools. Feeding of the bar stock through the collet is

Table 11.2   Machining Parameters for a Five-Station Indexing Machine

Station	K_s, m	t_{a_s}, s	C_{t_s}, \$	M_s, \$/s	t_{r_s}, s (for $v_{r_s} = 1$ m/s)
1	183	180	2	0.003	65
2	243	60	3	0.0027	65
3	61	120	2	0.0038	65
4	91	120	2	0.003	65
5	122	240	1	0.003	65

carried out intermittently after each machined component has been cut off, or, with the swiss-type automatic, the bar is rotated and fed continuously while the machining operations are carried out. Where feeding is intermittent, the machine is basically an automatic turret lathe; where feeding is continuous, the workpiece is fed past the various tools mounted radially around the working region.

Movement of the tool slides is often controlled by flat disk cams, which must be produced for the particular job. In general, in a single-spindle automatic, three cams are required, each cam being milled with an end mill of the same diameter as the cam follower. Clearly, the expense of producing cams for an automatic lathe can only be justified for large production runs.

Single-spindle automatic lathes with chucks are used for those components that cannot be machined from bar stock. In these machines the individual workpieces are loaded manually with one operator able to service a group of machines.

A final class of automatic lathe is the multispindle automatic. These lathes are basically flexible, rotary-transfer machines where each spindle holding a collet or chuck is indexed around the various tooling positions so that during each indexing cycle a completed component is produced. Drum cams instead of disk cams are used in these machines.

Another class of machine tool that can be mechanized is the internal or external cylindrical grinder. When fitted with mechanisms for loading workpieces automatically and with automatic wheel-dressing devices, these machines can continually produce finished components. The workpieces are often stacked in a magazine, and the operator simply ensures that the magazine is replenished with workpieces at suitable intervals. Because the components are small and the machining forces light, magnetic chucks are often employed to facilitate automatic work holding.

11.6.1 Economics of Automatic Machines

It will be assumed that one operator can service N_a automatic machines, that the operator's rate (including overheads) is W'_o, and that the rate for one machine (including overheads) is M'_t. The cost of production C_{pr} per component will then be given by

$$C_{pr} = \frac{C_b}{N_b} + (W'_o + M'_t)t_1 + \left(\frac{W'_o}{N_a} + M'_t\right)t_m$$

$$+ \left[(W'_o + M'_t)t_{ct} + C_t\right]\frac{t_m}{t} \qquad (11.11)$$

where

C_b = cost of setting up the machine (including manufacture of cams, etc.)
N_b = batch size
t_{ct} = tool-changing time
C_t = cost of providing one new cutting edge
t_m = machining time
t = tool life
t_1 = loading and unloading time

11.6.2 Example

Assume the following values apply to a bar-fed single-spindle automatic lathe (where t_1 is negligibly small) and one operator is servicing six machines: t_m = 30 s, t = 4000 s, t_{ct} = 60 s, W'_o = $2.20 × 10^{-3}/s, M'_t = $1.40 × 10^{-3}/s, C_t = $0.50, and C_b = $1000.
Substitution of these figures in Eq. (11.11) gives

$$C_{pr} = \frac{1000}{N_b} + \left[\left(\frac{2.2 \times 10^{-3}}{6} + 1.4 \times 10^{-3}\right)30\right]$$

$$+ \left[(2.2 \times 10^{-3} + 1.4 \times 10^{-3})60 + 0.5\right]\frac{30}{4000} = \frac{1000}{N_b} + 0.058$$

It can be seen that in this example a batch size of about 200,000 components is required before the set-up costs are reduced to 10 percent of the production cost per component.

11.7 NUMERICALLY CONTROLLED (NC) MACHINE TOOLS

11.7.1 Main Features of NC Systems

The complete NC machine tool system consists of the three basic elements shown in Fig. 11.3: the program of instructions, the controller unit, and the machine tool.

Program of Instructions

The program of instructions, or part program, as it is often called, is the detailed set of directions telling the machine tool what to do. It is a mixture of alphabetic codes and numerical data, which is interpreted by the NC controller. The program is fed to the controller, usually in the form of punched paper tape, but systems for direct electronic transfer of instructions are also available. The program is prepared independently of the machine tool by a part programmer, and programming an NC machine tool is essentially a specialized process-planning exercise. Some details of the preparation of NC part programs are discussed in Chap. 12.

The program contains instructions telling the NC controller, for example, how to move the machine slides, to generate the required surfaces on the workpiece. The displacements, velocities, and accelerations of the various machine tool components can usually be controlled. In addition, the various auxiliary functions of the machine tool can be controlled, including such items as coolant on or off, automatic tool change or turret index, and so on.

(a)   (b)   (c)
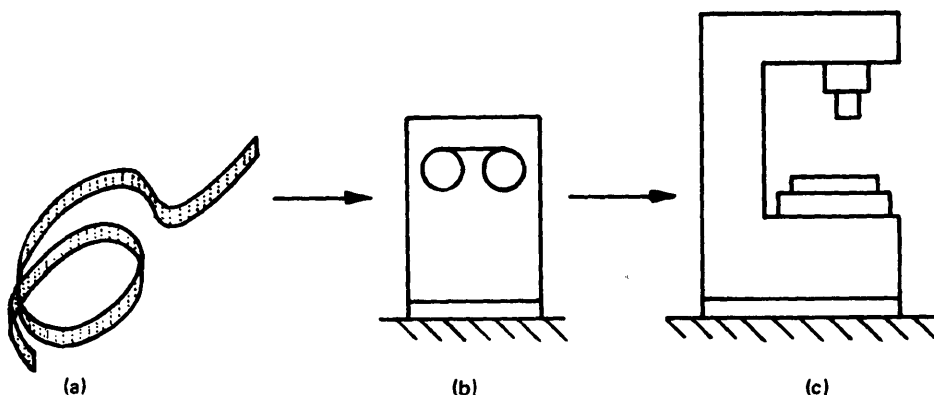
Figure 11.3 Basic components of a numerical control machine tool system. (a) Program; (b) controller; (c) machine tool.

Machine Tool Controller

The machine tool controller accepts the part program of instructions and converts these instructions into signals that control the various actions of the machine tool. The controller forms part of a feedback control system for the motions of the machine tool slideways.

The machine tool control system also performs a number of functions (Fig. 11.4). Input instructions are usually provided by the program but they can also be provided by the operator, who enters information manually from a control panel. The control panel also contains data displays for the operator. A tape reader is usually fitted to read the program instructions from the paper tape. Instructions are fed initially into a data input buffer, which stores a block of information. This represents one complete set of instructions for the next step in the machining sequence. Each block is usually terminated on the input tape by an end-of-block character, equivalent to the carriage return—line feed at the end of an instruction for a computer. Each instruction in the block is then decoded and the information is stored within the controller and acted upon.

Other main functions of the controller are interpolation and feed rate generation. In order to machine complex curved surfaces at a constant feed rate, instructions must be fed to the drives for the various slides and spindles so that the sum of their individual motions produces the required
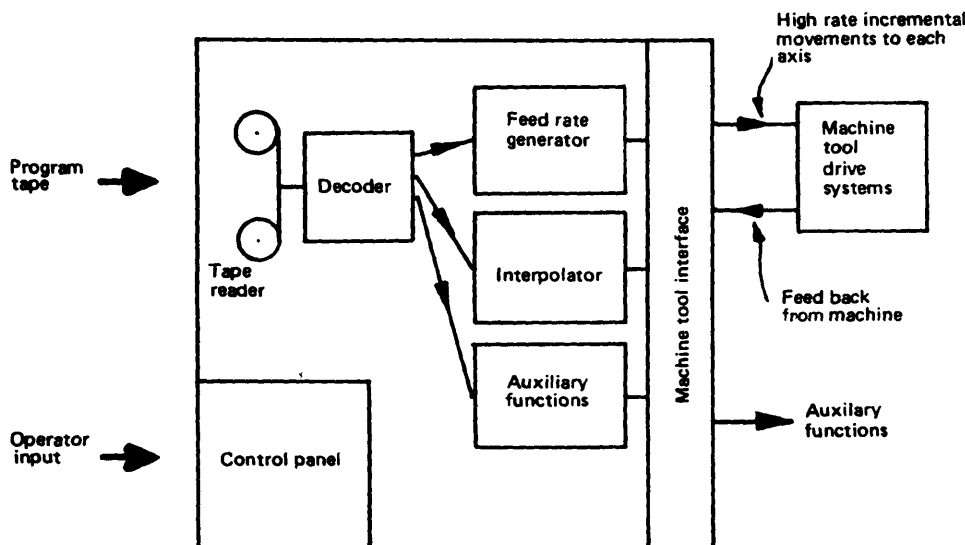
Figure 11.4 NC controller functions.

shape. The controller breaks down (interpolates) these curves into small individual increments for each controlled motion of the machine tool.

Finally, signal input–output channels connect the controller to the drive motors, transducers, and other controls of the machine tool.

Machine Tool

The third element of the NC system is the machine tool itself. This is a general-purpose machine tool fitted with drive motors and controls to operate the spindle and slides automatically and to switch on or off the various auxiliary functions of the machine. Transducers are fitted to feed back data on the position and velocity of, for example, the slideways, to the controller.

Numerically controlled machine tools range in complexity from simple drilling machines to complex machines that utilize a number of controlled motions. The most complex NC machine tools are so-called NC machining centers. These machines incorporate multiaxis control and are usually horizontal- or vertical-spindle milling machines, fitted with high-capacity tool magazines and automatic tool changers. The objective in using these machines is to carry out a large amount of machining in one workpiece fixturing, and they are capable of performing a wide variety of operations including milling, drilling, tapping, and boring. Additional motions, using, for example, indexing tables, are usually possible so that several orientations of the workpiece can be presented during the program.

11.7.2   NC Motions

There are three basic types of NC motions (Fig. 11.5), as follows:

Point-to-Point or Positional Control

In point-to-point control the machine tool elements (tools, table, etc.) are moved to programmed locations and the machining operations performed after the motions are completed. The path or speed of movement between locations is unimportant; only the coordinates of the end points of the motions are accurately controlled. This type of control is suitable for drill presses and some boring machines, where drilling, tapping, or boring operations must be performed at various locations on the workpiece.

Straight-Line or Linear Control

Straight-line control systems are able to move the cutting tool parallel to one of the major axes of the machine tool at a controlled rate suitable for machining. It is normally only possible to move in one direction at a time, so angular cuts on the workpiece are not possible. Consequently, for mill-

Types of NC Machine

Positional (point to point)	Paraxial (straight line)	Continuous path (contouring)

Workpiece Examples

Positional

Straight Line

Contouring

2½ Axis (2CL)

2 Axis (2C)

3 Axis (3C)
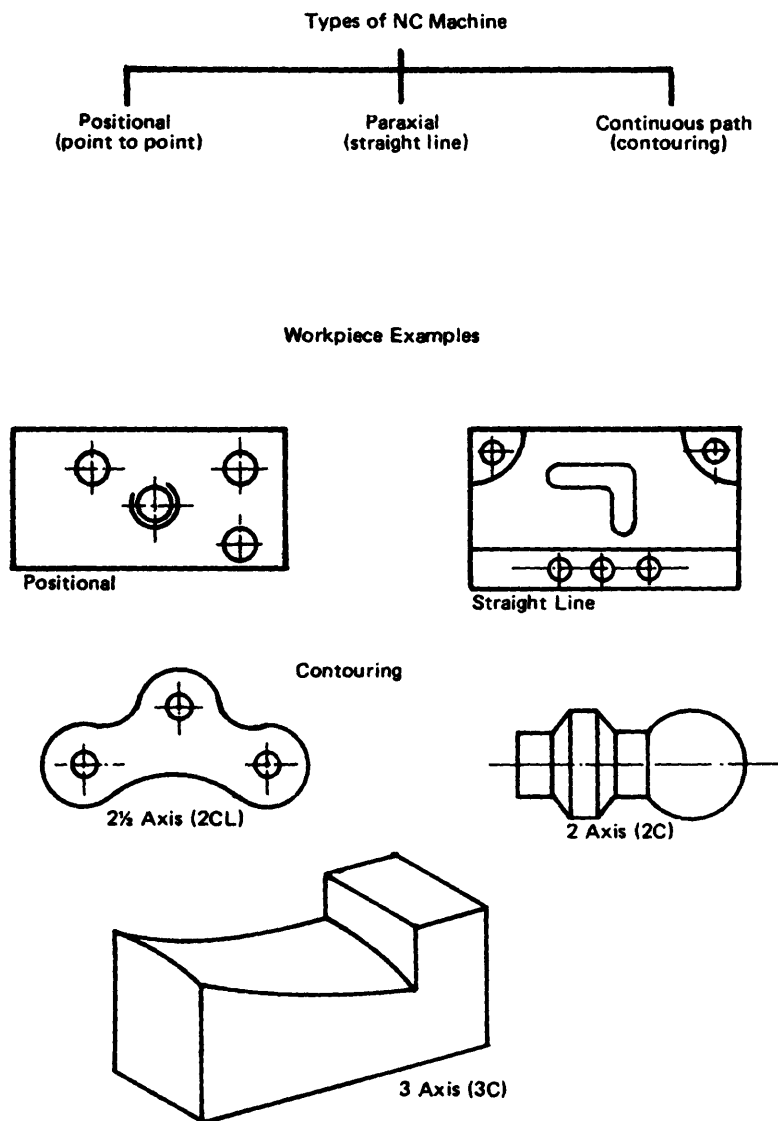
Figure 11.5   Types of NC machine motions and workpiece examples.

ing machines, only rectangular configurations can be machined or for lathes only surfaces parallel or perpendicular to the spindle axis can be machined. This type of controlled motion is often referred to as linear control or a half-axis of control (see below). Machines with this form of control are also capable of point-to-point control.

Continuous Path or Contouring Control

In continuous path control the motions of two or more of the machine axes are controlled simultaneously, so that the position and velocity of the tool are changed continuously. In this way curves and surfaces can be machined at a controlled feed rate. It is the function of the interpolator in the controller to determine the increments of the individual controlled axes of the machines necessary to produce the desired motion. This type of control is referred to as continuous control or a full axis of control.

Some terminology concerning controlled motions for NC machines has been introduced. For example, some machines are referred to as four- or five- or even six-axis machines. For a vertical milling machine three axes of control are fairly obvious, these being the usual X, Y, Z coordinate directions. A fourth or fifth axis of control would imply some form of rotary table to index the workpiece or possibly to provide angular motion of the workhead. Thus, in NC terminology an axis of control is any controlled motion of the machine elements (spindles, tables, etc). A further complication is use of the term half-axis of control; for example, many milling machines are referred to as 2½-axis machines. This means that continuous control is possible for two motions (axes) and only linear control is possible for the third axis. Applied to vertical milling machines, 2½-axis control means contouring in the X, Y plane and linear motion only in the Z direction. With these machines three-dimensional objects have to be machined with water lines around the surface at different heights. With an alternative terminology the same machine could be called a 2CL machine (C for continuous, L for linear control). Thus, a milling machine with continuous control in the X, Y, Z directions could be termed a three-axis machine or a 3C machine. Similarly, lathes are usually two axis or 2C machines. Figure 11.5 illustrates some of this terminology and the corresponding shape-producing capabilities.

11.7.3 Computers in Numerical Control

Rapid developments in and increased availability of low cost, high-speed computing systems has influenced the development and operation of NC systems. Early NC controllers were control systems with all the functions handled by hardware, logic circuits, switches, relays, and so on. Adaptation of these controllers to applications where more axes of control are ac-

quired involved the addition of more hardware. The development of microcomputer systems based on large-scale integrated-circuit chips has allowed many of the functions to be provided by software programs in modern NC systems. These systems are referred to as CNC systems, meaning computer numerical control systems. Practically all modern NC controllers are of this type.

The external appearance of a CNC machine is very similar to that of older NC machines. The tape reader is still the basic input channel for programs. However, the tape is normally read into the system only once for each batch of workpieces, rather than for each part as with older systems. The program is then stored in memory within the CNC controller. The various internal functions of the controller, interpolation, decoding, and so on, are carried out by software rather than hardware. Thus, CNC systems are sometimes referred to as soft-wired systems. Computer numerical control machine tools offer greater flexibility over older NC machine tools; particularly because the user can edit programs at the machine and can use special program macros provided for frequently used cutting sequences.

Another development in the use of computers in NC systems is direct numerical control (DNC), a manufacturing system in which a number of machines are controlled by a central computer through direct connection. The individual machines are supplied with control instructions and data as required. Direct numerical control can be effected at various levels; the simplest and most common form is to simply bypass the tape reader on each individual machine controller. This is called a behind-the-tape reader (BTR) mode of DNC. This mode eliminates the use of paper tape input, which is relatively unreliable, and programs are down-loaded from the central computer to the individual CNC systems as required. This is a relatively inexpensive form of DNC since data transfer rates are low and less costly serial communications lines can be used. Also, feedback in real time of data from the machine tool operation is possible with such systems, which is important for management reporting. With some DNC applications a few of the individual NC functions, such as interpolation, are also centralized but this results in the need for higher data transfer rates and more expensive communications links.

A further refinement of numerical control is adaptive control. This type of control can adapt itself to the prevailing circumstances. These circumstances are measured by the system itself and might include the power required for the machining operation, the wear of the cutting tool or grinding wheel, the forces generated, or the onset of chatter or instability. The system would ideally be designed for automatic adjustment of the feed, speed, or tool position to produce components at minimum cost and

within the tolerances specified. Such systems would be very expensive and have not yet found wide application mainly because of the difficulties of making continuous measurements of tool-wear rate during machining.

A relatively simple adaptive control system can be developed that automatically varies the cutting speed and feed in such a way as to maximize metal removal rates without exceeding predetermined cutting forces and power consumption. Systems of this type are relatively inexpensive and can machine under near-optimum conditions; they are referred to as adaptive control constraint systems.

11.7.4 Economics of Numerically Controlled Machines

For NC machines the cost of the preparations for machining a batch of components C_b will mostly consist of programming and tape preparation costs. There is generally a direct relationship between these costs and the machining time t_m as follows:

$$C_b = K_p t_m \tag{11.12}$$

where K_p is the cost of programming and tape preparation per unit machining time.

The production cost per component is therefore given by

$$C_{pr} = \frac{K_p t_m}{N_b} + M(t_1 + t_m) + \frac{t_m}{t}(M t_{ct} + C_t) \tag{11.13}$$

where

    N_b = batch size
    M = total machine and operator rate
    C_{ct} = cost of a sharp tool
    t = tool life
    t_m = loading and unloading and tool advance and tool withdrawal time
    t_1 = tool-changing time

11.7.5 Example

Consider a large NC turret lathe. The tools are fitted with disposable carbide inserts costing $0.50 per cutting edge and taking an average of 60 s to reset. The cost of tape preparation per unit of machining time would typically be $0.10/s, and a total cycle time of 300 s is assumed of which 50 percent is spent on actual chip removal. The lathe initially cost $125,000

with a payback period of 2 years, operator's wages are \$4.00/hr, and 100 percent overheads are applied to the machine and operator. The total machine rate M therefore becomes

$$M = \frac{2 \times 125{,}000}{2 \times 50 \times 40 \times 3600} + \frac{2 \times 4}{3600} = {\sim}\$0.02/s$$

Finally, the loading and unloading time is assumed to be 150 s and the tool life 300 s. Substitution of these figures in Eq. (11.13) gives

$$C_{pr} = \frac{0.1 \times 150}{N_b} + 0.02(150 + 150)$$

$$+ \frac{150}{300}\left[(0.02 \times 60) + 0.5\right] = \frac{15}{N_b} + 9.85$$

This result shows clearly that the system is economic for small batches and that the cost of programming and tape preparation ($15/N_b$) falls below 10 percent of the total production cost per component when the batch size is greater than 15.

11.8 COMPARISON OF THE ECONOMICS OF VARIOUS AUTOMATION SYSTEMS

Selection of the appropriate level of automation for a particular manufacturing situation is determined largely by the batch sizes and variety of parts to be processed. This can be illustrated by considering the economics of the manufacture of representative types of components on equivalent machines with the different types of automation fitted. Figure 11.6 shows a typical result [2] that compares the use of a center (engine) lathe, a turret lathe and an NC turret lathe for manufacturing a typical component.

The more automated machines are not economic for very small batches because the preproduction costs for setup and programming must be spread over a small number of components. For larger batches, the reduced cycle times for the automated equipment compensates for the greater preproduction costs. This result is typical and shows that manual machines are most suitable when only a few components are required and that NC machines are economic for medium-batch quantities, with more dedicated automation restricted to large-quantity production.
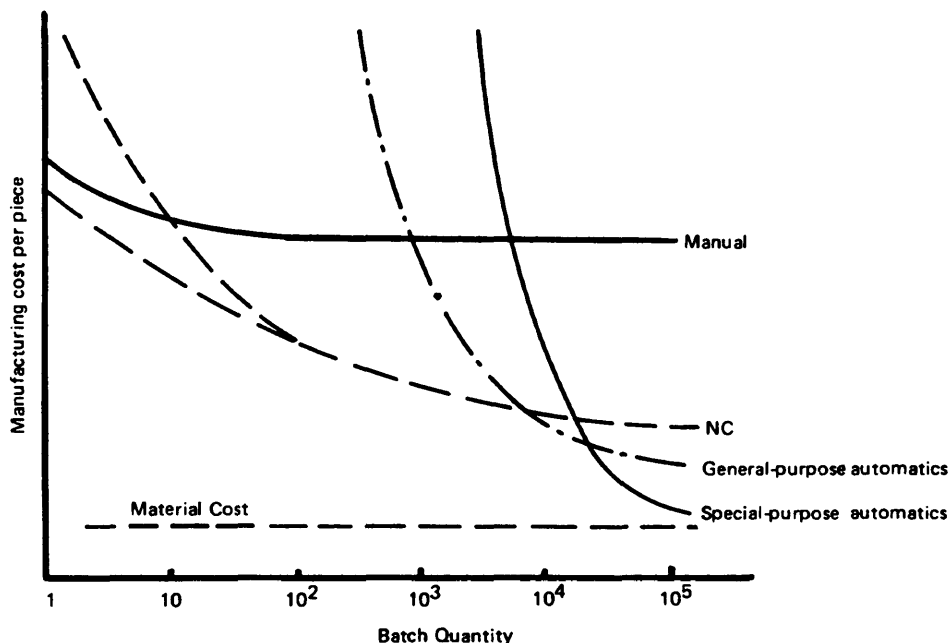
Figure 11.6 Variation of manufacturing cost with batch size for different levels of automation.

11.9 HANDLING OF COMPONENTS IN BATCH PRODUCTION

It has been mentioned that batch production can be automated only by using programmable devices that are preferably controlled by a central computer. One of the greatest problems in realizing the objective of complete computer-controlled manufacturing facilities is the development of general-purpose, programmable handling devices. One such device is an industrial robot such as that depicted in Fig. 11.7. This robot is capable of six axes of motion and of handling objects weighing as much as 120 kg (300 1b). Such robots are being increasingly employed in the loading and unloading of groups of machine tools.

Industrial robots are essentially programmable handling devices, which have several degrees of freedom and which can be fitted with tooling for a variety of tasks including welding, paint spraying, and so on. A gripper or hand is required to handle workpieces and a wide variety of grippers have been devised for holding various items. In adapting a robot to a new task, the grippers must usually be redesigned to accommodate the new item to be handled, and the robot must be reprogrammed.
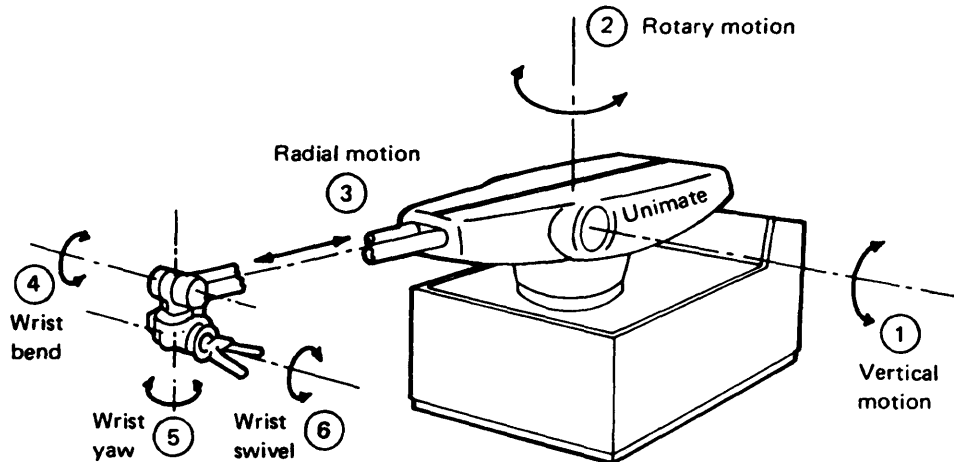
Figure 11.7 Six axes of motion of an industrial robot. (Courtesy of Unimation, Inc.)

A common task for robots is loading workpieces into the machine tool and unloading the machined components. However, most applications of robots to date have been for dedicated or large-batch production tasks, rather than the small- to medium-batch production that their inherent programmability would suggest. This is partly because the grippers and tooling must be adapted to a new task, even though reprogramming the robot may be relatively simple. The use of robots along with NC machines in a cellular layout is attractive provided adaptation of the tooling and grippers to new parts can be made efficient. Engleberger [3] states "if parts are classified into families and machines aggregated into complimentary families the handling of the parts throughout the manufacturing process becomes robot work." However, the grippers must be designed to handle the family of component parts without need modification.

Figure 11.8 shows a small cell of machines, serviced by a robot, used in the manufacture of commercial vehicle gearbox components [4]. The group of machines that form the automated manufacturing cell is made up of an automatic straightening press, two CNC cylindrical-grinding machines, and a pallet shuttle system. There are four basic families of components produced in the cell, with over 100 different components in all.

11.10   FLEXIBLE MANUFACTURING SYSTEMS

A logical step from the concepts of group layout and of NC machine tools and robotics are computer-controlled interlinked multistation machining
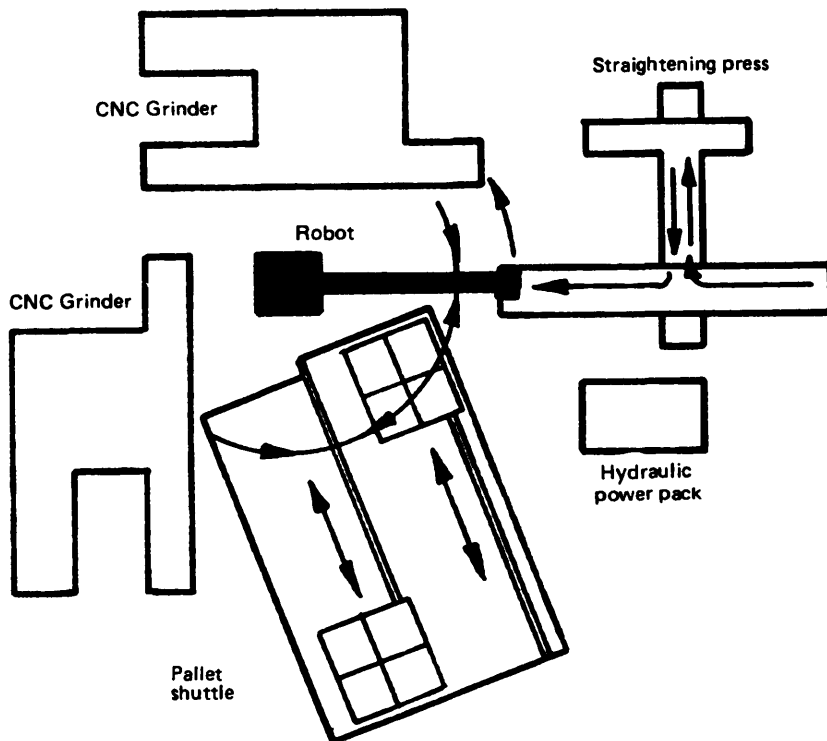
Figure 11.8 Robot work handling in a small cell. (From
[4].)

complexes, or flexible manufacturing systems (FMS) as they have become
called. Such systems can be looked upon as highly automated cells
manufacturing families of components.

The concept of FMS is not a new one; the first proposals were made in
the mid 1960s [5–7]. In recent years we have seen a growth in the number
of systems, particularly in Japan, such that it is estimated that in excess of
a hundred systems have been installed worldwide [8]. A flexible manufac-
turing system contains a number of features as follows:

1. Interlinked NC workstations operating on a limited range or family of
    workpieces. In early proposals the machines were of modular con-
    struction, but in recent systems general-purpose NC machines, in par-
    ticular machining centers, are most commonly used.
2. Automatic transportation, loading and unloading of workpieces and
    tools, using automatic guided vehicles (AGVs), robots, etc.

3. Workpieces mounted on pallets for transportation, partly to overcome the problems of new setups at each workstation

4. Centralized NC or DNC, together with overall computer control of the system

5. Operation for significant periods of time with little or no manual intervention

With FMS the term *flexibility* means the ability to process a variety of components without having to adjust machine setups or change tooling. High flexibility implies that a large family of different components can be produced by the particular system. Figure 11.9 shows that several variants of the basic FMS concept exist [9]. These are:

1. *Flexible manufacturing cells (FMCs):* These are basically machining centers but with the addition of a pallet pool or magazine (Fig. 11.10). The aim is to machine the workpiece with one setup. This type of machine can be operated unmanned for long periods of time, with the palletized workpieces transferred automatically to and from the machine. Flexible manufacturing cells of this type must be served by machines or operators engaged in blank preparation and palletization of workpieces. These cells are highly flexible in operation, having the ability to deal with a wide range of parts (40 to 800), in small batches of from 15 to 500.
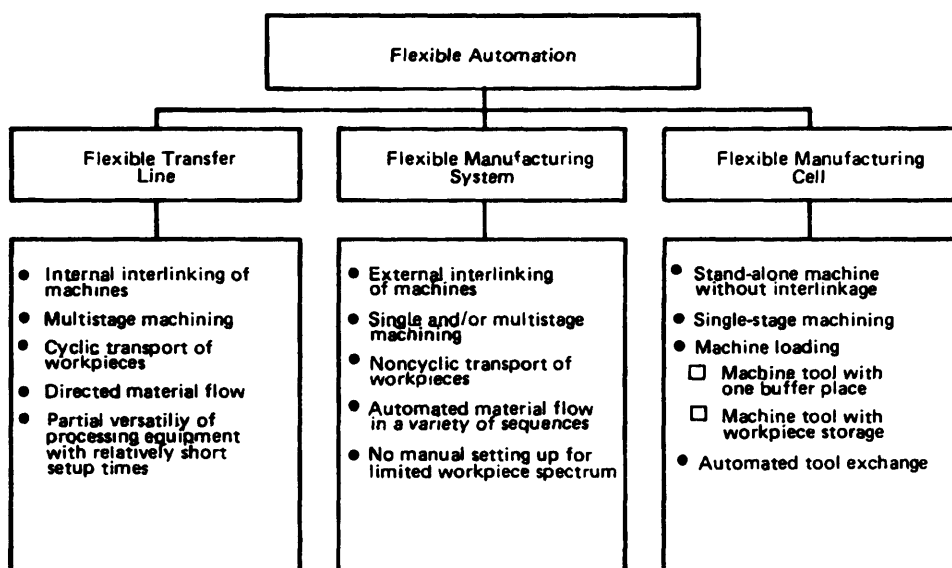
Figure 11.9 Variants of the FMS concept. (Adapted from Spur and Mertins [9].)
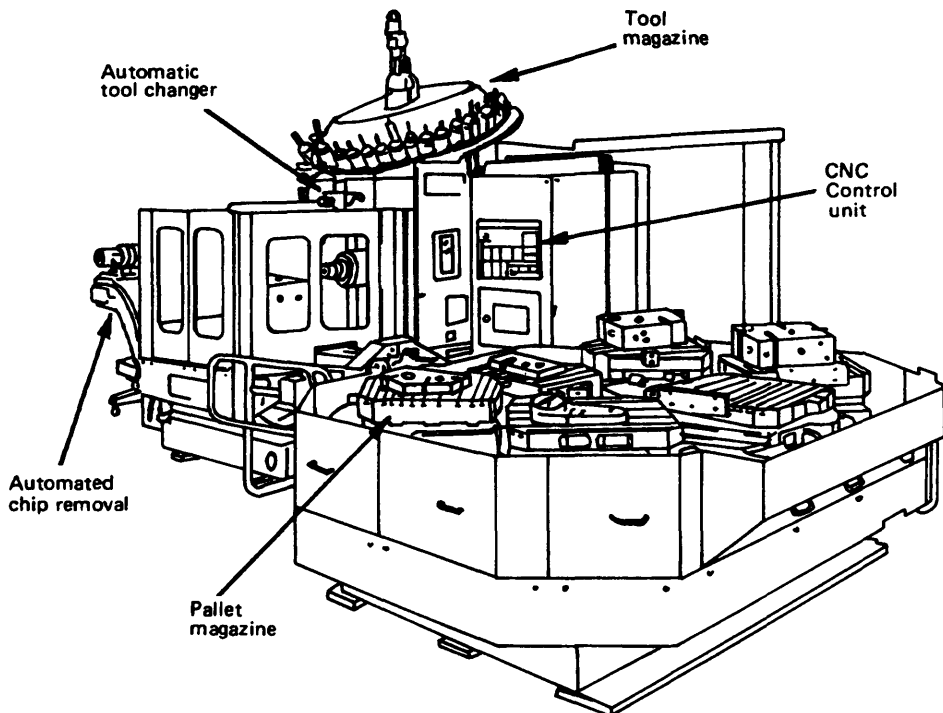
Figure 11.10 Typical machining center designed for unmanned operation with pallet and tool magazines and CNC controller able to communicate with host computers.

2. *Flexible transfer lines (FTLs)*. These systems consist of a number of NC or head-changeable machine tools connected by automatic material transfer systems. The system can machine different components but without flexible routing of the workpieces. The family of components is relatively small (<20) and the components must be quite similar to one another, as the overall flexibility of the system is too low for a larger variety to be accommodated. In consequence, the work cycles at each station must be quite well balanced. Figure 11.11 shows a typical system of this type. Production quantities must be quite large for economic use of these system (1500 to 15,000 per annum for each component).

3. *Flexible manufacturing systems (FMSs)*. In these systems NC workstations are linked by automatic workpiece transfer and handling, with flexible routing and automatic workpiece loading and unloading. Machining times at each station can differ considerably. The number of dif-
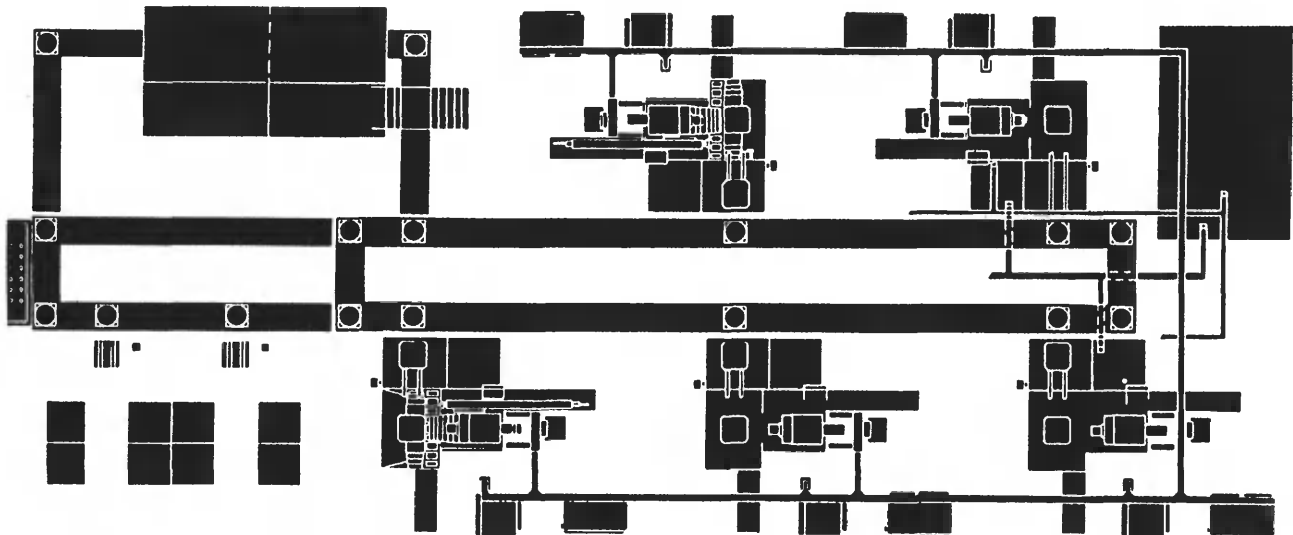
Figure 11.11 Flexible transfer line. (From Popplewell and Schmoll [10].)

ferent components that can be processed by these systems is from 10 to 150 in general and moderate quantities can be produced (15 to 500 components per annum for type).

11.10.1   Machine Tools in FMSs

The majority of FMSs developed have been for the processing of prismatic components [8], with a smaller number for rotational components. The most common machine tool type included in these systems is the horizontal-spindle machining center, but head-changing or head-indexing machines are also frequently used [11]. The latter machines are used for the drilling, tapping, and so on, of multiple holes, and operate using multispindle heads capable of processing several holes simultaneously. Separate heads are required for each workpiece processed.

The choice of machine tools for a FMS is influenced by a number of factors, but above all should be based on a detailed analysis of the family of components to be processed. Some of these factors are illustrated in Fig. 11.12 [11]. The flexibility of the system is increased by using horizontal machining centers with high-capacity tool magazines, as these are able to process a wide variety of components without modification. Flexibility is also increased by having several identical machine tools in the system, as this increases the availability of machine tools on which to process a particular component at any given time. Machining centers are relatively inefficient for the machining large numbers of holes, since only one tool can be used at a time. Consequently, head-changing or head-indexing machines may be introduced to improve productivity if numerous holes must be machined. However, the overall flexibility of the system is thereby reduced, as these machines are suitable for only a relatively small variety of components. A requirement for high precision would also dictate the inclusion of a precision boring machine in the system.

11.10.2   Work Handling for FMSs

Workpieces are usually mounted on standard pallets for processing in FMSs and these pallets locate automatically at each workstation in the system. A variety of work-handling devices are used to transport parts, pallets, and tools around the system. Some of these are as follows:

1. *Tow carts:* These are the most common devices used; they consist of a simple platform on castors and are towed around the system by engagement with underfloor, continuously moving chains. Carts stop at workstations by means of a mechanism that releases the tow pin at the appropriate time. Branches and loops are controlled in a similar manner to railway systems. The main advantage of tow carts is their simplicity and

Machine alternatives

General comments   Main component influence

| First choice for flexibility | Horizontal machining center | Suitable for large variety |

| Improved production rate for hole patterns, improved precision for bores | Head indexer | Limited variety, hole and bore patterns |
| | Head changer | Large variety, hole and bore patterns |

| Limited flexibility | Vertical turret lathe | Significant larger bores to be machined |

| Specialized System | Vertical gantry type, machining center | Large components with surface machining |

| Rarely used within system | Specialized machines | Incorporated to meet particular requirements |

Figure 11.12 Factors affecting machine tool selection for FMS. (From Hannam [11].)

low cost, since no on-board power is required for their movement or control. Facilities must be available at each workstation to load and unload pallets from the carts. Also, the circulation of carts must be undirectional.

2. *Automatic guided vehicles (AGVs)*. These devices are usually designed to follow wires buried in the floor of the plant or lines painted on the floor. On-board power and control is required for both movement and steering and for the handling of pallets. Automatic guided vehicles are more expensive than tow carts and are both larger and heavier. The main advantage of AGVs is their greater flexibility of operation. These devices may move in either direction, but for ease of control, circulation is usually restricted to one direction only in practice.

3. *Rail carts:* These carts move on rails and are generally restricted to backward and forward motion along straight tracks. Power and control instructions are transferred by overhead conductors or extra rails. Rail carts often accommodate two pallets to allow for pallet exchange at the system workstations.

4. *Roller conveyors:* Most of the early FMS developments utilized powered-roller conveyors for moving workpieces from station to station. The use of these conveyors in modern systems is less common. Roller conveyors are expensive to install and occupy valuable floor space. In addition, these conveyors are relatively inflexible in operation and difficult to alter if the overall system is expanded.

5. *Industrial robots:* Robots are used in FMSs but not extensively unless the cell consists of only a few machines. They may be used as secondary handling devices, particularly for turned workpieces, which may be transported around the system in batches on pallets by other handling devices and then transferred to the machine tool by robots at each workstation. Gripper designs suitable for handling a wide variety of components are important in this case.

11.10.3 Layouts for FMSs

A variety of different layouts for the machine tools in FMSs have been adopted. The choice depends on the scope of the system and the type of handling devices used for transporting workpieces from workstation to workstation. The use of rail carts mean that a straight track must be used, with machines located at the side of the track. Figure 11.13 shows the layout of a typical rail-cart-based system. Early systems using roller conveyors usually employed a simple loop configuration, with branches to the workstations.

The increased use of tow carts and AGVs has resulted in more complex multiloop or tree-type layouts being used. The latter type is most suitable for AGVs and is particularly useful if expansion of the system with additional workstations is anticipated. Figure 11.14 shows a typical multiloop layout using tow carts, and Fig. 11.15 shows a typical layout where AGVs are used for work handling.

11.10.4 Tooling in FMSs

The need for large numbers of tools in a FMS tends to restrict flexibility. Sufficient tools must be available to process all the component types. As explained earlier, overall flexibility can be increased by installing several machine tools of the same type, but if any component can be processed on any of these machines, this means that all the required tools must be available on all the machines. This leads to the requirement for very large
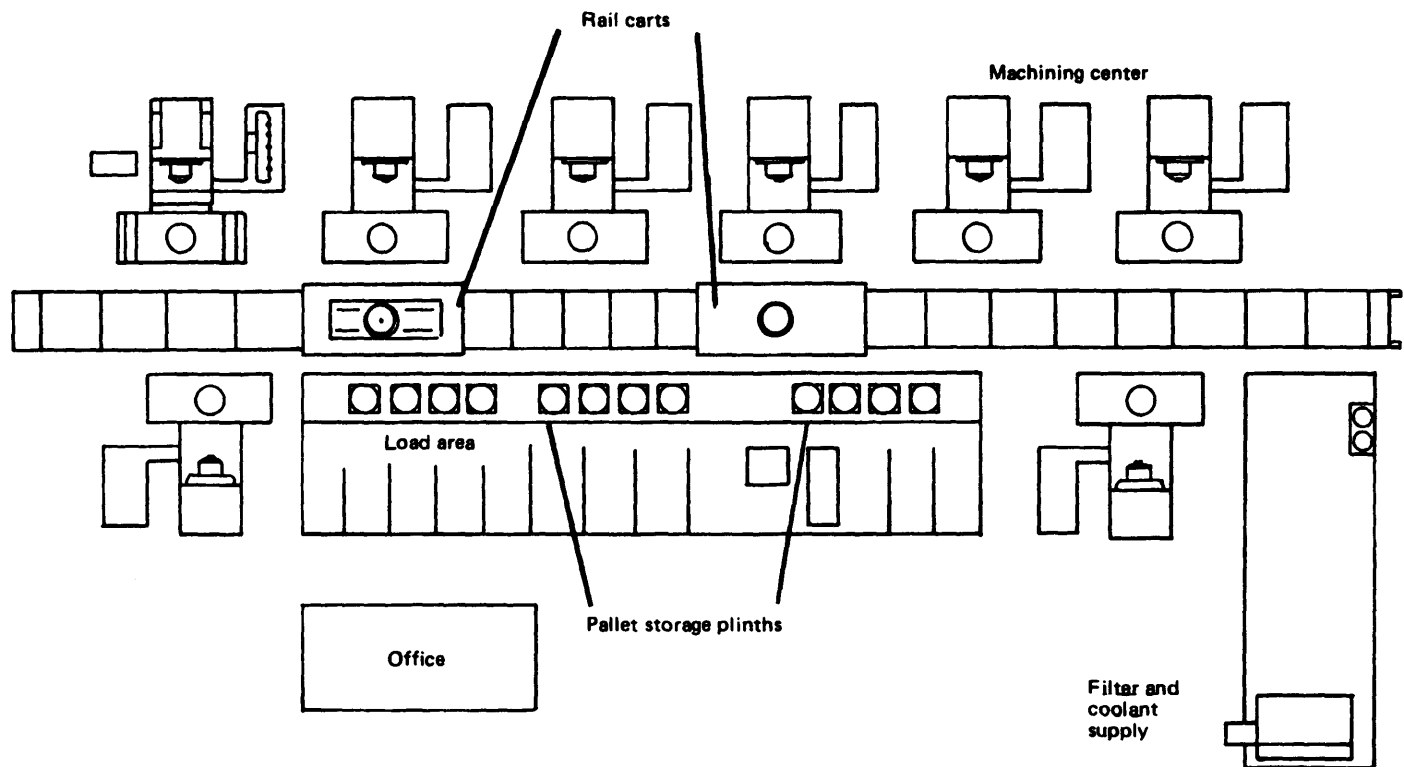
Figure 11.13 In-line rail-cart layout with eight horizontal machining centers and a load/unload area alongside the track. (From Hannam [11].)
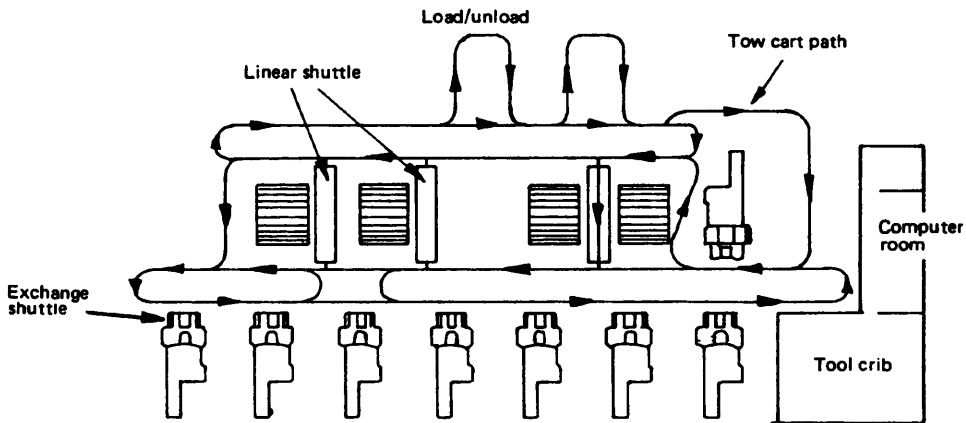
Figure 11.14 Typical tow-cart layout with eight horizontal machining centers and four head changers. (From Hannam [11].)

capacity tool magazines capable of accommodating up to 250 tools or more on each machine. Without such high tool capacity other solutions must be adopted that tend to reduce the overall flexibility of the system. These solutions include:

1. Dedication of some machines to a restricted range of components
2. Restricted times for processing subgroups of components, with the tooling in the system changed within the allowed time.

Long-term solutions may require a means of automatically changing the tools available in the system, but this results in considerable additional capital expenditure and development costs. Approaches being adopted include:

1. Interchangeable tool magazine carousels
2. Automated tool transfer from fixed to moving carousels at each workstation
3. Automatic handling of tools and components individually, and supplying these together at each workstation.

11.10.5 Pallets and Fixtures for FMSs

The pallets used to transport workpieces around FMSs are precision items and represent a significant capital investment. The pallets usually require some form of fixturing for locating and holding the workpiece. This leads to a requirement for multiple identical fixtures if several
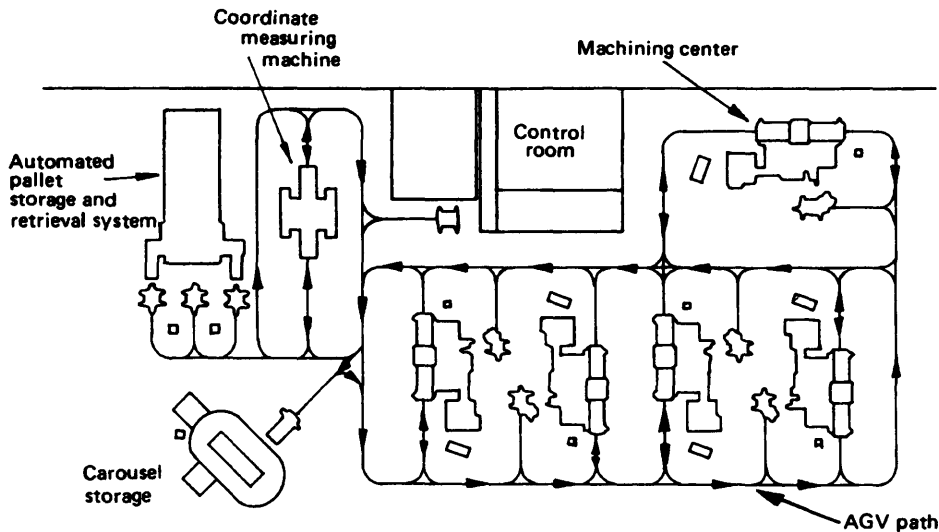
Figure 11.15 A typical automatic guided-vehicle layout with five horizontal machining centers, a coordinate measuring machine, automatic pallet storage and retrieval system, and carousel storage. (From Hannam [11].)

workpieces of the same configuration are to be processed at the same time. In conventional batch production only one fixture item is generally required for each machine tool. This leads to the need for forms of flexible fixturing that can be readily rebuilt or adapted to the range of workpieces being processed by FMS.

PROBLEMS

1. A rotary-transfer machine is designed to drill six 25-mm-diameter holes in a workpiece. At the feed employed it requires 1000 revolutions of a drill to complete the operation. Each drill costs \$6.00 and can be reground on average 10 times at a cost of \$2.00. The time taken to remove and replace each drill is 100 s. If the total machine rate including the operator and overheads is \$0.012/s, the indexing time is 3 s, and the time for advance and withdrawal of the tools is 5 s, estimate the minimum cost of production for each component and the corresponding production time. (Assume that the Tayor tool-life relation for the high-speed steel drill is

$$v \cdot t^{0.125} = 2.65$$

where v is the cutting speed, in meters per second (m/s), and t is the tool life, in seconds (s).

2. A numerically controlled milling machine has a linear interpolating control system for continuous contouring that will accept information from a punched tape prepared by the programmer. The programming time for this system is estimated to be 600 s per change point and the hourly charges of the programmer are $0.00139/s including overheads. The job under consideration has 20 change points and the total distance of cutter travel is 1.02 m. The appropriate feed speed for the particular cutter and work material is 1 mm/s and the total set-up time for each component is 300 s. If the total machine rate is $0.0033/s including operator costs and overheads, what minimum batch size is required for economic use of the numerically controlled machine tool? (Assume that on a hand-operated milling machine the set-up time and machine time per component are 300 s and 2.7 ks, respectively, and that the total machine rate is $0.00278/s.)

REFERENCES

1. Gallagher, C. C., and W. A. Knight: *Group Technology Production Methods in Manufacture,* Ellis Horwood, Ltd., Chichester, England, 1986.
2. Koenigsberger, F., and A. E. De Barr: *The Selection of Machine Tools,* Institution of Production Engineers, London, 1979.
3. Engleberger, J. F.: *Robotics in Practice,* Kogen-Page, London, 1980.
4. Department of Industry: *A Human Guide to Robots,* Her Majesty's Stationery Office, United Kingdom, p. 18, 1980.
5. Ohmi, T., Y. Ito, and Y. Yoshida: Flexible Manufacturing Systems in Japan— Present Status, Proc. 1st International Conference on Flexible Manufacturing Systems, p. 23, Brighton, U.K., Oct 20–22 1982.
6. Ranky, P. C.: *Computer Integrated Manufacturing,* Prentice-Hall, Englewood Cliffs, N.J., 1986.
7. Hitomi, K.: *Manufacturing Systems Engineering,* Taylor and Francis, London. 1979.
8. Steinhilper, R.: Step-by-Step Access to Flexible Automation in Manufacturing, Proc. 2nd European Conference on Automated Manufacturing, Birmingham, p. 299, 1983.
9. Spur, G., and K. Mertins: Flexible Manufacturing Systems in Germany; Conditions and Development Trends, Proc. 1st International Conference on Flexible Manufacturing Systems, p. 37, Brighton, U.K., Oct 20–22 1982.
10. Popplewell, F., and P. Schmoll: The Road to FMS, Proc. 1st International Conference on Flexible Manufacturing Systems, p. 501, Brighton, U.K., Oct 20–22 1982.
11. Hannam, R. G.: Alternatives in the Design of Flexible Manufacturing Systems for Prismatic Parts, *Proc. Inst. Mech. Eng.,* vol. 198, no. 82, p. 111, 1985.

12
Computer-Aided Manufacturing

12.1 INTRODUCTION

Computers are used extensively in the scientific and commercial fields. Recent developments in microelectronics have led to computer systems that combine high computing power with high reliability, small size, and low cost, making their use viable in increasing ranges of applications. These computer developments have made possible the rapid performance of tasks that are complicated and time-consuming to do manually. Computers can be programmed to carry out complex calculations and to process and store large amounts of data with high speed and efficiency. As a result, computers are being used increasingly in both design and manufacture, leading to the concepts of computer-aided design (CAD) and computer-aided manufacture (CAM) or CAD/CAM for short. The objective is to increase the efficiency of all aspects of design and manufacture and to integrate these activities by means of shared data bases, together with automatic data transfer between the various design and planning activities to be carried out. In this chapter only those aspects of CAD/CAM concerned with the technological aspects of machine tool application are considered in detail; in particular, process planning and numerical control (NC) programming applications are discussed. Details of other CAD/

353

CAM applications can be found in a variety of publications [1–3]. Before proceeding with details of computer-aided process planning and NC processing systems, an outline of the scope of CAD/CAM applications will be given.

12.2   SCOPE OF CAD/CAM

Computer-aided design is the use of computer systems to facilitate the creation, modification, analysis, and optimization of a design [1]. In this context the term *computer system* means a combination of hardware and software. Computer-aided manufacturing is the use of a computer system to plan, manage, and control the operation of a manufacturing plant. An appreciation of the scope of CAD/CAM can be obtained by considering the stages that must be completed in the design and manufacture of a product, as illustrated by the product cycle shown in Fig. 12.1. The inner loop of this figure includes the various steps in the product cycle and the outer loop shows some of the functions of CAD/CAM superimposed on the product cycle.

Based on market and customer requirements, a product is conceived, which may well be a modification of previous products. This product is then designed in detail, including any required design analysis, and drawings and parts lists are prepared. Subsequently, the various components and assemblies are planned for production, which involves the selection of sequences of processes and machine tools and the estimation of cycle times, together with the determination of process parameters, such as feeds and speeds. When the product is in production, scheduling and control of manufacture take place, and the order and timing of each manufacturing step for each component and assembly is determined to meet an overall manufacturing schedule. The actual manufacturing and control of product quality then takes place according to the schedule and the final products are delivered to the customers.

Computer-based procedures have been or are being developed to facilitate each of these stages in the product cycle, and these are shown in the outer loop of Fig. 12.1. Computer-aided design and drafting techniques have been developed. These allow a geometric model of the product and its components to be created in the computer. This model can then be analyzed using specialized software packages, such as those for finite element stress analysis, mechanisms design, and so on. Subsequently, drawings and parts lists can be produced with computer-aided drafting software and plotters. Computer-aided process-planning systems, including the preparation of NC programs, are available that produce work plans, estimates, and manufacturing instructions automatically from geometric descriptions of the components and assemblies.
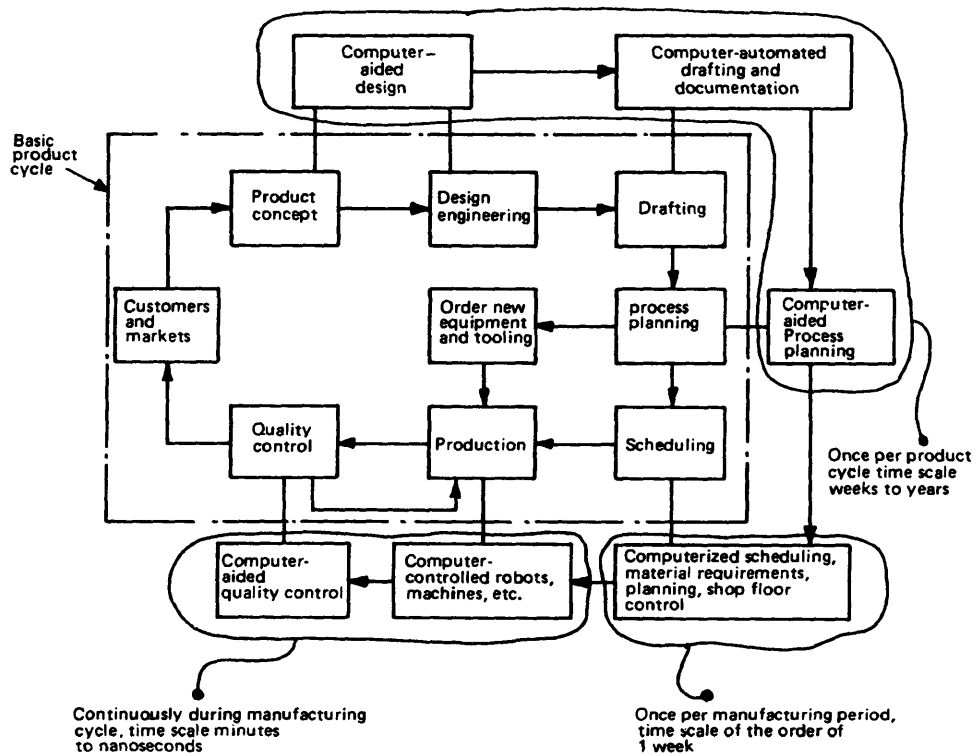
Figure 12.1 Product cycle with computer-aided procedures superimposed. (Adapted from Groover and Zimmers [1].)

For scheduling and production control, large amounts of data and numerous relatively simple calculations must be carried out. One example is the determination of order quantities by subtracting stock levels from forecasts of the number of items required during a particular manufacturing period. Many commercial software packages are available for scheduling, inventory control, and shop floor control, including materials requirements planning (MRP) systems [2]. At the shop-floor level computers are used extensively for the control and monitoring of individual machines (see the description of CNC machines in Chap. 11).

There is a difference in the time scale required for processing data and the issuing of instructions for these various applications of computers in the product cycle. For example, design and process-planning functions are carried out once for each new product and the time scale required is on the order of weeks to years for the completion of the whole task. Scheduling and production control tasks will be repeated once every production

period (usually one week) throughout the year. At the machine-control level instructions must be issued continually with a time scale of micro- or nanoseconds in many cases.

One of the major objectives of CAM is the integration of the various activities in the product cycle into one unified system, in which data is transferred from one function to another automatically. This leads to the concept of computer-integrated manufacture (CIM), with the final objective being the "paperless" factory. Several developments have taken place, but no totally integrated CIM systems have yet been achieved. Since the design and process-planning functions are carried out once in the product cycle, these are the most suitable functions for integration. This integration is particularly desirable because the geometric data generated during the design process is one of the basic inputs used by process planning when determining appropriate manufacturing sequences and work plans. Consequently, various activities in design and process planning can share a common design and manufacturing data base, as illustrated in Fig. 12.2. With such a system, geometric models of the products and components are created during the design process. This data is then accessed by various downstream activities, including NC programming, process planning, and robot programming. The programs and work plans generated by these activities are also added to the data base. Production control and inventory control programs can then access the work plans, time estimates, and parts lists (bill of materials file), in preparing the manufacturing schedules, for example.

12.3 PROCESS-PLANNING TASKS

Process planning has been defined by the Society of Manufacturing Engineers as "the systematic determination of the methods by which a product is to be manufactured, economically and competitively." Process plans are used to specify the sequence of production operations and the required tools and facilities that transform raw stock into finished parts. Process planning requires detailed knowledge of both the manufacturing processes available (e.g., machining, forming) and the production capabilities of the specific plant in which the parts are to be manufactured.

Figure 12.3 shows the sequence of steps in the design and planning for manufacture of a product and its component parts. The first three steps are concerned with the design of the items to be produced, and CAD systems are aimed at increasing the efficiency of these tasks. In manual systems the output of these stages is in the form of component and assembly drawings, specifications, and parts lists. In integrated computer-based systems, this information is stored in a common data base which includes geometric modeling information and a bill of materials (BOM) files.
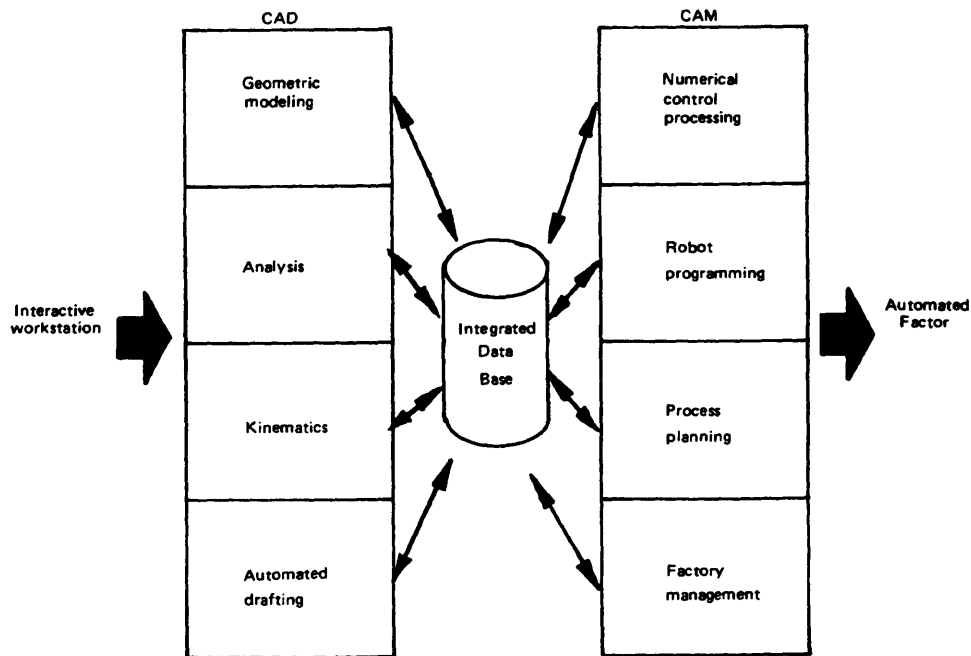
Figure 12.2   Integrated design and manufacturing data base. (From Knox [2].)

Steps 4 to 9 in Fig. 12.3 describe the main steps required in process planning. The process planner converts the geometric information (drawings) about the items to be manufactured into appropriate sequences of manufacturing operations and determines the processing parameters (e.g., feeds and speeds) for each operation, taking into consideration the part geometry, material, and quantities required. The first stage is to determine the operation sequence in general terms, followed by the selection of the machines for each operation. It is at this stage that the level of automation of the machines will be determined and, as explained in Chap. 11, this will be largely based on estimates of the quantities required for the product.

Steps 6 to 9 are concerned with the detailed planning of each operation on each machine and include the selection of work-holding methods, sequences of operations and tools and finally the determination of cutting data such as feeds and speeds, together with estimates of cycle times. At this stage the machinability of the material and economics of the process must be considered in determining the most appropriate cutting parameters. The output at step 9 is in the form of detailed work plans, which list all operations to be carried out in sequence, together with the processing

		Idea	
1	Product conception		Computer-Aided Design
2	Calculation	$f = \dfrac{pl^3}{48EI}$	
3	Design		
4	Machining sequence	Saw Turn Mill	
5	Sequence of machines		
6	Clamping device		
7	Sequence of operations		
8	Tool selection		
9	Cutting data	Speed Dia	
10	Tool paths		Computer-Aided Process Planning
11	Tool location		
12	Tool setting distance and collision checks		
13	Postprocessing		
14	Machining		

Figure 12.3   Stages in design and process planning.

parameters and operation times. Computer-aided process-planning systems have been or are being developed to deal with most of the steps 4 to 9 in Fig. 12.3.

For NC machines further steps are necessary to determine the tool paths necessary to machine the objects and to prepare the programs that drive the machines. Many computer-aided programming systems for NC machines have been developed. Initially these systems dealt mainly with the geometric calculations required to determine tool paths to machine the workpiece, but increasingly the automatic selection of tools and cutting conditions are determined by these systems, so that steps 7 to 9 in Fig. 12.3 are also incorporated into the programs.

For manual process planning, engineering part drawings are examined to develop manufacturing process plans and instructions. The process relies to a great extent on experienced planners to develop economical and feasible plans. The process planner must manage and retrieve a great deal of data and many documents, including established standards, machinability data, machine specifications, tooling inventories, stock availability, and existing process plans. Thus, process planning is an information-processing task to which the computer is well suited. In addition, because process planning involves many interrelated activities, determining the most appropriate plan for a particular case may require several iterations. The use of the computer enables alternatives to be readily explored. Another advantage of computer-aided process planning is greater consistency in the plans determined. This is a particularly important feature because the process-planning task involves the interpretation of the design features of a component to meet its manufacturing requirements. It is well known that in most companies a variety of different sequences exist for basically similar parts [4,5] and these have been generated by different process planners at different times. Similarly, giving the same component to several different planners will usually result in several different work plans being determined, dependent on the experience and choice of the individual planners [5].

Process planning is not an easy task to computerize because it is not an activity that can easily be flow-charted. The planner must consider many parameters simultaneously and make involved and detailed decisions that are difficult to structure in an ordered manner. Ideally the computer-aided process-planning system should follow the planning logic of an experienced planner.

12.4 COMPUTER-AIDED PROCESS PLANNING

Computer-aided process planning systems are aimed at carrying out the planning tasks outlined above and shown in Fig. 12.3. Two basic ap-

proaches to computer-aided systems for work planning have evolved: (1) the variant or retrieval approach and (2) the generative approach [4,6].

The variant approach utilizes the principles of Group Technology [6], and work plans are based on families of similar parts. In this manner the plan for a new part can be obtained more or less automatically from relatively small amounts of input data and with little interaction by the user of the system. Such systems are generally very efficient, but it may not be possible to develop systems using this approach for the whole range of parts to be processed.

The variant approach is an extension of manual planning. Plans for new parts are developed through recalling, identifying, and retrieving existing plans for similar parts and making necessary modifications. In some variant systems, standard plans for each family of parts are developed and filed using code numbers based on group technology principles. Upon entering the code number for a proposed new part, the standard plan for the family is retrieved to be either used or modified. A great deal of preliminary work is necessary to establish the standard plans, categorize the family of parts groupings, and establish the classification and coding systems. The computer, acting much like a word processor, then helps to assemble and edit appropriate plans for a new part. During the planning stage, various subroutines or canned programs can be called up to help the planner with the many decisions that must be made, generally in an interactive, conversational mode at a computer terminal. A number of variant or retrieval planning systems have been developed, including that prepared for CAM-I [7], as illustrated in Fig. 12.4. A similar system, based on the storage, retrieval, and editing of work plans for similar parts, identified by a classification system, has been developed by the Organization for Industrial Research and is shown in Fig. 12.5 [8].

Generative process-planning systems attempt to synthesize a unique plan for each individual part from general-purpose procedures, algorithms, and stored manufacturing knowledge, that define the various technological decisions that must be made. For truly generative systems, the sequence of operations as well as the process parameters are established without reference to previous work plans stored in the system. The system synthesizes or generates a specific process plan for a specific part, and relies on sophisticated decision algorithms, part data, and the specific manufacturing capabilities available. From an input of the component geometry, decision algorithms identify geometric features and the specific processes required to produce them.

Ideally this approach would allow a planner to present any part to the system and receive a complete, automatically determined plan. Processes would be selected, machine tools specified, processing sequences es-
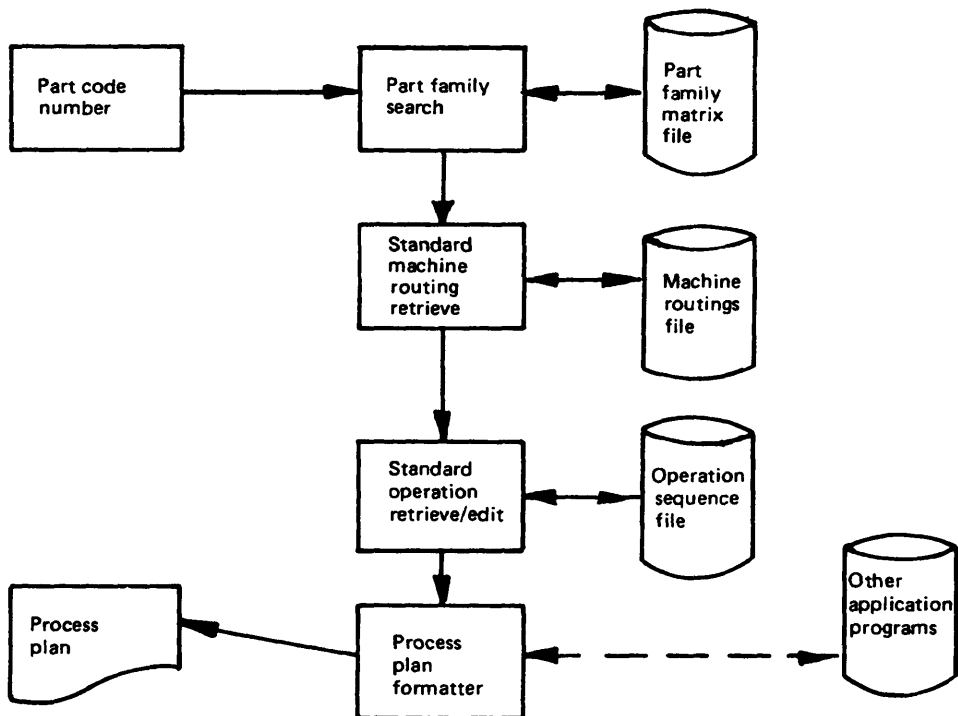
Figure 12.4 Retrieval process-planning system. (From Link [7].)

tablished, and process parameters determined. However, the decision logic for such systems is complex; it varies from industry to industry and company to company, and often process parameters need to be adjusted interactively to suit particular cases. Although considerable progress has been made in the development of generative process-planning systems, they are still in the early stages of development and use. Current systems tend to be restricted to specific operations or a particular type of manufacturing process (e.g., for rotational machined components) and still require considerable interaction by the user in selecting the appropriate sequences. This will probably be the case for some time to come, although considerable development work is in progress.

Several generative process-planning systems are available but these are generally restricted to limited ranges of component types or processes. Many of the developed systems are able to handle only the machining of rotational parts [9]. As an example, the AUTAP system, developed at the University of Aachen, is able to process operation plans only for rota-
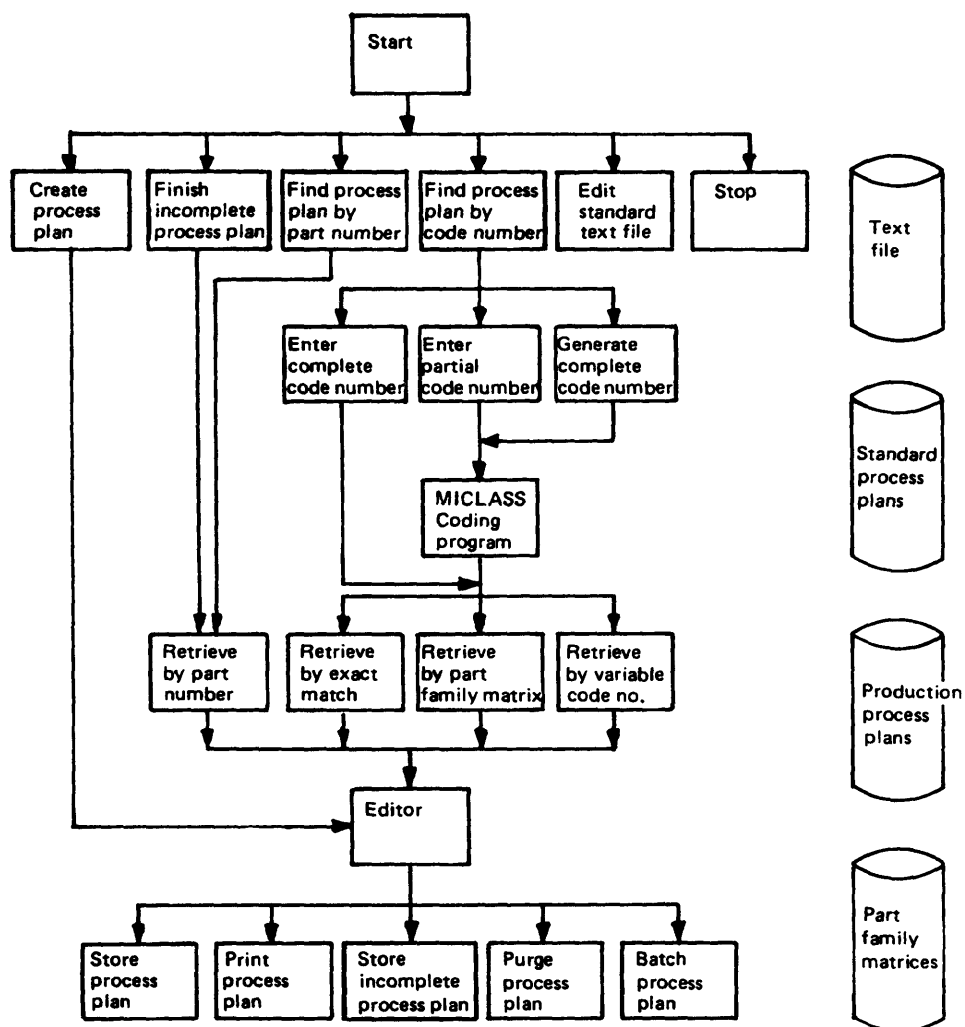
Figure 12.5   Retrieval or variant process-planning system. (From Houtzeel [8].)

tional parts and simple sheet metal parts. The general structure of the AUTAP system is shown in Fig. 12.6. The workpiece geometry is defined in terms of individual shape elements, which have associated manufacturing operations and sequences. On the basis of the individual elements present in the workpiece, the overall machining sequence is determined, and this is followed by the calculation of machining and set-up times for the individual operations. The final stage is to determine the quality control and inspection processes, followed by issuing the operation plan. This basic approach has been extended to prismatic parts in a separate system [10]. The overall structure of this latter system is shown in Fig. 12.7. Again the basic description of the component is in terms of detailed shape elements, which have an associated manufacturing sequence. The relationship between the shape features and associated processing sequences is illustrated in Fig. 12.8. The geometric description must follow a prescribed sequence, in which the overall shape is defined first, followed by the secondary shape features. Combination of the processes associated with each shape element can result in several alternative overall sequences from which the most economic is selected.

As explained previously, the development of computer-aided process-planning systems for widespread application is difficult, mainly because the planning decision logic varies from industry to industry, company to company, and so on. In addition, heavy reliance on experienced planners in determining suitable process plans is frequently required. For these reasons, recent concentration has been on applying expert systems programming methods to process planning. This approach is attractive because in expert systems the manufacturing decision rules can be isolated in a knowledge base, rather than incorporated into complex algorithms. It is then possible to alter and add to the rule base, without altering the inference logic of the system. Thus, the overall system should be readily adaptable to different manufacturing environments.

12.5 PROCESSING OF NC PROGRAMS

Numerical control programming is a specialized work planning process, as the programmer must make similar decisions and use similar information to that the process planner works with but with the additional complication that such work as the detailed geometric calculation of tool paths must be done. Numerical control machines may be programmed by manual methods, using the basic instruction set of the machine controller or a computer-aided NC processing system. Both methods require a good deal of skill and experience on the part of the programmer. Many computer NC processing systems have been developed, and the most widely
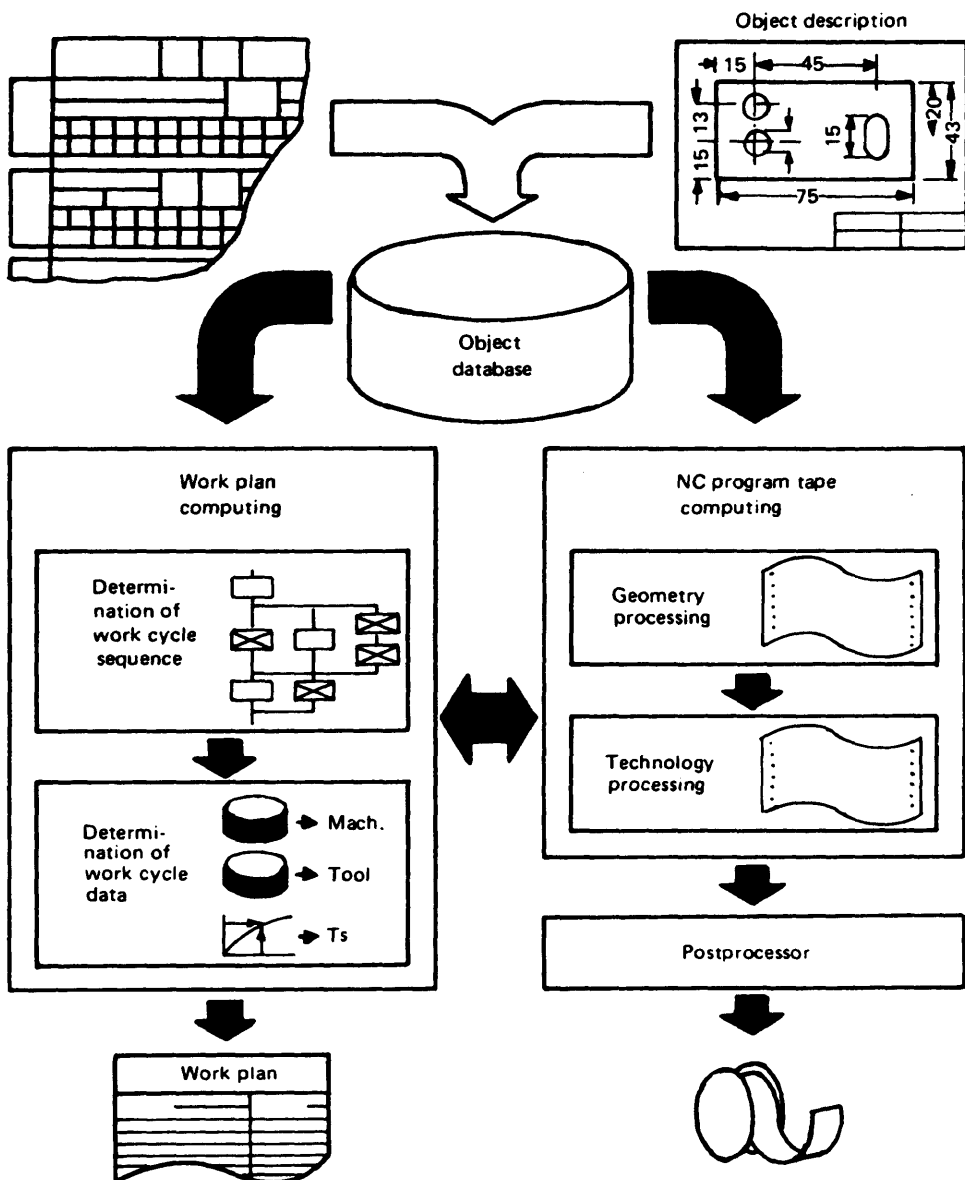
Figure 12.6 Basic structure of the AUTAP process-planning systems. (From Spur and Krause [10].)
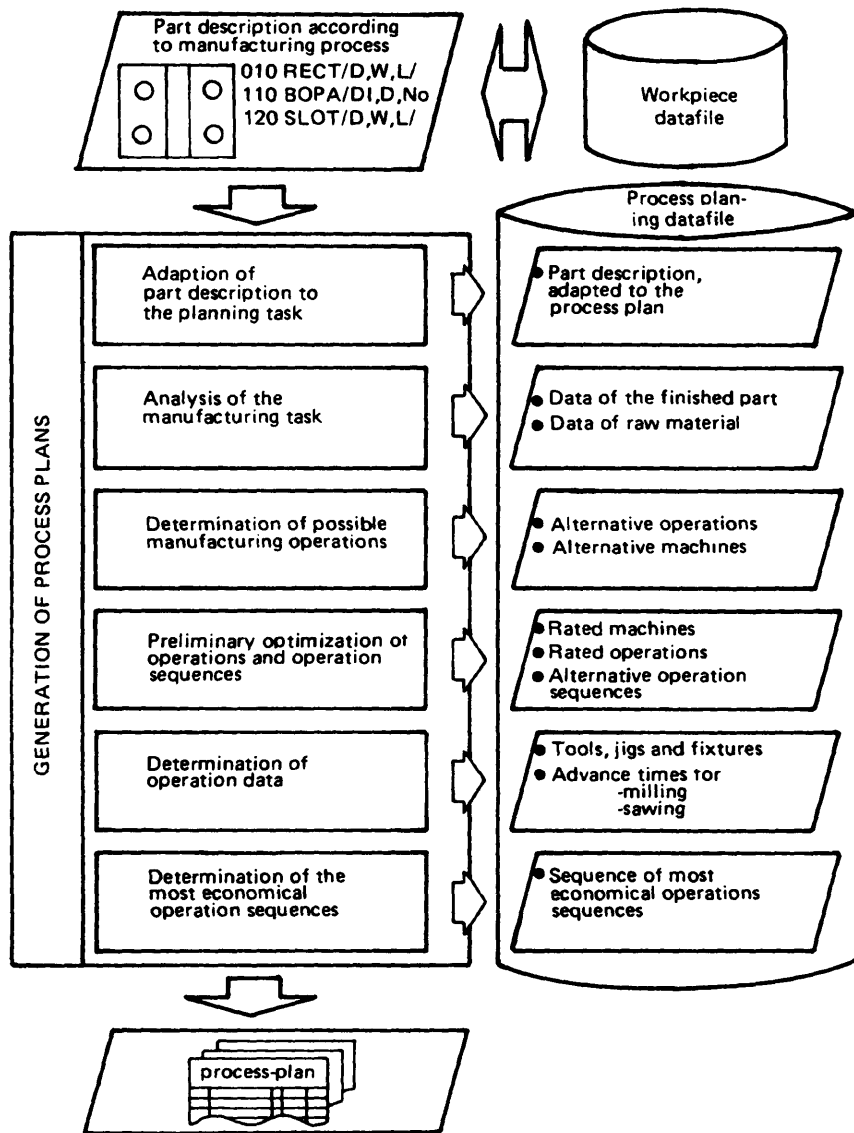
Figure 12.7   Basic structure of process-planning system for prismatic parts. (From Eversheim [11].)
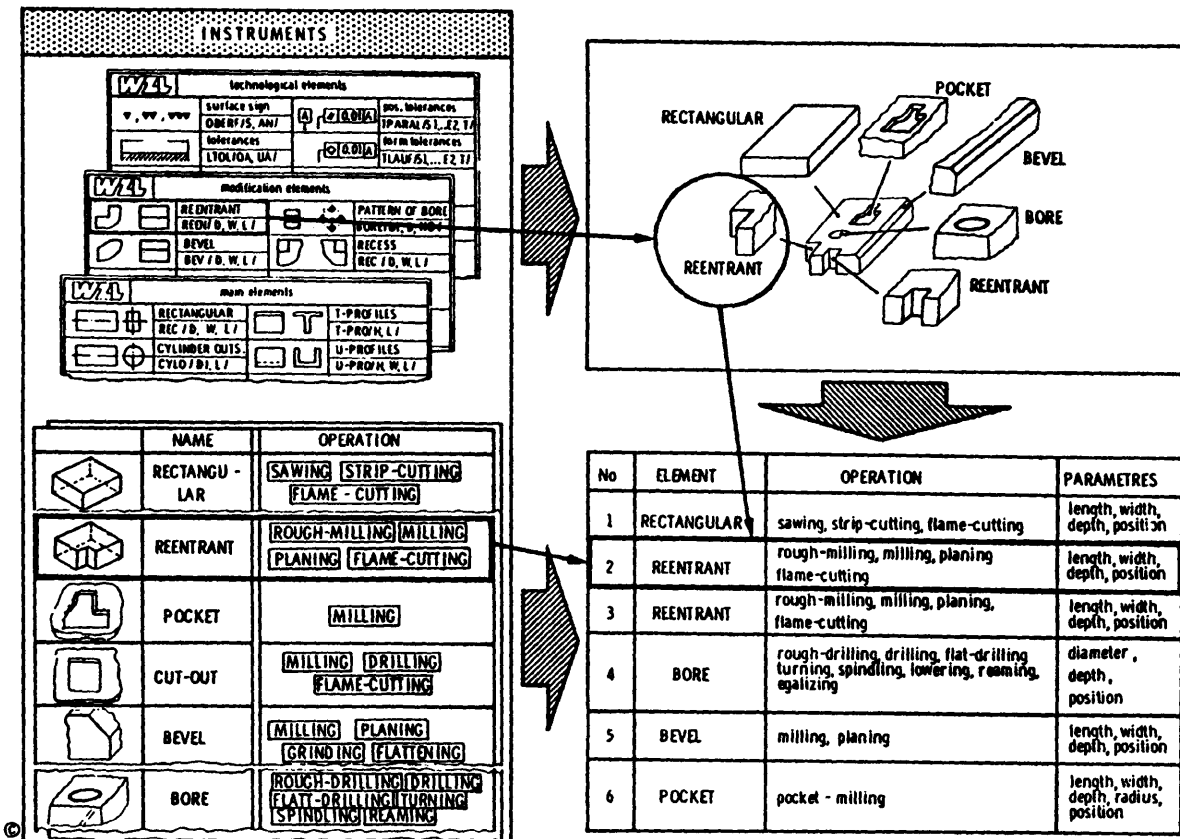
Figure 12.8 Relationship between shape functions and operation sequences for process planning. (From Eversheim [11].)

used are based on the language structure of the APT system [11]. With such systems the geometry of the part and tool motions is described by the programmer in the language of the system, and then the tool paths, and similar calculations, are determined by the processing system. Although simpler than manual programming for all but simple parts, NC processing systems still require significant experience and effort to use effectively.

The programming of NC machines involves the following tasks. (Fig. 12.3):

1. Determination of the sequence of operations required to machine the workpiece. This involves examining the shape features of the component to be produced and selecting the sequence of machining operations to produce these features.
2. Choice of cutting tools and order of use, corresponding to the sequence of operations.
3. Determination of feeds and cutting speeds for each operation. The appropriate values of feed and speed are dependent on the materials of the workpiece and of the selected cutting tools and can be selected using the economic models described in Chap. 8.
4. Determination of tool path coordinates, including both cutting and rapid traverse motions, taking into account possible collisions as with clamps. Tool path coordinates are offset from the surface of the workpiece, so that when the paths are followed, the correct size and shape of the workpiece is produced. This is necessary because the program point of the tool does not correspond to the point of contact between the tool and workpiece. Figure 12.9 shows the program point, that is, the point that traces out the tool path, for end milling cutters and lathe tools. For all but simple components, determination of the tool path coordinates involves time-consuming, repetitive, and often difficult geometric calculations.
5. Setting of program auxiliary functions, including tool changes, spindle starts and stops, coolant flow on and off, and so on.

To accomplish these tasks the following information sources are used:

1. Drawings of the component
2. Data on machine tool capabilities
3. Catalogs of machinability data for materials, recommended feeds, and cutting speeds
4. Catalogs of available cutting tools, which should be standardized as much as possible
5. Standard geometric formulas.
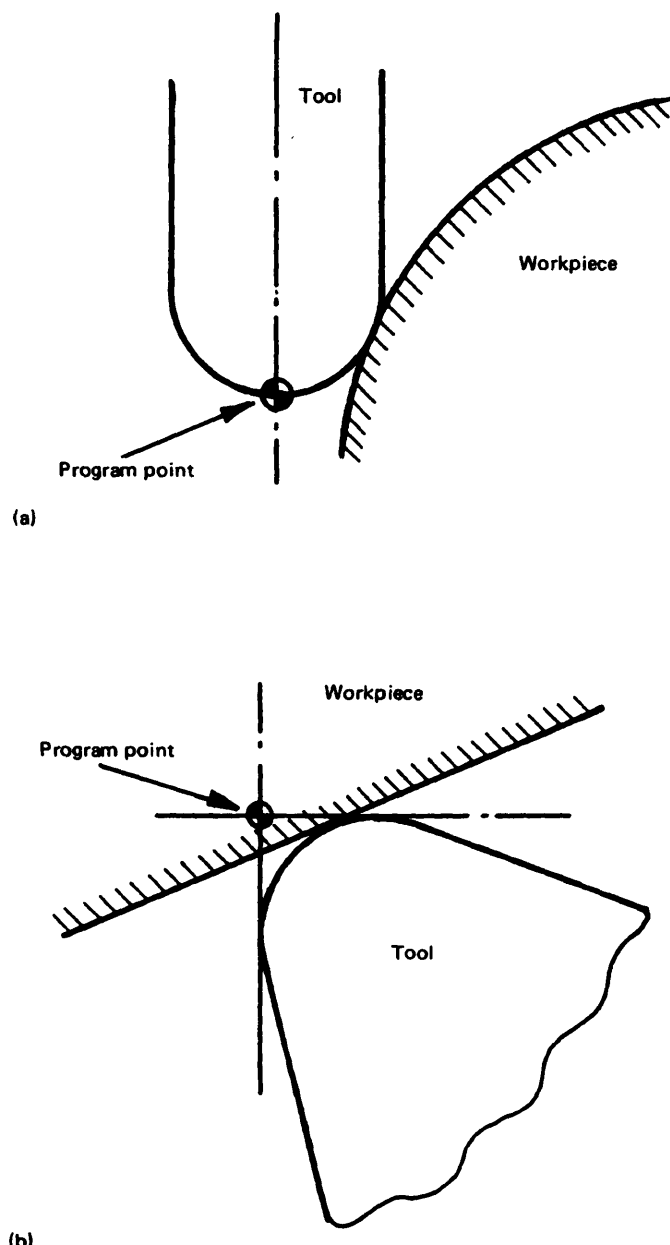
Figure 12.9 Tool program points for tool path determination. (a) Ball-ended milling cutter; (b) lathe tool. The program point sweeps out the offset tool path.

12.6 MANUAL PROGRAMMING OF NC MACHINES

Numerical control machines are programmed by means of a series of coded instructions, commonly entered into the controller using punched paper tape. The format of the basic instructions is now largely standardized and modern controllers utilize what is known as a word address format [12]. Older machines may use other tape code formats but these will not be described here.

Each set of instruction codes that the machine acts upon is called a NC block and is terminated on the tape by means of an end of block character (eob), which corresponds to the carriage return, line feed character of a teletype machine. The NC machine acts upon each block of coded instructions in turn. A typical block of instruction is of the following form:

n001 g80 x 07500 y 06500 z 100 f612 s16 t001 m03 eob

The individual instructions are conventionally entered in this order, but with word address format any order can be used, except for the first item (n001). This is because earlier controllers required the codes to be entered in a specified order. Each instruction consists of a letter code, which tells the controller the type of data to follow and indicates the address to which this data is to go, hence the term *word address format*. The explanations of each word or code type are as follows:

1. *Sequence number (n-codes):* This is an identification number for each block of instructions and increases sequentially through the program.

2. *Preparatory function (g-codes):* These instructions tell the controller what type of motion or action is to be carried out. These codes are largely standardized and Table 12.1 shows a typical list. An example of a preparatory function is g02, which indicates that the next motion will be circular interpolation in a clockwise direction. Many of the preparatory functions can indicate what are called canned cycles, as explained in more detail later.

3. *Coordinate data (x,y,z-codes, etc.)* These indicate the coordinates for the tool to move to, in the manner indicated by the preparatory function currently in force. The position of the decimal point in numerical data is not usually given, but is implied at a fixed position from the right in the number. The x,y,z-codes indicate the conventional cartesian coordinates. In four- and five- axis machines, other codes (a,b,c) may be used to indicate angular positions. For circular interpolation i,j,k-codes may be used to indicate the center of the circular arc to be followed.

4. *Feed rate (f-code):* This specifies the feed rate for the operation. The

Table 12.1 Preparatory Functions (EIA Standard RS-273)

Code	Function
g00	Point to point, positioning
g01	Linear interpolation
g02	Circular interpolation arc CW
g03	Circular interpolation arc CCW
g04	Dwell
g05	Hold
g06 & g07	Unassigned
g08	Acceleration
g09	Deceleration
g10	Linear interpolation (long dimensions)
g11	Linear interpolation (short dimensions)
g12	Unassigned
g13–g16	Axis selection
g17	xy plane selection
g18	zx plane selection
g19	yz plane selection
g20	Circular interpolation arc CW (long dimensions)
g21	Circular interpolation arc CW (short dimensions)
g22–g24	Unassigned
g25–g29	Permanently unassigned
g30	Circular interpolation arc CCW (long dimensions)
g31	Circular interpolation arc CCW (short dimensions)
g32	Unassigned
g33	Thread cutting, constant lead
g34	Thread cutting increasing lead
g35	Thread cutting, decreasing lead
g36–g39	Reserved for control use only
g40	Cutter compensation cancel
g41	Cutter compensation—left
g42	Cutter compensation—right
g43–g49	Cutter compensation if used; otherwise unassigned
g50–g59	Unassigned
g60–g79	Reserved for positioning only
g80	Fixed cycle cancel
g81	Fixed cycle 1
g82	Fixed cycle 2
g83	Fixed cycle 3
g84	Fixed cycle 4
g85	Fixed cycle 5
g86	Fixed cycle 6
g87	Fixed cycle 7
g88	Fixed cycle 8
g89	Fixed cycle 9
g90–g99	Unassigned

units are usually inches or millimeters per minute, with the decimal point again implied at a fixed position from the right.

5. *Spindle speed (s-code):* This specifies the spindle speed to be used for the operation and may be an actual value (in rpm) or a code for a fixed spindle speed.

6. *Tool number (t-code):* This indicates to the controller which tool is being used for the operation. In machines with manual tool-changing facilities, changing the t-word may simply tell the controller which previously stored tool length compensation data to use.

7. *Miscellaneous functions (m-codes):* These codes program various auxiliary functions on the machine tool. For example, mo3 starts the spindle with clockwise rotation. Miscellaneous functions are again largely standardized and Table 12.2 shows a typical list. The miscellaneous functions may be acted upon at the start or end of the motion described by a block of instructions. For example, m03, spindle rotation, is carried out before the motion takes place and m05, spindle off, occurs after the motion takes place.

With the word address format, information need not be repeated in successive blocks if it is to remain the same for subsequent blocks. For example,

n001 g01 x07500 y06550 z 100 f612 s16 m03 eob

n002 x08752 y06750

In this case the g-, z-, f-, s-, and m-codes remain the same for the second block. For safety reasons some preparatory functions are canceled after the block is acted upon and must be repeated in a subsequent block if required. This is generally the case for circular interpolation (g02, g03) and codes for thread cutting.

12.6.1 Fixed or Canned Cycles

Many NC machines can be programmed using what are called fixed or canned cycles. Preparatory codes from g80 upwards are usually assigned to these cycles. On modern CNC machines the user can define his own fixed cycles of commonly used operations. Many drilling and 2½ axis milling machines are programmed largely with fixed cycles. Figure 12.10 shows two typical fixed cycles for a drilling–milling machine. The first, g81, is a drilling cycle and the second, g84, is a tapping cycle. Each fixed cycle causes a sequence of motions to take place.

Using the preparatory function g81 will cause a drill to move at rapid traverse above the work surface to a specified *x,y* position, then to drill

Table 12.2 Miscellaneous Functions (EIA Standard RS-273)

Code	Function
m00	Program stop
m01	Optional (planned) stop
m02	End of program
m03	Spindle CW
m04	Spindle CCW
m05	Spindle OFF
m06	Tool change
m07	Coolant No. 2 ON
m08	Coolant No. 1 ON
m09	Coolant OFF
m10	Clamp
m11	Unclamp
m12	Unassigned
m13	Spindle CW & coolant ON
m14	Spindle CCW & coolant ON
m15	Motion+
m16	Motion−
m17–m24	Unassigned
m25–m29	Permanently unassigned
m30	End of tape
m31	Interlock bypass
m32–m35	Constant cutting speed
m36–m39	Unassigned
m40–m45	Gear changes if used; otherwise unassigned
m46–m49	Reserved for control use only
m50–m99	Unassigned

down to the specified z depth at the specified feed rate, followed by rapid retraction to just above the work surface. The g84 cycle is similar except the spindle is reversed and the tool feeds out at the appropriate tapping feed.

12.6.2   Tool Path Coordinates

The NC programmer must carry out the tasks outlined in Sec. 12.4. Determination of the tool path coordinates is an important part of NC programming and is a task that involves numerous repetitive calculations, many of which may be quite complex. As explained above, the tool paths are offset from the surface of workpiece, as it is the program point of the
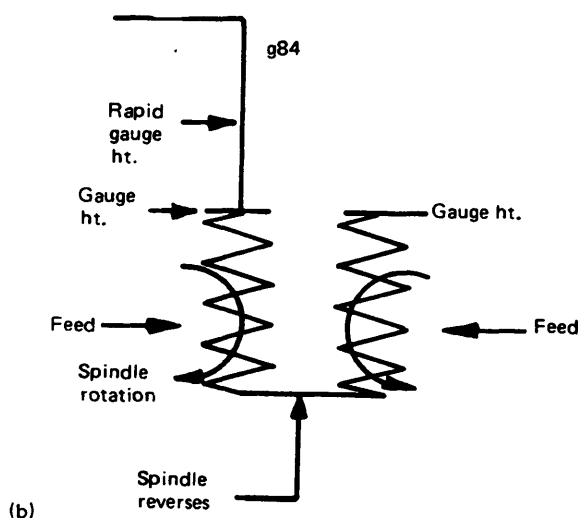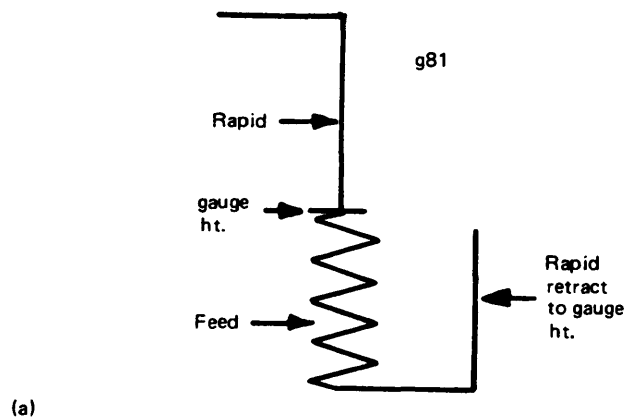
Figure 12.10 Fixed or canned cycles for a NC milling–drilling machine. (a) Drilling cycle; (b) tapping cycle.

tool that is driven along the tool path to machine the workpiece. Each path will be made up generally of linear or circular arc (circular interpolation) line segments. Thus, the manual programmer must determine the coordinates of the change points between each of these line segments. This can be illustrated by Fig. 12.11, which shows a milling operation in which an end mill is required to machine the outside profile of the workpiece. The change point coordinates that must be determined by the programmer are shown as the centers of the dotted circles, which represent the tool positions. In addition, the coordinates of the centers of the circular arcs in the profile must be determined. It can be seen that even in this fairly simple case, some relatively complicated calculations must be carried out to determine the required tool path coordinates. Determination of the required tool paths from complex three-dimensional surfaces is obviously difficult to do manually.

In many cases the programmer must carry out large numbers of relatively simple repetitive calculations in determining the relevant tool paths. Three such cases are illustrated in Fig. 12.12. In drilling operations (Fig. 12.12a) with complex patterns of holes, many coordinate positions must be determined. For roughing cuts in both milling and turning, many change points must be determined. Figure 12.12b shows the layers of
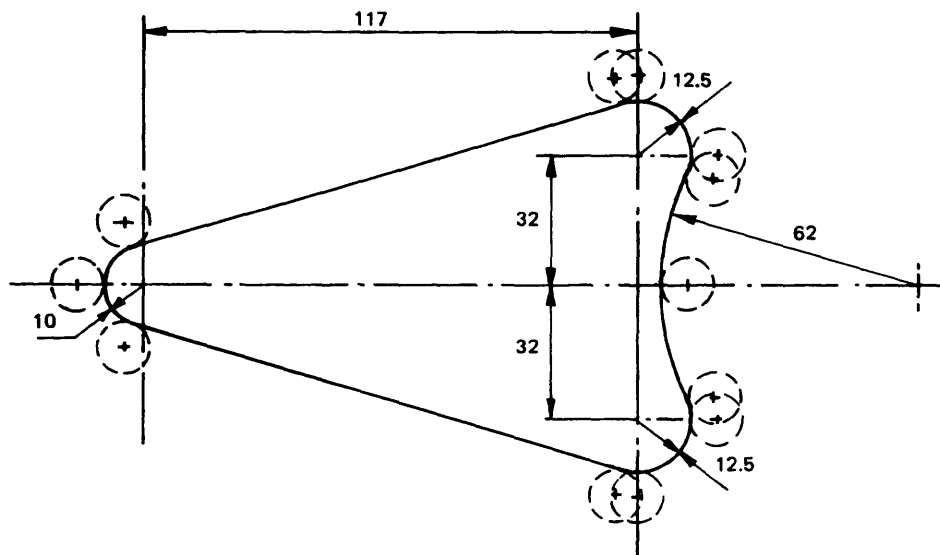
Figure 12.11   Tool path segment change points, for milling operation in which end mill machines outside profile of workpiece.

cuts necessary for a rough turning operation, and Fig. 12.12c illustrates the clearance of an area using an end mill. In both cases many tool path coordinates must be determined, using relatively simple repetitive calculations.

12.7 COMPUTER-AIDED NC PROCESSING

Computer-aided NC processing systems have been developed to facilitate the programming of NC machines. The objective of these systems is to carry out some or all of the programming tasks listed in Sec. 12.6, using stored data on tools, materials, machines, and geometric algorithms, from an input of the geometric description of the component to be machined. Computer-aided NC processing systems are economically justified for companies having a number of NC machine tools installed. Additionally, such systems may be the only practical way of preparing programs for the machining of complex workpieces, involving three-dimensional surfaces.

Computer-aided NC processing is carried out in two or sometimes three stages (Fig. 12.13). Input description of the part geometry is in a certain format called a NC language. The program that carries out the main geometric calculations is called a *processor*. The NC processor may have two stages. First, a geometric processing stage is required, which determines the offset tool path positions to machine the workpiece. This may be followed by a technological processing stage, which selects tools and determines appropriate feeds and speeds. For this latter purpose, files of standard tool data and materials data must be accessed. The main output from the processor is a file, called a cutter location (CL) file, containing mainly the coordinates of the tool positions in a standard format.

The NC processor program is largely independent of the machine tool that will be used to machine the workpiece. Consequently, a further program, called a *postprocessor*, must be used to convert the general CL data into the specific input instructions for the particular NC machine to be used. A different postprocessor is required for each of the various machine tool models for which the main NC processor may be used.

The functions of a postprocessor program are:

1. Read in CL data.
2. Convert data to the machine tool coordinate system.
3. Convert data to absolute or increment coordinates as required.
4. Check for machine limitations (slide travel, interference, allowable feeds and speeds, etc.).
5. Develop appropriate feeds and speeds for the machine.
6. Develop motion commands for the specific machine and controller.
7. Allow for interpolator type.
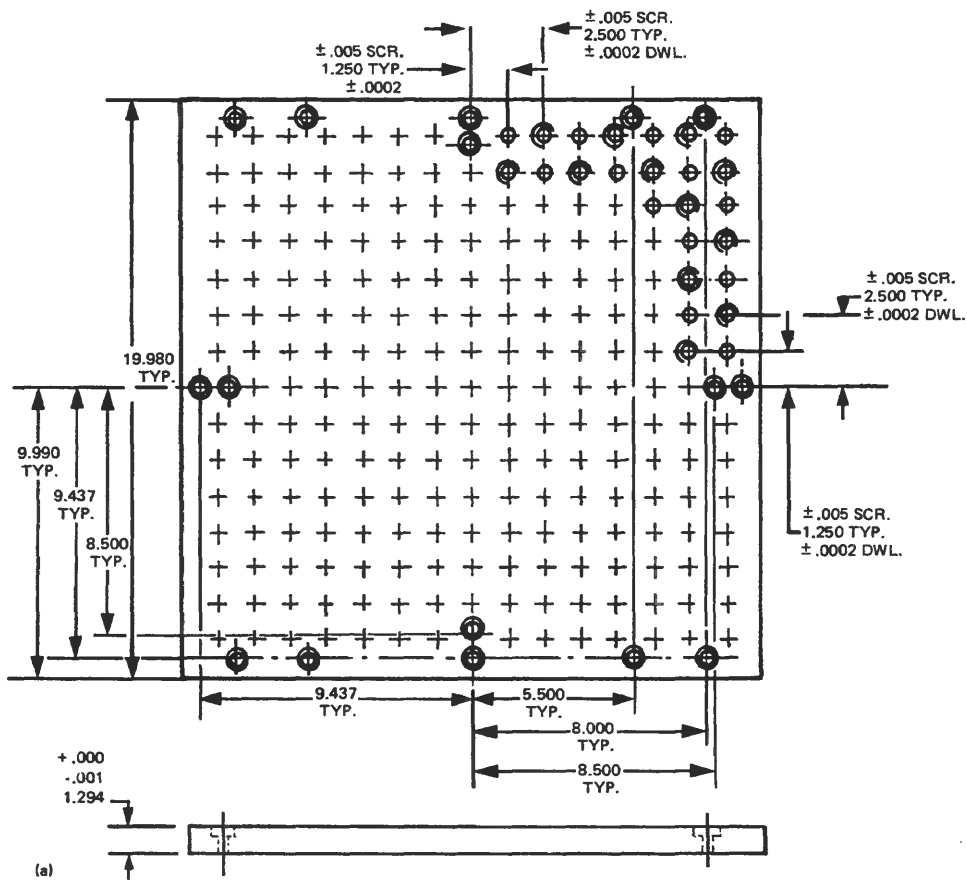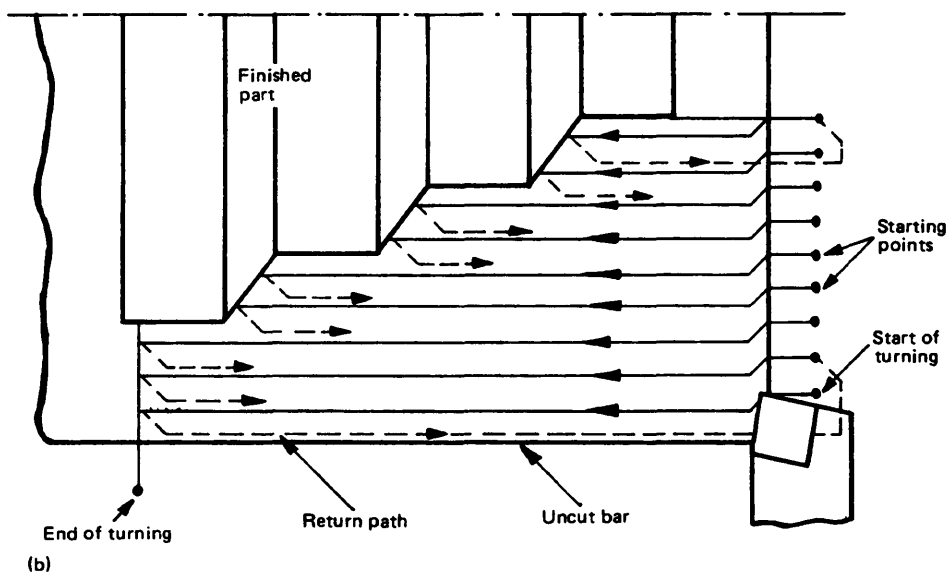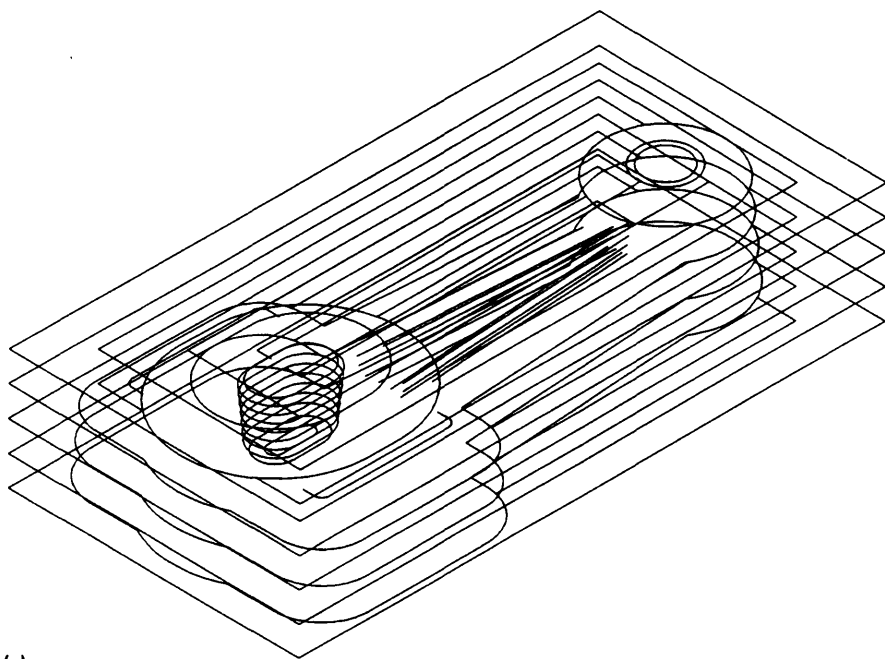
Figure 12.12 Examples of tool position and paths for NC machining operations. (a) Drilled hole patterns; (b) layers of cuts for rough-turning operation; and (c) area clearance for milling operation.

(b)

(c)
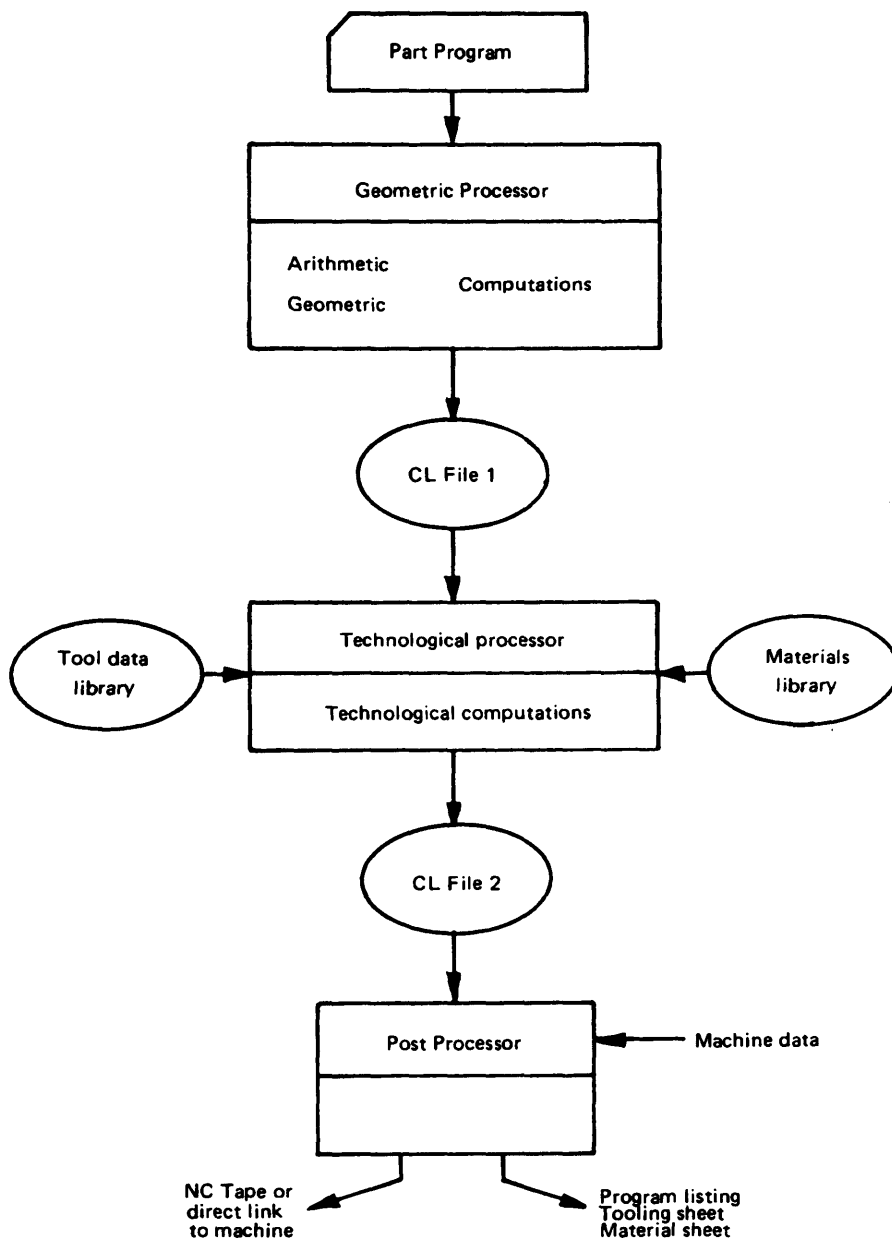
Figure 12.13   Processing stages for computer-aided NC program preparation.

8. Output the machine tool program type in appropriate block format and code set.
9. Print out listing of program for checking.
10. Print out error codes and diagnostics.

12.8 NUMERICAL CONTROL PROCESSING LANGUAGES

A large number of NC processing languages have been developed and these may be classified in various ways, based on the input information required and the internal similarities of these languages.

12.8.1 Input Information Level

Group I

With this group of languages, the basic input is the finished part geometry and the cutter location data is determined from this. The programmer specifies all motions and selects feeds, speeds, tools, and so on. Most of the early-developed NC languages fall within this group, including ADAPT and early versions of the APT processor.

Group II

With this group of languages, the basic input is the same as for group I, but with the additional specification of details of the initial workpiece geometry. The program contains routines for the automatic processing of tool paths for area clearance, pocket milling, machining patterns of holes, and so on. Feeds, speeds, and tools are selected by the programmer. This group includes languages such as APT, NELAPT, IFAPT, and COMPACT II.

Group III

With this group of languages, technological decisions such as tool selection and feed and speed selection are made by the program, based on files of tool and material data. The basic input is the same as in group II, with the addition of details of the workpiece material. Sequences of tools and operations are determined automatically by the processor. For example, specification of the tapping of a hole at a certain location in a rough surface will lead to the selection of a sequence of operations, including spot facing, center drilling, core drilling and tapping, together with the tools, feeds, and speeds corresponding to each operation. Languages such as the EXAPT processors and MITURN are in this group of languages.

12.8.2   Similarity of Language Structure

Available NC processing languages can also be classified according to the similarity of their structures, in particular, in free- and fixed-format languages.

Free-Format Languages

Free-format languages are similar in concept to high-level computer programming languages such as BASIC or FORTRAN. The free-format system incorporates a vocabulary of words that can be used in a variety of ways to describe both part geometry and tool motions. For example, there will be a variety of definitions for points, lines, and circles and these can be used in many different ways to define a particular part geometry. Consequently, free-format NC languages are generally flexible to use, but require considerable programming skill and training to be used effectively. It is relatively easy to add more facilities to free-format languages and to use the system for a variety of different machine tool types.

Fixed-Format Languages

With fixed-format languages, programming is simplified by restricting the input to a series of numbers and codes that must be entered in a predetermined sequence. Generally these languages are for a particular machine tool type, such as lathes. The aim is to produce an easy-to-use language so that machines can be programmed with very little training required. These languages are much less flexible to use than free-format languages and it is difficult to expand their facilities. Less computer power is required for fixed-format than for similar free-format languages. However, the majority of languages in common use are free-format.

NC programming languages can also be divided into:

1. APT-based languages (free-format) based on the APT language structure, which is described in more detail later. Included in this group of languages are APT, ADAPT, NELAPT, IFAPT, EXAPT, and others.
2. Non-APT languages, including COMPACT II, AUTOSPOT, SPLIT, and others.

The APT-based languages are very commonly used, as is the COMPACT II system.

12.9   NC PROGRAMMING USING APT-BASED LANGUAGES

Development of the APT (Automatically Programmed Tools) processor began at MIT in the early 1950s and has continued gradually since then.

The full APT processor can deal with the programming of machine tools having five or more axes of control, but several systems of more limited capabilities with the same language structure have been developed. For example, ADAPT is restricted to programming these machines having 2½ axes of control.

12.9.1 Language Structure

The APT language contains more than 300 English-like words, which can be used in a variety of ways to describe the component geometry and tool motions.

Geometric Statements

The APT language contains a large number of ways of defining the geometry of the component or the workpiece in terms of the points, lines, circles, surfaces, and so on, which make up this geometry. Each geometric statement is of the form:

SYMBOL (NAME) = WORD/MODIFIER, MODIFIER, . . .

For example, a point can be defined by

P = POINT/10, 20, 40

or a circle as:

CIRC1 = CIRCLE/CENTER, P, RADIUS, 57.75

There are a large number of ways of defining each type of geometry, with many of the definitions being in terms of previously defined geometry. For example, Fig. 12.14 shows some of the available ways of defining points. Further details of the variety of geometry definitions in APT can be found elsewhere [11].

12.9.2 Motion Statements

These commands describe how previously defined geometry is to be machined. Each statement is of the form:

motion command/descriptive data (modifier)

A simple point-to-point motion statement is

GOTO/P1

	P1 = POINT/20,10	
	P1 = POINT/INTOF,L1,L2	

	P1 = POINT/XSMALL,INTOF,4,C1	
	P1 = POINT/XSMALL,INTOF,C1,C2	

	P1 = POINT/C1,ATANGL,75	
	P1 = POINT/CENTER,C1	

	P1 = POINT/INTOF,L1,TAB1,P2	
	P1 = POINT/P2,CLW,C1,30	

	P1 = POINT/L1, XCORD,40	
	P1 = POINT/P2,XSMALL,L1,60	

	P1 = POINT/P2,DELTA,35,-25	
	P1 = POINT/P2,THETAR,28,90	

	P1 = POINT/INTOF, TAB1,P1,TAB2,P3	
	P1 = POINT/P2,XSMALL,TAB1,45	
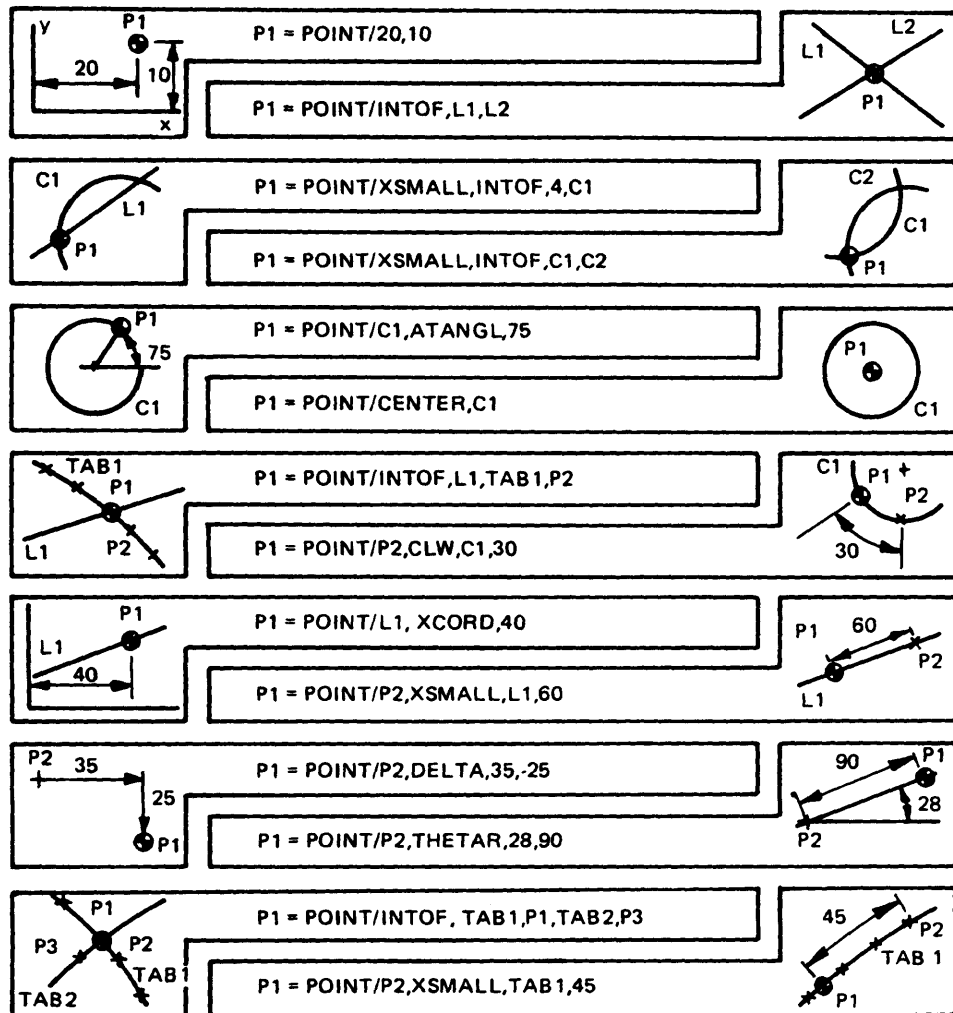
Figure 12.14 Some POINT definitions for the APT system.

and this would cause the tool to move from the current position to the previously defined coordinates of point P1. Incremental motions are specified using the statement GODLTA. For example, GODLTA/2.0, 3.0, 4.0 moves the tool 2.0, 3.0, and 4.0 increments in the x, y, z directions, respectively.

For contouring operations, the general method for specifying motions is in terms of three intersecting surfaces and the procedure can be illustrated by considering the orthogonal surfaces shown in Fig. 12.15. The three surfaces are as follows:

1. *Drive surface:* This is the surface that the axis of the tool moves parallel to during cutting so that the side of the cutter remains in contact with this surface.
2. *Part surface:* This is the surface that the end of the tool remains in contact with during cutting.
3. *Check surface:* This is the surface the tool is brought up to in order to end the cuts.
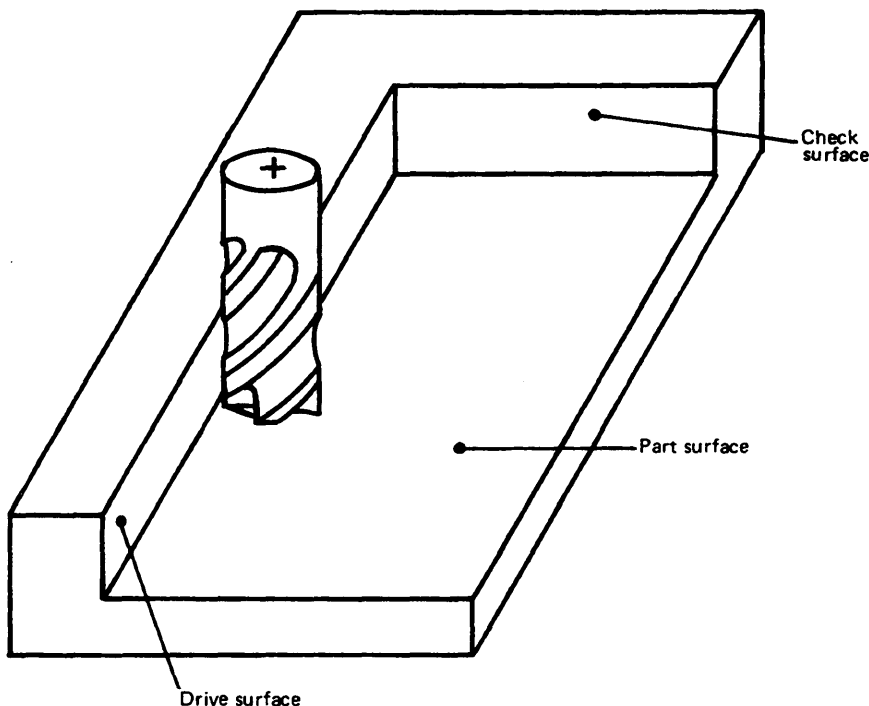
Figure 12.15 Surfaces for APT motion statements for contouring operations.

For the more general case, the drive, part, and check surfaces may be three-dimensional curved surfaces but the basic principle is the same as for orthogonal surfaces. The APT processor determines the appropriate tool path, which is offset from the drive and part surfaces so that the side of the tool remains in contact with the drive surface and the end of the tool remains in contact with the part surface.

In general, the tool follows the drive surface, leaving the part surface cut until it reaches the check surface. Once a cut has been initiated subsequent cuts can be specified by the following motion commands (Fig. 12.16):

GOLFT, GOFWD, GOUP, GORGHT, GOBACK, GODOWN

In using these commands the programmer must know the direction of approach of the tool after the previous tool path segment.

Motion commands may have several modifiers. In particular, these designate the finishing position at the check surface. The main modifiers are: TO, ON, PAST, and TANTO. The effects of these commands are illustrated in Fig. 12.17.
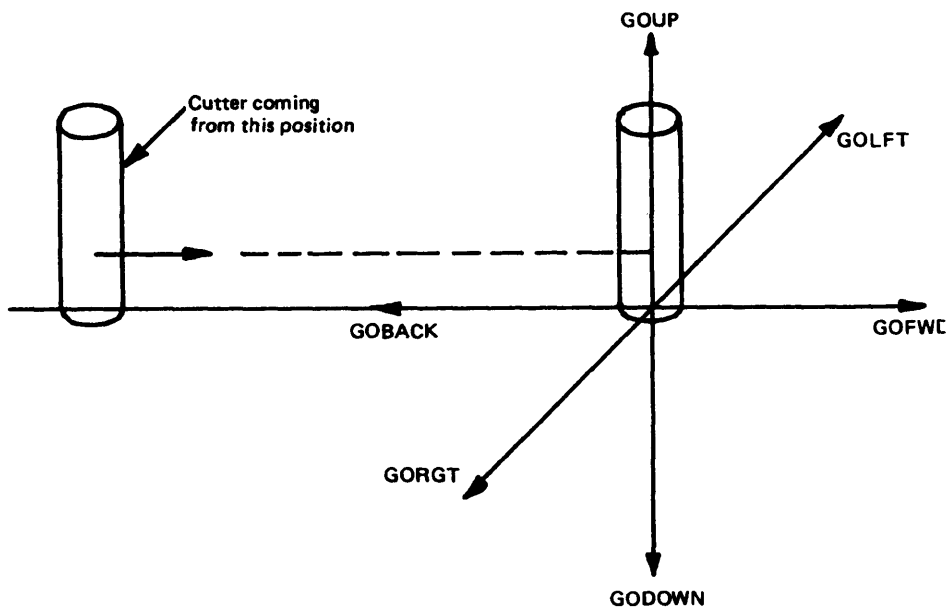
Figure 12.16   Motion commands for the APT system.
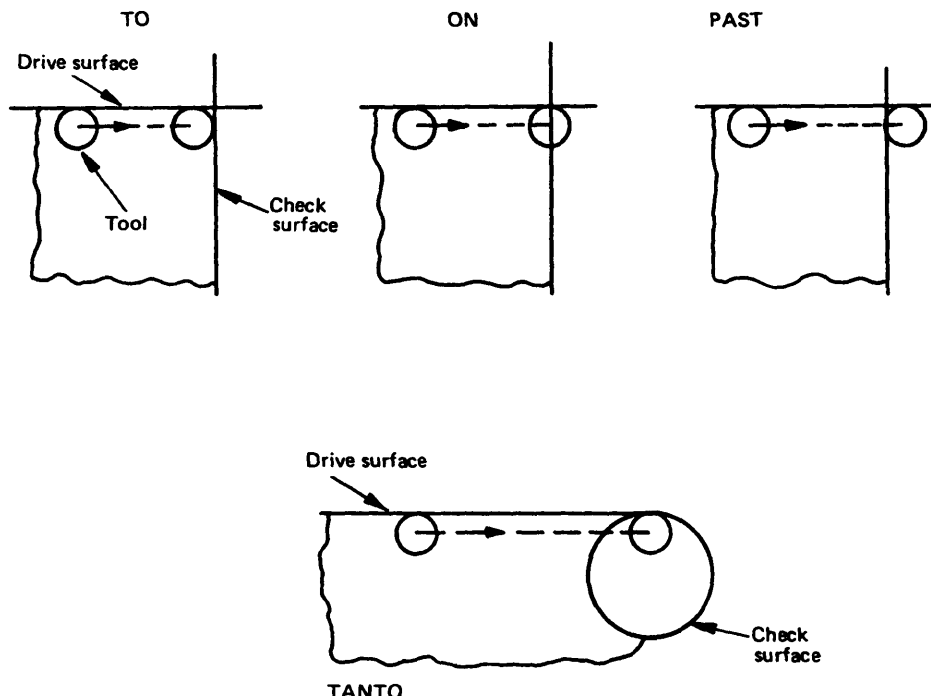
Figure 12.17 Motion command modifiers for the APT system.

12.9.3 Auxiliary Statements

Auxiliary statements include:

PARTNO, INTOL/, OUTTOL/, CUTTER/, etc.

The cutter specification is important since one of the main functions of the APT processor is to determine the offset tool paths, and for this the tool geometry must be known. For milling and drilling operations the general CUTTER specification is shown in Fig. 12.18. The default values of many of the parameters is zero and consequently the statement:

CUTTER/.500

defines a 0.5-in-diameter end-milling cutter.

Cutter D, r, E, F, α, β, h   Cutter - 50, 12
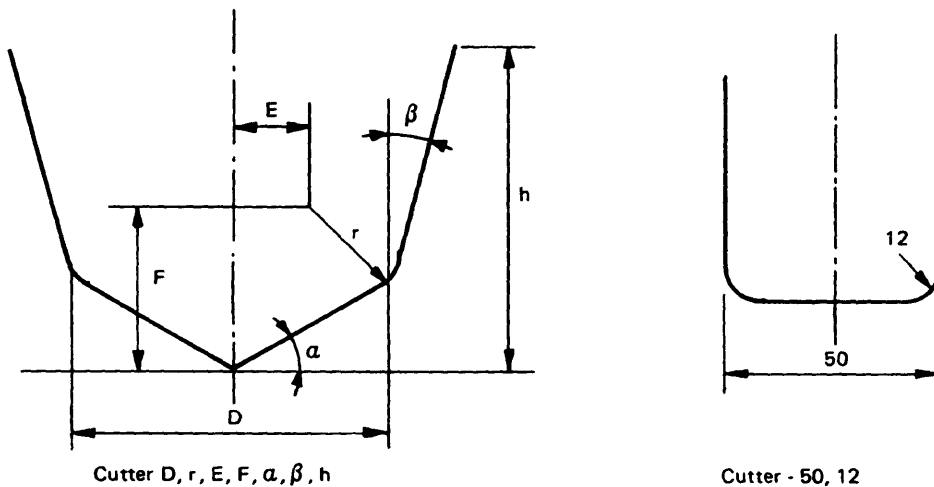
Figure 12.18   Cutter definitions in the APT system.

12.9.4   Postprocessor Statements

Programs in the APT language contain other statements which are passed directly to the postprocessor, including COOLNT/, RAPID, SPINDL/, FEDRAT/, TURRET/, MACHIN/, and so on. The words FEDRAT and SPINDLE specify the feed rate and spindle speed, respectively. The values for these are chosen by the programmer for most of the APT-based systems.

12.9.5   Programming Example in APT

The preceding discussion has given a brief overview of the APT language, which can be further illustrated by considering the example shown in Fig. 12.11. The outside profile of this component is to be machined with a 25 mm-diameter end-milling cutter. The APT program to generate the NC program to machine the part are shown in Table 12.3. Statements 1 to 9 are header and postprocessor statements. The tool, feed, and speed are selected by the programmer and specified by these commands.

Statements 10 to 21 are the geometry statements the programmer has decided to use to define the component geometry. Figure 12.19 shows the geometry specified by the geometry statements. The geometry defined at this stage is "unbounded"; that is, the planes and lines extend to infinity and complete circles are defined. The geometry is converted to the profile required by the tool motions specified by the motion commands.

Statements 22 to 31 are the motion commands. The programmer specifies that the tool start from the point SP, be brought to line L1, and then follow the profile in a counterclockwise direction. These motion commands convert the unbounded geometry into the required profile. This can be illustrated by considering the effect of statement 27 (Fig. 12.20). This causes the tool to move from the tangency point between circles C3 and C4 to the tangency point between circles C4 and C2. Only the arc between these two points is cut, as required for the profile of the component.

As can be seen, the part geometry is defined and the offset tool positions are determined by the APT processor. The tool path points shown in Fig. 12.11 for manual programming do not need to be determined by the programmer in this case. This is a relatively simple example, but the programmer is relieved from some fairly difficult calculations. For more complex parts, the saving in programming time is considerably greater. Many of the processors that utilize the APT language have facilities for automatically determining tool paths for machining processes which require many tool path points to be calculated. For example, area clearance routines are normally included for rough-turning operations, pocket milling, and so on. With these routines the profile to be machined and the original workpiece shape are defined. The various tool path points to clear out the required area are then determined automatically.

12.10 TECHNOLOGICAL NC PROCESSING SYSTEMS

With many of the APT-based NC processing systems the programmer selects the sequences of operations, tools, and cutting processing parameters. The EXAPT (which stands for extended subset of APT) series of processors, developed in West Germany [13, 14], include procedures for making technological decisions on sequences, cutting tools, and process parameters. Thus, several of the basic process-planning tasks are incorporated into the NC processing system (Fig. 12.21). Three separate systems exist: EXAPT1 for drilling and boring operations and the others for 2½-axis milling and turning operations [13].

The processing of programs using EXAPT is similar to that of the other APT-based systems, except that a technological processing stage is added after the geometric processing. At the technological processing stage, operation sequences, tools, and cutting process parameters are determined utilizing files of tools, materials, and operation sequences (Fig. 12.22). Additional instructions are included in the language, which use the same basic APT language format. These instructions enable both single operations and sequences of operations to be defined. In response

Table 12.3 APT Program for part shown in Fig. 12.11.

PART No. ERROR FLAGS	SEQ. No.	Stop Plate (DRG. No. AJ001X5)	
		INPUT STATEMENT	
	1	PART No.	STOP PLATE (DRG. No. AJ001X5)
	2	REMARK	HEADING STATEMENTS FOLLOW
	3		NOPOST
	4		FULIST/ON
	5		CLPRNT
	6		CUTTER/25
	7		SPINDL/350
	8		TOLER/0.03
	9		FEDRAT/15
	10	REMARK	GEOMETRIC STATEMENTS FOLLOW
	11	P1	= POINT/0, 0, 6
	12	P2	= POINT/117, 32, 6
	13	P3	= POINT/117, 32, 6
	14	C1	= CIRCLE/CENTER, P1, RADIUS, 10
	15	C2	= CIRCLE/CENTER, P2, RADIUS, 12.5
	16	C3	= CIRCLE/CENTER, P3, RADIUS, 12.5
	17	L1	= LINE/RIGHT, TANTO, C1, RIGHT, TANTO, C3
	18	L2	= LINE/LEFT, TANTO, C1, LEFT, TANTO, C2
	19	C4	= CIRCLE/XLARGE, OUT, C2, OUT, C3, RADIUS, 62
	20	SP	= POINT/−25, −25, 25
	21	PL1	= PLANE/P1, P2, P3

Header (seq. 1–9)

Geometry statements (seq. 10–21)

```
22   REMARK   MOTION STATEMENTS FOLLOW
23            FROM/SP
24            GO/TO, L1, TO, PL1
25            GORGT/L1, TANTO, C3
26            GOFWD/C3, TANTO, C4
27            GOFWD/C4, TANTO, C2
28            GOFWD/C2, TANTO, L2
29            GOFWD/L2, TANTO, C1
30            GOFWD/C1, TANTO, L1
31            GOTO/SP
32            STOP
33            PRINT/3, ALL
34            FINI
```

Motion
statement

12-19 Remark Geometric Statements Follow
P1 = POINT/0, 0, 6
P2 = POINT/117, 32, 6
P3 = POINT/117,-32, 6
C1 = CIRCLE/CENTER, P1, RADIUS, 10
C2 = CIRCLE/CENTER, P2, RADIUS, 12.5
C3 = CIRCLE/CENTER, P3, RADIUD, 12.5
L1 = LINE/RIGHT, TANTO, C1, RIGHT, TANTO,C3
L2 = LINE/LEFT,TANTO, C1, LEFT, TANTO', C2
C4 = CIRCLE, X LARGE, OUT, C2, OUT, C3, RADIUS, 62
SP = POINT/ -25, -25, 25
PL1 = PLANE/ P1, P2, P3
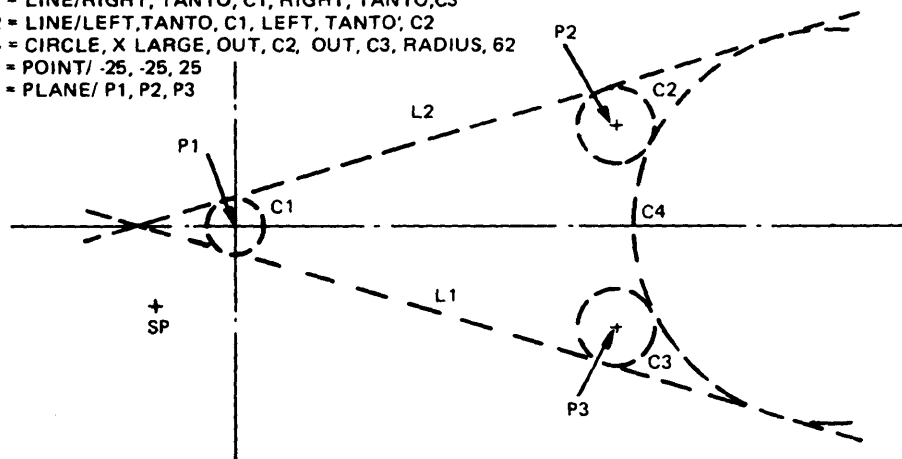
Figure 12.19 Geometric statements in APT for the milling operation shown in Fig. 12.11.

FROM/SP
GO/TO L1, TO P1
GO RGT/ L1, TANTO, C3
Go
GO FWD/ C3, TANTO, C4
GO FWD/ C4, TANTO, C2
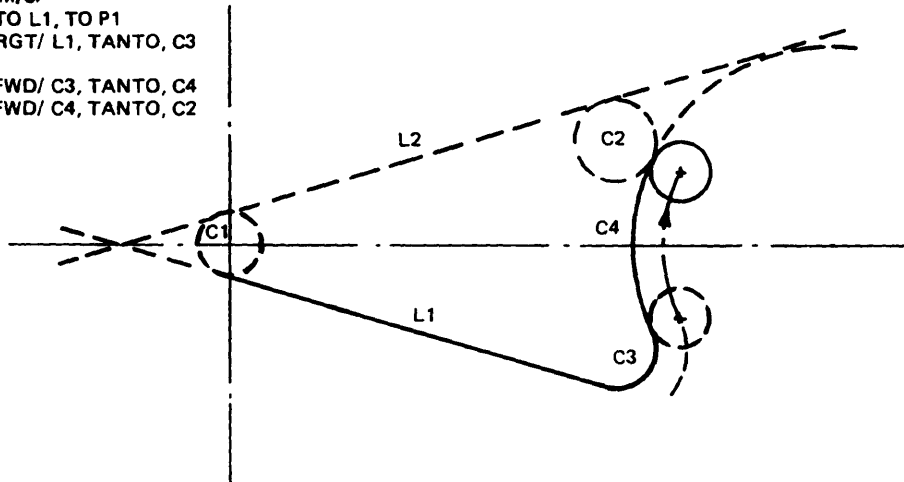
Figure 12.20 Motion statements convert the unbounded geometry into the required part profile.

Computer-aided design

Selection of sequence
of operations

Machine selection

Selection of jigs and
fixtures

Selection of machining
cycles

Selection of tools

Selection of
machining parameters

Calculation of
tool paths

Tool collision
checks

Selection of feed rate
and spindle speeds

Programming of tool
path

EXAPT 1

EXAPT 11

EXAPT 2

BASIC EXAPT

Boring   Milling   Turning

Figure 12.21   Scope of the EXAPT suite of NC processors. (From Rembold and
Epple [13].)
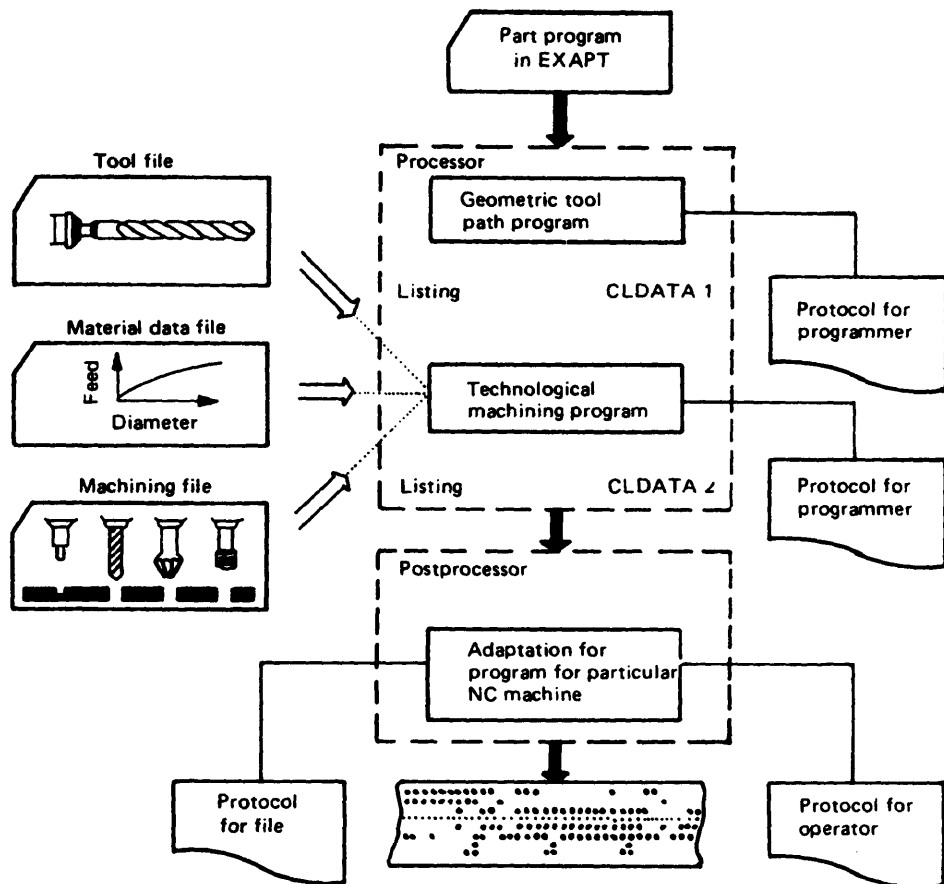
Figure 12.22 Sequence of programming a NC machine with EXAPT. (From Rembold and Epple [13].)

to these instructions, the tools and cutting-process parameters are selected from the files associated with the system. The material of the workpiece and its surface condition may also be specified. For example, the production of a reamed hole in a workpiece will require a sequence of operations, including center drilling, spot facing if the work surface is rough, drilling, predrilling for large-diameter holes, and finally reaming. Figure 12.23 shows a flow diagram for deciding this sequence, and rules for each decision are incorporated into the program [14]. For each operation in the sequence the appropriate tools will be chosen from the tool file and the feeds and speeds selected to suit the operation and workpiece materials.
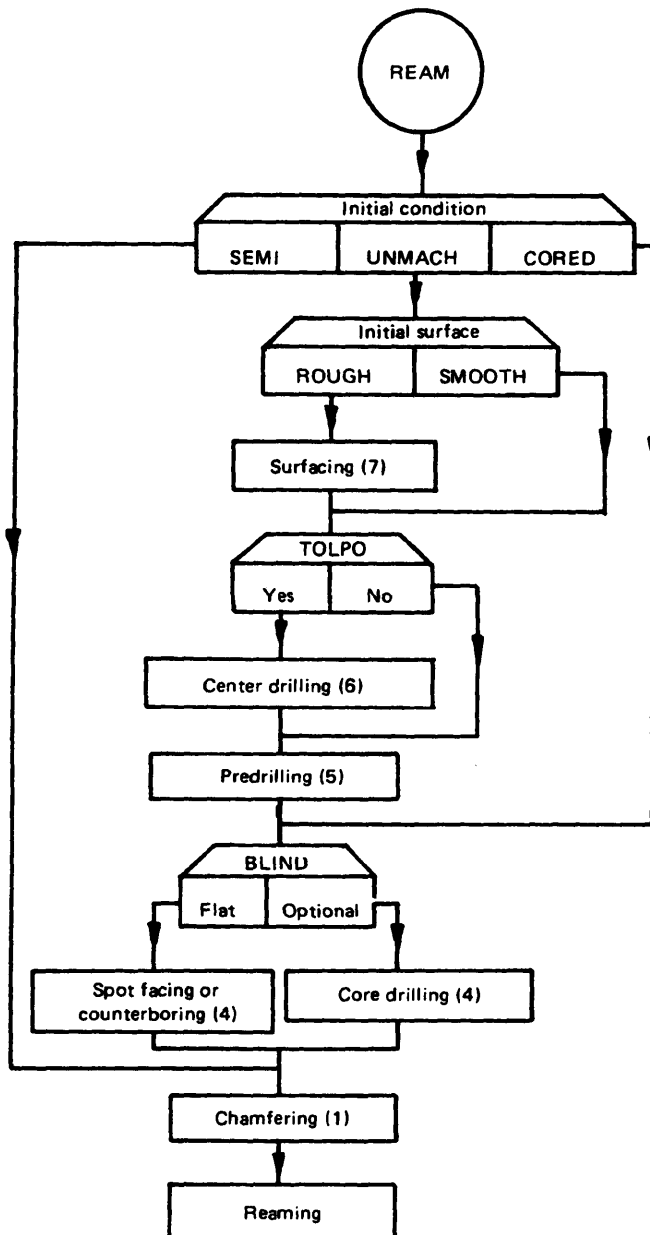
Figure 12.23 Flow diagram for determining the sequence of operations for reamed hole in EXAPT 1. (From Opitz and Simon [14].)

As an illustration of the use of the EXAPT systems, Fig. 12.24 shows a workpiece requiring some drilling, boring, and tapping operations and Table 12.4 lists the EXAPT I program required for its machining. The geometry statements (lines 4 to 7) are similar to those of the other APT-based processors. Statement 7 defines the pattern of four holes arranged on a 110-mm-diameter pitch circle. Statements 8 to 15 include the machining technology definitions. In statement 8 the material is specified, and this allows access to a file of material machinability recommendations for determining the feeds and speeds for the various operations. In statements 10 to 14 single operations for drilling, boring, tapping, and reaming are defined. In some cases tool numbers are included in the definition, but for others no tools are specified and the appropriate tools are then selected by the program from the tool files associated with the system. For all operations feeds and speeds will be determined that are appropriate to the operations, tools, and workpiece materials.

Statements 15 to 23 specify the operations to be carried out. For example, statements 22 and 23 indicate that the drilling and countersinking operations defined in statements 12 and 13, respectively, will be done at each hole position in the pattern of holes defined in statement 7. Similar appropriate machining technology definitions are included in the other EXAPT modules for milling and turning operations, including area clearance routines.

12.11   MANUAL DATA INPUT NC PROGRAMMING

Most CNC systems on modern machine tools incorporate a facility for manual data input (MDI), which enables the user to program the machine on site by entering instructions from a terminal at the machine. A simple interactive language is often included to facilitate operator programming of the machines. The facility is relatively simple to operate and represents a relatively easy way for small machine shops to begin to utilize NC machines. The main limitation is that the programs must usually be relatively short and simple for the following reasons:

1. As no hard copy of the program exists, there is a limit to the length and complexity of program that the operator can visualize.
2. Only 20 to 25 lines can normally be displayed on the terminal screen, adding to the operator's visualization problems.
3. The machine cannot be used while the program is being entered; therefore large amounts of production time can be lost while complex workpieces are being programmed.
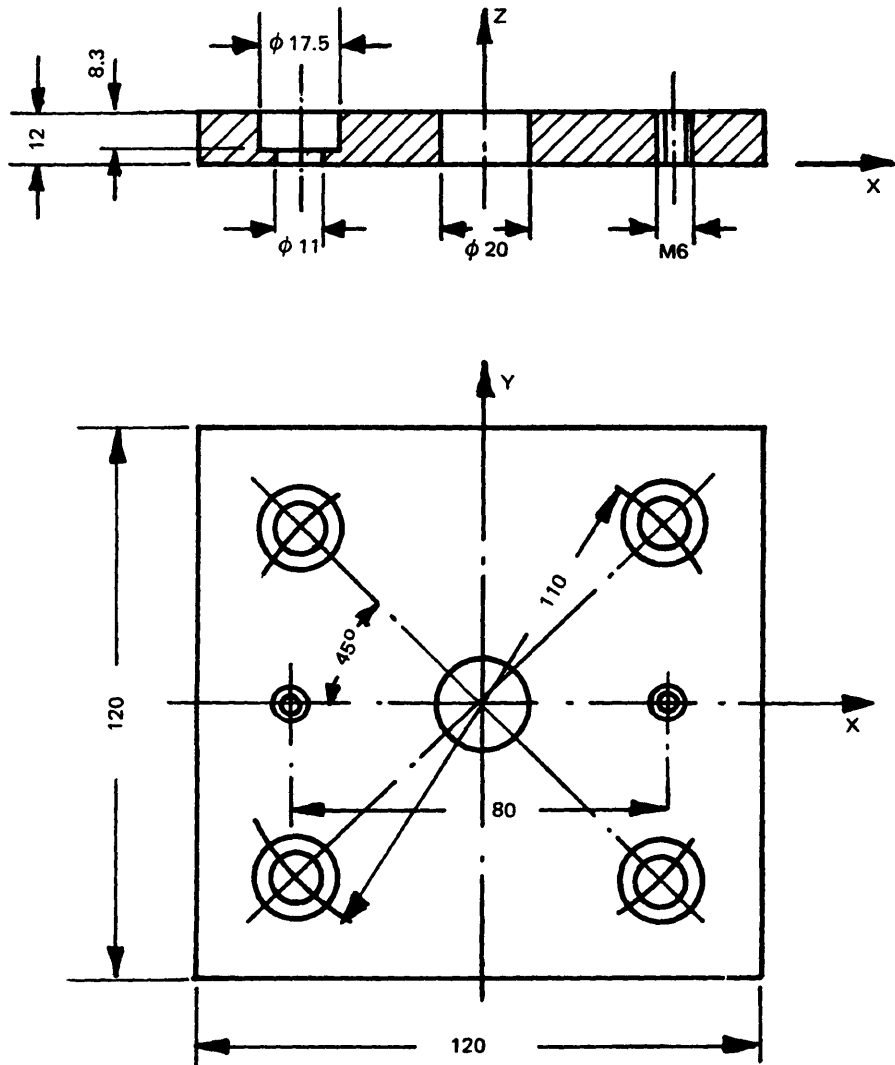
Figure 12.24 Sample workpiece for programming using EXAPT 1.

Table 12.4   EXAPT I Program for Workpiece of Fig. 12.24

1	PARTNO/PLATTE	
2	MACHIN/BOHR	Header
3	TRANS/200,100,0	
4	ZSURF/12	
5	MP = POINT/0,0,12	Geometrical
6	C1 = CIRCLE/CENTER,MP,RADIUS,55	definition
7	PAT = PATTERN/ARC, C1,45,CCLW,4	
8	PART/MATERL,12	
9	CLDIST/0.8	
10	BOHR1 = DRILL/SQ,DIAMET,5,DEPTH,12,TOOL,315	Technological
11	GEWIND = TAP/SQ,DIAMET,6,DEPTH,12,TOOL,416	definition
12	BOHR2 = DRILL/SQ,DIAMET,11,DEPTH,12	
13	SENK = SINK/SQ,DIAMET,17.5,DEPTH,8.3	
14	REIB = REAM/DIAMET,20,DEPTH,12	
15	COLLNT/ON	
16	FROM/−100,0,100	
17	WORK/BOHR1,GEWIND	Executive
18	GOTO/−40,0,12	definition
19	GOTO/40,0,12	
20	WORK/REIB	
21	GOTO/MP	
22	WORK/BOHR2,SENK	
23	GOTO/PAT	
24	FINI	End

REFERENCES

1. Groover, M. P. and E. W. Zimmers: *CAD/CAM: Computer-Aided Design and Manufacturing,* Prentice-Hall, Englewood Cliffs, N.J., 1984.
2. Knox, P.: *CAD/CAM Systems Planning and Implementation,* Marcel Dekker, New York, 1983.
3. Besant, C. B., and C. W. K. Lui: *Computer-Aided Design and Manufacture,* Ellis Horwood, Ltd., Chichester, England, 1986.
4. Gallagher, C. C., and W. A. Knight: *Group Technology Production Methods in Manufacture,* Ellis Horwood, Ltd., Chichester, England, 1986.
5. Halevi, G.: *The Role of Computers in Manufacturing Processes,* Wiley, New York, 1980.
6. Tultoff, J.: Process Planning: An Historical Review and Future Prospect, Proc. 19th CIRP International Seminar on Manufacturing Systems, Pennsylvania State University, University Park, June 1–2, 1987, p. 207.
7. Link, K. H.: Computer-Aided Process Planning (CAPP), *SME Technical Paper,* MS 77-314, 1977.
8. Houtzeel, A.: The many faces of group technology, *Amer. Mach.,* vol. 123, p. 115, 1979.
9. Hori, S.: *APT Part Programming, ITT Research Institute,* McGraw-Hill, New York, 1967.
10. Spur, G. and F. L. Krause: Technological planning for manufacture methodology of process planning, in *Computer-Aided Design and Manufacture,* U. Rembold, and R. Dillman, eds. Springer Verlag, New York, 1986, p.65.
11. Eversheim, W.: Automated generation of process plans for prismatic parts, *Ann. of CIRP,* vol. 32, p. 361, 1983.
12. Pressman, R. S. and J. E. Williams: *Numerical Control and Computer-Aided Manufacturing,* Wiley, New York, 1977.
13. Rembold, U. and W. Epple: Present state and future trends in the development of programming languages for manufacturing, in *Computer-Aided Design and Manufacturing,* U. Rembold and R. Dillman, eds. Springer Verlag, New York, 1986, p. 279.
14. Opitz, H. and W. Simon: EXAPT I Part Programmer Reference Manual, NEL Report No. 293, East Kilbride, June, 1967.

13
Design for Machining

13.1 INTRODUCTION

Many techniques are available to reduce manufacturing costs and increase manufacturing productivity. These measures include using:

1. Improved materials, tools, and processes
2. More effective organization and factory layout, materials handling, and assembly techniques
3. Automation, wherever it contributes to greater efficiency

Unfortunately, designers often consider that their job is to design the product for performance, appearance, and possibly reliability and that it is the manufacturing engineer's job to produce whatever has been designed. There is often a natural reluctance to change a proven design for the sake of a reduction in manufacturing cost, and although designers generally assert that they take manufacturing problems into account whenever possible, the fact is that as a subject, design for manufacture is hardly recognized compared with design for performance. Sometimes design for manufacture is mentioned briefly in textbooks on manufacturing, but only rarely is it mentioned in textbooks on design.

Many companies ensure that their designers obtain some manufac-

turing experience, and many university engineering programs include courses in manufacturing. All this is beneficial, but design for manufacture is one of those subjects a person is expected to assimilate through experience rather than learn from a textbook or instructor. This chapter explains one important aspect of this subject: design for machining.

For obvious reasons machining is a wasteful process, and many engineers feel that the main concern should be to design components that do not require machining. Since 80 to 90 percent of manufacturing machines are designed to machine metal, the view that machining should be avoided must be considered impracticable for the immediate future. However, the trend toward the use of "near net shape" processes that conserve material is clearly increasing, and when large-volume production is involved, this approach should be foremost in the designer's mind.

The following discussion deals first with standardization, then the choice of raw material for the component, the form of the raw material, the ways in which this form can be readily changed to the desired form by machining, and the ways in which the surfaces of the component are finished. Finally, an introduction to early cost estimating for designers is presented.

In the discussion, certain design principles that can help to simplify the machining of components and reduce manufacturing costs are introduced; these are summarized in the chapter.

The terms workpiece, part, piece part, component, or component part are often used interchangeably in describing the machined object. In this chapter, to avoid confusion, the object being machined will be termed a workpiece; after machining is complete, it will be called a component.

13.2 STANDARDIZATION

Provided it has been established that a separate component is necessary, perhaps the first rule in designing for machining is to use standard components as much as possible. Many small components, such as nuts, washers, bolts, screws, seals, bearings, gears, and sprockets, are manufactured in large quantities and standard sizes that should be employed wherever possible. The cost of these components is much lower than that of similar, nonstandard components. Clearly, the designer will need catalogues of the standard items available; these can be obtained from suppliers. Supplier information is provided in standard trade indexes, where companies are listed under products.

A second rule is to minimize the amount of machining by preshaping the workpiece if possible. Workpieces can sometimes be preshaped by

using castings or welded assemblies or metal deformation processes, such as extrusion, deep drawing, blanking, or forging. Obviously, the justification for the preforming of workpieces depends on the size of the batch (the number of components to be produced). In general, for small batches the tendency is to produce the desired shapes by machining. Again, standardization can play an important part when workpieces are to be preformed. The designer may be able to use preformed workpieces designed for a previous similar job, because the necessary patterns for castings or the tools and dies for metal-forming processes are already available.

Finally, even if standard components or standard preformed workpieces are not available, the designer should attempt to standardize the machined features to be incorporated in the design. Standardizing machined features means that the appropriate tools, jigs, and fixtures will be available, which can reduce manufacturing costs considerably. Examples of standardized machined features might include screw threads, keyways, seatings for bearings, splines, and so on. Information on standard features can be found in various reference books, for example, *Machinery's Handbook* [1].

13.3   CHOICE OF WORK MATERIAL

When choosing the material for a component, the designer must consider applicability, cost, availability, machinability, and the amount of machining required. Each of these factors influences the others, and the final optimum choice will generally be a compromise between conflicting requirements. The applicability of various materials will depend on the component's eventual function and will be decided by such factors as strength, resistance to wear, appearance, corrosion resistance, and so on. These features of the design process are outside the scope of this chapter, but once the choice of material for a component has been narrowed by the application of these criteria, the designer must then consider factors that help to minimize the final cost of the component. It should not be assumed, for example, that the least-expensive work material will automatically result in minimum cost for the component. For example, it might be more economical to choose a material that is less expensive to machine (more machinable) but has a higher purchase cost. In a constant-cutting-speed, rough-machining operation, the production cost C_{pr} per component is given by

$$C_{pr} = Mt_l + MKv^{-1} + Kt_r^{-1}v_r^{-1/n}(Mt_{ct} + C_t)v^{(1-n)/n} \qquad (13.1)$$

where

M = total machine and operator rate
t_l = nonproductive time
K = constant for the machining operation
v_r = cutting speed for a tool life of t_r
t_{ct} = tool changing time
C_t = cost of a sharp tool
v = cutting speed
n = constant depending mainly on the tool material

It was shown that the cutting speed v_c for minimum cost is given by

$$v_c = v_r\left(\frac{t_r}{t_c}\right)^n \tag{13.2}$$

where t_c is the tool life for minimum cost and is given by

$$t_c = \left(\frac{1}{n} - 1\right)\left(t_{ct} + \frac{C_t}{M}\right) \tag{13.3}$$

Thus, if Eqs. (13.1) through (13.3) are combined, the minimum cost of production $C_{\min}$ is given by

$$C_{\min} = Mt_l + \frac{MK}{(1 - n)v_r}\left(\frac{t_c}{t_r}\right)^n \tag{13.4}$$

The first term in this expression is the cost of the nonproductive time on the machine tool and is not affected by the work material chosen or by the amount of machining carried out on the workpiece. The second term is the cost of the actual machining operation, and for a given machine and tool design depends on the values of n, v_r, t_r, and K. The factor n depends mainly on the tool material (for high-speed steel $n = 0.125$ and for carbide $n = 0.25$ approximately); $v_r t_r^n$ is a measure of the machinability of the material; K is proportional to the amount of machining to be carried out on the workpiece and can be regarded as the distance traveled by the tool corner relative to the workpiece during the machining operation. For a given operation on a given machine tool and with a given tool material it is shown in Eq. (13.3) that the tool life for minimum cost would be constant and hence [from Eq. (13.4)] that the machining costs would be inversely proportional to the value of $v_r t_r^n$. Since v_r is the cutting speed giving a tool life of t_r, more readily machined materials have a higher value of $v_r t_r^n$ and hence give a lower machining cost.

Taking, for example, a machining operation using high-speed steel tools (n = 0.125) and typical figures of M = \$0.002 83/s, t_l = 300 s, t_c = 3000 s, K = 183 m (600 ft), and v_r = 0.76 m/s (150 ft/min) when t_r = 60 s, then from Eq. (13.4) the minimum production cost per component C_{min} is \$2.14. If, however, an aluminum workpiece for which a typical value of v_r is 3.05 m/s (600 ft/min) when t_r is 60 s could be used, the use of aluminum would reduce the production cost to \$1.17. In other words, an additional amount equal to the difference between these two costs could be spent for each workpiece in order to employ the more machinable material (i.e., as much as \$0.97 additional per workpiece). For a workpiece 25 mm (1 in.) in diameter, a value of K of 183 m (600 ft) would correspond to the finish-machining of a component of about 1.64×10^{-5} m (1 in.^{3}) in volume. Since the cost per unit volume of aluminum rod is only a few cents higher than the cost per unit volume of mild-steel rod, the total cost of the machined component would be much less for the aluminum material.

Clearly, the designer should select work materials that will result in minimum component cost.

13.4 SHAPE OF WORK MATERIAL

With the exception of workpieces that are to be partially formed before machining, such as forgings, castings, and welded structures, the choice of the shape of the work material depends mainly on availability. Metals are generally sold in plate, sheet, bar, or tube form (Table 13.1) in a wide range of standard sizes. The designer should check on the standard shapes and sizes from the raw material supplier and then design components that require the minimum of machining.

Components manufactured from a circular or hexagonal bar or tube are generally machined on machine tools that apply a rotary primary motion to the workpiece; these types of components are called rotational components. The remaining components are manufactured from square or rectangular bar, plate, or sheet and are called nonrotational components. Components partially formed before machining can also be classified as either rotational or nonrotational components.

13.5 SHAPE OF COMPONENT

13.5.1 Classification

As mentioned above, component shapes can be classified as rotational and nonrotational. The rotational components are those whose basic shape can be machined on lathes, boring mills, cylindrical grinders, or

Table 13.1 Standard Material Shapes and Ranges of Sizes

Name	Size	Shape
Plate	6–75 mm (0.25–3 in.)	
Sheet	0.1–5 mm (0.004–0.2 in.)	
Round bar or rod	3–200 mm dia. (0.125–8 in. dia.)	
Hexagonal bar	6–75 mm (0.25–3 in.)	
Square bar	9–100 mm (0.375–4 in.)	
Rectangular bar	3 × 12–100 × 150 mm (0.125 × 0.5–4 × 6 in.)	
Tubing	5 mm dia., 1 mm wall–100 mm dia., 3 mm wall (0.187 5 in. dia., 0.035 in. wall–4 in. dia., 0.125 in. wall)	

any other machine tool that applies a rotary primary motion to the workpiece. In defining a component shape as rotational, the important factor is that in machining its basic shape, the workpiece is rotated. The nonrotational category includes all shapes other than rotational shapes (and, of course, in machining its basic shape, the motion of the workpiece is linear). The basic shape of a rotational component is a plain cylinder with dimensions sufficiently large to enclose the final shape (Fig. 13.1a); the basic shape of a nonrotational component is a right-rectangular prism with dimensions sufficiently large to enclose the final shape (Fig. 13.1b).

In considering design for machining, it is important to know the ways in which the basic shapes can be readily changed by machining processes. Before proceeding, however, it will be helpful to describe briefly a method of classifying machined components developed by Opitz [2]. This classification system allows components to be identified by geometric code numbers for the purposes of analysis of complete production systems. The code number depends on the types of machining process required to produce the component and therefore provides a suitable basis for discussion of the ways in which basic shapes can be changed by machining. The main use of the classification system is to be able to categorize and group those components having similar features and requiring similar sequences of machining operations. This information allows manufacturing engineers to plan efficiently the layout of machines in the factory to reduce the handling and transfer of components as much as possible, as described in Chap. 11. However, it will also assist the designer who wishes to
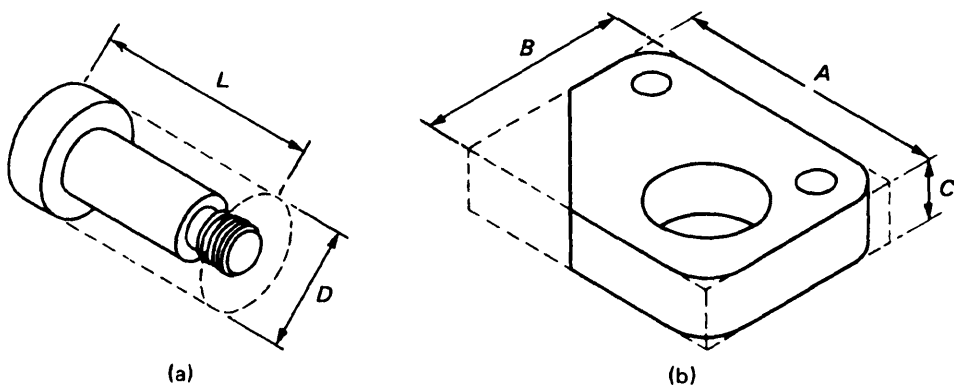
Figure 13.1   Basic component shapes. (a) Rotational; (b) nonrotational.

standardize components and avoid specifying machined features the company is not equipped to handle.

The basic geometric code number consists of five digits, the first digit describing the component class (either rotational or nonrotational) and the proportions of the overall shape, the remaining digits describing the variations from this shape. Table 13.2 shows the general basis of this coding system and the means of determining the first digit. Thus, for example, if the rotational component shown in Fig. 13.1a has a length-to-diameter (L/D) ratio of 2, the first digit in the code number is 1; if the nonrotational component shown in Fig. 13.1b has ratios A/B of 1.2 and A/C of 4.5, it is classified as a flat component, and the first digit in the code number is 6. (In labeling the basic rectangular prism the largest side is given the length A and the smallest the length C.) Components with first digits of 3 or 4 are those rotational components machined from other than cylindrical shapes (hexagonal bar, for example), and components with first digits of 5 or 9 are those that do not fit within the other categories. For components with first digits of 0, 1, 2, 6, 7, and 8 the determination of the remaining digits is shown in Tables 13.3 through 13.5.

A supplementary code can also be employed. This supplementary code consists of four further digits: the first gives the basic dimension of the component (D for a rotational component and A for a nonrotational component), the second specifies the material used, the third specifies the form of the raw material, and the fourth specifies the accuracy of the machined surfaces. For a complete description of the classification system the reader should see Ref. 2.

The rotational component shown in Fig. 13.1a can be machined from a bar by gripping one end in a lathe chuck, turning to form the steps, and then generating the screw thread. A second digit of 2 describes such a shape (a step to one end with a screw thread), and since the component has no internal shape, no plane-surface machining, and no auxiliary holes or gear teeth, the third, fourth, and fifth digits are all zero. Thus, the code number for this component is 12000. For the nonrotational component shown in Fig. 13.1b a second digit of 1 describes a plane component with one angular deviation, a third digit of 1 describes one smooth principal bore, a fourth digit of 0 describes no plane-surface machining, and a fifth digit of 3 describes a component with no gear teeth or forming and two or more holes drilled in one direction and related by a drilling pattern. Thus, the code number would be 61103. It should be noted that the rounding of the corners of the basic rectangular shape is ignored in deciding the geometric code.

From these brief examples it can be seen that the coding system is based on the more common machining techniques used to alter the initial

Table 13.2 Geometric Code Devised by Opitz [2] for Classification of Machined Components.

	1st digit component class	2d digit overall or main shape	3d digit rotational surface machining	4th digit plane surface machining	5th digit auxiliary holes, gear teeth, forming

Table content (Rotational components):

0	$\frac{L}{D} \leqslant 0.5$	External shape, external shape elements	Internal shape, internal shape elements	Plane surface machining	Auxiliary holes and gear teeth
1	$0.5 < \frac{L}{D} < 3$				
2	$\frac{L}{D} > 3$				
3	$\frac{L}{D} \leqslant 2$ with deviation	Overall shape	Rotational machining, internal and external shape elements	Plane surface machining	Auxiliary holes, gear teeth, forming
4	$\frac{L}{D} > 2$ with deviation				
5	Specific	Overall shape			

Nonrotational components:

6	$\frac{A}{B} < 3, \frac{A}{C} > 4$ Flat components	Overall shape	Principal bores	Plane surface machining	Auxiliary holes, gear teeth, forming
7	$\frac{A}{B} > 3$ Long components	Overall shape			
8	$\frac{A}{B} < 3, \frac{A}{C} < 4$ Cubic components	Overall shape			
9	Specific				

Table 13.3 Geometric Code for Rotational Components[a]

1st digit		2d digit		3d digit		4th digit	5th digit
Component class		**External shape, external shape elements**		**Internal shape, internal shape elements**		**Plane surface machining**	**Auxiliary hole(s) and gear teeth**
0	$\frac{L}{D} \leq 0.5$	0	Smooth, no shape elements	0	Without through bore blind hole	0 — No surface machining	0 — No auxiliary hole(s)
1	$0.5 < \frac{L}{D} < 3$	1	*(Stepped to one end or smooth)* No shape elements	1	*(Smooth or stepped to one end)* No shape elements	1 — External plane surface and/or surface curved in one direction	1 — Axial hole(s) not related by a drilling pattern
2	$\frac{L}{D} > 3$	2	With screwthread	2	With screwthread	2 — External plane surfaces related to one another by graduation around a circle	2 — Axial holes related by a drilling pattern
		3	With functional groove	3	With functional groove	3 — External groove and/or slot	3 — Radial hole(s) not related by a drilling pattern
		4	*(Stepped to both ends (multiple increases))* No shape elements	4	*(Stepped to both ends (multiple increases))* No shape elements	4 — External spline and/or polygon	4 — Holes axial and/or radial and/or in other directions not related
		5	With screwthread	5	With screwthread	5 — External plane surface and/or slot and/or groove, spline	5 — Holes axial and/or radial and/or in other directions related by drilling pattern
		6	With functional groove	6	With functional groove	6 — Internal plane surface and/or groove	6 — Spur gear teeth
		7	Functional taper	7	Functional taper	7 — Internal spline and/or polygon	7 — Bevel gear teeth
		8	Operating thread	8	Operating thread	8 — External and internal splines and/or slot and/or groove	8 — Other gear teeth
		9	Others (> 10 functional diameters)	9	Others (> 10 functional diameters)	9 — Others	9 — Others

Note: In the 1st digit column, the label "Rotational components" runs vertically. In the 2d/3d digit columns, "No gear teeth" applies to codes 0–5 and "With gear teeth" applies to codes 6–9 of the 5th digit.

[a]After Opitz [2]. © Verlag Wu. Girardet 1970. Reprinted by permission.

Table 13.4 Second Digit[a] of Geometric Code for Flat and Long Nonrotational Components[b]

1st digit	2d digit	1st digit	2d digit
Component class	Overall shape	Component class	Overall shape
	Plane 0 Rectangular		**Uniform cross section** 0 Rectangular
	1 Rectangular, with one deviation (right angle or triangular)		**Shape axis (straight)** 1 Rectangular with one deviation (right angle or triangular)
	2 Rectangular with angular deviations		2 Any cross section other than 0 and 1
	3 Rectangular with circular deviation		**Varying cross section** 3 Rectangular
	4 Any flat shape other than 0 to 3		4 Rectangular with one deviation (right angle or triangular
	5 Flat components, rectangular or right angled with small deviations due to casting, welding, forming		5 Any cross section other than 3 and 4
6 Flat components $\frac{A}{B} < 3,\ \frac{A}{C} > 4$	6 Flat components, round or any shape other than position 5		**Shape axis curved (bent)** 6 Rectangular, angular, and other cross sections
	7 Flat components regularly arched or dished	7 **Nonrotational components** Long components $\frac{A}{B} > 3$	7 Formed component
	8 Flat components irregularly arched or dished		8 Formed component with deviations in the main axis
	9 Others		9 Others

[a]For the third, fourth, and fifth digits, see Table 13.5.
[b]After Opitz [2]. © Verlag Wu. Girardet 1970. Reprinted by permission.

Table 13.5 Geometric Code for Cubic Components[a]

1st digit	2d digit	3d digit	4th digit	5th digit
Component class	Overall shape	Principal bore, rotational surface machining	Plane surface machining	Auxiliary hole(s), forming, gear teeth
	Block and blocklike components 0 Rectangular prism	0 No rotational machining or bore(s)	0 No surface machining	0 No auxiliary holes, gear teeth, and forming
	1 Rectangular with deviations (right angle or triangular)	1 One principal bore, smooth	1 Functional chamfers (e.g., welding prep.)	**No gear teeth, no forming** 1 Holes drilled in one direction only
	2 Compounded of rectangular prisms	2 One principal bore stepped to one or both ends	2 One plane surface	2 Holes drilled in more than one direction
	3 Components with a mounting or locating surface and principal bore	3 One principal bore with shape elements	3 Stepped plane surfaces	**No gear teeth, Related by a drilling pattern** 3 Holes drilled in one direction only
	4 Components with a mounting or locating surface, principal bore with dividing surface	4 Two principal bores, parallel	4 Stepped plane surfaces at right angles, inclined and/or opposite	4 Holes drilled in more than one direction
	5 Components other than 0 to 4	5 Several principal bores, parallel	5 Groove and/or slot	**Forming, no gear teeth** 5 Formed, no auxiliary holes
	Box and boxlike components — **Not split** 6 Approximate or compounded of rectangular prisms	6 Several principal bores, other than parallel	6 Groove and/or slot and 4	6 Formed, with auxiliary holes
7 Nonrotational components	7 Components other than 6	7 Machined annular surfaces, annular grooves	7 Curved surface	7 Gear teeth, no auxiliary hole(s)
8 Cubic components $\frac{A}{B} < 3$, $\frac{A}{C} < 4$	**Split** 8 Approximate or compounded of rectangular prisms	8 7 + principal bore(s)	8 Guide surfaces	8 Gear teeth, with auxiliary hole(s)
	9 Components other than 8	9 Others	9 Others	9 Others

[a]After Opitz [2]. © Verlag Wu. Girardet 1970. Reprinted by permission.

workpiece shape. Some of these machining techniques will now be described and will help to illustrate further design rules for machined components.

13.5.2 Rotational Components [(L/D) ⩽ 0.5]

Rotational components where the length-to-diameter ratio is less than or equal to 0.5 have a first digit of 0 and may be classified as disks. For diameters to approximately 300 mm (12 in.) the workpiece is generally gripped in a lathe chuck; for larger diameters it is necessary to clamp the workpiece on the table of a vertical borer. The simplest operations that could be performed would be machining of the exposed face and drilling, boring, and threading a concentric hole. All these operations could be performed on one machine without regripping the workpiece (Fig. 13.2). The realization that neither the unexposed face nor a portion of the outer cylindrical surface can be machined leads to a further general guideline for design: If possible, design the component so that machining is not necessary on the unexposed surfaces of the workpiece when it is gripped in the work-holding device. Also, the diameters of the external features should gradually increase, and the diameters of the internal features should gradually decrease from the exposed face.

Of course, with the examples shown in Fig. 13.2 it would probably be necessary to reverse the workpiece in the chuck to machine the opposite face. However, if the diameter of the workpiece were less than about 50 mm (2 in.), the desired surfaces could probably be machined on the end of a piece of bar stock and the component then separated from the bar by a

| Stepped surface | Bore | Stepped bore | Threaded bore | Typical |
| (facing) | (drilling) | (counterboring) | (threading or tapping) | component |
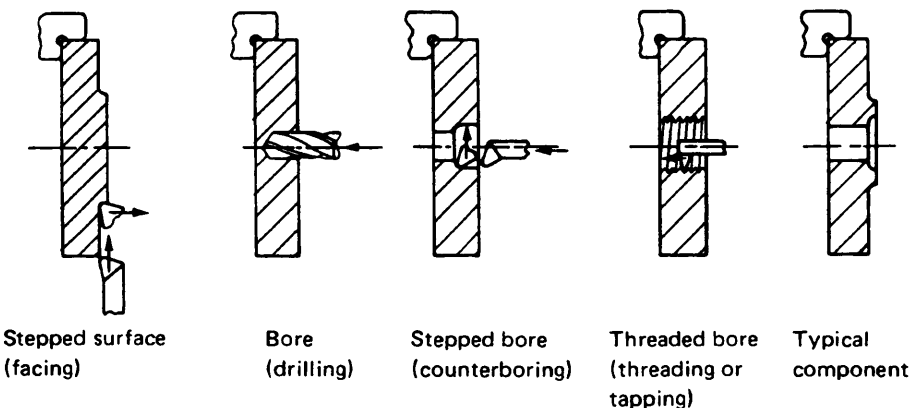
Figure 13.2   Some ways of machining a disk-shaped workpiece.

parting or cut-off operation (Fig. 13.3). It should be remembered that when a workpiece must be reversed in the chuck, the concentricity of features will be difficult to maintain (Fig. 13.4).

Consideration of the machining processes in Figs. 13.2 and 13.3 leads to further conclusions regarding the design of rotational components. First, because the slideways on a lathe are arranged either parallel or perpendicular to the axis of workpiece rotation, the easiest surfaces to generate are concentric cylindrical surfaces and plane surfaces normal to the workpiece axis. With the exception of short tapers or chamfers that can be machined by using the compound rest on a lathe, other types of surfaces should be avoided if possible. Sometimes, however, it is necessary to machine a functional conical (taper) surface (Fig. 13.5a), and this process requires the use of a taper turning attachment on a lathe, adding to the cost of production. Surfaces whose section is curved require special form tools (Fig. 13.5b) and cannot be justified unless large quantities of the components are to be manufactured.

When machined surfaces intersect to form an edge, the edge is square; when surfaces intersect to form an internal corner, however, the edge is rounded to the shape of the tool corner. Thus, the designer should always specify radii for internal corners. When the two intersecting faces are to form seatings for another component in the final assembly, the matching corner on the second component should be chamfered to provide clearance (Fig. 13.6). Chamfering ensures proper seating of the two parts and presents little difficulty in the machining operations. These corners or chamfers do not affect the geometric code of the components.

On rotational components some features may be necessary that can
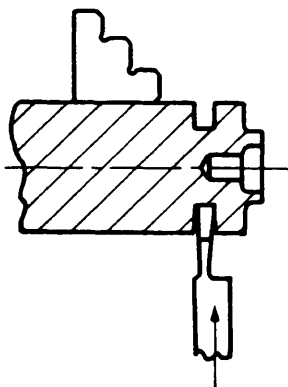
Figure 13.3   Parting finished components from bar stock.

Difficult to
maintain concentricity
of these surfaces
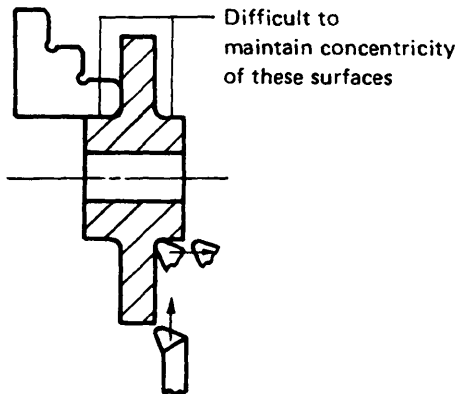
Figure 13.4   Machining of components stepped to both ends.

only be produced by machine tools other than those that rotate the workpiece. Consequently, the batch of workpieces requiring these features will have to be stacked temporarily and then transferred to another machine tool that may be in another part of the factory. This storage and transfer of workpieces around a factory presents a major organizational problem and adds considerably to manufacturing costs. Thus, if possible, the components should be designed to be machined on one machine tool only.

Plane-machining operations may also be required on a rotational

(a)   (b)
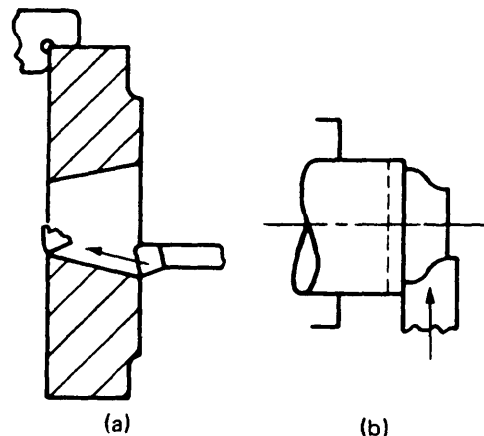
Figure 13.5   Machining of surfaces other than cylindrical or flat. (a) Machining of a functional taper; (b) form turning.
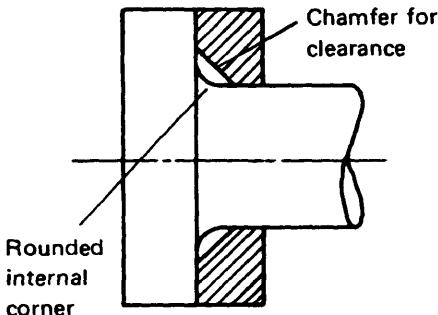
Figure 13.6 Rounded corners and chamfers.

component. Such operations might be carried out on a shaper (or slotter) or milling machine. A typical example is a keyway in the bore of one of the disk-shaped parts discussed earlier. Such a keyway could be readily machined in a shaper, as shown in Fig. 13.7. Finally, auxiliary holes (those not concentric with the component axis) and gear teeth may be required. Auxiliary holes would be machined on a drill press and would generally form a pattern as shown in Fig. 13.8. It should be noted that axial auxiliary holes are usually the easiest to machine because one of the flat surfaces on the workpiece can be used to orient it on the work-holding surface. Thus, the designer should avoid auxiliary holes inclined to the workpiece axis. Gear teeth would be generated on a special gear-cutting machine, and this process is generally slow and expensive.
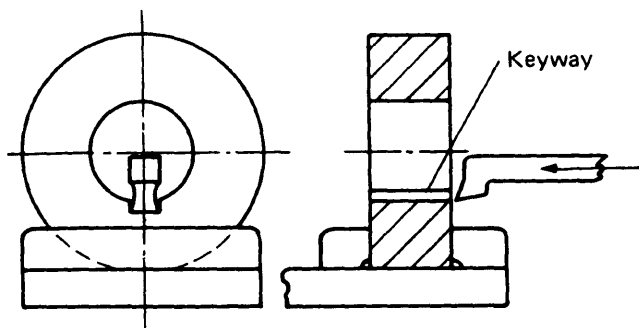
Figure 13.7 Machining a keyway on a shaper.
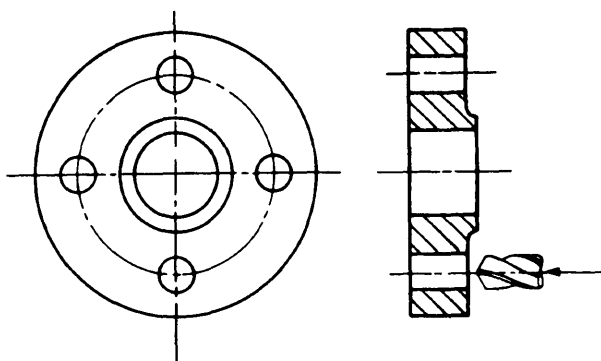
Figure 13.8 Drilling a pattern of auxiliary holes.

13.5.3 Rotational Components [0.5 < (L/D) < 3]

The class of rotational components having a length-to-diameter ratio of between 0.5 and 3 are short, cylindrical components. They have a first digit of 1 and are the most suitable for machining on engine and turret lathes. The workpieces from which these components are produced would often be in the form of bar stock, and the machined component would be separated from the workpiece by parting or cutoff, as was shown in Fig. 13.3. The whole of the outer surface of this type of component can be machined without interference by the jaws of the chuck. However, it is important with this type of component for the designer to ensure (if possible) that the diameters of a stepped internal bore are gradually decreasing from the exposed end of the workpiece (Fig. 13.9) and that no recesses or grooves are required on the surface produced in the parting or cutoff operation.

13.5.4 Rotational Components [(L/D) ⩾ 3]

The class of rotational components having a length-to-diameter ratio greater than or equal to 3 are long, cylindrical components. They have a first digit of 2 and would be machined on an engine lathe. These components would be supported between centers or gripped at the headstock end by a chuck and supported by the tailstock center at the other end. If the L/D ratio is too large, the flexibility of the workpiece creates a problem because of the forces generated during machining. Thus, the designer should ensure that the workpiece, when supported by the work-holding devices, is sufficiently rigid to withstand the machining forces.
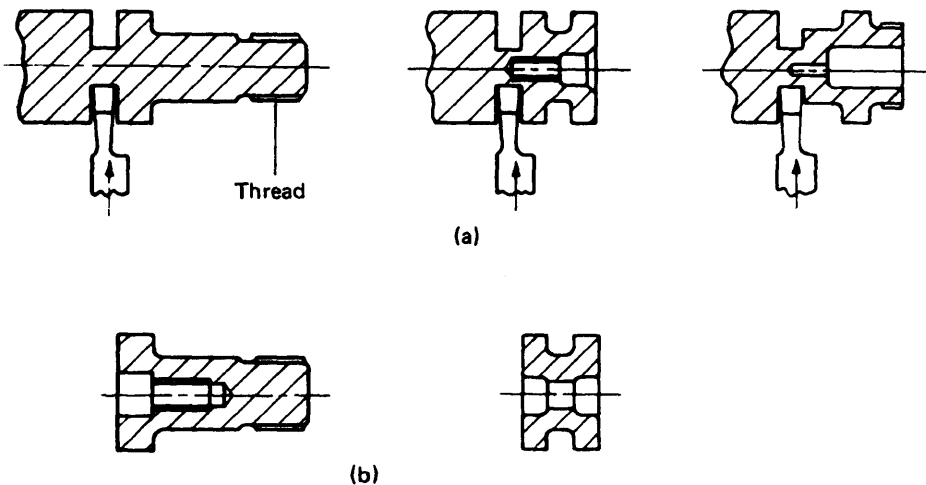
Figure 13.9 Machining components from bar stock. (a) Components that can be parted off complete; (b) components that cannot be parted off complete.

When a rotational component must be supported at both ends for machining of the external surfaces, internal surfaces of any kind cannot be machined at the same time. In any case, with slender components, concentric bores would necessarily have large length-to-diameter ratios and would be difficult to produce. Thus, the designer should try to avoid specifying internal surfaces for rotational components having large L/D ratios.

A common requirement on a long, cylindrical component is a keyway, or slot. A keyway is usually milled on a vertical-milling machine using an end-milling cutter (Fig. 13.10a) or on a horizontal-milling machine using a side- and face-milling cutter (Fig. 13.10b). The shape of the end of the keyway is determined by the shape of the milling cutter used and thus the designer, in specifying this shape, is specifying the machining process.

Before the ways of changing the basic nonrotational shapes by machining operations are discussed, some general points should be noted regarding undesirable features on rotational components. These undesirable design features can be categorized as follows:

1. Features impossible to machine
2. Features extremely difficult to machine that require the use of special tools or fixtures
3. Features expensive to machine even though standard tools can be used
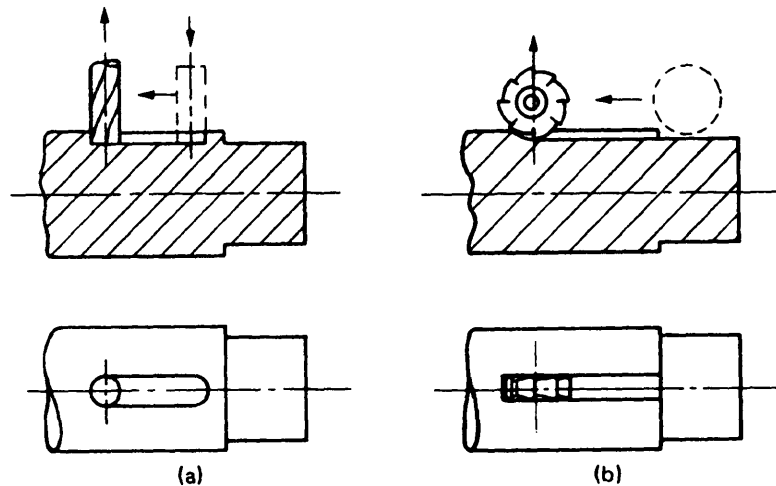
Figure 13.10 Machining of a keyway. (a) Vertical milling; (b) horizontal milling.

In considering the features of a particular design it should be realized that

1. Surfaces to be machined must be accessible when the workpiece is gripped in the work-holding device.
2. When the surface of the workpiece is being machined, the tool and tool-holding device must not interfere with the remaining surfaces on the workpiece.

Figure 13.11a shows an example of a component with external surfaces impossible to machine. This is because during the machining of one of the cylindrical surfaces, the tool would interfere with the other cylindrical surface. Figure 13.11b shows a component that would be extremely difficult to machine on a lathe because when the hole was drilled, the workpiece would have to be supported in a special holding device. Even if the workpiece were transferred to a drill press for the purpose of drilling the hole (in itself an added expense), a milled preparation would be required (Fig. 13.11c) to prevent the drill from deflecting sideways at the beginning of the drilling operation. Figure 13.11 also illustrates the difficulties that may arise when nonconcentric cylindrical surfaces are specified.

Figure 13.12 shows two examples where the tool or tool holder would interfere with other surfaces on the workpiece. The small radial hole shown in Fig. 13.12a would be difficult to machine because a special long
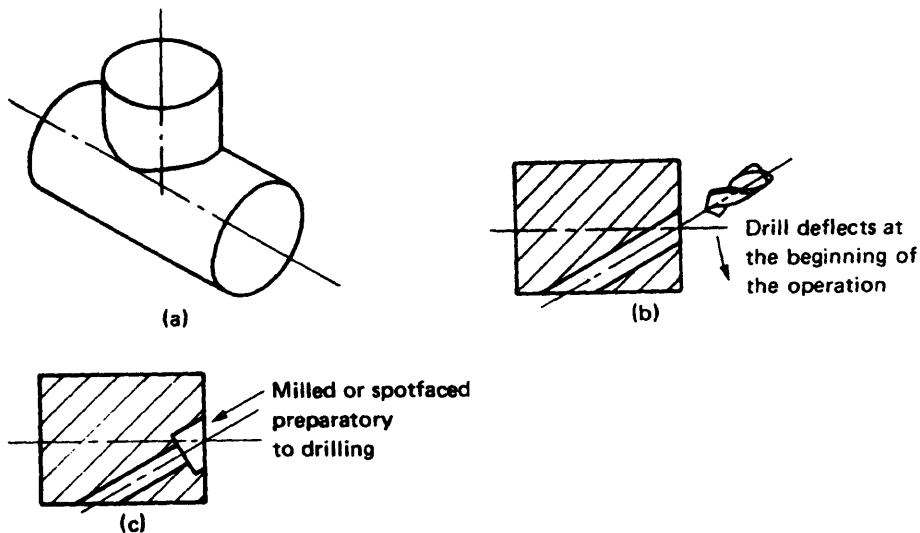
Figure 13.11 Difficulties arising when nonconcentric cylindrical surfaces are specified. (a) Impossible to machine; (b) difficult to machine; (c) can be machined on a drill press.
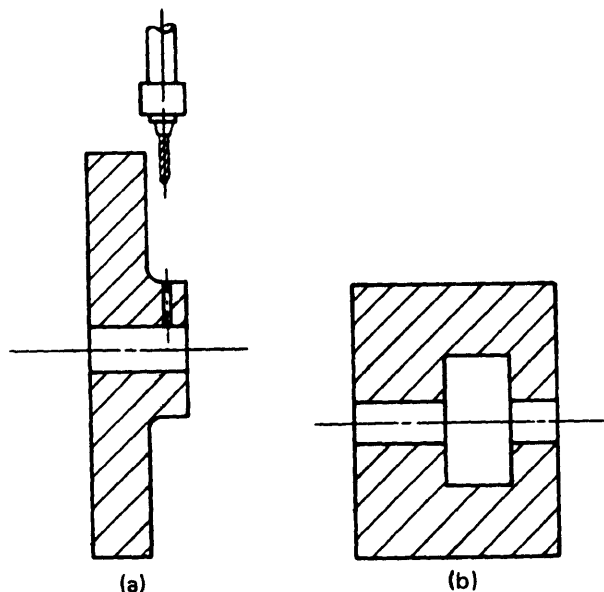
Figure 13.12 Design features to avoid in rotational parts. (a) Special drill required to machine radial hole; (b) impossible to machine internal recess.
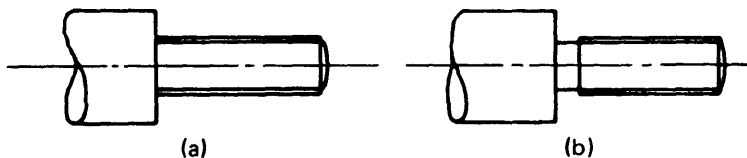
Figure 13.13 Provision of run-out groove for screw threads. (a) wrong; (b) right.

drill would be required. The internal recess shown in the component in Fig. 13.12b could not be machined because it would be impossible to design a cutting tool that would reach through the opening of the bore.

Figure 13.13a shows a screw thread extending to a shoulder. Extending a screw thread to a shoulder would be impossible because when the lathe carriage is disengaged from the lead screw at the end of each pass, the threading tool generates a circular groove in the workpiece. Thus, it is necessary to provide a run-out groove (Fig. 13.13b) so that the threading tool will have clearance and not interfere with the remaining machined surfaces.

Table 13.6 summarizes the rotational-workpiece features readily provided by machining. It should be kept in mind, however, that the relative difficulty of providing some of these features depends on the component's *L/D* ratio. For example, internal features, most readily machined when the *L/D* ratio is small, become increasingly difficult to machine as this ratio is increased. Also, components with a thin section become flexible and difficult to grip firmly; hence, very small or very large *L/D* ratios should be avoided where possible. In general, the features listed in Table 13.6 are placed in increasing order of machining cost.

Table 13.7 summarizes rotational-workpiece features that are more expensive to machine; these features, too, are listed approximately in increasing order of machining cost. Features not in Tables 13.6 and 13.7 should be examined carefully by the designer to see whether an alternative design would save manufacturing costs.

13.5.5 Nonrotational Components [$(A/B) \leqslant 3$, $(A/C) \geqslant 4$]

Nonrotational components having proportions such that the ratio *A/B* is less than or equal to 3 and the ratio *A/C* is greater than or equal to 4 are categorized as flat components and have a first digit of 6. Extremely thin, flat components should be avoided because of the difficulty of work holding in machining external surfaces. Many flat components are machined from plate or sheet stock and initially require machining of the outer

Table 13.6 Readily Provided Machined Features on Rotational Components
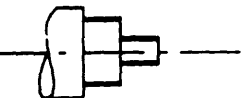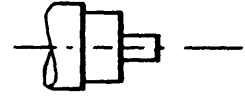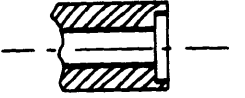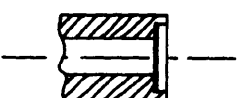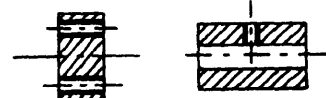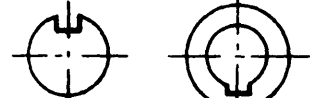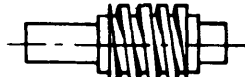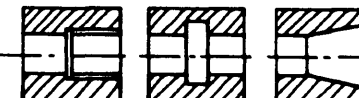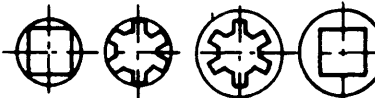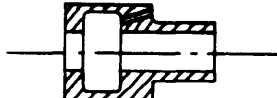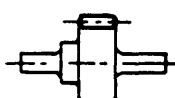
Machine	Type of surface	Orientation and nature of surface	Example
Lathe or vertical-boring machine	External surfaces (exposed when the workpiece is gripped in work-holding device)	Cylindrical concentric surfaces increasing in diameter from the exposed end of the workpiece	
		Plane surfaces normal to the workpiece axis	
	Internal surfaces (accessible when the workpiece is gripped in work-holding device)	Cylindrical, concentric surfaces decreasing in diameter from the exposed end of the workpiece	
		Plane surfaces normal to the workpiece axis	
Drill press	Auxiliary holes	Cylindrical holes radial or parallel to the workpiece axis and in accessible positions	
Milling machine or shaper	Auxiliary plane surfaces	Plane surfaces parallel to workpiece axis and in accessible positions	

Table 13.7 More Expensive Machined Features on Rotational Components

Machine	Type of surface	Orientation and nature of surface	Example
Lathe or vertical-boring machine	External surfaces (concentric)	Screw thread, functional groove, conical surface	
		Operating thread	
	Internal surfaces (concentric)	Screw thread, functional groove, conical surface	
		Operating thread	
Milling machine or broacher	Auxiliary plane surfaces	External spline or polygon section, internal through spline or polygon section	
Drill press	Auxiliary holes	Cylindrical holes not parallel or perpendicular to workpiece axis but in accessible positions	
Gear-cutting machine	Gear teeth	Concentric gear teeth	

edges. Outer edges are generally machined on either a vertical- or horizontal-milling machine. Figure 13.14 shows the simplest shapes that can be generated on the edge of a flat component. It can be seen that internal corners must have radii equal to the radius of the milling cutter used.

In general, the minimum diameter of cutters for horizontal milling [about 50 mm (2 in.) for an average machine] is much larger than the minimum diameter of cutters for vertical milling [about 12 mm (0.5 in.)]. Thus, small internal radii would necessitate vertical milling. However, as can be seen from Fig. 13.14, a flat workpiece that must be machined around the entire periphery will generally be bolted to the machine worktable with a spacer beneath the workpiece smaller than the finished component. This means of work holding will require at least two bolt holes to be provided in the workpiece. In horizontal milling the workpiece can be gripped in a vise. The worktable feed motions in milling machines are generally parallel and perpendicular to the machine spindle, and thus mutually perpendicular flat surfaces are the easiest to machine. The inclined surfaces shown in Fig. 13.14 are more difficult to machine because the workpiece must be reclamped for the purpose.

With flat components required in reasonably large batch sizes, manufacturing costs can often be considerably reduced by simultaneous

(a)   (b)
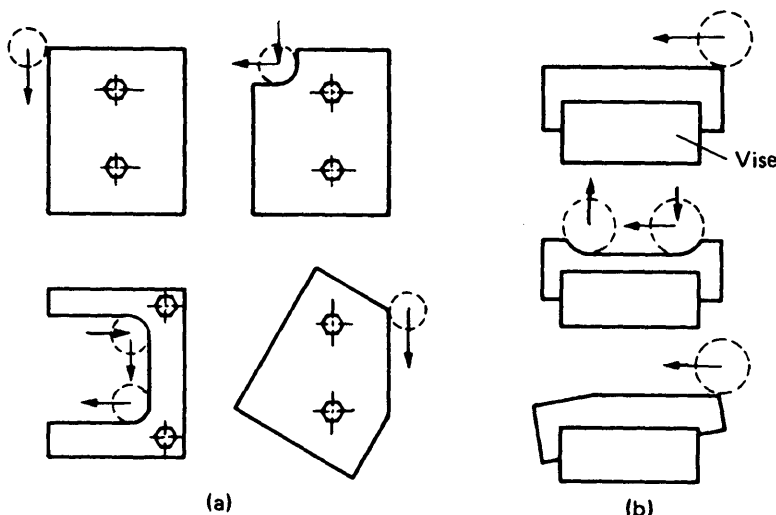
Figure 13.14 Milling external shape of flat components. (a) Vertical milling (plan view); (b) horizontal milling (front view).

machining of a stack of workpieces. A shaper might be used economically for the machining of a stack of workpieces (Fig. 13.15a) and would allow a greater variety of outer shapes to be produced because of the less severe limitations on the radii of inside corners. Also, for flat workpieces that can be stacked for machining and that are required in large quantities, form-milling cutters for horizontal milling can provide almost any outer shape other than undercuts (Fig. 13.15b).

Sometimes, large holes (principal bores) are required in nonrotational components. These principal bores are generally normal to the two large surfaces on the component and require machining by boring. This operation could be performed on a lathe (Fig. 13.16a), where the workpiece would be bolted to a faceplate, or on a vertical borer (Fig. 13.16b), where the workpiece would be bolted to the rotary worktable. For small parts, however, where high accuracy is required, the bores would be machined on a jig borer. A jig borer is similar to a vertical-milling machine, but the spindle is fed vertically and can hold a boring tool (Fig. 13.16c). From these examples it can be seen that where possible, principal bores should be cylindrical and normal to the base of the component. It can also be

(a)

(b)
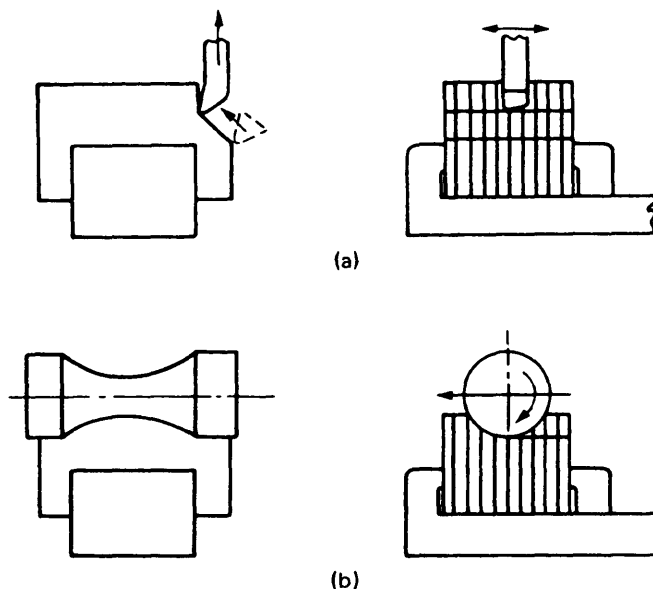
Figure 13.15 Machining of stacked workpieces. (a) Shaping; (b) horizontal milling.
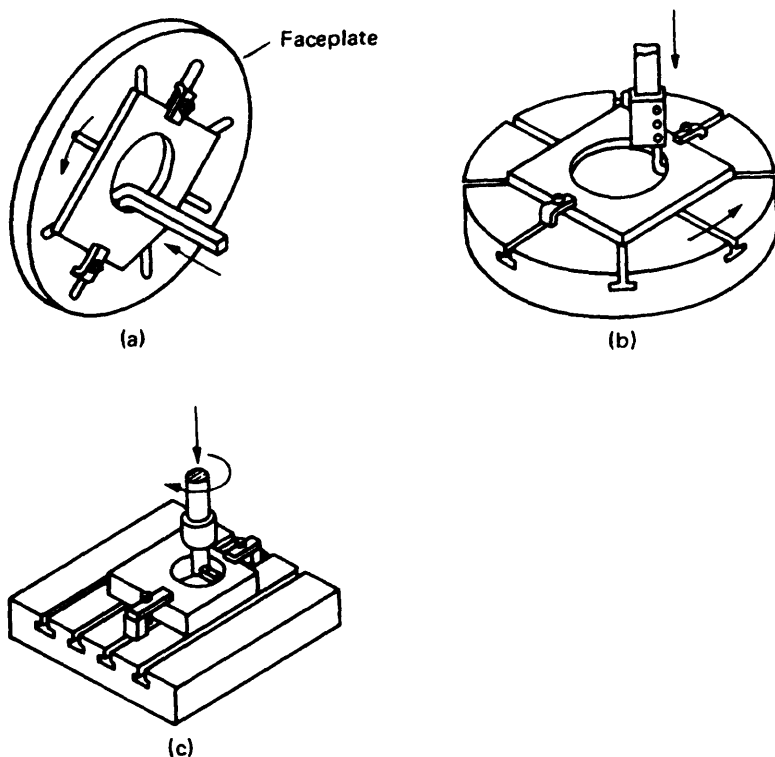
Figure 13.16 Machining of principal bores in nonrotational workpieces. (a) Lathe; (b) vertical borer; (c) jig borer.

seen that a spacer is required between the workpiece and the workholding surface.

The next type of secondary machining operation to be considered is the provision of a series of plane surfaces (represented by the fourth digit in the geometric code). These include the machining of steps, slots, and so on, in one of the large surfaces on the workpiece. If possible, plane-surfacing machining should be restricted to one surface of the component only, thus avoiding the need for reclamping the workpiece. Plane surfaces might be machined on milling machines, shapers, or, in very large workpieces (such as machine beds), on planing machines. Figure 13.17 shows a variety of plane-surface machining operations, and it can be seen that plane-machined surfaces should, if possible, be either parallel or normal to the base of the component. Also, internal radii need not be
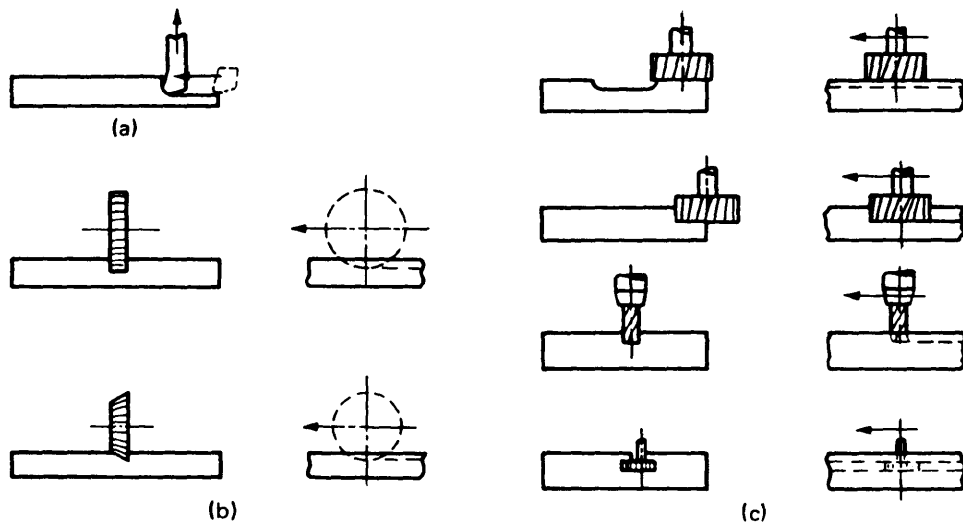
Figure 13.17 Plane-surface machining of flat components. (a) Shaping or planing; (b) horizontal milling; (c) vertical milling.

specified for the milling operations because the corners of the teeth on milling cutters are usually sharp.

Finally, auxiliary holes might be required in flat components, as in the case of disk-shaped, rotational components (Fig. 13.8); and these auxiliary holes would generally be machined on a drill press. Similar requirements to those discussed for the machining of auxiliary holes in disk-shaped rotational components apply. Thus, auxiliary holes should, if possible, be cylindrical and normal to the base of the component and preferably related by a pattern to simplify positioning of the workpiece for drilling.

13.5.6   Nonrotational Components [(A/B) > 3]

Nonrotational components having proportions such that the ratio A/B is greater than 3 are classifed as long components, have a first digit of 7, and are often machined from rectangular- or square-section bar stock. Extremely long components should be avoided because of the difficulties of work holding. The most common machining operations are drilling and milling. For obvious reasons, bored holes should be avoided because generally the workpiece cannot be rotated about the required axis. Also, machined surfaces parallel to the principal axis of the component should

be avoided because of the difficulties of holding down the entire length of the workpiece. Instead, the designer should, if possible, utilize work material preformed to the cross section required.

13.5.7 Nonrotational Components [(A/B) < 3, (A/C) < 4]

Nonrotational components having proportions such that the ratio A/B is less than 3 and the ratio A/C is less than 4 are classified as cubic components; they have a first digit of 8 and are often of quite complicated shape. Cubic components should be provided with at least one plane surface that can initially be surface-ground or milled to provide a base for work-holding purposes and a datum for further machining operations.

If possible, the outer machined surfaces of the component should consist of a series of mutually perpendicular plane surfaces parallel to and normal to its base. In this way, after the base has been machined, further machining operations can be carried out on external surfaces with minimum reclamping of the workpiece. Figure 13.18, for example, shows a cubic workpiece where the external exposed surfaces can all be machined on a vertical-milling machine without reclamping. This figure shows that sharp, internal corners parallel to the base can be machined readily but that sharp, internal corners normal to base should be avoided.

The workpiece shown in Fig. 13.18 is blocklike. However, many cubic components are boxlike, and some are split with flanges provided to allow the two split portions to be bolted together. When the split is provided at a main bore, this main bore is machined with the two sections bolted together. Main bores in cubic components are often machined on a
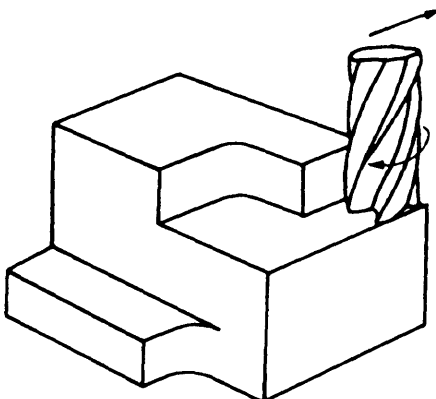
Figure 13.18 Milling outer surface of a cubic workpiece.

horizontal-boring machine. For ease of machining, internal cylindrical surfaces should be concentric and decrease in diameter from the exposed surface of the workpiece. Also, where possible, blind bores should be avoided because in horizontal boring the boring bar must usually be passed through the workpiece. Internal machined surfaces in a boxlike cubic component should be avoided unless the designer is certain that they will be accessible.

With small cubic components it is possible to machine pockets or internal surfaces using an end-milling cutter, as shown in Fig. 13.19. Again it can be seen that internal corners normal to the workpiece base must have a radius equal to that of the cutter. Also, the same cutter will be used to clear out the pocket after machining the outer shape, and the smaller the cutter diameter the longer it will take to perform this operation. Consequently, the cost of the operation will be related to the radii of the vertical internal corners. Thus, internal corners, normal to the workpiece base, should have as large a radius as possible.

Finally, cubic components will often have a series of auxiliary holes. Auxiliary holes should be cylindrical and either normal or parallel to the base of the component; they should also be in accessible positions and have L/D ratios that make it possible to machine them with standard

Cleared after
machining outline
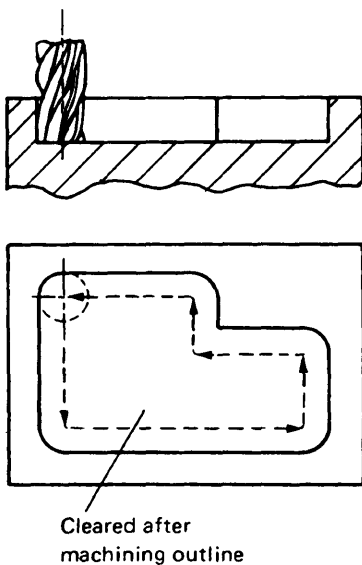
Figure 13.19 Milling a pocket in a blocklike cubic workpiece.

drills. In general, standard drills can produce holes having L/D ratios as large as 5.

Figure 13.20a shows examples of features that would be difficult and expensive to produce in nonrotational components. In the first case the internal vertical corners are shown sharp; these features cannot be produced with standard tools. In the second case the through hole has an extremely large L/D ratio and would be difficult to produce even with special deep-hole drilling techniques. Figure 13.20b shows examples of machined features virtually impossible to produce because a suitable tool cannot be designed that would reach all the internal surfaces. Figure 13.21 shows the design of some blind holes. A standard drill produces a hole with a conical blind end, and therefore the machining of a hole with a square blind end requires a special tool. Thus, the end of a blind hole should be conical. If the blind hole is to be provided with a screw thread, the screw thread will be tapped, and the designer should not specify a fully formed thread to the bottom of the blind hole since this type of screw thread is impossible to produce.

Holes that have a dogleg, or bend, should be avoided if possible. A curved hole (Fig. 13.21) is clearly impossible to machine; however, drilling a series of through holes and plugging unwanted outlets can often achieve the desired effect, although this operation is expensive.

Finally Fig. 13.22 shows an example of a boxlike cubic component

(a)

(b)
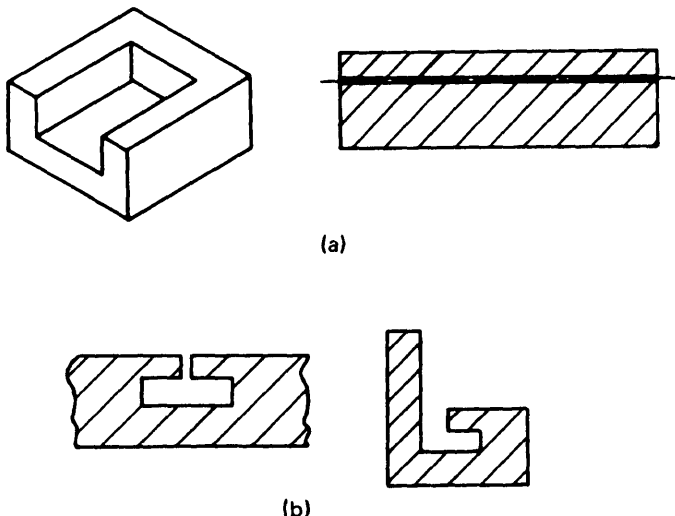
Figure 13.20 Design features to avoid in nonrotational components.

| Difficult | Easy | Impossible | Easy |

| Impossible | Impossible | Possible |
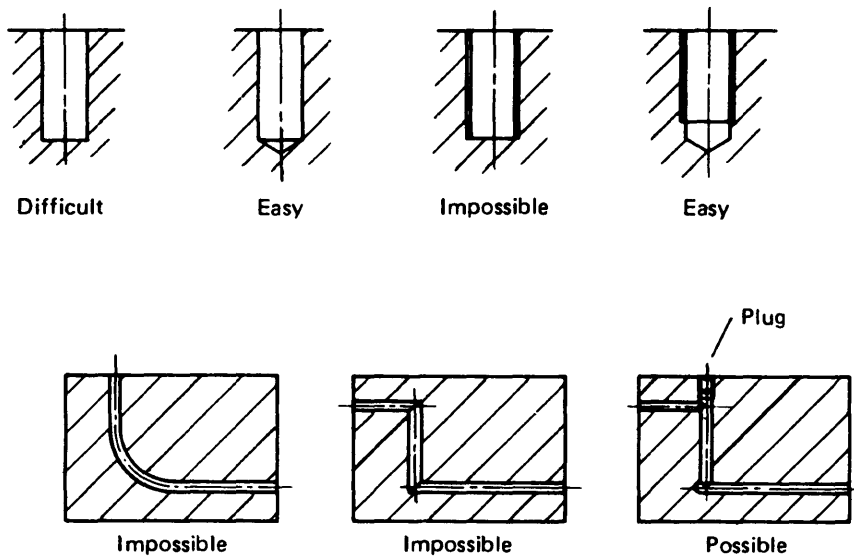
Figure 13.21 Design of blind holes.

Impossible to
machine these surfaces
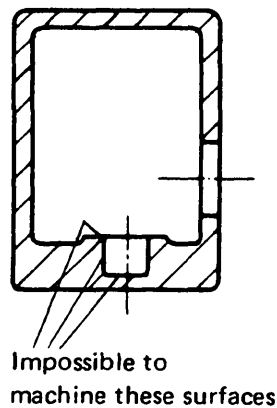
Figure 13.22 Inaccessible internal features in a boxlike cubic component.

Table 13.8 Readily Provided Machined Features on Nonrotational Components
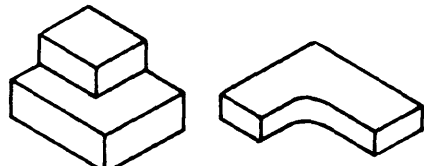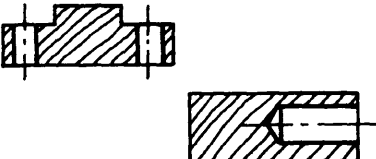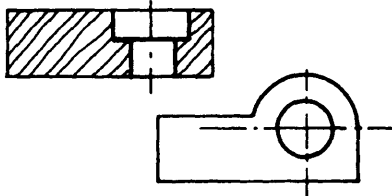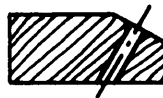
Machine	Type of surface	Orientation and nature of surface	Example
Milling machine shaper, or planer	External (exposed when workpiece is gripped in work-holding device)	Plane surfaces parallel and normal to base with no square internal corners normal to base	
	Plane-surface machining (on surfaces exposed when workpiece is gripped in work-holding device)	Rectangular slots or grooves parallel to base	
Drill press	Auxiliary holes	Cylindrical through holes normal to base Cylindrical blind holes with conical ends	
Lathe, vertical borer, jig borer, or horizontal borer	Principal bores	Cylindrical bores parallel or normal to base and decreasing in diameter from exposed surface of the workpiece	

Table 13.9 More Expensive Machined Features on Nonrotational Components

Machine	Type of surface	Orientation and nature of surface	Example
Milling machine, shaper, or planer	External	Accessible, inclined surfaces	
	Plane surface machining	Nonrectangular slots or grooves on accessible surfaces	
Vertical-milling machine		Accessible internal plane surfaces or pockets parallel or normal to base and with large radii specified for internal corners normal to base	
Drill press	Auxiliary holes	Accessible cylindrical holes inclined to base	
Lathe, vertical borer, jig borer, or horizontal borer	Principal bores	Cylindrical bores with functional grooves	
Gear-cutting machine	Gear teeth	In-line gear teeth on long components	

with internal features that cannot be machined because they are in-accessible.

Table 13.8 summarizes machined features that are relatively easy to provide on nonrotational workpieces in increasing order of cost; Table 13.9 presents machined features that would be more expensive to provide and should be avoided when possible. Again, it should be remembered that the relative difficulty of providing these features depends on the proportions of the component.

13.6 ASSEMBLY OF COMPONENTS

Most machined components must eventually be assembled, and the designer should give consideration to the assembly process. Design for ease of assembly is a separate subject [3]; however, there are one or two aspects of this subject that affect machining and can be mentioned here. The first requirement is, of course, that it should be physically possible to assemble the components. Obviously, the screw thread on a bolt or screw should be the same as the mating thread on the screwed hole into which the bolt or screw is to be inserted. Some assembly problems, however, are not quite so obvious. Figure 13.23 shows some impossible assembly situations, and it is left to the reader to decide why the components cannot be assembled properly.

A further requirement is that each operating machined surface on a component should have a corresponding machined surface on the mating component. For example, where flanges on castings are to be bolted together, the area around the bolt holes should be machined perpendicular to the hole (spot-faced, for example) to provide a proper seating for the bolt heads, nuts, or washers. Also, internal corners should not interfere with the external corner on the mating component. Figures 13.6 and 13.13 were examples of how this interference can be avoided. Finally, incorrect specification of tolerances can make assembly difficult or even impossible.

13.7 ACCURACY AND SURFACE FINISH

A designer will not generally want to specify an accurate surface with a rough finish or an inaccurate surface with a smooth finish. When determining the accuracy and finish of machined surfaces it is necessary to take into account the function intended for the machined surface. The specification of too-close tolerances or too-smooth surfaces is one of the major ways a designer can add unnecessarily to manufacturing costs. Such specifications could, for example, necessitate a finishing process,
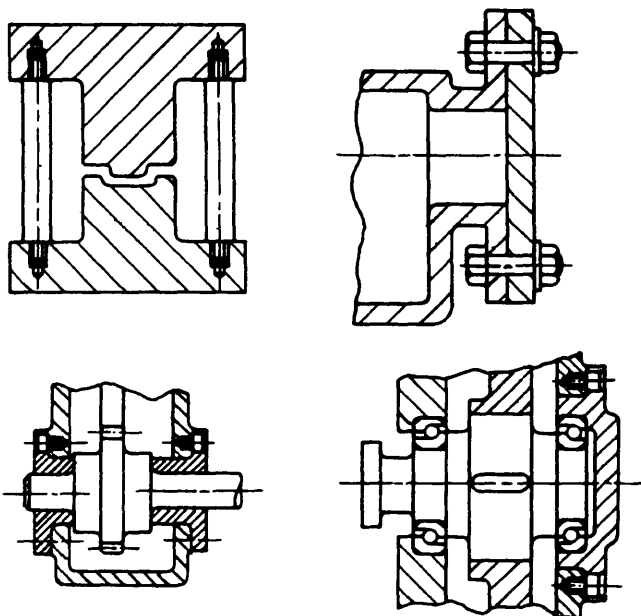
Figure 13.23 Components that cannot be assembled.

such as cylindrical grinding after rough turning, where an adequate accuracy and finish might have been possible using the lathe that performed the rough-turning operation. Thus, the designer should specify the widest tolerances and roughest surface that would give acceptable performance for operating surfaces.

As a guide to the difficulty of machining to within required tolerances it can be stated that

1. Tolerances from 0.127 to 0.25 mm (0.005 to 0.01 in.) are readily obtained.
2. Tolerances from 0.025 to 0.05 mm (0.001 to 0.002 in.) are slightly more difficult to obtain and increase production costs.
3. Tolerances 0.0127 mm (0.0005 in.) or greater require good equipment and skilled operators and add significantly to production costs.

Figure 13.24 illustrates the general range of surface finish that can be obtained in different operations. It can be seen that any surface with a specified surface finish of 1 μm (40 μ in.) arithmetical mean or better will generally require separate finishing operations, which substantially increases costs. Even when the surface can be finished on the same machine, a smoother surface requirement means increased costs.

Surface roughness, μin.

| 1 000 | 500 | 250 | 125 | 63 | 32 | 16 | 8 | 4 | 2 | 1 | 0.5 |

Snag, saw

Turn, shape, mill, bore

Drill

Ream

Grind

Hone

Lap, polish

| 25 | 12.5 | 6.3 | 3.2 | 1.6 | 0.8 | 0.4 | 0.2 | 0.1 | 0.05 | 0.025 | 0.012 5 |

Surface roughness, μm

☐ Typical   ⌐⌐ Less frequent
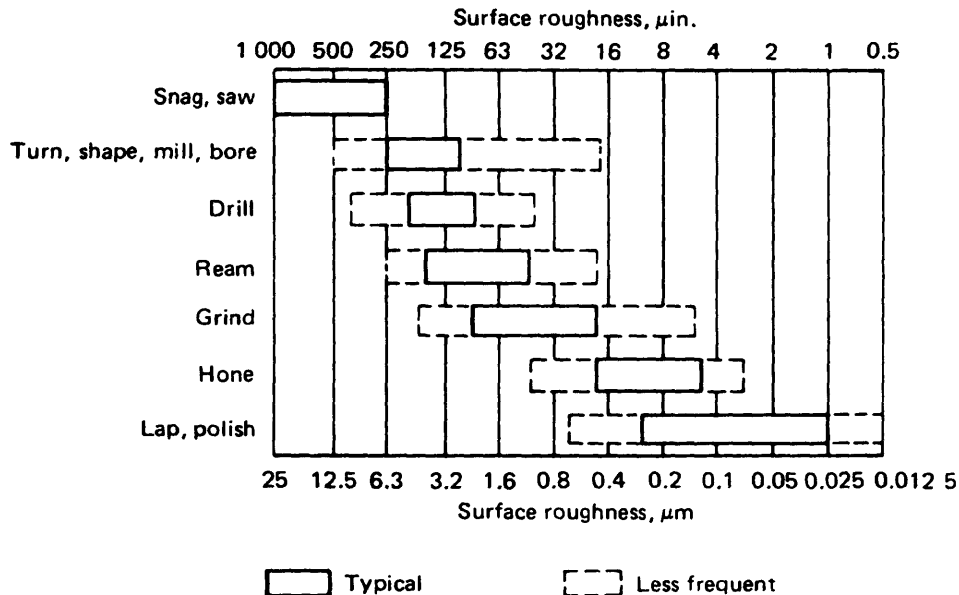
Figure 13.24 General range of surface roughness obtainable by various machining operations.

To illustrate the cost increase as the surface finish is improved, a simple turning operation can be considered. If a tool having a rounded-corner is used under ideal cutting conditions, the arithmetical-mean surface roughness R_a is related to the feed by

$$R_a = \frac{0.0321f^2}{r_\varepsilon} \tag{13.5}$$

where f is the feed and r_ε is the corner radius.

The machining time t_m is inversely proportional to the feed f and related by the equation

$$t_m = \frac{l_w}{fn_w} \tag{13.6}$$

where l_w is the length of the workpiece and n_w is the rotational frequency of the workpiece.

Substitution of f from Eq. (13.5) in (13.6) gives the machining time in terms of the specified surface finish:

$$t_m = \frac{0.18 l_w}{n_w (R_a r_\varepsilon)^{0.5}}$$ (13.7)

Thus, the machining time (and hence the machining cost) is inversely proportional to the square root of the surface finish. Figure 13.25 shows the relationship between production cost and surface finish for a typical turning operation. It can be seen that the costs rise rapidly when low values of surface finish are specified.

For many applications a smooth, accurate surface is essential. This smooth, accurate surface can most frequently be provided by finish grinding. When specifying finish grinding, the designer should take into account the accessibility of the surfaces to be ground. In general, surfaces to
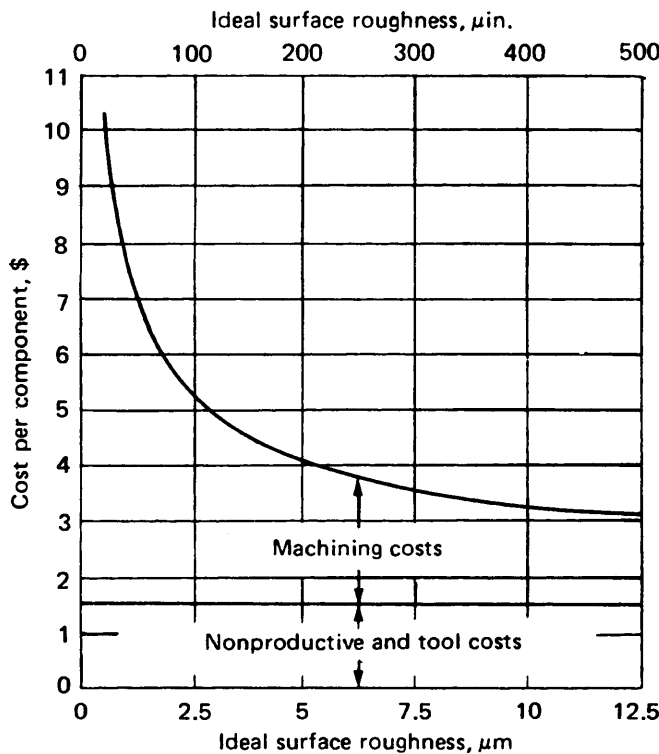
Figure 13.25 Effect of specified surface roughness on production costs in a turning operation, where the corner radius r_ε = 0.03 in. (0.762 mm), the rotational frequency of the workpiece n_w = 200 rpm (3.33 s^{-1}), and the length of the workpiece l_w = 34 in. (864 mm).
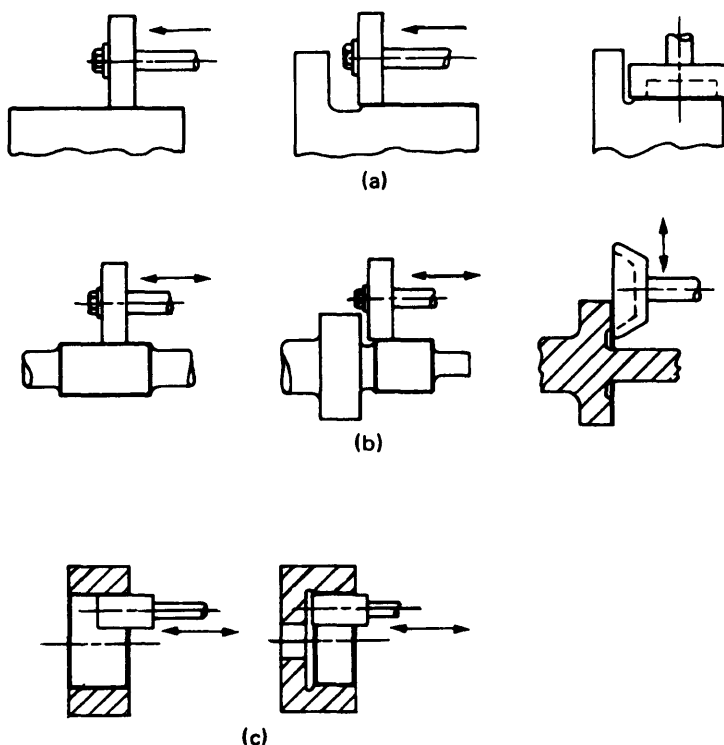
Figure 13.26 Surfaces that can readily be finish-ground. (a) Surface grinding; (b) cylindrical grinding; (c) internal grinding.

be finish-ground should be raised and should never intersect to form internal corners. Figure 13.26 shows the types of surfaces that are most readily finish-ground using standard-shaped abrasive wheels.

13.8   SUMMARY OF DESIGN GUIDELINES

This section lists the various design guidelines that have been developed. The section is intended to provide a summary of the main points a designer should keep in mind when considering the design of machined components.

Standardization

1.   Utilize standard components as much as possible.

2. Preshape the workpiece, if appropriate, by casting, forging, welding, and so on.
3. Utilize standard preshaped workpieces if possible.
4. Employ standard machined features wherever possible.

Raw Material

5. Choose raw materials that will result in minimum component cost (including cost of production and cost of raw material).
6. Utilize raw material in the standard forms supplied.

Component Design

a. General

7. Try to design the component so that it can be machined on one machine tool only.
8. Try to design the component so that machining is not needed on the unexposed surfaces of the workpiece when the component is gripped in the work-holding device.
9. Avoid machined features the company is not equipped to handle.
10. Design the component so that the workpiece, when gripped in the work-holding device, is sufficiently rigid to withstand the machining forces.
11. Verify that when features are to be machined, the tool, tool holder, work, and work-holding device will not interfere with one another.
12. Ensure that auxiliary holes or main bores are cylindrical and have L/D ratios that make it possible to machine them with standard drills or boring tools.
13. Ensure that auxiliary holes are parallel or normal to the workpiece axis or reference surface and related by a drilling patern.
14. Ensure that the ends of blind holes are conical and, in the case of a tapped blind hole, that the thread does not continue to the bottom of the hole.
15. Avoid bent holes or dogleg holes.

b. Rotational Components

16. Try to ensure that cylindrical surfaces are concentric and plane surfaces are normal to the component axis.
17. Try to ensure that the diameters of external features increase from the exposed face of the workpiece.
18. Try to ensure that the diameters of internal features decrease from the exposed face of the workpiece.

19. For internal corners on the component, specify radii equal to the radius of the rounded tool corner.
20. Avoid internal features for long components.
21. Avoid components with very large or very small *L/D* ratios.

c. Nonrotational Components

22. Provide a base for work holding and reference.
23. If possible, ensure that the exposed surfaces of the component consist of a series of mutually perpendicular plane surfaces parallel to and normal to the base.
24. Ensure that internal corners normal to the base have a radius equal to the tool radius. Also ensure that for machined pockets, the internal corners normal to the base have as large a radius as possible.
25. If possible, restrict plane surface machining (slots, grooves, etc.) to one surface of the component.
26. Avoid cylindrical bores in long components.
27. Avoid machined surfaces on long components by using work material preformed to the cross section required.
28. Avoid extremely long or extremely thin components.
29. Ensure that, in flat or cubic components, main bores are normal to the base and consist of cylindrical surfaces decreasing in diameter from the exposed face of the workpiece.
30. Avoid blind bores in large cubic components.
31. Avoid internal machined features in cubic boxlike components.

Assembly

32. Ensure that assembly is possible.
33. Ensure that each operating machined surface on a component has a corresponding machined surface on the mating component.
34. Ensure that internal corners do not interfere with a corresponding external corner on the mating component.

Accuracy and Surface Finish

35. Specify the widest tolerances and roughest surface that will give acceptable performance for operating surfaces.
36. Ensure that surfaces to be finish-ground are raised and never intersect to form internal corners.

13.9   EARLY COST ESTIMATING FOR MACHINED COMPONENTS

Designers normally have a reasonable knowledge of the factors to bear in mind when attempting to minimize manufacturing costs for machined

components, and the previous section listed some design rules that might be followed. Ultimately, however, the designer needs to know the magnitude of the effects of design decisions on manufacturing costs. The need for a method of estimating these costs is highlighted when considering the design of a product for ease of assembly. Techniques have been available for some time for analyzing an assembly in terms of the handling and insertion costs incurred as each part is added [3]. As a result of such analyses, many suggestions for design simplifications arise—often involving the elimination of individual parts or components. What has been lacking, however, are methods for quickly estimating the cost of these parts and the cost of tooling so that the total savings in products costs can be quantified.

Before embarking on a discussion of how an estimating method for designers might be developed, we should consider how the requirements for such a method differ from conventional cost-estimating procedures. These conventional procedures are meant to be applied after the component has been designed and its production planned. Thus, every step in production is known and can be estimated with a high degree of accuracy. During the early stages of design, however, the designer will not wish to specify, for example, all the work-holding devices and tools that might be needed; most likely, detailed design will not yet have taken place. Indeed, a final decision on the specific work material might not have been made at this stage. Thus, what is wanted is an approximate method requiring minimum information from the designer and assuming that the ultimate design will avoid unnecessary manufacturing expense and that the component will be manufactured under reasonably economic conditions.

Perhaps the simplest approach would be to have the designer specify the shape and size of the original workpiece and the quantity of material to be removed by machining. Then, with data on typical material costs per unit weight, an estimate can be made of the cost of the material needed to manufacture the component. If an approximate figure were available for the average cost of removal of each cubic inch of the material by machining, an estimate could also be made of the machining cost.

Unfortunately, this very simple approach will not take adequate account of the nonproductive costs involved in a series of maching operations. For example, if one cubic inch of material were to be removed in one pass by a simple turning operation, the nonproductive costs would be quite small—the component need only be loaded into the lathe and unloaded once—and the cutting tool need only be set and the feed engaged once. Compare this with one cubic inch of the same material removed by a combination of turning, screwing, milling, and drilling. In this case the nonproductive costs accumulate and become a highly significant factor in

Table 13.10 Approximate 1987 Costs (in cents/lb) for Various Metals[a]

Metal	Density lb/in^3	Mg/m^3	Bar	Rod	Sheet	Plate	Tube
Ferrous					<0.5 in	>0.5 in	
Carbon steel (cold-rolled)	0.283	7.83	51	51	36	42	92
Alloy steel	0.31	8.58	75	75	120	—	—
Stainless steel	0.283	7.83	150	150	250	250	—
Tool steel	0.283	7.83	644	644	—	644	—
Nonferrous							
Aluminum alloys	0.10	2.77	193	193	195	250	460
Brass	0.31	8.58	90	122	190	190	190
Nickel alloys	0.30	8.30	570	570	570	570	—
Magnesium alloys	0.066	1.83	335	335	606	606	335
Zinc alloys	0.23	6.37	150	150	150	150	—
Titanium alloy	0.163	4.51	1540	1540	2500	2500	—

[a]To convert to cents/kg multiply by 2.2.

Table 13.11 Loading and Unloading Times (s) versus Workpiece Weight[a]

Holding device	0–0.2 0–0.4	0.2–4.5 0.4–10	4.5–14 10–30	14–27 kg 30–60 lb	Crane
Angle plate (two U-clamps)	27.6	34.9	43.5	71.2	276.5
Between centers, no dog	13.5	18.6	24.1	35.3	73.1
Between centers, with dog	25.6	40.2	57.4	97.8	247.8
Chuck, universal	16.0	23.3	31.9	52.9	—
Chuck, independent (four jaws)	34.0	41.3	49.9	70.9	—
Clamp on table (three clamps)	28.8	33.9	39.4	58.7	264.6
Collet	10.3	15.4	20.9	—	—
Face Plate (three clamps)	31.9	43.3	58.0	82.1	196.2
Fixture, horizontal (three screws)	25.8	33.1	41.7	69.4	274.7
Fixture, vertical (three screws)	27.2	38.6	53.3	—	—
Hand-held	1.4	6.5	12.0	—	—
Jig	25.8	33.1	41.7	—	—
Magnet table	2.6	5.2	8.4	—	—
Parallels	14.2	19.3	24.8	67.0	354.3
Rotary table or Index plate (three clamps)	28.8	36.1	44.7	72.4	277.7
"V" Blocks	25.0	30.1	35.6	77.8	365.1
Vise	13.5	18.6	24.1	39.6	174.2

[a]After Fridriksson [4].

the ultimate cost of the machined component, especially when the machined component is relatively small.

What is needed is a method that forms a compromise between this oversimplified approach and the traditional detailed cost-estimating methods used by manufacturing and industrial engineers.

13.9.1 Material Cost

Often, the most important factor in the total cost of a machined component is the cost of the original workpiece. This material cost will frequently form more than 50 percent of the total cost and, therefore, should be estimated with reasonable care. Table 13.10 gives densities and approximate 1987 costs in cents per pound for a variety of materials in the basic shapes normally available. Provided the designer can specify the volume of material required for the original workpiece, the material cost can easily be estimated. Although the figures in Table 13.10 can be used as a rough guide, the designer can obtain more accurate figures from material suppliers.

13.9.2 Machine Loading and Unloading

Nonproductive costs are incurred every time the workpiece is loaded into (and subsequently unloaded from) a machine tool. An exhaustive study of loading and unloading times has been made by Fridriksson [4]; he found that these times can be estimated quite accurately for a particular machine tool and work-holding device if the weight of the workpiece is known. Some of Fridriksson's results are presented in Table 13.11, which can be used to estimate machine loading and unloading times. To these figures must be added the times for turning coolant on and off, cleaning the work-holding or clamping device, and so on.

13.9.3 Other Nonproductive Costs

For every pass, cut, or operation carried out on one machine tool, further nonproductive costs are incurred. In each case the tool must be positioned, perhaps the feed and speed settings changed, the feed engaged, and then, when the operation is completed, the tool withdrawn. If different tools are employed, the times for tool engagement or indexing must also be taken into account. Time elements for these tasks for different types of machine tools can be found in the literature. An averages time for these operations on a CNC turret lathe would be around 1.5 s.

13.9.4 Handling Between Machines

One of the costs to be considered is that incurred in moving batches of partially machined workpieces between machines. Fridriksson [4] made a

study of this by assuming that stacks of pallets of workpieces were moved around the factory using forklift trucks. He developed the following expression for t_f, the transportation time for a round trip by a forklift truck

$$t_f = 25.53 + 0.95 \, (l_p + l_{rd}) \text{ s} \tag{13.8}$$

where l_p is the length of the pathway between machines and l_{rd} is the distance the truck must travel to respond to a request (both lengths are measured in feet).

Assuming that $(l_p + l_{rd})$ is 139 m on average and that for every trip with a load of full pallets, a trip must be made with empty pallets, the total time is

$$t_f = 315 \text{ s} \tag{13.9}$$

If a full load of pallets and workpieces is 2000 lb, the number of workpieces of weight W transported will be $2000/W$ and the time per workpiece t_{tr} will be given by

$$t_{tr} = \frac{315}{2000/W} = 0.156W \text{ s} \tag{13.10}$$

Thus, for a workpiece weighing 10 lb, the effective transportation time is only 1.6 s, which is small compared with the loading and unloading time of between 19 and 43 s for that size of workpiece (Table 13.11). However, allowances for transportation time can be added to the loading and unloading times and these will become significant for large workpieces.

13.9.5 Material Type

The so-called machinability of a work material has been one of the most difficult factors to define and quantify. In fact, it is impossible to predict the difficulty of machining a material from a knowledge of its composition or its mechanical properties, without performing a machining test. Nevertheless, it is necessary for the purposes of cost estimating to employ published data on machinability. Perhaps the best source of such data, presented in the form of recommended cutting conditions, is the *Machining Data Handbook* [5].

13.9.6 Machining Costs

The machining cost for each cut, pass, or operation is incurred during the period between the feed being engaged and finally disengaged. It should

be noted that the tool is not cutting for the whole of this time because allowances for tool engagement and disengegement must be made—particularly for milling operations. However, typical values for these allowances can be found and are presented for lathe operations in Table 13.12 as correction factors to be applied to the actual machining time.

For an accurate estimation of actual machining time, it is necessary to know the cutting conditions, namely, cutting speed, feed and depth of cut in single-point tool operations, and feed speed, depth of cut, and width of cut in multipoint tool operations. Tables giving recommended values for these parameters for different work materials can fill large volumes such as the Metcut *Machining Data Handbook* [5].

Analysis of the selection of optimum machining conditions shows that the optimum feed (or feed per tooth) is the largest that the machine tool and cutting tool can withstand. Then, selection of the optimum cutting speed can be made by minimizing machining costs. The resulting combination of cutting speed and feed in a single-point tool operation gives a rate for the generation of the machined surface that can be measured in in.^{2}/min, for example. The inverse of such rates are presented by Ostwald [6] for a variety of workpiece and tool materials and for different roughing and finishing operations. A problem arises, however,

Table 13.12   Allowances for Tool Approach Engagement and Disengagement[a]

Operations	Allowances	
English units		
Turn, face, cutoff, bore, groove, thread	$t'_m = t_m + 5.4$	$d_a > 2$
	$t'_m = t_m + 1.35d_a^2$	$d_a < 2$
Drill (twist) (approach)	$t'_m = t_m(1 + 0.5d_a/l_m)$	
Drill (twist) (start)	$t'_m = t_m + (88.5/R_{sg})d_a^{1.67}$	
Metric units		
Turn, face, cutoff, bore, groove, thread	$t'_m = t_m + 5.4$	$d_a > 0.05$
	$t'_m = t_m + 2200d_a^2$	$d_a < 0.05$
Drill (twist) (approach)	$t'_m = t_m(1 + 0.5d_a/l_m)$	
Drill (twist) (start)	$t'_m = t_m + (25.9/R_{sg})d_a^{1.67}$	

[a]Adapted from Ostwald [2].
t_m = machining time, s; d_a = diameter of work surface, diameter of drilled hole, or diameter of machined surface, in.(m); l_m = length of machined surface in direction of cutting, in.(m); R_{sg} = rate of surface generation, in.^{2}/min (m^2/min) (Table 13.13).

when applying the figures for roughing operations. For example, Ostwald recommends a cutting speed of 500 ft/min (2.54 m/s) and a feed of 0.02 in. (0.51 mm) for the rough machining of low-carbon steel (170 Bhn) with a carbide tool. For a depth of cut of 0.3 in. (7.6 mm) this would mean a metal removal rate of 36 in.^{3}/min (9.82 µm^3/s). The *Machining Data Handbook* [5] quotes a figure of 1.35 hp min/in.^{3} (3.69 GJ/m^3) (unit power) for this work material. Thus, the removal rate obtained in this example would require almost 50 hp (36 kW). Since a typical medium-sized machine tool would have a 5 to 10 hp motor (3.7 to 7.5 kW) and an efficiency of around 70 percent, it can be seen that the recommended conditions could not be achieved except for small depths of cut. Under normal rough machining circumstances, therefore, a better estimate of machining time would be obtained from the unit horsepower (specific cutting energy) for the material, the volume of material to be removed, and the typical power available for machining.

For multipoint tools such as milling cutters, finishing and roughing costs are not usually distinguished. The chip load (feed per tooth) and the cutting speed are usually recommended for given tool materials. However, in these cases the machining time is not directly affected by the cutting speed but by the feed speed, which is controlled independently of the cutter speed. Thus, assuming that the optimum cutting speed is being employed, the feed speed that will give the recommended feed per tooth can be used to estimate the machining time. Again, a check must be made that the power requirements for the machine tool are not excessive.

13.9.7 Tool Replacement Costs

Every time a tool needs replacement because of wear, two costs are incurred: (1) the cost of machine idle time while the operator replaces the worn tool, and (2) the cost of providing a new cutting edge or tool. The choice of the best cutting speed for particular conditions is usually made by minimizing the sum of the tool replacement costs and the machining costs since both of these are affected by changes in the cutting speed.

Neglecting nonproductive costs, the cost of machining a feature in one component on one machine tool can be expressed by:

$$C_m = Mt_m + \frac{Q(Mt_{c_t} + C_t)t_m}{t} \qquad (13.11)$$

where

M = machine and operator rate

t_m = machining time (time the machine tool is operating)

Q = proportion of t_m for which a point on the tool cutting edge is contacting the workpiece

t = tool life while the cutting edge is contacting the workpiece

t_{c_t} = tool-changing time

C_t = cost of providing a new cutting edge

Now the machining time t_m is given by

$$t_m = \frac{k}{v} \tag{13.12}$$

where k is a constant for the particular operation and v is the cutting speed. Also, the tool life t is given by Taylor's tool-life equation:

$$vt^n = v_r t_r^n \tag{13.13}$$

where v_r and t_r are the reference cutting speed and tool life, respectively, and n is the Taylor tool-life index, which is dependent mainly on the tool material. Usually, for high-speed steel tools n is assumed to be 0.125 and for carbide tools, 0.25.

If Eqs. (13.12) and (13.13) are substituted into Eq.(13.11), the resulting expression is differentiated to give the cutting speed for minimum cost, and finally the optimum cutting speed is substituted in Eq. (13.11) to give the minimum cost of machining C_{min}, it can be shown that

$$C_{min} = \frac{Mt_{m_c}}{1 - n} \tag{13.14}$$

where t_{m_c} is the machining time when the optimum cutting speed is used.

It can be seen that the factor $1/(1 - n)$ applied to the machining time will allow for tool replacement costs provided that the cutting speed for minimum cost is always employed. The factor would be 1.14 for high-speed steel tooling and 1.33 for carbides. Under those circumstances, where use of optimum cutting conditions would not be possible because of power limitations, it is usually recommended that cutting speed be reduced. This is because greater savings in tool costs will result than if the feed were reduced. When cutting speed has been reduced, with a corresponding increase in machining time, the correction factor given by Eq. (13.14) will overestimate tool costs. If t_{m_p} is the machining time where the

cutting speed v_{p_o} giving maximum power is used, the machining cost C_p will be given by

$$C_p = Mt_{m_p} + \frac{Q(Mt_{c_t} + C_t)t_{m_p}}{t_{p_o}} \tag{13.15}$$

where t_{p_o} is the tool life obtained under maximum-power conditions which, from Taylor's tool-life equation, is

$$t_{p_o} = t_c \left(\frac{v_{p_o}}{v_c} \right)^{(1/n)} \tag{13.16}$$

The tool-life t_c under minimum-cost conditions is given by

$$t_c = \left[\frac{1-n}{n} \right] Q \left(t_{c_t} + \frac{C_t}{M} \right) \tag{13.17}$$

Substituting Eqs. (13.16) and (13.17) in Eq. (13.15) and using the relation in Eq. (13.12) gives

$$C_p = Mt_{m_p} \left[1 + \left(\frac{n}{1-n} \right) \left(\frac{t_{m_c}}{t_{m_p}} \right)^{(1/n)} \right] \tag{13.18}$$

Thus, Eq. (13.18) can be used instead of Eq. (13.14) when the cutting speed is limited by the power available on the machine tool.

13.9.8 Machining Data

In order to employ the approach described above, it is necessary to be able to estimate, for each operation, the machining time t_{m_c} for minimum-cost conditions and the machining time t_{m_p} where the cutting speed is limited by power availability. We saw earlier that machining data for minimum cost presented in handbooks can be expressed in terms of the rate at which machined surfaces can be generated. Table 13.13 gives typical values of the surface generation rates R_{sg} for several material classifications selected and for rough-turning operations with HSS tools or brazed-carbide tools. These values were adapted from the data in the *Machining Data Handbook* [5]. Analysis of the handbook data shows that if dis-posable-insert carbide tools are to be used, then the data for brazed-carbide tools can be multiplied by an average factor of 1.17.

When turning a workpiece of diameter d_a for a length l_m, the figures for

Table 13.13 Machining Data for a Variety of Metals[a,b]

Material	Hardness (Bhn)	Turning and boring			Drilling and reaming (1 in.)	
		R_{sg} (in.^{2}/min)			R_{sg} (in.^{2}/min)	
		HSS	Brazed Carb.	p_s(hp/in.^{3}/min)	HSS	p_s(hp/in.^{3}/min)
Low-carbon steel (free machining)	150–200	25.6	100	1.1	33.0	0.95
Low-carbon steel	150–200	22.4	92	1.35	13.4	1.2
Medium- and high-carbon steel	200–250	18.2	78	1.45	15.1	1.4
Alloy steel (free machining)	150–200	23.7	96	1.3	16.4	1.15
Stainless, ferritic (annealed)	135–185	12.6	48	1.55	9.4	1.35
Tool steels	200–250	12.8	54	1.45	6.2	1.4
Nickel alloys	80–360	9	42	2.25	14.3	2.0
Titanium alloys	200–275	12.6	24	1.35	7.9	1.25
Copper alloys (soft) (free-machining)	40–150	76.8	196	0.72	38.4	0.54
Zinc alloys (die cast)	80–100	58.5	113	0.3	51.1	0.2
Magnesium and alloys	40–90	162	360	0.18	75.2	0.18
Aluminum and alloys	30–80	176	352	0.28	79.8	0.18

Factor	Function	Turning, facing, boring								
k_f	finishing	0.60								
k_i	disposable insert	1.17								

Factor	Function	Tool diameter (in.) (mm)								
		1/16	1/8	1/4	1/2	3/4	1	1.5	2	in.
k_h	Drilling	1.59	3.18	6.35	12.7	19.1	25.4	38.1	50.8	mm
		0.08	0.19	0.35	0.60	0.83	1.00	1.23	1.48	

Factor	Function	Length/diameter ratio					
		<2	3	4	5	6	8
k_d	Deep holes	1.00	0.81	0.72	0.56	0.52	0.48

[a]Adapted from Machining Data Handbook [3].

[b]To convert in.^{2}/min to m^2/min, multiply by 6.45×10^{-4}. To convert hp · min/in.^{3} to GJ/m^3, multiply by 2.73.

Notes: (1) All data are for rough machining. For finish machining, multiply by k_f. (2) The term *carbide* refers to tools with brazed-carbide inserts. For tools with disposable carbide inserts, multiply by k_i. (3) Data for drilling are for 1.0-in.-diameter tools with hole depth/diameter less than 2. For other diameters, multiply by k_h. For deep holes also multiply by k_d.

R_{sg} given in Table 13.13 would be divided into the surface area ($A_m = (\pi)l_m d_a$) to give the machining time t_{m_c}. Thus

$$t_{m_c} = \frac{60 A_m}{R_{sg}} \text{ s} \tag{13.19}$$

If the operation is one of facing, it can be assumed that the conditions giving minimum cost at the start of the cut are used.

For an estimate of the machining time t_{m_p} for maximum power it is necessary to know the power available for machining and the unit power p_s (specific cutting energy) for the work material. Table 13.13 gives average values of p_s for the selection of work materials employed here.

When estimating the power available for machining P_m, it should be realized that small components will generally be machined on small machines with low power available, whereas larger components will be machined on large, higher-powered machines. For example, a small engine lathe may have less than 2 hp available for machining whereas an average-sized lathe may have 3 to 5 hp available. A larger vertical lathe will perhaps have 10 to 30 hp available. Typical power values for some CNC lathes are presented in Fig. 13.27, where the horsepower available for machining P_m is plotted against the typical weight capacity of the machine.

The machining time for maximum power is given by

$$t_{m_p} = \frac{60 V_m p_s}{P_m} \text{ s} \tag{13.20}$$

where V_m is the volume of material to be removed in the turning operation. If a_p is the depth of cut, then V_m would be given approximately by $\pi d_a l_m a_p$. However, for a facing or cutoff operation, the power limitations apply only at the beginning of the cut and the machining time will be longer than that given by Eq. (13.20). If d_a is the outer diameter and d_b is the inner diameter for the facing operation, it can be shown that a multiplying factor of $2d_a/(d_a + d_b)$ must be applied to the machining time. Thus, with a cutoff operation for a solid bar the correction factor will be 2, meaning that the machining time will be twice that obtained by assuming maximum power usage throughout the operation. This same correction factor can also be employed when considering the machining time t_{m_c} based on the machined surface area to be generated.
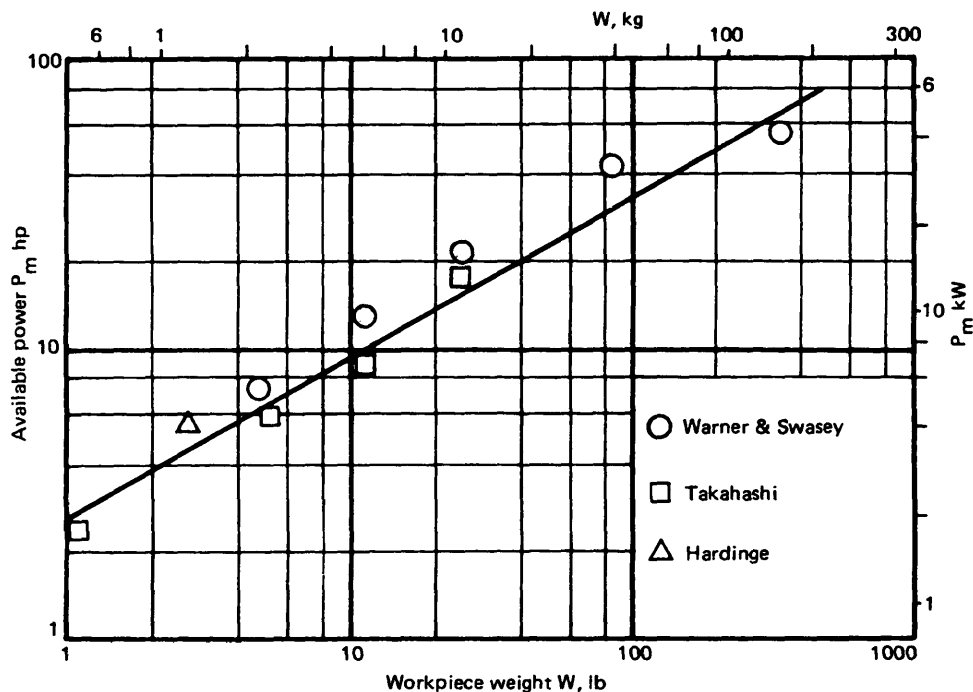
Figure 13.27 Relation between horsepower and workpiece weight for some CNC lathes.

13.9.9 Example

We shall estimate the machining cost for a facing operation on a free-machining steel bar 3 in. (76.2 mm) diameter and 10 in. (254 mm) long, where 0.2 in. (5.1 mm) is to be removed from the end of the bar using a brazed-type carbide tool. The surface area to be generated is

$$A_m = \left(\frac{\pi}{4}\right)(3)^2 = 7.05 \text{ in.}^2 \text{ (4.5 mm}^2\text{)}$$

and the volume of metal to be removed is

$$V_m = \left(\frac{\pi}{4}\right)(3)^2(0.2) = 1.41 \text{ in.}^3 \text{ (23.1 } \mu\text{m}^3\text{)}$$

For this work material–tool material combination, Table 13.13 gives a value of the surface generation rate R_{sg} of 100 in.^{2}/min (0.065 m^2/min) and from Eq. (13.19) the machining time is

$$t_{m_c} = 60(2)\left(\frac{7.07}{100}\right) = 8.5 \text{ s}$$

where the factor of 2 is applied for a facing or cutoff operation.
The weight of the workpiece is estimated to be

$$W = \frac{\pi}{4}(3)^2(10)(0.28) = 20 \text{ lb } (9.07 \text{ kg})$$

From Fig. 13.27 the power available for machining on a CNC chucking lathe would be approximately given by

$$P_m = 15 \text{ hp } (11.2 \text{ kW})$$

Table 13.13 gives a value of specific cutting energy (unit power) of 1.1 hp · min/in.^{3} (3 GJ/m^3) and so, from Eq. (13.20), the machining time at maximum power is

$$t_{m_p} = 60(2)(1.1)\left(\frac{1.41}{15}\right) = 12.4 \text{ s}$$

Again, the factor of 2 has been applied for facing a solid bar.
It can be seen that in this case the conditions for minimum cost cannot be used because of power limitations and that a machining time of 12.4 s will be required. Now we can apply the factor given by Eq. (13.18) to allow for tool costs.
For carbide tools the Taylor tool-life index is approximately 0.25, and since the ratio t_{m_c}/t_{m_p} is 8.5/12.4 or 0.69, the correction factor is

$$\left[1 + \left(\frac{0.25}{1 - 0.25}\right)(0.69)^{(1/0.25)}\right] = 1.07$$

and the corrected machining time is 12.4(1.07) or approximately 13.3 s.
In this example the correction factor for tool costs is fairly small because cutting speeds below those giving minimum costs are being employed. If optimum speeds could be used, the correction factor would be 1.33 and and the corrected machining time would be 11.2 s.
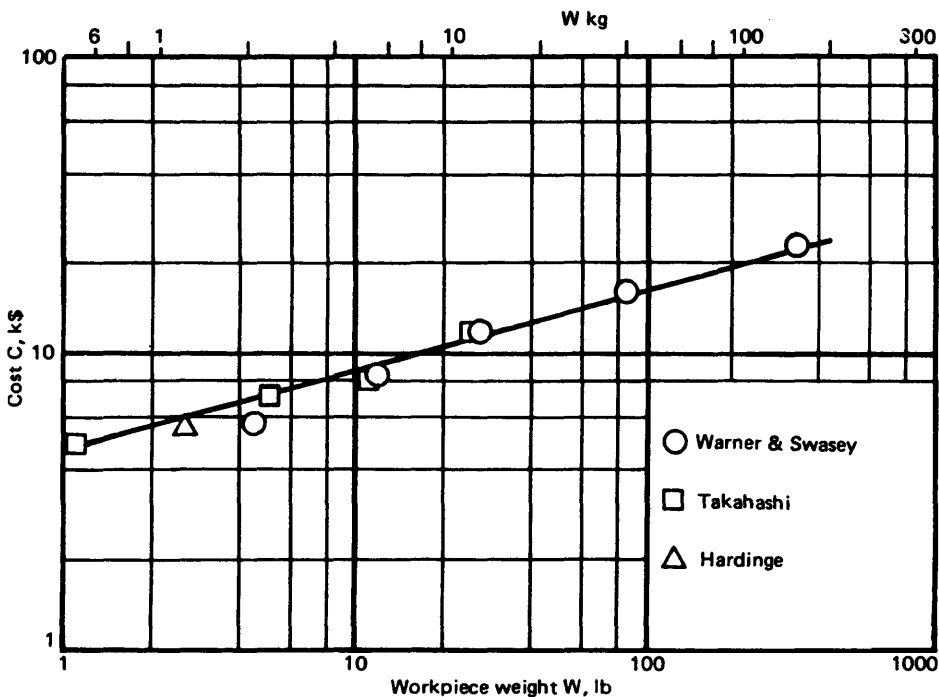
Figure 13.28 Relation between cost and workpiece weight for some CNC lathes.

Finally, in Fig. 13.28, data is presented on the typical cost of CNC lathes, where it can be seen that for the present example, a cost of about $10,000 would be appropriate. Assuming that the total rate for the operator and the machine would be $30 per hour or $0.0083 per second, the machining cost for the facing operation would be $0.11.

13.9.10 Approximate Cost Model for Turning

Figure 13.27 presented some data for CNC lathes. It can be seen that the power P_m available for machining can be expressed by

$$P_m = aW^b \tag{13.21}$$

where W is the initial weight of the workpiece and a, b are constants for the machine tool type.

The machining time for roughing operations, where maximum power is used, is therefore given by

$$t_{m_p} = \frac{60 r_v p_s W}{\rho a W^b} = \left(\frac{60 r_v p_s}{\rho a}\right) W^{(1-b)} \text{ s} \qquad (13.22)$$

where r_v is the proportion of the initial volume (or weight) of the workpiece to be removed by machining, p_s is the specific cutting energy or unit power for the work material, and ρ is the density of the work material.

The nonproductive time t_{np} is given by

$$t_{np} = \frac{t_{sa} + n_t t_{sb}}{B_s} + t_{ln} + n_o t_{pt} \text{ s} \qquad (13.23)$$

where t_{sa} is the basic set-up time, t_{sb} is the set-up time per tool, B_s is the batch size, t_{ln} is the loading and unloading time, t_{pt} is the tool-positioning time per operation, n_t is the number of tools, and n_o is the number of operations.

The loading and unloading time t_{ln} depends on the weight of the workpiece. Typical values for workpieces weighing less than 60 lb (27 kg), were presented in Table 13.11, and for chucking lathes this data when adjusted by adding the times for chuck cleaning and similar operations, can be expressed approximately by

$$t_{ln} = c + dW \qquad (13.24)$$

where c and d are constants equal to 38 and 1.1, respectively, when W is in pounds.

Approximate figures for the cost of CNC lathes were presented in Fig. 13.28, where it can be seen that the cost C_t of a machine tool can be expressed by

$$C_t = e W^f \text{ k\$} \qquad (13.25)$$

where e and f are constants.

If this cost is to be amortized over n_y years and the number of shifts is n_s, then the total rate R_t for the machine and operator is

$$R_t = \frac{k_m e W^f}{2 n_y n_s} + k_o R_o \qquad (13.26)$$

where R_o is the direct labor rate and k_m, k_o are factors to allow for machine and operator overheads, respectively.

If finish machining is to be carried out with a single-point tool, it can be assumed that this will be done under recommended conditions. These

conditions can be described by a machinability factor R_{sg} for the material, which is the product of speed and feed and is the rate at which the machined surface is generated. The finish machining time t_{m_c} will then be given by

$$t_{m_c} = \frac{60A_m}{R_{sg}} \text{ s} \tag{13.27}$$

where A_m is the surface area to be generated.

Worn-tool replacement costs can be significant when operating under optimum (minimum cost) conditions. It was shown earlier that these costs can be allowed for by modifying Eq. (13.27) as follows:

$$t'_{m_c} = \frac{60A_m}{R_{sg}} \left(\frac{1}{1-n}\right) \tag{13.28}$$

where n is the Taylor tool-life index.

When machining is carried out at maximum power, the corrected value of t_{m_p} to allow for tool replacement costs is

$$t'_{m_p} = t_{m_p}\left[1 + \left(\frac{n}{1-n}\right)\left(\frac{t_{m_c}}{t_{m_p}}\right)^{1/n}\right] \text{ s} \tag{13.29}$$

when $t_{m_c}/t_{m_p} < 1$. However, this correction will be small unless maximum-power conditions are close to the recommended conditions, which will usually not be the case for finishing operations.

13.9.11 Typical Rotational Component

As an example we can consider a rotational component machined on a CNC turret lathe. In a study of the turning requirements for British Industry [7] it was found that the average ratio r_v of the weight of metal removed to initial workpiece weight was 0.62 for light engineering. Also, in light engineering, only 2 percent of workpieces weighed over 60 lb (27 kg) and therefore required lifting facilities and 75 percent of the workpieces were turned from bar. Usually, the proportion of initial volume of material removed by internal machining v_i is relatively small for geometrical reasons. Taking a typical figure of 0.07 for r_i would leave a proportion $r_e = 0.55$ typically to be removed by external machining.

The British survey [7] also showed a direct correlation between the length-to-diameter ratio l_r and the diameter d_w(in.) of turned parts as follows:

$$l_r = \frac{1.67}{d_w^{0.68}} \tag{13.30}$$

or

$$l_r = \frac{1.26}{W^{0.29}} \tag{13.31}$$

for steel workpieces and where W is the weight of the workpiece (lb). Thus, a 10-lb (4.5-kg) cylindrical workpiece would typically have a length-to-diameter ratio of 0.64.

For free-machining low-carbon steel the *Machining Data Handbook* [5] gives a specific cutting energy p_s of 1.1 hp · min/in^3 (3 GJ/m^3) and the material density ρ is 0.283 lb/in.^{3} (7.83 Mg/m^3). Thus, with $r_u = 0.62$, the uncorrected machining time under maximum power given by Eq. (13.22) becomes

$$t_{m_p} = 49.9 W^{0.47} \tag{13.32}$$

The characteristics of typical CNC lathes are presented in Figs. 13.27 and 13.28, where it is found that the constants in Eqs. (13.21) and (13.25) are

$$a = 2.9, \quad b = 0.53, \quad e = 45, \quad f = 0.27$$

According to Ostwald [6], the basic set-up time for a CNC turret lathe is approximately 1.5 ks and the additional set-up time per tool is 0.54 ks. If the number of tools n_t is 5, the batch size B_s is 100, the number of operations n_o is 5, and the tool-positioning time t_{pt} for a CNC lathe is 1.5 s, then Eq. (13.23) becomes

$$t_{np} = 90.5 + 1.1 W \text{ s} \tag{13.33}$$

If the machine is to be depreciated over $n_y = 10$ years and worked on one shift ($n_s = 1$), and if the operator rate R_o is \$12.50 per hour and both overhead factors k_m and k_o are equal to 2, Eq. (13.26) becomes

$$R_t = 25 + 4.5 W^{0.27} \text{ \$/hr} \tag{13.34}$$

Finally, if we assume that all the surfaces on the workpiece are to be finished, including a through bore, it can be shown that the relation between the effective area A_m (in.^{2}) to be machined and the weight W (lb) of the workpiece is approximately given by

$$A_m = 3.7\left(\frac{1 - r_i}{2l_r} + 1 + r_{m_i}^{0.5} - \frac{r_{m_e}}{1.5}\right)l_r^{0.33}\frac{W^{0.67}}{\rho^{0.67}}$$ (13.35)

where l_r is the length–diameter ratio of the workpiece and r_{m_e}, r_{m_i} are the proportions of material removed by external and internal machining, respectively. For a steel workpiece where l_r is given by Eq. (13.31), $r_{m_e} = 0.55$ and $r_{m_i} = 0.07$, Eq. (13.35) becomes

$$A = 3.44 W^{0.67} + 8.36 W^{0.38}$$ (13.36)

From the *Machining Data Handbook* [5], for free-machining low-carbon steel and a carbide tool, the value of R_{tg} is 100 in.^{2}/min (0.065 m^2/min). Substitution of this value and Eq. (13.36) into Eq. (13.27) gives

$$t_{mc} = 2.06 W^{0.86} + 5.02 W^{0.57}$$ (13.37)

And finally, using Eqs. (13.28) and (13.29), the corrected values of t_{m_c} and t_{m_p} are

$$t_{m_c}' = 2.74 W^{0.86} + 6.68 W^{0.57}$$ (13.38)

$$t_{m_p}' = 49.9 W^{0.47} \text{ approx.}$$ (13.39)

The total machining cost is now given by

$$C_{m_t} = \frac{R_t(t_{m_p}' + t_{m_c}' + t_{np})}{36} \text{ cents}$$ (13.40)

and the material cost is given by

$$C_{\text{mat}} = C_w W \text{ cents}$$ (13.41)

where C_w is the cost per pound of the material.

It is now possible to study the effects of component size, work material, and other factors on the cost of a typical turned component.

13.9.12   Effects of Component Size

Figure 13.29 shows, for a low-carbon-steel turned component, the effect of the finished size of the component on the rough machining, finish machining, and nonproductive times per unit volume. It can be seen that as the size of the component is reduced below about 5 in.^{3} (82 µm^3), the time per unit volume and hence the cost per unit volume increases
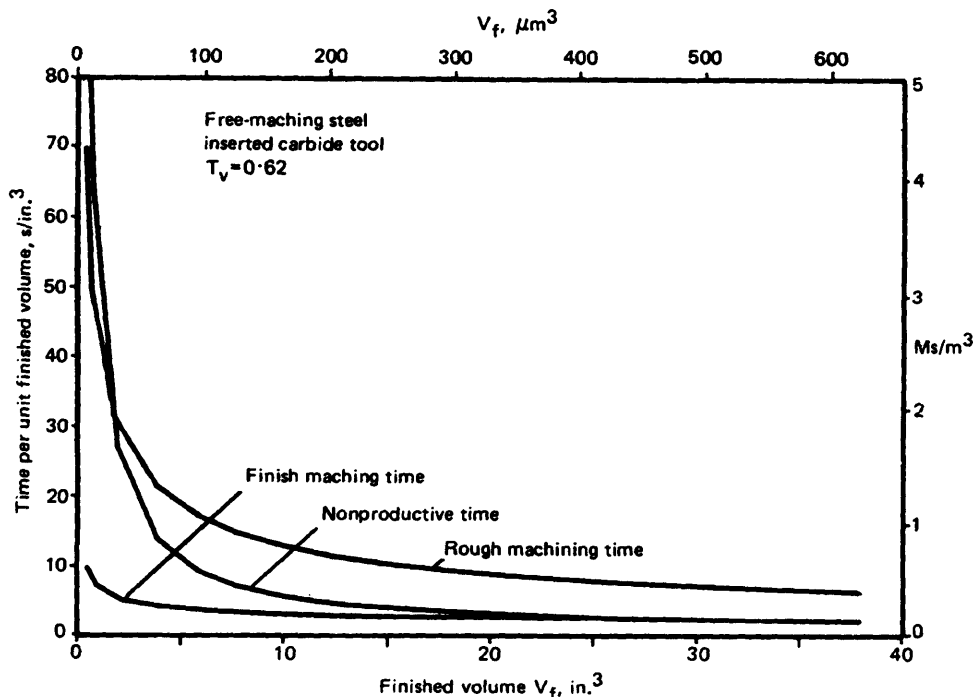
Figure 13.29 Effect of component size on rough machining, finish machining, and nonproductive times per unit volume.

dramatically—particularly for the nonproductive time. This increase is to be expected for the nonproductive time because it is not reduced in proportion to the weight of the component [Eq. (13.24)]. For example, even if the component size were reduced to almost zero, it would still take a finite time to place it in the machine, to set the speeds and feeds, and to turn the coolant on and off. For the rough-machining time, the higher times per unit volume for small components are a result of the reduced power available with the smaller machines used (Fig. 13.27). The finish-machining time is proportional to the area machined. It can be shown [Eq. (13.36)] that the surface area per unit volume (or weight) is higher for smaller components, thus leading to higher finish-machining times per unit volume.

These results have not taken into account the cost of the work material, and Fig. 13.30 shows how the total cost of the finished steel component varies with component size. This total cost is broken down into
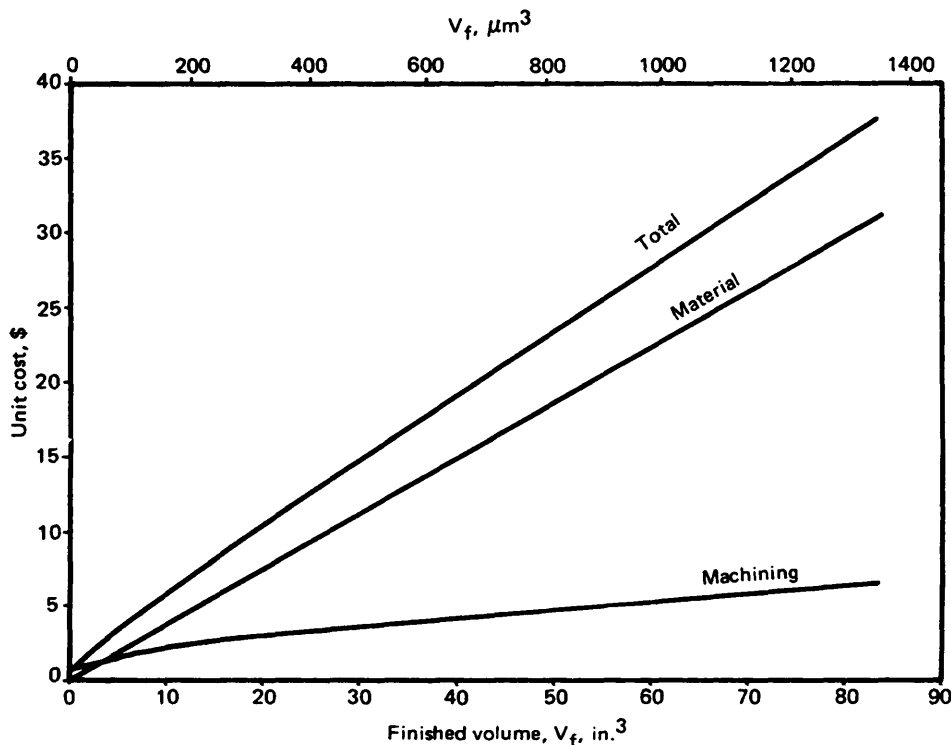
Figure 13.30 Effect of component size on total cost for machining a free-machining steel workpiece (cost 50 cents/lb) with an inserted carbide tool.

material cost and machining cost, and it can be seen that material cost is the most important factor contributing to the total cost even though 62 percent of the original workpiece was removed by machining—a figure that results in relatively high rough-machining costs. In fact, for the larger parts about 80 percent of the total cost is attributable to material costs.

13.9.13   Effects of Work Material

The work material affects the total cost of the component through four factors. The most important of these factors is the material cost. Estimates of the cost per unit volume of some representative materials are presented in Fig. 13.31. Next, the principal material factors affecting rough-machining costs and finish-machining costs are, respectively, the specific cutting energy (unit power) p_s and the recommended value of the surface generation rate R_{sg}. Comparisons of the magnitudes of these values for the same
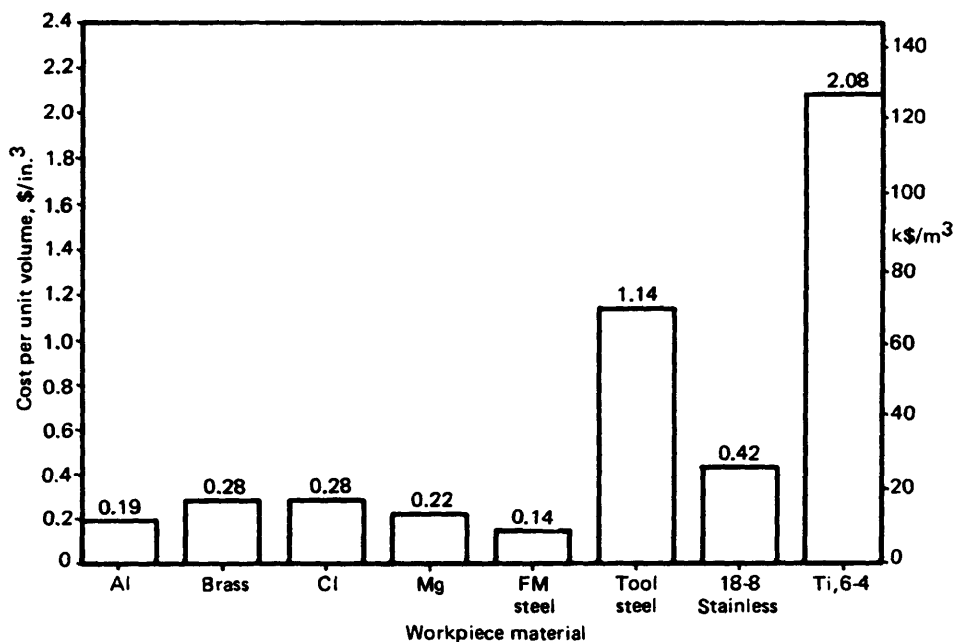
Figure 13.31 Cost per unit volume of some representative work materials.
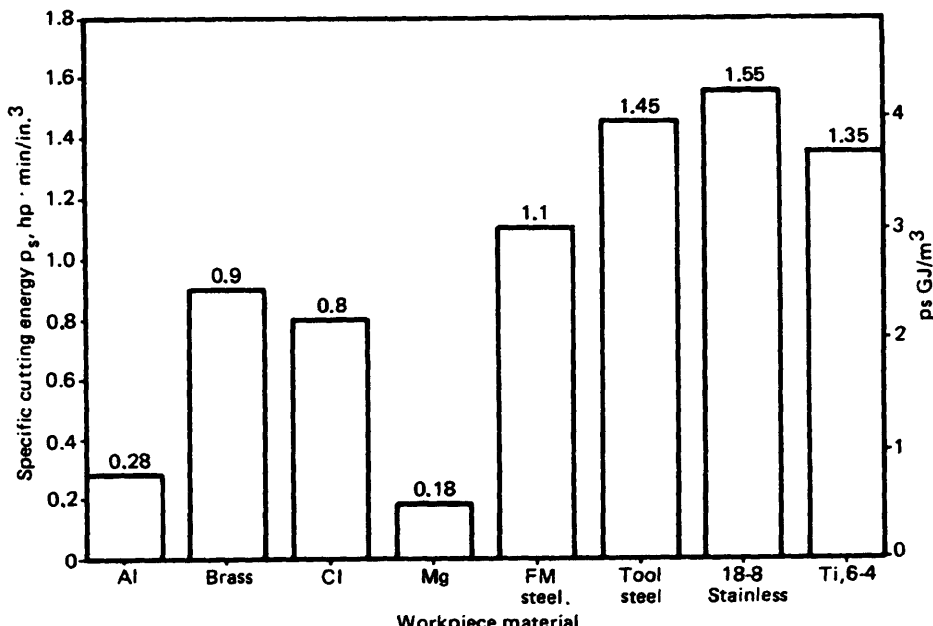
Figure 13.32 Specific cutting energy (unit power) p_s for some representative materials.
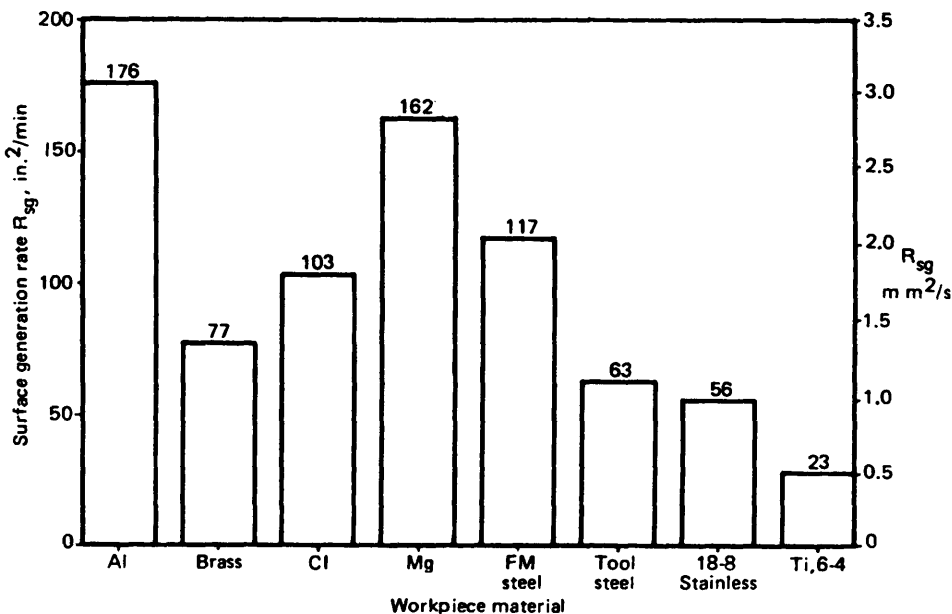
Figure 13.33 Rate of surface-area generation R_{sg} under recommended conditions for some representative materials.

representative materials are presented in Figs. 13.32 and 13.33. A fourth factor of rather less importance is the material density; this affects the weight of the workpiece and hence the handling time.

Figure 13.34 shows how the unit cost varies with finished workpiece size for each of the representative materials. It can be seen that the finished costs of low-carbon steel and aluminum workpieces are roughly the same even though the cost per unit volume of aluminum is about 30 percent higher than that of low-carbon steel. Also, the results for cast iron and brass are indistinguishable and about 15 percent higher than those for low-carbon steel and aluminum. At the high-cost end of the scale the total cost of large titanium components is about ten times that for low-carbon steel and for small components about five times. Material cost per unit volume for titanium is about 15 times that for low-carbon steel (Fig. 13.31).

13.9.14 Some General Observations

From the results of applying the approximate-cost models for components turned on CNC machines it is possible to make the following observations.
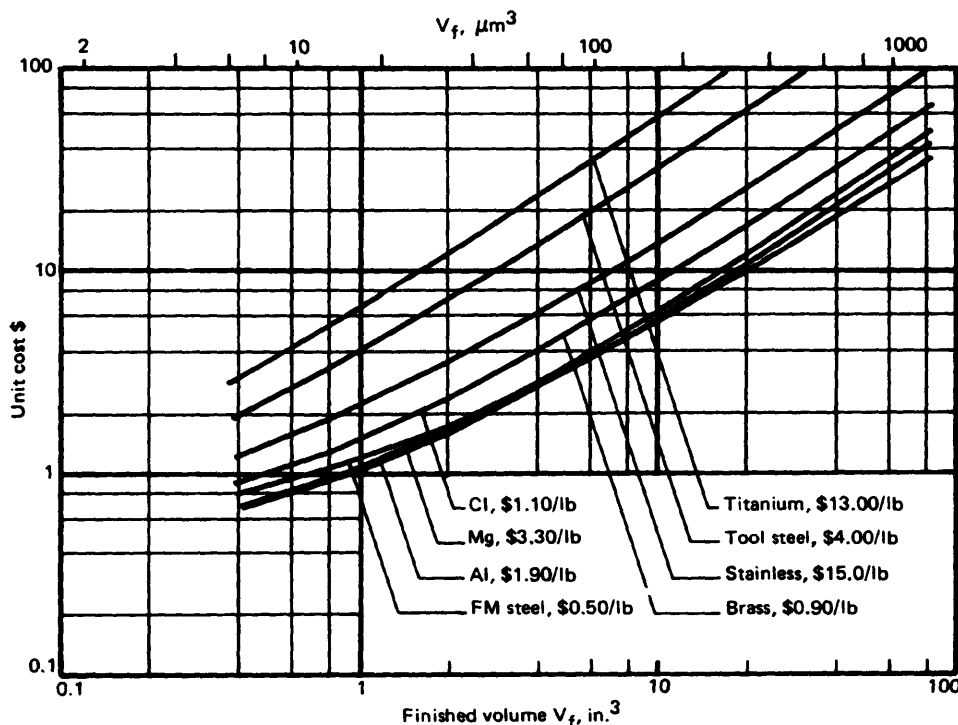
Figure 13.34 Effect of size on the unit cost of typical turned components.

1. For medium-sized and large workpieces, the cost of the original workpiece mainly determines the total manufactured cost of the finished component.

2. The cost per unit volume or per unit weight of small components (less than about 5 in.^{3} or 82 μm^3) increases rapidly as size is reduced because:

   a. The nonproductive times do not reduce in proportion to the smaller component size.

   b. The power available and hence the metal removal rate is lower for smaller components

   c. The surface area per unit volume to be finish-machined is higher for smaller components.

3. The choice of tool materials and optimum machining conditions affects only the finish-machining time. Since finish machining represents only about 25 percent of the total manufacturing cost, which in turn represents only about 20 percent of the total component cost, for

larger components the effects of changes in tool materials or recommended conditions can be negligible under many conditions.

4. The factors to be taken into account in estimating machining costs are as follows:

a. The amount of material to be removed. This factor directly affects the material costs per unit volume of the finished product and less importantly, the rough-machining time.

b. The rate for the machine tool and operator.

c. The power available for machining and the specific cutting energy of the work material.

d. The nonproductive times, especially for smaller components.

e. The surface area to be finish-machined.

f. The recommended finish-machining conditions, which are in turn affected by the work material and tool material used.

It should be noted that to reduce the high cost per unit weight of smaller components in practice, bar-fed automatic lathes are employed instead of CNC lathes—provided sufficient quantities are required. With these machines the nonproductive times and costs are significantly reduced.

From studies of the kind presented here it should be possible to generate data useful to the product designer who wishes to make early estimates of component costs at the conceptual stage of product design.

PROBLEMS

1. A batch of 10,000 rectangular blocks 50 × 25 × 25 mm is to be slab-milled on all faces. The material can be either mild steel costing $4,900/m³ or aluminum costing $6,100/m³. Estimate the total cost of the batch of components in each material if the average nonproductive time for each face = 60 s, the tool-changing time = 600 s, the cost of a sharp tool = $20.00, the machine and operator rate = $0.004/s, the tool-life index n = 0.125, the cutting speed for 60 s of tool life is 1 m/s for mild steel and 4 m/s for aluminum, the feed per revolution of the cutter = 1.25 mm, and the working engagement (depth of cut) = 2 mm. (Assume that the distance traveled by the 50-mm-diameter, 38-mm-wide cutter for each face of the workpiece is 5 mm greater than the length of the face.)

2. Aluminum rod is available in diameters of 1-mm increments to 25-mm diameter and in 2-mm increments from 26- to 50-mm diameter. In the design of a particular shaft it has been determined that its finished diameter D should be within the range
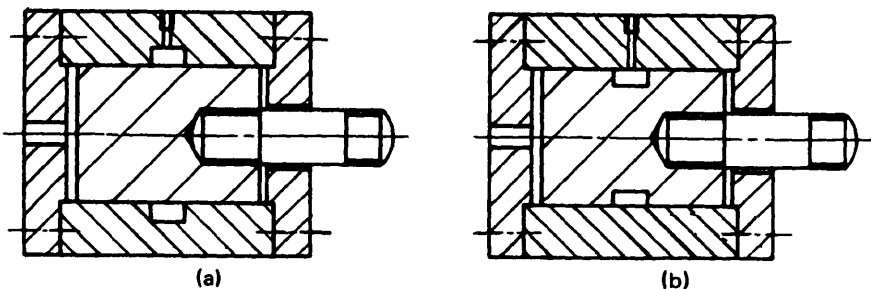
Figure 13.35 Alternative designs of cylinder assembly.

$$33 - \frac{(L - 229)^2}{84.75} > D > 27.43 + \frac{(L - 254)^2}{127}$$

where L is the length of the shaft. If an allowance of 2 mm in diameter is to be allowed for machining, what finished diameter should be chosen for the shaft?

3. Write the geometric code number for each of the components shown in Fig. 13.9, noting that run-out grooves for screw threads do not affect the coding.

4. Which of the two designs for a cylinder assembly shown in Fig. 13.35 would be preferable from the manufacturer's point of view? Also, list other manufacturing and assembly aspects of both designs that could be improved. (Note that the omission of details of the bolting arrangements for the cylinder ends is not to be considered an error.)

5. The end covers shown in Fig. 13.36 are to be milled from 10-mm-thick aluminum plate. Which of these two designs is preferable from the manufacturer's point of view? Also, what other aspects of the designs should be changed?

6. A designer has specified a surface finish on turned shafts of 0.4-μm arithmetical mean when a surface finish of 1.6 μm would suffice. Estimate the cost of this mistake when 2000 shafts are to be produced with a tool with a rounded corner if the machining time per component = 600 s, the number of components produced between tool regrinds = 4, the cost of a sharp tool = \$2.00, the machine and operator rate = \$0.003 3/s, the tool-changing time = 120 s, and the nonproductive time per component = 240 s.
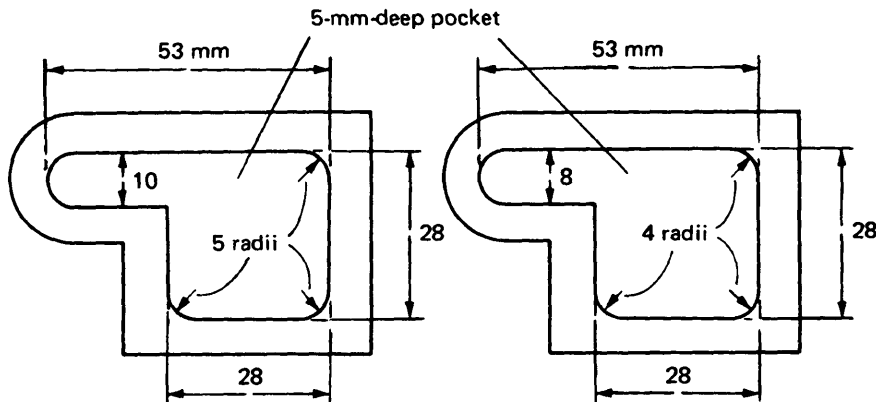
Figure 13.36 Alternative designs of an end cover.

REFERENCES

1. *Machinery's Handbook,* 19th ed., Industrial Press, Inc., New York, 1973.
2. Opitz, H.: *A Classification System to Describe Workpieces,* Pergamon Press, New York, 1970.
3. Boothroyd, G., and P. Dewhurst: *Product Design for Assembly,* Boothroyd Dewhurst, Inc., Wakefield, Rhode Island, 1987.
4. Fridriksson, L., Non-productive Time in Conventional Metal Cutting, Report No. 3, Design for Manufacturability Program, University of Massachusetts, Amherst, February, 1979.
5. *Machining Data Handbook,* 3rd ed., vols. 1, 2, Metcut Research Associates Inc., 1980.
6. Ostwald, P.F., AM Cost Estimator, McGraw-Hill, New York, 1985/1986.
7. Production Engineering Research Association, *Survey of Turning Requirements in Industry,* 1963.

14

Nonconventional Machining Processes

14.1 INTRODUCTION

The recent increase in the use of hard, high-strength, and temperature-resistant materials in engineering has made it necessary to develop many new machining techniques. With the exception of grinding, conventional methods of removing material from a workpiece are not readily applicable to these new materials. Even when such machining is possible, it is usually slow and highly inefficient. Although most of the new machining processes have been developed specifically for materials that are difficult to machine, some of them have found use in the production of complex shapes and cavities in softer, more readily machined materials.

Descriptions of the main nonconventional machining processes are given in this chapter. More detailed descriptions of these processes and several others can be found elsewhere [1].

Nonconventional machining processes may be used as alternatives to the more traditional processes for a number of reasons, including the following [2]:

1. *Machinability of the workpiece material:* Many workpiece materials are difficult to machine by conventional methods because of high hard-

467

ness, high thermal resistance, or high abrasive wear. For these materials many of the nonconventional machining processes are suitable.

2. *Shape complexity of the workpiece:* Many shape features are difficult or impossible to produce by conventional machining methods. For example, it is usually relatively simple to produce a cylindrical hole in a workpiece, but to produce a square, sharp-cornered hole of similar size is much more difficult. Nonconventional machining processes are often capable of machining complex shape features with comparative ease—even in materials that are normally difficult to machine.

3. *Surface integrity:* Conventional machining processes can result in surface cracks and residual stresses in the workpiece. Many nonconventional machining processes can remove material without causing these effects.

4. *Precision:* Many nonconventional processes are capable of high levels of precision, which cannot be achieved by conventional machining.

5. *Miniaturization:* Some nonconventional processes are capable of producing very small shape features and fine detail not possible by conventional machining (e.g., the machining of deep holes with very small diameters).

6. *Automatic data communication and computer integration:* Many nonconventional processes can be computer-controlled and linked directly to CAD/CAM systems in an integrated manufacturing environment.

14.2 RANGE OF NONCONVENTIONAL MACHINING PROCESSES

The nonconventional machining processes utilize a variety of energy sources for removing the workpiece material. Some of the more important processes are shown schematically in Fig. 14.1, grouped according to the energy source used. The three main processes that utilize a mechanical action for removing material are ultrasonic machining, abrasive-jet machining, and water-jet machining, including abrasive water-jet machining. Four processes can be characterized as electrothermal processes: electrodischarge machining, including wire-electrodischarge machining; laser-beam machining, electron-beam machining, and plasma-beam machining. The remaining processes are basically chemical: chemical machining and electrochemical machining, including electrochemical grinding. There are several other less commonly used processes also available [1], but these will not be discussed here.

A number of the processes shown in Fig. 14.1 remove material by means of a narrow jet or beam projected at the workpiece. A useful property of these processes is the ability to cut sheet or plate material with a very narrow "kerf" width. The kerf width is the width of the slit cut in the material, which determines the amount of waste material from the process and the intricacy of detail of the profile that may be cut by the process.

14.3 ULTRASONIC MACHINING

Ultrasonic machining is a valuable process for the precision machining of hard, brittle materials [3]. Material is removed by the abrasive action of a grit-loaded slurry circulating between the workpiece and a tool vibrating at ultrasonic frequencies. The tool is gradually fed into the workpiece to form a cavity corresponding to the tool shape. Frequencies of 20 to 40 kHz are most commonly used. A typical arrangement for ultrasonic machining is shown schematically in Fig. 14.2. The main elements are:

1. A high frequency generator
2. A transducer, which utilizes the piezoelectric or magnetostrictive effect
3. A transformer, which is shaped to amplify the vibration output of the transducer
4. A tool holder and tool
5. An abrasive slurry, which is circulated into the small gap between the tool and workpiece.

14.3.1 Transducers

A transducer converts energy from one form to another. Transducers used in ultrasonic machining convert electrical energy into mechanical motion, and they are based on piezoelectric or magnetostrictive principles. The amplitude of vibration possible depends on the length of the transducer and the strength of the material used, the limit being approximately 0.025 mm in practice.

Piezoelectric Transducers

Certain crystals, such as quartz, undergo small dimensional changes when subjected to a changing electrical current. Application of an alternating voltage to the crystal causes vibrations to occur and the amplitude is greatest at the resonant frequency of the crystal. For resonance, the length of the crystal must be equal to half the wavelength of sound in the crystal [4]. For quartz, Young's modulus $E = 5.2 \times 10^{10}$ N/m^2, the density $\rho = 2.6 \times 10^3$ kg/m^3, and hence the velocity of sound $C_s = E/\rho = 4480$ m/s.

Mechanical processes

Ultrasonic
machining (USM)

Water-jet
machining (WJM)

Abrasive-jet
machining (AJM)

Electrothermal processes

Electro-discharge
machining (EDM)

Laser-beam
machining (LBM)

Electron-beam
machining
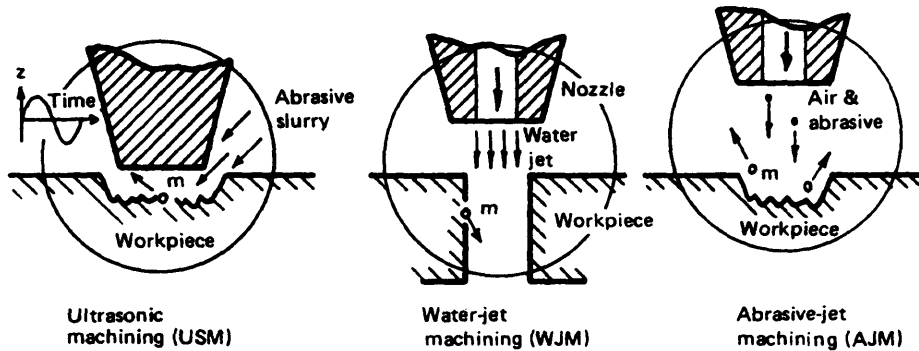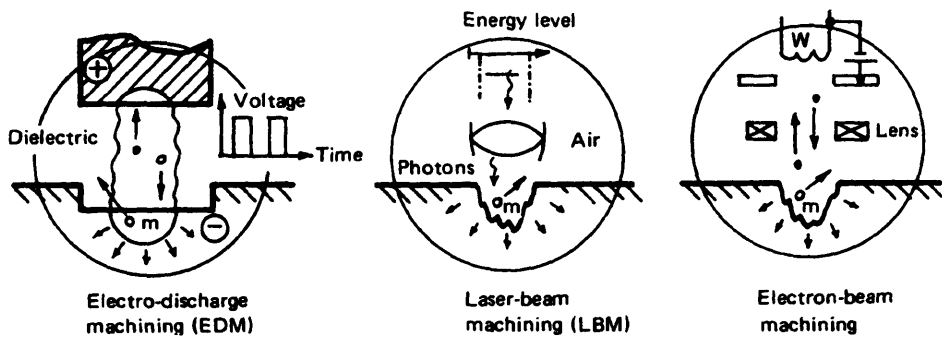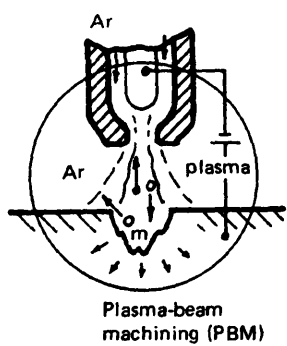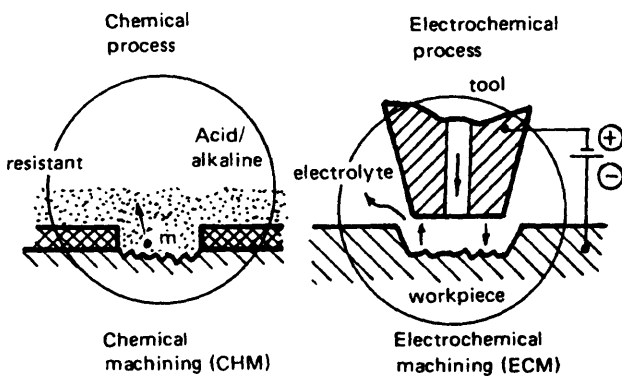
Figure 14.1 Schematics of various nonconventional machining processes. (Adapted from Snoeys [2].)

Chemical machining (CHM)

Electrochemical machining (ECM)

Plasma-beam
machining (PBM)
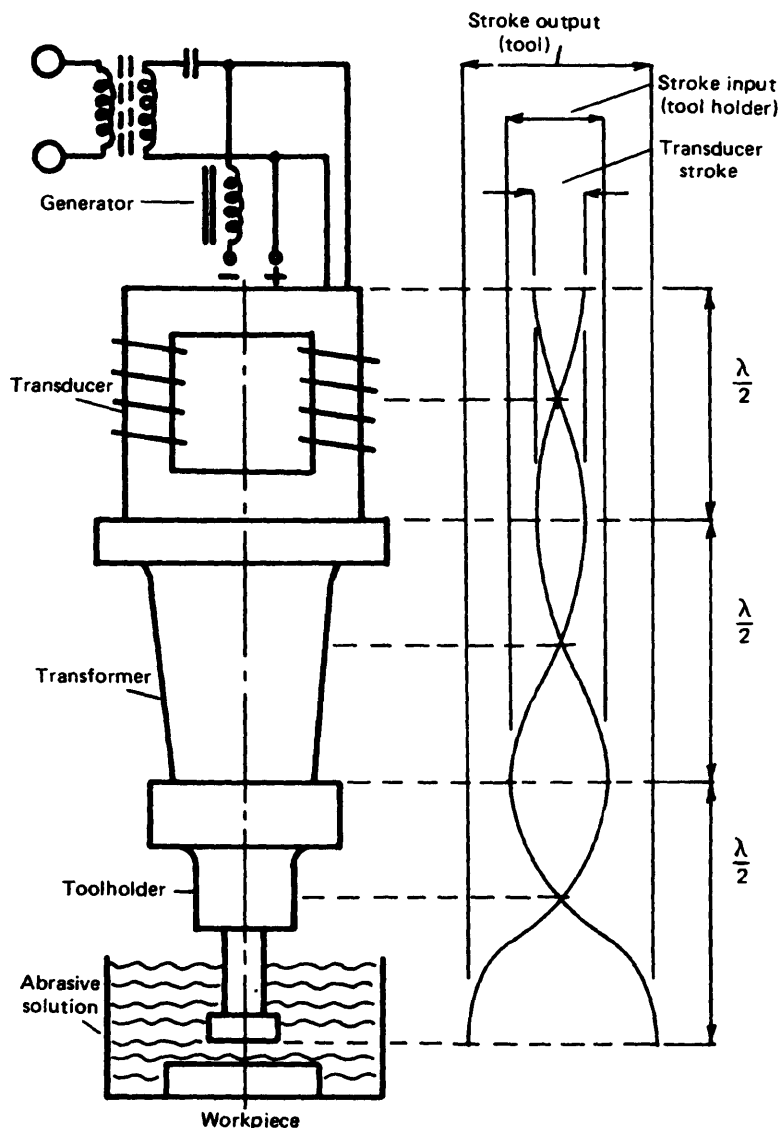
Figure 14.2 Basic features of the ultrasonic-machining process.
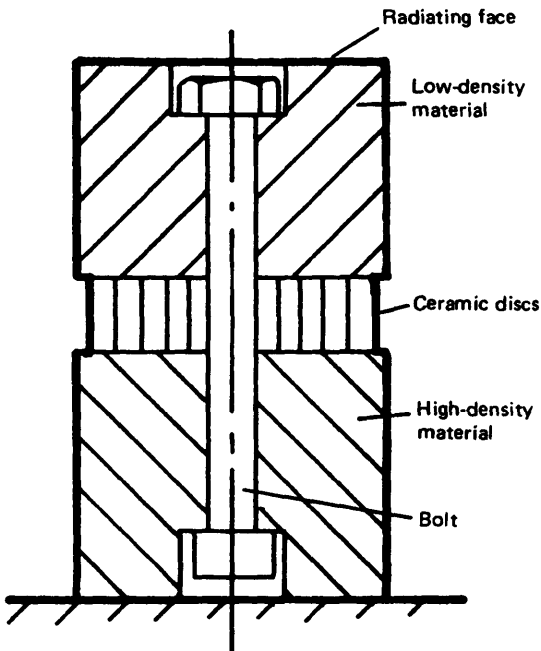
Figure 14.3 Piezoelectric ultrasonic transducers.

Finally, at a frequency f_s of 20 kHz, the wavelength $= C_s/f_s = 0.228$ m and therefore the required crystal length is 110 mm.

Polycrystalline ceramics such as barium titanate are also used as transducers; they have a sandwich construction and lengths of 75 to 100 mm. A typical transducer (Fig. 14.3) consists of a stack of ceramic disks, sandwiched between a high-density base and a lower-density block of material, which provides the radiating face of the transducer. The action of the transducer is based on the fact that, from momentum conservation, the velocity and amplitude of vibration are high in a lower density material. Such transducers are capable of converting electrical energy into vibrational energy at 96 percent efficiency and consequently do not require cooling.

Magnetostrictive Transducers

When ferromagnetic materials, such as nickel and nickel alloys, are magnetized, an expansion occurs. Application of an alternating current to coils surrounding the material (Fig. 14.4) causes vibrations at the applied frequency. The magnetic material is laminated to reduce eddy current losses, but the energy conversion efficiencies are only 20 to 35 percent;

Energizing coils

Laminated pack
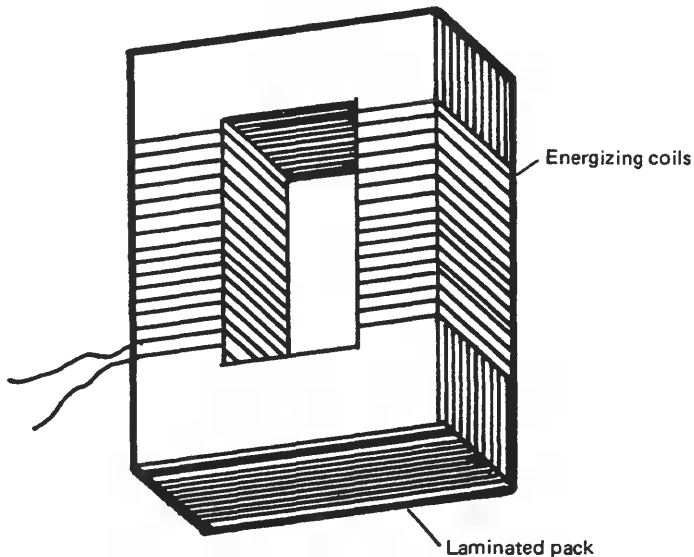
Figure 14.4   Magnetostrictive ultrasonic transducer.

consequently, water cooling is required to remove waste heat from the transducer.

14.3.2   Transformer and Tool Holder

The purpose of the transformer in ultrasonic machining is to increase the vibration amplitude. The transformer's length is half the wavelength of sound in the transformer material. The reduction in cross-sectional area causes amplification of the vibration, which increases in inverse proportion to the area ratio between the upper and lower ends of the transformer. Amplitide may be increased by as much as 600 percent with a suitably shaped transformer. A similar increase in amplitude at the tool face can occur in the tool holder, and final amplitudes at the tool face are usually in the range of 0.013 to 0.1 mm.

14.3.3   Tools

The shape of the tools is the inverse of the cavity to be eroded. Relatively ductile tool materials, such as stainless steel, brass, and mild steel are generally used to minimize tool wear. The tools are usually brazed to the tool holder to reduce possible fatigue problems associated with screwed fasteners.

14.3.4 Abrasive Slurry

The slurry consists of small abrasive particles mixed with water or sometimes oil, with the abrasive having a concentration of 30 to 60 percent by weight. Commonly used abrasive materials are boron carbide, silicon carbide, and aluminum oxide. The grit size is usually about the same as the amplitude of vibration being used.

14.3.5 Applications

Ultrasonic machining can be used to produce cavities in most materials whether conductive, nonconductive, metallic, ceramic, or composite. It is most effective on materials that are harder than $50R_c$. Material removal rates are low, usually less than 1.5 cm^3/min. Holes as small as 0.076 mm can be drilled and the upper limit on cavity size is approximately 75 mm. Machining depths of 50 mm or more are possible, but in practice depths are usually less than 5 mm. Tolerances of ±0.25 mm and surface finishes of 0.25 μm can routinely be obtained.

14.4 WATER-JET MACHINING

14.4.1 General Discussion

In water-jet machining, material is removed through the erosion effects of a high-velocity, small-diameter jet of water [1,5]. The process is primarily used for drilling and slitting operations on materials in sheet or slab form. Intricate shapes can be readily cut with a very narrow kerf width. The equipment (Fig. 14.5) used for water-jet machining consists of a high-pressure intensifier and pumping unit, capable of delivering water at pressures up to 400 MPa, a delivery system to route the high-pressure water to the work area, a nozzle to form the jet, and a positioning system that moves either the nozzle or the workpiece to bring about the cutting action.

The nozzle conventionally contains a sapphire insert to form the small-diameter jet to resist wear, but some success has been achieved with metallic nozzle inserts made from tungsten carbide (Fig. 14.6) [2,6]. Jet diameters are usually in the range 0.07 to 0.5 mm, and the typical life of the nozzle inserts is from 250 to 500 hours. The stand-off distance of the nozzle from the workpiece is usually in the range 3 to 25 mm. The choice of positioning system used for the tool or workpiece depends on the application of the process. In many applications the nozzle or workpiece is moved manually and the process is then similar to conventional band sawing. Water-jet cutting machines are also available with numerically
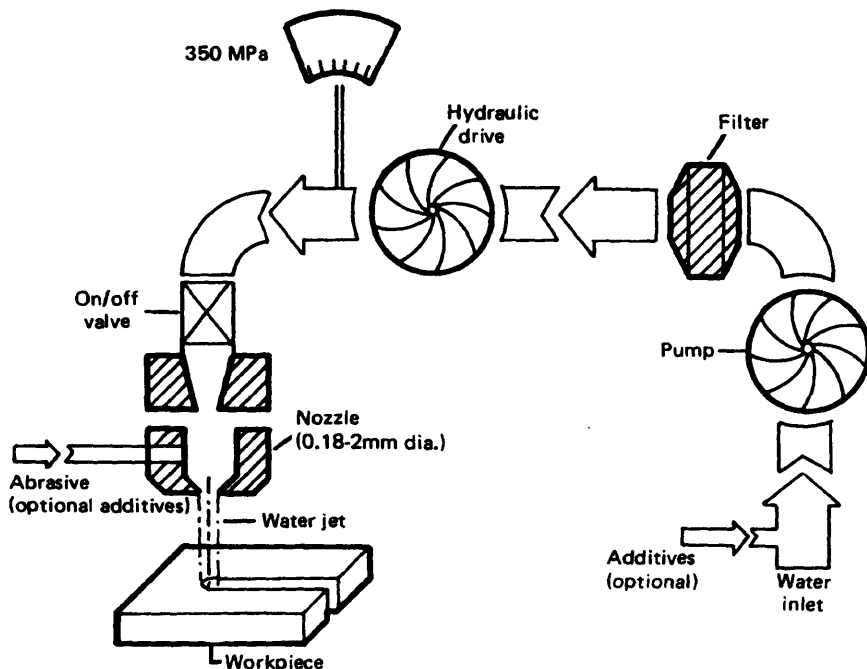
Figure 14.5 Basic features of water-jet and abrasive water-jet machining.
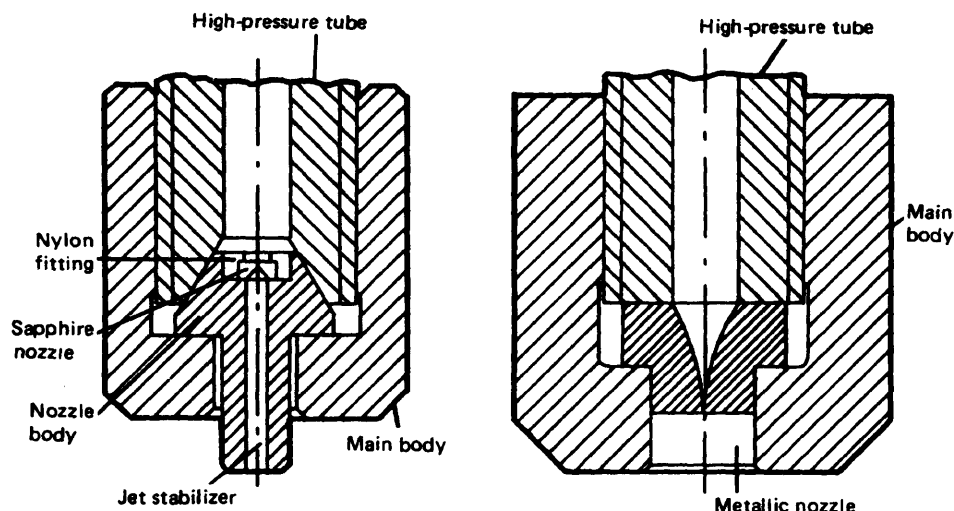
Figure 14.6 Nozzles for water-jet machining. (a) Conventional sapphire nozzle;
(b) metallic nozzle.

controlled workable motions or with the nozzle moved with an industrial robot.

Water-jet machining is mainly used for machining soft nonmetallic materials such as paper, wood, leather, and foam. High cutting rates are possible with no thermal damage to the work material. An adaptation of the basic process, which enables it to be used for machining hard materials, is the introduction of abrasive particles into the fluid stream after the jet; the process is then referred to as abrasive water-jet machining. The remainder of the equipment is essentially the same as in conventional water-jet machining. Commonly used abrasives for this process are garnet, silicon, and silicon carbide grains [1].

14.4.2 Application

Water-jet machining is used to cut soft, nonmetallic materials in sheet form, often in multilayer stacks. Table 14.1 shows some water-jet cutting rates for different materials [1]. Force levels on the workpiece are low, allowing crushable materials to be cut effectively without damage. The kerf width is approximately 0.28 mm larger than the nozzle diameter, enabling close nesting of the shapes to be cut from the sheet materials. Predrilling of starting holes is not necessary. The jet can pierce the material at any location and then cutting can be carried out in any direction. The surface finish of the cut edges is good, with no burrs and no thermal damage. Tolerances are a function of the material type and thickness, and they are usually within ±0.1 to 0.2 mm.

Abrasive water-jet machining is a considerable enhancement of the basic process, making it possible for a much wider range of materials to be cut. Virtually all materials, regardless of hardness, reflectivity, and con-

Table 14.1 Water-Jet Cutting Rates[a]

Material	Thickness (mm)	Pressure (MPa)	Nozzle diameter (mm)	Speed (m/min)
ABS plastic	2.2	379	0.15	1.0
	3.8	379	0.15	0.2
Cardboard	1.4	379	0.10	6.1
Cheese	100	379	0.20	22.8
Foam rubber	76	207	0.10	300
Leather	1.5	275	0.13	76.2
Plexiglas	3	379	0.13	0.9
Wood	3.2	379	0.13	1.0

[a]Adapted from Benedict [1].

Table 14.2 Abrasive Water-Jet Cutting Rates[a]

Material	Thickness (mm)	Pressure (MPa)	Nozzle diameter (mm)	Speed (mm/min)
Acrylic	3.5	NA[b]	NA	1200
	13	NA	NA	460
Aluminum	3.3	207	0.45/1.5	900
	25	207	0.45/1.5	51
	152	207	0.45/1.5	10
Boron	0.33	207	0.33/1.2	305
Cast iron	8.1	207	NA	150
Glass	10	207	0.45/1.5	915
Graphite	51	NA	NA	125
Steel	20	207	0.45/1.5	51
Titanium	3.4	NA	NA	300

[a]Adapted from Benedict [1].
[b]NA, not available.

ductivity, can be successfully cut. Most metals can be readily machined, with thicknesses of up to 100 mm. Table 14.2 lists some cutting speeds for various materials machined by abrasive water-jet machining [1]. Kerf widths are usually between 1.5 and 2.3 mm and the cut surfaces reveal no thermal or mechanical damage. Some tapering of the cut slit does occur and its extent increases with the material thickness. Brittle materials such as acrylic, graphite, and silica glass can be cut without damage, leaving the cut edges free from cracks. Porous materials such as concrete can be cut at thicknesses up to 300 mm. A growing application of abrasive water-jet machining is the trimming of cured fiber composite and laminated materials, because the materials do not delaminate during cutting and ragged fibers are not left protruding from the cut edges.

14.5 ABRASIVE-JET MACHINING

14.5.1

Abrasive-jet machining removes material through the eroding action of a high-velocity stream of abrasive-laden gas [7]. An abrasive jet is formed by microabrasive particles being entrained in an inert gas stream and propelled through a small nozzle at pressures up to 0.7 MPa, which results in jet velocities of up to 300 m/s. Material is removed from the workpiece by a

chipping action that is particularly effective on hard, brittle materials such as glass, silicon, tungsten, and ceramics.

In an abrasive-jet machining system the gas is first compressed and mixed with the abrasive powder in a mixing chamber (Fig. 14.7). The mixing chamber consists of a convergent–divergent inlet nozzle, followed by a chamber where the abrasive powder is drawn into the gas stream, before passing through the outlet nozzle to the work surface. The delivery nozzle, made of either tungsten carbide or sapphire, has a useful life of about 30 hours. Jet diameters are usually 0.12 to 1.25 mm. The most commonly used
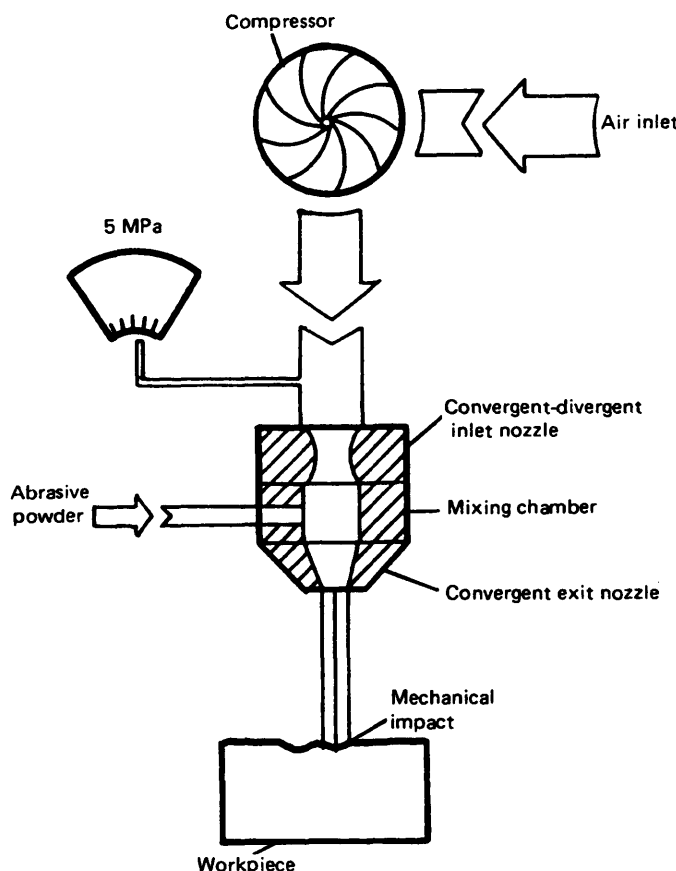
Figure 14.7 Basic features of abrasive-jet machining.

abrasives are aluminum oxide, silicon carbide, and sodium bicarbonate, with particle sizes varying from 10 to 50 μm.

14.5.2 Applications

The process can be used for performing intricate cutting, drilling, polishing, and etching operations on delicate workpieces because of the relatively low overall forces generated. The cooling action of the gas stream ensures that no thermal damage is experienced by the workpiece material. When abrasive-jet machining is not used as a cutting or drilling process, material removal rates are low—in the region of 0.015 cm³/min. Slots as small as 0.12 to 0.25 mm in width can be produced. For cutting and drilling operations, the process is restricted to metal foils and thin sections of ceramics and glass. Tolerances of ±0.12 mm are readily maintained, together with surface finishes ranging from 0.25 to 1.25 μm. Future development of the process is likely to be for microgrit-blasting applications such as deburring, cleaning, polishing, and etching. Typical applications are the etching of shallow, intricate holes in electronic components such as resistor paths in insulators and patterns in semiconductors. The engraving of characters on toughened-glass automobile windows is another significant application of the process.

14.6 CHEMICAL MACHINING

In chemical machining a strong acid or alkaline solution is used to dissolve materials selectively, resulting in controlled material removal [1]. A chemically resistant coating known as a mask is selectively applied to the workpiece to protect surfaces that are not to be machined. Chemical machining can be divided into two basic subprocesses: chemical milling and chemical blanking. In chemical milling, erosion of the material is used to produce pockets and channels in the workpiece surfaces or to remove material over large areas of the surfaces of a workpiece, for weight reduction, for example. In chemical blanking, holes and slots that penetrate entirely through the material are produced, usually in thin sheet materials.

The five steps in chemical machining are as follows:

1. *Part preparation:* cleaning
2. *Masking:* application of chemically resistant material
3. *Etching:* dip or spray exposure to the etchant
4. *Mask removal:* stripping the maskant and cleaning the part
5. *Finishing:* inspection and other processing

Three basic types of masks are used: cut-and-peel masks, screen-resist masks, and photoresist masks.

Cut-and-Peel Masks

A film of the chemically resistant material is applied to the workpiece by dipping, spraying, or flow coating, producing a dry film up to 0.13 mm thick. The materials most commonly used are vinyl, styrene, and butadiene. The rubbery film is then cut and peeled away selectively. The most common way of cutting the mask is by hand scribing using templates, but other methods, including laser cutting of the mask material, have been used [2]. Manual scribing of the mask material usually achieves an accuracy of ±0.13 to ±0.75 mm. The high mask thickness produced by the dipping or spraying of the mask material makes it possible for depths of as much as 13 mm to be cut.

Screen-Resist Masks

For a screen-resist mask, the mask material is applied to the workpiece surface by printing, using stencils and a fine polyester or stainless steel mesh screen. Screen printing is a fast, economical method of applying the mask material. Relatively thin coatings with tolerances held to ±0.05 to ±0.18 mm are obtained by screen printing. Etching depths are restricted to about 1.5 mm because of the thinness of the coating.

Photoresist Masks

Chemical machining using photoresist masks is quite widely used and is often referred to as photochemical machining. The process produces intricate and finely detailed shapes in materials by using a light-activated resist material. The workpiece is coated with the photoresist material and a master transparency is held against the workpiece, while exposure to ultraviolet light takes place (Fig. 14.8). The light activates the photoresist material in those areas corresponding to the transparent portions of the master negative. The areas corresponding to the opaque parts of the negative are dissolved away during the etching process.

Photoresist is the most accurate of the available masking methods and can be used to produce shapes with tolerances of ±0.025 to ±0.005 mm, but typically feature sizes cannot be less than the material thickness.

14.6.1   Etchants

A variety of materials are used for dissolving the workpiece material and selection of the most appropriate chemicals depends on a number of factors [1,8], including:

1. Sketch of desired part

2. Prepare plastic artwork (1 to 100 times)

3. Photographically reduce to actual size

4. Coat metal sheet with photopolymer

5. Place transparency on waxed sheet and expose to ultraviolet light

6. Develop exposed photopolymer

7. Etch part from metal sheet

8. Remove polymer

Finished part
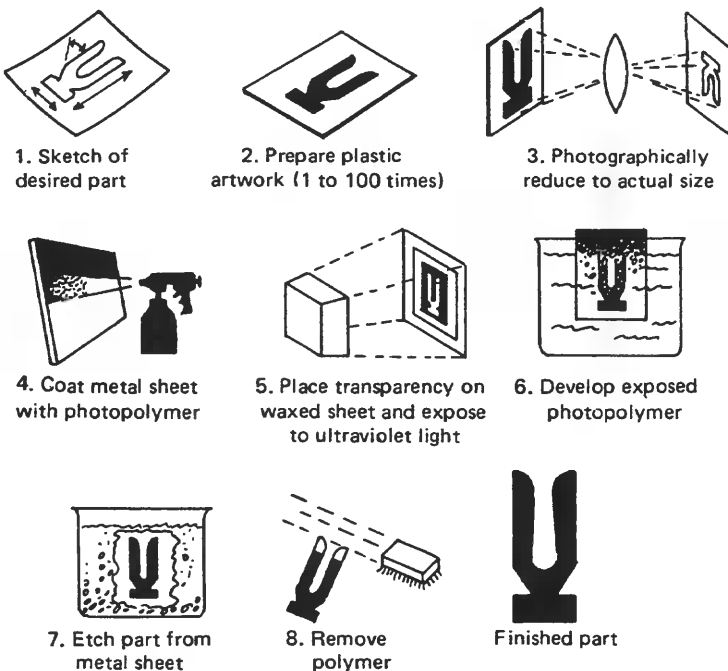
Figure 14.8 Process steps for photochemical machining.

1. The workpiece material
2. The mask material
3. The depth of etch required
4. The surface finish required, as some etchants attack the grain boundaries of some materials
5. The material removal rates required
6. The heat-treated condition of the material
7. The potential damage to the work material and the metallurgical properties required
8. Economic considerations.

14.6.2 Applications

Chemical machining using cut-and-peel masking is usually applied in the removal of material from large workpieces, for example, in the removal of material in selected areas for the lightening of aircraft wing panels and structural members.

Chemical blanking, using photoresists or screen-printed masks, is
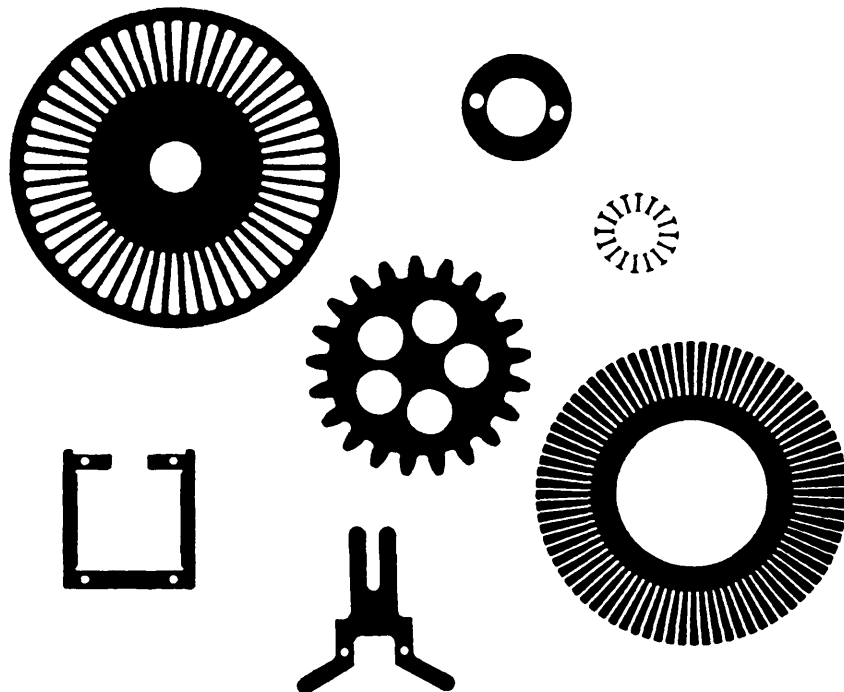
Figure 14.9 Some part profiles produced by photochemical blanking (From Benedict [1].)

used for producing delicate shapes in thin materials. Figure 14.9 shows some intricate parts produced by photochemical blanking [1]. The process can be used to produce burr-free shapes for which conventional blanking die costs would be very high. Another advantage of the process is that the workpiece material can be hard and brittle, so that it could not be blanked by conventional methods. In addition to sheet metal applications, photochemical machining is used routinely for the production of printed-circuit boards. The unwanted copper deposited on the board is removed photochemically, leaving the required pattern of connections on the nonmetallic backing material of the board.

14.7 ELECTROCHEMICAL MACHINING

Electrochemical machining (ECM) refers to the process of metal removal in which electrolytic action is utilized to dissolve the workpiece metal. It is,

in effect, the reverse of electroplating. A modification of the process is electrolytic grinding, which will be discussed later.

The ECM process is illustrated in Fig. 14.10. The workpiece (which must be a conductor of electricity) is placed in a tank on the machine table and connected to the positive terminal of a high-current, low-voltage dc supply. The tool electrode, shaped to form the required cavity in the workpiece, is connected to the negative terminal of the supply. An electrolyte flows through the gap between the tool and the workpiece and is then pumped back to the working zone, either through the tool or externally, depending on the application.

The action of the current flowing through the electrolyte is to dissolve the metal at the anode, that is, the workpiece. The electrical resistance is lowest (and hence the current is highest) in the region where the tool and workpiece are closest. Since the metal is dissolved from the workpiece most rapidly in this region, the form of the tool will be reproduced on the workpiece, as the tool is fed gradually toward the workpiece.

There is no mechanical contact between the workpiece and the tool.
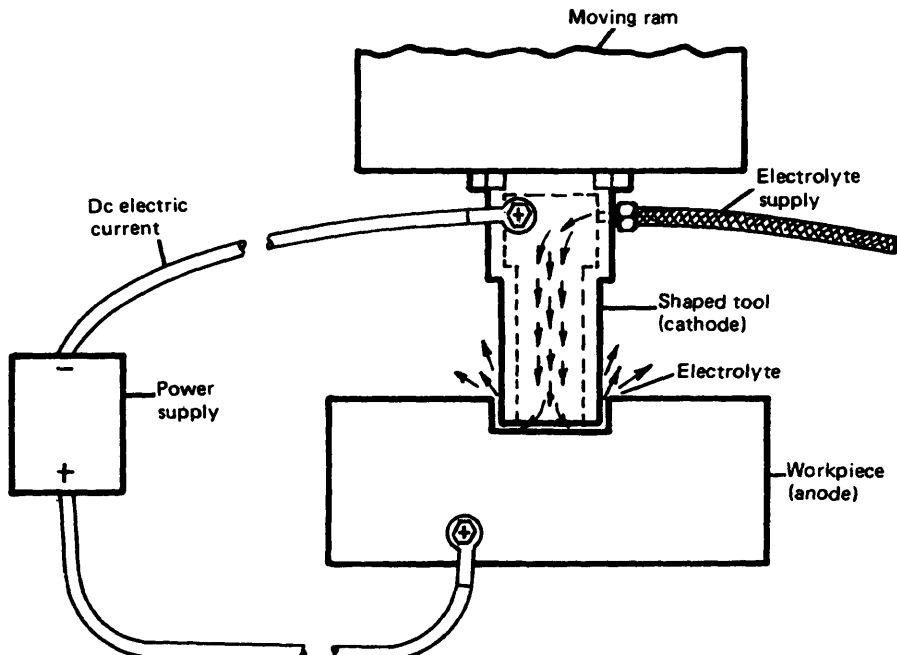
Figure 14.10   Schematic of electrochemical machining.

The fast-moving electrolyte removes the deplated material while it is in solution, before it can become plated on the tool (the cathode). Hence, there is neither tool wear nor plating of the workpiece material on the tool so that one tool can produce a large number of components during its life.

The electrolyte serves two important functions in ECM. First, the electrolyte provides the medium by which electrolysis takes place; and second, it removes the heat that is generated in the working zone as a result of the high current flow through the electrodes and the electrolyte.

The electrolyte most commonly used is brine; other salt solutions have been used in specific applications. The corrosive nature of the electrolytes used necessitates that the parts of the machine exposed to the electrolyte be manufactured from stainless steel or plastic or be coated with corrosion-resistant paint.

14.7.1 Metal Removal Rates

The rate at which material is removed from the workpiece in ECM can be predicted from a knowledge of its electrochemical equivalent.

The metal removal rate may be expressed as follows:

$$Z_{w_e} = \frac{\eta_e e I}{\rho} \tag{14.1}$$

where

Z_{w_e} = volume of metal removed electrolytically per unit time
e = electrochemical equivalent of the work material
I = current
η_e = current efficiency (i.e., fraction of the current actually effective in electrolysis)
ρ = density of the work material

The metals cobalt, iron, nickel, molybdenum, chromium, and tungsten, common constituents of engineering alloys, all have values of e/ρ in the range 32.5 to 37.4 p · m^3/As (0.119 to 0.137 $in.^3$/min/1000 A). The current efficiency η_e is usually on the order of 0.75 to 0.90, so that a good approximate figure for metal removal by ECM is 27.3 p · m^3/As (0.1 $in.^3$/min/1000 A) [9].

From Eq. (14.1) the tool feed speed is given by

$$v_f = \frac{Z_{w_e}}{A} = \eta_e \frac{e}{\rho} \frac{I}{A} \tag{14.2}$$

where

v_f = tool feed speed
A = area of work surface exposed to electrolysis
I/A = current density

Thus, to obtain the highest machining rate, the highest permissible current density should be used. The current density is limited by the capacity of the supply as well as the capacity of the work material, the tool material, and the electrolyte to carry the current. The current should not be so high as to produce excessive heat in the tool and the work or to cause electrical breakdown or decomposition of the electrolyte. A figure of 1.5 MA/m^2 (1000 $A/in.^2$) can usually be safely assumed, while quite often a current density as high as 4.5 MA/m^2 (3000 A/in^2) is permissible. Thus, when the maximum possible cutting rate is desired, the highest permissible current for the particular job must be determined by experiment. Table 14.3 shows the material removal rates for a range of different materials [1].

If the permissible current density for a particular job limits the total current to a level well below the machine and supply capacities, the possibility of two or more pieces being worked simultaneously may be considered. In this way the machine can be used to its full capacity and the overhead cost per component kept low.

Table 14.3 ECM Removal Rates[a]

Material	Density (g/cm³)	Removal rate (cm³/min)
Aluminum	2.7	1.9
Beryllium	1.8	1.3
Cobalt	8.9	1.9
Copper	8.9	3.9
Iron	7.8	2.1
Lead	11.3	5.0
Molybdenum	10.1	1.8
Nickel	8.9	1.9
Titanium	4.5	1.9
Tungsten	19.3	0.8
Uranium	19.0	1.8
Zirconium	6.5	1.9

[a]Adapted from Benedict [1].

14.7.2 Nature of the Machined Surface

The fact that metal removal in ECM is not achieved by mechanical shearing (as in conventional machining) or by melting and vaporization of the metal (as in EDM, Sec. 14.9) means that no thermal damage occurs and no residual stresses are produced on the worked surface. For this reason, ECM is often selected for highly stressed or fatigue-sensitive applications in the aerospace industries. The only heat generated results from electrical resistance, and the temperature cannot be allowed to rise above the boiling point of the electrolyte.

14.7.3 Effect of Tool Feed Speed and Supply Voltage on Accuracy

The predominant resistance to the current flow in ECM is that due to the electrolyte, and hence the current may be expressed as follows:

$$I_c = \frac{V_s}{R_e} = \frac{A V_s}{r_e a_g} \tag{14.3}$$

where

V_s = supply voltage
R_e = resistance owing to the electrolyte
r_e = specific resistivity of the electrolyte
a_g = gap between tool and work surfaces
A = area of work surface exposed to electrolysis

An expression for the gap width may now be obtained from Eqs. (14.2) and (14.3):

$$a_g = \frac{\eta_e V_s}{r_e \rho v_f} \tag{14.4}$$

Equation (14.4) shows that as the feed speed is increased, the gap width decreases. A smaller gap between the tool and the workpiece means higher accuracy of reproduction; therefore a higher feed speed (and hence a higher rate of removal) gives greater accuracy.

From Eq. (14.4) it is also seen that an increase in the applied voltage V_s increases a_g and hence reduces the accuracy of reproduction. However, as V_s is progressively increased with a given feed speed v_f [hence a constant current, by Eq. (14.2)], the increase in gap width a_g causes an increase in resistance. The increased heat generation and consequent temperature

rise lead to an increase in resistivity r_e so that the linear relationship between a_g and V_s no longer holds; the effect of this nonlinearity is to reduce the increase of a_g with V_s at constant v_f [10].

The supply voltage commonly used in ECM ranges from 5 to 20 V [7], the lower values being used for finish machining and the higher values for rough machining.

14.7.4 Tools for Electrochemical Machining

Tools for ECM are made from materials resistant to the electrolyte and also relatively easy to machine. Commonly used materials are brass, copper, stainless steel, and titanium. Tool design is often based upon experience with the process.

If a vertical-sided tool electrode is used to form a cavity in a workpiece, the sides of the cavity produced will not be vertical. This lack of conformity is a result of the current flowing between the sides of the tool and the sides of the cavity. To eliminate this effect it is usual to cover the sides of the tool with insulating material [2]. When the sides of the cavity required are not parallel to the direction of tool feed, such insulation may be unnecessary. The desired cavity shape may then be obtained by correcting the tool form, with the amount of the correction determined from practical experience with the process.

A most important factor in ECM tool design is provision of a suitable passage through the tool for efficient electrolyte flow through the cutting gap and to prevent stagnation areas.

14.7.5 Applications

The main applications of ECM are in the machining of complex shapes in difficult-to-machine materials, such as those used in high-temperature service. The removal rate for such materials can be much higher than that obtained with conventional machining, if conventional machining can be used at all. The removal rate for softer and more ductile materials is lower than that possible with conventional machining processes; but even for softer, more ductile materials ECM can be useful for producing complex shapes accurately.

The ECM process has been applied successfully to the following:

1. Machining of through holes of any cross section, usually by trepanning
2. Machining of blind holes with parallel sides
3. Machining of shaped cavities (i.e., forging dies)
4. Wire cutting of large slugs of metal

5. Machining of complex external shapes (i.e., turbine blade root profiles).

14.8   ELECTROLYTIC GRINDING

Electrolytic grinding is a modification of the ECM process described above [11]. The tool electrode consists of a rotating abrasive wheel, usually a metal-bonded diamond wheel, that can conduct electricity. The electrolyte is fed between the wheel and the work surface in the direction of movement of the wheel periphery so that it is carried past the work surface by the action of the wheel rotation. The abrasive particles help to maintain a constant gap between the wheel and the workpiece. In addition, the abrasive continually removes electrically resistant films from the work surface, which otherwise tend to impede the electrolytic action. (See Fig. 14.11.)

Thus, the metal removal rate can be expressed as

$$Z_w = Z_{w_e} + Z_{w_a} \qquad\qquad (14.5)$$

where

Z_w = total metal removal rate
Z_{w_e} = metal removed electrolytically per unit time
Z_{w_a} = metal removed by mechanical abrasion per unit time

The value of Z_{w_e} can be obtained from a knowledge of the current flowing, the electrochemical equivalent of the work material, and the current efficiency. For current densities up to approximately 1 MA/m² (700 A/in.²) the current efficiency can be assumed to be 1.00. Usually in practice Z_{w_e} constitutes 90 percent and Z_{w_a} 10 percent of the total metal removal rate Z_w [12].

In electrolytic grinding the predominance of the electrolytic action reduces wheel wear to a negligible amount and makes it possible to grind hard materials rapidly. Moreover, the wheel can be used for long periods without dressing. The temperature rise and mechanical forces are very small, and hence thermal damage and surface cracks, common in conventional grinding, are eliminated [12]. The surfaces are also free from scratches and burrs.

In applying electrolytic grinding it is desirable to design the operation in such a way that the area of contact between the wheel and the work is as large as possible [9]. This large contact area gives the highest rate of removal for a given current density and allows full use to be made of the
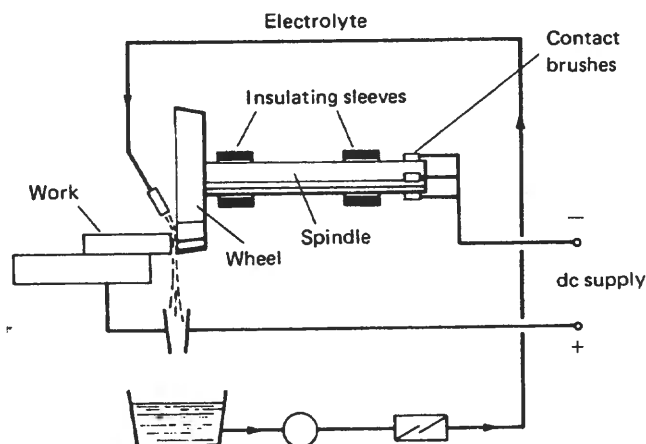
Figure 14.11 Electrolytic grinding.

available current capacity. Thus, applications that would conventionally require multipass grinding can be performed with a single pass by electrolytic grinding.

Electrolytic grinding has been used very successfully in the grinding of hard materials, which must also be electrically conductive. One of the most successful applications of the process is in the grinding of carbide-tool inserts [1], where the absence of grinding cracks in the ground tip and the high rate of removal are a great advantage. The saving in wheel wear also constitutes a major economy. Surface finishes of the order of 0.1 μm (4 μin.) have been obtained when carbide inserts are ground.

14.9 ELECTRICAL-DISCHARGE MACHINING

Electrical-discharge machining (EDM), or spark machining, as it is also called, removes material with repetitive spark discharges from a pulsating dc power supply, with a dielectric flowing between the workpiece and the tool.

The principle of the EDM process is illustrated by the simplified diagram in Fig. 14.12. The tool is mounted on the chuck attached to the machine spindle whose motion is controlled by a servo-controlled feed drive. The workpiece is placed in a tank filled with a dielectric fluid; a depth of at least 50 mm (2 in.) over the work surface is maintained to eliminate the risk of fire. The tool and workpiece are connected to a pulsating dc power supply. Dielectric fluid is circulated under pressure by a pump, usually through a hole (or holes) in the tool electrode. A spark gap of about 0.025 to 0.05 mm (0.001 to 0.002 in.) is maintained by the servomotor.

In power supplies for EDM the input power is first converted into continuous dc power by conventional solid-state rectifiers. The flow of this dc power is then controlled by a bank of power transistors which are switched by a digital multivibrator oscillator circuit. The high-power pulsed output is then applied to the tool and workpiece to produce the sparks responsible for material removal.

Each spark generates a localized high temperature on the order of 12,000°C in its immediate vicinity. This heat causes part of the surrounding dielectric fluid to evaporate; it also melts and vaporizes the metal to form a small crater on the work surface. Since the spark always occurs between the points of the tool and work that are closest together, the high spots of the work are gradually eroded, and the form of the tool is reproduced on the work. The condensed metal globules, formed during the process, are carried away by the flowing dielectric fluid. As the metal is eroded, the tool is fed toward the workpiece by a servo-controlled feed mechanism.
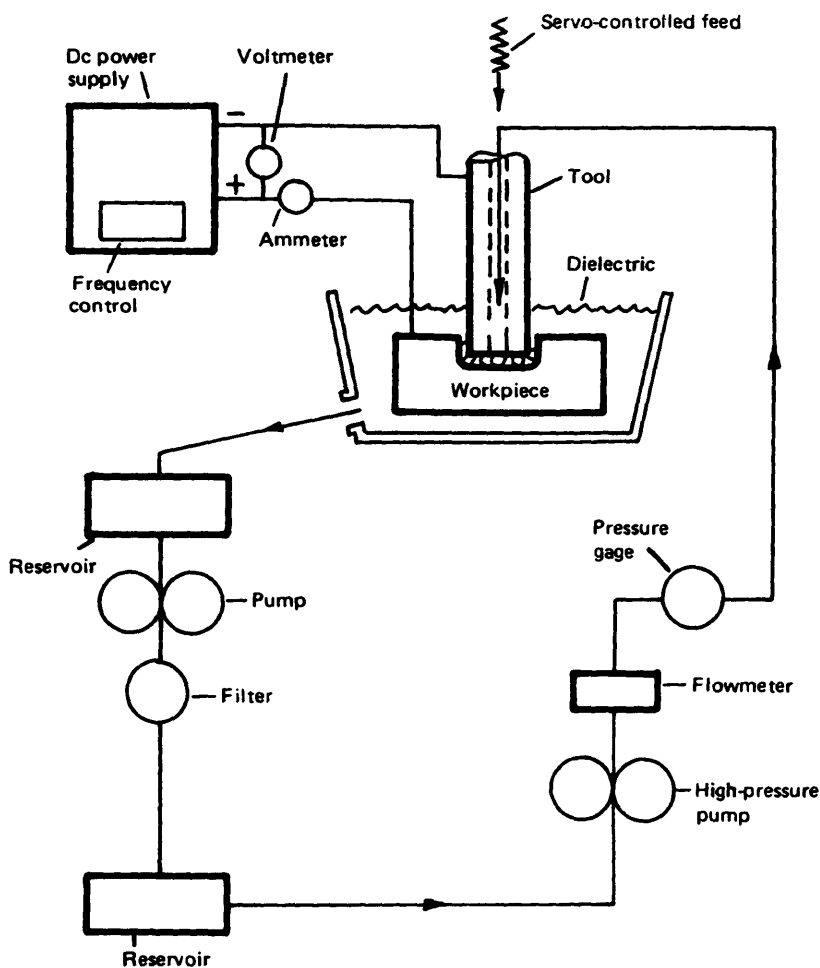
Figure 14.12   Basic features of electrical-discharge machining.

Each pulse in the EDM cycle lasts for only a few microseconds. Repeated pulses, at rates up to 100,000 per second, result in uniform erosion of material from the workpiece and from the electrode. As the process progresses, the electrode is advanced by the servodrive toward the workpiece to maintain a constant gap distance until the final cavity is produced.

The servomechanism that controls the infeed of the tool into the workpiece, shown in its simplest form in Fig. 14.13, consists of a reversible servomotor connected between one terminal of the condenser (D) and the slider of a variable resistance (B). A and C are at the same potential; if the mean value of the voltage V_c (Fig. 14.13) is equal to the preset voltage between A and B, the potentials at B and D are equal, and the servomotor remains stationary. If, however, the mean value of the voltage V_c changes because of changes in gap width, the potential at D will change, and the servomotor will rotate until the required gap is again obtained. In this way the servosystem maintains the mean spark-gap voltage (and hence the gap width) at a constant value. The motor must be reversible because if the servomechanism overshoots or short-circuits as a result of the accumulation of swarf in the gap, the tool must be withdrawn. A constant gap of about 0.025 to 0.05 mm (0.001 to 0.002 in.) is usually maintained [1]; the exact gap value may be varied by changing the setting of the variable resistance. Other types of control used in practice usually operate by sensing either the gap voltage or the gap capacitance.

14.9.1 Tool Materials and Tool Wear

The EDM electrode shape determines the shape of the hole or cavity which is sunk into the workpiece. Many materials have been successfully used as EDM electrodes. The main requirements of a tool material for EDM are as follows:

1. Electrically conductive
2. Exhibits low wear rates
3. Is easily machinable
4. Provides good surface finish on the workpiece

Each spark discharge removes material from both the workpiece and the electrode, and consequently the electrode gradually wears during the machining process. The wear ratio, defined as the volume of metal lost from the tool divided by the volume of metal removed from the work, depends on the tool and work materials used. For example, with a brass tool and a brass workpiece the ratio is approximately 0.5, whereas for a brass tool and a hardened-carbon-steel workpiece it is approximately
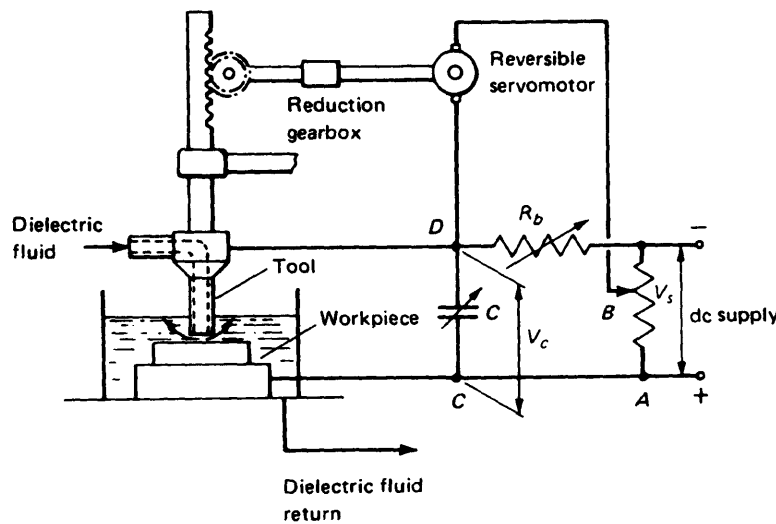
Figure 14.13 Basic features of EDM tool-feed control.

unity and for a brass tool and a tungsten carbide workpiece the ratio may be as high as 3. With suitably chosen materials wear ratios as low as 0.1 can be achieved [1,13].

The volume of material removed per discharge decreases rapidly as the melting point of the material increases (Fig. 14.14); thus high values of the wear ratio are obtained by having a high melting point for the tool material relative to the melting point of the work material [13]. Table 14.4 gives some properties of commonly used EDM tool materials. Graphite and copper graphite are by far the most common materials used. Graphite is easily machined and, because it vaporizes at very high temperatures relative to most metals, the wear rates of graphite electrodes are very low. Copper is added to graphite to form copper graphite, mainly to increase the conductivity of the electrode material. Copper and brass are also used as tool materials, but exhibit relatively high wear rates. Copper tungsten provides greatly improved wear rates, but is a much more difficult material to machine. Tungsten wire is often preferred over other materials
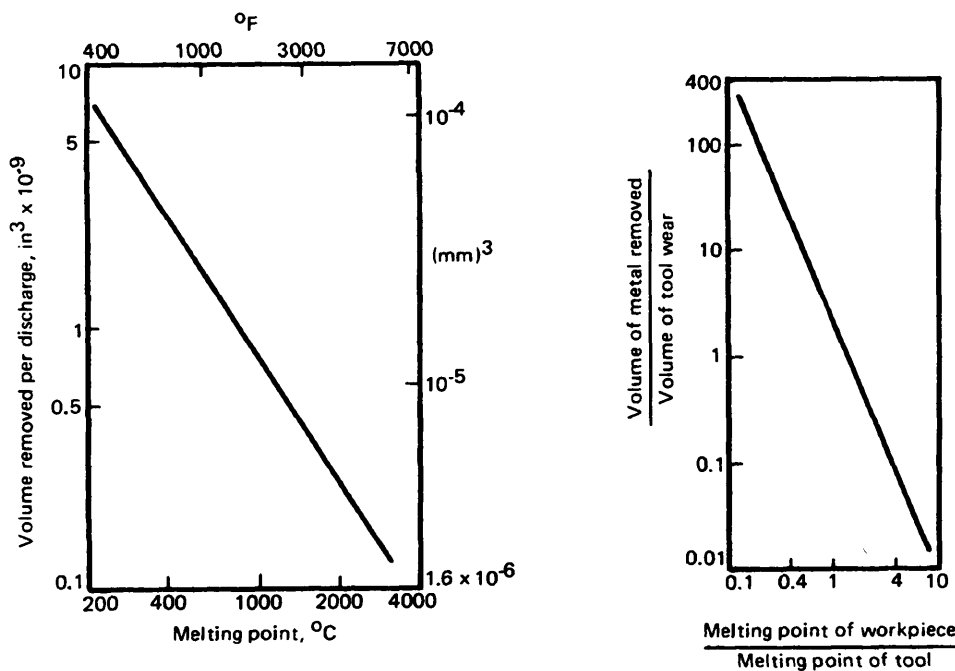
Figure 14.14 EDM metal removal and tool wear. (a) Volume removed per discharge as a function of melting point; (b) wear ratio as a function of workpiece to tool melting-point ratio.

Table 14.4 Some Physical Properties of Electrical Discharge Machining (EDM) Electrode Materials[a]

Property	Copper	Graphite	Tungsten	Iron
Melting point	1083	b	3395	1535
Boiling point	2580	>4000	>5930	>2800
Heat to vaporize from room temperature, cal/cm³	12,740	about 20,000	about 22,680	about 16,900
Thermal conductivity, Ag = 100%	94.3	30.3	29.6	16.2
Electrical conductivity, Ag = 100%	96.5	0.1	48.1	16.2
Strength, N/mm²	241	34	4134	275
Modulus of elasticity, N/mm² × 10³	124	5.9	351	186

[a]From Kalpajian [13].
[b]Sublimes or boils before melting at atmospheric pressure.

for drilling deep holes of small diameter because it can better withstand the tendency of the wire to buckle as a result of shock waves produced by the spark discharge or physical contact with the workpiece in the case of overshoot.

14.9.2 Dielectric Fluid

The dielectric fluid used must remain nonconducting until breakdown occurs; when the critical voltage is reached, it must break down rapidly and then deionize rapidly as each spark is discharged. The latent heat of vaporization of the dielectric fluid must be high so that only a small quantity vaporizes and the spark channel is confined to a small area. The dielectric fluid must have sufficiently low viscosity to flow easily and remove the metal globules effectively from the working zone. The dielectric fluid also acts as a coolant to carry away the heat generated by each spark.

The dielectric fluids commonly used are paraffin oil and transformer oil. Both these fluids are hydrocarbons and it has been found [14] that the hydrogen in these fluids provides the deionizing action necessary for the fluid to become an effective insulator after each discharge.

The dielectric fluid may be fed through nozzles near the working zone, but where possible, and especially when deep holes are drilled, the fluid is fed or drawn through the tool itself. In electrode design it is

necessary to provide sufficient passages through the tool to ensure adequate flushing of the tool–workpiece gap and prevent debris buildup, which can result in short circuits. Before the dielectric fluid is recirculated to the working zone, it is necessary to filter it to remove the metal particles produced in the process.

14.9.3   Process Parameters

Metal removal rates, surface finish, and accuracy are influenced mainly by the choice of electrical parameters. As the current is increased, each individual spark removes a larger crater of workpiece material (Fig. 14.15a), which increases the metal removal rate but also increases the surface roughness. Similar effects occur with increased spark voltage. Increasing the spark frequency, while keeping the other parameters constant, results in a decrease in surface roughness (Fig. 14.15b), because the energy available is shared between more sparks, and smaller-sized surface craters are produced in the workpiece. The frequency range of modern EDM machines is from 180 Hz, for roughing cuts, to several hundred kilohertz, for fine finishing. When the sparking frequency becomes very high, the dielectric fluid cannot deionize at a sufficiently high rate, placing an

(a)

1 amp   2 amp   3 amp   4 amp

(b)
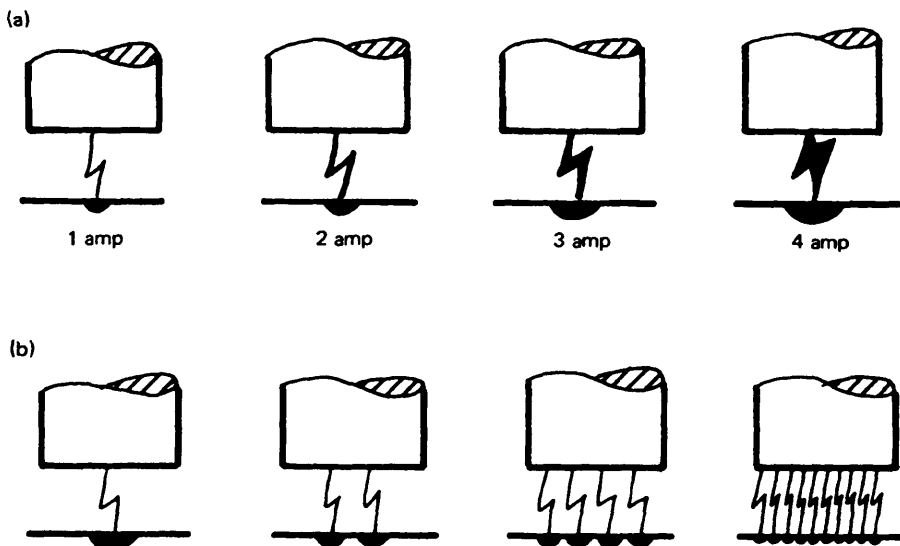
Figure 14.15   Influence of current and pulse frequency on metal removal and surface finish. (Adapted from Benedict [1].)

upper limit on the frequencies possible. Volumetric removal rates vary from 0.001 to 0.1 cm^3/hr [1].

The accuracy of the process is closely related to the spark-gap width; the smaller the gap the higher the accuracy, but a smaller gap results in a lower working voltage and a lower removal rate. A compromise is thus necessary. Typical spark gaps range from 0.012 to 0.05 mm. As the gap decreases, efficient flushing of the gap becomes more difficult to achieve.

Other factors affecting the accuracy of the process are the accuracy of the tool electrode itself and the allowance made on it for the spark gap. A cause of inaccuracy when deep parallel-sided cavities and holes are produced is the taper produced by sparks occurring between the sides of the electrode and the sides of the cavity. This sparking is assisted by any eroded particles that pass between the electrode and the sides of the cavity and effectively reduces the breakdown voltage of the dielectric fluid. The taper produced in this manner, on the order of 0.05 mm (0.002 in.) per side on the total depth of the cavity, becomes an asset in the machining of molds, blanking dies, and so on, where a small draw angle is required [2]. If the taper is not desirable, the tool form can be corrected by suitably relieving it behind the tip.

The spark-machined surface, having a matte appearance similar to a shot-blasted surface, consists of very small spherical craters as a result of the metal being removed by individual sparks. The finish is therefore nondirectional and very suitable for holding a lubricant [15]. Surface finishes of 0.25 μm (10 μin.) and better have been obtained. A layer of melted and resolidified material, known as recast, is left on the surface produced by EDM. This layer tends to be very hard and brittle (greater than $65R_c$ hardness). This recast layer is usually from 0.0025 to 0.05 mm in thickness and may have to be removed by other processes if high levels of fatigue resistance are required.

14.9.4 Applications

Electrical-discharge machining can be used for all electrically conducting materials regardless of hardness. The process is most suited to the sinking of irregularly shaped holes, slots, and cavities. Fragile workpieces can be machined without breakage. Holes can be of various shapes and can be produced at shallow angles in curved surfaces without problems of tool wander [1].

The EDM process finds greatest application at present in toolmaking, particularly in the manufacture of press tools, extrusion dies, forging dies, and molds. Graphite electrodes produced by copy milling from patterns are often used.

A great advantage of EDM is that the tool or die can be machined after it is hardened and hence great accuracy can be achieved. Tools of cemented carbide can be machined after final sintering, which eliminates the need for an intermediate partial sintering stage, thus eliminating the inaccuracies resulting from final sintering after holes, slots, and so on, are machined [15].

Electrical-discharge machining can be used effectively to drill small high-aspect-ratio holes. Diameters as small as 0.3 mm in materials 20 mm or more in thickness can be readily achieved. With efficient flushing, holes with aspect ratios as high as 100:1 have been produced. The process has been used successfully to produce very-small-diameter holes in hardened fuel-injector nozzles. Varying numbers of holes in a precise pattern can be drilled around the injector tip [1].

14.10   WIRE ELECTRICAL-DISCHARGE MACHINING

Wire electrical-discharge machining (wire-EDM) is an adaptation of the basic EDM process, which can be used for cutting complex two- and three-dimensional shapes through electrically conducting materials. Wire-EDM utilizes a thin, continuously moving wire as an electrode (Fig. 14.16). It is a relatively new process and applications have grown rapidly, particularly in the toolmaking field [16].

The wire electrode is drawn from a supply reel and collected on a take-up reel. This continuously delivers fresh wire to the work area. The wire is guided by sapphire or diamond guides and kept straight by high tension, which is important to avoid tapering of the cut surface.

High-frequency dc pulses are delivered to the wire and workpiece, causing spark discharges in the narrow gap between the two. A stream of dielectric fluid is directed, usually coaxially with the wire, to flood the gap between the wire and the workpiece. The power supplies for wire-EDM are essentially the same as for conventional EDM, except the current-carrying capacity of the wire limits currents to less than 20 A, with 10 A or less being most normal. In addition, the spark frequencies are higher, up to 1 MHz, to give a fine surface finish on the workpiece.

The workpiece is moved under computer numerical control (CNC) (Fig. 14.17) relative to the wire, and this enables complex-shaped profiles to be cut through sheet and plate materials. Many machines incorporate further angular positioning of the wire, thus allowing varying degrees of taper on the cut surface to be obtained. Adaptive control, based on gap-voltage sensing, is necessary to avoid contact between the wire and the work material. Short circuits must be sensed and the wire backed off along the programmed path to reestablish the correct gap for efficient cutting.
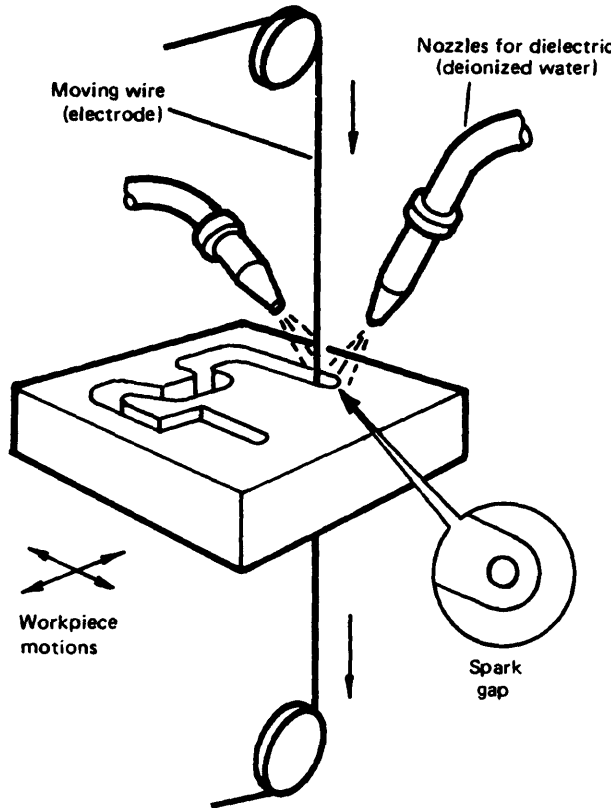
Figure 14.16   Basic features of wire-EDM.

Deionized water is the dielectric used for wire-EDM because it has low viscosity, presents no fire hazard, and results in high cooling rates and high material removal rates [1]. A low viscosity is important to ensure adequate flow through the wire–workpiece gap to ensure efficiency of flushing. Copper and brass wires are commonly used for the electrodes, when the wire diameter is relatively large (0.15 to 0.30 mm). If very fine wire is required for high-precision cutting (0.03 to 0.15 mm), molybdenum-steel wire is used for increased strength. The wire–workpiece gap usually ranges from 0.025 to 0.05 mm and consequently the kerf width of cut made by wire-EDM is less than 0.1 mm plus the wire diameter.

Wire-EDM is most commonly used for the fabrication of press stamping dies, extrusion dies, powder composition dies, profile gages, and templates. Complicated cutouts can be made in difficult-to-machine metals
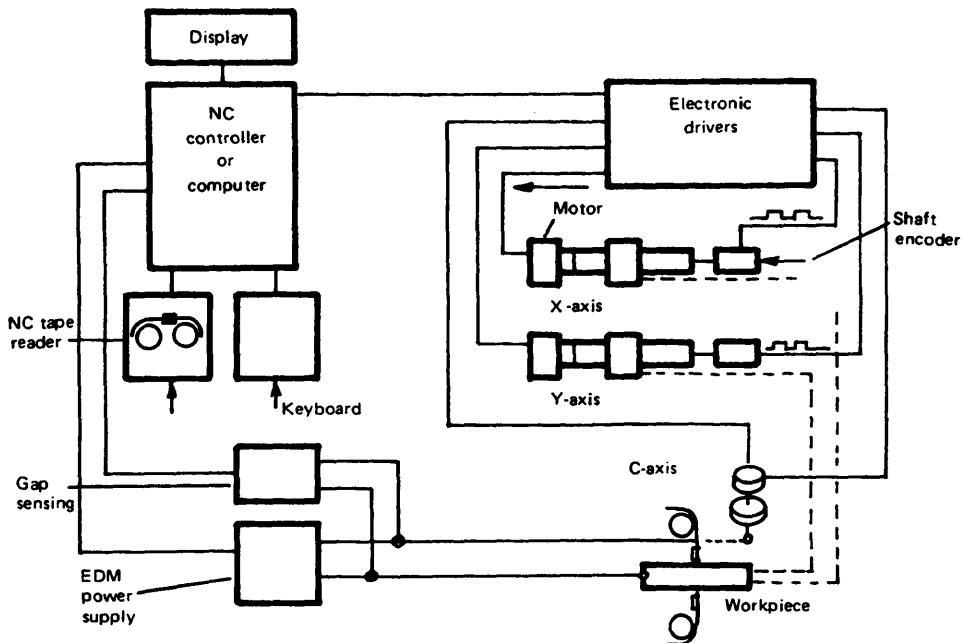
Figure 14.17 Schematic of wire-EDM system.

without the need for high-cost grinding or expensive shaped EDM elec-
trodes. Linear cutting rates are relatively low, ranging, for example, from
38 to 115 mm/hr in 25 mm thick steel. However, the linear speed is de-
pendent on the material being cut and not on the shape of the cut.
Although wire-EDM is a relatively slow cutting process, this is compen-
sated for by the complexity and accuracy of the profiles that can be cut.
Machines for wire-EDM are designed to operate unattended for long
periods of time (often for several days).

Accuracies in the cut-out profile of ±0.007 mm can be routinely ob-
tained with wire-EDM, and this figure can be further reduced with special
care, including ensuring uniformity of the wire diameter. The minimum
internal corner radius possible is limited only by the wire diameter being
used. External corners can be produced with radii as small as 0.038 mm.

14.11   LASER-BEAM MACHINING

Laser-beam machining can be used for the cutting, drilling, slotting, and
engraving of most materials. Material is removed rapidly by means of a
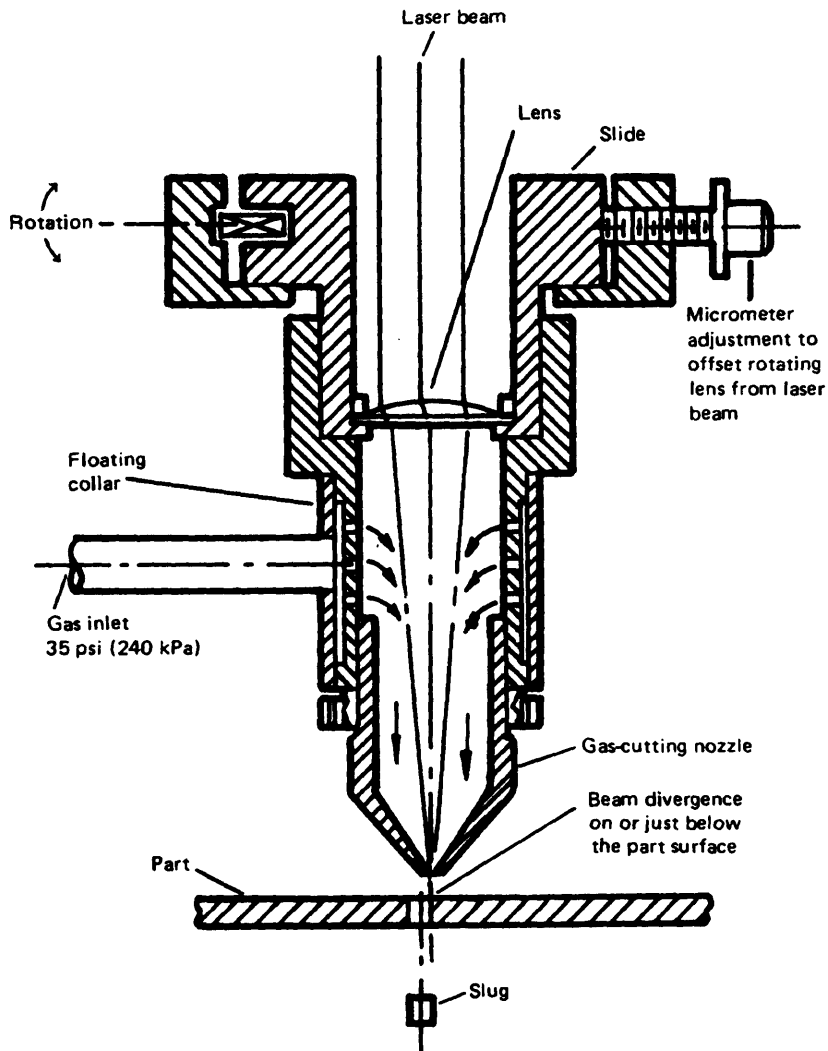
Figure 14.16   Typical laser cutting-head configuration.

high-energy coherent beam of light of a single wavelength. A typical cutting-head configuration is shown in Fig. 14.18. The beam is focused by the lens to a short distance from the nozzle of the cutting head. The high concentration of light at the focus produces energy densities as high as 10^6 W/mm^2 and lasers of less than 100 W power are capable of vaporizing or melting most materials [1]. Cutting and drilling can be achieved with no force applied to the workpiece and with only a small heat-affected zone.

14.11.1 Types of Laser

Table 14.5 lists the main types of laser used for drilling and cutting [1]. They differ mainly in the power output and wavelength of light used. A high proportion (over 70 percent) of industrial applications use either Nd:YAG or CO_2 lasers, mainly because of the higher power capabilities. The higher power lasers are capable of both pulsed or continuous generation. High-rate pulsing or continuous operation is required for cutting applications.

14.11.2 Percussion Drilling of Small Holes

Percussion drilling is the simplest technique for producing small holes. The laser beam is focused near to the workpiece surface and a short duration pulse from the laser causes a small volume of material to melt and partially vaporize. The explosive escape of the vapor removes most of the melted material in the form of a spray of molten droplets. Multiple pulses can be used to penetrate thick materials that cannot be drilled with one pulse.

Holes produced by this process are generally tapered (Fig. 14.19) and are only approximately round, but the hole size is highly repeatable. The depth of recast layer on the surface of the hole produced is very small. Holes can be drilled in times varying from 1 ms to 2 s dependent on the

Table 14.5   Industrial Laser Characteristics[a]

Laser type	Mode of operation	Power (W)
Ruby	Pulsed	50
Nd:glass	Pulsed	50
Nd:YAG	CW/pulsed	600
Alexandrite	CW/pulsed	100
CO_2	CW/pulsed	25,000

[a]From Benedict [1].
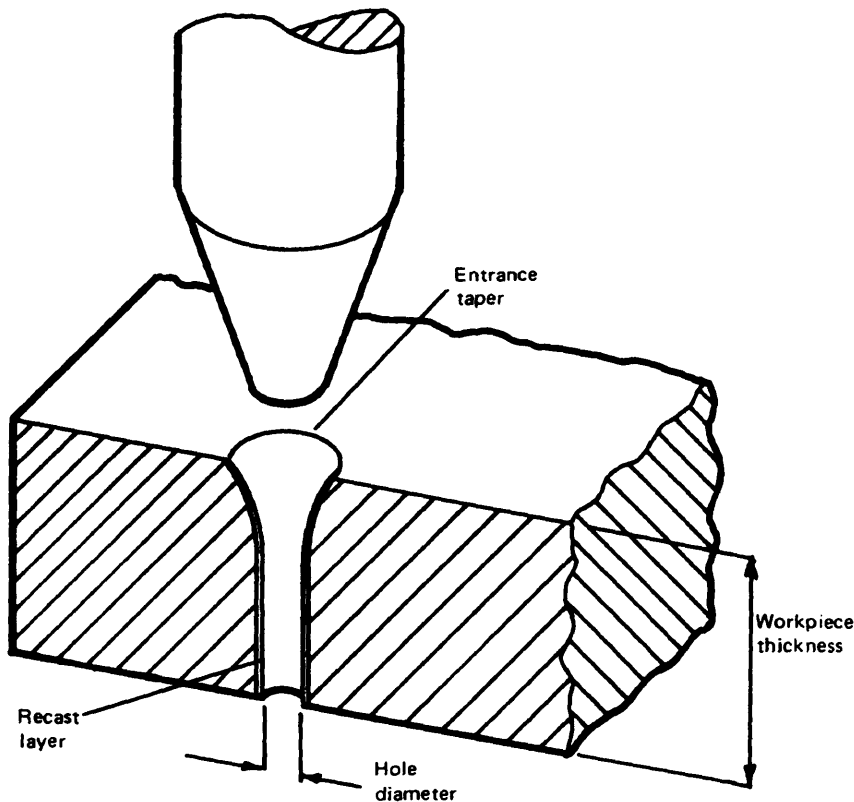
Figure 14.19 Hole configuration for laser percussion drilling.

material thickness; the maximum hole diameter that can be drilled is about 1.3 mm. Larger holes require defocusing of the beam, which decreases the illumination intensity and produces uneven melting of the workpiece material.

14.11.3 Trepanning or Cutting Operations

In the cutting or trepanning mode of operation, the laser pulses rapidly or operates continuously and a jet of gas is introduced through the cutting head around the focused beam (Fig. 14.18). The jet of gas can assist the melting of the material and facilitate the clearing of molten material from the cut, together with keeping debris from contaminating the focusing lens. The most commonly used gases are oxygen, air, and argon. Oxygen is used for materials that oxidize, such as carbon steels. The oxygen assists

the melting process and results in high cutting speeds, particularly for thin materials (Fig. 14.20). The cut edges left are oxidized and have a significant heat-affected zone.

Air is much less expensive to use than oxygen, but cutting rates are reduced because of the much lower oxygen content. Argon is used when shielding of the cut surfaces from oxidation is required, but results in cutting speeds about 25 percent lower than when using air.

Laser cutting machines are often fitted with numerical control for moving the workpiece relative to the workhead. These machines are able to cut complex profiles and holes with high precision and high cutting speeds; without the requirement for complex tooling, kerf widths as low as 0.64 mm can be achieved in thin materials.

14.11.4   Applications

Lasers are used for a variety of drilling and cutting applications. A wide range of materials can be cut with high precision and a small heat-affected zone. A typical drilling application is the formation of a pattern of small holes in gas turbine blades that provide cooling airflow through the blade surface. The small-diameter holes are readily produced in the high-temperature-resistant materials used for the blades. In addition, the holes can be drilled at shallow angles to the surface, without the problems of tool breakage and slippage that result with other mechanical methods of drilling.

Laser cutting machines are now used quite extensively for cutting complex profiles in sheet and plate materials. Hard materials can be cut, without the problems of tool wear. A typical application is the high-speed blanking of radial saw blades from plate stock. This can be achieved without the need for complex tooling. Numerous different profiles can be stored in the CNC positioning systems used and recalled as required [17].

14.12   ELECTRON-BEAM MACHINING

In electron-beam machining, material is removed by means of a focused beam of high-velocity electrons that strike the workpiece. The kinetic energy of the electrons is converted into heat that is sufficient to cause rapid melting and vaporization of the workpiece material. Figure 14.21 illustrates the main elements of an electron-beam machine. To eliminate scattering of the beam of electrons, the work is done in a high-vacuum chamber (10^{-5} mm of mercury or less). Electrons are emitted from an electron gun and are accelerated to speeds of about 75 percent of the speed of light,
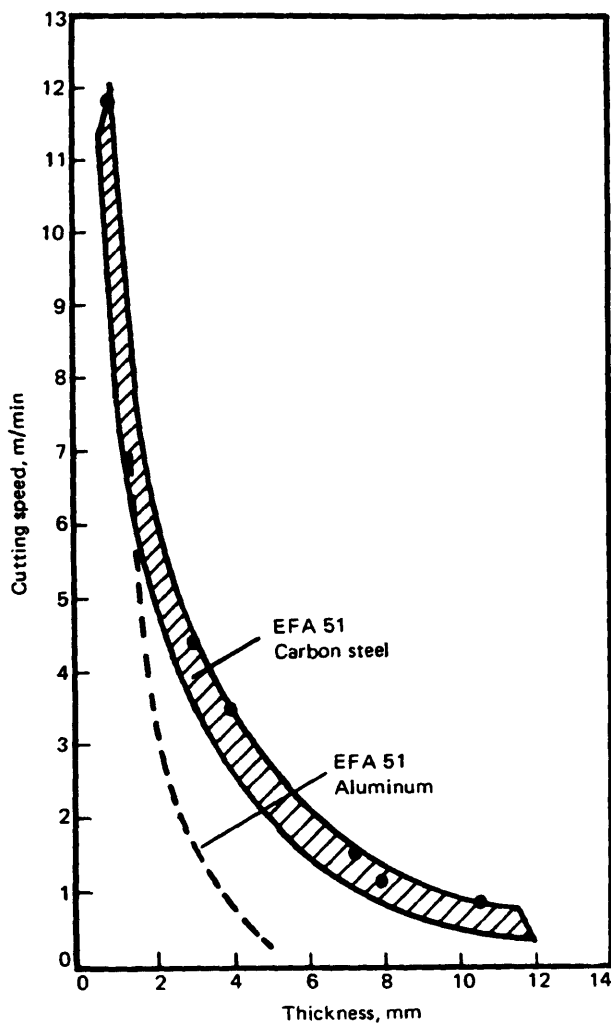
Figure 14.20 Cutting speeds in aluminum and carbon steel for a 100-W CO_2 laser. (Adapted from Benedict [1].)
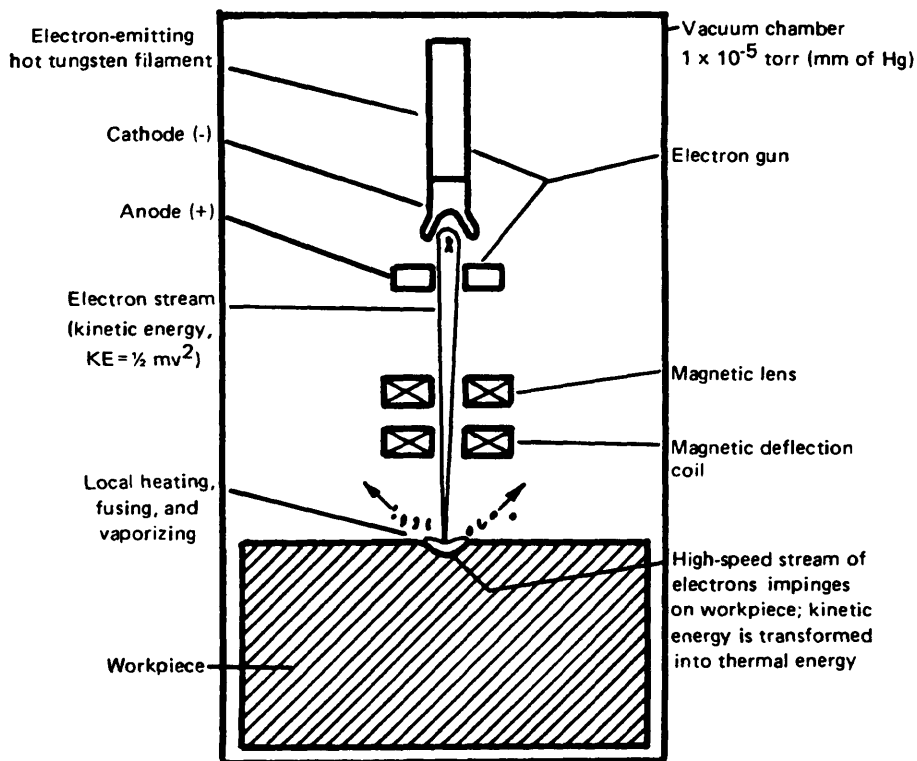
Figure 14.21 Basic features of electron-beam machining.

by voltages as high as 50 kV between the anode and cathode. A magnetic lens focuses the electron beam onto the workpiece, and energy densities of the order of 10^8 W/cm^2, which is sufficient to melt and vaporize any material, are produced.

The action of electron-beam drilling is illustrated in Fig. 14.22 [1]. The focused beam from an electron pulse strikes the workpiece and melting and vaporization of some of the material occurs. The pressure of the escaping vapor is sufficient to form and maintain a small capillary channel into the work material. The beam and capillary channel rapidly penetrate the workpiece until an organic or synthetic backing material is reached at which time the backing material vaporizes rapidly with an explosive release of vapor. The relatively high vapor pressure of the backing material vapor expells the molten walls of the capillary in a shower of sparks leaving a hole in the work material.

A single pulse is often used to produce a single hole, but for thick

| The sharply focused electron beam strikes the material to be drilled: local heating and fusion of the surface | The high power density of the electron beam produces a deepening metal vapor capillary encircled by molten material | The electron beam has drilled through the material being pierced and penetrates up to a certain depth into the auxilliary material | As a result of the high vapor pressure of the auxilliary material, the molten part of the material being drilled is expelled |

Figure 14.22 Action of electron-beam drilling.

materials multiple pulses may be required. Pulsing rates of up to 100 pulses per second are possible and deflection coils under program control can be used to move the beam around to cut holes of any shape.

A wide range of materials can be processed by electron-beam machining. As a result of the extremely high energy density of the beam and the short duration of beam–workpiece interaction, thermal effects on the workpiece material are limited to a heat-affected zone that seldom exceeds 0.025 mm in depth. The high beam-power density also enables high aspect ratio holes to be drilled, often as large as 15 to 1. For example, hole diameters of 0.1 to 1.4 mm can be drilled in materials up to 10 mm thick. Because no force is applied to the workpiece, brittle and fragile materials can be processed without fracture. Holes can be drilled at shallow angles to the work surface, as low as 20 deg if required. A minimum spacing between holes of twice the diameter of the hole is normal, but this restriction still allows up to 1000 holes per square centimeter to be drilled if required.

The most suitable application of electron-beam machining is for workpieces requiring large numbers of simple small holes to be drilled, or for drilling of holes in materials that are hard and difficult to machine by other processes. A typical example of the application of electron-beam machining [1] is the drilling of turbine engine combustor domes in Cn Nc Co Mo W steel. These parts have a wall thickness of 1.1 mm, and almost 4000 holes of 0.9 mm diameter are drilled in 60 min by electron-beam machining.

The equipment for electron-beam machining is very expensive and

the necessity to work in a vacuum adds considerably to floor-to-floor machining time. However, for certain highly specialized workpieces, electron-beam machining may be the only feasible method of production.

14.13   PLASMA-ARC CUTTING

14.13.1   General Discussion

Plasma-arc cutting is used mainly for cutting thick sections of electrically conductive materials. A high-temperature plasma stream interacts with the workpiece causing rapid melting. Any gas heated to extremely high temperatures dissociates into free electrons, ions, and neutral atoms and this condition is known as plasma. In the plasma state the material has electrical conductivity and the condition can be sustained by the application of electrical power.

The basic configuration of a plasma-arc torch is shown in Fig. 14.23. The electrically conductive workpiece material is positively charged and the electrode is negatively charged. An electric arc is maintained between the electrode and the workpiece. Gas flowing coaxially is heated to form the plasma stream, which has a peak temperature of approximately 33,-000°C. Air and nitrogen are the most commonly used gases for the plasma stream. The gas flow is delivered to the nozzle at pressures up to 1.4 MPa, producing a plasma stream that flows toward the workpiece at several hundred meters per second. The secondary gas flow around the nozzles helps constrain the plasma flow into a narrow jet and cleans the cut of molten material. The highest quality cuts can be obtained by injecting water around the main plasma jet. Some of the water vaporizes to produce a thin layer of steam that constricts the plasma. The benefits of this water constriction include a smaller heat-affected zone and increased nozzle life.

14.13.2   Applications

Using plasma-arc cutting, materials up to 200 mm in thickness can be cut [1]. However, most practical applications are for materials in the thickness range of 3 to 75 mm. Relatively high cutting speeds can be achieved, depending on the thickness and type of material being cut. Table 14.6 shows some typical cutting speeds for different materials. Tolerances of ±0.8 mm can be achieved in materials of thicknesses less than 25 mm, and tolerances of ±3 mm are obtained for greater thicknesses. The heat-affected zone for plasma-arc cutting varies between 0.7 and 5 mm in thickness.

Most applications of plasma-arc cutting are in the metal fabrication
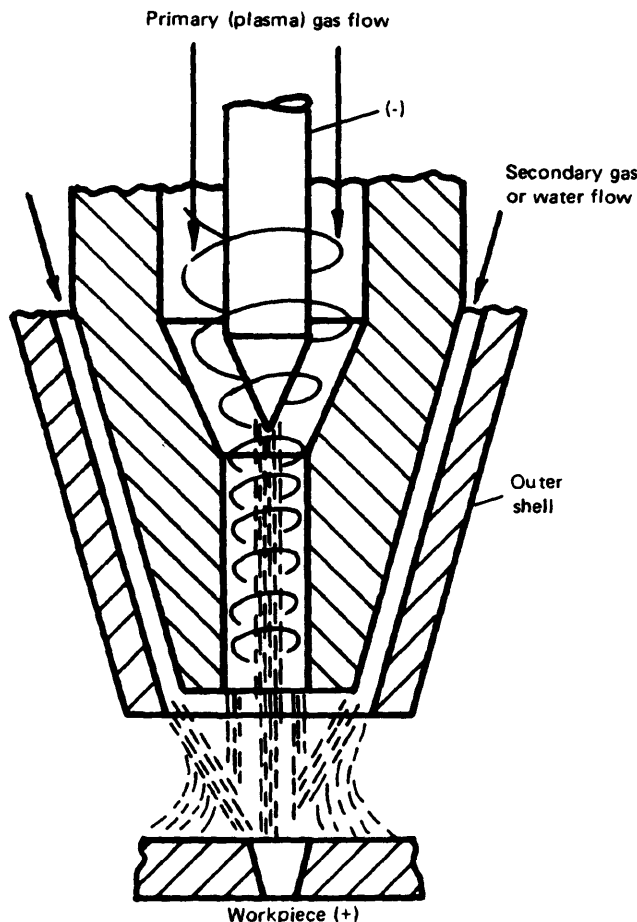
Figure 14.23 Basic features of a plasma-arc tool.

Table 14.6 Plasma Arc Cutting Speeds
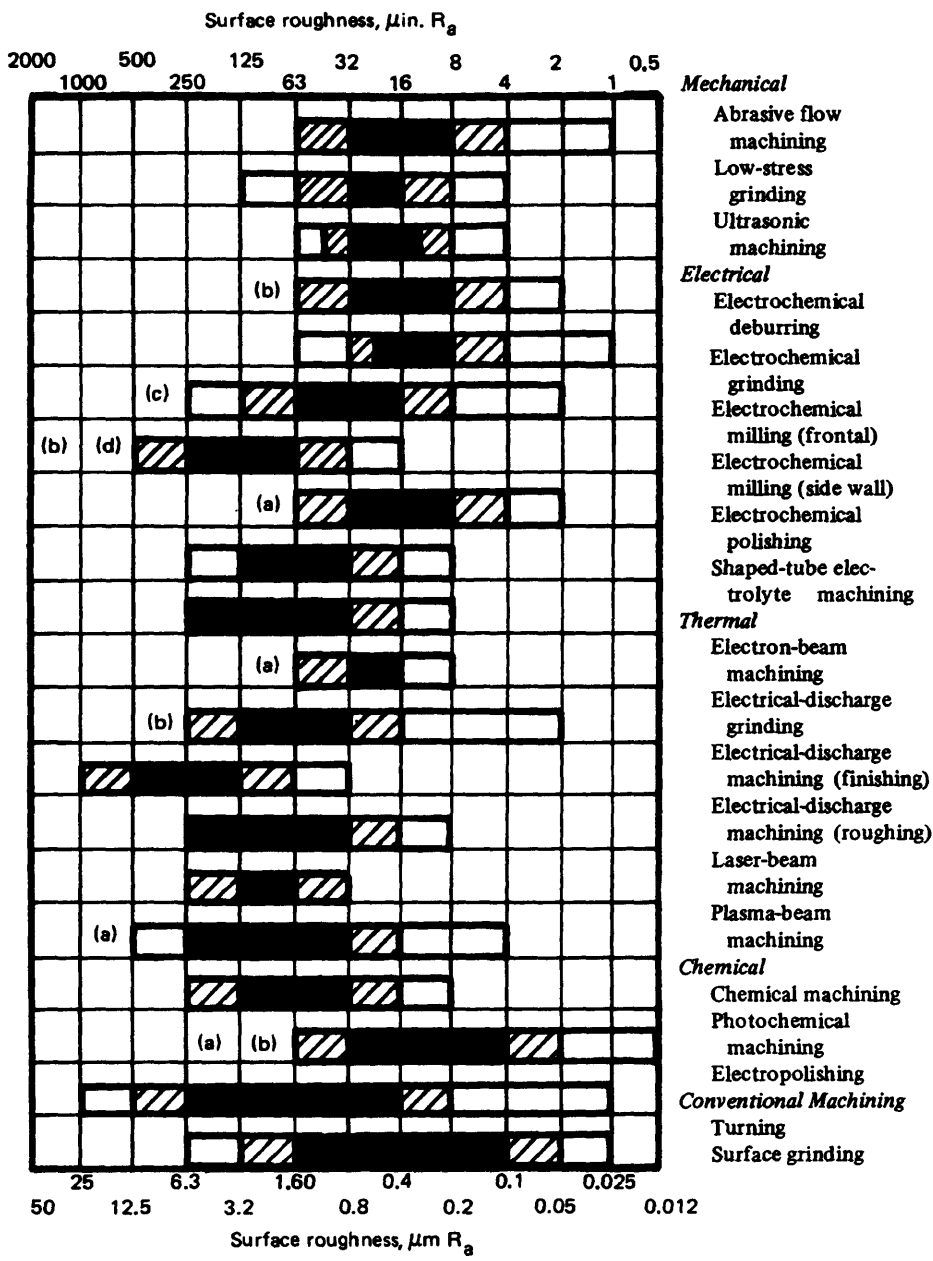
Material	Thickness (mm)	Arc current (A)	Cutting speed (mm/min)
Stainless steel	75	800	380
	130	1000	150
Aluminum	75	900	760
	180	1000	180
Brass	13	400	1780
Titanium	13	400	2285

and metal plate industries. A wider variety of materials can be cut than for flame cutting with an oxyacetylene torch. Plasma-arc nozzles can be fitted to cutting machines with both numerical and optical-line-following controls, so that relatively complex profiles can be readily cut.

14.14 COMPARATIVE PERFORMANCE OF CUTTING PROCESSES

As described in this chapter, a variety of cutting processes are available in addition to the more conventional hard-tool and abrasive machining processes. Some of these processes are only suitable for the machining of particular types of workpieces and applications, but some general comparison of the relative performance of the available processes is useful.

Figure 14.24 compares the surface finish and tolerances obtainable by various material removal processes. However, the rate at which material can be removed and the cost of removing material are also important considerations in the selection of processes. Table 14.7 compares typical metal removal rates for some of the available processes, together with the approximate power consumption per unit volume of material removed. It can be seen that conventional machining processes in general remove material faster and with less power consumption than the less conventional processes. Table 14.7 also shows values of the ratio of the capital equipment costs to the metal removal rates, relative to conventional machining. Again it can be seen that the capital costs associated with removing material by nonconventional processes are much higher than for conventional machining. However, many of the nonconventional processes may be the only viable way to produce some workpieces and shape features, particularly in hardened materials.

Surface roughness, μin. R_a

2000	500	125	32	8	2	0.5
1000	250	63	16	4	1	

Mechanical
 Abrasive flow
  machining
 Low-stress
  grinding
 Ultrasonic
  machining
Electrical
 Electrochemical
  deburring
 Electrochemical
  grinding
 Electrochemical
  milling (frontal)
 Electrochemical
  milling (side wall)
 Electrochemical
  polishing
 Shaped-tube elec-
  trolyte machining
Thermal
 Electron-beam
  machining
 Electrical-discharge
  grinding
 Electrical-discharge
  machining (finishing)
 Electrical-discharge
  machining (roughing)
 Laser-beam
  machining
 Plasma-beam
  machining
Chemical
 Chemical machining
 Photochemical
  machining
 Electropolishing
Conventional Machining
 Turning
 Surface grinding

25	6.3	1.60	0.4	0.1	0.025	
50	12.5	3.2	0.8	0.2	0.05	0.012

Surface roughness, μm R_a

Notes   (a) Depends on state of starting surface
         (b) Titanium alloys are generally rougher than nickel alloys
         (c) High current density areas.
         (d) Low current density areas.
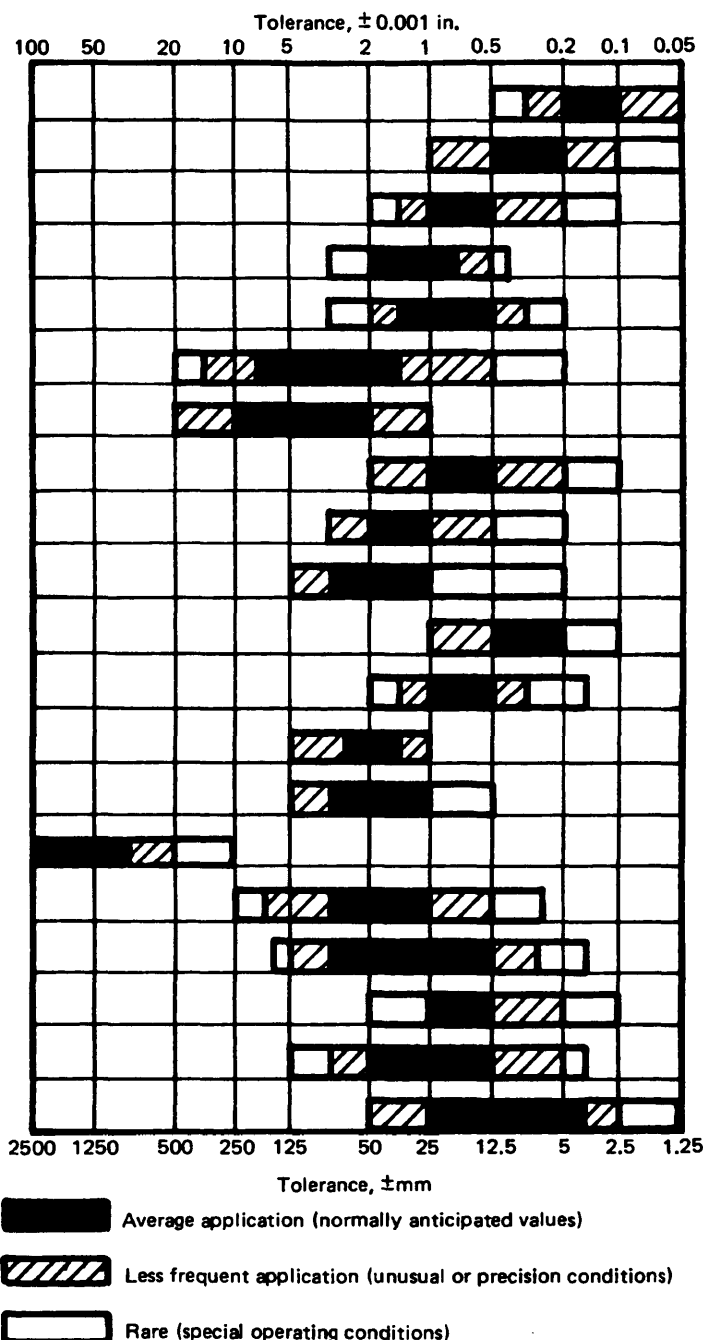
Figure 14.24 Surface roughness and tolerances for various material removal processes. (From Kalpajian [13].)

Table 14.7 Typical Removal Rates and Capital Costs for Various Machining Processes[a]

Process	Metal removal rate (cm³/s)	Approximate unit power (specific cutting energy) (GJ/m³)	Relative capital equipment cost per unit material removal rate
Edge-tool machining	14	3	1
Abrasive machining	8	30	2
Plasma jet	1.5	10	—
ECM	1.0	500	60
EDM	0.10	150	40
Ultrasonic machining	0.005	150	600
Electron beam	0.001	1,500	40,000
Abrasive jet	0.0001	10,000	—
Laser	0.0001	150,000	160,000

[a]Adapted from Wager [18].

PROBLEMS

1. Calculate the feed speed possible when drilling a 25-mm-diameter hole with electrochemical machining when a supply current of 5 kA is available. Assume that the electrochemical equivalent of the work material is 0.2 m · g/As, that its density is 8 M · g/m³, and that a current efficiency of 80 percent is obtainable.
2. Estimate the time taken to grind a 1-mm layer from the face of a carbide insert 15 mm square by electrolytic grinding. Assume that the current efficiency is 0.95, that the mass of metal removed mechanically is 10 percent of the total mass of metal removed, that a current density of 1 MA/m³ is used, and that the ratio of the electrochemical equivalent to the density of the work material is 26 p · m³/As.

REFERENCES

1. Benedict, G.: *Nontraditional Manufacturing Processes,* Marcel Dekker, New York, 1987.
2. Snoeys, R., I. Stuchens, and W. Dekeyser: Current trends in non-conventional material removal processes, *Ann. CIRP,* vol. 35, no.2, p. 467, 1986.
3. Bellows, G. and J.B. Kohls: Drilling without drills, *Am. Mach.,* Special Report No. 743, p.187, March, 1982.
4. Bradford, J. D., and D. B. Richardson: *Production Engineering Technology,* 3rd ed., Macmillan, London, 1980.
5. Hashish, M., and J. M. Reichmen: Analysis of Waterjet Cutting at High

Traverse Rates, Proc. 5th International Symposium on Jet Cutting Technology, BHRA Fluid Engineering, Cranfield, England, p. 57, 1980.

6. Koenig, W., and C. Wulf: Wasserstrahlschneiden, *Ind. Anz.*, vol. 106, no. 92, 1984.

7. Dombrowski, T. J.: The how and why of abrasive jet machining, *Modern Machine Shop*, p. 76, January, 1983.

8. Dini, J. W.: Fundamentals of chemical milling, *Am. Mach.*, Special Report 7.68, 1984.

9. Williams, L. A.: How to apply electrolytic machining, *Tool Eng.*, p. 43, December, 1959.

10. Opitz, H.: Electrical Machining Processes, International Research in Production Engineering, 1963, p. 225 (presented at the International Production Engineering Research Conference, Pittsburgh, 1963).

11. Phillips, R. E.: Electrochemical grinding—What is it? How does it work?, *SME Technical Paper*, MR 85-383, 1985.

12. Krabacher, E. J., W. A. Haggerty, C. R. Allison, and M. F. Davis: Electrical methods of machining, International Research in Production Engineering, 1963, p. 232 (presented at the International Production Engineering Research Conference, Pittsburgh, 1963).

13. Kalpajian, S.: *Manufacturing Processes for Engineering Materials*, Addison-Wesley, Reading, Mass., 1984.

14. Rudorff, D. W.: Principles and applications of spark machining, *Proc. IME*, vol. 171, p. 495, 1957.

15. *Spark Machining*, Machinery Publishing Co., Brighton, England, 1960.

16. Foster, R. F.: Evolution of wire-EDM, *Tooling Prod.*, p. 90, March, 1982.

17. Wilson, M. J.: Laser speeds saw cutting, *Production*, p. 52, June, 1984.

18. Wager, J. G.: New Metal Shaping Processes—Product Demands, Research Avenues and Assessment Criteria, Proc. 2nd International Conference on Production Research, Copenhagen, 1973, p. 231.

Nomenclature

A area of the work surface exposed to electrolysis in electrochemical machining (ECM)

A_a apparent area of contact between two surfaces

A_c cross-sectional area of the uncut chip; i.e., the cross-sectional area of the layer of material being removed by one cutting edge measured normal to the resultant cutting direction

A_g relative contact area of grains during grinding, percent

A_m area of machined surface

A_r real area of contact between two surfaces

A_s area of shear or area of shear plane

A_α tool flank; i.e., the surface over which the surface produced on the workpiece passes

A_γ tool face; i.e., the surface over which the chip flows

a characteristic linear dimension

a_c undeformed chip thickness; i.e., the thickness of the layer of

material being removed by one cutting edge at the selected point measured normal to the resultant cutting direction

a_{cav} mean undeformed chip thickness; i.e., the mean value of a_c

a_{cmax} maximum undeformed chip thickness; i.e., the maximum value of a_c

a_d depth of dress for grinding wheel; i.e., the amount of penetration of the dressing tool

a_e working engagement; i.e., the instantaneous engagement of the complete tool with the workpiece, measured in the working plane P_{fe} and perpendicular to the direction of feed motion (previously known as depth of cut in a slab-milling operation)

a_f feed engagement; i.e., the instantaneous engagement of the tool cutting edge with the workpiece, measured in the working plane P_{fe} and in the direction of feed motion (in single-point tool operations it is equal to the feed f; in multipoint tool operations, it is equal to the feed per tooth)

a_g gap between the tool and workpiece in ECM

a_h in-phase component of harmonic receptance

a_{hmin} maximum negative in-phase value of operative receptance

a_o chip thickness, i.e., the thickness of the chip produced during machining

a_p back engagement, i.e., the instantaneous engagement of the complete tool with the workpiece, measured perpendicular to the working plane, P_{fe} (previously known as depth of cut in a single-point tool operation and width of cut in a slab-milling operation)

a_r ratio of the inner to the outer radius of surface to be faced

a_t total depth of material to be removed in a machining operation

a_v amplitude of vibration

a_{vmax} maximum amplitude of vibration, i.e., the maximum value of a_v

a_w width of chip, i.e., the width of the chip produced during machining or the width of the uncut chip

a_{wmax} maximum chip width, i.e., the maximum value of a_w

B_s batch size for one set-up

b_h out-of-phase component of harmonic receptance

b_w width of the machined surface; width of the workpiece

b_{wm} width of cut along asymptote to stability chart

b_{wo} width of cut for unconditional stability

C cutting speed for 1 min of tool life (in feet per minute)

C_b cost of setting up and preparing for the machining of a batch of components

C_c ratio of k_2/k_1, assumed a constant

C_g number of active grains per unit area on a grinding-wheel surface

C_m cost of machining, neglecting non-productive costs

C_{mat} cost of material for one workpiece

C_{min} minimum cost of production, i.e., the minimum value of C_{pr}

C_{mt} total machining cost

C_p cost of machining when maximum power is used

C_{pr} production cost, i.e., the average cost of producing each component on one machining tool

C_s velocity of sound

C_t cost of sharp tool, i.e., the average cost of providing the machine operator with a sharp tool or cutting edge, including regrinding costs or the cost of the insert and the tool or tool-holder depreciation

C_w cost per lb of workpiece material

c specific heat capacity

c_d damping force per unit velocity, i.e., the viscous damping constant

dF_r variation in resultant cutting force

dF_1 force variation in-phase with tool displacement

dF_2 force variation out-of-phase with tool displacement

d_a	outer diameter of workpiece
d_b	inner diameter of workpiece
d_e	equivalent wheel diameter in grinding
d_g	average diameter of the grains in a grinding wheel
d_m	diameter of the machined surface
d_t	diameter of the cutting tool or abrasive wheel
d_{tr}	diameter of the transient surface
d_w	diameter of a cylindrical workpiece; diameter of a work surface
E	Young's Modulus
E_g	proportion of total energy flowing into workpiece during grinding
e	electrochemical equivalent of the work material
e_n	chip-breaker land width (Fig. 8.9)
F	instantaneous value of the external harmonic force
F_c	cutting component of the resultant tool force, F_r
F_c'	cutting component of resultant force F_r' acting on the chip-tool interface region
F_f	frictional force on the tool face; frictional force between sliding surfaces
F_{max}	maximum, or peak, value of the external harmonic force
F_n	normal force on the tool face; normal load between surfaces
F_{ns}	normal force on shear plane
F_o	maximum or peak value of external force per unit mass
F_p	plowing force
F_r	resultant tool force
F_r'	resultant force acting on the chip-tool interface region
F_s	force required to shear the work material on the shear plane
F_t	thrust component of the resultant tool force F_r
F_t'	thrust component of the resultant force F_r' acting on the chip-tool interface region

F_{to}	threshold thrust force in grinding, i.e., the minimum value of the thrust force F_t to give grinding by cutting
F_u	harmonic force in u direction
F_v	harmonic force in v direction
f	feed, i.e., the displacement of the tool relative to the workpiece, in the direction of feed motion, per stroke or per revolution of the workpiece or tool
f_d	feed during the dressing of a grinding wheel
f_s	frequency (*Hz*)
G	plan-setting angle (Fig. 7.14)
G_r	grinding ratio, i.e., the ratio of the volume of metal removed to the volume of wheel removed during grinding
H	elevation-setting angle (Fig. 7.14)
H_n	grinding-wheel hardness number
h	chip-breaker height (Fig. 8.3)
I	current in ECM
i	$\sqrt{-1}$
K	constant for a machining operation; can be regarded as the distance traveled by the tool in relation to the workpiece during the machining time t_m
K_p	cost of programming and tape preparation per unit machining time
KT	crater depth (Fig. 4.3)
k	thermal conductivity
k_m	factor to allow for machine overheads
k_o	factor to allow for operator overheads
k_1	chip thickness coefficient or cutting stiffness
k_2	out-of-phase force coefficient
L	roll-setting angle (Fig. 7.14)
l_c	length of chip
l_f	contact length between the chip and tool

l_m	length of machined surface
l_n	chip-breaker distance (Fig. 8.3)
l_p	length of pathway between machines
l_r	length to diameter ratio of workpiece
l_{rd}	distance travelled by fork lift truck in responding to a request
l_s	length of the shear plane
l_{st}	sticking-contact length
l_t	length of a tool or broach
l_w	length of the workpiece or hole to be machined
l_o	dimensionless length of contact between the chip and tool
M	total machine and operator rate (cost per unit time), including machine depreciation M_t, operator's wage W_o and machine and operator overheads
M_s	rate for each station on a transfer machine, including overheads (cost per unit time)
M_t	machine-tool depreciation rate (cost per unit time)
M_t'	machine-tool rate including overheads (cost per unit time)
m	number of revolutions of the workpiece during spark-out in plunge cylindrical grinding
m_c	mass of the chip specimen
m_e	equivalent mass of a machine-tool system
N	number of teeth on the cutting tool
N_a	number of automatic machines serviced by one operator
N_b	batch size, i.e., the number of components in the batch to be machined
N_c	number of chips produced per unit time in grinding
N_d	average number of cutting edges in cut
N_s	number of stations on a transfer machine
N_t	number of tool changes necessary during the machining of a batch of components

NB	wear on tool flank measured normal to the cutting direction
n	constant in Taylor's tool life equation
n_o	number of operations
n_r	frequency of reciprocation
n_s	rotational frequency of a machine-tool spindle; number of shifts
n_{sc}	rotational frequency of a machine-tool spindle for minimum production cost
n_{sef}	rotational frequency of a machine-tool spindle for maximum efficiency (maximum rate of profit)
n_{sp}	rotational frequency of a machine-tool spindle for minimum production time
n_t	rotational frequency of the cutting tool or abrasive wheel; number of tools used
n_w	rotational frequency of the workpiece
n_y	amortization period (years)
P	heat source
P_e	electrical power consumed by the machine tool during a machining operation
P_f	rate of heat generation in the secondary deformation zone
P_f	assumed working plane (Fig. 7.8)
P_{fe}	working plane (Fig. 7.10)
P_g	tool-face orthogonal plane (Figs. 7.4 and 7.14)
P_m	power required to perform the machining operation
P_n	cutting edge normal plane (Figs. 7.9 and 7.11)
P_o	tool orthogonal plane (Fig. 7.6)
P_p	tool back plane (Fig. 7.8)
P_{pe}	working back plane (Fig. 7.10)
P_r	rate of profit (cost per unit time)
P_r	tool reference plane (Figs. 7.8 and 7.9)
P_{re}	working reference plane (Figs. 7.10 and 7.11)

P_s	rate of heat generation in the primary deformation zone
P_s	tool cutting edge plane (Fig. 7.9)
P_{se}	working cutting edge plane (Fig. 7.11)
p_s	specific cutting energy, i.e., the work required to remove a unit volume of metal.
Q	proportion of machining time t_m during which the tool cutting edge is engaged with the workpiece
q_n	chip-breaker groove radius (Fig. 8.2)
R	thermal number
R_a	arithmetical mean value of surface roughness
R_b	ballast resistance in electrical-discharge machining (EDM)
R_c	Rockwell hardness number (C scale)
R_e	resistance of the electrolyte in ECM
R_{max}	maximum height of surface irregularities
R_o	operator rate
R_{sg}	surface generation rate during machining
R_t	total machine and operator rate
R_{uu}	direct harmonic receptance in the u direction
R_{uv}, R_{vu}	cross harmonic receptance between u and v directions
R_{vv}	direct harmonic receptance in the v direction
r	radius at which cutting is taking place
r_c	cutting ratio
r_{chip}	radius of the chip curvature
r_e	specific resistivity of the electrolyte in ECM
r_g	grain-aspect ratio in grinding
r_i	inside radius of the workpiece surface to be faced
r_{me}	ratio of workpiece volume removed externally by machining
r_{mi}	ratio of workpiece volume removed internally be machining
r_o	outside radius of the workpiece surface to be faced

r_v	proportion of initial workpiece volume to be removed in machining
r_e	corner radius, i.e., the radius of a rounded tool corner
S	amount received for machining one component
S	tool major cutting edge (Fig. 7.1)
S'	tool minor cutting edge (Fig. 7.1)
S_e	effective spring stiffness of the machine-workpiece-tool system (restoring force per unit displacement)
S_i	stiffness of the wheel and work in grinding
S_n	grinding-wheel-structure number
S_t	stiffness of the wheel support system in grinding
S_w	stiffness of the work support system in grinding
T	time between successive tool passes or revolutions of the workpiece
t	tool life, i.e., life of the tool cutting edge while the cutting edge is engaged with the workpiece
t'	time
t_c	tool life for minimum production cost
t_a	tool-changing time, i.e., the average machine time to change a worn tool or to index (and, if necessary, replace) a worn insert
t_{ef}	tool life for maximum efficiency (maximum rate of profit)
t_f	transportation time for a round trip with a fork lift truck
t_l	nonproductive time, i.e., the average machine time to load and unload a component and to return the cutting tool to the beginning of the cut
t_{ln}	loading and unloading time
t_m	machining time, i.e., the machine time to machine a component
t_{mc}	machining time for minimum production cost
t'_{mc}	machining time for minimum cost corrected for tool replacement
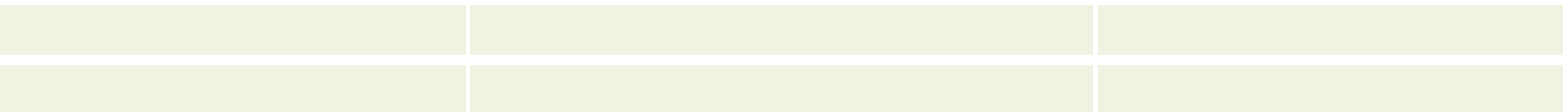
t_{mp} machining time when maximum power is used

t'_{mp} machining time for maximum power corrected for tool replacement

t_p tool life for maximum production rate (or minimum production time)

t_{pr} production time, i.e., the average time to produce one component on one machine tool

t_{po} tool life when maximum power is used

t_{pt} tool positioning time

t_r tool life for a cutting speed of v_r

t_s time for spark-out in grinding

t_{sa} basic set-up time per batch

t_{sb} set-up time per tool

t_t transfer time for a transfer machine

t_{tr} transportation time per workpiece

V_b percentage volume of bond material in a grinding wheel

V_c condenser voltage in EDM

V_g gap breakdown voltage in EDM

V_o volume of chip produced in grinding

V_s supply voltage in EDM and ECM

VB average width of the flank wear land in the central portion of the active cutting edge (zone B in Fig. 4.3)

VB_{max} maximum width of the flank wear land in the central portion of the active cutting edge (zone B in Fig. 4.3)

$(VB)_m$ width of the flank wear land when the tool must be reground

$(VB)_o$ increase in the flank wear land width in zone B during the production of one component

VC width of the flank wear land at the tool corner (zone C in Fig. 4.3)

V_m volume of material removed in machining

VN	width of the flank wear land at the wear notch (zone N in Fig. 4.3)
v	cutting speed, i.e., the instantaneous velocity of the primary motion of the selected point on the cutting edge relative to the workpiece
v_{av}	mean cutting speed, i.e., the average value of v along the major cutting edge
v_c	cutting speed for minimum cost
v_e	resultant cutting speed, i.e., the instantaneous velocity of the resultant cutting motion of the selected point on the cutting edge relative to the workpiece
v_{ef}	cutting speed for maximum efficiency (maximum rate of profit)
v_f	feed speed, i.e., the instantaneous velocity of the feed motion of the selected point on the cutting edge relative to the work-piece
v_i	machine infeed rate in grinding
v_{max}	maximum cutting speed, i.e., the maximum value of v
v_{po}	cutting speed when maximum power is used
v_r	cutting speed giving a tool life of t_r
v_o	velocity of chip flow
v_p	cutting speed for minimum production time
v_t	surface speed of the wheel during grinding
v_{trav}	traverse speed in grinding
v_w	surface speed of workpiece during grinding
W	weight of workpiece
W_o	operator's wage (cost per unit time)
W_o'	operator's wage (wage plus overheads) (cost per unit time)
w_o	dimensionless width of secondary deformation zone
Z_t	wheel-removal rate in grinding
Z_w	metal-removal rate, i.e., the total volume of metal removed per unit time

Z_{wa}	metal-removal rate owing to abrasive in electrolytic grinding
Z_{we}	metal-removal rate owing to electrolysis
Z_{wmax}	maximum metal-removal rate, i.e., the maximum value of Z_w
α	half angle between excitation directions u and v
α_n	tool normal clearance (Fig. 7.12)
α_{n_e}	working normal clearance (Fig. 7.13)
β	mean angle of friction on tool face
β_c	phase angle between successive waves cut on the workpiece surface
β_e	instantaneous cutting direction during oscillatory cutting
β_n	normal wedge angle (Fig. 7.12)
β_R	angle between resultant displacement direction and vertical direction
Γ	proportion of heat generated in primary deformation zone conducted into workpiece
γ_f	tool side rake (Fig. 7.5)
γ_g	tool geometric rake (Fig. 7.4)
γ_m	proportion of real contact area over which metallic contact occurs
γ_n	tool normal rake (Fig. 7.12)
γ_{n_e}	working normal rake (Fig. 7.13)
γ_o	tool orthogonal rake (Fig. 7.6)
γ_p	tool back rake (Fig. 7.5)
γ_{set}	angle set on the vise to grind the tool back rake
δ_c	work-surface slope, i.e., the inclination of the work surface relative to the mean cutting direction
δ_R	resultant displacement in the R direction
δ_t	total relative deflection of the workpiece, wheel, and supports under steady-state grinding conditions
δ_u	response (deflection) in the u direction

δ_v	response (deflection) in the v direction
δ_w	amount to be removed from the workpiece in grinding
ε_r	tool-included angle (Fig. 7.12)
ε_{re}	working included angle (Fig. 7.13)
ζ	damping ratio
η	resultant cutting speed angle, i.e., the angle between the direction of primary motion and the resultant cutting direction
η_e	current efficiency in ECM
η_m	overall efficiency of the machine-tool motor and drive systems
θ	temperature
θ_c	angle between resultant cutting force F_r and normal to the cut surface
θ_f	average temperature rise of the chip owing to frictional heat source
θ_m	temperature rise of material passing through the secondary deformation zone
θ_{max}	maximum temperature along the tool face
θ_s	temperature rise of material passing through the primary deformation zone
θ_o	initial workpiece temperature
κ_r	tool cutting edge angle (Fig. 7.12)
κ_r'	tool minor cutting edge angle (Fig. 7.12)
κ_{re}	working cutting edge angle (Fig. 7.13)
κ_{re}'	working minor cutting edge angle
Λ_t	wheel-removal parameter in grinding, i.e., the volume of wheel removed per unit time per unit thrust force
Λ_w	workpiece-removal parameter in grinding, i.e., the volume of metal removed per unit time per unit thrust force
λ_s	tool cutting edge inclination (Fig. 7.12)
λ_{se}	working cutting edge inclination (Fig. 7.13)
λ_γ	chip-flow angle (Fig. 7.3)

μ	coefficient of friction
μ_c	overlap factor between successive cuts of the tool
ρ	density of work material
σ	chip-breaker wedge angle (Fig. 8.3)
σ_f	normal stress on the tool face
σ_{fmax}	maximum normal stress on the tool face
σ_s	normal stress on the shear plane
σ_y	yield pressure of softer material
τ_f	shear stress on the tool face; shear strength of softer metal
τ_s	apparent shear strength of the work material (shear stress on shear plane)
τ'_s	shear stress on the shear plane corrected for the tool-nose force F_p
τ_{st}	shear stress on the tool face in sticking region
τ_{s0}	shear stress on the shear plane with zero normal stress applied
τ_1	shear strength of softer metal in boundary lubrication
τ_2	shear strength of softer lubricant layer in boundary lubrication
Φ_c	rate of heat transportation into the chip
Φ_t	rate of heat conduction into the tool
Φ_w	rate of heat conduction into the workpiece
ϕ	shear angle
ϕ_f	phase difference between disturbing force and resulting motion
ϕ_x	angle between normal to the cut surface and the vertical direction
ψ	angle between exciting force and vertical direction
Ω	rotational speed of the workpiece (rad/s)
ω	angular frequency of vibration
ω_f	angular frequency of external harmonic force
ω_n	natural angular frequency

page_530

Index

A

Start of Citation[PU]Marcel Dekker, Inc.[/PU][DP]1989[/DP]End of Citation

page_532

Horizontal milling machine, 33-40

Horizontal spindle surface grinding machine, 49-52

Hot hardness of tool materials, 143

I

Infeed in grinding, 49, 53, 56, 57

International Standards Organization (*see* ISO)

Internal grinding machine, 57-8

ISO

    recommended roughness values, 173

    standard for tool life testing, 134

    standard marking system for grinding wheels, 286

    system for tool nomenclature, 205

    tool life test for turning, 149

L

Languages for NC processing, 379-87

    APT, 379, 380-87

    EXAPT, 379, 387-94

Laser beam machining, 501-5

    applications of, 505

    cutting operations with, 504-5

APPROVED